

The impact of smoking-associated aldehyde exposure on the molecular regulation of mitochondrial function in epithelial cells of the airways and lungs

Citation for published version (APA):

Tulen, C. B. M. (2023). *The impact of smoking-associated aldehyde exposure on the molecular regulation of mitochondrial function in epithelial cells of the airways and lungs: implications for COPD*. [Doctoral Thesis, Maastricht University]. Maastricht University. <https://doi.org/10.26481/dis.20230420ct>

Document status and date:

Published: 01/01/2023

DOI:

[10.26481/dis.20230420ct](https://doi.org/10.26481/dis.20230420ct)

Document Version:

Publisher's PDF, also known as Version of record

Please check the document version of this publication:

- A submitted manuscript is the version of the article upon submission and before peer-review. There can be important differences between the submitted version and the official published version of record. People interested in the research are advised to contact the author for the final version of the publication, or visit the DOI to the publisher's website.
- The final author version and the galley proof are versions of the publication after peer review.
- The final published version features the final layout of the paper including the volume, issue and page numbers.

[Link to publication](#)

General rights

Copyright and moral rights for the publications made accessible in the public portal are retained by the authors and/or other copyright owners and it is a condition of accessing publications that users recognise and abide by the legal requirements associated with these rights.

- Users may download and print one copy of any publication from the public portal for the purpose of private study or research.
- You may not further distribute the material or use it for any profit-making activity or commercial gain
- You may freely distribute the URL identifying the publication in the public portal.

If the publication is distributed under the terms of Article 25fa of the Dutch Copyright Act, indicated by the "Taverne" license above, please follow below link for the End User Agreement:

www.umlib.nl/taverne-license

Take down policy

If you believe that this document breaches copyright please contact us at:

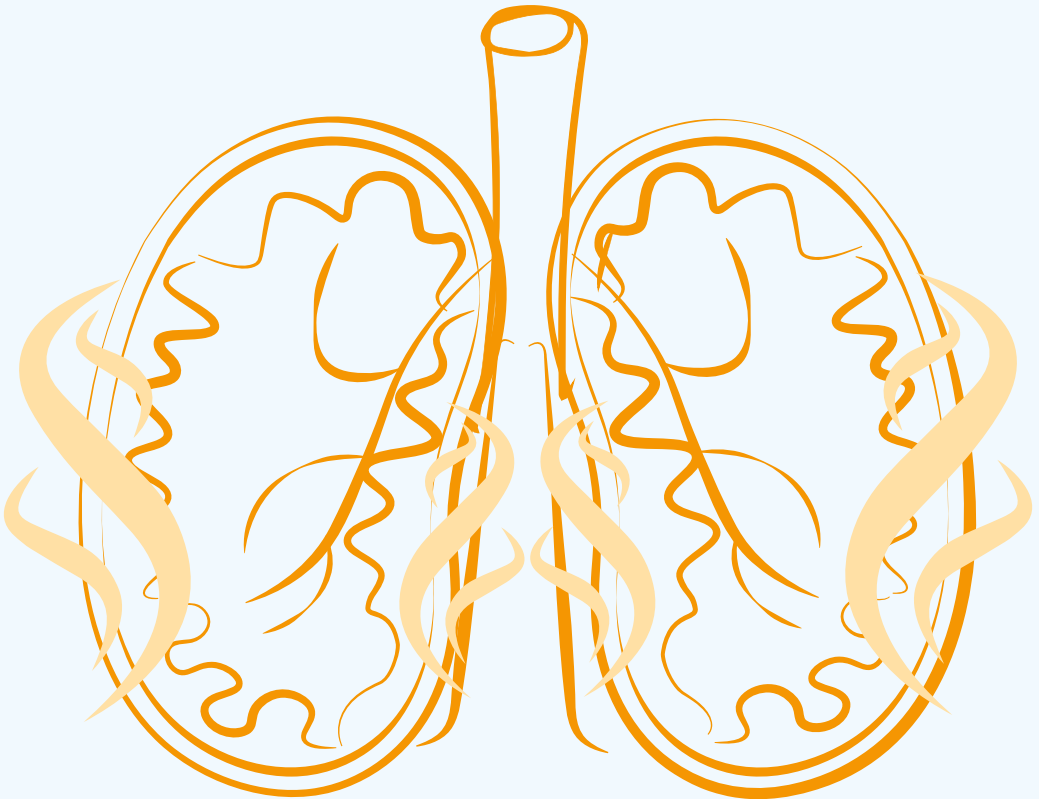
repository@maastrichtuniversity.nl

providing details and we will investigate your claim.

Download date: 10 May. 2024

The impact of smoking-associated aldehyde exposure on the molecular regulation of mitochondrial function in epithelial cells of the airways and lungs

Implications for COPD



Christy B.M. Tulen

**The impact of smoking-associated aldehyde
exposure on the molecular regulation of
mitochondrial function in epithelial cells
of the airways and lungs**

Implications for COPD

Christy B.M. Tulen

© Christy B.M. Tulen, Maastricht 2023

Provided by thesis specialist Ridderprint, ridderprint.nl

Printing: Ridderprint

Layout and design: Wiebke Keck, persoonlijkproefschrift.nl

ISBN: 978-94-6469-291-4

All rights are reserved. No parts of this book may be reproduced or transmitted in any form or by any means, without the written permission of the author.

The impact of smoking-associated aldehyde exposure on the molecular regulation of mitochondrial function in epithelial cells of the airways and lungs

Implications for COPD

PROEFSCHRIFT

ter verkrijging van de graad van doctor aan de Universiteit Maastricht
op gezag van de Rector Magnificus, Prof. dr. Pamela Habibović
volgens het besluit van het College van Decanen,
in het openbaar te verdedigen
op donderdag 20 april 2023 om 16.00 uur

door

Christy Bavonia Maria Tulen

geboren op 28 augustus 1993 te Leiden, Nederland

Promotores

Prof. dr. F.J. van Schooten

Prof. dr. A. Opperhuizen

Copromotor

Dr. A.H.V. Remels

Beoordelingscommissie

Prof. dr. M.K.C. Hesselink (voorzitter)

Prof. dr. D.J. Conklin (University of Louisville, United States of America)

Prof. dr. F. Franssen

Prof. dr. H.I. Heijink (University of Groningen, UMCG, the Netherlands)

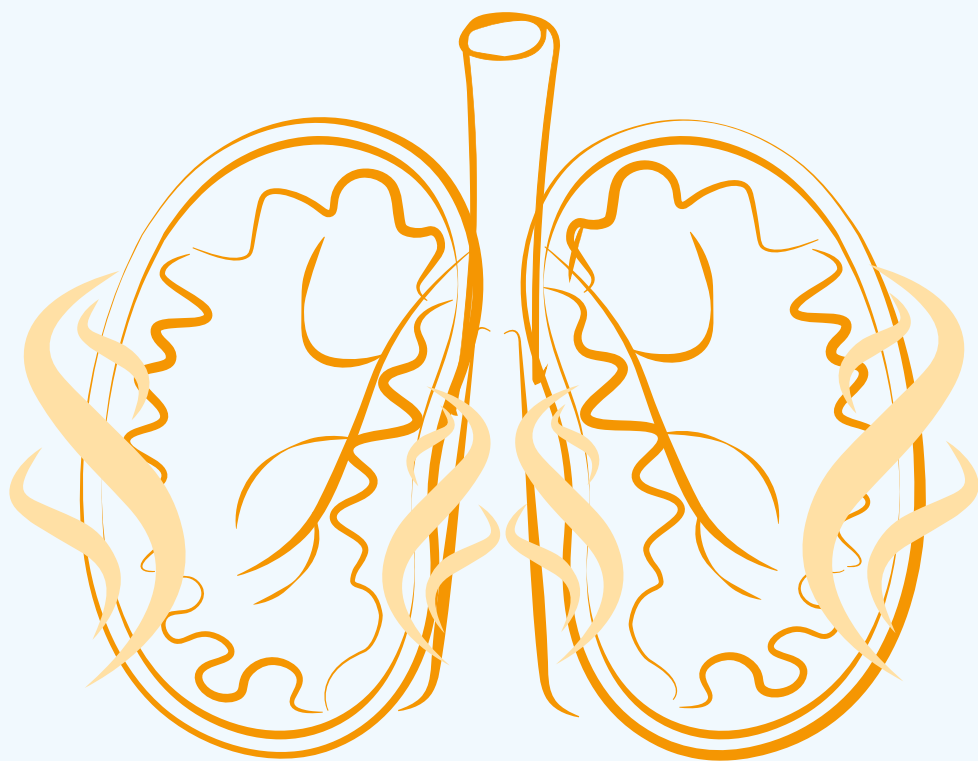
Prof. dr. D.T.H.M. Sijm

The research described in this thesis was conducted at NUTRIM School of Nutrition and Translational Research in Metabolism at Maastricht University in collaboration with the National Institute for Public Health and the Environment (RIVM) and the Netherlands Food and Consumer Product Safety Authority (NVWA).

The research was funded by the Netherlands Food and Consumer Product Safety Authority (NVWA).

Table of contents

Chapter 1	Introduction	7
Chapter 2	Alterations in the transcript abundance of molecules controlling mitochondrial turnover in peripheral lung tissue from chronic obstructive pulmonary disease patients	33
Chapter 3	Dysregulated mitochondrial metabolism upon cigarette smoke exposure in various human bronchial epithelial cell models	83
Chapter 4	Acrolein inhalation acutely affects the regulation of mitochondrial metabolism in rat lung	159
Chapter 5	Impact of sub-acute acrolein inhalation on the molecular regulation of mitochondrial metabolism in rat lung	207
Chapter 6	Smoking-associated exposure of human primary bronchial epithelial cells to aldehydes: Impact on molecular mechanisms controlling mitochondrial content and function	245
Chapter 7	Summary and general discussion	301
	Impact paragraph	331
	Nederlandse samenvatting	341
	Dankwoord	353
	About the author	363
	- Curriculum vitae	364
	- List of publications	365



Chapter 1

Introduction

The research described in this thesis concerns the toxicity of smoking-associated aldehydes on the molecular regulation of mitochondrial content, function and metabolism in cells of the airways and lungs, in the context of chronic obstructive pulmonary disease (COPD). This mechanistic knowledge into the impact of aldehydes on the molecular mechanisms controlling mitochondrial function is needed to contribute to the ultimate research aim to provide scientific evidence which supports the future regulation of aldehydes content in cigarette smoke (CS) by mandated lowering by the World Health Organization (WHO). To reach our goals, we used several experimental *in vivo* and *in vitro* models of COPD as well as exposure to CS or aldehydes and evaluated readout parameters related to the molecular regulation of mitochondrial content, metabolism, mitochondrial biogenesis and mitophagy. We will introduce this topic and research questions in this chapter.

Aldehydes as component of cigarette smoke

The use of tobacco is the leading preventable cause of death globally, with a mortality rate of more than 8 million people/year including 1.2 million deaths due to second-hand tobacco smoke. The most common form of tobacco use is cigarette smoking (1). The WHO Framework Convention on Tobacco Control (FCTC) and the WHO Study Group on Tobacco Product Regulation (TobReg) address the tobacco epidemic by focusing on prevention of initiation of tobacco use, promotion of tobacco cessation and protection from second-hand tobacco smoke exposure. Besides these measures to reduce tobacco-related morbidity and mortality, the FCTC also acknowledges the need for the regulation of the contents and composition of emissions of tobacco products in Articles 9 and 10 of the convention which is aimed at reducing attractiveness, addictiveness and toxicity of tobacco products (2, 3).

The chemical composition of CS is complex, including more than 6000 different known components (4, 5). Of these thousands of chemicals, nine toxicants are currently prioritized for mandated lowering by WHO Study Group on TobReg. These include components in the particulate phase (e.g., specific nitrosamines and benzo(a)pyrene) and in the volatile phase (e.g., aldehydes; acetaldehyde, acrolein, formaldehyde, volatile organic compounds as benzene and 1,3-butadiene, and carbon monoxide). These toxicants were selected based on available toxicity data, toxicity indices, their potential for mandated lowering in smoke, representativeness of the chemicals present in volatile *versus* particulate phases of smoke and various chemical classes, and toxicity related with health risk for diseases such as cancer, cardiovascular- or respiratory disease (2).

In this thesis, the research is focused on the chemical class of aldehydes, mainly acetaldehyde, acrolein and formaldehyde and its effects on mitochondrial metabolism and health in airway/lung cells in the context of COPD pathogenesis. These short-chain

aldehydes have been identified to be formed during the pyrolysis and combustion of tobacco and, due to their chemical structure, are highly reactive electrophilic compounds. All three of these aldehydes have similar mechanisms of formation, molecular structures, and chemical properties and may be representative of the broader chemical class of aldehydes in smoke (2, 6-8). Risk assessment of these three individual aldehydes using computer models based on inhalation exposure risk factors resulted in a hazard ranking which concluded that acrolein, which is also the most studied aldehyde, represents the most harmful component of the three (7, 9). Moreover, based on a computational fluid dynamics modeling coupled to airway region-specific physiologically-based pharmacokinetic tissue models, the kinetics of acrolein, acetaldehyde and formaldehyde were analysed for human respiratory tracts and showed the highest local dose in oral and laryngeal tissues with penetration to the pulmonary tissues (7).

The amount of aldehydes present in CS depends on several factors such as (added) sugars present in the tobacco and smoking behavior/topography. To be more specific, the yield of aldehydes varies considerably due to the combustion and pyrolysis of sugars (e.g., caramelization) as well as the reaction between sugars and amines in tobacco (10-13). Also, the amount and type of sugars present in tobacco fluctuates due to different drying (curing) processes of unprocessed tobacco leaves and the addition of sugars and sugar-containing ingredients during the process of manufacturing (10, 14-17). The impact of these features on the amount of aldehydes per cigarette has been shown in a study by Pauwels *et al.* that reported a range of 36.7-1199.5 µg acetaldehyde, 1.3-121.7 µg acrolein and 0.7-54.9 µg formaldehyde per cigarette, with large variations depending on different tobacco brands and smoking regimes (18). Although inhalation of tobacco smoke is a major source of aldehydes exposure in humans, it is not the only source, as aldehydes are also endogenously formed and both environmental as well as occupational exposure of aldehydes takes place via, for example, air pollution, burning of fossil fuels, industrial waste and indoor via fireplaces and gas heaters/stove. Moreover, besides inhalation also dermal or oral exposure can be a route of exposure to aldehydes for example via cosmetics or diet. Exposure to these non-tobacco sources of aldehydes exposure however situate themselves in a low dose range compared to smoking-associated aldehydes exposure (19-22).

Detoxification of aldehydes is facilitated by the enzyme aldehyde dehydrogenase (ALDH), which is responsible for the reduction of aldehydes to less reactive forms (23). An important isoform of this enzyme is the mitochondrial enzyme ALDH2, which plays a major role in detoxifying aldehydes including acetaldehyde, acrolein and formaldehyde (24-26). Interestingly, although (isoforms of) ALDH enzymes are highly expressed in stem cells of all tissues, besides liver, heart and brain, levels of ALDH2 are observed to be expressed in stem cells of the airways and in lung tissue (27-30).

Aldehyde-induced respiratory toxicity is associated with the development of COPD

Inhalation of aldehydes, through for example cigarette smoking, results in exposure of the epithelial cells lining the respiratory tract and the alveoli and has been convincingly linked to respiratory toxicity.

Already many years ago, it was shown that sub chronic acrolein exposure in rat (up to 4 ppm, for 62 days: 6h/day 5 days/week) resulted in impaired lung function and structure (31). Due to its electrophilic nature, acrolein is also known to be involved in oxidation of DNA, RNA, protein and lipids in cells of the lungs (32, 33). The International Agency for Research on Cancer (IARC) has classified acrolein as '*probably carcinogenic to humans*' (Group 2A) based on sufficient evidence of carcinogenicity in experimental animals and strong mechanistic evidence (34). Limits of human occupational exposure varies per country: EU Occupational Exposure Limits (OEL) are: 0.02 ppm (8 hours time-weighted average; TWA) or 0.05 ppm (Short Term Exposure Limit; STEL), the current American Conference of Governmental Industrial Hygienists threshold limits: 0.1 ppm (35, 36), and the United States Environmental Protection Agency (US EPA) reference environmental exposure per day as follows: for inhalation 2×10^{-5} mg/m³ and oral 0.5 µg/kg (37). Moreover, a more recent mode-of-action analysis described the potential of acrolein to induce key cellular processes linked to respiratory toxicity that are associated with tobacco smoke exposure (38). These included interaction with proteins and other macromolecules, initiation of cell death (oncosis, necrosis and apoptosis), inflammation responses and oxidative stress, tissue remodeling and devastation, as well as impairments in the elasticity of the lung and enlarged airspace of the lung. Interestingly, all of these processes have also been recognized to be essentially involved in the airway pathogenesis of COPD (38, 39). Moreover, acrolein-exposed mice showed elevated transcript and protein levels as well as increased activity of lung matrix metalloproteinase 9, which was associated with increased transcript levels of genes involved in mucus production (MUC5AC) and mucin protein in lung tissue (both features associated with COPD) (40).

Although, like acrolein, it is known that acetaldehyde and formaldehyde can induce respiratory toxicity, the underlying cellular mechanisms involved have been less extensively studied and are only scarcely described in literature. The IARC has classified formaldehyde as '*carcinogenic to humans*' (Group 1) based on convincing toxicological and epidemiological evidence (41) and acetaldehyde as '*possibly carcinogenic to humans*' (Group 2B) which is based on limited human evidence and sufficient experimental animal evidence of carcinogenicity (42). Formaldehyde OEL limits of inhalation are 0.3 ppm (8 hours TWA) or 0.6 ppm for STEL (15 min) (43) and acetaldehyde human exposure limits are for occupational exposure 200 ppm for 8 hours TWA (Occupational Safety and Health Administration) (44). An *in vitro*

study by Cheah *et al.* observed differentially-expressed genes involved in apoptosis and DNA damage after exposure of lung alveolar epithelial cells to formaldehyde or acetaldehyde (45). Regarding the impact of formaldehyde specifically, a link has been shown between formaldehyde inhalation and respiratory toxicity manifested as an inflammatory response, cytotoxicity and genotoxicity (46). Interestingly, a recent study investigated the individual susceptibility to lung injury due to formaldehyde exposure by integrating analyses of the genome with molecular epidemiology. A link was shown between expression of the gene 5-hydroxytryptamine (serotonin) receptor 4 (*HTR4*), previously identified to be associated with airflow obstruction (47-49), and individual susceptibility to formaldehyde-induced adverse respiratory effects (progression and prevalence of COPD) (50). With respect to acetaldehyde, a hazard summary of the US EPA described the main acute and chronic effects upon inhalation exposure (51). Acute exposure to acetaldehyde was described to result in irritation of the respiratory tract in humans and higher levels of exposure have been shown to result in erythema, pulmonary edema and necrosis. Moreover, in animals, acute exposure to acetaldehyde resulted in a decline in breathing-rate and increased blood pressure (52). Although, acute inhalation of acetaldehyde resulted in low toxicity in rats, rabbits and hamsters, chronic inhalation revealed alterations in nasal mucosa and trachea in hamsters (52-54). In addition, acetaldehyde has been identified as being genotoxic and carcinogenic (51, 55, 56), but evidence is limited resulting in Group 2B classification by IARC as mentioned above. However, studies linking acetaldehyde inhalation to a potential increased risk for developing COPD are lacking.

Besides the role of individual aldehydes in inducing cellular mechanisms underlying lung injury, a few studies also investigated the impact of a mix of reactive aldehydes, which is more representative for CS, on these processes in (cells of) the airways. For example, van der Toorn *et al.* showed a critical role for aldehydes present in CS in mediating cytokine production as well as neutrophilic airway inflammation, while mononuclear inflammation was not affected in mice exposed to CS (including aldehydes) for 5 days (57). In addition, Zhang *et al.* have shown a synergistic impact of specific aldehydes on apoptosis, cytotoxicity and genotoxicity using an *in vitro* model of bronchial epithelial cells co-exposed to acrolein and/or formaldehyde (58-60). Also, Zulueta *et al.* exposed human bronchial epithelial cells to a mixture of nicotine (1 mM), acrolein (35 μ M), formaldehyde (80 μ M) and acetaldehyde (1 mM), which resulted in increased abundance of inflammatory cytokines and matrix metalloproteinase 9 (61). These findings illustrate the importance of not only focusing on individual aldehydes, but also taking into account the respiratory toxicity of the mixture.

To summarize, inhalation of these three short-chain aldehydes, as components of CS, has been convincingly associated with respiratory toxicity in which cellular mechanisms such as oxidative stress, tissue remodeling, inflammation, and cell death play a key role.

A link between exposure to aldehydes and the development of COPD has been suggested by several studies. Elevated acrolein levels have been observed in expired breath condensate and induced sputum (62) as well as in plasma from COPD patients (63). In addition, acrolein concentrations in supernatants of homogenized lung tissue as well as protein-bound acrolein have been detected in lung tissues of COPD patients and non-COPD smokers, compared to never-smokers (63) indicative of significant (CS-related) exposure. Furthermore, increased expression of ALDH enzymes, including ALDH2, has been observed in bronchoalveolar lavage fluid of COPD patients (64). Moreover, the presence of *ALDH2*2* (an inactive allele of ALDH2) has been associated with an increased risk of developing smoking-associated chronic airway obstruction in a Japanese population (65). In addition, Kuroda *et al.* also extensively studied the effect of this ALDH2 polymorphism on the lung using several *in vivo* and *in vitro* models. Firstly, they observed an association between the inactive form of the gene: *ALDH2*2* and reduced lung function parameters (FEV_1/FVC) in a population of healthy individuals. Secondly, antioxidant gene expression has been found to be decreased if *ALDH2* function was disturbed in human lungs. Lastly, conflicting results were shown in *Aldh2*2* Tg mice, as they were resistant to develop emphysema in response to chronic CS exposure (66). The susceptibility to inhalation toxicity of acetaldehyde was also studied in *Aldh2^{-/-}* mice exposed for 24 h/day during 14 days, and revealed more pronounced abnormalities to pathological features of the respiratory epithelium in larynx, pharynx, trachea and nose (67). With respect to other ALDH enzymes, it has been shown *in vitro* that expression of ALDH3A1 protects against cytotoxicity and DNA damage in CS extract-exposed epithelial cells of the airways (68).

In summary, these findings clearly indicate that smokers are highly exposed to aldehydes and that aberrations in the mechanisms responsible for detoxifying aldehydes are associated with an increased risk for abnormalities in lung function and development of obstructive airway/lung diseases such as COPD.

Mitochondrial function in healthy cells of the airways

Mitochondria are eukaryotic organelles, including a mitochondrial matrix surrounded by a double-membrane. Besides the nuclear genome, which is required for mitochondrial functionality, also specific mitochondrial DNA (mtDNA) is present in the mitochondrial matrix. mtDNA encodes for 37 genes and 13 proteins, which are mostly encoding for subunits of the complexes of the oxidative phosphorylation (69). Although mitochondria are the powerhouse of the cell driving ATP production from a traditional point of view, they are also important mediators in critical cellular processes such as inflammation, oxidative stress and cell death (70).

Interestingly, the cellular processes, as described above, that have been linked to acrolein-induced respiratory toxicity as well as the development of COPD, are known to be regulated by (dysfunction of) mitochondria. Indeed, mitochondrial dysfunction has been shown to induce cell death pathways, inflammation and oxidative stress in multiple cell types including airway and lung epithelial cells (70). Healthy and functional mitochondria are known to be important for normal function of cells of the lungs and airways as energy generation by these organelles is essential for maintaining specific cellular functions, such as, for example, cilia beating and production of surfactant and mucus (70, 71). In order to be able to respond to the energy demand of distinct cell types, which obviously depends on their function, the number of mitochondria as well as mitochondrial organization/location is variable in different types of airway epithelial cells, including basal-, ciliated-, club- or secretory goblet cells as well as in alveolar cells (70, 72). Moreover, mitochondria are also highly dynamic organelles capable to adapt to cellular stressors and changes in metabolic requirements to maintain mitochondrial morphology, homeostasis and ATP production (70). Processes regulating mitochondrial turnover, mitochondrial content and metabolism preserve homeostasis of the mitochondrial network. These processes include synthesis of new mitochondria (mitochondrial biogenesis) and mitochondrial dynamics including mitochondrial fusion, mitochondrial fission as well as targeted degradation of damaged or dysfunctional mitochondria (mitophagy). Mitochondrial biogenesis, fission/fusion and mitophagy are all continuously interacting with each other to orchestrate the complex, dynamic mitochondrial network in cells of the airways and lungs (70, 73).

The generation of new mitochondria, i.e., mitochondrial biogenesis, is accurately coordinated by nuclear- and mitochondria-specific regulatory mechanisms. Mitochondrial biogenesis is controlled by nuclear transcriptional coactivators of the peroxisome proliferator-activated receptor gamma, coactivator 1 (PPARGC1) family, respectively PPARGC1 alpha (PPARGC1A) and PPARGC1 beta (PPARGC1B), together with their upstream effectors and downstream regulators, such as nuclear respiratory factors (NRF), transcription factor a, mitochondrial (TFAM) and estrogen related receptor alpha (ESRRA). In addition, mitochondria-associated regulatory mechanisms are involved in regulating mitochondrial biogenesis, for example import of mitochondrial proteins (e.g., mitochondrial protein import machinery (TOMM)) and mtDNA replication, transcription and translation (74-77).

Fusion and fission are complement activities to ensure dynamic, healthy mitochondria by mediating inter-mitochondrial content exchange, mitochondrial distribution, and the release of intermembrane space proteins during apoptosis processes (78). GTPases of the dynamin superfamily facilitate the process of mitochondrial fusion, respectively outer-membrane fusion is regulated by outer-membrane proteins mitofusin 1 and mitofusin 2, while inner-membrane fusion is mediated by inner-membrane isoforms of OPA1, mitochondrial dynamin Like GTPase (Opa1). Mitochondrial fission is initiated

by dynamin-related protein 1 (DRP1), a large GTPase, upon recruitment to the outer-membrane by multiple receptor proteins such as fission protein 1 (FIS1), mitochondrial fission factor (MFF), mitochondrial dynamic protein 49 (MID49), and MID51 (73).

The selective degradation of damaged or defective mitochondria is tightly regulated by the mitophagy machinery, which requires specific autophagy proteins to support autophagosome formation. Two distinct mitophagy pathways have been identified: ubiquitin- and receptor-mediated mitophagy. Ubiquitin-mediated mitophagy is also called the PTEN-induced kinase 1 (PINK1)/Parkin RBR E3 ubiquitin protein ligase (PRKN) pathway. In healthy cells, the master regulator PINK1 is degraded upon recruitment of PRKN and translocation to the inner mitochondrial membrane. In contrast, cellular stress (e.g., hypoxia or energy stress) triggers depolarization of the mitochondrial membrane potential, followed by PINK1 stabilization and accumulation on the outer mitochondrial membrane. Altogether, subsequent phosphorylation of ubiquitin, recruitment and activation of PRKN and ubiquitination of mitochondrial receptor proteins, initiates the generation of an autophagosome to degrade the engulfed organelle. In addition, independently from the PINK1/PRKN pathway, receptor-mediated mitophagy is predominantly mediated by receptor proteins embedded in the outer mitochondrial membrane namely BCL2 interacting protein 3 (BNIP3), BNIP3-like (BNIP3L; NIX) and FUN14 domain containing 1 (FUNDC1). Due to the direct interaction of these membrane receptors with light chain 3 beta (LC3B) on the autophagosomal membrane, ubiquitination is superfluous in this pathway. In both pathways regulating mitophagy, ultimately, specific autophagy proteins ensure encapsulation and degradation of the mitochondria in an autophagosome, respectively autophagy-related genes, beclin-1, microtubule-Associated protein 1 light chain 3 beta, sequestosome 1 (77, 79, 80).

The interplay among mitochondrial biogenesis, fission and fusion and mitophagy is essential to maintain mitochondrial homeostasis for proper function of the lung cells.

Thus, mitochondria have an essential role in maintaining cellular homeostasis and function in epithelial cells of the airways and the periphery of the lung, and mitochondrial dysfunction triggers processes known to be involved in the pathogenesis of COPD. Therefore, it comes as no surprise that mitochondrial abnormalities, including changes in the molecular mechanisms involved in mitochondrial homeostasis, have been described in these cell types in COPD as described in more detail below.

Mitochondrial abnormalities in epithelial cells of the airways and lungs from COPD patients

Aberrant mitochondrial morphology has been observed in epithelial cells of the airways/lungs from COPD patients. Indeed, elongated and swollen mitochondria have been described in primary bronchial epithelial cells (PBEC) from ex-smoking COPD patients with very severe disease compared to never-smoking controls (81). In line with these observations, another study described fragmentation, branching and cristae depletion in PBEC from COPD patients relative to smokers without COPD (82). Also, a reduction in mitochondrial membrane potential, as well as higher mitochondrial reactive oxygen species (ROS) and lower superoxide dismutase 2 levels (a mitochondrially-located anti-oxidant) were shown in isolated mitochondria from bronchial biopsies from COPD patients with moderate disease (GOLDII) (83). Moreover, based on the hypothesis of an association between the release of extracellular mtDNA and mitochondrial dysfunction in COPD patients, mtDNA levels in urine were linked to increased respiratory symptom burden in particular among smokers without COPD and mtDNA levels in plasma were linked to baseline COPD status (84, 85). Collectively, these studies suggest abnormalities in mitochondrial morphology/content and oxidative responses in the lungs and airways of COPD patients.

Although studies investigating the molecular regulation of mitochondrial biogenesis in the airways/lungs of COPD patients are very limited, a few studies exist in which the abundance of specific molecules involved in mitochondrial biogenesis has been assessed in PBEC or (peripheral) lung tissue from COPD patients. Reduced expression of the master regulator controlling mitochondrial biogenesis, PPARGC1A, was observed in lung homogenates from moderate and severe COPD patients (GOLDII and GOLDIII), whereas elevated levels of PPARGC1A were observed in mild COPD patients (GOLDI) (86). In contrast to these findings, in PBEC of ex-smoking COPD GOLDIV patients, elevated transcript levels of *PPARGC1A* relative to non-smoking controls have been reported (81). Other studies have reported decreased or no alterations in levels of TFAM in lung tissue from moderate COPD patients compared to non-COPD patients (87) or in ex-smoking COPD GOLDIV patients compared to non-smoking controls respectively (81). Collectively, although scarce in number, these studies do suggest that the molecular regulation of mitochondrial biogenesis is altered in the airways and lungs of COPD patients.

With respect to the regulation of mitophagy in the lungs/airways in COPD, an increased expression of PINK1, involved in ubiquitin-mediated mitophagy, has been observed in lung tissue homogenates and in bronchial epithelial cells from COPD patients (81, 88). On the other hand, decreased protein levels of PRKN, another important regulator associated with the ubiquitin-mediated mitophagy pathway, were found in lung homogenates from COPD patients relative to non-COPD smokers (89). This decrease in PRKN protein levels was also demonstrated in isolated mitochondria of lung tissue from

COPD patients or smokers relative to non-smokers suggestive of an altered translocation of PRKN to the mitochondria in COPD, which may indicate impairments in the clearance of (damaged) mitochondria through the mitophagy pathway (90). Research assessing the molecular regulation of the receptor-mediated pathway in cells of the airways/lung from COPD patients is scarce. Besides the observed changes in the regulation of mitophagy in COPD patients, also upregulated expression of autophagy proteins as well as increased formation of autophagic vacuoles has been observed in lung tissue from COPD patients compared to non-smokers, respectively elevated at GOLD0 and sustained during disease progression up to GOLDII/IV (91).

Altogether, although not abundant in nature, these reports all suggest aberrations in the molecular pathways involved in mitochondrial content, mitochondrial function and mitochondrial quality control (mitochondrial biogenesis *versus* mitophagy) in cells of the airways in COPD. Additional research is required to investigate how the molecular pathways regulating mitochondrial turnover (mitochondrial biogenesis *versus* mitophagy) are implicated in COPD pathogenesis and whether differences herein exists in different compartment of the lungs and airways.

CS-induced mitochondrial dysfunction in epithelial cells of the airways and lungs

Given that smoking is the main risk factor for developing COPD and, as described above, several abnormalities at the level of the mitochondrion have been described in COPD patients, it is reasonable to assume a role for (components) of CS in these abnormalities. Indeed, multiple reviews have discussed studies which show a direct link between exposure of airway/lung epithelial cells to CS and disturbances in (the molecular regulation of) mitochondrial function both *in vivo* and *in vitro* (72, 92, 93). Key findings related to CS-induced alterations in mitochondrial morphology and processes involved in maintaining mitochondrial homeostasis are described below.

Firstly, abnormalities in the mitochondrial structure (e.g., fragmentation) have been convincingly demonstrated upon CS exposure of both bronchial- and alveolar epithelial cells (81, 82, 94, 95), which is similar to observations in COPD patients as described in the paragraph above.

Moreover, alterations in mitochondrial bioenergetic processes in response to CS exposure have been reported in several airway models. More specifically, decreased mitochondrial respiration, lower ATP production, elevated mitochondrial ROS levels, reduced mtDNA, altered abundance/activity of subunits of electron transport chain complexes and loss of mitochondrial membrane potential have been observed *in vitro* in alveolar and bronchiolar epithelial cells (primary cells or cell lines) in response

to CS extract (81, 82, 88, 94, 96-100). In addition to these *in vitro* studies, decreased mitochondrial respiration, lower ATP production while metabolizing glucose, altered glycolysis affecting the surfactant synthesis and increased expression/activity of (subunits of) oxidative phosphorylation complexes have been observed in isolated primary alveolar type II cells or mouse lung tissue from mice exposed to CS for 4 or 8 weeks (101, 102). Conflicting findings, suggesting an adaptive effect or compensatory response have also been reported in primary alveolar type II cells upon low, non-toxic doses of smoke or following 8 weeks of smoke exposure in mice (95, 102).

In line with the CS-induced abnormalities in mitochondrial morphology and function, studies have also shown that CS can impede on the molecular pathways involved in the control of mitochondrial quality processes. Indeed, both *in vitro* as well as *in vivo* CS exposure models convincingly showed alterations in the abundance of key molecules involved in these pathways.

More specifically, upregulated transcript levels of key regulators of the PPARGC1-network, respectively *PPARGC1A*, have been shown in bronchial epithelial cells acutely exposed to CS extract (103). In contrast, a decrease in expression of *PPARGC1A* has been observed in experimental animal models of CS-induced COPD, e.g., mice instilled with CS extract (104) or in mice instilled with LPS and CS (105).

With regard to mitophagy, in line with the observation in COPD patients, increased abundance of *PINK1* and decreased abundance of *PRKN* was observed in various *in vivo* and *in vitro* airway models of CS exposure (88-90, 97, 106, 107). Conflicting findings or no alterations in the abundance of these constituents were also reported in human or mice alveolar or bronchiolar cells exposed to CS (extract) (81, 88, 90, 94, 95, 97). The other mitophagy pathway, i.e., receptor-mediated mitophagy, is less well studied before and contradictory results were reported. Elevated abundance of receptor-mediated proteins have been observed both *in vivo* in a COPD mouse model (exposed to CS) and *in vitro* in bronchial epithelial cells following CS extract exposure (108, 109). Interestingly, a leading role for CS-induced receptor-mediated mitophagy in COPD has been suggested by Wen *et al.*, showing suppression of the development of COPD-like features in mice by silencing *FUNDC1* (109).

Whether or not CS-induced changes in mitophagy and autophagy in the airways and lungs can be considered as being protective or detrimental in the context of lung disease remains to be established. Illustrative of this complex regulation of mitophagy is the fact that *in vivo* and *in vitro* studies reported a protective role of both knockdown/knockout of *PINK1* or *PRKN* (88, 89, 110) as well as of overexpression of *PRKN* (89, 90, 110) against CS or extract thereof induced mitophagy or dysfunctional mitochondria. Future research is required to elucidate the exact role of these key regulators herein.

Mitochondrial fusion and fission are essential processes involved in the biogenesis of new organelles and in the degradation of defective mitochondria. In line with CS-induced abnormalities in these processes, CS has been shown to disrupt fusion and fission events. Indeed, CS exposure has been shown to lead to mitochondrial fragmentation (increased fission) and decreased fusion in epithelial cells of the airways, as shown in previous studies (82, 88, 94, 106, 107, 111, 112). Nevertheless, conflicting findings pointing towards decreased abundance of fission- and increased abundance of fusion-associated proteins or even no alterations are also reported upon CS extract or whole CS (condensate) exposure in cells of the lung and airways (81, 90, 95, 96). Possible explanations for these discrepancies could be the variation in models and duration of exposure illustrated by Walczak *et al.* (113), cell type specific effects and the fact that fission and fusion are dynamic processes operating as a flux. Further studies should investigate the functional impact of this disbalance.

Although the body of evidence described above clearly shows (CS-induced) abnormalities at the levels of the mitochondrion and the pathways regulating mitochondrial content and function in COPD, these studies do not provide evidence for a causal relationship between mitochondrial dysfunction in epithelial cells of the airways and lungs and the development of COPD. One study by Cloonan *et al.*, however, did provide causal evidence for this by demonstrating that prevention of CS-induced mitochondrial dysfunction in a mouse model of COPD significantly ameliorated CS-induced development of emphysema and bronchitis (114). This study further highlights the central role of mitochondria in development of COPD.

Thus far, it is unknown which exact chemical components present in CS are responsible for mitochondrial dysfunction. Aldehydes are suggested to be one of the chemicals involved, as outlined below.

Aldehydes-induced mitochondrial dysfunction in lung cells associated with COPD pathogenesis

In this paragraph, we describe evidence from *in vitro* and *in vivo* studies that suggest that aldehydes, as components of CS, may mediate CS-induced mitochondrial abnormalities as described above. As this is a relatively new vantage point, literature regarding this topic is limited and mainly centers around investigations of the impact of acrolein on mitochondrial metabolism *in vivo* and *in vitro*.

Abnormal mitochondrial morphology (e.g., fragmentation) has been shown upon exposure of human lung fibroblasts and alveolar epithelial cells to acrolein (115). Moreover, *Aldh2*^{-/-} mice, deficient in aldehyde detoxification mechanisms, have been shown to display aberrant mitochondrial morphology as well as elevated ROS levels

and less functional mitochondria in cells of the trachea and lung compared to WT mice, even in absence of exposure to CS (66).

Previous studies also described a negative impact of acrolein on the regulation of mitochondrial function and energy metabolism in the airways and lungs. For example, an *in vivo* study in which mice were exposed to 10 ppm acrolein revealed increased molecules associated with glycolysis and branched chain amino acid metabolism in acrolein-sensitive and acrolein-resistant mouse strains by metabolic profiling (116). Besides this *in vivo* evidence, *in vitro* exposure of alveolar epithelial cells to acrolein resulted in a metabolic shift, respectively from the glycolytic pathway to the pentose phosphate pathway, in mitochondria. This shift results in the use of palmitate from phosphatidylcholine as alternative substrate for mitochondrial respiration leading to decreased surfactant levels, respectively a feature often observed in lung diseases including COPD (117). In addition, acrolein exposure of lung alveolar cells was shown to induce cellular stress and apoptosis, which was mediated through the mitochondrial pathway mediated by ROS (118). Furthermore, mtDNA damage, reduced mitochondrial membrane potential, inhibited bioenergetics (decrease in mitochondrial respiration), and decreased mtDNA copy number has been observed in alveolar epithelial cells and fibroblasts following acute acrolein exposure (115). Lastly, exposure of human lung fibroblasts to low doses of acrolein for a prolonged period of 16 days resulted in significantly decreased mitochondrial membrane potential and downregulated expression of complex I, II, III and V of the mitochondrial electron transport chain (119). In summary, these findings show that acrolein exposure can disrupt the regulation of mitochondrial function and mitochondrial metabolism in cells of the airways and lungs.

Additional knowledge about the potential of aldehydes to disrupt mitochondrial metabolism and bioenergetic processes can be obtained from studies using cell types other than lung cells. In this regard, acrolein incubation of mitochondria isolated from rat liver resulted in dose-dependent inhibition of mitochondrial respiration, mitochondrial enzyme activity associated with complex I and II, pyruvate dehydrogenase, alpha-ketoglutarate dehydrogenase, as well as alteration of mitochondrial permeability transition and elevated protein carbonyls (120). Knowledge regarding the effect of acetaldehyde and formaldehyde on the regulation of mitochondrial metabolism in the airways is limited and mainly studied in non-lung cell types. One exception is the reported impaired cilia function and cilia beating in bovine bronchial epithelial cells upon acetaldehyde exposure implying disrupted mitochondrial energy metabolism (121, 122). To explain in more detail the findings in other cell types, dysregulated mitochondrial metabolism has been observed in acetaldehyde-exposed hepatocytes (123), upon formaldehyde and acetaldehyde exposure of rat liver mitochondria (124) and after formaldehyde exposure of neuroblastoma cells (125). Moreover, in macrophages, formaldehyde exposure resulted in increased glycolysis and hypoxia signaling (126).

In addition to acrolein, acetaldehyde and formaldehyde, a few studies assessed the impact of crotonaldehyde (which is also found in CS) on mitochondria in cells of the airways. Recently, *in vivo* chronic exposure of rats to crotonaldehyde by oral gavage induced apoptosis in lung tissue which was associated with inflammation and oxidative stress mediated via the mitochondrial pathways (127). Chronic crotonaldehyde exposure of rats by intragastric administration also resulted in mitochondrial dysfunction in the lungs evidenced by disrupted mitochondrial energy metabolism, oxidative stress and apoptosis (128). In addition, *in vitro* studies reported crotonaldehyde-triggered apoptosis (caspase dependent manner) as well as oxidative stress in human bronchial epithelial cells (129) and showed crotonaldehyde-induced apoptosis via intracellular calcium, mitochondria and P53 signalling in alveolar macrophages (130). In other cell types, it has been shown that short-term crotonaldehyde exposure of mice cardiomyocytes resulted in apoptosis, mitochondrial injury and inhibited regulatory pathways involved in mitochondrial oxidative capacity (131).

Interestingly, Clapp *et al.* demonstrated that dose-dependent exposure to cinnamaldehyde, yet another member of the aldehyde family of chemicals (present in e-cigarette liquids), impaired mitochondrial function, mitochondrial respiration, glycolysis and reduced intracellular ATP levels and suppressed ciliary beat frequency of differentiated human bronchial epithelial cells (132).

Although these studies clearly suggest a detrimental impact of different aldehydes, commonly associated with CS, on mitochondrial function and mitochondrial metabolism, limited information is available on whether or not aldehydes disturb (the regulation of) mitochondrial biogenesis and mitophagy. A decline in PPARGC1A protein levels has been reported *in vitro* in lung fibroblasts upon acrolein exposure (119). In addition, reduced PPARGC1A protein levels were also observed in mice cardiomyocytes upon short-term crotonaldehyde exposure (131). To the best of our knowledge, there are no previous studies available investigating the effect of acetaldehyde and formaldehyde on the molecular regulation of mitochondrial biogenesis in cells of the airways or lungs.

With respect to mitophagy, it has been shown in literature that aldehydes can induce autophagy and mitophagy, which is mainly studied in response to acrolein in non-primary human lung cells. *In vivo* studies reported augmented autophagosome number (and protein ratio MAP1LC3BII/I) in alveolar epithelial cells from rats upon sub-acute exposure to formaldehyde (133). Moreover, acrolein-induced autophagy and mitophagy has been demonstrated in human lung alveolar basal epithelial cells and fibroblasts (115).

In addition, the impact of acrolein on mitochondrial dynamics has been evaluated previously to a limited extent. Acrolein exposure induced (transcriptional regulation of) mitochondrial fission *in vitro* (in alveolar and lung fibroblast) (115).

To summarize, to our current knowledge, exposure to smoking-associated aldehydes, in particular acrolein, results in dysregulated mitochondrial (energy) metabolism, mitochondrial biogenesis and mitophagy in cells of the airways and lungs (Figure 1). It is however difficult to compare abovementioned findings in the distinct studies, because of differences in experimental set-up such as exposure dose, exposure regime and types of cells analysed (lung *versus* non-lung cells).

Whereas the abovementioned *in vivo* and *in vitro* studies focused on the impact of individual aldehydes, *in vivo* evidence is scarce and there is a lack of studies investigating the impact of a mixture of acetaldehyde, acrolein, formaldehyde (comparable to levels and proportions present in one cigarette) using a physiologically-relevant exposure regime.

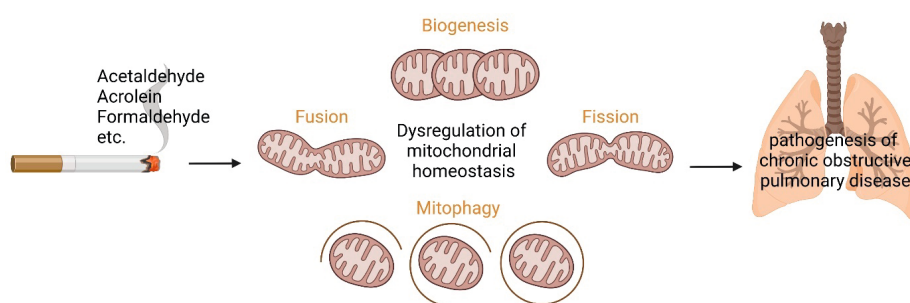


Figure 1. Aldehydes present in cigarette smoke are suggested to induce dysregulation of processes controlling mitochondrial homeostasis in cells of the airways and lungs, respectively the synthesis of new mitochondria (mitochondrial biogenesis) and mitochondrial dynamics including mitochondrial fusion/fission as well as targeted degradation of damaged or dysfunctional mitochondria (mitophagy). Based on previous *in vitro* and *in vivo* studies, aldehydes-induced mitochondrial dysfunction has been suggested to be involved in the pathogenesis of chronic obstructive pulmonary disease. Designed with Biorender.com.

Aims and outline of this thesis

In summary, as described in the paragraphs above, smoking of tobacco is the main risk factor for developing COPD. During the pyrolysis and combustion of tobacco, aldehydes are formed which include acetaldehyde, acrolein and formaldehyde. These short chain aldehydes have been shown to induce cellular mechanisms underlying respiratory toxicity. Emerging evidence suggests that dysfunctional mitochondria are mechanistically and causally involved in the development of CS-associated lung diseases such as COPD. Abnormalities in morphology and function of mitochondria have been described in the airways of COPD patients as well as in various experimental models in response to exposure to CS or extract thereof. However, if and to what extent the molecular pathways regulating mitochondrial turnover and health are disrupted in COPD patients and whether differences herein exists in different compartment of the

lungs/airways is unknown. Moreover, it is incompletely understood how exactly CS exposure affects the molecular regulation of mitochondrial quality control processes in airway epithelial cells. Furthermore, as CS consists of more than 6000 chemicals, it is unknown which particular components are the culprit of this indicated aberrant regulation of mitochondrial content and function. Aldehydes have been suggested to impede on mitochondrial metabolism as *in vitro* studies have indicated acrolein-induced mitochondrial dysfunction in cells of the airways. However, it is unknown if *in vivo* inhalation of acrolein (or other aldehydes) affects pathways controlling mitochondrial content or metabolism in cells of the airways or lungs. Unfortunately, previous *in vitro* studies have mainly focussed on the impact of individual aldehydes on the molecular regulation of mitochondrial metabolism and content, and have used cell lines and non-physiologically relevant exposure regimes.

Therefore, the aim of this thesis is to investigate the impact of several aldehydes (relevant for CS-exposure) on the molecular regulation of mitochondrial content, function and metabolism in epithelial cells of the airways and lungs, in the context of COPD. The rationale behind this study is to provide scientific evidence which supports the future regulation of aldehydes content in CS by mandated lowering by the WHO.

Our hypothesis is that the molecular mechanisms controlling mitochondrial content, function and metabolism are disrupted in airway/lung (epithelial) cells from COPD patients, as well as upon exposure to aldehydes emitted by CS. To investigate our hypothesis, we deployed several experimental *in vivo* and *in vitro* airway models of COPD as well as exposure to CS or aldehydes and evaluated read-out parameters related to the molecular regulation of mitochondrial metabolism, mitochondrial content, mitochondrial biogenesis and mitophagy.

Firstly, in **Chapter 2**, we assessed whether or not the abundance of constituents of the molecular pathways controlling mitochondrial turnover (mitochondrial biogenesis *versus* mitophagy) was changed in bronchial epithelial cells and peripheral lung tissue from COPD patients *versus* non-COPD patients. We hypothesized that the molecular regulation of these mitochondrial pathways are affected in (epithelial) cells of the airways from COPD patients. To explore this, we measured the protein and mRNA expression of key regulators involved in mitochondrial turnover processes and mitochondrial metabolic pathways in peripheral lung tissues as well as in isolated PBEC cultured submerged (undifferentiated; basal cells) or at air-liquid interface (differentiated; ciliated cells, secretory club cells, mucus-producing goblet cells) from non-COPD patients and COPD patients at different stages of disease progression.

In **Chapter 3**, the impact of CS on regulatory molecules involved in the control of mitochondrial metabolism and quality control processes was explored in several *in vitro* culture models of human PBEC from non-COPD donors. Our hypothesis described

a differential impact of smoke exposure on the abundance of a comprehensive panel of constituents involved in mitochondrial metabolism in PBEC, which depends on the variation in exposure time (acute *versus* repeated/ chronic), type of smoke exposure (whole CS *versus* CS extract) or PBEC model (undifferentiated *versus* differentiated). To be more specific, four experimental models of exposure to whole CS or CS extract in PBEC were deployed to address this hypothesis, including (1) differentiated PBEC cultures at air-liquid interface acutely exposed to whole CS, (2) PBEC cultures at air-liquid interface chronically exposed (during differentiation) to whole CS followed by smoking cessation, (3) undifferentiated PBEC cultured in submerged conditions acutely exposed to whole CS and (4) undifferentiated submerged PBEC cultures treated with CS extract. Protein and transcript levels as well as enzyme activity of essential molecules involved in the regulation of mitochondrial biogenesis, mitophagy, mitochondrial dynamics, mitochondrial content and mitochondrial energy metabolism were studied in these models.

In addition, we performed *in vivo* studies to reveal the effect of acute and sub-acute acrolein inhalation on the regulation of mitochondrial metabolism in rat lung in **Chapter 4** and **Chapter 5**. We hypothesized that *in vivo* acrolein inhalation lead to changes in the molecular pathways controlling mitochondrial metabolism, mitophagy and mitochondrial biogenesis in rat lung. To study this, rats were acutely exposed to acrolein by nose-only inhalation (**Chapter 4**) or sub-acutely exposed to acrolein by whole-body inhalation (**Chapter 5**). In both studies, the enzyme activity and abundance (protein and mRNA) of indices involved in mitochondrial metabolism, mitochondrial content, mitochondrial biogenesis and mitophagy were assessed in lung homogenates.

Subsequently, we aimed to obtain more insight into the impact of smoking-associated exposure to aldehydes on the molecular mechanisms controlling mitochondrial content and function using a physiologically-relevant *in vitro* model of the bronchial epithelium in **Chapter 6**. We hypothesized that acute exposure to a mixture of acetaldehyde, acrolein and formaldehyde, representative for CS, disrupts the molecular regulation of mitochondrial content and mitochondrial function in human PBEC. Therefore, fully differentiated human PBEC at air-liquid interface from multiple non-COPD patients were once exposed to air (control), CS (1 cigarette) or a mixture of acetaldehyde, acrolein, and formaldehyde in a continuous flow system using a puff-like exposure protocol. Post-exposure, we analyzed cytotoxicity, secretion of interleukins, cytokines and chemokines, protein and transcript abundance of key constituents involved in mitochondrial metabolic pathways and quality control processes as well as ciliary beating.

Finally, in **Chapter 7**, the findings of these five studies are discussed in a broader context considering the recent literature. Moreover, limitations and implications for regulation and future research are addressed.

References

1. World Health Organization. Factsheet Tobacco: WHO; 2022 [updated 05/24/2022. Available from: <https://www.who.int/news-room/fact-sheets/detail/tobacco>
2. Burns DM, Dybing E, Gray N, Hecht S, Anderson C, Sanner T, et al. Mandated lowering of toxicants in cigarette smoke: a description of the World Health Organization TobReg proposal. *Tob Control*. 2008;17(2):132-41.
3. World Health Organization & World Health Organization Tobacco Free Initiative. The scientific basis of tobacco product regulation: second report of a WHO study group. World Health Organization; 2008.
4. Talhout R, Schulz T, Florek E, van Benthem J, Wester P, Opperhuizen A. Hazardous compounds in tobacco smoke. *Int J Environ Res Public Health*. 2011;8(2):613-28.
5. Rodgman A, Perfetti TA. The chemical components of tobacco and tobacco smoke: CRC press; 2013.
6. Cheah NP. Volatile aldehydes in tobacco smoke: source fate and risk. [Ph.D. Dissertation Thesis]. Maastricht, The Netherlands: Maastricht University; 2016.
7. Corley RA, Kabilan S, Kuprat AP, Carson JP, Jacob RE, Minard KR, et al. Comparative Risks of Aldehyde Constituents in Cigarette Smoke Using Transient Computational Fluid Dynamics/ Physiologically Based Pharmacokinetic Models of the Rat and Human Respiratory Tracts. *Toxicol Sci*. 2015;146(1):65-88.
8. LoPachin RM, Gavin T. Molecular mechanisms of aldehyde toxicity: a chemical perspective. *Chem Res Toxicol*. 2014;27(7):1081-91.
9. Fowles J, Dybing E. Application of toxicological risk assessment principles to the chemical constituents of cigarette smoke. *Tob Control*. 2003;12(4):424-30.
10. Talhout R, Opperhuizen A, van Amsterdam JG. Sugars as tobacco ingredient: Effects on mainstream smoke composition. *Food Chem Toxicol*. 2006;44(11):1789-98.
11. Fagerson IS. Thermal degradation of carbohydrates; a review. *Journal of Agricultural and Food Chemistry*. 1969;17(4):747-50.
12. Mattonai M, Tamburini D, Colombini MP, Ribechini E. Timing in Analytical Pyrolysis: Py(HMDS)-GC/MS of Glucose and Cellulose Using Online Micro Reaction Sampler. *Anal Chem*. 2016;88(18):9318-25.
13. Mattonai M, Ribechini E. A comparison of fast and reactive pyrolysis with insitu derivatisation of fructose, inulin and Jerusalem artichoke (*Helianthus tuberosus*). *Anal Chim Acta*. 2018;1017:66-74.
14. Roemer E, Schorp MK, Piadé JJ, Seeman JI, Leyden DE, Haussmann HJ. Scientific assessment of the use of sugars as cigarette tobacco ingredients: a review of published and other publicly available studies. *Crit Rev Toxicol*. 2012;42(3):244-78.
15. Leffingwell J. BA basic chemical constituents of tobacco leaf and differences among tobacco types. Oxford UK: Blackwell Science; 1999. 265-84 p.
16. Cahours X, Verron T, Purkis S. Effect of sugar content on acetaldehyde yield in cigarette smoke. *Beiträge zur Tabakforschung International/Contributions to Tobacco Research*. 25(2):381-95.
17. Seeman JI, Laffoon SW, Kassman AJ. Evaluation of relationships between mainstream smoke acetaldehyde and “tar” and carbon monoxide yields in tobacco smoke and reducing sugars in tobacco blends of U.S. commercial cigarettes. *Inhal Toxicol*. 2003;15(4):373-95.

18. Pauwels C, Klerx WNM, Pennings JLA, Boots AW, van Schooten FJ, Opperhuizen A, et al. Cigarette Filter Ventilation and Smoking Protocol Influence Aldehyde Smoke Yields. *Chem Res Toxicol*. 2018;31(6):462-71.
19. Faroon O, Roney N, Taylor J, Ashizawa A, Lumpkin MH, Plewak DJ. Acrolein environmental levels and potential for human exposure. *Toxicol Ind Health*. 2008;24(8):543-64.
20. Rietjens I, Michael A, Bolt HM, Siméon B, Andrea H, Nils H, et al. The role of endogenous versus exogenous sources in the exposome of putative genotoxins and consequences for risk assessment. *Arch Toxicol*. 2022;96(5):1297-352.
21. Sinharoy P, McAllister SL, Vasu M, Gross ER. Environmental Aldehyde Sources and the Health Implications of Exposure. *Adv Exp Med Biol*. 2019;1193:35-52.
22. Kuykendall JR. 8.16 - Aldehydes. In: McQueen CA, editor. *Comprehensive Toxicology (Second Edition)*. Oxford: Elsevier; 2010. p. 291-330.
23. O'Brien PJ, Siraki AG, Shangari N. Aldehyde sources, metabolism, molecular toxicity mechanisms, and possible effects on human health. *Crit Rev Toxicol*. 2005;35(7):609-62.
24. Marchitti SA, Brocker C, Stagos D, Vasiliou V. Non-P450 aldehyde oxidizing enzymes: the aldehyde dehydrogenase superfamily. *Expert Opin Drug Metab Toxicol*. 2008;4(6):697-720.
25. Chen CH, Ferreira JC, Gross ER, Mochly-Rosen D. Targeting aldehyde dehydrogenase 2: new therapeutic opportunities. *Physiol Rev*. 2014;94(1):1-34.
26. Nakamura J, Holley DW, Kawamoto T, Bultman SJ. The failure of two major formaldehyde catabolism enzymes (ADH5 and ALDH2) leads to partial synthetic lethality in C57BL/6 mice. *Genes Environ*. 2020;42:21.
27. Ma I, Allan AL. The role of human aldehyde dehydrogenase in normal and cancer stem cells. *Stem Cell Rev Rep*. 2011;7(2):292-306.
28. Hegab AE, Ha VL, Bisht B, Darmawan DO, Ooi AT, Zhang KX, et al. Aldehyde dehydrogenase activity enriches for proximal airway basal stem cells and promotes their proliferation. *Stem Cells Dev*. 2014;23(6):664-75.
29. Hegab AE, Ha VL, Darmawan DO, Gilbert JL, Ooi AT, Attiga YS, et al. Isolation and in vitro characterization of basal and submucosal gland duct stem/progenitor cells from human proximal airways. *Stem Cells Transl Med*. 2012;1(10):719-24.
30. Dipple KM, Crabb DW. The mitochondrial aldehyde dehydrogenase gene resides in an HTF island but is expressed in a tissue-specific manner. *Biochem Biophys Res Commun*. 1993;193(1):420-7.
31. Costa DL, Kutzman RS, Lehmann JR, Drew RT. Altered lung function and structure in the rat after subchronic exposure to acrolein. *Am Rev Respir Dis*. 1986;133(2):286-91.
32. Pizzimenti S, Ciamporcerio E, Daga M, Pettazzoni P, Arcaro A, Cetrangolo G, et al. Interaction of aldehydes derived from lipid peroxidation and membrane proteins. *Front Physiol*. 2013;4:242.
33. Zarkovic N, Cipak A, Jaganjac M, Borovic S, Zarkovic K. Pathophysiological relevance of aldehydic protein modifications. *J Proteomics*. 2013;92:239-47.
34. IARC (International Agency for Research on Cancer). Acrolein, crotonaldehyde, and arecoline. Lyon, France: IARC Working Group; 2020.
35. European Commission. Commission Directive (EU) 2017/164 of 31 January 2017 establishing a fourth list of indicative occupational exposure limit values pursuant to Council Directive 98/24/EC, and amending Commission Directives 91/322/EEC, 2000/39/EC and 2009/161/EU. *OJ L* 27/115. 2017.

36. ACGIH (American Conference of Governmental Industrial Hygienists). Acrolein. Threshold limit values for chemical substances and physical agents and biological exposure indices. Cincinnati (OH), USA; 2019.
37. United States Environmental Protection Agency. Method 5030C. Purge-and-trap for aqueous samples. 2003.
38. Yeager RP, Kushman M, Chemerynski S, Weil R, Fu X, White M, et al. Proposed Mode of Action for Acrolein Respiratory Toxicity Associated with Inhaled Tobacco Smoke. *Toxicol Sci.* 2016;151(2):347-64.
39. Moretto N, Volpi G, Pastore F, Facchinetti F. Acrolein effects in pulmonary cells: relevance to chronic obstructive pulmonary disease. *Ann N Y Acad Sci.* 2012;1259:39-46.
40. Deshmukh HS, Shaver C, Case LM, Dietsch M, Wesselkamper SC, Hardie WD, et al. Acrolein-activated matrix metalloproteinase 9 contributes to persistent mucin production. *Am J Respir Cell Mol Biol.* 2008;38(4):446-54.
41. IARC (International Agency for Research on Cancer). Chemical Agents and Related Occupations. IARC Working Group; 2012.
42. IARC (International Agency for Research on Cancer). Allyl Compounds, Aldehydes, Epoxides and Peroxides. Lyon, France; 1985.
43. ECHA (European Chemicals Agency). Worker exposure to formaldehyde and formaldehyde releasers. Finland; 2019.
44. OSHA Occupational Chemical Database Acetaldehyde, [Internet]. [cited 08/19/2022]. Available from: <https://www.osha.gov/chemicaldata/570>.
45. Cheah NP, Pennings JL, Vermeulen JP, van Schooten FJ, Opperhuizen A. In vitro effects of aldehydes present in tobacco smoke on gene expression in human lung alveolar epithelial cells. *Toxicol In Vitro.* 2013;27(3):1072-81.
46. Bernardini L, Barbosa E, Charão MF, Brucker N. Formaldehyde toxicity reports from in vitro and in vivo studies: a review and updated data. *Drug Chem Toxicol.* 2020:1-13.
47. Wilk JB, Shrine NR, Loehr LR, Zhao JH, Manichaikul A, Lopez LM, et al. Genome-wide association studies identify CHRNA5/3 and HTR4 in the development of airflow obstruction. *Am J Respir Crit Care Med.* 2012;186(7):622-32.
48. Hancock DB, Eijgelsheim M, Wilk JB, Gharib SA, Loehr LR, Marcianti KD, et al. Meta-analyses of genome-wide association studies identify multiple loci associated with pulmonary function. *Nat Genet.* 2010;42(1):45-52.
49. Repapi E, Sayers I, Wain LV, Burton PR, Johnson T, Obeidat M, et al. Genome-wide association study identifies five loci associated with lung function. *Nat Genet.* 2010;42(1):36-44.
50. Tian M, Xia P, Yan L, Gou X, Giesy JP, Dai J, et al. Toxicological Mechanism of Individual Susceptibility to Formaldehyde-Induced Respiratory Effects. *Environ Sci Technol.* 2022;56(10):6511-24.
51. U.S. Environmental Protection Agency. Acetaldehyde: Hazard Summary-Created in April 1992; Revised in January 2000.; 2000.
52. U.S. Environmental Protection Agency. Health Assessment Document for Acetaldehyde. Environmental Criteria and Assessment Office, Office of Health and Environmental Assessment, Office of Research and Development, Research Triangle Park, NC.; 1987. Contract No.: EPA/600/8-86-015A.
53. U.S. Department of Health and Human Services. Registry of Toxic Effects of Chemical Substances (RTECS, online database). National Toxicology Information Program, National Library of Medicine, Bethesda, MD; 1993.

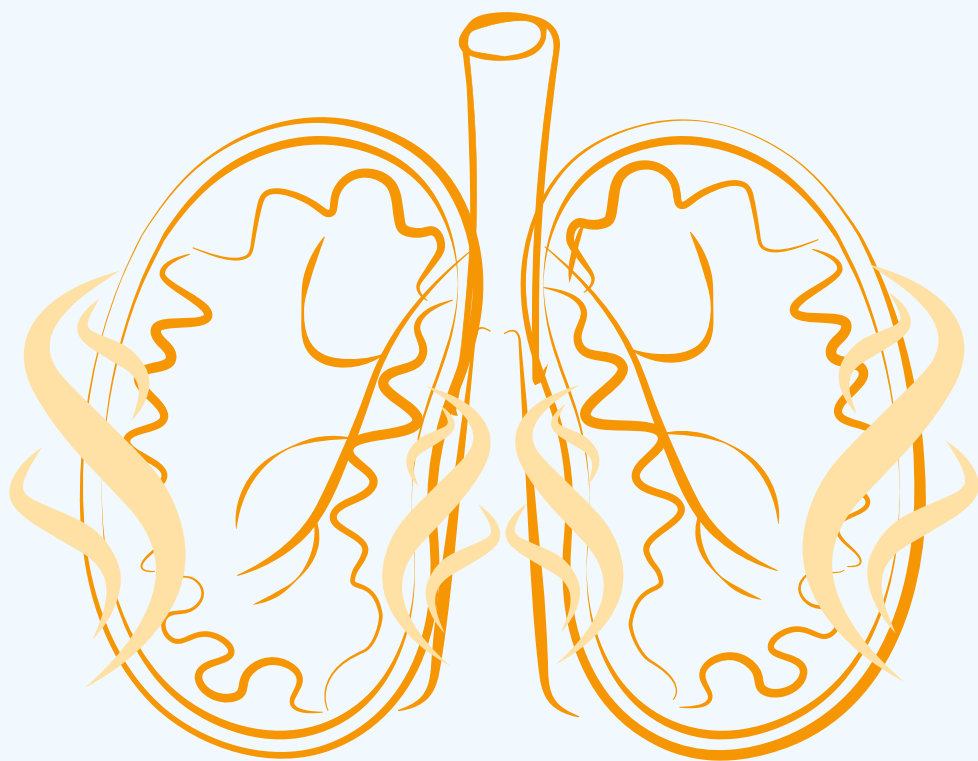
54. U.S. Environmental Protection Agency. Integrated Risk Information System (IRIS) on Acetaldehyde. National Center for Environmental Assessment, Office of Research and Development, Washington, D.C. National Center for Environmental Assessment, Office of Research and Development, Washington, D.C. ; 1999.
55. National Research Council (US) Committee. Emergency and Continuous Exposure Guidance Levels for Selected Submarine Contaminants. Washington (DC): National Academies Press (US); 2009.
56. IARC (International Agency for Research on Cancer). Acetaldehyde. Re-evaluation of Some Organic Chemicals, Hydrazine and Hydrogen Peroxide (Part Two). Lyon, France; 1999.
57. van der Toorn M, Slebos DJ, de Bruin HG, Gras R, Rezayat D, Jorge L, et al. Critical role of aldehydes in cigarette smoke-induced acute airway inflammation. *Respir Res.* 2013;14(1):45.
58. Zhang S, Chen H, Wang A, Liu Y, Hou H, Hu Q. Combined effects of co-exposure to formaldehyde and acrolein mixtures on cytotoxicity and genotoxicity in vitro. *Environ Sci Pollut Res Int.* 2018;25(25):25306-14.
59. Zhang S, Zhang J, Chen H, Wang A, Liu Y, Hou H, et al. Combined cytotoxicity of co-exposure to aldehyde mixtures on human bronchial epithelial BEAS-2B cells. *Environ Pollut.* 2019;250:650-61.
60. Zhang S, Zhang J, Cheng W, Chen H, Wang A, Liu Y, et al. Combined cell death of co-exposure to aldehyde mixtures on human bronchial epithelial BEAS-2B cells: Molecular insights into the joint action. *Chemosphere.* 2020;244:125482.
61. Zulueta A, Caretti A, Campisi GM, Brizzolari A, Abad JL, Paroni R, et al. Inhibitors of ceramide de novo biosynthesis rescue damages induced by cigarette smoke in airways epithelia. *Naunyn Schmiedebergs Arch Pharmacol.* 2017;390(7):753-9.
62. Corradi M, Pignatti P, Manini P, Andreoli R, Goldoni M, Poppa M, et al. Comparison between exhaled and sputum oxidative stress biomarkers in chronic airway inflammation. *Eur Respir J.* 2004;24(6):1011-7.
63. Yasuo M, Droma Y, Kitaguchi Y, Ito M, Imamura H, Kawakubo M, et al. The relationship between acrolein and oxidative stress in COPD: in systemic plasma and in local lung tissue. *Int J Chron Obstruct Pulmon Dis.* 2019;14:1527-37.
64. Tu C, Mammen MJ, Li J, Shen X, Jiang X, Hu Q, et al. Large-scale, ion-current-based proteomics investigation of bronchoalveolar lavage fluid in chronic obstructive pulmonary disease patients. *J Proteome Res.* 2014;13(2):627-39.
65. Morita K, Masuda N, Oniki K, Saruwatari J, Kajiwarra A, Otake K, et al. Association between the aldehyde dehydrogenase 2*2 allele and smoking-related chronic airway obstruction in a Japanese general population: a pilot study. *Toxicol Lett.* 2015;236(2):117-22.
66. Kuroda A, Hegab AE, Jingtao G, Yamashita S, Hizawa N, Sakamoto T, et al. Effects of the common polymorphism in the human aldehyde dehydrogenase 2 (ALDH2) gene on the lung. *Respir Res.* 2017;18(1):69.
67. Oyama T, Isse T, Ogawa M, Muto M, Uchiyama I, Kawamoto T. Susceptibility to inhalation toxicity of acetaldehyde in Aldh2 knockout mice. *Frontiers in Bioscience-Landmark.* 2007;12(5):1927-34.
68. Jang JH, Bruse S, Liu Y, Duffy V, Zhang C, Oyamada N, et al. Aldehyde dehydrogenase 3A1 protects airway epithelial cells from cigarette smoke-induced DNA damage and cytotoxicity. *Free Radic Biol Med.* 2014;68:80-6.
69. Mishra P, Chan DC. Mitochondrial dynamics and inheritance during cell division, development and disease. *Nat Rev Mol Cell Biol.* 2014;15(10):634-46.

70. Cloonan SM, Choi AM. Mitochondria in lung disease. *J Clin Invest.* 2016;126(3):809-20.
71. Cloonan SM, Kim K, Esteves P, Triantafyllidis T, Barnes PJ. Mitochondrial dysfunction in lung ageing and disease. *Eur Respir Rev.* 2020;29(157).
72. Aghapour M, Remels AHV, Pouwels SD, Bruder D, Hiemstra PS, Cloonan SM, et al. Mitochondria: at the crossroads of regulating lung epithelial cell function in chronic obstructive pulmonary disease. *Am J Physiol Lung Cell Mol Physiol.* 2020;318(1):L149-l64.
73. Mishra P, Chan DC. Metabolic regulation of mitochondrial dynamics. *J Cell Biol.* 2016;212(4):379-87.
74. Jornayvaz FR, Shulman GI. Regulation of mitochondrial biogenesis. *Essays Biochem.* 2010;47:69-84.
75. Lin J, Handschin C, Spiegelman BM. Metabolic control through the PGC-1 family of transcription coactivators. *Cell Metab.* 2005;1(6):361-70.
76. Scarpulla RC. Metabolic control of mitochondrial biogenesis through the PGC-1 family regulatory network. *Biochim Biophys Acta.* 2011;1813(7):1269-78.
77. Ploumi C, Daskalaki I, Tavernarakis N. Mitochondrial biogenesis and clearance: a balancing act. *Febs j.* 2017;284(2):183-95.
78. Detmer SA, Chan DC. Functions and dysfunctions of mitochondrial dynamics. *Nature Reviews Molecular Cell Biology.* 2007;8(11):870-9.
79. Gomes LC, Scorrano L. Mitochondrial morphology in mitophagy and macroautophagy. *Biochim Biophys Acta.* 2013;1833(1):205-12.
80. Fritsch LE, Moore ME, Sarraf SA, Pickrell AM. Ubiquitin and Receptor-Dependent Mitophagy Pathways and Their Implication in Neurodegeneration. *J Mol Biol.* 2020;432(8):2510-24.
81. Hoffmann RF, Zarrintan S, Brandenburg SM, Kol A, de Bruin HG, Jafari S, et al. Prolonged cigarette smoke exposure alters mitochondrial structure and function in airway epithelial cells. *Respir Res.* 2013;14:97.
82. Hara H, Araya J, Ito S, Kobayashi K, Takasaka N, Yoshii Y, et al. Mitochondrial fragmentation in cigarette smoke-induced bronchial epithelial cell senescence. *Am J Physiol Lung Cell Mol Physiol.* 2013;305(10):L737-46.
83. Haji G, Wiegman CH, Michaeloudes C, Patel MS, Curtis K, Bhavsar P, et al. Mitochondrial dysfunction in airways and quadriceps muscle of patients with chronic obstructive pulmonary disease. *Respiratory Research.* 2020;21(1):262.
84. Zhang WZ, Hoffman KL, Schiffer KT, Oromendia C, Rice MC, Barjaktarevic I, et al. Association of plasma mitochondrial DNA with COPD severity and progression in the SPIROMICS cohort. *Respiratory Research.* 2021;22(1):126.
85. Zhang WZ, Rice MC, Hoffman KL, Oromendia C, Barjaktarevic IZ, Wells JM, et al. Association of urine mitochondrial DNA with clinical measures of COPD in the SPIROMICS cohort. *JCI Insight.* 2020;5(3):e133984.
86. Li J, Dai A, Hu R, Zhu L, Tan S. Positive correlation between PPARgamma/PGC-1alpha and gamma-GCS in lungs of rats and patients with chronic obstructive pulmonary disease. *Acta Biochim Biophys Sin.* 2010;42(9):603-14.
87. Peng H, Yang M, Chen ZY, Chen P, Guan CX, Xiang XD, et al. Expression and methylation of mitochondrial transcription factor a in chronic obstructive pulmonary disease patients with lung cancer. *PLoS One.* 2013;8(12):e82739.

88. Mizumura K, Cloonan SM, Nakahira K, Bhashyam AR, Cervo M, Kitada T, et al. Mitophagy-dependent necroptosis contributes to the pathogenesis of COPD. *J Clin Invest*. 2014;124(9):3987-4003.
89. Ito S, Araya J, Kurita Y, Kobayashi K, Takasaka N, Yoshida M, et al. PARK2-mediated mitophagy is involved in regulation of HBEC senescence in COPD pathogenesis. *Autophagy*. 2015;11(3):547-59.
90. Ahmad T, Sundar IK, Lerner CA, Gerloff J, Tormos AM, Yao H, et al. Impaired mitophagy leads to cigarette smoke stress-induced cellular senescence: implications for chronic obstructive pulmonary disease. *Faseb j*. 2015;29(7):2912-29.
91. Chen ZH, Kim HP, Sciurba FC, Lee SJ, Feghali-Bostwick C, Stolz DB, et al. Egr-1 regulates autophagy in cigarette smoke-induced chronic obstructive pulmonary disease. *PLoS One*. 2008;3(10):e3316.
92. Hikichi M, Mizumura K, Maruoka S, Gon Y. Pathogenesis of chronic obstructive pulmonary disease (COPD) induced by cigarette smoke. *J Thorac Dis*. 2019;11(Suppl 17):S2129-S40.
93. Prakash YS, Pabelick CM, Sieck GC. Mitochondrial Dysfunction in Airway Disease. *Chest*. 2017;152(3):618-26.
94. Sundar IK, Maremanda KP, Rahman I. Mitochondrial dysfunction is associated with Miro1 reduction in lung epithelial cells by cigarette smoke. *Toxicol Lett*. 2019;317:92-101.
95. Ballweg K, Mutze K, Königshoff M, Eickelberg O, Meiners S. Cigarette smoke extract affects mitochondrial function in alveolar epithelial cells. *Am J Physiol Lung Cell Mol Physiol*. 2014;307(11):L895-907.
96. Park EJ, Park YJ, Lee SJ, Lee K, Yoon C. Whole cigarette smoke condensates induce ferroptosis in human bronchial epithelial cells. *Toxicol Lett*. 2019;303:55-66.
97. Wu K, Luan G, Xu Y, Shen S, Qian S, Zhu Z, et al. Cigarette smoke extract increases mitochondrial membrane permeability through activation of adenine nucleotide translocator (ANT) in lung epithelial cells. *Biochem Biophys Res Commun*. 2020;525(3):733-9.
98. van der Toorn M, Rezayat D, Kauffman HF, Bakker SJ, Gans RO, Koëter GH, et al. Lipid-soluble components in cigarette smoke induce mitochondrial production of reactive oxygen species in lung epithelial cells. *Am J Physiol Lung Cell Mol Physiol*. 2009;297(1):L109-14.
99. Valdivieso Á G, Dugour AV, Sotomayor V, Clauzure M, Figueroa JM, Santa-Coloma TA. N-acetyl cysteine reverts the proinflammatory state induced by cigarette smoke extract in lung Calu-3 cells. *Redox Biol*. 2018;16:294-302.
100. Malinska D, Szymanski J, Patalas-Krawczyk P, Michalska B, Wojtala A, Prill M, et al. Assessment of mitochondrial function following short- and long-term exposure of human bronchial epithelial cells to total particulate matter from a candidate modified-risk tobacco product and reference cigarettes. *Food Chem Toxicol*. 2018;115:1-12.
101. Agarwal AR, Yin F, Cadenas E. Short-term cigarette smoke exposure leads to metabolic alterations in lung alveolar cells. *Am J Respir Cell Mol Biol*. 2014;51(2):284-93.
102. Agarwal AR, Zhao L, Sancheti H, Sundar IK, Rahman I, Cadenas E. Short-term cigarette smoke exposure induces reversible changes in energy metabolism and cellular redox status independent of inflammatory responses in mouse lungs. *Am J Physiol Lung Cell Mol Physiol*. 2012;303(10):L889-98.
103. Vanella L, Li Volti G, Distefano A, Raffaele M, Zingales V, Avola R, et al. A new antioxidant formulation reduces the apoptotic and damaging effect of cigarette smoke extract on human bronchial epithelial cells. *Eur Rev Med Pharmacol Sci*. 2017;21(23):5478-84.

104. Wang S, He N, Xing H, Sun Y, Ding J, Liu L. Function of hesperidin alleviating inflammation and oxidative stress responses in COPD mice might be related to SIRT1/PGC-1 α /NF- κ B signaling axis. *J Recept Signal Transduct Res*. 2020;1-7.
105. Wang XL, Li T, Li JH, Miao SY, Xiao XZ. The Effects of Resveratrol on Inflammation and Oxidative Stress in a Rat Model of Chronic Obstructive Pulmonary Disease. *Molecules*. 2017;22(9).
106. Kyung SY, Kim YJ, Son ES, Jeong SH, Park JW. The Phosphodiesterase 4 Inhibitor Roflumilast Protects against Cigarette Smoke Extract-Induced Mitophagy-Dependent Cell Death in Epithelial Cells. *Tuberc Respir Dis*. 2018;81(2):138-47.
107. Son ES, Kim SH, Ryter SW, Yeo EJ, Kyung SY, Kim YJ, et al. Quercetogetin protects against cigarette smoke extract-induced apoptosis in epithelial cells by inhibiting mitophagy. *Toxicol In Vitro*. 2018;48:170-8.
108. Zhang M, Shi R, Zhang Y, Shan H, Zhang Q, Yang X, et al. Nix/BNIP3L-dependent mitophagy accounts for airway epithelial cell injury induced by cigarette smoke. *J Cell Physiol*. 2019;234(8):14210-20.
109. Wen W, Yu G, Liu W, Gu L, Chu J, Zhou X, et al. Silencing FUNDC1 alleviates chronic obstructive pulmonary disease by inhibiting mitochondrial autophagy and bronchial epithelium cell apoptosis under hypoxic environment. *J Cell Biochem*. 2019;120(10):17602-15.
110. Araya J, Tsubouchi K, Sato N, Ito S, Minagawa S, Hara H, et al. PRKN-regulated mitophagy and cellular senescence during COPD pathogenesis. *Autophagy*. 2019;15(3):510-26.
111. Aravamudan B, Kiel A, Freeman M, Delmotte P, Thompson M, Vassallo R, et al. Cigarette smoke-induced mitochondrial fragmentation and dysfunction in human airway smooth muscle. *Am J Physiol Lung Cell Mol Physiol*. 2014;306(9):L840-54.
112. Song C, Luo B, Gong L. Resveratrol reduces the apoptosis induced by cigarette smoke extract by upregulating MFN2. *PLoS One*. 2017;12(4):e0175009.
113. Walczak J, Malińska D, Drabik K, Michalska B, Prill M, John S, et al. Mitochondrial Network and Biogenesis in Response to Short and Long-Term Exposure of Human BEAS-2B Cells to Aerosol Extracts from the Tobacco Heating System 2.2. *Cell Physiol Biochem*. 2020;54(2):230-51.
114. Cloonan SM, Glass K, Laucho-Contreras ME, Bhashyam AR, Cervo M, Pabon MA, et al. Mitochondrial iron chelation ameliorates cigarette smoke-induced bronchitis and emphysema in mice. *Nat Med*. 2016;22(2):163-74.
115. Wang HT, Lin JH, Yang CH, Haung CH, Weng CW, Maan-Yuh Lin A, et al. Acrolein induces mtDNA damages, mitochondrial fission and mitophagy in human lung cells. *Oncotarget*. 2017;8(41):70406-21.
116. Fabisiak JP, Medvedovic M, Alexander DC, McDunn JE, Concel VJ, Bein K, et al. Integrative metabolome and transcriptome profiling reveals discordant energetic stress between mouse strains with differential sensitivity to acrolein-induced acute lung injury. *Mol Nutr Food Res*. 2011;55(9):1423-34.
117. Agarwal AR, Yin F, Cadenas E. Metabolic shift in lung alveolar cell mitochondria following acrolein exposure. *Am J Physiol Lung Cell Mol Physiol*. 2013;305(10):L764-73.
118. Roy J, Palapati P, Bettaieb A, Tanel A, Averill-Bates DA. Acrolein induces a cellular stress response and triggers mitochondrial apoptosis in A549 cells. *Chem Biol Interact*. 2009;181(2):154-67.

119. Luo C, Li Y, Yang L, Feng Z, Li Y, Long J, et al. A cigarette component acrolein induces accelerated senescence in human diploid fibroblast IMR-90 cells. *Biogerontology*. 2013;14(5):503-11.
120. Sun L, Luo C, Long J, Wei D, Liu J. Acrolein is a mitochondrial toxin: effects on respiratory function and enzyme activities in isolated rat liver mitochondria. *Mitochondrion*. 2006;6(3):136-42.
121. Sisson JH, Tuma DJ, Rennard SI. Acetaldehyde-mediated cilia dysfunction in bovine bronchial epithelial cells. *Am J Physiol*. 1991;260(2 Pt 1):L29-36.
122. Wyatt TA, Schmidt SC, Rennard SI, Tuma DJ, Sisson JH. Acetaldehyde-stimulated PKC activity in airway epithelial cells treated with smoke extract from normal and smokeless cigarettes. *Proc Soc Exp Biol Med*. 2000;225(1):91-7.
123. Farfán Labonne BE, Gutiérrez M, Gómez-Quiroz LE, Konigsberg Fainstein M, Bucio L, Souza V, et al. Acetaldehyde-induced mitochondrial dysfunction sensitizes hepatocytes to oxidative damage. *Cell Biol Toxicol*. 2009;25(6):599-609.
124. Van Buskirk JJ, Frisell WR. Inhibition by formaldehyde of energy transfer and related processes in rat liver mitochondria. II. Effects on energy-linked reactions in intact mitochondria and phosphorylating particles. *Arch Biochem Biophys*. 1969;132(1):130-8.
125. Zerín T, Kim JS, Gil HW, Song HY, Hong SY. Effects of formaldehyde on mitochondrial dysfunction and apoptosis in SK-N-SH neuroblastoma cells. *Cell Biol Toxicol*. 2015;31(6):261-72.
126. Ma H, Lin J, Li L, Ding Z, Huang P, Song X, et al. Formaldehyde reinforces pro-inflammatory responses of macrophages through induction of glycolysis. *Chemosphere*. 2021;282:131149.
127. Li S, Wei P, Zhang B, Chen K, Shi G, Zhang Z, et al. Apoptosis of lung cells regulated by mitochondrial signal pathway in crotonaldehyde-induced lung injury. *Environ Toxicol*. 2020;35(11):1260-73.
128. Zhang S, Zhang B, Zhang Q, Zhang Z. Crotonaldehyde exposure induces liver dysfunction and mitochondrial energy metabolism disorder in rats. *Toxicol Mech Methods*. 2021;31(6):425-36.
129. Liu XY, Yang ZH, Pan XJ, Zhu MX, Xie JP. Crotonaldehyde induces oxidative stress and caspase-dependent apoptosis in human bronchial epithelial cells. *Toxicol Lett*. 2010;195(1):90-8.
130. Yang BC, Pan XJ, Yang ZH, Xiao FJ, Liu XY, Zhu MX, et al. Crotonaldehyde induces apoptosis in alveolar macrophages through intracellular calcium, mitochondria and p53 signaling pathways. *J Toxicol Sci*. 2013;38(2):225-35.
131. Pei Z, Zhuang Z, Sang H, Wu Z, Meng R, He EY, et al. α,β -Unsaturated aldehyde crotonaldehyde triggers cardiomyocyte contractile dysfunction: role of TRPV1 and mitochondrial function. *Pharmacol Res*. 2014;82:40-50.
132. Clapp PW, Lavrich KS, van Heusden CA, Lazarowski ER, Carson JL, Jaspers I. Cinnamaldehyde in flavored e-cigarette liquids temporarily suppresses bronchial epithelial cell ciliary motility by dysregulation of mitochondrial function. *Am J Physiol Lung Cell Mol Physiol*. 2019;316(3):L470-186.
133. Liu QP, Zhou DX, Lv MQ, Ge P, Li YX, Wang SJ. Formaldehyde inhalation triggers autophagy in rat lung tissues. *Toxicol Ind Health*. 2018;748233718796347.

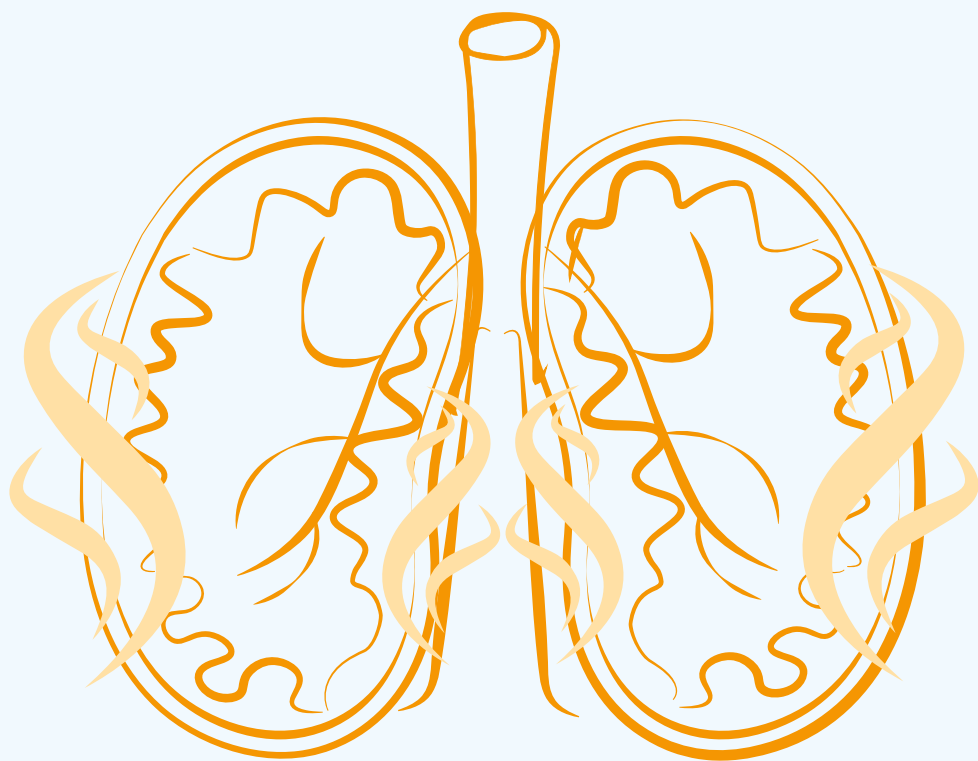


Chapter 2

Alterations in the transcript abundance of molecules controlling mitochondrial turnover in peripheral lung tissue from chronic obstructive pulmonary disease patients

Christy B.M. Tulen, Cheryl van de Wetering, Caspar H.J. Schiffrs, Birke J. Benedikter, Pieter A. Leermakers, Juliana H. Boukhaled, Marie-José Driittij, Bernd T. Schmeck, Niki L. Reynaert, Antoon Opperhuizen, Frederik-Jan van Schooten, Alexander H.V. Remels

Submitted



Chapter 3

Dysregulated mitochondrial metabolism upon cigarette smoke exposure in various human bronchial epithelial cell models

Christy B.M. Tulen*, Ying Wang*, Daan Beentjes, Phyllis J.J. Jessen, Dennis K. Ninaber, Niki L. Reynaert, Frederik-Jan van Schooten, Antoon Opperhuizen, Pieter S. Hiemstra, Alexander H.V. Remels

*These authors contributed equally to this work

Disease Models & Mechanisms. 2022 Mar 1; 15(3):dmm049247
DOI: [10.1242/dmm.049247](https://doi.org/10.1242/dmm.049247)

Abstract

Exposure to cigarette smoke (CS) is the primary risk factor for developing chronic obstructive pulmonary disease. The impact of CS exposure on the molecular mechanisms involved in mitochondrial quality control in airway epithelial cells is incompletely understood. Undifferentiated or differentiated primary bronchial epithelial cells were acutely/chronically exposed to whole CS (WCS) or CS extract (CSE) in submerged or air-liquid interface conditions. Abundance of key regulators controlling mitochondrial biogenesis, mitophagy and mitochondrial dynamics was assessed. Acute exposure to WCS or CSE increased the abundance of components of autophagy and receptor-mediated mitophagy in all models. Although mitochondrial content and dynamics appeared to be unaltered in response to CS, changes in both the molecular control of mitochondrial biogenesis and a shift toward an increased glycolytic metabolism were observed in particular in differentiated cultures. These alterations persisted, at least in part, after chronic exposure to WCS during differentiation and upon subsequent discontinuation of WCS exposure. In conclusion, smoke exposure alters the regulation of mitochondrial metabolism in airway epithelial cells, but observed alterations may differ between various culture models used.

Keywords: autophagy, cell model, cigarette smoke, culture methods, human primary bronchial epithelial cells, mitochondrial metabolism

Introduction

Exposure to cigarette smoke (CS) is the most important risk factor for developing chronic obstructive pulmonary disease (COPD), a leading cause of mortality and burden of disease worldwide (1, 2). However, whereas much has been learnt about the role of oxidative stress and CS-induced inflammation, our insight into the molecular mechanisms driving smoke-induced COPD pathogenesis still has various knowledge-gaps, including those related to mitochondrial function.

Recent studies have suggested a crucial role for mitochondrial dysfunction in the pathogenesis of smoking-related lung diseases such as COPD (3-8). Indeed, a variety of studies have identified abnormal mitochondrial morphology, e.g., swelling and fragmentation, in airway epithelial cells of COPD patients, which was recapitulated in various *in vivo* and *in vitro* experimental exposure models with CS or CS extract (CSE), respectively (3, 9-17). Moreover, in mice, amelioration of CS-induced mitochondrial dysfunction alleviated COPD-associated pathological features (3).

Mitochondrial function and content are regulated by a series of crucial cellular quality control processes, including mitochondrial biogenesis and mitophagy. Mitochondrial biogenesis is essentially regulated via the peroxisome proliferator-activated receptor gamma, coactivator 1 (PPARGC1) signaling network which includes a myriad of transcription factors and transcriptional co-activators (18-20) that cooperatively drive the genesis of new organelles. On the other hand, defective/damaged mitochondria can be degraded by selective autophagy, i.e., mitophagy, which is modulated by two specific pathways (21): (1) receptor-mediated mitophagy, initiated by mitochondrial receptors, such as BCL2/adenovirus E1B 19 kDa protein-interacting protein 3 (BNIP3), BNIP3-like (BNIP3L), and FUN14 domain containing 1 (FUNDCl); and (2) ubiquitin-mediated mitophagy, triggered by a loss of mitochondrial membrane potential, accumulation of PTEN induced kinase 1 (PINK1) and recruitment of parkin RBR E3 ubiquitin protein ligase (PRKN) in the outer mitochondrial membrane. Evidently, both mitophagy pathways require general autophagy proteins, such as GABA type A receptor associated protein like 1 (GABARAPL1), microtubule-associated protein 1B light chain 3 (MAP1LC3) alpha and beta, and sequestosome 1 (SQSTM1), to facilitate formation of the autophagosomal membrane around the mitochondrion (22).

Autophagy has been suggested to be critically involved in COPD pathogenesis (23). Previous research indicated that markers of autophagy and mitophagy are induced in lung tissue of COPD patients (9, 24-26). This was confirmed in various models of CS(E) exposure of (human) airway epithelial cells, however most studies deployed cell lines or submerged undifferentiated cultures of primary human airway epithelial cells (9, 11, 16, 24-32), which are not an accurate representation of the complex *in vivo* cellular architecture of the human airway epithelium.

Because epithelial cells that line the respiratory tract are the first cells to be exposed to inhaled toxicants, the relevance of studying the impact of exposure to CS on mitochondrial function and content in airway epithelial cells is obvious (33). However, the epithelial lining of the airways consists of several distinct cell types not all of which are included in most studied cell lines or submerged culture models. Studying the variety of cell types is essential because individual cell types differ in number and intracellular organization of mitochondria, which may be related to their function and corresponding energy demand (6). Therefore, a differentiated pseudostratified layer of primary airway epithelial cells, including ciliated-, club- and goblet cells, is needed to study these processes in culture models (34). However, previous studies used cell lines or submerged undifferentiated primary bronchial epithelial cells (PBEC) cultures (more representative of a basal-like cell type reflecting damaged epithelium) to assess the impact of CSE on autophagy and mitophagy (9, 11, 16, 24-32). Applying a more physiologically relevant model consisting of the various epithelial cell types differentiated by culture at the air-liquid interface (ALI), which allows exposure to whole CS (WCS) (including gaseous and particulate mainstream CS components) instead of an aqueous CSE, has the potential to provide better insight into the impact of CS on the regulation of critical mitochondrial quality control processes. Importantly, we previously reported that differentiation of PBEC at the ALI is accompanied by a marked increase in expression of genes involved in xenobiotic metabolism and increases metabolic activity (35). This is relevant for studying effects of CS exposure on PBEC cultures, because such biotransformation reactions may contribute to both detoxification of CS components as well as to formation of (more) reactive species. Therefore, comparison of such more advanced models to more simple conventional models using submerged cultures and CSE is needed to establish whether or not the use of more complex models is warranted over the use of more simple *in vitro* models.

In addition to these considerations, most available *in vitro* studies evaluated the impact of acute CS(E) exposure on mitochondrial quality control systems in airway epithelial cells. Given that COPD develops as a result of chronic exposure to CS, it is important to characterize the impact of acute *versus* chronic CS exposure on these cellular processes. Moreover, only a few *in vitro* studies investigated the long-lasting impact on parameters relevant to COPD pathophysiology after termination of CS exposure. These studies demonstrated recovery of epithelial differentiation markers (36), while inflammation (37, 38), apoptosis (39) and alterations in mitochondrial morphology and function (11) have been shown to persist upon smoking cessation *in vivo* in epithelial cells derived from former-smoking COPD patients as well as in *in vitro* airway culture models. However, the impact of smoking cessation on mechanisms that underlie these (CS-induced) mitochondrial aberrations (i.e. mitochondrial biogenesis and mitophagy) are incompletely understood. In addition, whether and to what extent, changes in these processes persist after smoking cessation is unknown.

Therefore, our study investigated, for the first time, the abundance of a comprehensive panel of key regulatory molecules involved in mitochondrial metabolism in various *in vitro* models of CS exposure using human PBEC from multiple (non-COPD) donors (n=3/4 donors/model). These cells were either cultured and exposed in a submerged, undifferentiated status or were differentiated by culture in an ALI culture system and subsequently exposed to CSE or WCS, respectively. In addition to assessing the acute response of mitochondrial quality control processes to CS exposure, we also studied the impact of repeated/chronic WCS exposure during differentiation as well as recovery of mitochondria following cessation of WCS exposure in our ALI-PBEC (undifferentiated PBEC cultured at the ALI to induce differentiation) model. This way, we obtained insight into differences and similarities between the effects of CS on the regulation of mitochondrial metabolism in four different epithelial culture models.

Materials and methods

PBEC isolation and expansion

PBEC of four non-COPD donors for the CSE exposure experiments of undifferentiated PBEC were provided by the Primary Lung Culture (PLUC) facility at Maastricht University Medical Center + (Maastricht, the Netherlands) and PBEC of four non-COPD donors for the WCS exposure experiments of (un-)differentiated PBEC were obtained from Leiden University Medical Center (Leiden, the Netherlands). Approval of the use of PBEC for research provided by the PLUC facility was confirmed by the scientific board of the Maastricht Pathology Tissue Collection (MPTC) under code MPTC2010-019 and the local Medical Ethic Committee code 2017-0087. PBEC were isolated, expanded and differentiated as previously described (40-43). Use of such lung tissue that became available for research within the framework of patient care at MUMC+ and LUMC was in line with the 'Human Tissue and Medical Research: Code of conduct for responsible use' (2011) (www.federa.org), which describes the opt-out system for coded anonymous further use of patient data and tissue collection, storage and further use. Characteristics of the PBEC donors are shown in Table 1.

Table 1. Characteristics of PBEC donors.

Experiment	Acute WCS ALI-PBEC	Chronic WCS ALI-PBEC	Acute WCS S-PBEC	CSE-treated S-PBEC
N	4	3	3	4
Male/female	3/1	2/1	2/1	3/1
Age (years)	58.50 ± 4.15	57.33 ± 5.13	57.33 ± 5.13	69.75 ± 4.03
BMI	30.55 ± 1.41	30.07 ± 1.31	30.07 ± 1.31	28 ± 8.76
Pack-years (years)	15 ± 12.25	7.5 ± 7.50	7.5 ± 7.50	35.00 ± 21.21**
FEV ₁ /FVC	70.36 ± 5.49*	68.49 ± 5.89*	68.49 ± 5.89*	76.06 ± 4.12
VC (l)	4.51 ± 0.40	4.44 ± 0.44	4.44 ± 0.44	3.55 ± 0.69

*Missing value for one donor. **Missing value for two donors. Characteristics of human PBEC donors used in the experiments: acute WCS-exposed ALI-PBEC, chronic WCS-exposed ALI-PBEC followed by smoking cessation, acute WCS-exposed S-PBEC, CSE-treated S-PBEC. Data are presented as mean±s.d. BMI, body mass index; CSE, cigarette smoke extract; FEV₁, forced expiratory volume in the first second; FVC, forced vital capacity; PBEC, primary bronchial epithelial cells; VC, vital capacity; WCS, whole cigarette smoke.

In brief, PBEC were isolated from tumor-free resected bronchus rings obtained from lung cancer patients undergoing resection surgery at MUMC+ or LUMC. After isolation, PBEC were seeded and expanded in keratinocyte-serum-free medium (Life-technologies Europe B.V., the Netherlands) containing 0.2 ng/ml epidermal growth factor (Gibco, USA), 25 µg/ml bovine pituitary extract (Gibco or Life Technologies Europe B.V.), 1 µM isoproterenol (Sigma-Aldrich, USA) and 100 µg/ml primocin (InvivoGen, the Netherlands) or mycozap (0.2%) (Lonza, USA) on six-well plates (Corning Costar, USA) coated with 5 µg/ml or 10 µg/ml human fibronectin (Promocell, Germany or Sigma-Aldrich), 30 µg/ml PureCol (Advanced BioMatrix, USA) and 10 µg/ml bovine serum albumin (BSA; Fraction V; Sigma-Aldrich or Thermo Fisher Scientific, USA) diluted in Hank's balanced salt solution (HBSS; no calcium, no magnesium, no Phenol Red) (Gibco) or phosphate-buffered saline (PBS; Fresenius Kabi, Netherlands). When cells reached confluence, PBEC (mycoplasma-free) were harvested by trypsinization and frozen in liquid nitrogen until use.

Submerged PBEC culture and CSE treatment

PBEC of four non-COPD donors (MUMC+) were thawed (5×10^5 cells, passage 1), seeded and further expanded in supplemented keratinocyte-serum-free medium with mycozap in pre-coated T75 flasks (Greiner Bio-One, the Netherlands) as mentioned above and previously described (42), including some minor adaptations. Subsequently, PBEC were seeded at a density of 7000 cells/cm² in passage 3-4 on a 12- or 24-well plates (i.e., 1.9 cm² or 3.8 cm²) (Corning Costar). The next day, PBEC were washed with HBSS (no calcium,

no magnesium, no Phenol Red) (Gibco) and cultured in Lonza Bronchial Epithelial Basal Medium supplemented with Bronchial Epithelial Cell Growth Medium singlequots (except gentamycin) (Lonza) and 1% penicillin/streptomycin (Gibco). Undifferentiated PBEC were cultured in submerged conditions (further referred to as S-PBEC) for ~3 days upon 60-70% confluency. S-PBEC were starved for 4 h prior to treatment, by replacing the proliferation medium with starvation medium consisting of Lonza Bronchial Epithelial Basal Medium supplemented with Bronchial Epithelial Cell Growth Medium singlequots, except gentamycin, epidermal growth factor and bovine pituitary extract (Lonza), and including 1% penicillin/streptomycin (Gibco).

CSE was generated by using 3R4F research cigarettes (University of Kentucky, Lexington, KY, USA) according to the protocol previously described by Carp and Janoff (1978) (44). In short, after removal of the filters, a cigarette was smoked until the filter paper line by bubbling air (2 ml/s) in HBSS (2 ml) (Gibco) using a linear pump following the regime of 5 s smoking 10 ml, 5 s pause. The ~4 h-starved PBEC were exposed in technical triplicates to fresh sterile filtered CSE (1-2%) diluted in HBSS or control (HBSS; 0% CSE) in Lonza starvation medium for 4 h, 24 h or 48 h.

Submerged and ALI-PBEC culture and WCS treatment

After thawing PBEC of four non-COPD donors (based on pre-surgery spirometry; LUMC), cells were further expanded in supplemented keratinocyte serum-free medium with 1% penicillin/streptomycin (Gibco) replacing primocin in T75 flasks (Greiner Bio-One) as mentioned above and previously described (42). Next, 40,000 cells at passage 2 were transferred to 12-insert transwells coated with the same supplements as mentioned above. Apical and basal sides of transwells were filled with a mixture of 50% Bronchial Epithelial Cell Medium-basal (ScienCell, Sanbio) and 50% Dulbecco's modified Eagle's medium (STEMCELL Technologies, Germany) (referred to as B/D medium), supplemented with 12.5 mM HEPES, bronchial epithelial cell growth supplement, 100 U/ml penicillin, 100 ug/ml streptomycin (all from ScienCell) and 2 mM glutaMAX (Thermo Fisher Scientific).

Undifferentiated PBEC were cultured in submerged conditions using medium supplemented with 1 nM of the synthetic retinoid EC23 (Tocris, Abingdon, UK) (referred to as S-PBEC) for ~6 days to reach confluence before WCS or air exposure, or cultured at the ALI to induce mucociliary differentiation (referred to as ALI-PBEC) as previously described (45). After confluence was reached, the apical medium was removed and cells were cultured at the ALI in B/D medium as described above with 50 nM EC23 for 2 weeks; three times a week the basal medium was refreshed and the apical side was washed with PBS to remove excess mucus.

For WCS exposure, S-PBEC or ALI-PBEC cultures cultured on transwells were exposed to either fresh air (control) or WCS from one 3R4F research cigarette using an exposure

chamber specifically designed for cell culture experiments as previously described (46). In S-PBEC, apical medium was removed shortly before WCS exposure. Fresh air or WCS derived from one cigarette in the holder was pumped into the exposure chamber until one cigarette burned out. After that, fresh air was used to remove residual WCS from the chamber for 10 min. The weight difference of a filter placed between the pump and exposure chamber before and after exposure was recorded to measure the amount of smoke infused inside the exposure chamber. Approximately 2 mg CS-derived particles were deposited on the filter as determined by measuring the filter of different exposures. After WCS or air exposure, apical medium was added to undifferentiated cultures. Cultures were harvested at 6 h and 24 h after exposure according to experimental requirements.

For chronic WCS exposure and cessation, after reaching confluence on the inserts, ALI-PBEC were apically washed every day to remove mucus at 4 h prior to daily WCS exposure and exposed to either fresh air or WCS during differentiation at the ALI for a total of 14 days (chronic exposure model), followed up by a cessation period of 10 days. Cells and basal medium were harvested on Day 14, 16, 19 and 23 to isolate proteins and mRNA as well as measure the levels of L-lactate.

Separation of luminal and basal cell-enriched fractions

ALI-PBEC were separated into luminal and basal cell fractions at 6 h after WCS or air exposure as described previously, using calcium depletion followed by trypsinization (46). Successful separation was identified by measuring gene expression of a basal cells marker (*TP63*) and an early progenitor cell marker (cytokeratin-8, *KRT8*).

RNA isolation, cDNA synthesis and real-time quantitative PCR analysis

CSE-treated undifferentiated PBEC were lysed after 4 h, 24 h or 48 h in 200-400 μ L RLT lysis buffer including 1% 2-Mercaptoethanol (Sigma-Aldrich) and processed according to the RNeasy® Mini Kit manufacturer's protocol (Catalog number 74104 and 74106, Qiagen, USA). WCS-exposed S-PBEC or ALI-PBEC were lysed using RNA lysis buffer, and total RNA was robotically isolated using Maxwell® 16 simply RNA tissue kit (Promega, the Netherlands). A NanoDrop ND 1000 UV-visible spectrophotometer (Isogen Life Sciences, the Netherlands or NanoDrop Technologies, USA) was used to analyze the quantity and purity of the RNA samples. Total RNA (CSE experiments, 25-140 ng; WCS experiments, 500 ng) was reverse transcribed using iScript™ cDNA synthesis method (Bio-Rad, the Netherlands). The cDNA was diluted in Milli-Q (CSE, 1:17.86-1:100; WCS, 1:50) in order to have an equal original input of 25 ng or 10 ng RNA per experiment and stored at -20°C until further analysis.

Expression of genes of interest was analyzed in all samples by real-time quantitative PCR (qPCR) by mixing diluted cDNA, target- and human-specific primers (Eurofins, the Netherlands or Invitrogen, USA) and a 2xSensiMix™ SYBR® & Fluorescein Kit (Bioline,

the Netherlands) or IQ SYBR Green Supermix (Bio-Rad) in white 384-multiwell plates (Roche, Switzerland or BIOplastics BV, the Netherlands). Subsequently, the thermal cycling protocol (10 min at 95°C, 55 cycles of 10 s at 95°C, 20 s at 60°C) was run on a Roche LightCycler 480 machine (Roche). The following software programs were used to perform melt curves and gene expression analysis: LightCycler480 software (Roche) and LinRegPCR software 2014.x (the Netherlands), respectively. Moreover normalization of the expression of mRNA transcripts of interest was conducted by using GeNorm software 3.4 (Primerdesign, USA), which calculated a correction factor based on the expression of a combination of reference genes (*ACTB*, *B2M*, *PPIA*, *RPL13A*, *ATP5B* (also known as *ATP5F1B*)). Used target and human-specific primer sequences are listed in Table S1.

DNA isolation and mitochondrial DNA (mtDNA) copy number analysis

Following exposures, CSE was kept with the cells for 24 h or 48 h, or cells were cultured for 6 h or 24 h after short WCS treatment. Next, PBEC were lysed in 250-400 µl lysis buffer (0.1 M Tris-HCl pH 8.5, 0.005 M EDTA pH 8.0, 0.2% (w/v) sodium dodecyl sulphate, 0.2 M NaCl) at room temperature. To isolate DNA, addition of Proteinase K (10 mg/ml) (Qiagen) to the lysates (1:50) was required, followed by overnight incubation at 55°C. The next day, lysates were centrifuged at 20,000 x g for 15 min. Thereafter, 500 µl isopropanol was added to the supernatant, facilitating DNA precipitation by vigorously shaking. Following two washes of the DNA pellets with 70% ethanol, dry DNA pellets were dissolved in 125 µl TE buffer (10 mM Tris-HCl pH 8.0, 1 mM EDTA). The DNA samples were subsequently incubated at 55°C for 2 h, overnight at 4°C and finally stored at -20 °C until use. DNA quantity and purity was determined by using the NanoDrop ND 1000 UV-visible spectrophotometer (Isogen Life Sciences). DNA samples were diluted in TE buffer (1:50) followed by qPCR analysis (see 'RNA isolation, cDNA synthesis and real-time quantitative PCR analysis' section). mtDNA copy numbers were assessed by investigating the ratio of the expression of mtDNA, mitochondrially-encoded cytochrome C oxidase II (*MT-CO2*), and genomic DNA, *ACTB* (Table S1).

Western Blotting

Whole-cell lysates for western blotting were generated by lysis of treated PBEC in 200 µL whole-cell lysis buffer (20 mM Tris-HCl pH 7.4, 150 mM NaCl, 1% Nonidet P40 in Milli-Q) or Pierce RIPA buffer (Thermo Fisher Scientific), including fresh PhosSTOP Phosphatase and cOmplete, Mini, EDTA-free protease inhibitor cocktail tablets (both Roche). The whole-cell lysates were rotated and subsequently centrifuged at 20,000 x g both for 30 min at 4°C. Assessment of the total protein content in the whole-cell lysate fraction was conducted according to the manufacturer's protocol of the Pierce™ BCA Protein Assay Kit range 20-2000 µg/mL (Thermo Fisher Scientific). The whole-cell lysate supernatant was consecutively diluted to similar concentration within experiments (range 0.0667-1 µg/µl) in a final concentration of 1x Laemmli buffer (0.25 M Tris-HCl pH

6.8, 8% (w/v) sodium dodecyl sulphate, 40% (v/v) glycerol, 0.4 M dithiothreitol, 0.02% (w/v) Bromophenol Blue), boiled at 100°C for 5 min and stored at -80°C pending analysis.

Samples (1-10 µg of protein per lane) and at least two protein ladders (Precision Plus Protein™ All Blue Standards #161-0373, Bio-Rad) were run on each gel in 1x MES running buffer (Bio-Rad) on a Criterion XT Precast 4-12 or 12% Bis-Tris gel (Bio-Rad). Separation of the proteins was achieved by electrophoresis (100-130 V for 1 h), followed by electroblotting (Bio-Rad Criterion Blotter) (100 V for 1 h) to transfer the proteins from the gel to a 0.45 µM nitrocellulose transfer membrane (Bio-Rad). To quantify total protein content, the nitrocellulose membranes were stained using 0.2% (w/v) Ponceau S in 1% (v/v) acetic acid (Sigma-Aldrich) for 5 min, followed by a Milli-Q wash and imaging using the Amersham™ Imager 600 (GE Healthcare, the Netherlands). After removal of the Ponceau S staining, non-specific binding sites on the membranes were blocked for 1 h in 3% (w/v) non-fat dry milk (Campina, the Netherlands) in Tween20 Tris-buffered saline (TBST; 20 mM Tris, 137 mM NaCl, 0.1% (v/v) Tween20, pH 7.6). Subsequently, a TBST wash was followed by overnight incubation of the membranes at 4°C with a target-specific primary antibody (Table S2) diluted 1:500-1:2000 in TBST with 3% (w/v) BSA or non-fat dry milk. The next day, membranes were washed and incubated with a horseradish peroxidase-conjugated secondary antibody (Table S2) diluted 1:10,000 in 3% (w/v) non-fat dry milk in TBST for 1 h at room temperature. Thereafter, membranes were washed again and incubated for 3 min with either 0.25 x Supersignal West FEMTO or 0.5 x Supersignal West PICO Chemiluminescent Substrate (Thermo Fisher Scientific) to visualize the target proteins using the Amersham™ Imager 600 (GE Healthcare). Quantification of images was performed using Image Quant software (GE Healthcare). Absolute protein quantification was calculated by correcting for total protein loading content assessed by Ponceau S staining over the entire size range of proteins (10 kDa - 250 kDa). For western blot analysis, in each of the models described in Fig. 1, based on the respective molecular mass, the following proteins were loaded on the same gel, implying that, for the quantification of these proteins, normalization was based on the same Ponceau S staining (Gel I: HK2, DNMI1L, OXPHOS, SQSTM1; Gel II: PRKN, BNIP3L, BNIP3, FUNDC1, PINK1, MAP1LC3B; Gel III: PPARGC1A, NRF1, TFAM, GABARAPL1, ESRRA). The western blot images presented in the figures of this paper have been equally adjusted for brightness and contrast throughout the picture. Selected images reflecting changes in one PBEC donor are representative for the group of donors/experiment (n=3/4 donors/experiment).

Metabolic enzyme activity assays

Metabolic enzyme activity lysates were generated by lysis of treated PBEC in 100 µl 0.5% Triton X-100 (Sigma-Aldrich) for 15 min on ice, followed by scraping (on ice). Subsequently, the lysates were centrifuged at 20,000 x g for 2 min at 4°C. Supernatants were aliquoted for protein analysis or diluted in 5% BSA in Milli-Q (1:4) for metabolic enzyme activity analysis, both stored at -80°C. Total protein content in the supernatant

fraction was evaluated following the manufacturer's protocol of the Pierce™ BCA Protein Assay Kit range 20-2000 µg/mL (Thermo Fisher Scientific).

After running the three assays (citrate synthase, hydroxyacyl-coenzyme A dehydrogenase (HADH) and phosphofructokinase 1 (PFK1), analysis of the samples was spectrophotometrically conducted at 340 nM (HADH/PFK1) or 412 nM (citrate synthase) at 37°C using a Multiskan Spectrum plate reader (Thermo Labsystems, the Netherlands). Enzyme activity was calculated by slope determination and correction for total protein content of the samples. Details of the analyses were as follows:

Citrate synthase. Citrate synthase activity was assessed as previously described (IUBMB Enzyme Nomenclature EC 2.3.3.1) (47) by mixing undiluted samples with reagent (100 mM Tris, 0.1 mM DNTB, 40 µM acetyl coenzyme A), followed by initiation of the reaction by addition of oxaloacetic acid (25 mM).

HADH. HADH enzyme activity was assessed as previously described (IUBMB Enzyme Nomenclature EC 1.1.1.35) (48). After mixing the undiluted samples with reagent (0.22 mM NADH, 100 mM tetrapotassium pyrophosphate pH 7.3), the reaction was initiated by addition of 2.3 mM acetoacetyl-CoA.

PFK1. As previously described (IUBMB Enzyme Nomenclature EC 2.7.1.11) (49), PFK1 enzyme activity was evaluated by mixing undiluted samples with reagent (48.8 mM Tris, 7.4 mM MgCl₂·6H₂O, 74 mM KCl, 384 µM KCN, 2.8 mM ATP, 1.5 mM DTT, 0.3 mM NADH, 0.375 U/mL aldolase, 0.5625 U/mL glycerol-3-phosphate dehydrogenase and 7.425 U/mL triose phosphate isomerase, pH 8.0). To initiate the reaction, fructose-6-phosphate (30.6 mM) in Tris buffer (49.5 mM, pH 8.0) was added to the mix of undiluted sample and reagent.

Lactate assay

Levels of L-lactate in apical and basal medium collected from S-PBEC and the basal medium of ALI-PBEC at 24 h after acute/chronic WCS exposure were measured using a Lactate Colorimetric/Fluorometric Assay Kit (K607-100, BioVision, USA). In brief, 50 µl diluted samples in Lactate Assay Buffer were mixed with 50 µl Reaction Mix (Lactate Enzyme Mix, Probe and Lactate Assay Buffer) and incubated for 30 min. The absorbance at OD 570 nm was measured in a microplate reader (Bio-Rad).

Immunofluorescence staining and confocal microscopy

Immunofluorescence staining of ALI-PBEC cultures on inserts was performed as mentioned before (45). At indicated time points after acute WCS exposure, membranes with attached ALI-PBEC were washed and PBEC fixed in 4% (w/v) paraformaldehyde in PBS for 30 min at room temperature. Membranes were washed once and stored in PBS at 4°C until use. Before staining for intracellular antigens, ice-cold methanol was added

for 10 min at 4°C. Blocking and permeabilization buffer for non-specific binding sites was PBS/1% (w/v) BSA/0.3% (w/v) Triton-X-100 (PBT) buffer. After incubation for 30 min at 4°C, specific binding sites were stained with rabbit anti-LC3B antibody (1:100; Cell Signaling Technology, USA) together with mouse anti-MUC5AC antibody (1:200; Thermo Fisher Scientific), anti-acetylated α -tubulin antibody (1:500; Sigma-Aldrich), anti-CC-10 antibody (1:50; Hycult Biotech, the Netherlands) or anti-NGFR antibody (1:100; Abcam, UK) for 1 h at room temperature. After washing, secondary antibodies (donkey anti-rabbit and donkey anti-mouse Alexa Fluor antibodies; all diluted 1:200, Thermo Fisher Scientific) and 4',6-diamidino-2-phenylindole (DAPI; 1:50, Sigma-Aldrich) were added to the cells in the dark for 30 min at room temperature. Next, membranes with ProLongTM Gold Antifade Mountant (Thermo Fisher Scientific) were placed on glass slides and covered with a coverslip. Slides were viewed using a Leica TCS SP8 confocal microscope (Leica Microsystems, Germany) at 630 x original magnification.

Statistical analysis

Prism 8.0.1 software (GraphPad, USA) was used to perform statistical analyses and graph the data. Data are presented as mean fold change of independent donors compared to control (air, 0% CSE or Day 14) \pm standard error of the mean (s.e.m.). In the CSE-exposed S-PBEC experiments, each donor reflects the mean of technical triplicates. Outliers were excluded based on quality assessment of gene expression melt curve/peak analysis using LightCycler480 Software (Roche), and western blot analysis. Statistical testing of differences between acute WCS and air exposures in S-PBEC or ALI-PBEC was performed using a two-tailed paired parametric t-test. Moreover, a two-tailed paired parametric t-test was conducted to test differences in WCS *versus* air exposures after smoking cessation in ALI-PBEC on each day (e.g., WCS Day 14 *versus* air control). If comparison of various groups was required in case of the CSE exposure (CSE 1% or 2% *versus* 0% CSE) or in WCS chronic smoking cessation experiments (WCS Day 16, 19, 23 *versus* WCS Day 14), assuming a Gaussian distribution and using Geisser-Greenhouse correction, one-way ANOVA (matched/repeated measures) followed by Sidak's post-hoc test for multiple comparisons was conducted, and, in the case of missing values, mixed-effects modeling was performed. Statistical significance was considered if $p < 0.05$ and a trend was indicated if $p < 0.1$.

Results

We deployed four models of exposure of PBEC to WCS or CSE. These included, respectively, (1) differentiated ALI-PBEC acutely exposed to WCS, (2) ALI-PBEC chronically exposed (during differentiation) to WCS followed by smoking cessation, (3) undifferentiated S-PBEC (PBEC cultured in submerged conditions) acutely exposed to WCS and (4) undifferentiated S-PBEC treated with CSE (Fig. 1). ALI-PBEC cultures were differentiated and included several distinct cell types present in the pseudostratified epithelium, mimicking the ‘healthy’ normal airway epithelium (36). Undifferentiated S-PBEC, on the other hand, consisted of basal cells, reflecting injured/damaged airway epithelium. Collectively, these models allowed us not only to test our hypothesis that WCS exposure has a differential impact on mitochondrial quality control systems in undifferentiated (predominantly basal-like cell type) *versus* differentiated (including ciliated, club and goblet cells) human PBEC cultures, but also allowed us to compare the effect of an aqueous extract of CS (CSE) to that of WCS (particles and gaseous components) and assess the potential influence of smoking cessation.

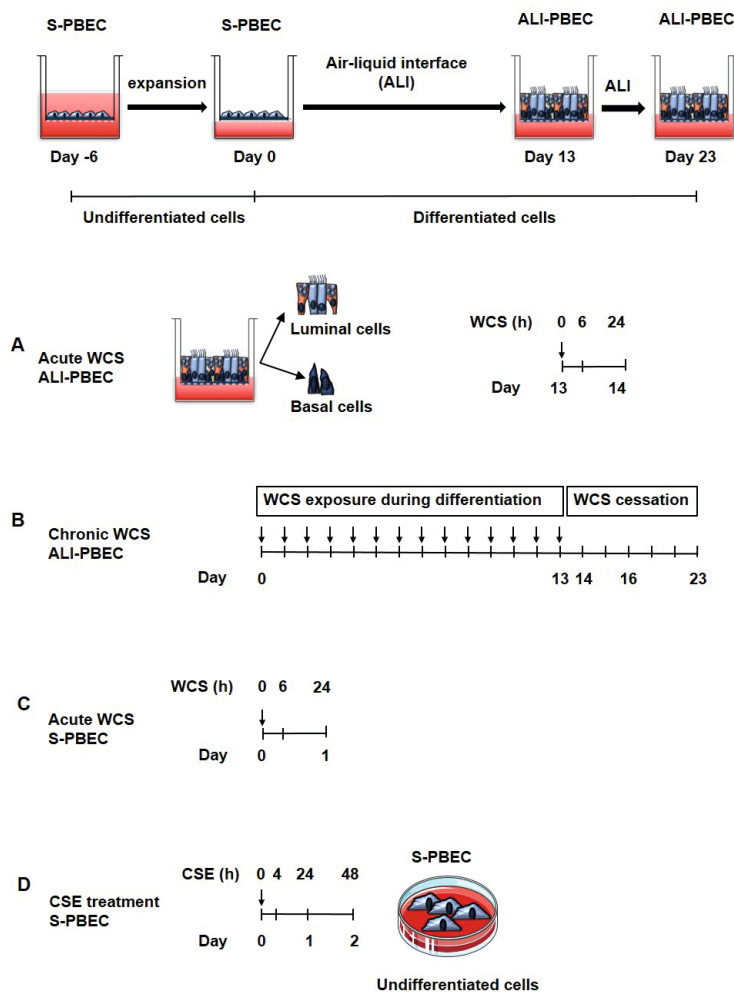


Figure 1. Experimental cigarette smoke (CS)-exposed cell models. Models A, B and C were primary bronchial epithelial cells (PBEC) cultured on transwells to allow apical exposure to fresh air or whole CS (WCS), whereas the model shown in D was PBEC cultured on tissue culture plastic requiring submerged exposure to CS extract (CSE). **(A)** Acute WCS-exposed ALI-PBEC: after 2-weeks of differentiation, ALI-PBEC (undifferentiated PBEC cultured at the air-liquid interface (ALI) to induce differentiation) were exposed to fresh air or WCS from one 3R4F cigarette (University of Kentucky, 2 mg). Subsequently, whole-cell lysates were harvested after 6 h and 24 h, and the basal and luminal fractions were harvested only at 6 h post-exposure (n=3 donors/group). **(B)** Chronic WCS-exposed (during differentiation) ALI-PBEC followed by smoking cessation: ALI-PBEC were 1x daily exposed to fresh air or WCS from one 3R4F cigarette (University of Kentucky, 2 mg) during differentiation for 14 days, followed by a cessation period of up to 10 days. Cells were harvested on Day 14 (24 h after the last WCS exposure), 16, 19 and 23 (n=3 donors/group). **(C)** Acute WCS-exposed S-PBEC: undifferentiated S-PBEC (PBEC cultured in submerged conditions) were exposed, after removal of apical medium, to fresh air or WCS from one 3R4F cigarette (University of Kentucky, 2 mg), followed by harvesting of whole-cell lysates after 6 h and 24 h recovery (n=3 donors/group). **(D)** CSE-treated S-PBEC: undifferentiated S-PBEC were submerged treated with CSE from one 3R4F cigarette (University of Kentucky) diluted in HBSS (0.1-2%) in Lonza starvation medium for 4 h, 24 h or 48 h (n=4 donors/group).

Increase in autophagy markers in response to CS exposure

As autophagy proteins play a key role in facilitating mitochondrial quality control (i.e. breakdown) by the autophagosomal pathways, we studied the effect of WCS exposure in ALI-PBEC on the expression of several autophagy-related proteins. Firstly, as it has been reported that activation of autophagy, as a cytoprotective mechanism, is related to oxidative stress (50), and to verify that our CS exposures were able to elicit a cellular response indicative of successful exposure in the different models, we investigated the oxidative stress response to WCS or CSE by measuring anti-oxidant gene expression in our four models. Elevated mRNA levels of superoxide dismutase 1 (*SOD1*) were observed in ALI-PBEC following acute WCS exposure and 24 h after chronic WCS exposure during differentiation (Figs S1A, C). Separation of cellular fractions revealed that the acute WCS-induced upregulation of *SOD2* expression originated from both the luminal and basal cell fraction (Fig. S1B). The separation of basal and luminal cell fractions was validated by measuring gene expression of the basal cell marker *TP63* and early progenitor cell marker *KRT8* (Fig. S2), respectively. In contrast to changes observed in ALI-PBEC exposed to WCS, in S-PBEC exposed to CSE only, *SOD1* transcript levels were induced (in a dose-dependent manner) whereas *SOD2* transcript levels were decreased, which was not observed in S-PBEC exposed to WCS (Fig. S1D). Our previous results also showed that acute WCS exposure resulted in increased expression of genes involved in the antioxidant defense, including heme oxygenase 1 and NAD(P)H quinone oxidoreductase 1 in ALI-PBEC (51). In accordance with these previous data, our results collectively point to a cellular response to oxidative stress indicative of successful exposure to CS(E) in the different models.

Next, we assessed the impact of exposure of the cells to CS constituents on the expression of autophagy-related proteins. As shown in Fig. 2A-C, both protein and transcript levels of the adaptor proteins SQSTM1 and GABARAPL1, as well as the marker of the accumulation of autophagosomes (LC3BII; also known as MAP1LC3B2), were increased after WCS exposure in ALI-PBEC. These increases were most pronounced at 6 h post-WCS exposure and were largely dissipated after 24 h. Similar results were obtained in S-PBEC exposed to WCS or CSE (Fig. S3), although it appeared that induction of transcript expression of autophagy markers in response to CSE was delayed and more pronounced compared to these changes in ALI-PBEC cultures stimulated with WCS (Fig. S3C). Importantly, to further determine the cellular location of the increased expression of these autophagy markers in response to WCS, we isolated basal and luminal cells from WCS-exposed ALI-PBEC cultures. By comparison, both basal and luminal cell fractions of ALI-PBEC expressed higher mRNA levels of autophagy markers after WCS exposure indicating that both fractions were similarly affected by WCS exposure (although responses appeared to be slightly more pronounced in the basal fraction) (Fig. 2D). To further investigate and validate these findings, an immunofluorescence assay was conducted, using staining with the anti-LC3B (also known as MAP1LC3B) antibody as autophagy indicator; co-staining with anti-MUC5AC, anti-acetylated α -tubulin, anti-

CC-10 (also known as SCGB1A1) and anti-NGFR was used to detect goblet cells, ciliated cells, club cells and basal cells, respectively. As depicted in Fig. 2E, the presence of cell differentiation markers demonstrates differentiation of air- and WCS-exposed PBEC in our model. WCS exposure enhanced the number of LC3B⁺ puncta in ALI-PBEC (Fig. 2E), which was most pronounced in basal cells and goblet cells. Furthermore, the pronounced induction in abundance of autophagy markers in acute WCS models was largely absent in the chronic WCS-exposed ALI-PBEC cultures. Moreover, even a decreased ratio of LC3BII/I was observed 24 h after the last exposure which was recovered after WCS cessation (Fig. 2F-H).

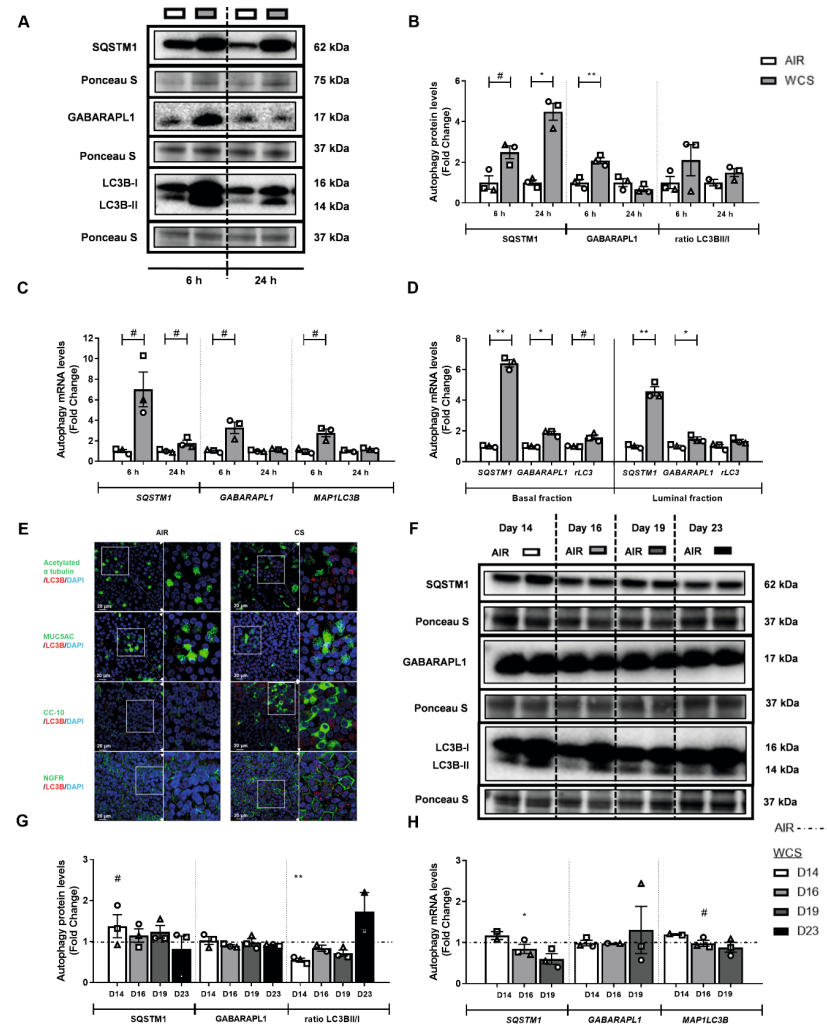


Figure 2. See next page for legend.

Figure 2. Increase in abundance of autophagy markers in WCS-exposed ALI-PBEC. After 2-weeks of differentiation, ALI-PBEC were exposed to fresh air or WCS from one 3R4F cigarette (University of Kentucky, 2 mg), and whole-cell lysates were harvested after 6 h and 24 h, and the basal and luminal fractions were harvested only at 6 h post-exposure (n=2-3 donors/group). **(A-D)** Protein **(A, B)** and transcript **(C, D)** levels of autophagy regulators SQSTM1, GABARAPL1, MAP1LC3B and ratios of LC3BII/I or MAP1LC3B/A (rLC3) in whole-cell lysates or in basal/luminal cell fractions post-exposure are presented. Data are presented as mean fold change compared to control (air)±s.e.m.. Independent donors are represented by open circles, triangles or squares. Statistical differences between WCS *versus* air were tested using a two-tailed paired parametric t-test (*p<0.1, *p<0.05 and **p<0.01). **(E)** Immunofluorescence staining and confocal microscopy were conducted post-WCS exposure in differentiated ALI-PBEC using antibodies for anti-LC3B (red) together with anti-MUC5AC (green), anti-acetylated α -tubulin (green), anti-CC-10 (green) and anti-NGFR (green) in combination with 4',6-diamidino-2-phenylindole (DAPI;blue) for nuclear staining. Immunofluorescence images shown are representative for three donors with 630 x original magnification. Scale bars: 20 μ m. ALI-PBEC were 1x daily exposed to fresh air or WCS from one 3R4F cigarette (University of Kentucky, 2 mg) during differentiation for 14 days, followed by a cessation period of up to 10 days. Cells were harvested on Day 14 (24 h after the last exposure), 16, 19 and 23 (n=2-3 donors/group). **(F-H)** Protein **(F, G)** and mRNA levels **(H)** of autophagy regulators SQSTM1, GABARAPL1 and ratio LC3BII/I or MAP1LC3B were analyzed in whole-cell lysates. Representative western blots, including representative parts of the Ponceau S staining, are shown. Data are presented as mean fold change compared to control (air or WCS Day 14)±s.e.m.. Independent donors are represented by open circles, triangles or squares. Statistical differences between WCS and air after smoking cessation in ALI-PBEC on each day were tested using a two-tailed paired parametric t-test (e.g., WCS Day 14 *versus* air). Comparison of various groups to test the difference between WCS Day 16, 19, 23 and Day 14 in WCS chronic smoking cessation experiments was conducted using one-way ANOVA followed by Sidak's post-hoc test for multiple comparisons, and, in case of missing values, mixed-effects modeling was performed. Statistical significance is indicated as #p<0.1, *p<0.05 and **p<0.01 compared to control (air or WCS Day 14).

Taken together, acute WCS exposure of well-differentiated ALI-PBEC (representing an intact epithelial layer) resulted in an elevated abundance of autophagy markers associated with accumulation of autophagosomes and expression of ubiquitin-binding autophagic adaptors localized in both basal and luminal cells. Similar findings were made in undifferentiated S-PBEC exposed to CSE or WCS (representing damaged epithelium). Importantly, these changes were reversible as they were no longer observed after cessation in our chronic ALI-PBEC WCS exposure model.

Modulation of mitophagy-specific markers in response to CS exposure

Because we observed a potent increase in the abundance of general autophagy markers in response to WCS exposure, and because these proteins are also essential for mitochondrial-specific autophagy (mitophagy), we next investigated whether the specific receptor- and ubiquitin-mediated mitophagy pathways involved in the removal of damaged or dysfunctional mitochondria, were also affected by WCS exposure.

As illustrated in Fig. 3, protein levels of BNIP3 and mRNA levels of *BNIP3L* and *FUNDC1* were significantly increased 24 h after acute WCS exposure in differentiated ALI-PBEC (Fig. 3A-C). In contrast, we observed a transient decrease in mRNA levels of *FUNDC1* at 6 h post-WCS exposure in these cultures (Fig. 3C). To study the impact of acute WCS exposure on regulators of mitophagy in specific epithelial cell types, we also

investigated transcript levels of those regulators in the basal and luminal fractions of these differentiated ALI-PBEC cultures at 6 h post-WCS exposure. In line with the whole-cell lysate data, increased *BNIP3(L)* and decreased *FUNDC1* mRNA expression were observed in both fractions (Fig. 3D). The chronic WCS exposure model revealed that increases in BNIP3 protein levels in response to WCS were persistent 24 h after chronic WCS exposure, whereas changes in the transcript abundance of other regulators of mitophagy were more transient in nature (Fig. 3E-G). Although CSE exposure of undifferentiated S-PBEC yielded similar results as in ALI-PBEC cultures (i.e. increased BNIP3 protein), WCS exposure of these cells revealed only significantly decreased *BNIP3* mRNA levels (Fig. S4).

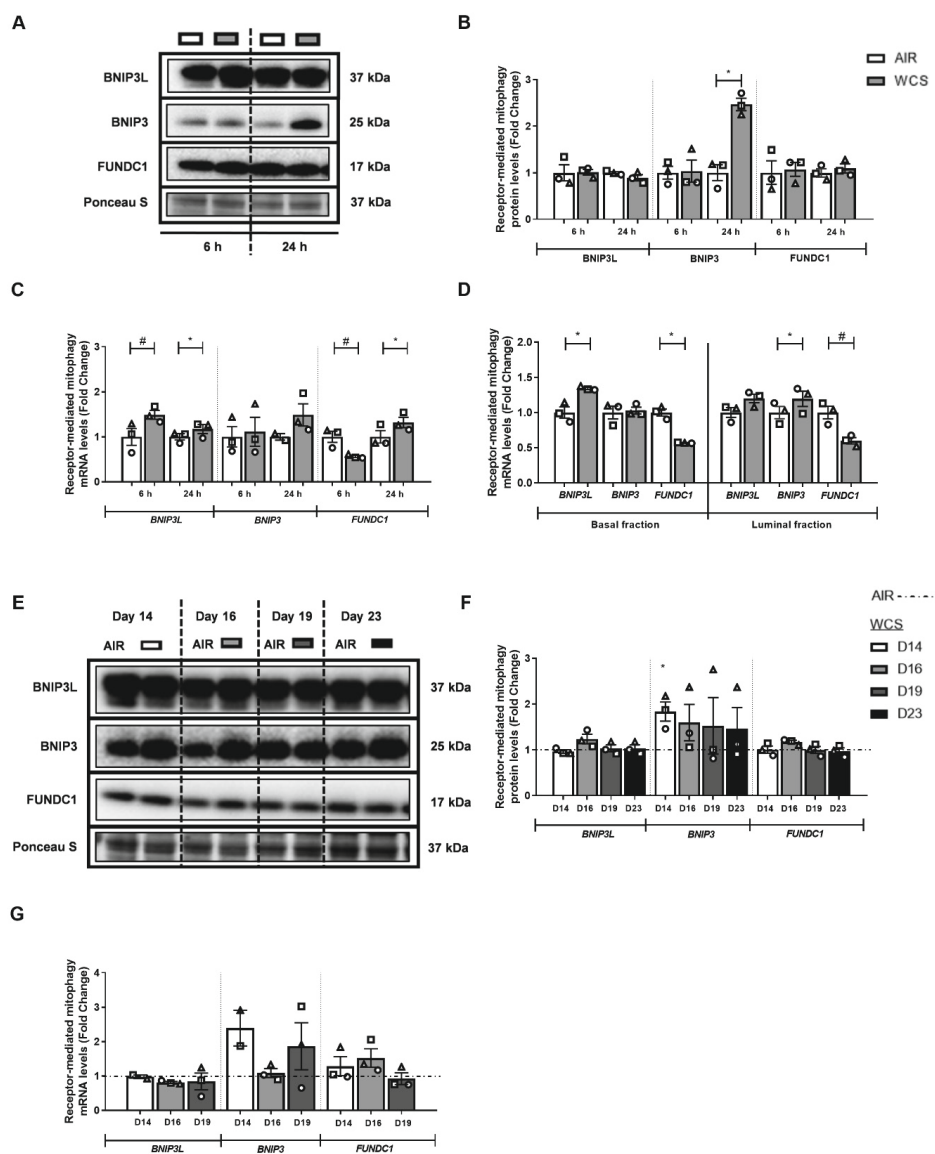


Figure 3. See next page for legend.

Figure 3. WCS-induced changes in protein and mRNA levels of constituents involved in the receptor-mediated mitophagy machinery in ALI-PBEC. After 2-weeks of differentiation, ALI-PBEC were exposed to fresh air or WCS from one 3R4F cigarette (University of Kentucky, 2 mg), and whole-cell lysates were harvested after 6 h and 24 h, and the basal and luminal fractions were harvested only at 6 h post-exposure (n=2-3 donors/group). **(A-D)** Protein **(A, B)** as well as mRNA **(C, D)** levels of constituents involved in receptor-mediated mitophagy - BNIP3L, BNIP3, FUNDC1 - were analyzed in whole-cell lysates or basal/luminal cell fractions post-exposure. Data are presented as mean fold change compared to control (air)±s.e.m.. Independent donors are represented by open circles, triangles or squares. Statistical differences between WCS and air were tested using a two-tailed paired parametric t-test (*p<0.1 and *p<0.05). ALI-PBEC were 1x daily exposed to fresh air or WCS from one 3R4F cigarette (University of Kentucky, 2 mg) during differentiation for 14 days, followed by a cessation period of up to 10 days. Cells were harvested on Day 14 (24 h after the last exposure), 16, 19 and 23 (n=2-3 donors/group). **(E-G)** Protein **(E, F)** and mRNA **(G)** levels of receptor-mediated mitophagy regulators BNIP3L, BNIP3, and FUNDC1 were analyzed in whole-cell lysates. Representative western blots, including representative parts of the Ponceau S staining, are shown. Data are presented as mean fold change compared to control (air or WCS Day 14)±s.e.m.. Independent donors are represented by open circles, triangles or squares. Statistical differences between WCS and air after smoking cessation in ALI-PBEC on each day were tested using a two-tailed paired parametric t-test (e.g., WCS Day 14 *versus* air). Comparison of various groups to test the difference of WCS Day 16, 19, 23 and Day 14 in WCS chronic smoking cessation experiments was conducted using one-way ANOVA followed by Sidak's post-hoc test for multiple comparisons, and, in the case of missing values, mixed-effects modeling was performed. Statistical significance is indicated as *p<0.05 compared to control (air or WCS Day 14).

Because the abundance of the ubiquitin-binding autophagic adaptor SQSTM1 was increased in response to acute WCS exposure (Fig. 2), we further investigated the expression levels of ubiquitin-dependent mitophagy regulators PINK1 and PRKN. In general, PRKN abundance was significantly decreased in response to acute WCS exposure in ALI-PBEC and upon CSE treatment in S-PBEC, whereas PINK1 protein and transcript levels showed a trend to increase in acute WCS-exposed ALI-PBEC as well as upon smoking cessation (Fig. 4; Fig. S5).

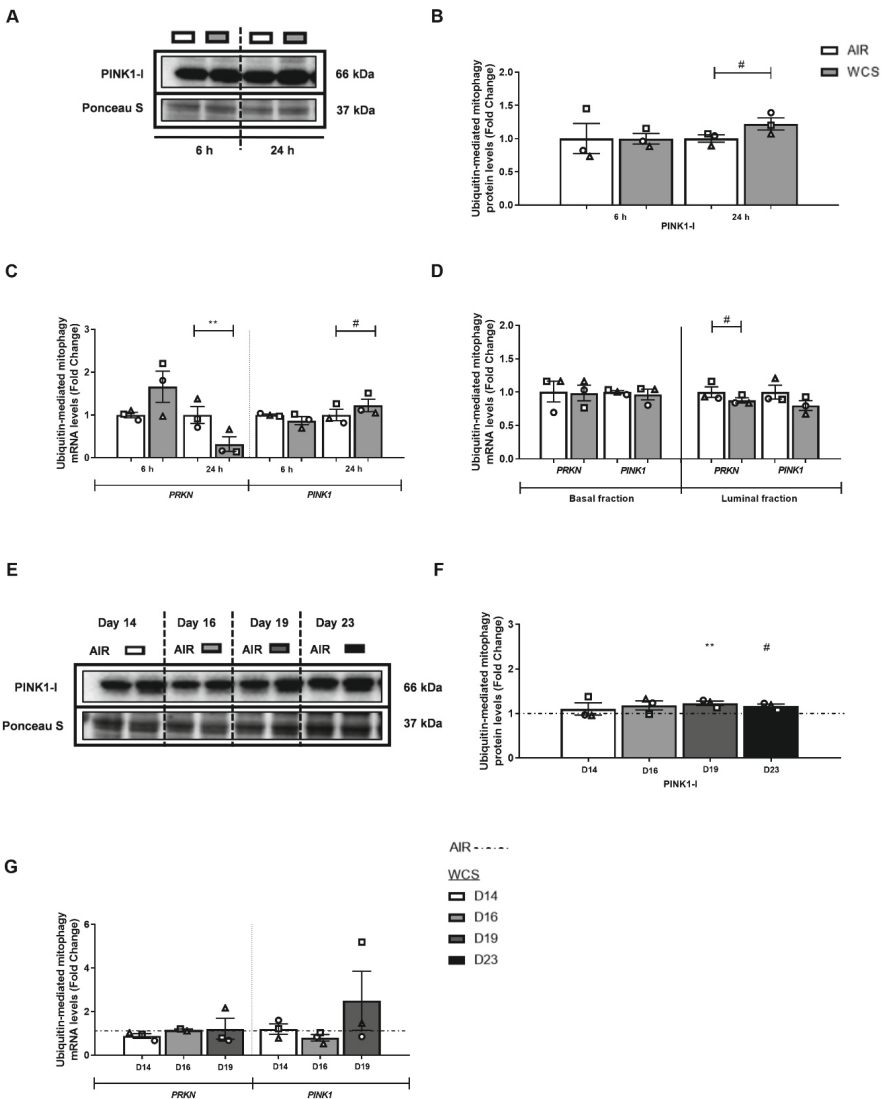


Figure 4. See next page for legend.

Figure 4. Alterations in the abundance of constituents associated with ubiquitin-mediated mitophagy in ALI-PBEC. After 2-weeks of differentiation, ALI-PBEC were exposed to fresh air or WCS from one 3R4F cigarette (University of Kentucky, 2 mg), and whole-cell lysates were harvested after 6 h and 24 h, and the basal and luminal fractions were harvested only at 6 h post-exposure (n=3 donors/group). (A-D) Protein (A, B) as well as mRNA (C, D) levels of constituents involved in ubiquitin-mediated mitophagy, PRKN and PINK1, were analyzed in whole-cell lysates or basal/luminal cell fractions post-exposure. Data are presented as mean fold change compared to control (air)±s.e.m.. Independent donors are represented by open circles, triangles or squares. Statistical differences between WCS and air were tested using a two-tailed paired parametric t-test (*p<0.1 and **p<0.01). ALI-PBEC were 1x daily exposed to fresh air or WCS from one 3R4F cigarette (University of Kentucky, 2 mg) during differentiation for 14 days, followed by a cessation period of up to 10 days. Cells were harvested on Day 14 (24 h after the last exposure), 16, 19 and 23 (n=2-3 donors/group). (E-G) Protein (E, F) and mRNA (G) levels of mitophagy regulators PRKN and PINK1 were analyzed in whole-cell lysates. Western blot analysis revealed one distinct band for PINK1 protein corresponding with the expected molecular mass for PINK1-I (66 kDa). Representative western blots, including representative parts of the Ponceau S staining, are shown. Data are presented as mean fold change compared to control (air or WCS Day 14)±s.e.m.. Independent donors are represented by open circles, triangles or squares. Statistical differences between WCS and air after smoking cessation in ALI-PBEC on each day were tested using a two-tailed paired parametric t-test (e.g, WCS Day 14 *versus* air). Comparison of various groups to test the difference between WCS Day 16, 19, 23 and Day 14 in WCS chronic smoking cessation experiments was conducted using one-way ANOVA followed by Sidak's post-hoc test for multiple comparisons, and, in case of missing values, mixed-effects modeling was performed. Statistical significance is indicated as #p<0.1 and **p<0.01 compared to control (air or WCS Day 14).

In conclusion, these results indicate that WCS, as well as CSE, stimulation specifically affects the regulation of receptor-mediated mitophagy, which was consistently observed in all models and, at least to some degree, persists upon chronic WCS exposure and smoking cessation.

WCS-induced alterations in the molecular machinery controlling mitochondrial biogenesis

As both mitophagy and mitochondrial biogenesis play an essential role in maintaining mitochondrial homeostasis, we next investigated the impact of CS on the abundance of constituents involved in the genesis of mitochondria.

Firstly, in ALI-PBEC, we evaluated whether acute WCS exposure affected the abundance of transcriptional co-activators of the PPARGC1 network, a critical signaling cascade involved in the regulation of mitochondrial biogenesis and mitochondrial energy metabolism (20). No significant changes were observed in protein and transcript levels of most investigated transcriptional co-activators of the PPARGC1 network (i.e. PPARGC1A and PPARGC1B) in whole-cell lysates in all models (Fig. 5; Fig. S6). However, elevated peroxisome proliferator-activated receptor gamma coactivator-related protein 1 (*PPRC1*) mRNA levels were observed in response to acute WCS exposure in both basal and luminal fractions of WCS-exposed ALI-PBEC (Fig. 5D). Similar responses, although not all statistically significant, likely due to interdonor variation, were observed in whole-cell lysates after WCS-exposure of both differentiated ALI-PBEC and undifferentiated S-PBEC (Fig. 5C; Fig. S6C). Remarkably, abundance of *PPARGC1B*

mRNA levels showed a transient response to acute WCS exposure, whereas we observed a decline in response to CSE in S-PBEC (Fig. 5C,D; Fig. S6C). In contrast to the response to acute WCS exposure, *PPARGC1A* mRNA levels were significantly decreased upon chronic WCS exposure (Fig. 5G).

Thereafter, we examined the impact of WCS exposure on abundance of transcription factors associated with the PPARGC1 network. Protein and transcript levels of PPARGC1-coactivated transcription factors, either transcription factor A, mitochondrial (TFAM), nuclear respiratory factor 1 (NRF1) or estrogen-related receptor alpha (ESRRA), were largely unaltered upon acute WCS exposure and slightly decreased upon chronic WCS exposure and cessation in differentiated ALI-PBEC cultures (Fig. 6). Interestingly though, in line with increased levels of *PPRC1* as described above, fractionation of basal and luminal fractions revealed increased mRNA levels of *ESRRA* and *TFAM* in response to WCS (Fig. 6D).

Variable, but minor, changes of the abundance of indices involved in mitochondrial biogenesis were observed in response to WCS (increases) and CSE (decreases) in undifferentiated S-PBEC cultures (Fig. S7).

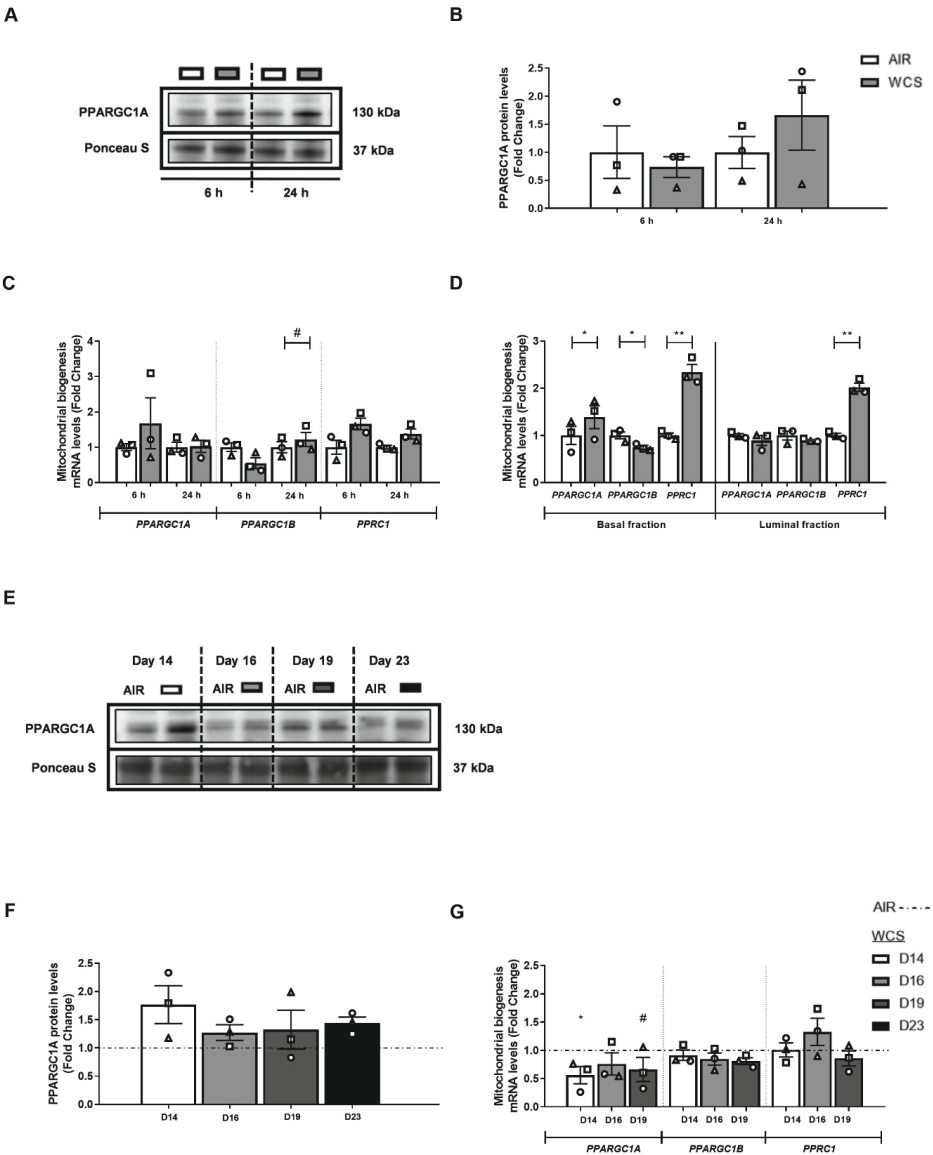


Figure 5. See next page for legend.

Figure 5. Changes in transcription factors associated with mitochondrial biogenesis in response to WCS exposure in ALI-PBEC. After 2-weeks of differentiation, ALI-PBEC were exposed to fresh air or WCS from one 3R4F cigarette (University of Kentucky, 2 mg), and whole-cell lysates were harvested after 6 h and 24 h, and the basal and luminal fractions were harvested only at 6 h post-exposure (n=3 donors/group). **(A-D)** Protein **(A, B)** and mRNA **(C, D)** levels of transcriptional co-activators of the PPARGC1 network, i.e. PPARGC1A, PPARGC1B and PPRC1, were analyzed in whole-cell lysates or basal/luminal cell fractions post-exposure. Data are presented as mean fold change compared to control (air)±s.e.m.. Independent donors are represented by open circles, triangles or squares. Statistical differences between WCS and air were tested using a two-tailed paired parametric t-test (*p<0.1, *p<0.05 and **p<0.01). ALI-PBEC were 1x daily exposed to fresh air or WCS from one 3R4F cigarette (University of Kentucky, 2 mg) during differentiation for 14 days, followed by a cessation period of up to 10 days. Cells were harvested on Day 14 (24 h after the last exposure), 16, 19 and 23 (n=3 donors/group). **(E-G)** Protein **(E, F)** and mRNA levels **(G)** of indices involved in the PPARGC1 network are depicted. Representative western blots, including representative parts of the Ponceau S staining, are shown. Data are presented as mean fold change compared to control (air or WCS Day 14)±s.e.m.. Independent donors are represented by open circles, triangles or squares. Statistical differences between WCS and air after smoking cessation in ALI-PBEC on each day were tested using a two-tailed paired parametric t-test (e.g, WCS Day 14 *versus* air). Comparison of various groups to test the difference of WCS Day 16, 19, 23 and Day 14 in WCS chronic smoking cessation experiments was conducted using one-way ANOVA followed by Sidak's post-hoc test for multiple comparisons, and, in the case of missing values, mixed-effects modeling was performed. Statistical significance is indicated as #p<0.1, *p<0.05 compared to control (air or WCS Day 14).

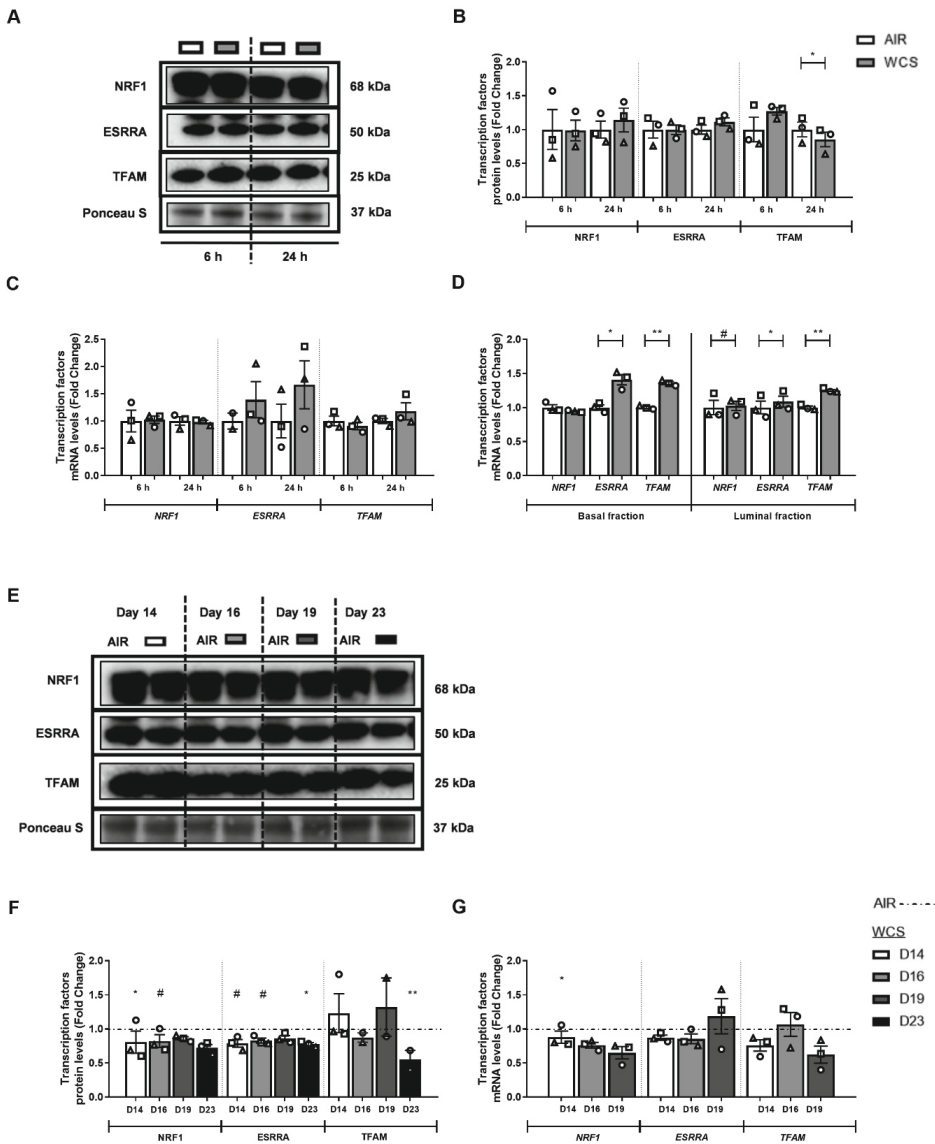


Figure 6. Alterations in the abundance of PPARGC1-coactivated transcription regulators in WCS-exposed ALI-PBEC. After 2-weeks of differentiation, ALI-PBEC were exposed to fresh air or WCS from one 3R4F cigarette (University of Kentucky, 2 mg), and whole-cell lysates were harvested after 6 h and 24 h, and the basal and luminal fractions were harvested only at 6 h post-exposure (n=2-3 donors/group). (A-D) Protein (A, B) as well as mRNA (C, D) levels of PPARGC1-coactivated transcription regulators: NRF1, ESRRA, TFAM were analyzed in whole-cell lysates or basal/luminal cell fractions post-exposure. Data are presented as mean fold change compared to control (air)±s.e.m.. Independent donors are represented by open circles, triangles or squares. Statistical differences between WCS and air were tested using a two-tailed paired parametric t-test (*p<0.1, *p<0.05 and **p<0.01). ALI-PBEC were 1x daily exposed to fresh air or WCS from one 3R4F cigarette (University of Kentucky, 2 mg) during differentiation for 14 days, followed by a cessation period of up to 10 days. Cells were harvested on Day 14 (24 h after the last exposure), 16, 19 and 23 (n=2-3 donors/group). (E-G) Protein (E, F) and transcript (G) levels of PPARGC1-coactivated transcription regulators are presented. Representative western blots, including representative parts of the Ponceau S staining, are shown. Data are presented as mean fold change compared to control (air or WCS Day 14)±s.e.m.. Independent donors are represented by open circles, triangles or squares. Statistical differences between WCS and air after smoking cessation in ALI-PBEC on each day were tested using a two-tailed paired parametric t-test (e.g., WCS Day 14 *versus* air). Comparison of various groups to test the difference between WCS Day 16, 19, 23 and Day 14 in WCS chronic smoking cessation experiments was conducted using one-way ANOVA followed by Sidak's post-hoc test for multiple comparisons, and, in the case of missing values, mixed-effects modeling was performed. Statistical significance is indicated as #p<0.1, *p<0.05 and **p<0.01 compared to control (air or WCS Day 14).

Collectively, these data show that expression of transcriptional co-activators involved in mitochondrial biogenesis was largely unaltered in whole-cell lysates, while increased expression was observed in specific cell fractions of acute WCS-exposed ALI-PBEC and in basal cells of WCS-exposed S-PBEC. Moreover, a different response was observed in the other *in vitro* CS exposure models. However, the observed increases, in particular in PPRC1, and also alterations in the levels of some transcription factors associated with these co-activator molecules following CS exposure, may suggest a compensatory cellular response to induce mitochondrial biogenesis.

Changes in the regulation of mitochondrial fusion and fission in response to WCS exposure

Because of the observed changes in these mitochondrial quality control mechanisms in the different models and the fact that these processes require mitochondrial fusion and fission, we examined the impact of WCS exposure on key molecules involved in the regulation of mitochondrial dynamics. Acute WCS-treatment resulted in upregulation of the mitochondrial fusion markers mitofusin 1 (*MFN1*) in ALI-PBEC (Fig. S8A-E). However, CSE or WCS exposure had no pronounced impact on the regulation of fission or fusion markers in S-PBEC (Fig. S9). Also, no pronounced alterations were observed in the abundance of mitochondrial dynamic regulators upon chronic WCS exposure and the smoking cessation period (Fig. S8F-H).

Disruption of the metabolic phenotype upon WCS exposure

We next investigated whether CS-induced changes in the regulation of mitochondrial biogenesis and mitophagy were accompanied by changes in mitochondrial content and mitochondrial metabolic pathways. To this end, we investigated the effects of WCS exposure on the activity of critical metabolic enzymes and abundance of proteins involved in mitochondrial metabolic pathways.

Acute WCS exposure of differentiated ALI-PBEC cultures as well as CSE exposure of undifferentiated S-PBEC did not affect mitochondrial content as assessed by mtDNA copy number (Fig. S10A; Fig. S11A). Also, protein and mRNA levels of nuclear-encoded and mitochondrial-encoded proteins and genes of electron-transport chain (ETC) subunits were unaltered after acute or chronic exposure of ALI-PBEC to WCS (Fig. S10B-H). Some minor, but variable, alterations were found in transcript and protein levels of analyzed subunits of ETC complexes in undifferentiated S-PBEC cultures exposed to CSE or WCS (Fig. S11B-D). Although we did observe some slight alterations in the abundance of ETC subunits in the different models, in general, our data indicate no marked changes in indices of mitochondrial content in all models after acute or chronic exposure to CS.

We also examined the impact of CS exposure on the activity and expression of constituents of the fatty acid β -oxidation and tricarboxylic acid cycle. Besides downregulated HADH enzyme activity in acute WCS-exposed ALI-PBEC, we also observed increased citrate synthase activity in CSE-treated S-PBEC (Fig. S12A,E). Similar changes at mRNA level were found in the basal fraction of WCS-exposed ALI-PBEC, while conflicting, but transient, gene expression was found in S-PBEC CS models (Fig. S12B-D,F).

Finally, we explored whether CS exposure may affect the metabolic program in PBEC. First, lactate production was measured in the basal medium of WCS-exposed ALI-PBEC. We observed an increase in L-lactate levels after acute and chronic WCS exposure of differentiated ALI-PBEC cultures compared to air control, which persisted after WCS cessation, indicating a shift to a glycolytic metabolism (Fig. 7A,F). In line with this, mRNA abundance of hexokinase 2 (HK2), the enzyme responsible for the first step in glycolysis, was found to be elevated in acute and chronic WCS-exposed ALI-PBEC and in S-PBEC (Fig. 7E,H; Fig. S13E). Activity or expression levels of other markers of glycolysis (PFK1 enzyme activity and HK2 abundance) showed no significant differences in response to acute or chronic WCS-exposed ALI-PBEC (Fig. 7B-D,G). No significant differences were observed in L-lactate levels after acute WCS exposure in undifferentiated S-PBEC (Fig. S13A) or in activity of PFK1 and expression of HK2 in CSE-exposed S-PBEC (Fig. S13B-E).

Collectively, these results demonstrate that CS exposure does not affect mtDNA copy number or the abundance of constituents of the ETC, but do suggest a shift to a more glycolytic metabolism in fully differentiated PBEC cultures, but not in damaged epithelium.

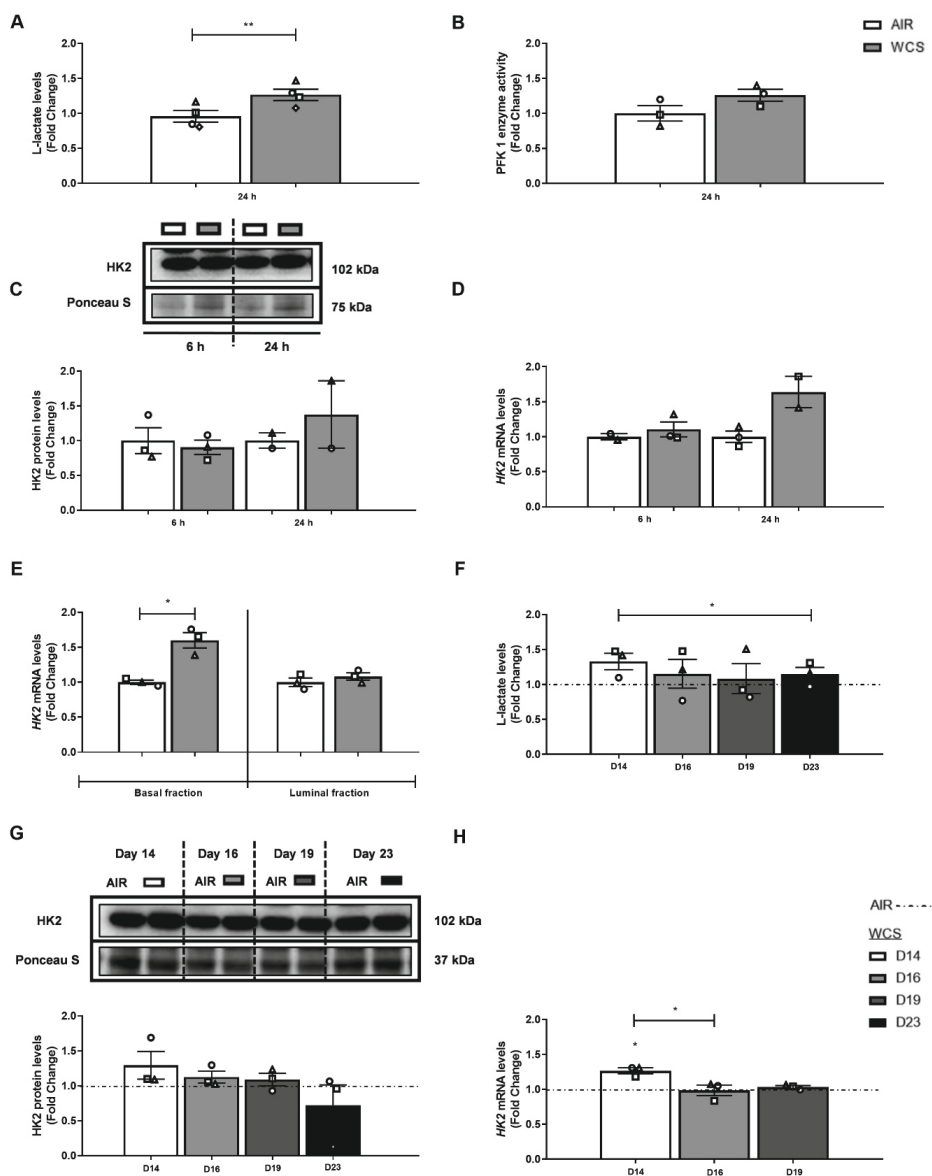


Figure 7. See next page for legend.

Figure 7. WCS-induced shift to anaerobic glycolysis in ALI-PBEC. After 2-weeks of differentiation, ALI-PBEC were exposed to fresh air or WCS from one 3R4F cigarette (University of Kentucky, 2 mg), and basal medium was collected after 24 h, and whole-cell lysates were harvested after 6 h and 24 h, and the basal and luminal fractions were harvested only at 6 h post-exposure (n=2-4 donors/group). **(A-E)** L-lactate in basal medium (n=4 donors/group) **(A)**, PFK1 activity (n=3 donors/group) **(B)**, and HK2 protein **(C)** and mRNA **(D, E)** (n=2-3 donors/group) levels were analyzed in whole-cell lysates or basal/luminal cell fractions post-exposure. Data are presented as mean fold change compared to control (air)±s.e.m.. Independent donors are represented by open circles, triangles, squares or diamonds. Statistical differences between WCS and air were tested using a two-tailed paired parametric t-test (*p<0.05 and **p<0.01). ALI-PBEC were 1x daily exposed to fresh air or WCS from one 3R4F cigarette (University of Kentucky, 2 mg) during differentiation for 14 days, followed by a cessation period of up to 10 days. Basal medium and cells were harvested on Day 14 (24 h after the last exposure), 16, 19 and 23 (n=3 donors/group). **(F-H)** L-lactate **(F)**, and HK2 protein **(G)** and transcript **(H)** levels are shown. Representative western blots, including representative parts of the Ponceau S staining, are shown. Data are presented as mean fold change compared to control (air or WCS Day 14)±s.e.m.. Independent donors are represented by open circles, triangles or squares. Statistical differences between WCS and air after smoking cessation in ALI-PBEC on each day were tested using a two-tailed paired parametric t-test (e.g, WCS Day 14 *versus* air). Comparison of various groups to test the difference between WCS Day 16, 19, 23 and Day 14 in WCS chronic smoking cessation experiments was conducted using one-way ANOVA followed by Sidak's post-hoc test for multiple comparisons, and, in the case of missing values, mixed-effects modeling was performed. Statistical significance is indicated as *p<0.05 compared to control (air or WCS Day 14).

Discussion

In our study, for the first time, we examined the impact of acute WCS and CSE exposure on the molecular mechanisms regulating mitochondrial content and function in multiple PBEC models, ranging from undifferentiated cells that were exposed to CSE in a submerged culture to well-differentiated cultures exposed to WCS in an ALI system. In addition to studying acute effects of exposure, we also evaluated the persistence of these effects following chronic WCS exposure during differentiation and potential recovery upon cessation of WCS exposure.

First and foremost, we observed a potent increase in the abundance of general autophagy proteins in differentiated cultures acutely exposed to WCS, in both basal and luminal cell fractions. Interestingly, these changes were largely absent in PBEC repeatedly exposed to WCS during differentiation. This autophagy response to acute smoke exposure was also observed in undifferentiated PBEC, both in response to acute WCS and CSE exposure. Also, mitophagy-related protein and transcript expression, specifically for those involved in receptor-mediated mitophagy, increased in response to smoke exposure in several of our models. Increases in the expression of proteins involved in receptor-mediated mitophagy were mainly observed in differentiated cultures, persisted after chronic exposure and remained elevated for the duration of the smoke cessation protocol. Analysis of markers of mitochondrial content and mitochondrial dynamics revealed no pronounced changes in response to WCS or CSE in any of our models. We did observe, however, that differentiated PBEC cultures acutely exposed to WCS displayed minor changes in the abundance of proteins involved in mitochondrial biogenesis, as well as a metabolic shift towards a more glycolytic phenotype. These findings are summarized in Table 2, which also shows several differences in the response of our different PBEC cultures to WCS or CSE. This highlights the importance of tailoring the *in vitro* model to the research question with regard to studying the impact of (chemical) exposure-induced mitochondrial abnormalities in the context of respiratory disease.

Table 2. Summary of changes in the molecular regulation of mitochondrial metabolism in four PBEC models of CS exposure. Summary of the protein and transcript expression of regulators involved in mitochondrial metabolism (e.g., biogenesis *versus* mitophagy) analyzed by western blotting and real-time qPCR in four PBEC models of exposure to WCS or CSE. These included (1) differentiated ALI-PBEC acutely-exposed to WCS (including whole-cell lysates and separated basal and luminal fractions), (2) ALI-PBEC chronically-exposed (during differentiation) to WCS followed by smoking cessation, (3) undifferentiated S-PBEC acutely-exposed to WCS, and (4) undifferentiated S-PBEC treated with CSE (submerged). The effect of acute CS exposure in the PBEC models (WCS and CSE, S-PBEC and ALI-PBEC) was assessed by comparison to fresh air or 0% CSE, except in the chronic WCS cessation model, in which we also compared WCS exposure at Day 16, 19, 23 to 24 h post-chronic WCS exposure (WCS Day 14). Arrows indicate the direction of change; one arrow means indicates fold change <2 and two arrows indicates fold change >2 for treatment *versus* control (air, 0 % CSE or WCS Day 14). ‘↓/↑’ indicates a differential response of various markers. ‘=’ indicates no change in response to smoke exposure compared to control. Only significant differences are indicated. ALI-PBEC, undifferentiated PBEC cultured at the air-liquid interface to induce differentiation; CS, cigarette smoke; CSE, CS extract; PBEC, primary bronchial epithelial cells; WCS, whole CS; S-PBEC, PBEC cultured in submerged conditions.

Processes involved in mitochondrial quality control		ALI-PBEC			S-PBEC	
		Acute WCS	Chronic WCS	Chronic WCS cessation	Acute WCS	CSE treatment
Autophagy		↑↑	↑ / ↓	=	↑↑	↑↑
Mitophagy	Receptor mediated	↑	↑	=	=	↑
	Ubiquitin mediated	↓	=	=	=	↓
Mitochondrial biogenesis	PPARGC1 co-activators	↑	↓	=	↑	↓
	PPARGC1 co-activated transcription factors	↑	↓	=	↑	↓
Glycolytic metabolism		↑	↑	↓	↑	=
Mitochondrial dynamics	Fission	=	=	=	↑	=
	Fusion	↑	=	=	↑	=
Mitochondrial content		=	=	=	↑	↑ / ↓

We observed increases in the abundance of both protein and transcript levels of key constituents of autophagy in luminal as well as basal fractions of differentiated cultures as well as in whole-cell lysates of non-differentiated cultures. Collectively, this implies that this is a robust response of different bronchial epithelial cell types to CS constituents and is reflected in both intact as well as damaged epithelium (both of which are present in the airways of COPD patients). These data are in line with previous findings in CS(E)-treated human airway epithelial cells (24, 25, 29, 30, 52), in lung homogenates of (a majority of ex-smoking) COPD patients (24, 53) and in CS-exposed

mice (9, 24, 53). Furthermore, they provide further support for the hypothesis that imbalanced autophagy, and in particular excessive autophagy induction, contributes to the pathogenesis of COPD by resulting in programmed cell death of epithelial cells and subsequent development of pulmonary emphysema (54).

Induction of autophagy likely results from (sub)cellular damage by oxidative components present in CS (54, 55). In line with this notion and with previous studies (25), we did observe modulation of cellular anti-oxidant systems in response to WCS in our models. Although a robust induction of autophagy markers was observed in our acute exposure models, chronic exposure to WCS resulted in a decreased ratio of LC3BII/I in differentiating PBEC, which recovered during smoke cessation. In line with this observation, a recent study showed low amounts of LC3B-positive cells in cultured PBEC from severe COPD patients, possibly associated with a decreased number of club cells (56). As a persistent loss of the club cell marker SCGB1A1 has previously been demonstrated in our chronic WCS model (36), the differential effects of chronic *versus* acute WCS exposure on autophagy markers and recovery upon cessation could potentially be explained by both oxidative stress and aberrant differentiation and/or loss of club cells in response to chronic smoke exposure (36). These speculations on the relationship between autophagy and aberrant epithelial cell differentiation are supported by observations showing that autophagy inhibits ciliated cell differentiation (57) and regulates mucin production by goblet cells in the airway epithelium (58). Although blocking induction of autophagy (e.g. after smoke exposure) may improve epithelial function (30, 59), autophagy may also serve a protective function by enabling adequate restoration of airway epithelial function after an insult (60, 61). Collectively, these studies indicate that CS-induced increases in autophagy contribute to aberrant epithelial differentiation upon smoke exposure.

Mitophagy is a form of targeted autophagy that can contribute to the clearance of damaged mitochondria that have been found following exposure to CS in multiple human and mice airway epithelial cell types in lung tissue as well as in PBEC cultures from COPD patients (25, 26, 62). In our study, we found an increased abundance of proteins involved in receptor-mediated mitophagy following both acute and chronic stimulation with WCS or CSE in different cell populations, which persisted during the cessation period. To the best of our knowledge, only a few studies have investigated the impact of CS on regulation of receptor-mediated mitophagy in airway epithelial cells. These studies reported an increase in receptor-mediated mitophagy proteins in response to smoke exposure both *in vivo* and *in vitro* (30, 59).

Interestingly, it has been shown that cellular hypoxia-related signaling (i.e. hypoxia-inducible factor (HIF1 α)) is activated by smoke exposure in these airway epithelial cell models (63-65). Moreover, it is known that hypoxia activates receptor-mediated mitophagy in various cell types (66-71), as HIF1 α has been recognized as an upstream

regulator of BNIP3(L) (67, 72, 73). Therefore, it can be speculated that CS-induced hypoxia partly contributes to the observed CS-induced elevated receptor-mediated mitophagy. Moreover, indicative of a contribution of CS-induced activation of receptor-mediated mitophagy to COPD pathology, one study reported amelioration of COPD-like features in mice with genetically blocked receptor-mediated mitophagy (59). In contrast to the observed robust changes in receptor-mediated mitophagy in response to CS in our models, changes in mediators of ubiquitin-mediated mitophagy were less pronounced. In general, we observed that PINK1 protein and transcript levels tended to be increased in response to acute CS exposure, whereas PRKN levels decreased. This is in line with the literature, as CS-induced increases in PINK1 levels and decreased PRKN abundance have been described in several *in vitro/vivo* (airway) models (9, 16, 25, 26, 31, 32) and in peripheral lung tissue and bronchial epithelial cells of (ex-smoking) COPD patients (9, 11, 25, 26). However, other studies reported no changes or even increases in the levels of these constituents of ubiquitin-mediated mitophagy in response to CS in various *in vitro* and *in vivo* models of exposure of cells of the airways to CS as well as in lungs of COPD patients (9-11, 16, 26, 62).

In general, whether or not mitophagy serves a protective or detrimental role in CS-induced COPD development remains controversial. Indeed, previous studies have reported that knockdown/knockout of PINK1 or PRKN (9, 25, 31, 74), as well as overexpression of PRKN (25, 26, 74), protected against CSE-induced mitophagy or mitochondrial dysfunction in *in vitro* or *in vivo* models, highlighting the complexity of regulation of mitophagy. Seemingly discrepant findings regarding CS-induced mitophagy in the literature may stem from differences in dose and time of exposure of cells to CS constituents (mild *versus* severe CS stress) or from the dynamic (flux) nature of mitophagy. The fact that, in our study, the induction of receptor-mediated mitophagy was more pronounced than ubiquitin-mediated mitophagy and that *in vivo* models of smoke exposure (or COPD) often describe activation of this PINK1/PRKN pathway (9, 25, 26), may be related to the fact that our *in vitro* models lack the inflammatory cells that are present *in vivo* in smoke-induced COPD. An important consideration is that inflammation is linked to mitochondrial dysfunction (75, 76) and inflammatory mediators may activate the PINK1/PRKN pathway in epithelial cells (77). Further studies focusing on the molecular mechanisms of the pathway-specific regulation of mitophagy in epithelial cell types need to be conducted.

Besides clearance of damaged mitochondria by mitophagy, mitochondrial biogenesis is crucial in maintaining mitochondrial homeostasis. Interestingly, we observed that some proteins involved in mitochondrial biogenesis were increased in response to acute WCS exposure, while both CSE and chronic WCS exposure resulted in a decrease in these molecules. In line with our findings, previous studies also observed differential effects of short-term or long-term CS exposure on mitochondrial biogenesis. For example, whereas short-term CSE treatment of cultured human bronchial epithelial

cells increased transcript abundance of the mitochondrial biogenesis-associated marker PPARGC1A (78), PPARGC1A was non-detectable after long-term CSE exposure (11). Similar findings were also observed in lung tissue from COPD patients at different disease stages, ranging from increased PPARGC1A abundance in mild or ex-smoking COPD patients to decreased abundance in moderate and severe COPD lung tissue (11, 79). Collectively, increased mitochondrial biogenesis in acute WCS models might indicate an adaptive cellular response, whereas decreased mitochondrial biogenesis upon chronic WCS exposure might reflect an inability to compensate for these changes.

We did not find pronounced differences in the abundance of fusion and fission indices after CS exposure in our models. Previous studies have found that short- or long-term CSE exposure can induce changes in proteins regulating mitochondrial dynamics with effects on mitochondrial morphology (9, 62). These effects were found to range from swollen, fragmented organelles to mitochondrial hyperfusion (9, 10, 17, 28, 31, 32, 62, 80), and the variability in CSE preparation (including type of cigarette used, concentration and generation of CSE) may explain the conflicting findings in *in vitro* studies. As we did not assess mitochondrial morphology in our study, no solid conclusions can be drawn about the impact of CS exposure in our models.

mtDNA damage and disturbed mitochondrial metabolism, including impaired respiratory capacity and abundance/activity of subunits of ETC complexes, have been described in multiple *in vitro* or *in vivo* (airway) models in response to CS(E) (3, 6, 9-11, 16, 29). Importantly, several studies showed that CS-induced mitochondrial dysfunction contributes to altered epithelial function (81) as well as development of COPD (3). In our study, we did not observe large changes in mtDNA copy number or the abundance of oxidative phosphorylation complexes. As mtDNA copies vary per cell type, and only selected subunits of various complexes were analyzed, additional studies are required. We cannot exclude the possibility that increased mitochondrial biogenesis may have compensated for potential loss of mitochondria in our models.

In line with prior evidence reporting CS-induced metabolic reprogramming of airway epithelial cells (13, 82), mouse lungs (83) or in COPD (84-87), we observed increased lactate production in our models in response to WCS, which persisted during chronic WCS exposure and cessation. Although we did not assess mitochondrial function by respirometry or complex activity analysis, and therefore cannot decisively conclude about the impact of CS on mitochondrial function, the fact that lactate increases does suggest abnormalities in mitochondrial oxidative metabolism. Moreover, metabolic reprogramming is suggested to be a driver of CS-induced inflammatory lung diseases (88). Furthermore, it has been reported that lactate, here found to be increased after smoke exposure as a result of smoke-induced deregulation of cellular metabolism, directly binds to transmembrane domain of mitochondrial antiviral-signalling protein (MAVS) and thus prevents MAVS aggregation. This is an important step in antiviral

signalling, and it was reported that lactate inhibits type I interferon production, impairs anti-viral responses and enhances viral replication (89). Because it is well established that cigarette smoking increases susceptibility to viral infections (90), which was replicated in various *in vitro* epithelial culture models (including our WCS for rhinovirus infection) (91-93), these data suggest that increased lactate production upon WCS exposure may contribute to CS-induced increases in epithelial susceptibility to viral infections.

To better understand the impact of CS on mitochondrial quality control processes in simple and advanced *in vitro* PBEC models, we included four models that cover a variation in type and duration of CS exposure, epithelial cell types and read-out parameters. Obviously, the different exposure scenarios influence the results because, during WCS (that includes volatiles) exposure, the cells are directly and shortly exposed, whereas via incubating with CSE (only dissolved, aqueous components) in the medium, the contact time with CS components will be longer. Although a similar response in these two exposure models can be explained by the impact of aqueous CS components (present in both CS and CSE), a conflicting response could be due to the continuous exposure of CSE (e.g. receptor-mediated mitophagy) or additional volatiles present in WCS. However, in general, the non-standardized methods of WCS or CSE preparation, e.g. variability in type of cigarette, concentration determination and generation (often in-house developed systems), make it difficult to compare results of different smoke exposure studies.

The strength of our study is the investigation, for the first time, of a comprehensive panel of markers involved in the regulation of mitochondrial metabolism in various relevant CS exposure *in vitro* primary human airway epithelial cell models. The novelty of our findings is multifaceted (Fig. 8). Firstly, the use of human PBEC from multiple donors (Table 1) to assess CS-induced changes in mitochondrial homeostasis is a strength as many studies in this area use immortalized or tumor lines or rodent exposure studies. Secondly, we exposed fully differentiated cultures of PBEC directly and shortly to WCS (gas and particulate phase, short- and long-lived CS constituents) in an ALI system, which adequately mimics the real-life exposure. Reports using this model and exposure system are very limited (likely due to the complexity of the culture- and exposure system), and most studies using primary cells employed undifferentiated submerged cultures that were exposed to CSE rather than WCS. Moreover, the combination of these various models (CSE and WCS, undifferentiated S-PBEC and differentiated ALI-PBEC) adds important novelty and insight to the field. Third, we analyzed changes in the regulation of mitochondrial homeostasis in both luminal and basal cell fractions of the differentiated pseudostratified epithelium, which has not previously been reported. Fourth, whereas studies usually examined a selection of markers related to one or two mitochondrial processes, we here investigated for the first time a comprehensive panel of markers involved in all important processes associated with the regulation of

mitochondrial metabolism in our *in vitro* CS exposure models of PBEC. Lastly, studying this subset of molecules involved in mitochondrial metabolism in four relevant *in vitro* CS exposure models of PBEC allows important comparisons not only between our four different models, but also with data present in the literature. The relevance of our findings is enhanced by using PBEC cultured in both (un)differentiated submerged and ALI conditions and comparison of different type and duration of CS exposure.

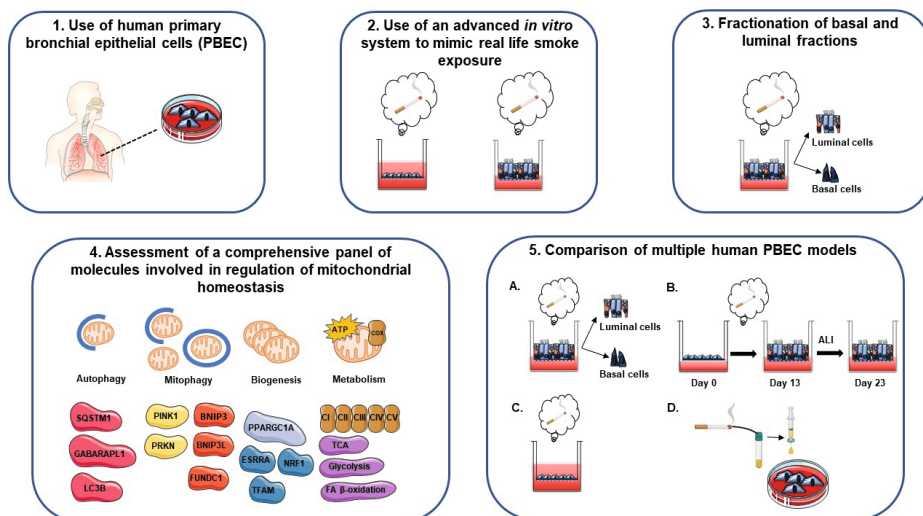


Figure 8. Overview of experimental approach. Schematic representation of the novelty and strengths of the study. (1) Use of human primary bronchial epithelial cells (PBEC): human PBEC (differentiated or undifferentiated) from multiple donors (non-chronic obstructive pulmonary disease (COPD) patients) were used to assess cigarette smoke (CS)-induced changes in mitochondrial homeostasis. (2) Use of an advanced *in vitro* system to mimic real-life smoke exposure: fully differentiated cultures of PBEC were directly and shortly exposed to whole CS (WCS) in an air-liquid interface (ALI) system. (3) Fractionation of basal and luminal fractions: changes in the regulation of mitochondrial homeostasis in basal and luminal fractions of WCS-exposed differentiated PBEC were investigated. (4) Assessment of a comprehensive panel of molecules involved in regulation of mitochondrial homeostasis: a comprehensive panel of markers involved in all important processes associated with the regulation of mitochondrial metabolism was investigated in our *in vitro* CS exposure models of PBEC. (5) Comparison of multiple human PBEC models (A-D): studying a subset of molecules involved in mitochondrial metabolism in four relevant *in vitro* CS exposure models of PBEC allows important comparisons not only between our four different models, but also with data present in literature.

The differentiated epithelial cultures used in the present study mimics an intact pseudostratified epithelium relevant to study responses to inhalation toxicants of an intact epithelial layer, while the undifferentiated PBEC model represents a basal cell-like structure relevant to study responses of a damaged, partly denuded epithelial layer. Moreover, chronic WCS exposure of a differentiating epithelial layer followed by cessation of exposure, provided the opportunity to investigate repair. Strikingly, we

observed abnormalities at the level of mitochondrial quality control mechanisms in all models, suggestive of a role for CS-induced mitochondrial dysfunction in different areas of the bronchial epithelium relevant for COPD. The different responses that we observed highlight the importance of making considered choices for (un)differentiated cell models, type of CS exposure and duration of smoking in future respiratory inhalation (toxicology) studies tailored to the research question.

Inevitably, our study obviously also has several limitations. First, a limited number of donors was investigated. Second, although our short-term CS exposure models may mimic changes in airway epithelial cells from chronic smokers, including autophagy, differences between molecular changes in response to acute *versus* chronic smoke exposure or with changes in lung homogenates from COPD patients were observed, as illustrated by the findings on mitochondrial biogenesis or ubiquitin-mediated mitophagy. Furthermore, as mitochondrial biogenesis, mitophagy, and mitochondrial dynamics are dynamic processes, the fact that our analyses only represent a snapshot of these processes is a limitation. Because our current research aimed to compare CS-induced alterations in the molecular mechanisms underlying mitochondrial function between four different models, we did not focus on their contribution to CS-induced changes in epithelial function related to, for instance, repair, differentiation and remodelling, as well as, for example, epithelial barrier function, antimicrobial responses, cilia beating and mucus production. However, the impact of acute and chronic CS exposure on the abovementioned aspects of epithelial function has previously been reported by us in the models used in the present study (36, 41, 93-96) and by other research groups (97-101). In addition, direct associations between mitochondrial dysfunction, deregulated autophagy and lactate production and epithelial function have previously been reported (3, 30, 57-59, 81, 102). Whereas we only separated basal and luminal cells in our differentiated ALI-PBEC model that includes several epithelial cell types (36), additional research should evaluate the impact of CS exposure in individual luminal cell types, as well as in alveolar cells, as those are also markedly affected in COPD. Furthermore, further research is needed to delineate the effects of CS exposure on mitochondrial quality control processes, using advanced state-of-the-art *in vitro* models and more realistic WCS exposure methods, including varying puff-topography regimes reflecting human smoking behavior.

Our model is limited to (differentiated) epithelial cells, and did not include other cell types such as immune cells. However, our observations are supported by findings in lung tissue of COPD patients showing mitochondrial alterations and increased autophagy. Moreover, other studies reported similar molecular changes of mitochondrial metabolism in *in vivo* smoke exposure models and have demonstrated that these are not only associated with, but also causally related to, functional and structural abnormalities in the bronchial and alveolar compartment reminiscent of COPD lung/airway pathology (3, 9, 24). Future studies using more complex models

such as co-culture (103), lung on chips (104) or *ex vivo* precision-cut lung slices (105) to investigate the individual molecular changes at global, single-cell and tissue levels, have the potential to overcome some of these limitations. We have previously reported the feasibility of such an approach by showing that macrophages support epithelial repair in our WCS exposure model using co-cultures of epithelial cells and monocyte-derived macrophages (106). Moreover, although our study has a targeted approach, future studies could focus on a more 'global' multi-omics approach to investigate the impact of smoke exposure on mitochondrial metabolism. Other studies have used such approaches; for example, metabolomics has been used to elucidate the role of smoke-induced metabolic reprogramming in the pathogenesis of lung diseases (88), lipidomics was used by us to show that polyunsaturated fatty acid metabolism is affected by exposure of ALI-PBEC to WCS and altered in sputum from COPD patients compared to controls (107), and transcriptomics analysis of CS-exposed ALI-cultures reported critical molecular pathways involved in aberrant tissue remodelling and lung disease-associated pathways (108). Interestingly, a multi-omics approach has also been applied in repeated CS-exposed co-cultures of bronchial tissue, revealing alterations in molecular pathways involved in airway diseases (109). However, these studies did not compare the different culture or exposure models used in the present study.

In conclusion, in this study, differences were observed in the regulation of mitochondrial metabolic processes in the four investigated models reflecting damaged, intact, differentiating or repairing airway epithelium, and multiple CS exposure regimes. The results highlight the robust model-independent impact of CS exposure on the abundance of key molecules involved in autophagy and receptor-mediated mitophagy. These alterations were, at least in part although less pronounced, recapitulated after chronic exposure of differentiating epithelial cells to CS. Differences observed in the regulation of mitochondrial metabolic processes, such as mitochondrial biogenesis, in the investigated models, reflecting various cell types of the epithelium and CS exposure regimes, supports the importance of tailoring the experimental model to the research question.

Acknowledgements

The authors would like to thank Mieke Dentener and Nico Kloosterboer of the Primary Lung Culture Facility (PLUC; Maastricht University Medical Center+) for providing donor cells, advice, and protocols.

Competing interests

The authors have declared that no competing interests consist.

Funding

This research is supported by the Netherlands Food and Consumer Product Safety Authority (NVWA) and by a fellowship from the China Scholarship Council.

Data availability

N/A

Authors' contribution

Conceptualization and design: Christy B.M. Tulen, Ying Wang, Pieter S. Hiemstra, Alexander H.V. Remels

Methodology: Dennis K. Ninaber, Niki L. Reynaert

Formal analysis: Christy B.M. Tulen, Ying Wang, Daan Beentjes, Phyllis J.J. Jessen

Investigation: Christy B.M. Tulen, Ying Wang, Daan Beentjes, Phyllis J.J. Jessen

Data curation: Christy B.M. Tulen, Ying Wang, Daan Beentjes, Phyllis J.J. Jessen

Writing – original draft: Christy B.M. Tulen, Ying Wang

Writing – review & editing: Frederik-Jan van Schooten, Antoon Opperhuizen, Pieter S. Hiemstra, Alexander H.V. Remels

Visualization: Christy B.M. Tulen, Ying Wang,

Supervision: Pieter S. Hiemstra, Alexander H.V. Remels

References

1. Celli BR, Wedzicha JA. Update on Clinical Aspects of Chronic Obstructive Pulmonary Disease. *N Engl J Med*. 2019;381(13):1257-66.
2. WHO. The top 10 causes of death: World Health Organization; 2020 [Available from: <https://www.who.int/news-room/fact-sheets/detail/the-top-10-causes-of-death>.]
3. Cloonan SM, Glass K, Laucho-Contreras ME, Bhashyam AR, Cervo M, Pabon MA, et al. Mitochondrial iron chelation ameliorates cigarette smoke-induced bronchitis and emphysema in mice. *Nat Med*. 2016;22(2):163-74.
4. Cloonan SM, Choi AM. Mitochondria in lung disease. *J Clin Invest*. 2016;126(3):809-20.
5. Prakash YS, Pabelick CM, Sieck GC. Mitochondrial Dysfunction in Airway Disease. *Chest*. 2017;152(3):618-26.
6. Aghapour M, Remels AHV, Pouwels SD, Bruder D, Hiemstra PS, Cloonan SM, et al. Mitochondria: at the crossroads of regulating lung epithelial cell function in chronic obstructive pulmonary disease. *Am J Physiol Lung Cell Mol Physiol*. 2020;318(1):L149-l64.
7. Pan S, Conaway S, Jr., Deshpande DA. Mitochondrial regulation of airway smooth muscle functions in health and pulmonary diseases. *Arch Biochem Biophys*. 2019;663:109-19.
8. Hiemstra PS, van der Does AM. Reprogramming of cellular metabolism: driver for airway remodelling in COPD? *Eur Respir J*. 2017;50(5).
9. Mizumura K, Cloonan SM, Nakahira K, Bhashyam AR, Cervo M, Kitada T, et al. Mitophagy-dependent necroptosis contributes to the pathogenesis of COPD. *J Clin Invest*. 2014;124(9):3987-4003.
10. Sundar IK, Maremanda KP, Rahman I. Mitochondrial dysfunction is associated with Miro1 reduction in lung epithelial cells by cigarette smoke. *Toxicol Lett*. 2019;317:92-101.
11. Hoffmann RF, Zarrintan S, Brandenburg SM, Kol A, de Bruin HG, Jafari S, et al. Prolonged cigarette smoke exposure alters mitochondrial structure and function in airway epithelial cells. *Respir Res*. 2013;14:97.
12. Malinska D, Szymanski J, Patalas-Krawczyk P, Michalska B, Wojtala A, Prill M, et al. Assessment of mitochondrial function following short- and long-term exposure of human bronchial epithelial cells to total particulate matter from a candidate modified-risk tobacco product and reference cigarettes. *Food Chem Toxicol*. 2018;115:1-12.
13. Agarwal AR, Yin F, Cadenas E. Short-term cigarette smoke exposure leads to metabolic alterations in lung alveolar cells. *Am J Respir Cell Mol Biol*. 2014;51(2):284-93.
14. Valdivieso Á G, Dugour AV, Sotomayor V, Clauzure M, Figueroa JM, Santa-Coloma TA. N-acetyl cysteine reverts the proinflammatory state induced by cigarette smoke extract in lung Calu-3 cells. *Redox Biol*. 2018;16:294-302.
15. van der Toorn M, Rezayat D, Kauffman HF, Bakker SJ, Gans RO, Koëter GH, et al. Lipid-soluble components in cigarette smoke induce mitochondrial production of reactive oxygen species in lung epithelial cells. *Am J Physiol Lung Cell Mol Physiol*. 2009;297(1):L109-14.
16. Wu K, Luan G, Xu Y, Shen S, Qian S, Zhu Z, et al. Cigarette smoke extract increases mitochondrial membrane permeability through activation of adenine nucleotide translocator (ANT) in lung epithelial cells. *Biochem Biophys Res Commun*. 2020;525(3):733-9.
17. Hara H, Araya J, Ito S, Kobayashi K, Takasaka N, Yoshii Y, et al. Mitochondrial fragmentation in cigarette smoke-induced bronchial epithelial cell senescence. *Am J Physiol Lung Cell Mol Physiol*. 2013;305(10):L737-46.

18. Jornayvaz FR, Shulman GI. Regulation of mitochondrial biogenesis. *Essays Biochem.* 2010;47:69-84.
19. Lin J, Handschin C, Spiegelman BM. Metabolic control through the PGC-1 family of transcription coactivators. *Cell Metab.* 2005;1(6):361-70.
20. Scarpulla RC. Metabolic control of mitochondrial biogenesis through the PGC-1 family regulatory network. *Biochim Biophys Acta.* 2011;1813(7):1269-78.
21. Gomes LC, Scorrano L. Mitochondrial morphology in mitophagy and macroautophagy. *Biochim Biophys Acta.* 2013;1833(1):205-12.
22. Fritsch LE, Moore ME, Sarraf SA, Pickrell AM. Ubiquitin and Receptor-Dependent Mitophagy Pathways and Their Implication in Neurodegeneration. *J Mol Biol.* 2020;432(8):2510-24.
23. Hikichi M, Mizumura K, Maruoka S, Gon Y. Pathogenesis of chronic obstructive pulmonary disease (COPD) induced by cigarette smoke. *J Thorac Dis.* 2019;11(Suppl 17):S2129-S40.
24. Chen ZH, Kim HP, Sciurba FC, Lee SJ, Feghali-Bostwick C, Stolz DB, et al. Egr-1 regulates autophagy in cigarette smoke-induced chronic obstructive pulmonary disease. *PLoS One.* 2008;3(10):e3316.
25. Ito S, Araya J, Kurita Y, Kobayashi K, Takasaka N, Yoshida M, et al. PARK2-mediated mitophagy is involved in regulation of HBEC senescence in COPD pathogenesis. *Autophagy.* 2015;11(3):547-59.
26. Ahmad T, Sundar IK, Lerner CA, Gerloff J, Tormos AM, Yao H, et al. Impaired mitophagy leads to cigarette smoke stress-induced cellular senescence: implications for chronic obstructive pulmonary disease. *Faseb j.* 2015;29(7):2912-29.
27. Mizumura K, Justice MJ, Schweitzer KS, Krishnan S, Bronova I, Berdyshev EV, et al. Sphingolipid regulation of lung epithelial cell mitophagy and necroptosis during cigarette smoke exposure. *Faseb j.* 2018;32(4):1880-90.
28. Song C, Luo B, Gong L. Resveratrol reduces the apoptosis induced by cigarette smoke extract by upregulating MFN2. *PLoS One.* 2017;12(4):e0175009.
29. Park EJ, Park YJ, Lee SJ, Lee K, Yoon C. Whole cigarette smoke condensates induce ferroptosis in human bronchial epithelial cells. *Toxicol Lett.* 2019;303:55-66.
30. Zhang M, Shi R, Zhang Y, Shan H, Zhang Q, Yang X, et al. Nix/BNIP3L-dependent mitophagy accounts for airway epithelial cell injury induced by cigarette smoke. *J Cell Physiol.* 2019;234(8):14210-20.
31. Kyung SY, Kim YJ, Son ES, Jeong SH, Park JW. The Phosphodiesterase 4 Inhibitor Roflumilast Protects against Cigarette Smoke Extract-Induced Mitophagy-Dependent Cell Death in Epithelial Cells. *Tuberc Respir Dis.* 2018;81(2):138-47.
32. Son ES, Kim SH, Ryter SW, Yeo EJ, Kyung SY, Kim YJ, et al. Quercetin protects against cigarette smoke extract-induced apoptosis in epithelial cells by inhibiting mitophagy. *Toxicol In Vitro.* 2018;48:170-8.
33. Hiemstra PS, Grootaers G, van der Does AM, Krul CAM, Kooter IM. Human lung epithelial cell cultures for analysis of inhaled toxicants: Lessons learned and future directions. *Toxicol In Vitro.* 2018;47:137-46.
34. Mertens TC, Karmouty-Quintana H, Taube C, Hiemstra PS. Use of airway epithelial cell culture to unravel the pathogenesis and study treatment in obstructive airway diseases. *Pulm Pharmacol Ther.* 2017;45:101-13.
35. Boei J, Vermeulen S, Klein B, Hiemstra PS, Verhoosel RM, Jennen DGJ, et al. Xenobiotic metabolism in differentiated human bronchial epithelial cells. *Arch Toxicol.* 2017;91(5):2093-105.

36. Amatngalim GD, Schrumpf JA, Dishchekenian F, Mertens TCJ, Ninaber DK, van der Linden AC, et al. Aberrant epithelial differentiation by cigarette smoke dysregulates respiratory host defence. *Eur Respir J*. 2018;51(4):1701009.
37. Wang Y, Xu J, Meng Y, Adcock IM, Yao X. Role of inflammatory cells in airway remodeling in COPD. *Int J Chron Obstruct Pulmon Dis*. 2018;13:3341-8.
38. Rutgers SR, Postma DS, ten Hacken NH, Kauffman HF, van Der Mark TW, Koeter GH, et al. Ongoing airway inflammation in patients with COPD who Do not currently smoke. *Chest*. 2000;117(5 Suppl 1):262s.
39. Hodge S, Hodge G, Holmes M, Reynolds PN. Increased airway epithelial and T-cell apoptosis in COPD remains despite smoking cessation. *European Respiratory Journal*. 2005;25(3):447-54.
40. Schrumpf JA, Ninaber DK, van der Does AM, Hiemstra PS. TGF- β 1 Impairs Vitamin D-Induced and Constitutive Airway Epithelial Host Defense Mechanisms. *J Innate Immun*. 2020;12(1):74-89.
41. Amatngalim GD, van Wijck Y, de Mooij-Eijk Y, Verhoosel RM, Harder J, Lekkerkerker AN, et al. Basal cells contribute to innate immunity of the airway epithelium through production of the antimicrobial protein RNase 7. *J Immunol*. 2015;194(7):3340-50.
42. van Wetering S, Zuyderduyn S, Ninaber DK, van Sterkenburg MAJA, Rabe KF, Hiemstra PS. Epithelial differentiation is a determinant in the production of eotaxin-2 and -3 by bronchial epithelial cells in response to IL-4 and IL-13. *Mol Immunol*. 2007;44(5):803-11.
43. van Wetering S, van der Linden AC, van Sterkenburg MA, de Boer WI, Kuijpers AL, Schalkwijk J, et al. Regulation of SLPI and elafin release from bronchial epithelial cells by neutrophil defensins. *Am J Physiol Lung Cell Mol Physiol*. 2000;278(1):L51-8.
44. Carp H, Janoff A. Possible mechanisms of emphysema in smokers. In vitro suppression of serum elastase-inhibitory capacity by fresh cigarette smoke and its prevention by antioxidants. *Am Rev Respir Dis*. 1978;118(3):617-21.
45. Wang Y, Ninaber DK, van Schadewijk A, Hiemstra PS. Tiotropium and Fluticasone Inhibit Rhinovirus-Induced Mucin Production via Multiple Mechanisms in Differentiated Airway Epithelial Cells. *Front Cell Infect Microbiol*. 2020;10:278.
46. Amatngalim GD, Schrumpf JA, Dishchekenian F, Mertens TCJ, Ninaber DK, van der Linden AC, et al. Aberrant epithelial differentiation by cigarette smoke dysregulates respiratory host defence. *Eur Respir J*. 2018;51(4).
47. Shepherd D, Garland P. The kinetic properties of citrate synthase from rat liver mitochondria. *Biochem J*. 1969;114(3):597-610.
48. Bergmeyer H, Gawehn K, Grassl M. 3-Hydroxyacyl-CoA dehydrogenase. Methods of enzymatic analysis. 1974;1:474.
49. Ling K, Paetkau V, Marcus F, Lardy HA. [77a] Phosphofructokinase: I. Skeletal Muscle. *Methods in enzymology*. 9: Elsevier; 1966. p. 425-9.
50. Yun HR, Jo YH, Kim J, Shin Y, Kim SS, Choi TG. Roles of Autophagy in Oxidative Stress. *Int J Mol Sci*. 2020;21(9):3289.
51. Zarcone MC, Duistermaat E, van Schadewijk A, Jedynska A, Hiemstra PS, Kooter IM. Cellular response of mucociliary differentiated primary bronchial epithelial cells to diesel exhaust. *Am J Physiol Lung Cell Mol Physiol*. 2016;311(1):L111-23.
52. Xu L, Li X, Wang H, Xie F, Liu H, Xie J. Cigarette smoke triggers inflammation mediated by autophagy in BEAS-2B cells. *Ecotoxicol Environ Saf*. 2019;184:109617.

53. Chen ZH, Lam HC, Jin Y, Kim HP, Cao J, Lee SJ, et al. Autophagy protein microtubule-associated protein 1 light chain-3B (LC3B) activates extrinsic apoptosis during cigarette smoke-induced emphysema. *Proc Natl Acad Sci U S A*. 2010;107(44):18880-5.
54. Ornatowski W, Lu Q, Yegambaram M, Garcia AE, Zemskov EA, Maltepe E, et al. Complex interplay between autophagy and oxidative stress in the development of pulmonary disease. *Redox Biol*. 2020;36:101679.
55. Yun HR, Jo YH, Kim J, Shin Y, Kim SS, Choi TG. Roles of Autophagy in Oxidative Stress. *Int J Mol Sci*. 2020;21(9).
56. Malvin NP, Kern JT, Liu T-C, Brody SL, Stappenbeck TS. Autophagy proteins are required for club cell structure and function in airways. *Am J Physiol Lung Cell Mol Physiol*. 2019;317(2):L259-L70.
57. Li K, Li M, Li W, Yu H, Sun X, Zhang Q, et al. Airway epithelial regeneration requires autophagy and glucose metabolism. *Cell Death Dis*. 2019;10(12):875.
58. Zhou JS, Zhao Y, Zhou HB, Wang Y, Wu YF, Li ZY, et al. Autophagy plays an essential role in cigarette smoke-induced expression of MUC5AC in airway epithelium. *Am J Physiol Lung Cell Mol Physiol*. 2016;310(11):L1042-52.
59. Wen W, Yu G, Liu W, Gu L, Chu J, Zhou X, et al. Silencing FUNDC1 alleviates chronic obstructive pulmonary disease by inhibiting mitochondrial autophagy and bronchial epithelium cell apoptosis under hypoxic environment. *J Cell Biochem*. 2019;120(10):17602-15.
60. Pampliega O, Cuervo AM. Autophagy and primary cilia: dual interplay. *Curr Opin Cell Biol*. 2016;39:1-7.
61. Li ZY, Wu YF, Xu XC, Zhou JS, Wang Y, Shen HH, et al. Autophagy as a double-edged sword in pulmonary epithelial injury: a review and perspective. *Am J Physiol Lung Cell Mol Physiol*. 2017;313(2):L207-117.
62. Ballweg K, Mutze K, Königshoff M, Eickelberg O, Meiners S. Cigarette smoke extract affects mitochondrial function in alveolar epithelial cells. *Am J Physiol Lung Cell Mol Physiol*. 2014;307(11):L895-907.
63. Daijo H, Hoshino Y, Kai S, Suzuki K, Nishi K, Matsuo Y, et al. Cigarette smoke reversibly activates hypoxia-inducible factor 1 in a reactive oxygen species-dependent manner. *Scientific reports*. 2016;6:34424-.
64. Zhang Q, Tang X, Zhang Z-F, Velikina R, Shi S, Le AD. Nicotine induces hypoxia-inducible factor-1 α expression in human lung cancer cells via nicotinic acetylcholine receptor-mediated signaling pathways. *Clin Cancer Res*. 2007;13(16):4686-94.
65. Yasuo M, Mizuno S, Kraskauskas D, Bogaard HJ, Natarajan R, Cool CD, et al. Hypoxia inducible factor-1 α in human emphysema lung tissue. *Eur Respir J*. 2011;37(4):775-83.
66. Ishihara M, Urushido M, Hamada K, Matsumoto T, Shimamura Y, Ogata K, et al. Sestrin-2 and BNIP3 regulate autophagy and mitophagy in renal tubular cells in acute kidney injury. *Am J Physiol Renal Physiol*. 2013;305(4):F495-509.
67. Bellot G, Garcia-Medina R, Gounon P, Chiche J, Roux D, Pouyssegur J, et al. Hypoxia-induced autophagy is mediated through hypoxia-inducible factor induction of BNIP3 and BNIP3L via their BH3 domains. *Mol Cell Biol*. 2009;29(10):2570-81.
68. Wu W, Li W, Chen H, Jiang L, Zhu R, Feng D. FUNDC1 is a novel mitochondrial-associated-membrane (MAM) protein required for hypoxia-induced mitochondrial fission and mitophagy. *Autophagy*. 2016;12(9):1675-6.

69. Wang L, Wang P, Dong H, Wang S, Chu H, Yan W, et al. Ulk1/FUNDC1 Prevents Nerve Cells from Hypoxia-Induced Apoptosis by Promoting Cell Autophagy. *Neurochem Res.* 2018;43(8):1539-48.
70. Lv M, Wang C, Li F, Peng J, Wen B, Gong Q, et al. Structural insights into the recognition of phosphorylated FUNDC1 by LC3B in mitophagy. *Protein Cell.* 2017;8(1):25-38.
71. Lee S-J, Kim H-P, Jin Y, Choi AMK, Ryter SW. Beclin 1 deficiency is associated with increased hypoxia-induced angiogenesis. *Autophagy.* 2011;7(8):829-39.
72. Allen GF, Toth R, James J, Ganley IG. Loss of iron triggers PINK1/Parkin-independent mitophagy. *EMBO reports.* 2013;14(12):1127-35.
73. Wang X, Yang H, Yanagisawa D, Bellier J-P, Morino K, Zhao S, et al. Mitochondrial ferritin affects mitochondria by stabilizing HIF-1 α in retinal pigment epithelium: implications for the pathophysiology of age-related macular degeneration. *Neurobiol Aging.* 2016;47:168-79.
74. Araya J, Tsubouchi K, Sato N, Ito S, Minagawa S, Hara H, et al. PRKN-regulated mitophagy and cellular senescence during COPD pathogenesis. *Autophagy.* 2019;15(3):510-26.
75. López-Armada MJ, Riveiro-Naveira RR, Vaamonde-García C, Valcárcel-Ares MN. Mitochondrial dysfunction and the inflammatory response. *Mitochondrion.* 2013;13(2):106-18.
76. Kampf C, Relova AJ, Sandler S, Roomans GM. Effects of TNF- α , IFN- γ and IL- β on normal human bronchial epithelial cells. *Eur Respir J.* 1999;14(1):84-91.
77. Liu Y, Li L, Pan N, Gu J, Qiu Z, Cao G, et al. TNF- α released from retinal Müller cells aggravates retinal pigment epithelium cell apoptosis by upregulating mitophagy during diabetic retinopathy. *Biochem Biophys Res Commun.* 2021;561:143-50.
78. Vanella L, Li Volti G, Distefano A, Raffaele M, Zingales V, Avola R, et al. A new antioxidant formulation reduces the apoptotic and damaging effect of cigarette smoke extract on human bronchial epithelial cells. *Eur Rev Med Pharmacol Sci.* 2017;21(23):5478-84.
79. Li J, Dai A, Hu R, Zhu L, Tan S. Positive correlation between PPARG γ /PGC-1 α and gamma-GCS in lungs of rats and patients with chronic obstructive pulmonary disease. *Acta Biochim Biophys Sin.* 2010;42(9):603-14.
80. Aravamudan B, Kiel A, Freeman M, Delmotte P, Thompson M, Vassallo R, et al. Cigarette smoke-induced mitochondrial fragmentation and dysfunction in human airway smooth muscle. *Am J Physiol Lung Cell Mol Physiol.* 2014;306(9):L840-54.
81. Yang D, Xu D, Wang T, Yuan Z, Liu L, Shen Y, et al. Mitoquinone ameliorates cigarette smoke-induced airway inflammation and mucus hypersecretion in mice. *Int Immunopharmacol.* 2021;90:107149.
82. Solanki HS, Babu N, Jain AP, Bhat MY, Puttamalles V, Advani J, et al. Cigarette smoke induces mitochondrial metabolic reprogramming in lung cells. *Mitochondrion.* 2018;40:58-70.
83. Agarwal AR, Zhao L, Sancheti H, Sundar IK, Rahman I, Cadenas E. Short-term cigarette smoke exposure induces reversible changes in energy metabolism and cellular redox status independent of inflammatory responses in mouse lungs. *Am J Physiol Lung Cell Mol Physiol.* 2012;303(10):L889-98.
84. Tu C, Mammen MJ, Li J, Shen X, Jiang X, Hu Q, et al. Large-scale, ion-current-based proteomics investigation of bronchoalveolar lavage fluid in chronic obstructive pulmonary disease patients. *J Proteome Res.* 2014;13(2):627-39.
85. Kao CC, Hsu JW, Bandi V, Hanania NA, Kheradmand F, Jahoor F. Glucose and pyruvate metabolism in severe chronic obstructive pulmonary disease. *J Appl Physiol.* 2012;112(1):42-7.

86. Pastor MD, Nogal A, Molina-Pinelo S, Meléndez R, Salinas A, González De la Peña M, et al. Identification of proteomic signatures associated with lung cancer and COPD. *J Proteomics*. 2013;89:227-37.
87. Agarwal AR, Kadam S, Brahme A, Agrawal M, Apte K, Narke G, et al. Systemic Immuno-metabolic alterations in chronic obstructive pulmonary disease (COPD). *Respir Res*. 2019;20(1):171.
88. Li L, Yang DC, Chen C-H. Metabolic reprogramming: A driver of cigarette smoke-induced inflammatory lung diseases. *Free Radic Biol Med*. 2021;163:392-401.
89. Zhang W, Wang G, Xu ZG, Tu H, Hu F, Dai J, et al. Lactate Is a Natural Suppressor of RLR Signaling by Targeting MAVS. *Cell*. 2019;178(1):176-89.e15.
90. Jiang C, Chen Q, Xie M. Smoking increases the risk of infectious diseases: A narrative review. *Tob Induc Dis*. 2020;18:60.
91. Duffney PF, McCarthy CE, Nogales A, Thatcher TH, Martinez-Sobrido L, Phipps RP, et al. Cigarette smoke dampens antiviral signaling in small airway epithelial cells by disrupting TLR3 cleavage. *Am J Physiol Lung Cell Mol Physiol*. 2018;314(3):L505-113.
92. Eddleston J, Lee RU, Doerner AM, Herschbach J, Zuraw BL. Cigarette smoke decreases innate responses of epithelial cells to rhinovirus infection. *Am J Respir Cell Mol Biol*. 2011;44(1):118-26.
93. Wang Y, Romeo PP, Nikkels J, Ninaber DK, Schrumpf JA, Van Der Does AM, et al. Effect of short-time smoking cessation on rhinovirus-induced innate immune responses in an airway epithelial culture model. *ERJ Open Research*. 2019;5(suppl 2):PP118.
94. Amatngalim GD, Broekman W, Daniel NM, van der Vlugt LE, van Schadewijk A, Taube C, et al. Cigarette smoke modulates repair and innate immunity following injury to airway epithelial cells. *PloS one*. 2016;11(11):e0166255.
95. Amatngalim GD, Schrumpf JA, Henic A, Dronkers E, Verhoosel RM, Ordonez SR, et al. Antibacterial defense of human airway epithelial cells from chronic obstructive pulmonary disease patients induced by acute exposure to nontypeable *Haemophilus influenzae*: modulation by cigarette smoke. *Journal of innate immunity*. 2017;9(4):359-74.
96. Luppi F, Aarbiou J, van Wetering S, Rahman I, de Boer WI, Rabe KF, et al. Effects of cigarette smoke condensate on proliferation and wound closure of bronchial epithelial cells in vitro: role of glutathione. *Respir Res*. 2005;6(1):140.
97. Heijink IH, Brandenburg SM, Postma DS, van Oosterhout AJ. Cigarette smoke impairs airway epithelial barrier function and cell-cell contact recovery. *European Respiratory Journal*. 2012;39(2):419-28.
98. Tatsuta M, Kan-o K, Ishii Y, Yamamoto N, Ogawa T, Fukuyama S, et al. Effects of cigarette smoke on barrier function and tight junction proteins in the bronchial epithelium: protective role of cathelicidin LL-37. *Respir Res*. 2019;20(1):251.
99. Cao X, Wang Y, Xiong R, Muskhelishvili L, Davis K, Richter PA, et al. Cigarette whole smoke solutions disturb mucin homeostasis in a human in vitro airway tissue model. *Toxicology*. 2018;409:119-28.
100. Gindele JA, Kiechle T, Benediktus K, Birk G, Brendel M, Heinemann F, et al. Intermittent exposure to whole cigarette smoke alters the differentiation of primary small airway epithelial cells in the air-liquid interface culture. *Sci Rep*. 2020;10(1):6257.
101. Aghapour M, Raei P, Moghaddam SJ, Hiemstra PS, Heijink IH. Airway Epithelial Barrier Dysfunction in Chronic Obstructive Pulmonary Disease: Role of Cigarette Smoke Exposure. *Am J Respir Cell Mol Biol*. 2018;58(2):157-69.

102. Fujita Y, Araya J, Ito S, Kobayashi K, Kosaka N, Yoshioka Y, et al. Suppression of autophagy by extracellular vesicles promotes myofibroblast differentiation in COPD pathogenesis. *J Extracell Vesicles*. 2015;4:28388.
103. Iskandar AR, Xiang Y, Frentzel S, Talikka M, Leroy P, Kuehn D, et al. Impact Assessment of Cigarette Smoke Exposure on Organotypic Bronchial Epithelial Tissue Cultures: A Comparison of Mono-Culture and Coculture Model Containing Fibroblasts. *Toxicol Sci*. 2015;147(1):207-21.
104. Bennet TJ, Randhawa A, Hua J, Cheung KC. Airway-On-A-Chip: Designs and Applications for Lung Repair and Disease. *Cells*. 2021;10(7):1602.
105. Donovan C, Seow HJ, Bourke JE, Vlahos R. Influenza A virus infection and cigarette smoke impair bronchodilator responsiveness to β -adrenoceptor agonists in mouse lung. *Clin Sci (Lond)*. 2016;130(10):829-37.
106. van Riet S, van Schadewijk A, de Vos S, Vandeghinste N, Rottier RJ, Stolk J, et al. Modulation of Airway Epithelial Innate Immunity and Wound Repair by M(GM-CSF) and M(M-CSF) Macrophages. *J Innate Immun*. 2020;12(5):410-21.
107. van der Does AM, Heijink M, Mayboroda OA, Persson LJ, Aanerud M, Bakke P, et al. Dynamic differences in dietary polyunsaturated fatty acid metabolism in sputum of COPD patients and controls. *Biochim Biophys Acta Mol Cell Biol Lipids*. 2019;1864(3):224-33.
108. Xiong R, Wu Y, Wu Q, Muskhelishvili L, Davis K, Tripathi P, et al. Integration of transcriptome analysis with pathophysiological endpoints to evaluate cigarette smoke toxicity in an in vitro human airway tissue model. *Arch Toxicol*. 2021;95(5):1739-61.
109. Ishikawa S, Matsumura K, Kitamura N, Takanami Y, Ito S. Multi-omics analysis: Repeated exposure of a 3D bronchial tissue culture to whole-cigarette smoke. *Toxicol In Vitro*. 2019;54:251-62.

Supplementary information

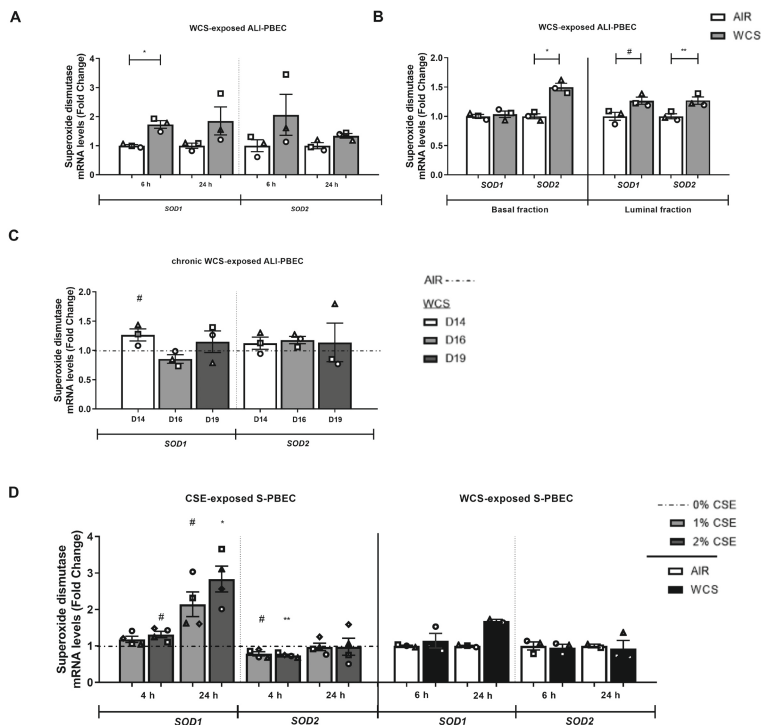


Fig. S1. Increase in expression of genes involved in anti-oxidant response after CS exposure in both ALI- and S-PBEC. After 2-weeks of differentiation, ALI-PBEC were exposed to fresh air or WCS from one 3R4F cigarette (University of Kentucky, 2 mg) and whole-cell lysates were harvested after 6 h and 24 h, and the basal and luminal fractions were harvested only at 6 h post-exposure (n=3 donors/group). Gene expression of *SOD1* and *SOD2* in whole-cell lysates of ALI-PBEC (A) and separated fractions (B) were analyzed by real-time qPCR. ALI-PBEC were 1x daily exposed to fresh air or WCS from one 3R4F cigarette (University of Kentucky, 2 mg) during differentiation for 14 days followed by a cessation period up to 10 days. Cells were harvested on Day 14 (24 h after the last WCS exposure), 16 and 19 (n=3 donors/group). mRNA levels of *SOD1* and *SOD2* (C) were analyzed in whole-cell lysates. Undifferentiated S-PBEC were treated with CSE from one 3R4F cigarette (University of Kentucky) diluted in HBSS (0-1-2%) in Lonza starvation medium for 4 h or 24 h (n=4 donors/group) or undifferentiated S-PBEC cultured on transwells were exposed, after removal of apical medium, to fresh air or WCS from one 3R4F cigarette (University of Kentucky, 2 mg) followed by harvesting of whole-cell lysates after 6 h or 24 h recovery (n=2-3 donors/group). mRNA levels of *SOD1* and *SOD2* (D) were analyzed in whole-cell lysates. Data are presented as mean fold change compared to control (air, 0% CSE or WCS Day 14) \pm s.e.m.. Independent donors are represented by open circles, triangles, squares or diamonds. In case of the CSE-exposed S-PBEC experiments, the symbols reflect the mean of technical triplicates. Statistical differences between WCS versus air or WCS versus air after smoking cessation in ALI-PBEC on each day (e.g., WCS Day 14 versus air), were tested using a two-tailed paired parametric t-test. If comparison of various groups was required in case of the CSE exposure (CSE 1% or 2% versus 0% CSE) or in WCS chronic smoking cessation experiments (WCS Day 16, 19 versus WCS Day 14), an one-way ANOVA (matched/repeated measures) followed by Sidak's post-hoc test for multiple comparisons was conducted, and in case of missing values the mixed-effects models was performed. Statistical significance is indicated as #p<0.1, *p<0.05 and **p<0.01 compared to control (air, 0% CSE or WCS Day 14).

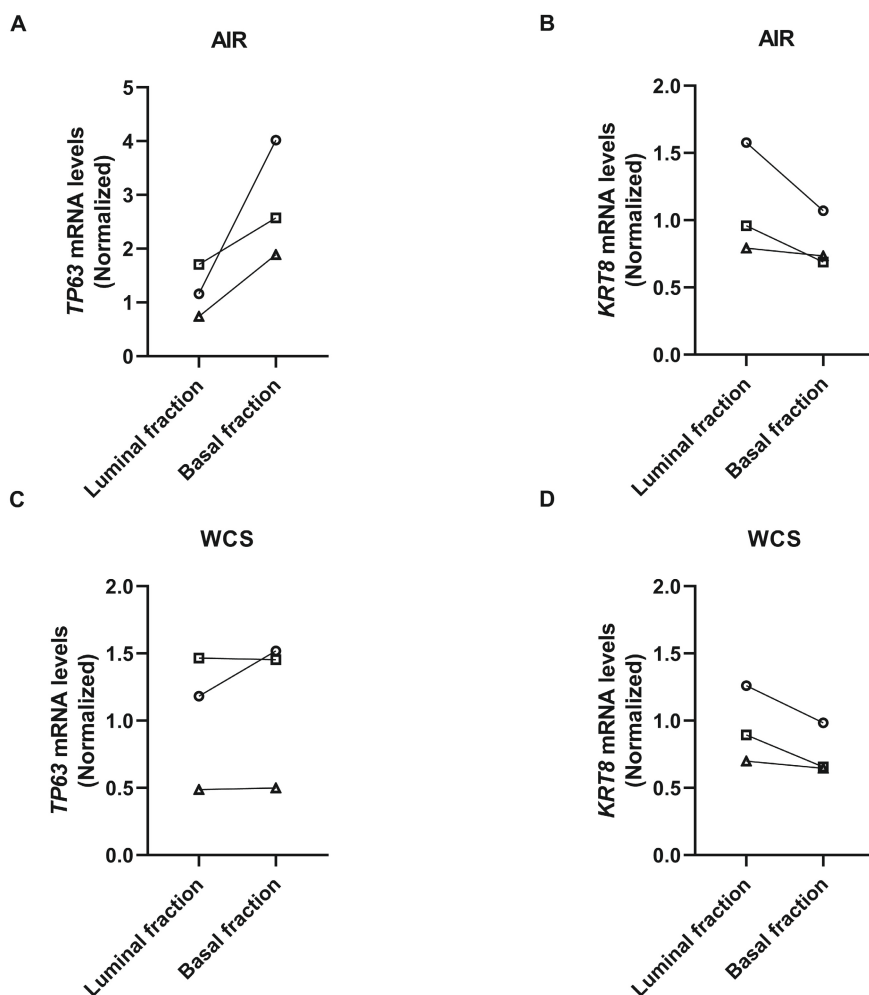


Fig. S2. Validation of separation of basal and luminal cell fractions from ALI-PBEC. After 2-weeks of differentiation, ALI-PBEC were exposed to fresh air or WCS from one 3R4F cigarette (University of Kentucky, 2 mg) and separated into luminal and basal cell fractions at 6 h post-exposure using calcium depletion followed by trypsinization (n=3 donors/group). Independent donors are represented by open circles, triangles or squares. Successful separation was identified by measuring gene expression of basal cells marker (TP63) (A, C) and early progenitor cell marker (cytokeratin-8, KRT8) (B, D).

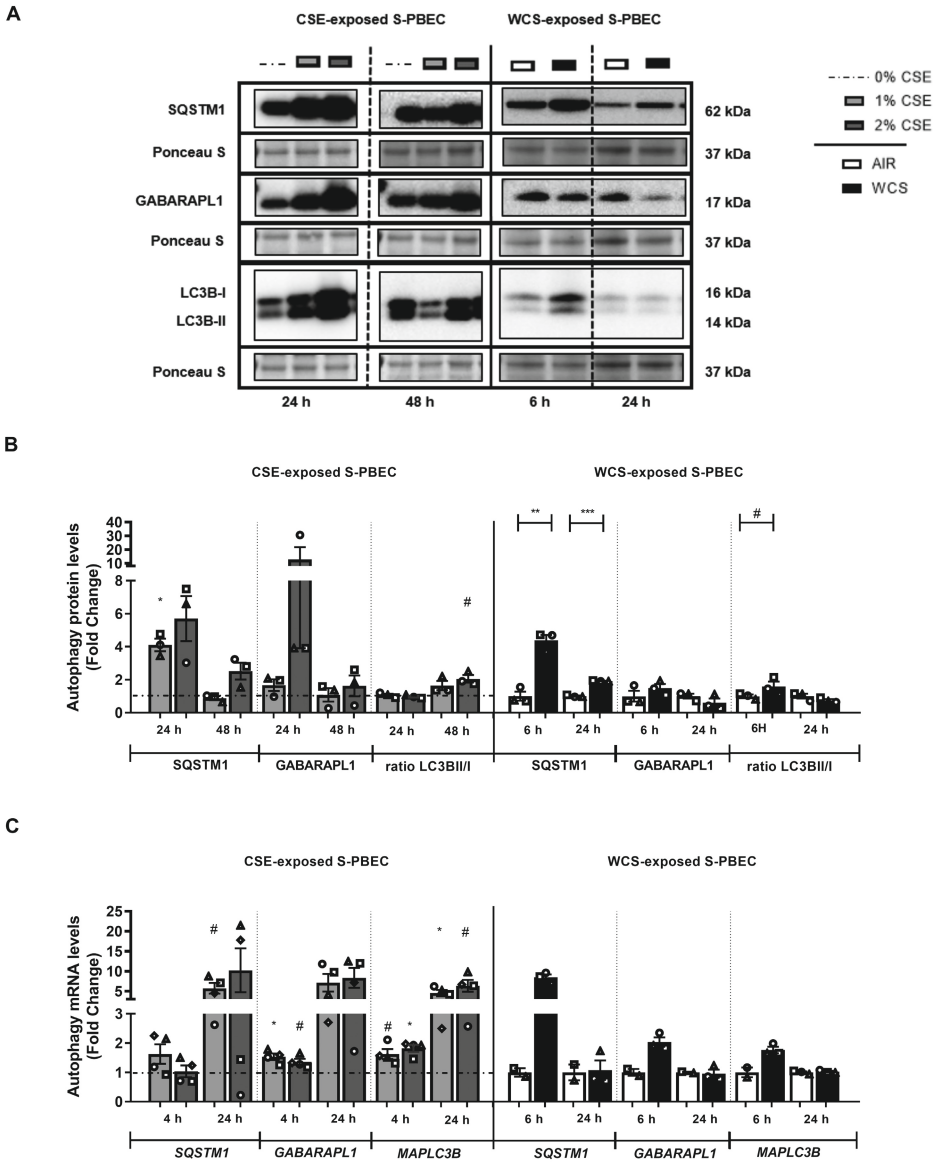
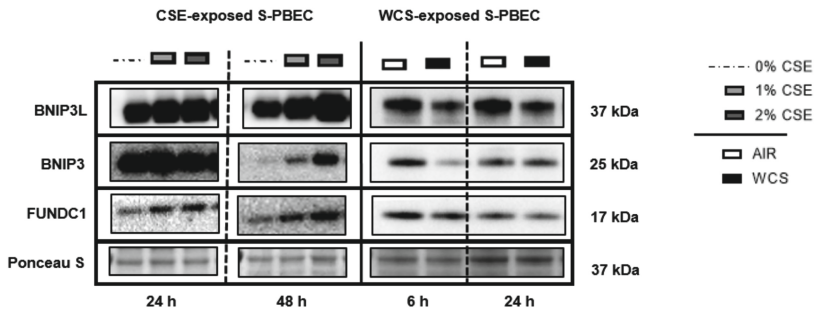


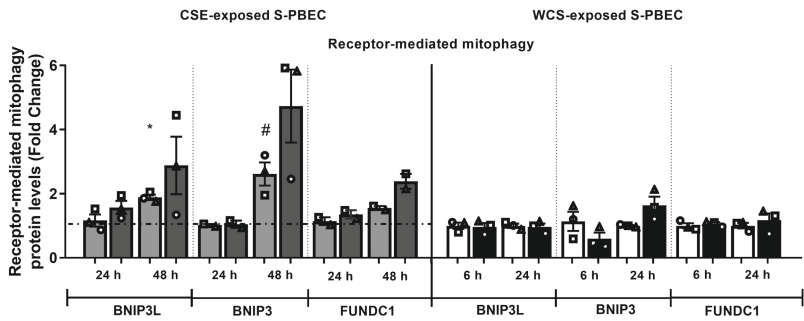
Figure S3. See next page for legend.

Fig. S3. Increase in abundance of key constituents involved in autophagy following acute CSE or WCS exposure in S-PBEC. Undifferentiated S-PBEC were treated with CSE from one 3R4F cigarette (University of Kentucky) diluted in HBSS (0.1-2%) in Lonza starvation medium for 4 h, 24 h or 48 h (n=3-4 donors/group) or undifferentiated S-PBEC cultured on transwells were exposed, after removal of apical medium, to fresh air or WCS from one 3R4F cigarette (University of Kentucky, 2 mg) followed by harvesting of whole-cell lysates after 6 h or 24 h recovery (n=2-3 donors/group). Protein (**A, B**) as well as transcript abundance (**C**) of autophagy regulators SQSTM1, GABARAPL1 and ratio LC3BII/I or MAP1LC3B were measured by western blot and real-time qPCR. Representative western blots, including representative parts of the Ponceau S Staining, are shown. Data are presented as mean fold change compared to control (0% CSE or air) \pm s.e.m.. Independent donors are represented by open circles, triangles, squares or diamonds. In case of the CSE-exposed S-PBEC experiments, the symbols reflect the mean of technical triplicates. Statistical differences between the various CSE exposure groups (CSE 1% or 2% *versus* 0% CSE) were tested using an one-way ANOVA (matched/repeated measures) followed by Sidak's post-hoc test for multiple comparisons, and in case of missing values the mixed-effects models was performed. WCS *versus* air was tested using a two-tailed paired parametric t-test. Statistical significance is indicated as *p<0.1, *p<0.05 and **p<0.01 compared to control (0% CSE or air).

A



B



C

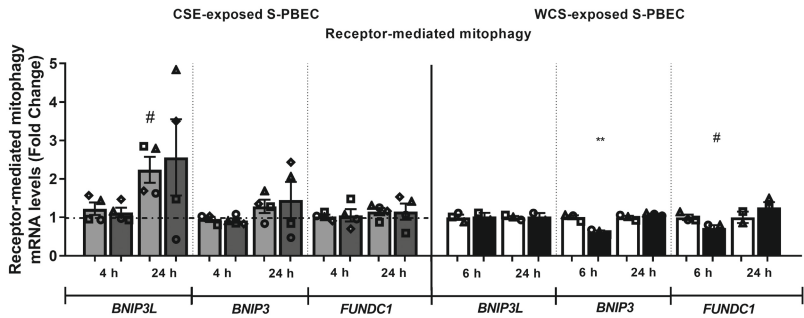
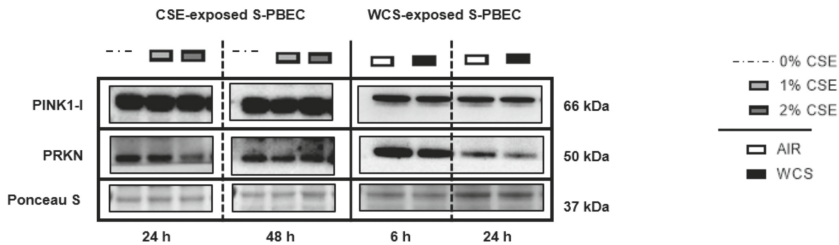


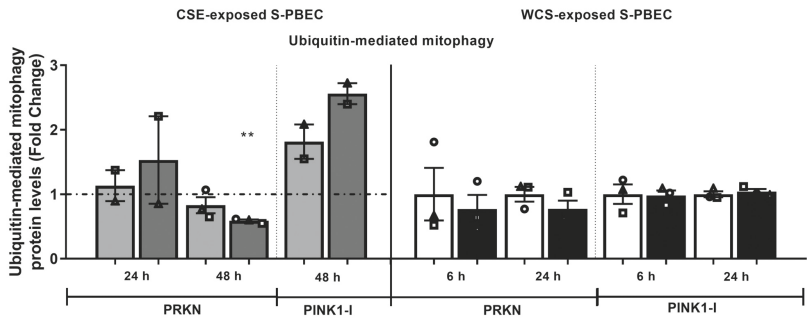
Figure S4. See next page for legend.

Fig. S4. Upregulation of constituents of the receptor-mediated mitophagy machinery in CS-exposed S-PBEC. Undifferentiated S-PBEC were treated with CSE from one 3R4F cigarette (University of Kentucky) diluted in HBSS (0.1-2%) in Lonza starvation medium for 4 h, 24 h or 48 h (n=2-4 donors/group) or undifferentiated S-PBEC cultured on transwells were exposed, after removal of apical medium, to fresh air or WCS from one 3R4F cigarette (University of Kentucky, 2 mg) followed by harvesting of whole-cell lysates after 6 h or 24 h recovery (n=2-3 donors/group). Protein (**A, B**) and mRNA levels (**C**) of regulators involved in receptor-mediated mitophagy (BNIP3L, BNIP3, FUNDC1) were analyzed in whole-cell lysates. Representative western blots, including representative parts of the Ponceau S Staining, are shown. Data are presented as mean fold change compared to control (0% CSE or air) \pm s.e.m.. Independent donors are represented by open circles, triangles, squares or diamonds. In case of the CSE-exposed S-PBEC experiments, the symbols reflect the mean of technical triplicates. Statistical differences between the various CSE exposure groups (CSE 1% or 2% *versus* 0% CSE) were tested using an one-way ANOVA (matched/repeated measures) followed by Sidak's post-hoc test for multiple comparisons, and in case of missing values the mixed-effects models was performed. WCS *versus* air was tested using a two-tailed paired parametric t-test. Statistical significance is indicated as # $p < 0.1$, * $p < 0.05$ and ** $p < 0.01$ compared to control (0% CSE or air).

A



B



C

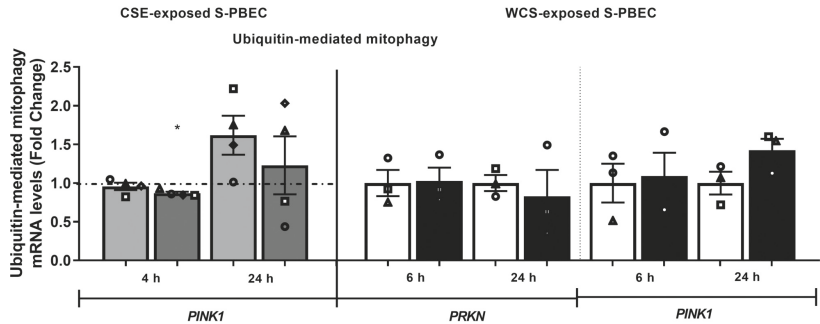
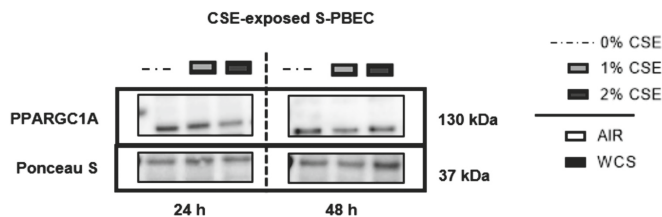


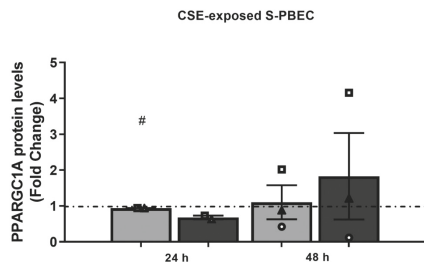
Figure S5. See next page for legend.

Fig. S5. Modulation of ubiquitin-mediated mitophagy markers in CS-exposed S-PBEC. Undifferentiated S-PBEC were treated with CSE from one 3R4F cigarette (University of Kentucky) diluted in HBSS (0.1-2%) in Lonza starvation medium for 4 h, 24 h or 48 h (n=2-4 donors/group) or undifferentiated S-PBEC cultured on transwells were exposed, after removal of apical medium, to fresh air or WCS from one 3R4F cigarette (University of Kentucky, 2 mg) followed by harvesting of whole-cell lysates after 6 h or 24 h recovery (n=3 donors/group). Protein (**A, B**) and mRNA levels (**C**) of regulators involved in ubiquitin-mediated mitophagy (PRKN, PINK1) were analyzed in whole-cell lysates. Western blot analysis revealed one distinct band for PINK1 protein corresponding with expected molecular weight for PINK1-I (66 kDa). Representative western blots, including representative parts of the Ponceau S Staining, are shown. Data are presented as mean fold change compared to control (0% CSE or air) \pm s.e.m.. Independent donors are represented by open circles, triangles, squares or diamonds. In case of the CSE-exposed S-PBEC experiments, the symbols reflect the mean of technical triplicates. Statistical differences between the various CSE exposure groups (CSE 1% or 2% *versus* 0% CSE) were tested using an one-way ANOVA (matched/repeated measures) followed by Sidak's post-hoc test for multiple comparisons, and in case of missing values the mixed-effects models was performed. WCS *versus* air was tested using a two-tailed paired parametric t-test. Statistical significance is indicated as * $p < 0.05$ and ** $p < 0.01$ compared to control (0% CSE or air).

A



B



C

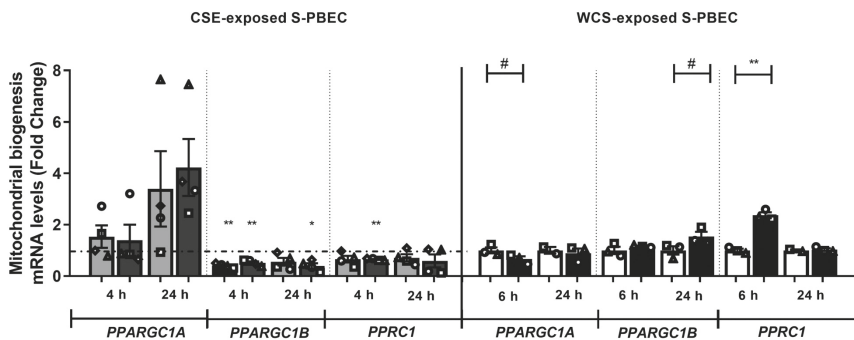
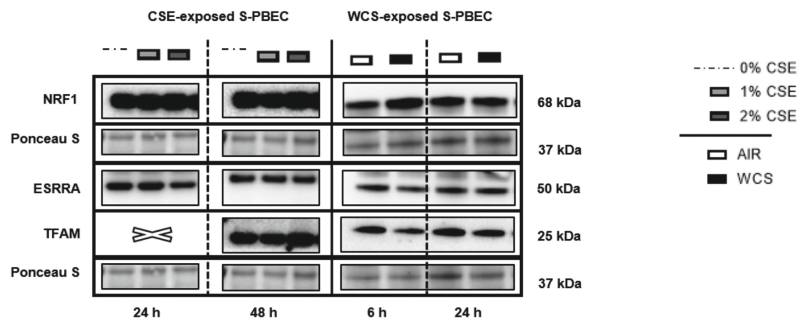


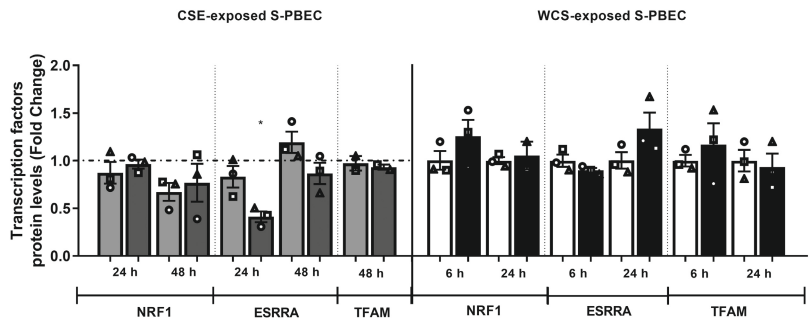
Figure S6. See next page for legend.

Fig. S6. Alterations in expression of transcript levels of transcriptional co-activators of the PPARGC1 network in response to acute CS exposure in S-PBEC. Undifferentiated S-PBEC were treated with CSE from one 3R4F cigarette (University of Kentucky) diluted in HBSS (0-1-2%) in Lonza starvation medium for 4 h, 24 h or 48 h (n=2-4 donors/group) or undifferentiated S-PBEC cultured on transwells were exposed, after removal of apical medium, to fresh air or WCS from one 3R4F cigarette (University of Kentucky, 2 mg) followed by harvesting of whole-cell lysates after 6 h or 24 h recovery (n=2-3 donors/group). Protein (**A, B**) as well as transcript abundance (**C**) of transcriptional co-activators involved in the PPARGC1 network (PPARGC1A, PPARGC1B, PPRC1) are presented. Representative western blots, including representative parts of the Ponceau S Staining, are shown. Data are presented as mean fold change compared to control (0% CSE or air) \pm s.e.m.. Independent donors are represented by open circles, triangles, squares or diamonds. In case of the CSE-exposed S-PBEC experiments, the symbols reflect the mean of technical triplicates. Statistical differences between the various CSE exposure groups (CSE 1% or 2% *versus* 0% CSE) were tested using an one-way ANOVA (matched/repeated measures) followed by Sidak's post-hoc test for multiple comparisons, and in case of missing values the mixed-effects models was performed. WCS *versus* air was tested using a two-tailed paired parametric t-test. Statistical significance is indicated as #p<0.1, *p<0.05 and **p<0.01 compared to control (0% CSE or air).

A



B



C

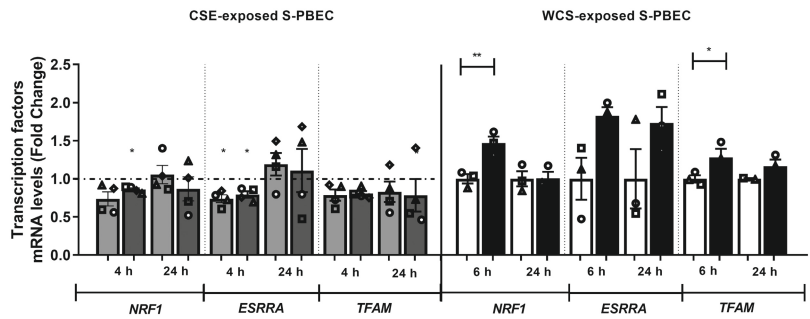


Figure S7. See next page for legend.

Fig. S7. Changes in the abundance of PPARGC1-coactivated transcription factors after CS exposure in S-PBEC. Undifferentiated S-PBEC were treated with CSE from one 3R4F cigarette (University of Kentucky) diluted in HBSS (0-1-2%) in Lonza starvation medium for 4 h, 24 h or 48 h (n=3-4 donors/group) or undifferentiated S-PBEC cultured on transwells were exposed, after removal of apical medium, to fresh air or WCS from one 3R4F cigarette (University of Kentucky, 2 mg) followed by harvesting of whole-cell lysates after 6 h or 24 h recovery (n=2-3 donors/group). Protein (**A, B**) and mRNA levels (**C**) of PPARGC1-coactivated transcription regulators, NRF1, ESRRA and TFAM, were measured by western blotting or real-time qPCR. Representative western blots, including representative parts of the Ponceau S Staining, are shown. Data are presented as mean fold change compared to control (0% CSE or air) \pm s.e.m.. Independent donors are represented by open circles, triangles, squares or diamonds. In case of the CSE-exposed S-PBEC experiments, the symbols reflect the mean of technical triplicates. Statistical differences between the various CSE exposure groups (CSE 1% or 2% *versus* 0% CSE) were tested using an one-way ANOVA (matched/repeated measures) followed by Sidak's post-hoc test for multiple comparisons, and in case of missing values the mixed-effects models was performed. WCS *versus* air was tested using a two-tailed paired parametric t-test. Statistical significance is indicated as * $p < 0.05$ and ** $p < 0.01$ compared to control (0% CSE or air).

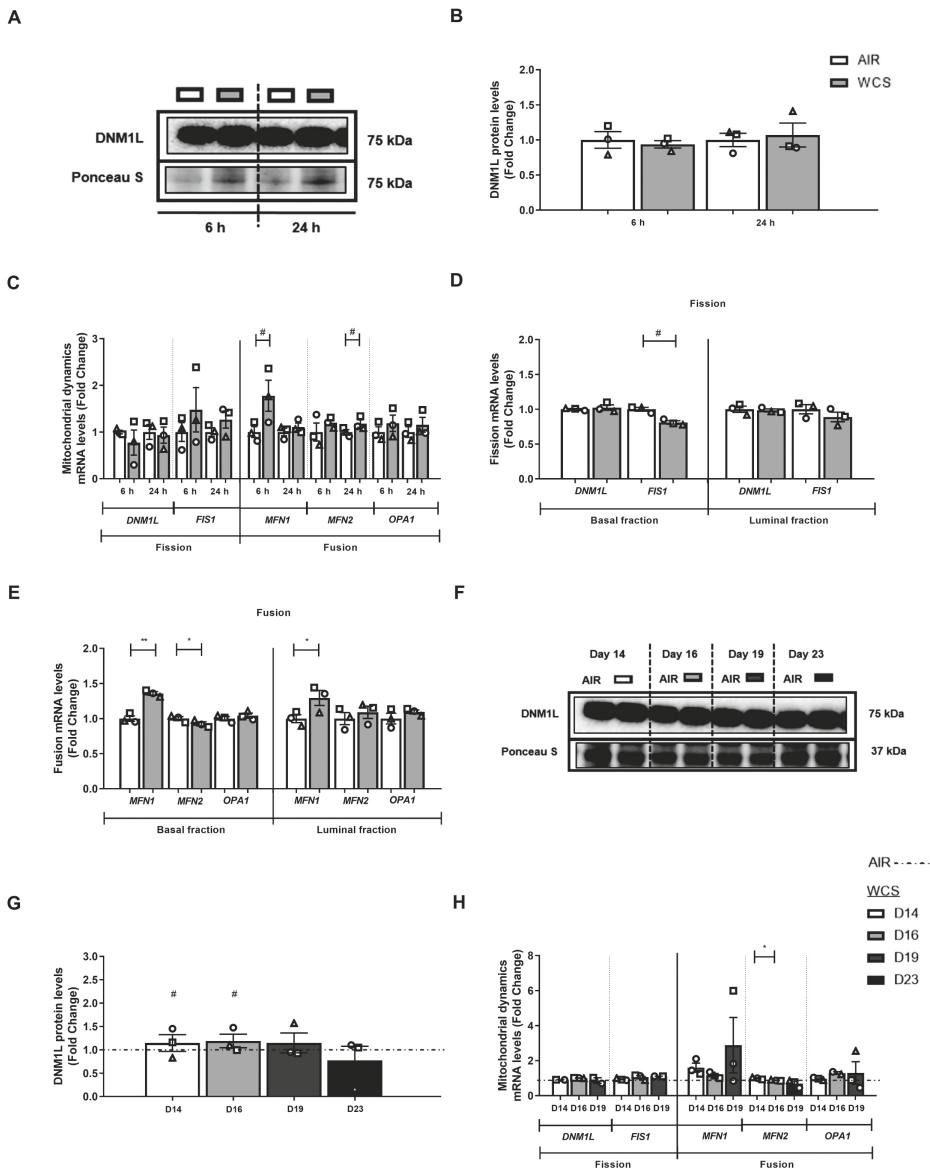


Figure S8. See next page for legend.

Fig. S8. Changes in mitochondrial dynamics markers in response to WCS exposure in ALI-PBEC.

After 2-weeks of differentiation, ALI-PBEC were exposed to fresh air or WCS from one 3R4F cigarette (University of Kentucky, 2 mg) and whole-cell lysates were harvested after 6 h and 24 h, and the basal and luminal fractions were harvested only at 6 h post-exposure (n=3 donors/group). Protein (**A, B**) and mRNA levels (**C, D, E**) of fission- and fusion-associated markers were analyzed in whole-cell lysates or basal/luminal cell fractions post-exposure. Data are presented as mean fold change compared to control (air) \pm s.e.m.. Independent donors are represented by open circles, triangles or squares. Statistical differences between WCS *versus* air were tested using a two-tailed paired parametric t-test, * $p < 0.1$, * $p < 0.05$ and ** $p < 0.01$. ALI-PBEC were 1x daily exposed to fresh air or WCS from one 3R4F cigarette (University of Kentucky, 2 mg) during differentiation for 14 days followed by a cessation period up to 10 days. Cells were harvested on Day 14 (24 h after the last exposure), 16, 19 and 23 (n=2-3 donors/group). Abundance of DNMI1L protein (**F, G**) and transcript abundance of fission and fusion regulators (**H**) are shown. Representative western blots, including representative parts of the Ponceau S Staining, are shown. Data are presented as mean fold change compared to control (air or WCS Day 14) \pm s.e.m.. Independent donors are represented by open circles, triangles or squares. Statistical differences between WCS *versus* air after smoking cessation in ALI-PBEC on each day was tested using a two-tailed paired parametric t-test (e.g., WCS Day 14 *versus* air). Comparison of various groups to test the difference of WCS Day 16, 19, 23 *versus* Day 14 in WCS chronic smoking cessation experiments was conducted using an one-way ANOVA followed by Sidak's post-hoc test for multiple comparisons, and in case of missing values the mixed-effects models was performed. Statistical significance is indicated as * $p < 0.1$ and * $p < 0.05$ compared to control (air or WCS Day 14).

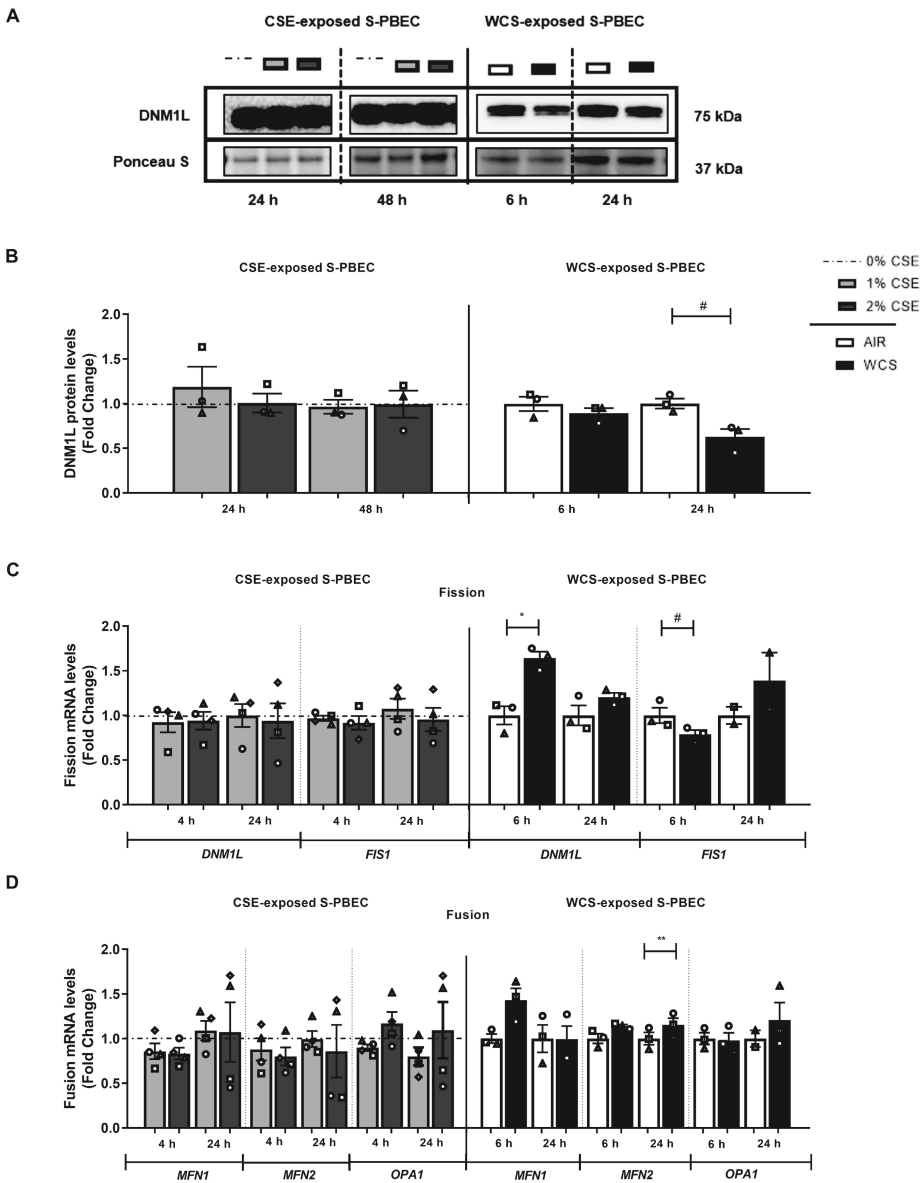


Figure S9. See next page for legend.

Fig. S9. Aberrant protein and transcript abundance of fission- and fusion-associated markers in S-PBEC. Undifferentiated S-PBEC were treated with CSE from one 3R4F cigarette (University of Kentucky) diluted in HBSS (0-1-2%) in Lonza starvation medium for 4 h, 24 h or 48 h (n=3-4 donors/group) or undifferentiated S-PBEC cultured on transwells were exposed, after removal of apical medium, to fresh air or WCS from one 3R4F cigarette (University of Kentucky, 2 mg) followed by harvesting of whole-cell lysates after 6 h or 24 h recovery (n=2-3 donors/group). Protein (**A, B**) and mRNA levels (**C**) of fission-associated markers (DNM1L, FIS1) and gene expression of fusion-associated markers (MFN1, MFN2, OPA1) (**D**) were measured using western blot and real-time qPCR. Representative western blots, including representative parts of the Ponceau S Staining, are shown. Data are presented as mean fold change compared to control (0% CSE or air) \pm s.e.m.. Independent donors are represented by open circles, triangles, squares or diamonds. In case of the CSE-exposed S-PBEC experiments, the symbols reflect the mean of technical triplicates. Statistical differences between the various CSE exposure groups (CSE 1% or 2% *versus* 0% CSE) were tested using an one-way ANOVA (matched/repeated measures) followed by Sidak's post-hoc test for multiple comparisons, and in case of missing values the mixed-effects models was performed. WCS *versus* air was tested using a two-tailed paired parametric t-test. Statistical significance is indicated as #p<0.1, *p<0.05 and **p<0.01 compared to control (0% CSE or air).

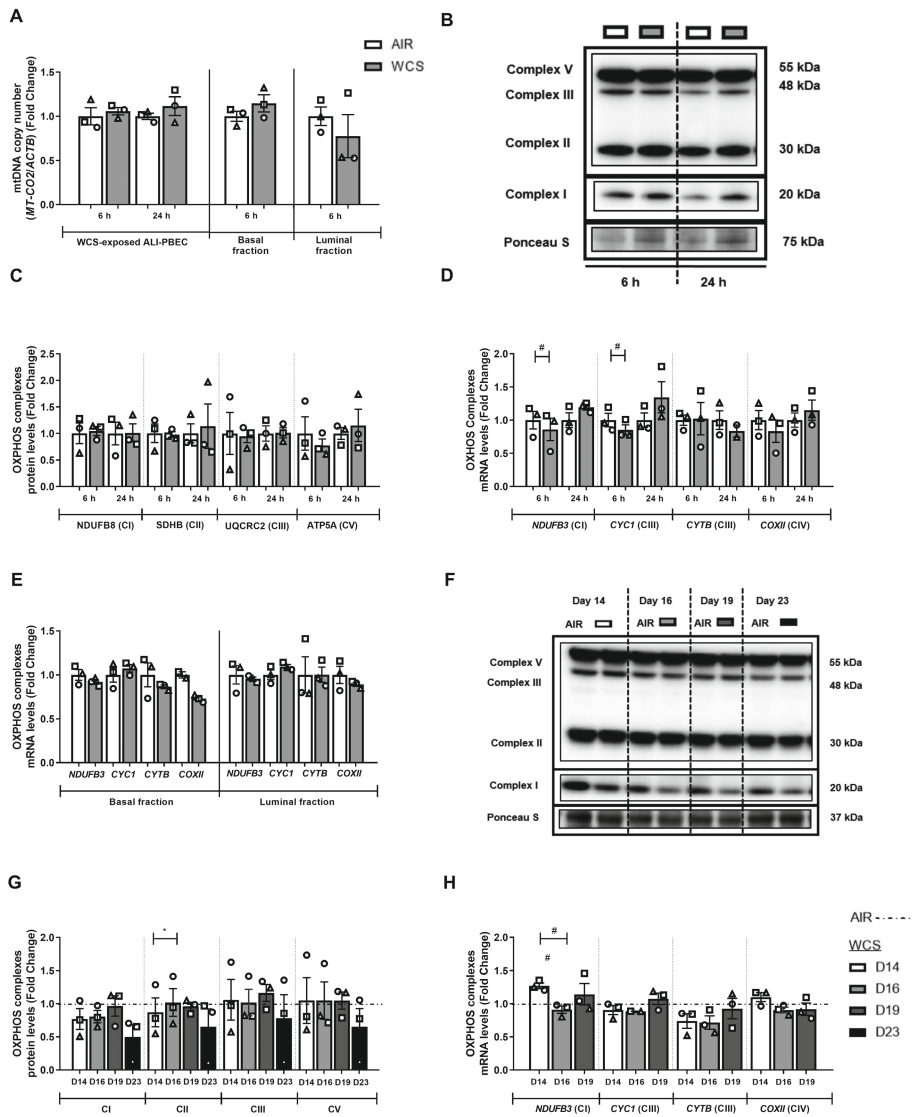


Figure S10. See next page for legend.

Fig. S10. Unaltered abundance of subunits of the electron transport chain in WCS-exposed ALI-PBEC.

After 2-weeks of differentiation, ALI-PBEC were exposed to fresh air or WCS from one 3R4F cigarette (University of Kentucky, 2 mg) and whole-cell lysates were harvested after 6 h and 24 h, and the basal and luminal fractions were harvested only at 6 h post-exposure (n=2-3 donors/group). Mitochondrial DNA copy number (**A**), protein (**B, C**) as well as transcript levels (**D, E**) of nuclear and mitochondrial-encoded subunits of the electron transport chain (Complex I (CI), Complex II (CII), Complex III (CIII), Complex IV (CIV), Complex V (CV)) were analyzed in whole-cell lysates or basal and luminal fractions post-exposure. Data are presented as mean fold change compared to control (air) \pm s.e.m.. Independent donors are represented by open circles, triangles or squares. Statistical differences between WCS *versus* air were tested using a two-tailed paired parametric t-test, *p<0.1. ALI-PBEC were 1x daily exposed to fresh air or WCS from one 3R4F cigarette (University of Kentucky, 2 mg) during differentiation for 14 days followed by a cessation period up to 10 days. Cells were harvested on Day 14 (24 h after the last exposure), 16, 19 and 23 (n=2-3 donors/group). Protein (**F, G**) and mRNA expression (**H**) of subunits of the electron transport chain are analyzed. Representative western blots, including representative parts of the Ponceau S Staining, are shown. Data are presented as mean fold change compared to control (air or WCS Day 14) \pm s.e.m.. Independent donors are represented by open circles, triangles or squares. Statistical differences between WCS *versus* air after smoking cessation in ALI-PBEC on each day was tested using a two-tailed paired parametric t-test (e.g. WCS Day 14 *versus* air). Comparison of various groups to test the difference of WCS Day 16, 19, 23 *versus* Day 14 in WCS chronic smoking cessation experiments was conducted using an one-way ANOVA followed by Sidak's post-hoc test for multiple comparisons, and in case of missing values the mixed-effects models was performed. Statistical significance is indicated as #p<0.1 and *p<0.05 compared to control (air or WCS Day 14).

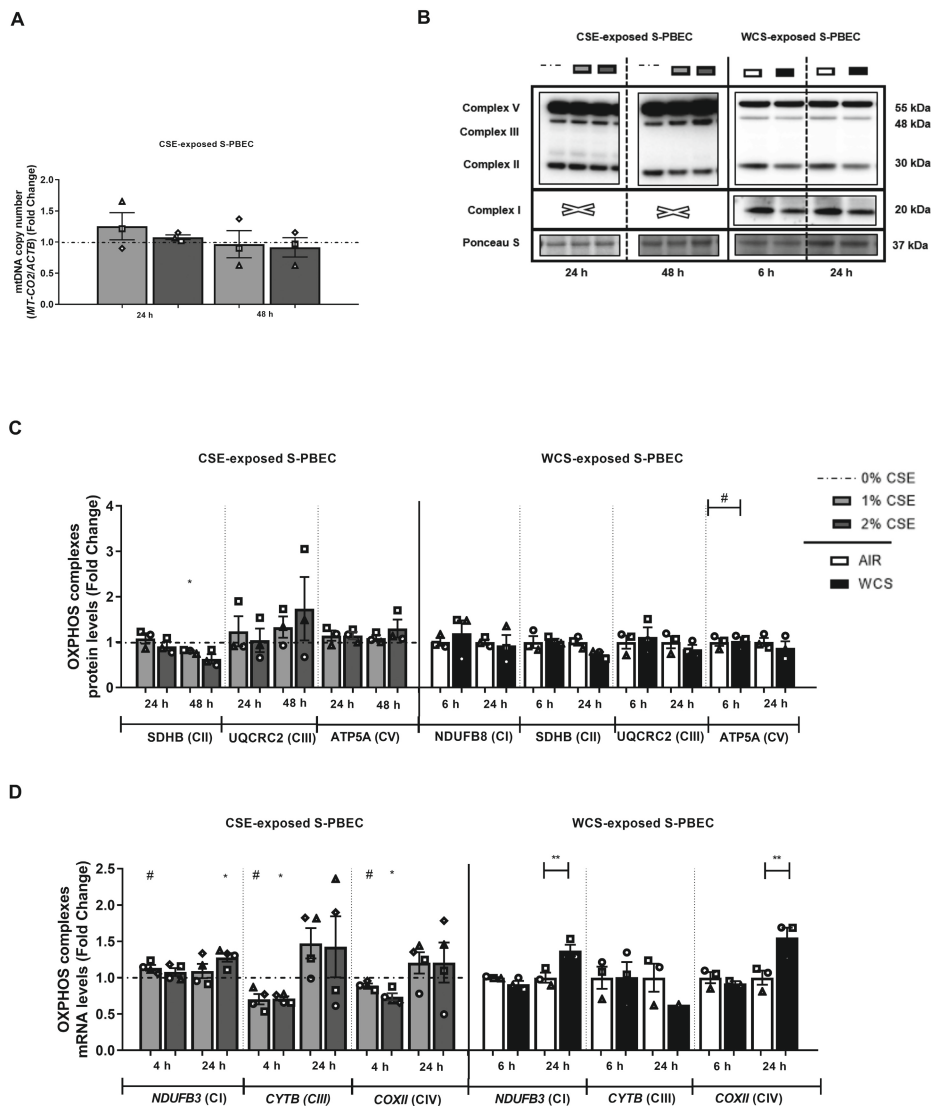


Figure S11. See next page for legend.

Fig. S11. Modulation in the abundance of subunits of the electron transport chain in CS-exposed S-PBEC. Undifferentiated S-PBEC were treated with CSE from one 3R4F cigarette (University of Kentucky) diluted in HBSS (0.1-2%) in Lonza starvation medium for 4 h, 24 h or 48 h (n=3-4 donors/group) or undifferentiated S-PBEC cultured on transwells were exposed, after removal of apical medium, to fresh air or WCS from one 3R4F cigarette (University of Kentucky, 2 mg) followed by harvesting of whole-cell lysates after 6 h or 24 h recovery (n=1-3 donors/group). Mitochondrial DNA copy number (**A**), protein (**B, C**) as well as transcript levels (**D**) of nuclear and mitochondrial-encoded subunits of the electron transport chain (Complex I (CI), Complex II (CII), Complex III (CIII), Complex IV (CIV), Complex V (CV)) were analyzed in whole-cell lysates. Representative western blots, including representative parts of the Ponceau S Staining, are shown. Data are presented as mean fold change compared to control (0% CSE or air) \pm s.e.m.. Independent donors are represented by open circles, triangles, squares or diamonds. In case of the CSE-exposed S-PBEC experiments, the symbols reflect the mean of technical triplicates. Statistical differences between the various CSE exposure groups (CSE 1% or 2% *versus* 0% CSE) were tested using an one-way ANOVA (matched/repeated measures) followed by Sidak's post-hoc test for multiple comparisons, and in case of missing values the mixed-effects models was performed. WCS *versus* air was tested using a two-tailed paired parametric t-test. Statistical significance is indicated as #p<0.1, *p<0.05 and **p<0.01 compared to control (0% CSE or air).

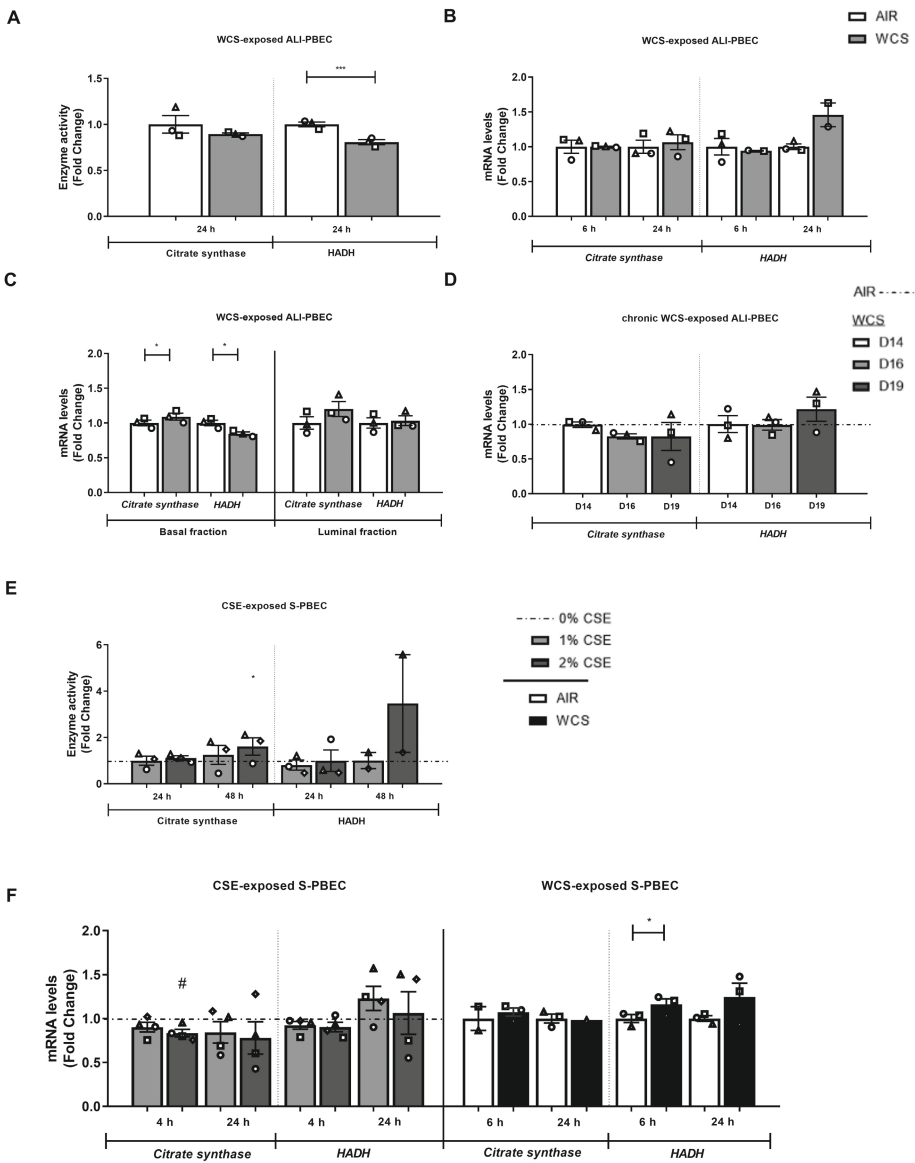


Figure S12. See next page for legend.

Fig. S12. Disruption of activity and abundance of key components involved in the fatty acid β -oxidation in CS-exposed ALI- and S-PBEC. After 2-weeks of differentiation, ALI-PBEC were exposed to fresh air or WCS from one 3R4F cigarette (University of Kentucky, 2 mg) and whole-cell lysates were harvested after 6 h and 24 h, and the basal and luminal fractions were harvested only at 6 h post-exposure (n=2-3 donors/group). Enzyme activities of citrate synthase and HADH (**A**) and related transcript abundance in whole-cell lysates (**B**) or basal and luminal fractions (**C**) were assessed in ALI-PBEC. Next, ALI-PBEC were 1x daily exposed to fresh air or WCS from one 3R4F cigarette (University of Kentucky, 2 mg) during differentiation for 14 days followed by a cessation period up to 10 days. Cells were harvested on Day 14 (24 h after the last exposure), 16 and 19 (n=3 donors/group). Transcript abundance (**D**) of *citrate synthase* and *HADH* were measured. Undifferentiated S-PBEC were treated with CSE from one 3R4F cigarette (University of Kentucky) diluted in HBSS (0-1-2%) in Lonza starvation medium for 4 h, 24 h or 48 h (n=4 donors/group) or undifferentiated S-PBEC cultured on transwells were exposed, after removal of apical medium, to fresh air or WCS from one 3R4F cigarette (University of Kentucky, 2 mg) followed by harvesting of whole-cell lysates after 6 h or 24 h recovery (n=1-3 donors/group). Cell lysates were used to measure enzyme activities of citrate synthase and HADH (**E**) and related transcript abundance (**F**). Data are presented as mean fold change compared to control (air, 0% CSE or WCS Day 14) \pm s.e.m.. Independent donors are represented by open circles, triangles, squares or diamonds. In case of the CSE-exposed S-PBEC experiments, the symbols reflect the mean of technical triplicates. Statistical differences between WCS *versus* air or WCS *versus* air after smoking cessation in ALI-PBEC on each day (e.g., WCS Day 14 *versus* air) were tested using a two-tailed paired parametric t-test. If comparison of various groups was required in case of the CSE exposure (CSE 1% or 2% *versus* 0% CSE) or in WCS chronic smoking cessation experiments (WCS Day 16, 19 *versus* WCS Day 14), an one-way ANOVA (matched/repeated measures) followed by Sidak's post-hoc test for multiple comparisons was conducted, and in case of missing values the mixed-effects models was performed. Statistical significance is indicated as *p<0.1, *p<0.05 and **p<0.01 compared to control (air, 0% CSE or WCS Day 14).

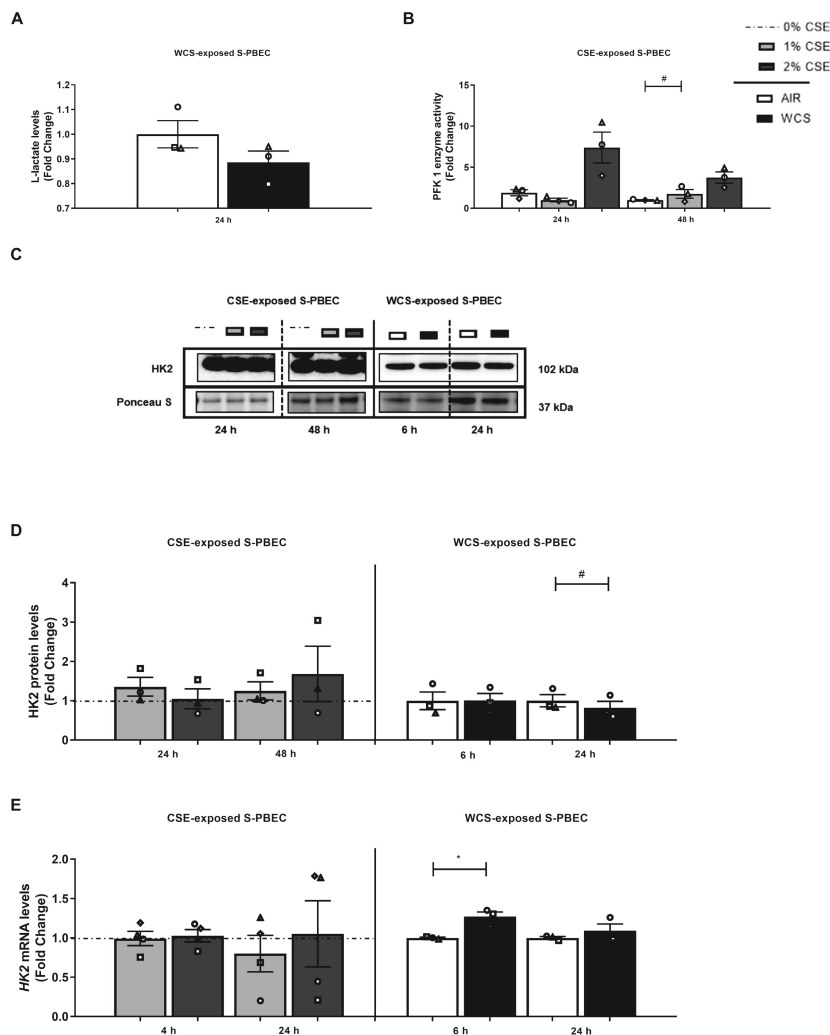


Figure S13. See next page for legend.

Fig. S13. Glycolytic shift after CS exposure in S-PBEC. Undifferentiated S-PBEC were treated with CSE from one 3R4F cigarette (University of Kentucky) diluted in HBSS (0.1-2%) in Lonza starvation medium for 4 h, 24 h or 48 h (n=3-4 donors/group) or undifferentiated S-PBEC cultured on transwells were exposed, after removal of apical medium, to fresh air or WCS from one 3R4F cigarette (University of Kentucky, 2 mg) followed by harvesting of whole-cell lysates after 6 h or 24 h recovery (n=3 donors/group). L-lactate levels (**A**), PFK1 enzyme activity (**B**) as well as protein (**C, D**) and mRNA levels (**E**) of HK2 were analyzed in S-PBEC. Representative western blots, including representative parts of the Ponceau S Staining, are shown. Data are presented as mean fold change compared to control (0% CSE or air) \pm s.e.m.. Independent donors are represented by open circles, triangles, squares or diamonds. In case of the CSE-exposed S-PBEC experiments, the symbols reflect the mean of technical triplicates. WCS *versus* air was tested using a two-tailed paired parametric t-test. Statistical differences between the various CSE exposure groups (CSE 1% or 2% *versus* 0% CSE) were tested using an one-way ANOVA (matched/repeated measures) followed by Sidak's post-hoc test for multiple comparisons, and in case of missing values the mixed-effects models was performed. Statistical significance is indicated as * $p < 0.1$ and * $p < 0.05$ compared to control (0% CSE or air).

Table S1. Human primers sequences used for real-time quantitative PCR analysis.

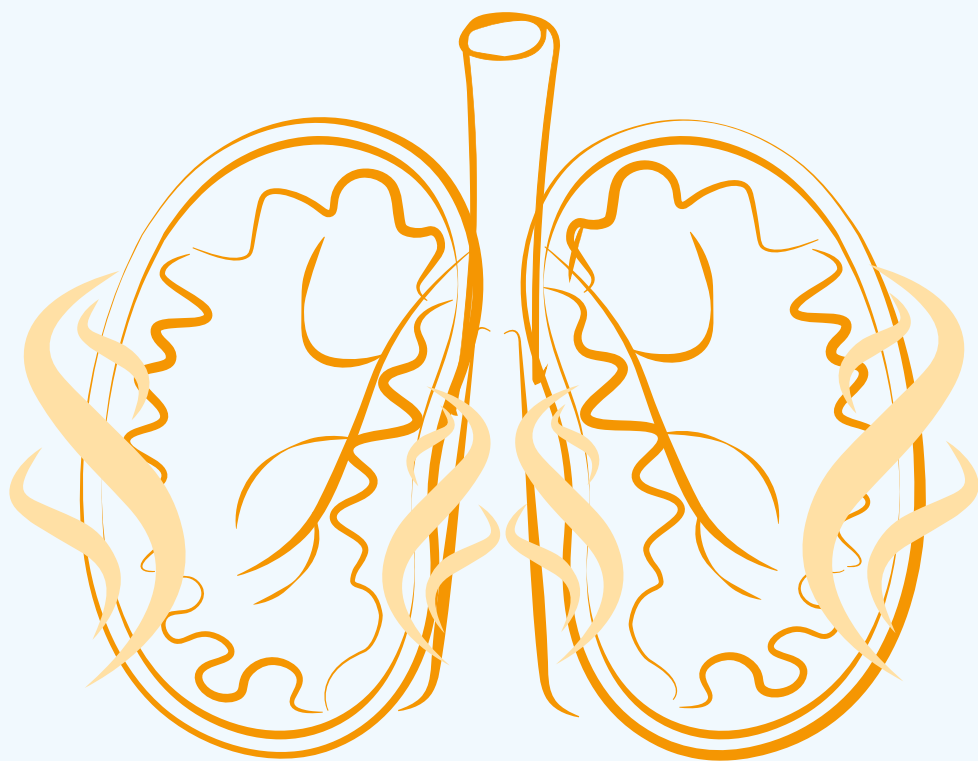
Gene	Sense primer (5'-3')	Antisense primer (3'-5')
Reference genes		
<i>ATP5B</i>	TCACCCAGGCTGGTTCAGA	AGTGGCCAGGGTAGGCTGAT
<i>B2M</i>	CTGTGCTCGCGCTACTCTCTCTT	TGAGTAAACCTGAATCTTTGGAGTACGC
<i>ACTB</i>	AAGCCACCCCACTTCTCTCTAA	AATGCTATCACCTCCCCCTGTGT
<i>PPIA</i>	CATCTGCACTGCCAAGACTGA	TTCATGCCTTCTTTCACTTTGC
<i>RPL13A_1</i>	CCTGGAGGAGAAGAGGAAAGAGA	TTGAGGACCTCTGTGTATTGTCAA
<i>RPL13A_2</i>	AAGGTGGTGGTCGTACGCTGTG	CGGGAAGGGTTGGTGTTCATCC
Target genes		
<i>BNIP3</i>	AGCGCCCGGGATGCA	CCCGTTCCCATTATTGCTGAA
<i>BNIP3L</i>	CTGCGAGGAAAATGAGCAGTCTCT	GCCCCCATTTTCCCATTG
<i>Citrate synthase</i>	GATGTGTGATGAGAAGTTACGAGACT	TGGCCATAGCCTGGAACAA
<i>COXII</i>	ACCTGCGACTCCTTGACGTT	GGGGGCTTCAATCGGGAGTA
<i>CYC1</i>	GAGCACGACCATCGAAAACG	CGATATGCCAGCTTCCGACT
<i>DNM1L</i>	CGACTCATTAATCATATTTTCTCATTGTGACG	TGCATTACTGCCTTTGGCACACT
<i>ESRRA</i>	TGCTGCTCACGCTACCGCTC	TCGAGCATCTCCAAGAACAGC
<i>FIS1</i>	CCTGTGCGGAGCAAGTACAA	TCCTTGCTCCCTTTGGGCAG
<i>FUNDC1</i>	GAAACGAGCGAACAAAGCAG	GCAAAAAGCCTCCACAAAT
<i>GABARPL1</i>	ATCGGAAAAAGGAAGGAGAAAAGATC	CAGGCACCCTGGCTTTTGG
<i>HADHA</i>	TGGCTTCCC GCCTTGTC	TGGAGCCGGTCCACTATCTTC
<i>HK2</i>	GTAAATACAGTGGATCTCAATCTTCGGG	CAAGGATTTGAGATGATTCGCTATTCA
<i>KRT8</i>	TCCTCAGGCAGCTATATGAAGAG	GGTTGGCAATATCCTCGTACTGT
<i>MAP1LC3A</i>	CCTGGACAAGACCAAGTTTGTG	GTCTTTCTCTGCTCGTAGATG
<i>MAP1LC3B</i>	ACCATGCCGTCGGAGAAGAC	TCTCGAATAAGTCGGACATCTTCTACTCT
<i>MFN1</i>	CTGAGGATGATTGTTAGCTCCACG	CAGGCGAGCAAAAAGTGGTAGC
<i>MFN2</i>	TGGACCACCAAGGCCAAGGA	TCTCGCTGGCATGTCTCCAC
<i>Mt-CytB</i>	ACCCCTAGGAATCACCTCC	GCCTAGGAGGTCTGGTGAGA
<i>NDUFB3</i>	TCAGATTGCTGTGACACATGG	TGGTGTCCCTTCTATCTTCCA
<i>NRF1</i>	AGGAACACGGAGTGACCCAA	TATGCTCGGTGTAAGTAGCCA
<i>OPA1</i>	TACCAAAGGCATTTTGTAGATTCTGAGTT	GCATGCGCTGTATACGCCAA
<i>PIGR</i>	CTCTCTGGAGGACCACCGT	CAGCCGTGACATTCCTCTG
<i>PINK1</i>	GAAAGCCGCACTACCAAGA	AGCACATTTGCGGCTACTCG
<i>PPARGC1A</i>	AAGCCACTACAGACACCGC	TCGTAGCTGTACATACCTGGG
<i>PPARGC1B</i>	GGCGCTTTGAAGTGTTTGGTGA	TGATGAAGCCGTACTTCTCGCCT
<i>PPRC1</i>	GCCCTTTGATCTCTGCTTTGGG	AAGTCTTCCCGGTTGGAGTCAAG
<i>PRKN</i>	GGTTTGCTTCTGCCGGAATG	CTTTCATCGACTCTGTAGGCCTG
<i>SDHB</i>	TGGGGCCTGCAGTTCTTATG	ATGGTGTGGCAGCGGTATAG
<i>SOD1</i>	GGTCCTCACTTAAATCCTCTAT	CATCTTTGTGACGAGTCACATT
<i>SOD2</i>	TGGACAAACCTCAGCCCTAACG	TGATGGCTTCCAGCAACTCCC
<i>SQSTM1</i>	GGTGCACCCCAATGTGATCT	CGCAGACGCTACACAAGTCG
<i>TFAM</i>	GAAAGATTCCAAGAAGCTAAGGGTGATT	TCCAGTTTTCTTTACAGTCTTCAGCTTTT
<i>TP63</i>	CCACCTGGACGTATTCCACTG	TCGAATCAAATGACTAGGAGGGG

Abbreviations: *ATP5B*: ATP synthase F1 subunit beta, *B2M*: beta-2 microglobulin, *ACTB*: actin B, *PPIA*: peptidylprolyl isomerase A, *RPL13A*: ribosomal protein L13A, *BNIP3*: BCL2 interacting protein 3, *BNIP3L*: BCL2 interacting protein 3-like, Citrate synthase, *COXII*: cytochrome c oxidase subunit II, *CYC1*: cytochrome c-1, *DNM1L*: dynamin 1-like, *ESRRA*: estrogen related receptor, alpha, *FIS1*: fission, mitochondrial 1, *FUNDC1*: FUN14 domain containing 1, *GABARAPL1*: GABA type A receptor associated protein like 1, *HADHA*: hydroxyacyl-CoA dehydrogenase trifunctional multienzyme complex subunit alpha, *HK2*: hexokinase 2, *KRT8*: keratin 8, *MAP1LC3A*: microtubule-associated protein 1 light chain 3 alpha, *MAP1LC3B*: microtubule-associated protein 1 light chain 3 beta, *MFN1*: mitofusin 1, *MFN2*: mitofusin 2, *Mt-CytB*: mitochondrial-encoded cytochrome beta, *NDUFB3*: NADH:ubiquinone oxidoreductase subunit B3, *NRF1*: nuclear respiratory factor 1, *OPA1*: OPA1, mitochondrial dynamin like GTPase, *PIGR*: Polymeric Immunoglobulin Receptor, *PINK1*: PTEN induced kinase 1, *PPARGC1A*: PPARG coactivator 1 alpha, *PPARGC1B*: PPARG coactivator 1 beta, *PPRC1*: PPARG related coactivator 1, *PRKN*: parkin RBR E3 ubiquitin protein ligase, *SDHB*: succinate dehydrogenase complex iron sulfur subunit B, *SOD1*: superoxide dismutase 1, *SOD2*: superoxide dismutase 2, *SQSTM1*: sequestosome 1, *TFAM*: transcription factor A, mitochondrial, *TP63*: tumor protein 63

Table S2. Antibodies used for western blotting.

Target	RRID	Company	Product number	Dilution factor
Primary antibodies				
BNIP3	AB_2259284	Cell Signaling Technology	Cat# 3769S	1:1000
BNIP3L	AB_2688036	Cell Signaling Technology	Cat# 12396	1:1000
DNM1L	AB_10950498	Cell Signaling Technology	Cat# 8570	1:1000
ESRRA	AB_1523580	Abcam	Cat# ab76228	1:1000
FUNDC1	AB_10609242	Santa Cruz Biotechnology	Cat# sc-133597	1:500
GABARAPL1	AB_2294415	Proteintech Group	Cat# 11010-1-AP	1:1000
HK2	AB_2232946	Cell Signaling Technology	Cat# 2867	1:1000
MAP1LC3B	AB_915950	Cell Signaling Technology	Cat# 2775	1:1000
NRF1	AB_2154534	Abcam	Cat# ab55744	1:1000
OXPHOS	AB_2629281	MitoScience LLC	Cat# MS604	1:1000
PINK1	AB_10127658	Novus Biologicals	Cat# BC100-494	1:2000
PPARGC1A	AB_10697773	Millipore	Cat# 516557	1:1000
PRKN	AB_2159920	Cell Signaling Technology	Cat# 4211	1:1000
SQSTM1	AB_10624872	Cell Signaling Technology	Cat# 5114	1:1000
TFAM	AB_10682431	Millipore	Cat# DR1071	1:1000
Secondary antibodies				
Goat Anti-Mouse IgG Antibody	AB_2827937	Vector Laboratories	Cat#BA-9200	1:10000
Goat Anti-Rabbit IgG Antibody	AB_2313606	Vector Laboratories	Cat#BA-1000	1:10000

Abbreviations: BNIP3: BCL2 interacting protein 3, BNIP3L: BCL2 interacting protein 3-Like, DNM1L: dynamin 1-like, ESRRA: estrogen related receptor, alpha, FUNDC1: FUN14 domain containing 1, GABARAPL1: GABA type A receptor associated protein like 1, HK2: hexokinase 2, MAP1LC3B (or LC3B): microtubule-associated protein 1 light chain 3 beta, NRF1: nuclear respiratory factor 1, OXPHOS: oxidative phosphorylation antibody cocktail (containing NDUFB8: NADH:ubiquinone oxidoreductase subunit B8, SDHB: succinate dehydrogenase complex iron sulfur subunit B, UQCRC2: ubiquinol-cytochrome C reductase core protein 2, MT-COI: mitochondrially encoded cytochrome C oxidase I, ATP5F1A: ATP synthase F1 subunit alpha), PINK1: PTEN induced kinase 1, PPARGC1A: PPARG coactivator 1 alpha, PRKN: parkin RBR E3 ubiquitin protein ligase, SQSTM1: sequestosome 1, TFAM: transcription factor A, mitochondrial



Chapter 4

Acrolein inhalation acutely affects the regulation of mitochondrial metabolism in rat lung

Christy B.M. Tulen, Samantha J. Snow, Pieter A. Leermakers,
Urmila P. Kodavanti, Frederik-Jan van Schooten,
Antoon Opperhuizen, Alexander H.V. Remels

Toxicology. 2022 Mar 15; 496(153129)

DOI: 10.1016/j.tox.2022.153129

Abstract

Exposure of the airways to cigarette smoke (CS) is the primary risk factor for developing several lung diseases such as Chronic Obstructive Pulmonary Disease (COPD). CS consists of a complex mixture of over 6000 chemicals including the highly reactive α,β -unsaturated aldehyde acrolein. Acrolein is thought to be responsible for a large proportion of the non-cancer disease risk associated with smoking. Emerging evidence suggest a key role for CS-induced abnormalities in mitochondrial morphology and function in airway epithelial cells in COPD pathogenesis. Although *in vitro* studies suggest acrolein-induced mitochondrial dysfunction in airway epithelial cells, it is unknown if *in vivo* inhalation of acrolein affects mitochondrial content or the pathways controlling this. In this study, rats were acutely exposed to acrolein by inhalation (nose-only; 0–4 ppm), 4 h/day for 1 or 2 consecutive days ($n = 6/\text{group}$). Subsequently, the activity and abundance of key constituents of mitochondrial metabolic pathways as well as expression of critical proteins and genes controlling mitochondrial biogenesis and mitophagy were investigated in lung homogenates. A transient decreasing response in protein and transcript abundance of subunits of the electron transport chain complexes was observed following acrolein inhalation. Moreover, acrolein inhalation caused a decreased abundance of key regulators associated with mitochondrial biogenesis, respectively a differential response on day 1 *versus* day 2. Abundance of components of the mitophagy machinery was in general unaltered in response to acrolein exposure in rat lung. Collectively, this study demonstrates that acrolein inhalation acutely and dose-dependently disrupts the molecular regulation of mitochondrial metabolism in rat lung. Hence, understanding the effect of acrolein on mitochondrial function will provide a scientifically supported reasoning to shortlist aldehydes regulation in tobacco smoke.

Keywords: pulmonary toxicity, acrolein, metabolism, mitochondria, molecular mechanisms, cigarette smoke

Introduction

Chronic obstructive pulmonary disease (COPD) is a leading cause of morbidity and mortality worldwide (1). Exposure to tobacco smoke, which consists of a complex mixture of over 6000 chemicals, is the main risk factor for developing COPD (2, 3). One particular class of chemicals formed during the pyrolysis and combustion of tobacco is aldehydes, such as acrolein, which, due to its α,β -unsaturated structure, is considered as one of the most reactive (4, 5). Levels of acrolein in cigarette smoke (CS) vary around 1.3-121.7 $\mu\text{g}/\text{cigarette}$ (i.e., 2.1-110.4 ppm) depending on brand and smoking regime (6).

Acrolein is a primary (respiratory) irritant and considered to represent approximately ninety percent of the smoking-associated known non-cancer disease risk (7-9). Previous literature suggested a link between acrolein exposure and abnormalities in structure and function of the airways (10). Moreover, acrolein is able to induce multiple cellular events considered to be central in COPD pathogenesis (e.g., inflammation, oxidative stress and tissue remodeling) (9). Importantly, recent human studies highlight a link between aldehyde dehydrogenase, an enzyme that detoxifies aldehydes (11), and lung function. This is illustrated by a study in a Japanese general population which identified an association between the presence of an inactive allele of aldehyde dehydrogenase and incidence of smoking-related chronic airway obstruction (12). Although these studies suggest an association between exposure of the airways to acrolein (as a component of CS), the underlying molecular mechanisms that lead to abnormalities in lung structure/function and initiation of COPD-associated cellular processes remain obscure.

In the last few years, mitochondrial dysfunction has been postulated as a key mechanism underlying the pathogenesis of several (smoking-related) lung diseases, including COPD (13, 14).

Indeed, mitochondrial dysfunction is known to trigger multiple cellular processes that are also central to COPD pathogenesis (13, 14) and abnormalities in mitochondrial morphology have been described in airway epithelial cells of COPD patients or in cells of the airways in response to CS extract exposure (15-20). Moreover, a study by Cloonan *et al.* supported that mitochondrial dysfunction is causally involved in COPD pathogenesis by demonstrating prevention of CS-induced mitochondrial dysfunction in cells of the airways of mice (e.g., *Irf2*-deficiency, low-iron diet) protected against the development of COPD-like features (21).

Mitochondria are dynamic organelles in which homeostasis is controlled by an interplay of processes including mitochondrial biogenesis, mitophagy, and mitochondrial fusion and fission (13). The process of mitochondrial biogenesis is tightly regulated by the Peroxisome Proliferator-Activated Receptor (PPAR) Gamma Coactivator 1

(PPARGC1) signaling cascade, in which Peroxisome Proliferator-Activated Receptor Gamma Coactivator 1 alpha (PPARGC1A) co-activators mediate numerous nuclear and mitochondrial transcription factors responsible for controlling the expression of mitochondrial metabolic constituents (22, 23). Mitophagy, on the other hand, is the process of selective degradation of damaged or defective mitochondria by autophagy driven by a family of specific proteins. Activation of mitochondrial receptors, such as BCL2 Interacting Protein 3 (BNIP3), BNIP3-Like (BNIP3L), and FUN14 Domain Containing 1 (FUNDC1), triggers receptor-mediated mitophagy, while a loss of mitochondrial membrane potential, accumulation of Phosphatase and tensin homolog (PTEN) Induced Kinase 1 (PINK1) and recruitment/activation of Parkin RBR E3 Ubiquitin Protein Ligase (PRKN) on the outer mitochondrial membrane act as signals to initiate ubiquitin-mediated mitophagy. Subsequently, both pathways require general autophagy proteins to prime proteins for elimination by the autophagic-lysosomal pathways (24).

As mitochondrial biogenesis and mitophagy require fusion and fission, specific fusion associated proteins Mitofusin 1 and 2 (MFN1 and MFN2), OPA1, Mitochondrial Dynamin Like GTPase (OPA1), and fission related proteins Dynamin-1-Like (DNM1L) and Fission, mitochondrial 1 (FIS1) are crucial to facilitate adequate mitochondrial quality control (25).

These processes, (i.e., mitochondrial biogenesis and mitophagy) are critical in maintaining mitochondrial quality control in response to inhaled toxicants in the airways. Although literature regarding the mechanisms of mitochondrial toxicity induced by acrolein is scarce, a few *in vitro* studies indicate that acrolein is able to impair mitochondrial morphology and mitochondrial function in cells of the airways (26-28). However, whether or not *in vivo* acrolein exposure affects mitochondrial content and the processes regulating this has been discussed to a limited extend in previous literature.

The primary aim of the current study is to assess the impact of acute acrolein inhalation *in vivo* on mitochondrial metabolic pathways as well as mitochondrial biogenesis and mitophagy in the lung. Therefore, rats were exposed to acrolein by nose-only inhalation (0-4 ppm; 4 h/day) for 1 or 2 consecutive days, after which activity and/or abundance of critical constituents of mitochondrial metabolic pathways as well as expression of key proteins and genes regulating the pathways of mitochondrial biogenesis and mitophagy were investigated in lung tissue.

Materials and methods

Acrolein exposure of rats

The animal exposure experiments were conducted at the United States Environmental Protection Agency (Durham, USA) as previously described by Snow *et al.* (29). All animal experiments were approved by the United States Environmental Protection Agency Institutional Animal Care and Use Committee.

Briefly, male Wistar rats (10-weeks old) were obtained from Charles Rivers Laboratories (Raleigh, North Carolina, USA). The rats were housed in a specific pathogen-free AAALAC-approved animal facility on a 12 h light/12 h dark cycle, in pairs in polycarbonate cages with hardwood chip bedding. Rats were provided *ad libitum* water and food (Rodent Chow 5001: Ralston Purina Laboratories, St Louis, Missouri, USA). After acclimation to nose-only exposure tubes (Lab Products, Seaford, Delaware, USA) for 2 consecutive days for 1 and 2 h respectively, adult Wistar rats (~12-weeks old) were nose-only exposed to air or acrolein (2 or 4 ppm), 4 h/day for 1 or 2 consecutive days (n=6/group; in total n=36) as previously described (29). The final desired concentrations of acrolein (CAS No. 107-02-8) were achieved by dilution of acrolein gas (1000 ppm cylinder) with filtered compressed air (supplied by a medical grade air compressor). During the nose-only exposure, chamber pressure, flow rates, temperature and relative humidity were controlled. The acute inhalation dose of 4 ppm acrolein is relevant as it is above the range of the environmental presence of acrolein (3.6 – 10.7 ppb) (30) and is in the (lower) range of levels found in one cigarette (i.e., 2.1-110.4 ppm) (6). Moreover, the concentration of acrolein used in this study is in line with prior *in vivo* acrolein exposure studies (9).

The rats were euthanized using an overdose of sodium pentobarbital (Fatal-Plus diluted 1:1 with saline; >200 mg/kg; I.P. Vortech Pharmaceuticals, Ltd., Dearborn, Michigan, USA) immediately (within 1 h) following 4 h of acrolein exposure at day 1 or immediately (within 1 h) following 2 days of consecutive acrolein exposure at day 2. The left lung lobe was dissected, snap-frozen in liquid nitrogen and stored at -80°C for further processing.

RNA isolation, cDNA synthesis and real-time quantitative PCR analysis

Lung tissues were crushed by a mortar while frozen. A handheld PRO Scientific Bio-Gen PRO200 homogenizer was used to homogenize approximately 50-100 mg of powdered lung tissue in 1 mL TRIzol™ Reagent (Invitrogen™, USA) for 2 x 10 s at maximum speed. Next, the homogenates were processed per the manufacturer's protocol (Catalog number 15596026 and 15596018, Invitrogen™). Quantity and purity of the RNA samples were determined by using the NanoDrop ND 1000 UV-visible spectrophotometer (Isogen Life Sciences, de Meern, the Netherlands).

RNA quality (i.e., degradation) was evaluated by running approximately 400-1000 ng RNA of each sample dissolved 1:10 in Loading Dye (Invitrogen™) in a 2% (w/v) agarose

gel in 0.5 x Tris-borate EDTA stained with Sybr Safe DNA gel Stain (Invitrogen™) for approximately 60 min and run at 100 Volt.

Reverse transcription of 400 ng of total RNA was conducted using iScript™ cDNA synthesis kit (Bio-Rad, Veenendaal, the Netherlands) according to the manufacturer's protocol including a no reverse transcription control and a no template control. The cDNA was diluted in Milli-Q (1:50) and stored at -20°C until use.

Real-time quantitative PCR amplification of genes of interest was conducted by mixing 4.4 µL of 1:50 diluted cDNA, 5 µL 2xSensiMix™ SYBR® & Fluorescein Kit (Bioline, Alphen aan de Rijn, the Netherlands) and 0.6 µL target and species-specific primers in white LightCycler480 384-multiwell plates (Roche, Basel, Switzerland). In accordance with the manufacturer's instructions, the following thermal cycling protocol was run on the Roche LightCycler480 machine (Roche): 10 min at 95°C, 55 cycles of 10 s at 95°C, 20 s at 60°C. Melt curves were analyzed using LightCycler480 software (Roche) and gene expression analysis was conducted using LinRegPCR software 2014.x (the Netherlands). In addition, a correction factor was calculated using GeNorm software 3.4 (Primerdesign, Southampton, USA) based on the expression of a combination of at least four reference genes (*B2m*, *Hprt1*, *Ppia*, *Rpl13A*, *Tuba1a*) in order to normalize the expression of mRNA transcripts of interest. A list of primers sequences used is shown in Table S1.

DNA isolation and mitochondrial DNA copy number

Approximately 10-30 mg of powdered left lung lobe was dissolved in 250 µL lysis buffer (0.1 M Tris/HCl pH 8.5, 0.005 M EDTA pH 8.0, 0.2% (w/v) sodium dodecyl sulphate, 0.2 M NaCl) at room temperature. Thereafter, Proteinase K (Qiagen, USA) (>600 mAU/mL) was added to the lysates (1:50). Following incubation overnight at 55°C, additional 250 µL lysis buffer was added to the lysates where after they were centrifuged at full speed 25,000 x g for 15 min. The supernatant was taken and DNA was precipitated by adding 500 µL isopropanol and shaking vigorously. The DNA pellets were subsequently washed twice using 70% ethanol. After evaporation of the ethanol, the DNA pellets were dissolved in 125 µL TE buffer (10 mM Tris/HCl pH 8.0, 1 mM EDTA pH 8.0) and incubated at 55°C for 2 h. Lastly, the samples were incubated overnight at 4°C and subsequently stored at -20°C until use.

Quantity and purity of the DNA samples were determined by using the NanoDrop ND 1000 UV-visible spectrophotometer (Isogen Life Sciences). Diluted DNA samples (1:50 in TE buffer) were analyzed for expression of mitochondrial DNA (mtDNA), *mitochondrially encoded cytochrome c oxidase II* (*Mt-co2*), and genomic DNA, *peptidylprolyl isomerase A* (*Ppia*), (Table S1) using real-time quantitative PCR (see 'RNA isolation, cDNA synthesis and real-time quantitative PCR analysis' section). Assessment of the ratio of mtDNA *versus* genomic DNA yielded mtDNA copy numbers.

Western blotting

Whole-cell lysates for western blotting were generated by homogenizing approximately 50 mg of powdered left lung lobe in 600 μ L Immunoprecipitation lysis buffer (50 mM Tris pH 7.4, 150 mM NaCl, 10% (v/v) glycerol, 0.5% Nonidet P40, 1 mM EDTA) including PhosSTOP Phosphatase and cOmplete, Mini, EDTA-free Protease Inhibitor cocktail tablets (both Roche) for 5 s at medium speed using a handheld PRO Scientific Bio-Gen PRO200 homogenizer. Following homogenizing, the whole tissue lysates were rotated for 30 min in the cold room and centrifuged at 20,000 \times g for 30 min at 4°C. The protein content was assessed in the supernatant of the whole tissue lysates with the Pierce™ BCA Protein Assay Kit according to the manufacturer's protocol (Catalog number 23225 and 23227, Thermo Fisher Scientific, Rockford, USA). The supernatant fraction was diluted (1 μ g/ μ L) in a final concentration of 1 \times Laemmli buffer (0.25 M Tris pH 6.8, 8% (w/v) sodium dodecyl sulphate, 40% (v/v) glycerol, 0.4 M dithiothreitol, 0.02% (w/v) Bromophenol Blue) and boiled for 5 min at 100°C before storage at -80°C until further analysis.

The samples were run, 10 μ g of protein per lane, through a Criterion XT Precast 4-12 or 12% Bis-Tris gel (Bio-Rad) in 1 \times MES running buffer (Bio-Rad). Two protein ladders or more were loaded on each gel (Precision Plus Protein™ All Blue Standards #161-0373, Bio-Rad). Electrophoresis (100-130 V for 1 h) was used to separate the proteins, followed by electroblotting (Bio-Rad Criterion Blotter) (100 V for 1 h) in order to transfer the proteins on the gel to a 0.45 μ M nitrocellulose transfer membrane (Bio-Rad). nitrocellulose membranes were stained with 0.2% Ponceau S in 1% acetic acid (Sigma-Aldrich, Zwijndrecht, the Netherlands) for 5 min, followed by a Milli-Q wash and imaging using the Amersham™ Imager 600 (GE Healthcare, Eindhoven, the Netherlands) in order to quantify total protein content. After washing off the Ponceau S staining, membranes were blocked for 1 h in 3% (w/v) non-fat dry milk (Campina, Eindhoven, the Netherlands) in Tween20 Tris-buffered saline (20 mM Tris, 137 mM NaCl, 0.1% (v/v) Tween20, pH 7.6). Thereafter, membranes were washed with Tween20 Tris-buffered saline and incubated overnight at 4°C with a target-specific primary antibody (Table S2) diluted 1:500-1:2,000 in Tween20 Tris-buffered saline with 3% (w/v) Bovine Serum Albumin or non-fat dry milk. Membranes were subsequently washed and incubated with a horseradish peroxidase-conjugated secondary antibody (Table S2) diluted 1:10,000 in 3% (w/v) non-fat dry milk in Tween20 Tris-buffered saline for 1 h at room temperature. Next, the membranes were washed and incubated for 3 min with either 0.25 \times Supersignal West FEMTO or 0.5 \times Supersignal West PICO Chemiluminescent Substrate (Thermo Fisher Scientific, Landsmeer, the Netherlands), and visualized using the Amersham™ Imager 600 (GE Healthcare). Original unaltered images were quantified with Image Quant software (GE Healthcare). Original western blots were corrected for total protein loading content assessed by Ponceau S staining over the entire size range of proteins (250 kDa - 10 kDa). Included representative images in the figures of this manuscript have been adjusted for brightness and contrast equally throughout

the picture. The 75 kDa Ponceau S band in the figures is representative for the whole Ponceau S staining, as well as the selected band of one animal is reflecting the changes observed in the whole group (n=6/group).

Metabolic enzyme activity assays

Lysates for assessment of metabolic enzyme activity were generated by homogenizing approximately 10-30 mg of powdered left lung lobe in 350 μ L SET buffer (pH 7.4: 250 mM sucrose, 2 mM EDTA, 10 mM Tris) for 5 s at medium speed using a handheld PRO Scientific Bio-Gen PRO200 homogenizer. Following homogenizing, the lysates were incubated on ice for 15 min and centrifuged at 20,000 x g for 10 min at 4°C. The Pierce™ BCA Protein Assay Kit was used to examine total protein content in the whole-cell lysate supernatant according to the manufacturer's protocol (Catalog number 23225 and 23227, Thermo Fisher Scientific). The supernatant of the homogenates were diluted in 5% Bovine Serum Albumin in Milli-Q (1:4) and stored at -80°C until further analysis of Hydroxyacyl-Coenzyme A Dehydrogenase (HADH) and Phosphofructokinase (PFK).

HADH

Assessment of HADH enzyme activity was conducted as previously described (EC 1.1.1.35) (31). Undiluted samples were mixed with reagent (0.22 mM NADH, 100 mM tetrapotassium pyrophosphate pH 7.3) followed by initiation of the reaction by addition of 2.3 mM acetoacetyl-CoA. Samples were spectrophotometrically analyzed in duplicate at 340 nM at 37°C using a Multiskan Spectrum plate reader (Thermo Labsystems, Breda, the Netherlands). Total protein content of the samples was used as correction factor in order to calculate HADH enzyme activity by slope determination.

PFK

PFK enzyme activity was assessed as previously described (EC 2.7.1.11) (32), by mixing undiluted samples with reagent (48.8 mM Tris, 7.4 mM $\text{MgCl}_2 \cdot 6\text{H}_2\text{O}$, 74 mM KCl, 384 μ M KCN, 2.8 mM ATP, 1.5 mM DTT, 0.3 mM NADH, 0.375 U/mL aldolase, 0.5625 U/mL glycerol-3-phosphate dehydrogenase and 7.425 U/mL triose phosphate isomerase, pH 8.0). Thereafter, the reaction was initiated by addition of fructose-6-phosphate (30.6 mM) in Tris buffer (49.5 mM, pH 8.0). Analysis of the samples was spectrophotometrically conducted in duplicate at 340 nM at 37°C using a Multiskan Spectrum plate reader (Thermo Labsystems). PFK enzyme activity was calculated by correction for total protein content of the samples.

L-lactate assay

Whole tissue lysates for assessment of L-lactate were generated by homogenizing approximately 10-30 mg of powdered left lung lobe in 250 μ L lactate assay buffer for 10-15 passes at medium speed using a handheld PRO Scientific Bio-Gen PRO200 homogenizer on ice. Next, the lysates were centrifuged at 20,000 x g for 5 min at 4°C. The supernatant was collected and the endogenous enzyme lactate dehydrogenase was

removed using perchloric acid and potassium hydroxide deproteinization by ensuring a final pH 6.5-8. Subsequently, L-lactate levels were examined in undiluted samples in duplicate according to the manufacturer's protocol (L-lactate Assay kit colorimetric, ab65331, Abcam, Cambridge, USA). Measurement of L-lactate was conducted at 450 nm.

Statistical analysis

Data are presented as mean fold change compared to air control \pm standard error of the mean (SEM). Extreme outliers were excluded in the mRNA data file based on both boxplot analysis (i.e., values more than three interquartile ranges from the end of a box) in IBM Statistics SPSS 25 and melt curve/peak analysis using LightCycler480 software (Roche). Statistical analyses were conducted in GraphPad Prism 8.0 software (La Jolla, California, USA). Statistical significance was assessed by testing normal distribution of the data with the Shapiro-Wilk test. The difference between three groups (2 or 4 ppm acrolein exposure *versus* air control) was analyzed in case of normal distributed data by one-way ANOVA and a Dunnett's post-hoc test for multiple comparisons or in case of non-normal distribution by a Kruskal-Wallis test followed by a Dunn's multiple comparisons test. In case of analysis of the difference between two groups (4 ppm acrolein exposure *versus* air control), a two-tailed unpaired parametric t-test was used. Statistical significance was considered if p-values were below 0.05 (* $p < 0.05$) or 0.01 (** $p < 0.01$) and a trend was indicated if # $p < 0.1$. GraphPad Prism 8.0 was used to graph the data.

Results

Altered transcript abundance of inflammation and oxidative stress markers in response to acute acrolein inhalation

In accordance with previous findings, showing the influx of inflammatory cells in response to acrolein exposure in rats (29), we observed that exposure to 4 ppm acrolein resulted in increased transcript levels of the inflammatory genes *NFκB inhibitor alpha* (*Nfkbia*) (1 Day: FC=2.34±0.56, $p<0.05$) and *C-C motif chemokine ligand 2* (*Ccl2*) (1 Day: FC=4.25±0.91, $p<0.01$ and 2 Day: FC=13.30±1.70, $p<0.01$) (Fig. S1A). In contrast, exposure to 2 ppm acrolein resulted in decreased mRNA levels of *Nfkbia* (2 Day: FC=0.60±0.03, $p<0.1$) (Fig. S1A). The mRNA levels of *C-X-C motif chemokine ligand 1* (*Cxcl1*), responsible for attracting neutrophils to the site of inflammation, were decreased after 2 days of 2 ppm (FC=0.55±0.05, $p<0.01$) and following 1 or 2 days of 4 ppm acrolein inhalation (1 Day: FC=0.71±0.09, $p<0.1$; 2 Day: FC=0.63±0.09, $p<0.05$) (Fig. S1B). Regarding transcript levels of anti-oxidant genes, although transcript abundance of *superoxide dismutase 1* (*Sod1*) was unaltered in response to acrolein inhalation, mRNA levels of *superoxide dismutase 2* (*Sod2*) were significantly elevated after 2 days of 4 ppm acrolein exposure (FC=1.56±0.17, $p<0.05$) (Fig. S1C). No significant differences were found in transcript abundance of *aldehyde dehydrogenase 2* (*Aldh2*) following acrolein exposure (Fig. S1D). Moreover, we have analyzed protein levels of cleaved caspase-3 as well as the abundance of the ratio of *BCL2 associated X, apoptosis regulator* and *Bcl2, apoptosis regulator* (*Bax/Bcl2*), all established markers of apoptosis, and observed that levels were unchanged or decreased (Cleaved caspase-3: 2 Day: 4 ppm: FC=0.54±0.12, $p<0.05$) suggesting no activation of apoptosis in response to acrolein in our study (Fig. S2).

Acrolein inhalation acutely affects mitochondrial and non-mitochondrial metabolic pathways in rats

To study the effect of acrolein exposure on indices of mitochondrial content and metabolism, we first assessed mtDNA copy number as a marker of mitochondrial content.

As depicted in Fig. 1A, although mtDNA levels appeared to be higher after 1 day of exposure (4 ppm: $p=0.18$), no significant differences in mtDNA copy number were observed in acrolein- versus air-exposed rats.

Next, the impact of acrolein inhalation on key constituents of mitochondrial and non-mitochondrial metabolic pathways in rat lung was evaluated by investigating the activity and/or abundance of components of the electron transport chain, fatty acid beta-oxidation pathway, tricarboxylic acid cycle, and glycolysis.

Firstly, when investigating protein levels of both nuclear-encoded and mitochondrial-encoded sub-units of electron transport chain complexes, protein levels of

mitochondrial-encoded sub-unit of complex IV as well as nuclear-encoded sub-units of complexes I and II were unaltered after acrolein exposure (Fig. 1B-D). In contrast, we observed that the protein abundance of nuclear-encoded sub-units associated with electron transport chain complexes III and V were significantly lower ($p < 0.05$) following 1 day of exposure to 4 ppm acrolein (Fig. 1B and D). In line, protein levels of Translocase Of Outer Mitochondrial Membrane 20 (TOMM20), a critical outer mitochondrial membrane receptor, were also significantly decreased ($p < 0.05$) in response to 1 day of acrolein exposure (4 ppm) (Fig. 1B and E). Strikingly, the observed differences in protein abundance of all of these mitochondrial proteins in response to 4 ppm acrolein were no longer observed after 2 days of exposure (Fig. 1B, D, and E). Inhalation of a lower dose of acrolein, 2 ppm, did not alter abundance of these analyzed proteins, with the exception of increased ($p < 0.1$) protein levels of complex III following exposure for 2 consecutive days (Fig. 1B and D).

In addition, evaluation of mRNA levels of nuclear-encoded genes of the respective electron transport chain sub-units revealed no alterations in transcript levels of those investigated nuclear-encoded electron transport chain constituents, except for *succinate dehydrogenase complex iron sulfur subunit B (Sdhb)* (subunit of complex II) mRNA levels which were significantly decreased ($p < 0.01$) in response to acrolein exposure (Fig. 1F). In addition, mRNA levels of *cytochrome c oxidase subunit 4i1 (Cox4i1)* (sub-unit of complex IV) were significantly elevated ($p < 0.01$) in rat lung after 2 consecutive days of 4 ppm acrolein exposure (Fig. 1F). In general, similar, but less pronounced, findings were shown in rats exposed to 2 ppm acrolein (Fig. 1F).

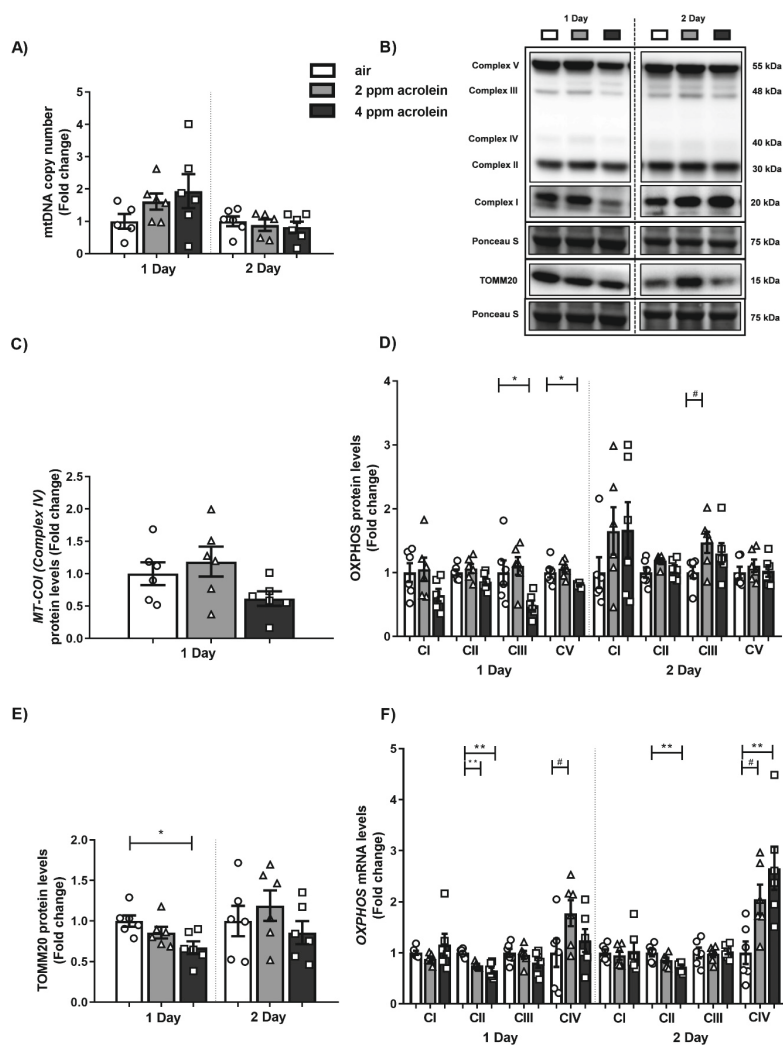


Figure 1. Acute acrolein exposure affects the abundance of sub-units of the electron transport chain in rat lung. Wistar rats were exposed by nose-only inhalation to air (control) or acrolein (2 or 4 ppm) for 4 h/day for 1 or 2 days (n=5-6/group). **(A)** Mitochondrial DNA (mtDNA) copy number, **(B-D)** protein and **(F)** mRNA levels of nuclear- and mitochondrial-encoded constituents of the electron transport chain (i.e., subunits of oxidative phosphorylation (OXPHOS) complexes I-V), as well as **(B, E)** protein abundance of TOMM20 in rat lung. Representative western blot images are shown of one animal/group reflective of the changes in the whole group as quantified in the corresponding graph. The dashed line indicates that the samples of day 1 and day 2 were loaded on (and selected from) different blots. Data are presented as mean fold change compared to air-exposed rats \pm SEM. Individual animals are represented by open circle (air), triangle (2 ppm acrolein) or square (4 ppm acrolein). Statistical differences between 2 or 4 ppm acrolein *versus* air were tested using an one-way ANOVA followed by a Dunnett's post-hoc test for multiple comparisons or in case of non-normal distribution a Kruskal-Wallis test followed by a Dunn's multiple comparisons test. Statistical significance is indicated as # $p < 0.1$, * $p < 0.05$ and ** $p < 0.01$ compared to air (control).

Besides assessing protein and transcript abundance of sub-units of the electron transport chain complexes, we also examined activity and abundance of constituents of the fatty acid beta-oxidation and tricarboxylic acid cycle. Exposure to acrolein did significantly alter activity levels of HADH, a rate-limiting enzyme in fatty acid beta-oxidation, in response to 2 ppm acrolein (1 Day: FC=0.78±0.07, $p<0.05$; 2 Day: FC=1.44±0.14, $p<0.05$), while acrolein did not affect transcript abundance of *hydroxyacyl-CoA dehydrogenase trifunctional multienzyme complex subunit alpha (Hadha)* and *acyl-CoA dehydrogenase, long chain (Acadl)* (Fig. S3A-C). On the other hand, transcript levels of *citrate synthase* were significantly increased in response to 4 ppm acrolein compared to control both after 1 and 2 days of exposure (1 Day: FC=1.48±0.14, $p<0.05$; 2 Day: FC=1.79±0.15, $p<0.05$) (Fig. S3D).

Subsequently, to examine the effect of acrolein exposure on glycolysis, we assessed activity and abundance of key components of the glycolytic pathway. While PFK activity was unaltered, L-lactate levels were significantly elevated ($p<0.05$) on day 1 in response to 4 ppm acrolein exposure (Fig. 2A and B). In addition, we evaluated protein and transcript abundance of Hexokinase 2 (HK2), responsible for the first step in glycolysis, and observed increases in HK2 protein as well as transcript levels of *Hk2* in response to 4 ppm acrolein exposure for 2 consecutive days ($p<0.05$ and $p<0.1$, respectively) (Fig. 2C and D).

Although no alterations were observed in the transcript abundance of *lactate dehydrogenase A (Ldha)*, *pyruvate kinase M1/2 (Pkm)*, *pyruvate dehydrogenase kinase 4 (Pdk4)* and *solute carrier family 2 member 1 (Slc2a1)* in acrolein-exposed rats compared to control, mRNA levels of *solute carrier family 2 member 4 (Slc2a4)* were lower following 1 day of 4 ppm acrolein exposure (FC=0.46±0.16, $p<0.1$) (Fig. S3E-H).

Overall, these results suggest alterations in the abundance and activity of constituents of key metabolic processes, especially at the level of the sub-units of electron transport chain complexes, as well as a shift towards a more glycolytic metabolism in acrolein-exposed rat lung.

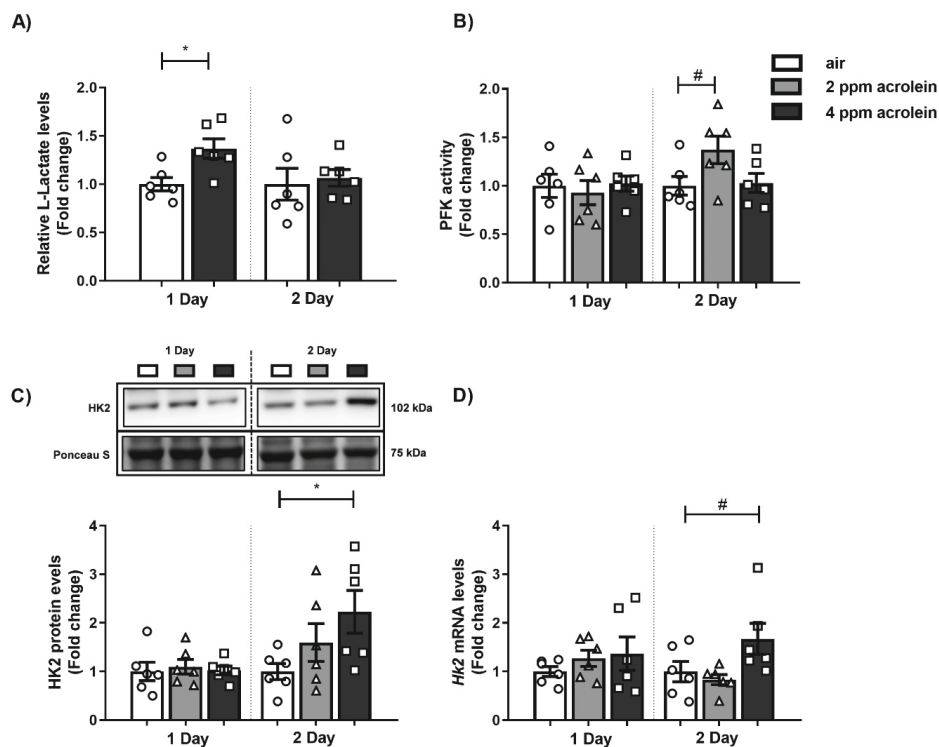


Figure 2. Alterations in activity and expression of key constituents of glycolysis in response to acrolein inhalation in rats. Wistar rats were exposed by nose-only inhalation to air (control) or acrolein (2 or 4 ppm) for 4 h/day for 1 or 2 days ($n=6/\text{group}$). (A) Relative L-Lactate levels are presented. Statistical differences between 4 ppm acrolein *versus* air were tested using a two-tailed unpaired parametric t-test. (B) PFK activity, (C) protein abundance of HK2, and (D) transcript levels of *Hk2* in rat lung homogenates. Representative western blot images are shown of one animal/group reflective of the changes in the whole group as quantified in the corresponding graph. The dashed line indicates that the samples of day 1 and day 2 were loaded on (and selected from) different blots. Statistical differences between 2 or 4 ppm acrolein *versus* air were tested using an one-way ANOVA followed by a Dunnett's post-hoc test for multiple comparisons. Data are presented as mean fold change compared to air-exposed rats \pm SEM. Individual animals are represented by open circle (air), triangle (2 ppm acrolein) or square (4 ppm acrolein). Statistical significance is indicated as * $p<0.1$, * $p<0.05$ and ** $p<0.01$ compared to air (control).

The molecular regulation of mitochondrial biogenesis is disrupted in rats acutely exposed to acrolein

In order to examine if the abovementioned alterations in mitochondrial metabolic pathways were associated with changes in regulation of mitochondrial biogenesis, we assessed the abundance of key regulators of mitochondrial biogenesis in response to acute acrolein exposure in rat lung.

Firstly, we studied the abundance of transcriptional co-activators of the PPARGC1 signaling cascade, a central network associated with the regulation of mitochondrial biogenesis and cellular mitochondrial energy metabolism. As shown in Fig. 3A and B respectively, only 4 ppm acrolein exposure resulted in decreased ($p < 0.1$) protein as well as transcript levels of PPARGC1A, respectively on day 1 and day 2. In contrast, transcript abundance of *Ppargc1b*, a homologue of *Ppargc1a*, was significantly elevated (2ppm: $p < 0.05$; 4 ppm: $p < 0.01$) following acrolein inhalation for 2 consecutive days (Fig. 3C), and no differences were observed in transcript levels of *PPARG related coactivator 1* (*Pprc1*) (Fig. S4A).

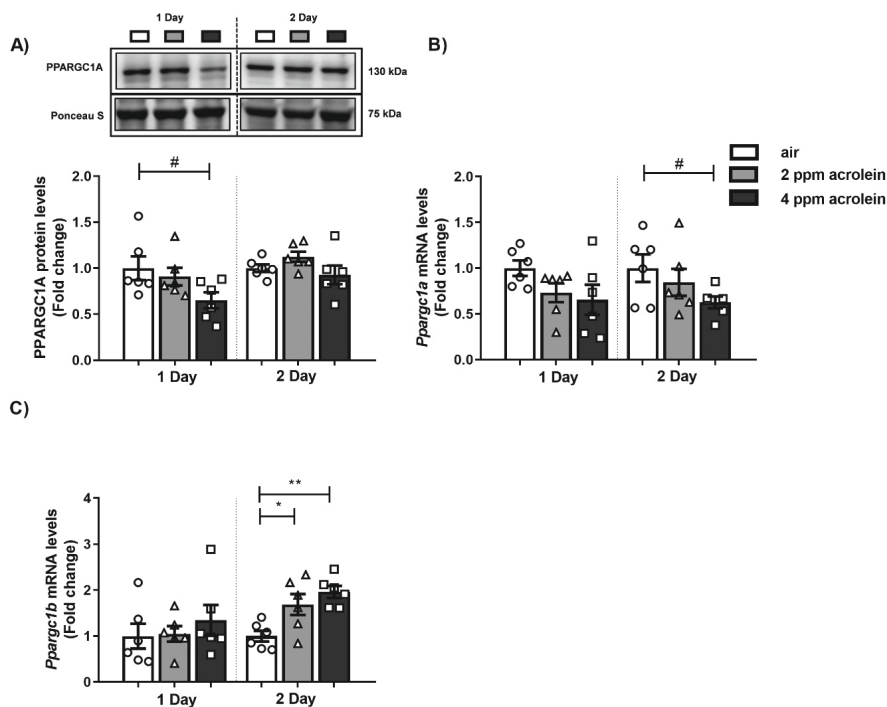


Figure 3. Abundance of PPARGC1 molecules is altered in rats acutely exposed to acrolein. Wistar rats were exposed by nose-only inhalation to air (control) or acrolein (2 or 4 ppm) for 4 h/day for 1 or 2 days ($n=6$ /group). Protein levels of **(A)** PPARGC1A and gene expression of **(B)** *Ppargc1a* and **(C)** *Ppargc1b* in rat lung. Representative western blot images are shown of one animal/group reflective of the changes in the whole group as quantified in the corresponding graph. The dashed line indicates that the samples of day 1 and day 2 were loaded on (and selected from) different blots. Data are presented as mean fold change compared to air-exposed rats \pm SEM. Individual animals are represented by open circle (air), triangle (2 ppm acrolein) or square (4 ppm acrolein). Statistical differences between 2 or 4 ppm acrolein *versus* air were tested using a one-way ANOVA followed by a Dunnett's post-hoc test for multiple comparisons or in case of non-normal distribution a Kruskal-Wallis test followed by a Dunn's multiple comparisons test. Statistical significance is indicated as * $p<0.1$, * $p<0.05$ and ** $p<0.01$ compared to air (control).

Next, we assessed whether acrolein exposure affected the abundance of PPARGC1-coactivated transcription factors involved in the regulation of mitochondrial biogenesis and mitochondrial energy metabolism. While protein as well as mRNA levels of some investigated transcription factors of the PPARGC1 network were largely unaltered (Fig. 4A, B, D, E; Fig. S4B-E), decreased mRNA levels of *nuclear respiratory factor 1* (*Nrf1*) (1 Day: 2 ppm: $p<0.1$; 2 Day: 2 ppm: $p<0.01$ and 4 ppm: $p<0.05$) and *peroxisome proliferator-activated receptor alpha* (*Ppara*) (1 Day: 2 ppm: $p<0.1$ and 4 ppm: $p<0.01$) were observed in response to exposure to acrolein as shown in Fig. 4C and F.

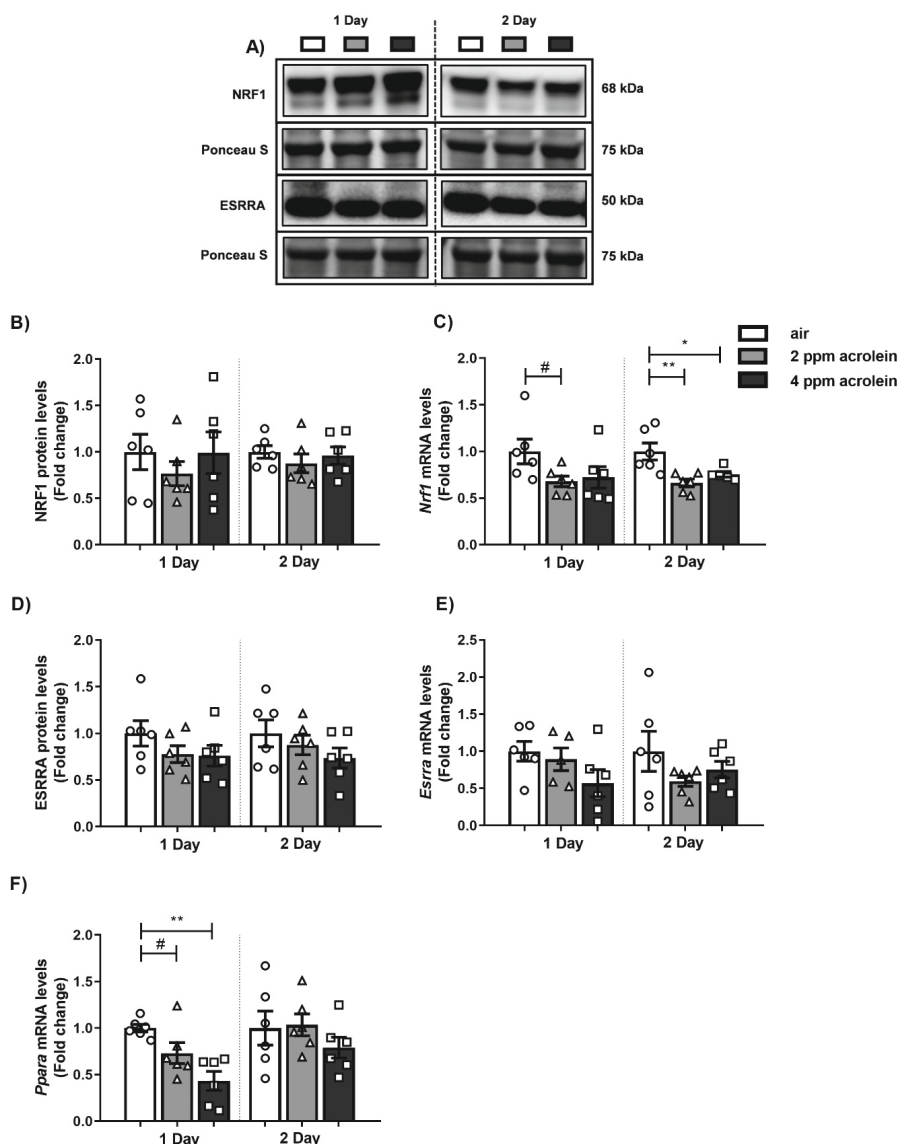


Figure 4. Acute acrolein inhalation affects the abundance of PPARGC1-coactivated transcription factors. Wistar rats were exposed by nose-only inhalation to air (control) or acrolein (2 or 4 ppm) for 4 h/day for 1 or 2 days (n=5-6/group). (A) Protein levels of (B) NRF1 and (D) ESRR as well as transcript abundance of (C) *Nrf1*, (E) *Esrra*, and (F) *Ppara* in rat lung. Representative western blot images are shown of one animal/group reflective of the changes in the whole group as quantified in the corresponding graph. The dashed line indicates that the samples of day 1 and day 2 were loaded on (and selected from) different blots. Data are presented as mean fold change compared to air-exposed rats \pm SEM. Individual animals are represented by open circle (air), triangle (2 ppm acrolein) or square (4 ppm acrolein). Statistical differences between 2 or 4 ppm acrolein versus air were tested using an one-way ANOVA followed by a Dunnett's post-hoc test for multiple comparisons. Statistical significance is indicated as * $p < 0.1$, * $p < 0.05$ and ** $p < 0.01$ compared to air (control).

In conclusion, these findings indicate that acute acrolein inhalation disrupts the molecular regulation of mitochondrial biogenesis, in particular at the level of the PPARGC1 signaling cascade.

The molecular regulation of mitophagy and mitochondrial dynamics following acute acrolein inhalation

Besides mitochondrial biogenesis, mitophagy (i.e., mitochondrial-specific autophagy) plays an essential role in regulating mitochondrial content and function. In order to study the impact of acrolein inhalation on mitophagy, we explored protein and mRNA levels of key regulators of receptor- and ubiquitin-mediated mitophagy.

As depicted in Fig. 5A, B, and D, BNIP3L protein levels were reduced in response to 4 ppm acrolein (1 Day: $p<0.1$; 2 Day: $p<0.01$), while BNIP3 protein abundance was increased (2 ppm: $p<0.1$; 4 ppm: $p<0.05$) in response to 2 days of acrolein exposure. In addition, mRNA transcript abundance of these two key receptor proteins involved in receptor-mediated mitophagy, were unaltered in response to acrolein (Fig. 5C and E). Moreover, protein and mRNA levels of FUNDC1, also a key constituent of receptor-mediated mitophagy, were not changed in rat lung after exposure to acrolein (Fig. 5A, F, and G). In addition, no significant changes in protein and mRNA levels of regulators of ubiquitin-mediated mitophagy (PINK1 and PRKN) were observed in rats following acute acrolein inhalation (Fig. S5).

As mitophagy requires general autophagy proteins in order to prime proteins for degradation by the autophagic-lysosomal pathways, we studied the abundance of general autophagy proteins. As shown in Fig. S6, protein and transcript levels of all investigated general autophagy-related constituents (GABA Type A Receptor Associated Protein Like 1 (GABARAPL1), (ratio) Microtubule-Associated Protein 1 Light Chain 3 Beta (MAP1LC3B), and *Becn1* (*Becn1*)) were unchanged in rats acutely exposed to acrolein, however, Sequestosome 1 (SQSTM1) protein levels were increased in response to the highest dose of acrolein for 2 consecutive days ($FC=1.47\pm0.12$, $p<0.01$).

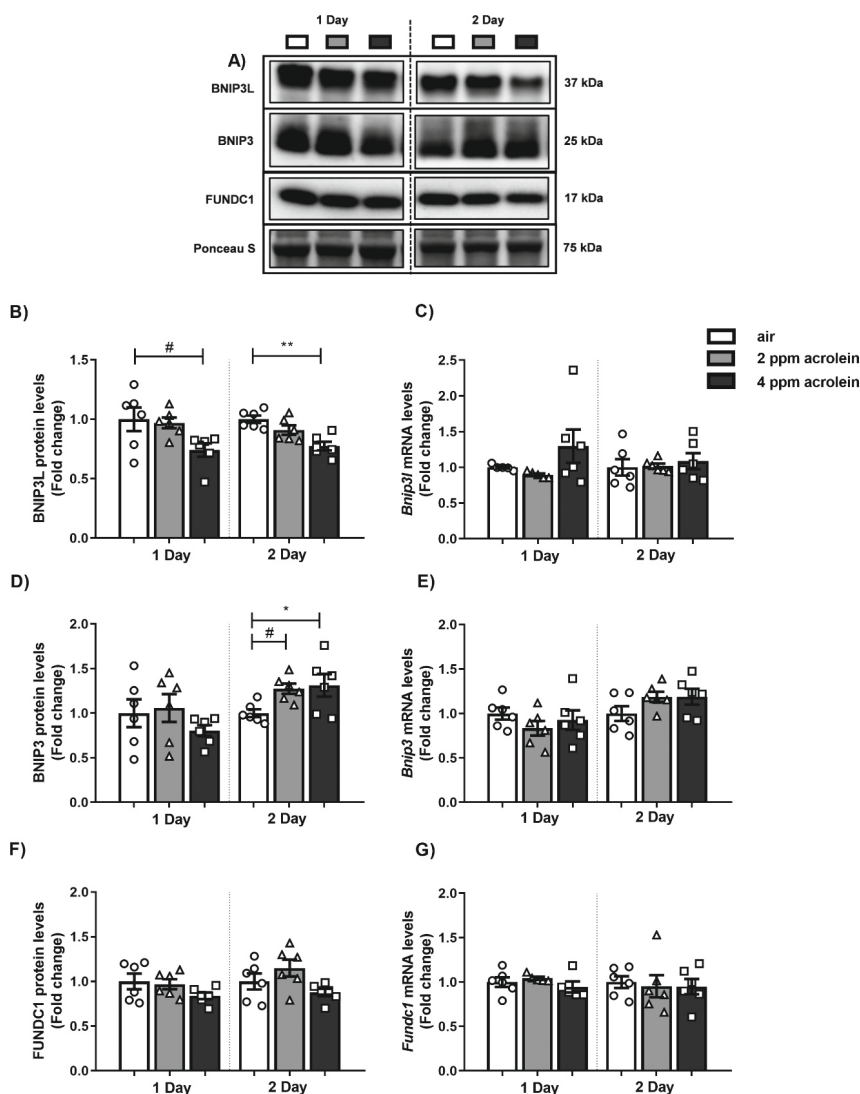


Figure 5. Altered abundance of key constituents of receptor-mediated mitophagy in response to acrolein exposure in rats. Wistar rats were exposed by nose-only inhalation to air (control) or acrolein (2 or 4 ppm) for 4 h/day for 1 or 2 days (n=5-6/group). Receptor-mediated mitophagy-associated (A) protein abundance of (B) BNIP3L, (D) BNIP3, and (F) FUNDC1, as well as transcript abundance of (C) *Bnip3l* and (E) *Bnip3*, and (G) *Fundc1* in rat lung tissue are presented. Representative western blot images are shown of one animal/group reflective of the changes in the whole group as quantified in the corresponding graph. The dashed line indicates that the samples of day 1 and day 2 were loaded on (and selected from) different blots. Data are presented as mean fold change compared to air-exposed rats \pm SEM. Individual animals are represented by open circle (air), triangle (2 ppm acrolein) or square (4 ppm acrolein). Statistical differences between 2 or 4 ppm acrolein *versus* air were tested using an one-way ANOVA followed by a Dunnett's post-hoc test for multiple comparisons or in case of non-normal distribution a Kruskal-Wallis test followed by a Dunn's multiple comparisons test. Statistical significance is indicated as * $p < 0.01$, * $p < 0.05$ and ** $p < 0.01$ compared to air (control).

In summary, these data suggest minor alterations in the molecular regulation of the mitophagy machinery, in particular in receptor-mediated mitophagy, while in general no changes were identified in the abundance of autophagy-related constituents in response to acute acrolein exposure in rats.

Considering the essential role of mitochondrial dynamics together with mitochondrial biogenesis and mitophagy to maintain mitochondrial homeostasis, we next aimed to explore the impact of acrolein exposure on abundance of key constituents of fusion and fission in rat lung.

Although mRNA levels of regulators of fusion *Mfn1* and *Mfn2* were not affected by acrolein inhalation, transcript abundance of *Opa1* was significantly increased ($p < 0.05$) in response to 4 ppm acrolein exposure for 1 day (Fig. 6A-C). In addition, with regard to fission, transcript levels of *Dnm1l* were significantly elevated after 2 days of acrolein exposure (2 ppm: $p < 0.05$; 4 ppm: $p < 0.01$), while *Fis1* mRNA levels were decreased ($p < 0.01$) in response to the highest dose of acrolein after 1 day (Fig. 6D and E). Collectively, these results indicate alterations in the molecular regulation of fusion and fission which are critical processes involved in mitochondrial dynamics.

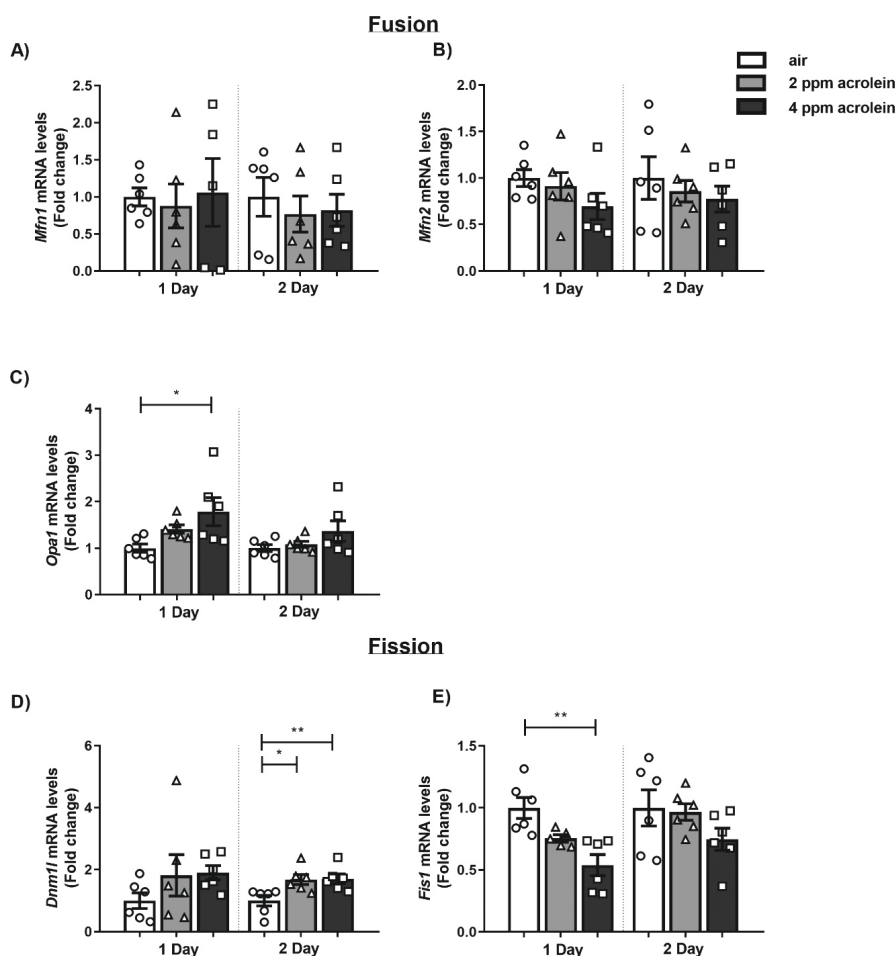


Figure 6. Transcript expression of regulators of mitochondrial dynamics is disrupted in rats exposed to acrolein. Wistar rats were exposed by nose-only inhalation to air (control) or acrolein (2 or 4 ppm) for 4 h/day for 1 or 2 days (n=5-6/group). Fusion-associated gene expression of (A) *Mfn1*, (B) *Mfn2*, and (C) *Opa1*, as well as transcript abundance of fission-associated genes (D) *Dnm1l* and (E) *Fis1* in rat lung. Data are presented as mean fold change compared to air-exposed rats \pm SEM. Individual animals are represented by open circle (air), triangle (2 ppm acrolein) or square (4 ppm acrolein). Statistical differences between 2 or 4 ppm acrolein *versus* air were tested using an one-way ANOVA followed by a Dunnett's post-hoc test for multiple comparisons or in case of non-normal distribution a Kruskal-Wallis test followed by a Dunn's multiple comparisons test. Statistical significance is indicated as * $p < 0.05$ and ** $p < 0.01$ compared to air (control).

Discussion

In this study, we investigated the acute effect of acrolein inhalation, a component of CS, on key regulators of mitochondrial content and function in rat lung. We observed that acrolein inhalation resulted in a dose-dependent and differential response on the activity and abundance of key constituents of mitochondrial metabolic pathways on day 1 *versus* day 2 in particular leading to a transient decrease in abundance of several subunits of electron transport chain complexes and to decreased protein levels of critical regulators involved in mitochondrial biogenesis.

Acrolein-induced inflammation and oxidative stress are well described in various *in vivo* and *in vitro* airway exposure models (9, 28, 33-38). In accordance to previous literature, acrolein exposure in our study induced inflammatory and *Sod2* gene expression, as well as a previously reported influx of inflammatory cells in bronchoalveolar and nasal lavage fluid illustrative of effective acrolein administration to the rat lungs (29). The observed decrease in expression of *Cxcl1* can be clarified by stress hormone-modulated neutrophilic inflammation and cell-specific extravasation of neutrophils as previously suggested by Snow *et al.* (29). Although, previous literature described the impact of acrolein inhalation on cell death and apoptosis *in vivo* (39, 40) and it has been shown that acrolein can induce apoptosis in cultured airway epithelial cells (26, 35, 41-43), we did not observe acrolein-induced apoptosis in our model.

Next, we focused on the impact of acrolein on the abundance of key constituents of mitochondrial metabolic pathways and observed in particular a decreased abundance of subunits of the electron transport chain. This is in line with previous studies reporting that acrolein exposure resulted in increased intracellular and mitochondrial ROS production, mtDNA damage, and disturbed mitochondrial metabolism in a variety of *in vitro* airway models and isolated rat liver mitochondria (26-28, 44). Interestingly, comparable findings have been described in multiple *in vitro* or *in vivo* (airway) models in response to CS (extract) (14-16, 21, 45, 46) or several aldehydes (47-49). The fact that mtDNA copy number did not change in our study while we did observe changes in the abundance of proteins involved in mitophagy and mitochondrial biogenesis could be explained by the fact that multiple copies of mtDNA exist in a mitochondrion, lack of evaluation of the activity of mitophagy and mitochondrial biogenesis *per se* (only the abundance of proteins involved in these processes) and timing of our analyses after exposure. Nevertheless, these results, in concert with data of our study, strongly suggest that aldehydes (i.e., acrolein) may mediate, at least part of, the detrimental effects that CS exerts on the molecular regulation of mitochondrial content and function in airway epithelial cells.

Furthermore, in light of the mentioned elevated ROS levels upon acrolein or CS exposure, interestingly in particular glycolysis is a susceptible process affected by changes in redox balances (50). This would be in line with our findings of elevated L-lactate levels

and increased abundance of HK2. Available literature also supports smoke-induced disruption of glycolytic metabolism, which has been described not only in cultured airway epithelial cells or *in vivo* models exposed to aldehydes (27, 44, 47, 51, 52) or CS (53, 54), but also in COPD (55-58). Our findings of unaltered mtDNA levels, decreased abundance of mitochondrial proteins (e.g., subunits of oxidative phosphorylation (OXPHOS) complexes) and increased lactate levels in response to acrolein suggest that mitochondria become less oxidative, while the number of mitochondria remains the same, which is at least partly in line with the findings from previous studies (26). Taken into account the above-mentioned findings, this can indicate an impaired aerobic respiration resulting in a shift to glycolytic energy metabolism.

To the best of our knowledge, there are only a few *in vitro* studies examining the effect of aldehydes on the regulation of mitochondrial biogenesis. In line with our data, these studies showed declined PPARGC1A protein levels in acrolein-exposed lung fibroblasts (28) or crotonaldehyde-exposed cardiomyocytes (48). Accordingly, while increased expression levels of PPARGC1A were observed in lung homogenates of mild COPD patients and in ex-smoking severe COPD patients or short-term CS extract-stimulated bronchial epithelial cells (18, 59, 60), decreased abundance of regulators of biogenesis were shown in moderate and severe COPD patients (60) and in *in vivo* subacute COPD models (61, 62). However, also opposite findings were reported (60, 63). Differences likely result from variation in duration of CS extract exposure, dose, and models investigated in those studies. Moreover, we observed a significantly increased transcript abundance of *Ppargc1b* after 2 days of exposure, which may be explained as a compensatory/repair response to mitochondrial damage elicited by acute acrolein exposure. The reductions in abundance of key regulators of mitochondrial biogenesis in response to acrolein that we observed in our study shed some light on the molecular mechanism potentially underlying acrolein-induced impairment of mitochondrial metabolism. Although a causal relationship between these reductions and impairment of mitochondrial metabolism upon exposure to acrolein cannot be concluded from our study, it is feasible that, due to the essential role of these regulators in the molecular control of the mitochondrial biogenesis program that is well described in mammalian cells (22, 23), these reductions serve as a molecular basis for these metabolic changes. In addition, it is well-known from studies in other cell types than lung cells that activation of the inflammatory NF- κ B pathway directly impedes on the activity of the PPARGC1 signaling network that controls mitochondrial biogenesis. For example, P65 (the main transcription factor mediating effects of NF- κ B activation) has been shown to be able to physically bind to PPARGC1 and reduces its expression thereby impeding its function (64) and blockade of the NF- κ B pathway prevented detrimental effects of inflammatory cytokines on mitochondrial metabolism (65). Although, the impact of acrolein on the NF- κ B pathway has been described as diverse and conflicting in literature depending on the dose and duration of acrolein exposure (9, 38, 66), it has been suggested that acrolein can induce an inflammatory response and activate the NF- κ B pathway (38),

e.g., as demonstrated in an *in vivo* study (67). Collectively, these findings suggest that inflammation-induced impairments in the PPARGC1 signaling network may well serve as the molecular mechanism underlying acrolein-induced abnormalities in mitochondrial metabolism as we observed in our study.

Although no striking differences were shown in the abundance of components of receptor- and ubiquitin-mediated mitophagy, elevated BNIP3 and reduced BNIP3L protein levels were observed in response to acrolein. To the best of our knowledge, only one study showed acute acrolein-induced mitophagy (26) as well as one study showed that CS-induced mitophagy is BNIP3L-dependent in human airway (epithelial) cells (68). More is known about ubiquitin-mediated mitophagy, as increased PINK1 and decreased PRK2 abundance has been demonstrated in various *in vitro/vivo* (airway) models of CS exposure (15, 19, 45, 69-71) as well as in lung tissue or bronchial epithelial cells of (ex-smoking) COPD patients (15, 18, 19, 71). However, whether or not mitophagy plays a protective role or contributes to CS-induced airway pathology remains to be established as illustrated in previous studies (15, 16, 19, 45, 69-73).

Previous research suggested increased autophagy in response to acrolein or crotonaldehyde in human lung epithelial cells or fibroblasts (26, 74, 75) and after formaldehyde inhalation in rats (76). Similar findings were reported in lung homogenates of COPD patients (77), in CS (extract)-exposed human cells of the airways (46, 68, 71, 77) and in CS-exposed mice (15, 77). However, autophagy-associated indices were mostly reported to be unchanged in our study suggestive of a different impact of acrolein and CS in various exposure models.

Due to the essential role of mitochondrial dynamics in controlling mitochondrial homeostasis, we further studied abundance of fusion and fission regulators. In line with our findings of increased *Dnm1l* transcript levels in response to acrolein inhalation, Wang *et al.* also demonstrated increased mitochondrial fission upon acrolein exposure in human lung cells (26). Collectively, previous studies have reported indications for reduced fusion and increased fission in COPD lung homogenates (15), alveolar epithelial cells of smokers (78), and *in vivo* (15) and *in vitro* smoke-exposure models (15-17, 20, 69, 70, 79). Discrepancies in abundance of regulators involved in mitochondrial dynamics in response to various types of CS in lung epithelial cells (18, 19, 46, 73), could be explained by variation in exposure models or duration of CS exposure as illustrated by Walczak *et al.* (63). Although we showed a disrupting effect of acrolein exposure on the transcriptional regulation of mitochondrial fusion and fission, further studies have to reveal the functional impact of acrolein on mitochondrial dynamics.

As our data, in concert with prior evidence, suggest acrolein-induced disruption of the molecular regulation of mitochondrial content/function and mitochondrial dysfunction

is being implicated in the pathogenesis of COPD, acrolein is an interesting potential target to be regulated in CS.

Acrolein, together with acetaldehyde and formaldehyde, are considered to be representative aldehydes for CS in all brands and human smoking regimes due to similar molecular structures, properties, precursors and mechanisms of formation and are extremely toxic due to local peak concentrations (5, 80-82). They are shortlisted for regulation by the World Health Organization Study Group on Tobacco Product Regulation due to their adverse impact on human health for which the current study provides more evidence (5, 80, 83). Potential reduction of aldehyde exposure per puff can be facilitated (5) e.g., by reducing sugar content (84), selection of type of tobacco (85), and cigarette design (6).

Previous studies indicated that the immunologic response and mechanism of cell death (apoptosis, oncosis or necrosis) following acrolein exposure may be dose- and cell type-related (9, 38). We found a lower induction of inflammatory gene expression after acute exposure to 2 ppm compared to 4 ppm acrolein. This coincided with the observed less pronounced changes in the expression of regulators of mitochondrial metabolism in response to 2 ppm acrolein, while exposure to 4 ppm resulted in significant deregulation of mitochondrial metabolism indicating that, not only the inflammatory response, but also modulation of other cellular processes depends on the dose and duration of exposure. Previous *in vivo* studies also reported dose-dependent biological effects ranging from lethal effects after short high dose acrolein exposure in rat up to 40,000 ppm (86) to lung inflammation and cell death in animals exposed up to 10 ppm (36, 40, 51). In general, the concentrations of acrolein (2 and 4 ppm) used in this study have been associated with milder effects on lung health in rat (30, 86) as for example depression of respiratory rate has been reported in animals exposed to 4.6 ppm (87) or 9.2 ppm (88).

This study, for the first time, provides a comprehensive overview of the impact of acrolein on the regulation of mitochondrial content and function in the lung. Nevertheless, our study has several limitations. Obviously, analyses were conducted in lung tissue homogenates which includes various cell types, so effects of acrolein on specific cell types cannot be dissected from this study. However, previous *in vitro* studies demonstrated a detrimental impact of acrolein exposure on the regulation of mitochondrial function and quality control (i.e., mitochondrial biogenesis and mitophagy) in various cell types, e.g., lung fibroblasts, alveolar or bronchial epithelial cells, suggesting that these cell types likely are also impacted by acrolein in our study (26-28, 41, 43, 89, 90). Secondly, reported changes in abundance of key regulators involved in the processes of mitochondrial biogenesis, mitophagy, fusion, and fission are not indicative for actual functional process or mitochondrial content changes, limiting conclusions that can be drawn from our data. Thirdly, different from human smokers exposed to CS, nose-only inhalation of acrolein in our model likely

primarily resulted in exposure in the nasal airways as suggested due to alteration of breathing parameters as protecting mechanism in response to acrolein (29, 82, 91-93). Nevertheless, from the (previous) reported inflammatory profile in the airways of the acrolein-exposed rats, it is still clear that acrolein reached the cells of the airways in our study (29). Fourthly, the continuous nose-only exposure model that we deployed does not accurately reflect the puff-topography that smokers usually display (81, 82). Fifthly, while no studies are investigating the impact of gender in response to acrolein exposure we cannot exclude that gender affect the observed differences in our study as previous literature reported a sex-dependent ozone-mediated inflammatory and physiological response (94, 95) and inflammation may damage mitochondrial metabolism (96). Besides gender, previous studies indicated age-related deterioration of mitochondrial function in lung disease (97, 98) suggesting an aggravated mitochondrial response following acrolein inhalation. However, by opting for a single gender (male) at a specific (young) age, we prevented confounding by these variables. Furthermore, no pronounced correlations were observed between analyzed parameters related to mitochondrial homeostasis (e.g., mitochondrial biogenesis, mitophagy) correlated with pathological hallmarks associated with inflammation, lung damage or apoptosis (0 *versus* 4 ppm acrolein; data not shown). Moreover, the differential time course effects observed in our study on 1 day *versus* 2 day could be explained by the immediate cellular effects analyzed at day 1 mediated by a stress response and cellular metabolic and immune alterations as previously shown in our ozone and acrolein-exposure studies (29, 99-101), while at day 2 a combination of immediate response including a peak inflammatory response are investigated. Also, conflicting changes were observed at mRNA and protein level in the analyzed markers of mitochondrial metabolism. Potential explanations for this could be that the time point (1 h post-exposure) may be sufficient to induce transcriptional changes but may be too short to pick up changes in protein levels at day 1, the low number of animals per group as well as the biological variation (SEM). In addition, it is known, albeit in other cell types, that acrolein is able to induce post-transcriptional (e.g., mRNA splicing (102)), and post-translational (e.g., protein-acrolein adducts (103)) modifications and can impact expression of miRNA's (104) potentially clarifying why mRNA changes not correlate with protein changes. Lastly, assessment of the effect of individual aldehydes on mitochondrial metabolism is not representative for exposure of cells of the airways to the complex combination of aldehydes present in CS, indicated to induce synergistic toxicity (90, 103, 105). Therefore, it is relevant to study co-exposure of aldehydes for regulation in the future.

In conclusion, our study shows that acute acrolein exposure has an impact on the molecular regulation of mitochondrial metabolism in rat lung. Further research should focus on assessing the effect of acrolein individually and in combination with acetaldehyde and formaldehyde, on mitochondrial function. Although mitochondrial dysfunction has been implicated in COPD pathogenesis, whether or not this can contribute to COPD development remains to be established. Hence, understanding the effect of acrolein on mitochondrial function will provide a scientifically supported reasoning to shortlist regulation of aldehydes in tobacco smoke.

COI/Funding

The authors report no conflict of interest.

This research is supported by the Netherlands Food and Consumer Product Safety Authority (NVWA).

Disclaimer: The research described in this article has been reviewed by the Center for Public Health and Environmental Assessment, U.S. Environmental Protection Agency, and approved for publication. Approval does not signify that the contents necessarily reflect the views and policies of the Agency, nor does the mention of trade names of commercial products constitute endorsement or recommendation for use.

References

- Mathers CD, Loncar D. Projections of Global Mortality and Burden of Disease from 2002 to 2030. *PLoS Med.* 2006;3(11):e442.
- Rodgman A, Perfetti TA. The chemical components of tobacco and tobacco smoke: CRC press; 2013.
- Mannino DM, Buist AS. Global burden of COPD: risk factors, prevalence, and future trends. *The Lancet.* 2007;370(9589):765-73.
- Stevens JF, Maier CS. Acrolein: sources, metabolism, and biomolecular interactions relevant to human health and disease. *Mol Nutr Food Res.* 2008;52(1):7-25.
- World Health Organization & World Health Organization Tobacco Free Initiative. The scientific basis of tobacco product regulation: second report of a WHO study group. World Health Organization; 2008.
- Pauwels C, Klerx WNM, Pennings JLA, Boots AW, van Schooten FJ, Opperhuizen A, et al. Cigarette Filter Ventilation and Smoking Protocol Influence Aldehyde Smoke Yields. *Chem Res Toxicol.* 2018;31(6):462-71.
- Haussmann H-J. Use of hazard indices for a theoretical evaluation of cigarette smoke composition. *Chem Res Toxicol.* 2012;25(4):794-810.
- Fowles J, Dybing E. Application of toxicological risk assessment principles to the chemical constituents of cigarette smoke. *Tob Control.* 2003;12(4):424-30.
- Yeager RP, Kushman M, Chemerynski S, Weil R, Fu X, White M, et al. Proposed Mode of Action for Acrolein Respiratory Toxicity Associated with Inhaled Tobacco Smoke. *Toxicol Sci.* 2016;151(2):347-64.
- Costa DL, Kutzman RS, Lehmann JR, Drew RT. Altered lung function and structure in the rat after subchronic exposure to acrolein. *Am Rev Respir Dis.* 1986;133(2):286-91.
- O'Brien PJ, Siraki AG, Shangari N. Aldehyde sources, metabolism, molecular toxicity mechanisms, and possible effects on human health. *Crit Rev Toxicol.* 2005;35(7):609-62.
- Morita K, Masuda N, Oniki K, Saruwatari J, Kajiwar A, Otake K, et al. Association between the aldehyde dehydrogenase 2*2 allele and smoking-related chronic airway obstruction in a Japanese general population: a pilot study. *Toxicol Lett.* 2015;236(2):117-22.
- Cloonan SM, Choi AM. Mitochondria in lung disease. *J Clin Invest.* 2016;126(3):809-20.
- Aghapour M, Remels AHV, Pouwels SD, Bruder D, Hiemstra PS, Cloonan SM, et al. Mitochondria: at the crossroads of regulating lung epithelial cell function in chronic obstructive pulmonary disease. *Am J Physiol Lung Cell Mol Physiol.* 2020;318(1):L149-164.
- Mizumura K, Cloonan SM, Nakahira K, Bhashyam AR, Cervo M, Kitada T, et al. Mitophagy-dependent necroptosis contributes to the pathogenesis of COPD. *J Clin Invest.* 2014;124(9):3987-4003.
- Sundar IK, Maremanda KP, Rahman I. Mitochondrial dysfunction is associated with Mirol reduction in lung epithelial cells by cigarette smoke. *Toxicol Lett.* 2019;317:92-101.
- Hara H, Araya J, Ito S, Kobayashi K, Takasaka N, Yoshii Y, et al. Mitochondrial fragmentation in cigarette smoke-induced bronchial epithelial cell senescence. *Am J Physiol Lung Cell Mol Physiol.* 2013;305(10):L737-46.
- Hoffmann RF, Zarrintan S, Brandenburg SM, Kol A, de Bruin HG, Jafari S, et al. Prolonged cigarette smoke exposure alters mitochondrial structure and function in airway epithelial cells. *Respir Res.* 2013;14:97.

19. Ahmad T, Sundar IK, Lerner CA, Gerloff J, Tormos AM, Yao H, et al. Impaired mitophagy leads to cigarette smoke stress-induced cellular senescence: implications for chronic obstructive pulmonary disease. *Faseb j*. 2015;29(7):2912-29.
20. Aravamudan B, Kiel A, Freeman M, Delmotte P, Thompson M, Vassallo R, et al. Cigarette smoke-induced mitochondrial fragmentation and dysfunction in human airway smooth muscle. *Am J Physiol Lung Cell Mol Physiol*. 2014;306(9):L840-54.
21. Cloonan SM, Glass K, Laucho-Contreras ME, Bhashyam AR, Cervo M, Pabon MA, et al. Mitochondrial iron chelation ameliorates cigarette smoke-induced bronchitis and emphysema in mice. *Nat Med*. 2016;22(2):163-74.
22. Lin J, Handschin C, Spiegelman BM. Metabolic control through the PGC-1 family of transcription coactivators. *Cell Metab*. 2005;1(6):361-70.
23. Scarpulla RC. Metabolic control of mitochondrial biogenesis through the PGC-1 family regulatory network. *Biochim Biophys Acta*. 2011;1813(7):1269-78.
24. Fritsch LE, Moore ME, Sarraf SA, Pickrell AM. Ubiquitin and Receptor-Dependent Mitophagy Pathways and Their Implication in Neurodegeneration. *J Mol Biol*. 2020;432(8):2510-24.
25. Mishra P, Chan DC. Mitochondrial dynamics and inheritance during cell division, development and disease. *Nat Rev Mol Cell Biol*. 2014;15(10):634-46.
26. Wang HT, Lin JH, Yang CH, Haung CH, Weng CW, Maan-Yuh Lin A, et al. Acrolein induces mtDNA damages, mitochondrial fission and mitophagy in human lung cells. *Oncotarget*. 2017;8(41):70406-21.
27. Agarwal AR, Yin F, Cadenas E. Metabolic shift in lung alveolar cell mitochondria following acrolein exposure. *Am J Physiol Lung Cell Mol Physiol*. 2013;305(10):L764-73.
28. Luo C, Li Y, Yang L, Feng Z, Li Y, Long J, et al. A cigarette component acrolein induces accelerated senescence in human diploid fibroblast IMR-90 cells. *Biogerontology*. 2013;14(5):503-11.
29. Snow SJ, McGee MA, Henriquez A, Richards JE, Schladweiler MC, Ledbetter AD, et al. Respiratory Effects and Systemic Stress Response Following Acute Acrolein Inhalation in Rats. *Toxicol Sci*. 2017;158(2):454-64.
30. De Woskin R, Greenberg M, Pepelko W, Strickland J. Toxicological review of acrolein; in support of summary information on the integrated risk information system (Iris). Washington, DC: US Environmental Protection Agency; 2003. Contract No.: EPA/635/R-03/003.
31. Bergmeyer H, Gawehn K, Grassl M. 3-Hydroxyacyl-CoA dehydrogenase. *Methods of enzymatic analysis*. 1974;1:474.
32. Ling K, Paetkau V, Marcus F, Lardy HA. [77a] Phosphofructokinase: I. Skeletal Muscle. *Methods in enzymology*. 9: Elsevier; 1966. p. 425-9.
33. Dwivedi AM, Upadhyay S, Johanson G, Ernstgard L, Palmberg L. Inflammatory effects of acrolein, crotonaldehyde and hexanal vapors on human primary bronchial epithelial cells cultured at air-liquid interface. *Toxicol In Vitro*. 2018;46:219-28.
34. Cichocki JA, Smith GJ, Morris JB. Tissue sensitivity of the rat upper and lower extrapulmonary airways to the inhaled electrophilic air pollutants diacetyl and acrolein. *Toxicol Sci*. 2014;142(1):126-36.
35. Xiong R, Wu Q, Muskhelishvili L, Davis K, Shemansky JM, Bryant M, et al. Evaluating Mode of Action of Acrolein Toxicity in an In Vitro Human Airway Tissue Model. *Toxicol Sci*. 2018;166(2):451-64.

36. Park JH, Ku HJ, Lee JH, Park JW. Idh2 Deficiency Exacerbates Acrolein-Induced Lung Injury through Mitochondrial Redox Environment Deterioration. *Oxid Med Cell Longev*. 2017;2017:1595103.
37. Zhang H, Forman HJ. Acrolein induces heme oxygenase-1 through PKC-delta and PI3K in human bronchial epithelial cells. *Am J Respir Cell Mol Biol*. 2008;38(4):483-90.
38. Moghe A, Ghare S, Lamoreau B, Mohammad M, Barve S, McClain C, et al. Molecular mechanisms of acrolein toxicity: relevance to human disease. *Toxicol Sci*. 2015;143(2):242-55.
39. Kitaguchi Y, Taraseviciene-Stewart L, Hanaoka M, Natarajan R, Kraskauskas D, Voelkel NF. Acrolein induces endoplasmic reticulum stress and causes airspace enlargement. *PLoS One*. 2012;7(5):e38038.
40. Kim JK, Park JH, Ku HJ, Kim SH, Lim YJ, Park JW, et al. Naringin protects acrolein-induced pulmonary injuries through modulating apoptotic signaling and inflammation signaling pathways in mice. *J Nutr Biochem*. 2018;59:10-6.
41. Roy J, Palapati P, Bettaieb A, Tanel A, Averill-Bates DA. Acrolein induces a cellular stress response and triggers mitochondrial apoptosis in A549 cells. *Chem Biol Interact*. 2009;181(2):154-67.
42. Yadav UCS, Ramana KV, Srivastava SK. Aldose reductase regulates acrolein-induced cytotoxicity in human small airway epithelial cells. *Free radical biology & medicine*. 2013;65:15-25.
43. Zhang S, Zhang J, Cheng W, Chen H, Wang A, Liu Y, et al. Combined cell death of co-exposure to aldehyde mixtures on human bronchial epithelial BEAS-2B cells: Molecular insights into the joint action. *Chemosphere*. 2020;244:125482.
44. Sun L, Luo C, Long J, Wei D, Liu J. Acrolein is a mitochondrial toxin: effects on respiratory function and enzyme activities in isolated rat liver mitochondria. *Mitochondrion*. 2006;6(3):136-42.
45. Wu K, Luan G, Xu Y, Shen S, Qian S, Zhu Z, et al. Cigarette smoke extract increases mitochondrial membrane permeability through activation of adenine nucleotide translocator (ANT) in lung epithelial cells. *Biochem Biophys Res Commun*. 2020;525(3):733-9.
46. Park EJ, Park YJ, Lee SJ, Lee K, Yoon C. Whole cigarette smoke condensates induce ferroptosis in human bronchial epithelial cells. *Toxicol Lett*. 2019;303:55-66.
47. Clapp PW, Lavrich KS, van Heusden CA, Lazarowski ER, Carson JL, Jaspers I. Cinnamaldehyde in flavored e-cigarette liquids temporarily suppresses bronchial epithelial cell ciliary motility by dysregulation of mitochondrial function. *Am J Physiol Lung Cell Mol Physiol*. 2019;316(3):L470-l86.
48. Pei Z, Zhuang Z, Sang H, Wu Z, Meng R, He EY, et al. α,β -Unsaturated aldehyde crotonaldehyde triggers cardiomyocyte contractile dysfunction: role of TRPV1 and mitochondrial function. *Pharmacol Res*. 2014;82:40-50.
49. Farfán Labonne BE, Gutiérrez M, Gómez-Quiroz LE, Königsberg Fainstein M, Bucio L, Souza V, et al. Acetaldehyde-induced mitochondrial dysfunction sensitizes hepatocytes to oxidative damage. *Cell Biol Toxicol*. 2009;25(6):599-609.
50. Mullarky E, Cantley LC. Diverting Glycolysis to Combat Oxidative Stress. In: Nakao K, Minato N, Uemoto S, editors. *Innovative Medicine: Basic Research and Development*. Tokyo: Springer Copyright 2015, The Author(s). 2015. p. 3-23.

51. Fabisiak JP, Medvedovic M, Alexander DC, McDunn JE, Concel VJ, Bein K, et al. Integrative metabolome and transcriptome profiling reveals discordant energetic stress between mouse strains with differential sensitivity to acrolein-induced acute lung injury. *Mol Nutr Food Res.* 2011;55(9):1423-34.
52. Novotny MV, Yancey MF, Stuart R, Wiesler D, Peterson RG. Inhibition of glycolytic enzymes by endogenous aldehydes: a possible relation to diabetic neuropathies. *Biochim Biophys Acta.* 1994;1226(2):145-50.
53. Agarwal AR, Yin F, Cadenas E. Short-term cigarette smoke exposure leads to metabolic alterations in lung alveolar cells. *Am J Respir Cell Mol Biol.* 2014;51(2):284-93.
54. Agarwal AR, Zhao L, Sancheti H, Sundar IK, Rahman I, Cadenas E. Short-term cigarette smoke exposure induces reversible changes in energy metabolism and cellular redox status independent of inflammatory responses in mouse lungs. *Am J Physiol Lung Cell Mol Physiol.* 2012;303(10):L889-98.
55. Tu C, Mammen MJ, Li J, Shen X, Jiang X, Hu Q, et al. Large-scale, ion-current-based proteomics investigation of bronchoalveolar lavage fluid in chronic obstructive pulmonary disease patients. *J Proteome Res.* 2014;13(2):627-39.
56. Kao CC, Hsu JW, Bandi V, Hanania NA, Kheradmand F, Jahoor F. Glucose and pyruvate metabolism in severe chronic obstructive pulmonary disease. *J Appl Physiol.* 2012;112(1):42-7.
57. Pastor MD, Nogal A, Molina-Pinelo S, Meléndez R, Salinas A, González De la Peña M, et al. Identification of proteomic signatures associated with lung cancer and COPD. *J Proteomics.* 2013;89:227-37.
58. Agarwal AR, Kadam S, Brahme A, Agrawal M, Apte K, Narke G, et al. Systemic Immuno-metabolic alterations in chronic obstructive pulmonary disease (COPD). *Respir Res.* 2019;20(1):171.
59. Vanella L, Li Volti G, Distefano A, Raffaele M, Zingales V, Avola R, et al. A new antioxidant formulation reduces the apoptotic and damaging effect of cigarette smoke extract on human bronchial epithelial cells. *Eur Rev Med Pharmacol Sci.* 2017;21(23):5478-84.
60. Li J, Dai A, Hu R, Zhu L, Tan S. Positive correlation between PPARGgamma/PGC-1alpha and gamma-GCS in lungs of rats and patients with chronic obstructive pulmonary disease. *Acta Biochim Biophys Sin.* 2010;42(9):603-14.
61. Wang S, He N, Xing H, Sun Y, Ding J, Liu L. Function of hesperidin alleviating inflammation and oxidative stress responses in COPD mice might be related to SIRT1/PGC-1alpha/NF-kappaB signaling axis. *J Recept Signal Transduct Res.* 2020:1-7.
62. Wang XL, Li T, Li JH, Miao SY, Xiao XZ. The Effects of Resveratrol on Inflammation and Oxidative Stress in a Rat Model of Chronic Obstructive Pulmonary Disease. *Molecules.* 2017;22(9).
63. Walczak J, Malińska D, Drabik K, Michalska B, Prill M, John S, et al. Mitochondrial Network and Biogenesis in Response to Short and Long-Term Exposure of Human BEAS-2B Cells to Aerosol Extracts from the Tobacco Heating System 2.2. *Cell Physiol Biochem.* 2020;54(2):230-51.
64. Alvarez-Guardia D, Palomer X, Coll T, Davidson MM, Chan TO, Feldman AM, et al. The p65 subunit of NF-kappaB binds to PGC-1alpha, linking inflammation and metabolic disturbances in cardiac cells. *Cardiovasc Res.* 2010;87(3):449-58.
65. Remels AHV, Gosker HR, Bakker J, Guttridge DC, Schols AMWJ, Langen RCJ. Regulation of skeletal muscle oxidative phenotype by classical NF-κB signalling. *Biochim Biophys Acta Mol Basis Dis.* 2013;1832(8):1313-25.

66. Yadav UC, Ramana KV. Regulation of NF- κ B-induced inflammatory signaling by lipid peroxidation-derived aldehydes. *Oxid Med Cell Longev*. 2013;2013:690545.
67. Sun Y, Ito S, Nishio N, Tanaka Y, Chen N, Isobe K. Acrolein induced both pulmonary inflammation and the death of lung epithelial cells. *Toxicol Lett*. 2014;229(2):384-92.
68. Zhang M, Shi R, Zhang Y, Shan H, Zhang Q, Yang X, et al. Nix/BNIP3L-dependent mitophagy accounts for airway epithelial cell injury induced by cigarette smoke. *J Cell Physiol*. 2019;234(8):14210-20.
69. Son ES, Kim SH, Ryter SW, Yeo EJ, Kyung SY, Kim YJ, et al. Quercetogetin protects against cigarette smoke extract-induced apoptosis in epithelial cells by inhibiting mitophagy. *Toxicol In Vitro*. 2018;48:170-8.
70. Kyung SY, Kim YJ, Son ES, Jeong SH, Park JW. The Phosphodiesterase 4 Inhibitor Roflumilast Protects against Cigarette Smoke Extract-Induced Mitophagy-Dependent Cell Death in Epithelial Cells. *Tuberc Respir Dis*. 2018;81(2):138-47.
71. Ito S, Araya J, Kurita Y, Kobayashi K, Takasaka N, Yoshida M, et al. PARK2-mediated mitophagy is involved in regulation of HBEC senescence in COPD pathogenesis. *Autophagy*. 2015;11(3):547-59.
72. Araya J, Tsubouchi K, Sato N, Ito S, Minagawa S, Hara H, et al. PRKN-regulated mitophagy and cellular senescence during COPD pathogenesis. *Autophagy*. 2019;15(3):510-26.
73. Ballweg K, Mutze K, Königshoff M, Eickelberg O, Meiners S. Cigarette smoke extract affects mitochondrial function in alveolar epithelial cells. *Am J Physiol Lung Cell Mol Physiol*. 2014;307(11):L895-907.
74. Wang L, Li X, Yang Z, Pan X, Liu X, Zhu M, et al. Crotonaldehyde induces autophagy-mediated cytotoxicity in human bronchial epithelial cells via PI3K, AMPK and MAPK pathways. *Environ Pollut*. 2017;228:287-96.
75. Wang L, Li X, Yang Z, Zhu M, Xie J. Autophagy induced by low concentrations of crotonaldehyde promotes apoptosis and inhibits necrosis in human bronchial epithelial cells. *Ecotoxicol Environ Saf*. 2019;167:169-77.
76. Liu QP, Zhou DX, Lv MQ, Ge P, Li YX, Wang SJ. Formaldehyde inhalation triggers autophagy in rat lung tissues. *Toxicol Ind Health*. 2018;748233718796347.
77. Chen ZH, Kim HP, Sciurba FC, Lee SJ, Feghali-Bostwick C, Stolz DB, et al. Egr-1 regulates autophagy in cigarette smoke-induced chronic obstructive pulmonary disease. *PLoS One*. 2008;3(10):e3316.
78. Kosmider B, Lin CR, Karim L, Tomar D, Vlasenko L, Marchetti N, et al. Mitochondrial dysfunction in human primary alveolar type II cells in emphysema. *EBioMedicine*. 2019;46:305-16.
79. Song C, Luo B, Gong L. Resveratrol reduces the apoptosis induced by cigarette smoke extract by upregulating MFN2. *PLoS One*. 2017;12(4):e0175009.
80. Burns DM, Dybing E, Gray N, Hecht S, Anderson C, Sanner T, et al. Mandated lowering of toxicants in cigarette smoke: a description of the World Health Organization TobReg proposal. *Tob Control*. 2008;17(2):132-41.
81. Cheah NP. Volatile aldehydes in tobacco smoke: source fate and risk. [Ph.D. Dissertation Thesis]. Maastricht, The Netherlands: Maastricht University; 2016.
82. Corley RA, Kabilan S, Kuprat AP, Carson JP, Jacob RE, Minard KR, et al. Comparative Risks of Aldehyde Constituents in Cigarette Smoke Using Transient Computational Fluid Dynamics/ Physiologically Based Pharmacokinetic Models of the Rat and Human Respiratory Tracts. *Toxicol Sci*. 2015;146(1):65-88.

83. World Health Organization Framework Convention on Tobacco Control. Partial guidelines for implementation of articles 9 and 10—regulation of the contents of tobacco products and regulation of tobacco product disclosures. 2012.
84. Talhout R, Opperhuizen A, van Amsterdam JG. Sugars as tobacco ingredient: Effects on mainstream smoke composition. *Food Chem Toxicol.* 2006;44(11):1789-98.
85. Baker RR, da Silva JRP, Smith G. The effect of tobacco ingredients on smoke chemistry. Part I: Flavourings and additives. *Food Chem Toxicol.* 2004;42:3-37.
86. Ashizawa A, Roney N, Taylor J. Toxicological profile for acrolein. 2007.
87. Bergers WWA, Beyersbergen van Henegouwen AG, Hammer AH, Bruijnzeel PLB. Breathing Patterns of Awake Rats Exposed to Acrolein and Perfluorobutylene Determined with an Integrated System of Nose-Only Exposure and Online Analyzed Multiple Monitoring of Breathing. *Inhal Toxicol.* 1996;8(1):81-93.
88. Cassee FR, Groten JP, Feron VJ. Changes in the nasal epithelium of rats exposed by inhalation to mixtures of formaldehyde, acetaldehyde, and acrolein. *Fundam Appl Toxicol.* 1996;29(2):208-18.
89. Moretto N, Facchinetti F, Southworth T, Civelli M, Singh D, Patacchini R. alpha,beta-Unsaturated aldehydes contained in cigarette smoke elicit IL-8 release in pulmonary cells through mitogen-activated protein kinases. *Am J Physiol Lung Cell Mol Physiol.* 2009;296(5):L839-48.
90. Zhang S, Zhang J, Chen H, Wang A, Liu Y, Hou H, et al. Combined cytotoxicity of co-exposure to aldehyde mixtures on human bronchial epithelial BEAS-2B cells. *Environ Pollut.* 2019;250:650-61.
91. Lee BP, Morton RF, Lee LY. Acute effects of acrolein on breathing: role of vagal bronchopulmonary afferents. *J Appl Physiol.* 1992;72(3):1050-6.
92. Perez CM, Hazari MS, Ledbetter AD, Haykal-Coates N, Carll AP, Cascio WE, et al. Acrolein inhalation alters arterial blood gases and triggers carotid body-mediated cardiovascular responses in hypertensive rats. *Inhal Toxicol.* 2015;27(1):54-63.
93. Corley RA, Kabilan S, Kuprat AP, Carson JP, Minard KR, Jacob RE, et al. Comparative computational modeling of airflows and vapor dosimetry in the respiratory tracts of rat, monkey, and human. *Toxicol Sci.* 2012;128(2):500-16.
94. Yaeger MJ, Reece SW, Kilburg-Basnyat B, Hodge MX, Pal A, Dunigan-Russell K, et al. Sex Differences in Pulmonary Eicosanoids and Specialized Pro-Resolving Mediators in Response to Ozone Exposure. *Toxicol Sci.* 2021.
95. Birukova A, Cyphert-Daly J, Cumming RI, Yu YR, Gowdy KM, Que LG, et al. Sex Modifies Acute Ozone-Mediated Airway Physiologic Responses. *Toxicol Sci.* 2019;169(2):499-510.
96. Kampf C, Relova AJ, Sandler S, Roomans GM. Effects of TNF-alpha, IFN-gamma and IL-beta on normal human bronchial epithelial cells. *Eur Respir J.* 1999;14(1):84-91.
97. Cloonan SM, Kim K, Esteves P, Trian T, Barnes PJ. Mitochondrial dysfunction in lung ageing and disease. *Eur Respir Rev.* 2020;29(157).
98. Mercado N, Ito K, Barnes PJ. Accelerated ageing of the lung in COPD: new concepts. *Thorax.* 2015;70(5):482-9.
99. Henriquez AR, Snow SJ, Schladweiler MC, Miller CN, Dye JA, Ledbetter AD, et al. Beta-2 Adrenergic and Glucocorticoid Receptor Agonists Modulate Ozone-Induced Pulmonary Protein Leakage and Inflammation in Healthy and Adrenalectomized Rats. *Toxicol Sci.* 2018;166(2):288-305.

100. Henriquez AR, Williams W, Snow SJ, Schladweiler MC, Fisher C, Hargrove MM, et al. The dynamicity of acute ozone-induced systemic leukocyte trafficking and adrenal-derived stress hormones. *Toxicology*. 2021;458:152823.
101. Miller DB, Snow SJ, Schladweiler MC, Richards JE, Ghio AJ, Ledbetter AD, et al. Acute Ozone-Induced Pulmonary and Systemic Metabolic Effects Are Diminished in Adrenalectomized Rats. *Toxicol Sci*. 2016;150(2):312-22.
102. Haberzettl P, Vladykovskaya E, Srivastava S, Bhatnagar A. Role of endoplasmic reticulum stress in acrolein-induced endothelial activation. *Toxicol Appl Pharmacol*. 2009;234(1):14-24.
103. LoPachin RM, Gavin T. Molecular mechanisms of aldehyde toxicity: a chemical perspective. *Chem Res Toxicol*. 2014;27(7):1081-91.
104. O'Toole TE, Abplanalp W, Li X, Cooper N, Conklin DJ, Haberzettl P, et al. Acrolein decreases endothelial cell migration and insulin sensitivity through induction of let-7a. *Toxicol Sci*. 2014;140(2):271-82.
105. Zhang S, Chen H, Wang A, Liu Y, Hou H, Hu Q. Combined effects of co-exposure to formaldehyde and acrolein mixtures on cytotoxicity and genotoxicity in vitro. *Environ Sci Pollut Res Int*. 2018;25(25):25306-14.

Supplementary information

Transcript abundance of regulators of inflammation and oxidative stress is altered in response to acute acrolein exposure in rat lung

Significantly elevated transcript abundance of the inflammatory marker *NFκB inhibitor alpha* (*Nfkbia*) (1 Day: FC=2.34±0.56, p<0.05), involved in inhibition of the NF-κB transcription, and chemokine *C-C motif chemokine ligand 2* (*Ccl2*) (1 Day: FC=4.25±0.91, p<0.01; 2 Day: FC=13.30±1.70, p<0.01) was observed after 1 or 2 days of 4 ppm acrolein exposure (Fig. S1A). In contrast, decreased mRNA levels of *Nfkbia* (FC=0.60±0.03, p<0.1) were observed following 2 ppm acrolein inhalation for 2 days (Fig. S1A). Transcript levels of *C-X-C motif chemokine ligand 1* (*Cxcl1*), responsible for attracting neutrophils to the site of inflammation, were downregulated in response to acute acrolein inhalation after 2 days of 2 ppm (FC=0.55±0.05, p<0.01) and following 1 or 2 days of 4 ppm acrolein inhalation (1 Day: FC=0.71±0.09, p<0.1; 2 Day: FC=0.63±0.09, p<0.05) (Fig. S1B). In addition, 4 ppm acrolein exposure affected mRNA expression of *superoxide dismutase 2* (*Sod2*) (2 Day: FC=1.56±0.17, p<0.05), encoding for a mitochondrial anti-oxidant protein, while no effect on transcript abundance of *superoxide dismutase 1* (*Sod1*) was observed in rat lung (Fig. S1C). As shown in Fig. S1D, mRNA levels of *aldehyde dehydrogenase 2* (*Aldh2*) were unaltered after acrolein exposure in rats. Furthermore, the abundance of established apoptosis regulators were analyzed. We observed significantly decreased levels of cleaved caspase-3 protein in response to 4 ppm acrolein inhalation for 2 days (FC=0.54±0.12, p<0.05), while transcript abundance of the ratio of *BCL2 associated X, apoptosis regulator* and *Bcl2, apoptosis regulator* (*Bax/Bcl2*) was unchanged following acrolein exposure, suggesting no activation of apoptosis in response to acrolein in our study (Fig. S2).

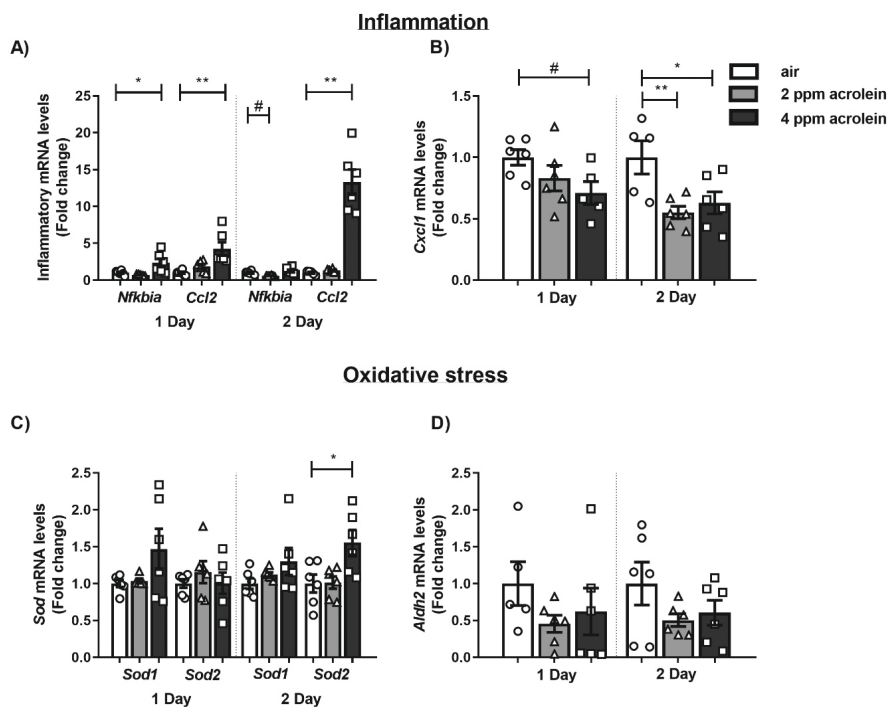


Figure S1. mRNA expression of inflammatory and oxidative stress markers in acrolein-exposed rats.

Wistar rats were exposed by nose-only inhalation to air (control) or acrolein (2 or 4 ppm) for 4 h/day for 1 or 2 days ($n = 4-6$ /group). Transcript abundance of (A) *Nfkb1a* and *Ccl2*, (B) *Cxcl1*, (C) *Sod1* and *Sod2*, and (D) *Aldh2* in rat lung. Data are presented as mean fold change compared to air-exposed rats \pm SEM. Individual animals are represented by open circle (air), triangle (2 ppm acrolein) or square (4 ppm acrolein). Statistical differences between 2 or 4 ppm acrolein versus air were tested using an one-way ANOVA followed by a Dunnett's post-hoc test for multiple comparisons or in case of non-normal distribution a Kruskal-Wallis test followed by a Dunn's multiple comparisons test. Statistical significance is indicated as $*p < 0.1$, $*p < 0.05$ and $**p < 0.01$ compared to air (control).

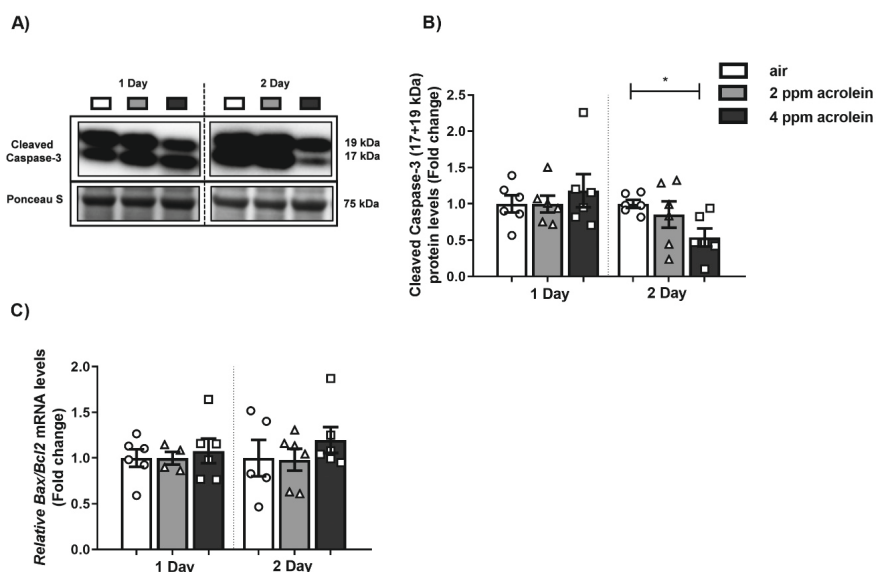


Figure S2. Abundance of apoptosis markers following acrolein exposure in rats. Wistar rats were exposed by nose-only inhalation to air (control) or acrolein (2 or 4 ppm) for 4 h/day for 1 or 2 days (n = 4-6/group). Protein levels of **(A, B)** cleaved caspase-3 as well as transcript abundance of **(C)** ratio *Bax/Bcl2* in rat lung. Western blot analysis revealed two distinct bands corresponding with expected molecular weights for cleaved caspase-3 protein (17 + 19 kDa). Representative western blot images are shown of one animal/group reflective of the changes in the whole group as quantified in the corresponding graph. The dashed line indicates that the samples of day 1 and day 2 were loaded on (and selected from) different blots. Data are presented as mean fold change compared to air-exposed rats \pm SEM. Individual animals are represented by open circle (air), triangle (2 ppm acrolein) or square (4 ppm acrolein). Statistical differences between 2 or 4 ppm acrolein *versus* air were tested using an one-way ANOVA followed by a Dunnett's post-hoc test for multiple comparisons or in case of non-normal distribution a Kruskal-Wallis test followed by a Dunn's multiple comparisons test. Statistical significance is indicated as *p<0.1, **p<0.05 and ***p<0.01 compared to air (control).

Acrolein inhalation acutely affects the activity and abundance of key components involved in fatty acid β -oxidation, tricarboxylic acid cycle and glycolysis in rats

We assessed the activity and transcript abundance of components of the fatty acid β -oxidation and tricarboxylic acid cycle. Activity of Hydroxyacyl-Coenzyme A Dehydrogenase (HADH) was altered following exposure to 2 ppm acrolein compared to control (1 Day: FC=0.78 \pm 0.07, p <0.05; 2 Day: FC=1.44 \pm 0.14, p <0.05) (Fig. S3A).

Moreover, no differences were found in expression of fatty acid β -oxidation related genes, i.e., *hydroxyacyl-CoA dehydrogenase trifunctional multienzyme complex subunit alpha* (*Hadha*) and *acyl-CoA dehydrogenase, long chain* (*Acadl*), in acrolein-exposed rats (Fig. S3B and C). Remarkably, transcript levels of the tricarboxylic acid cycle associated gene *citrate synthase* were observed to be significantly elevated in response to 4 ppm of acrolein (1 Day: FC=1.48 \pm 0.14, p <0.05; 2 Day: FC=1.79 \pm 0.15, p <0.05) (Fig. S3D).

Subsequently, we assessed the abundance of key constituents of the glycolytic pathway. Although mRNA levels of *lactate dehydrogenase A* (*Ldha*), *pyruvate kinase M1/2* (*Pkm*), *pyruvate dehydrogenase kinase 4* (*Pdk4*) and *solute carrier family 2 member 1* (*Slc2a1*) were unaltered in acrolein-exposed rats compared to control, decreased transcript abundance of *solute carrier family 2 member 4* (*Slc2a4*) was observed in response to 1 day of 4 ppm acrolein exposure (FC=0.46 \pm 0.16, p <0.1) (Fig. S3E-H).

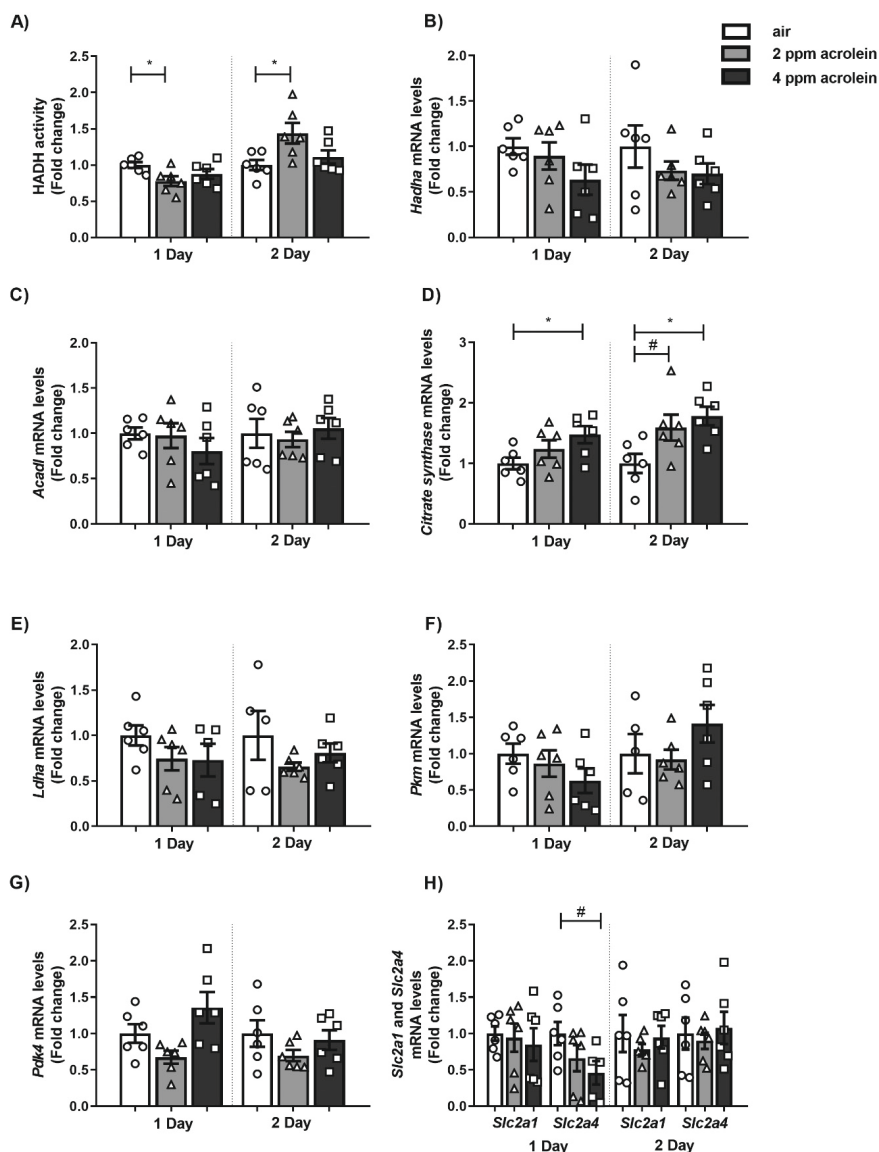


Figure S3. Alterations in activity and transcript abundance of key constituents of the fatty acid β -oxidation, tricarboxylic acid cycle and glycolysis in response to acute acrolein exposure in rats. Wistar rats were exposed by nose-only inhalation to air (control) or acrolein (2 or 4 ppm) for 4 h/day for 1 or 2 days ($n = 5-6$ /group). (A) HADH enzyme activity as well as mRNA expression of (B) *Hadha*, (C) *Acadl*, (D) *citrate synthase*, (E) *Ldha*, (F) *Pkm*, (G) *Pdk4*, and (H) *Slc2a1* and *Slc2a4* in rat lung. Data are presented as mean fold change compared to air-exposed rats \pm SEM. Individual animals are represented by open circle (air), triangle (2 ppm acrolein) or square (4 ppm acrolein). Statistical differences between 2 or 4 ppm acrolein versus air were tested using an one-way ANOVA followed by a Dunnett's post-hoc test for multiple comparisons or in case of non-normal distribution a Kruskal-Wallis test followed by a Dunn's multiple comparisons test. Statistical significance is indicated as * $p < 0.05$ and ** $p < 0.01$ compared to air (control).

The molecular regulation of mitochondrial biogenesis related constituents in rats acutely exposed to acrolein

We studied the impact of acute acrolein exposure on the abundance of Peroxisome Proliferator-Activated Receptor (PPAR) Gamma (PPARG) Coactivator 1 (PPARGC1) molecules and coactivated transcription factors involved in the molecular regulation of mitochondrial biogenesis and mitochondrial energy metabolism. As depicted in Fig. S4, protein abundance of Transcription factor A, Mitochondrial (TFAM) and mRNA levels of *PPARG related coactivator 1* (*Pprc1*), *Tfam*, *PPAR delta* (*Ppard*), and *GA binding protein transcription factor subunit alpha* (*Gabpa*) were unaltered in acrolein- versus air-exposed rats.

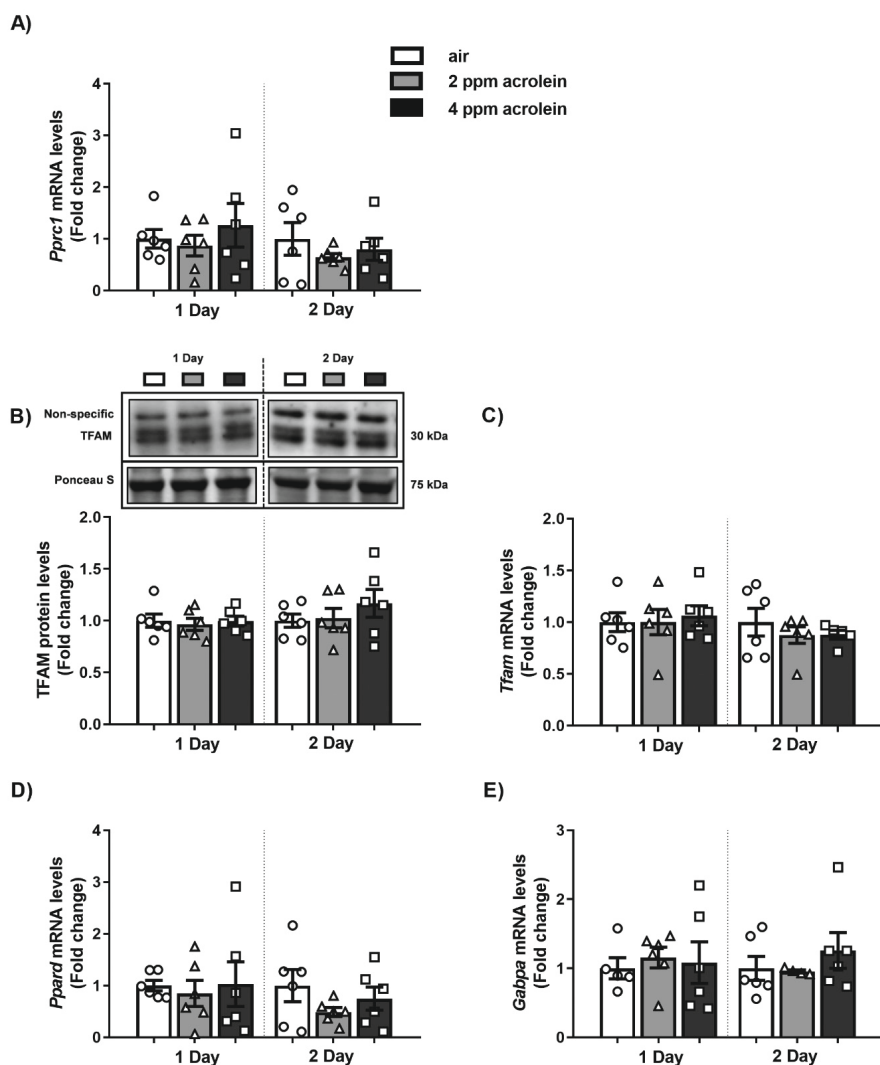


Figure S4. Abundance of mitochondrial biogenesis associated components is unaffected in response to acrolein inhalation in rats. Wistar rats were exposed by nose-only inhalation to air (control) or acrolein (2 or 4 ppm) for 4 h/day for 1 or 2 days ($n = 4-6/\text{group}$). Transcript abundance of PPARGC1 molecule (A) *Pprc1* and abundance of PPARGC1-coactivated transcription factor protein (B) TFAM as well as transcripts (C) *Tfam*, (D) *Ppard*, and (E) *Gabpa* in rat lung tissue homogenates. Representative western blot images are shown of one animal/group reflective of the changes in the whole group as quantified in the corresponding graph. The dashed line indicates that the samples of day 1 and day 2 were loaded on (and selected from) different blots. Data are presented as mean fold change compared to air-exposed rats \pm SEM. Individual animals are represented by open circle (air), triangle (2 ppm acrolein) or square (4 ppm acrolein). Statistical differences between 2 or 4 ppm acrolein *versus* air were tested using an one-way ANOVA followed by a Dunnett's post-hoc test for multiple comparisons or in case of non-normal distribution a Kruskal-Wallis test followed by a Dunn's multiple comparisons test. Statistical significance is indicated as * $p < 0.1$, * $p < 0.05$ and ** $p < 0.01$ compared to air (control).

Abundance of ubiquitin-mediated mitophagy and general autophagy-related constituents is unaltered in rats acutely exposed to acrolein

The impact of acute acrolein exposure on the abundance of key regulators involved in ubiquitin-mediated mitophagy and general autophagy, both essential for the selective breakdown of mitochondria, was evaluated in rat lung tissue. As shown in Fig. S5, protein and mRNA levels of constituents involved in ubiquitin-mediated mitophagy, i.e., Phosphatase and tensin homolog (PTEN) Induced Kinase 1 (PINK1) and Parkin RBR E3 Ubiquitin Protein Ligase (PRKN), were unchanged in rats acutely exposed to acrolein compared to air control. Next, we investigated the abundance of general autophagy proteins and transcripts, due to their essential role in facilitating the degradation of mitochondria by the autophagic-lysosomal pathways. While significant elevated protein levels of Sequestosome 1 (SQSTM1) were observed after 2 days of 4 ppm acrolein exposure ($FC=1.47\pm0.12$, $p<0.01$), no significant alterations in protein and transcript abundance of general autophagy-related constituents, i.e., GABA Type A Receptor Associated Protein Like 1 (GABARAPL1), (ratio) Microtubule-Associated Protein 1 Light Chain 3 Beta (MAP1LC3B), and *Becn1* (*Becn1*), were found following acute acrolein exposure in rats (Fig. S6).

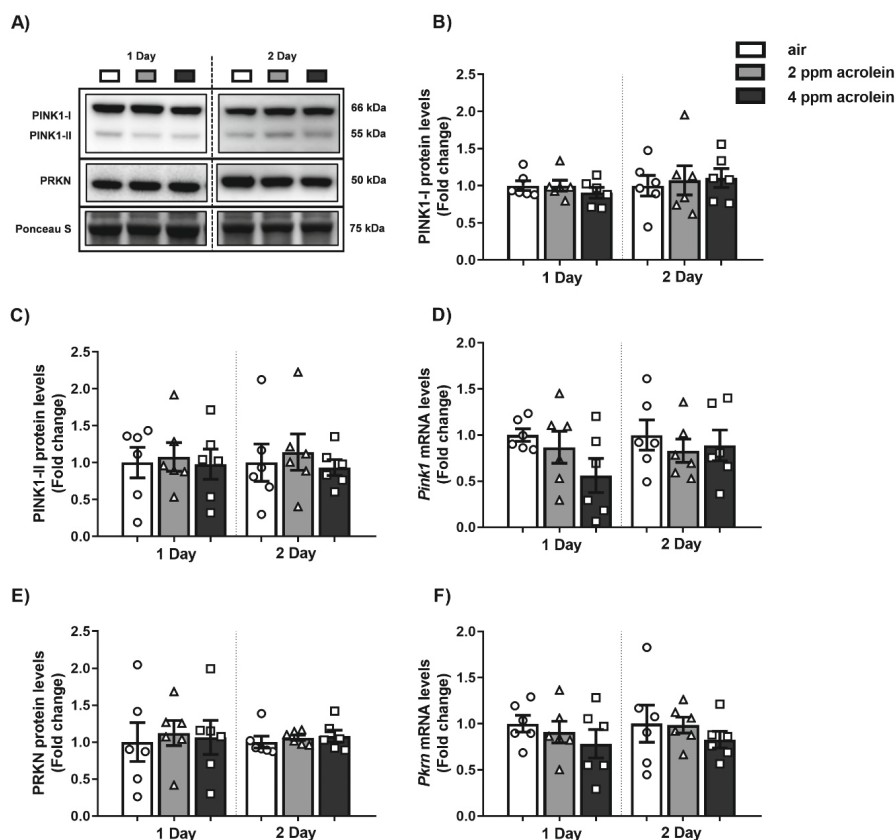


Figure S5. Unaltered abundance of key constituents of ubiquitin-mediated mitophagy in response to acrolein exposure in rats. Wistar rats were exposed by nose-only inhalation to air (control) or acrolein (2 or 4 ppm) for 4 h/day for 1 or 2 days ($n = 6/\text{group}$). Ubiquitin-mediated mitophagy-associated (A) protein abundance of (B) PINK1-I, (C) PINK1-II, and (E) PRKN, as well as transcript levels of genes encoding for (D) *Pink1* and (F) *Prkn* in rat lung. Western blot analysis revealed two distinct bands corresponding with expected molecular weights for PINK protein, entitled PINK1-I (66 kDa) and PINK1-II (55 kDa). Representative western blot images are shown of one animal/group reflective of the changes in the whole group as quantified in the corresponding graph. The dashed line indicates that the samples of day 1 and day 2 were loaded on (and selected from) different blots. Data are presented as mean fold change compared to air-exposed rats \pm SEM. Individual animals are represented by open circle (air), triangle (2 ppm acrolein) or square (4 ppm acrolein). Statistical differences between 2 or 4 ppm acrolein *versus* air were tested using an one-way ANOVA followed by a Dunnett's post-hoc test for multiple comparisons or in case of non-normal distribution a Kruskal-Wallis test followed by a Dunn's multiple comparisons test. Statistical significance is indicated as * $p < 0.1$, * $p < 0.05$ and ** $p < 0.01$ compared to air (control).

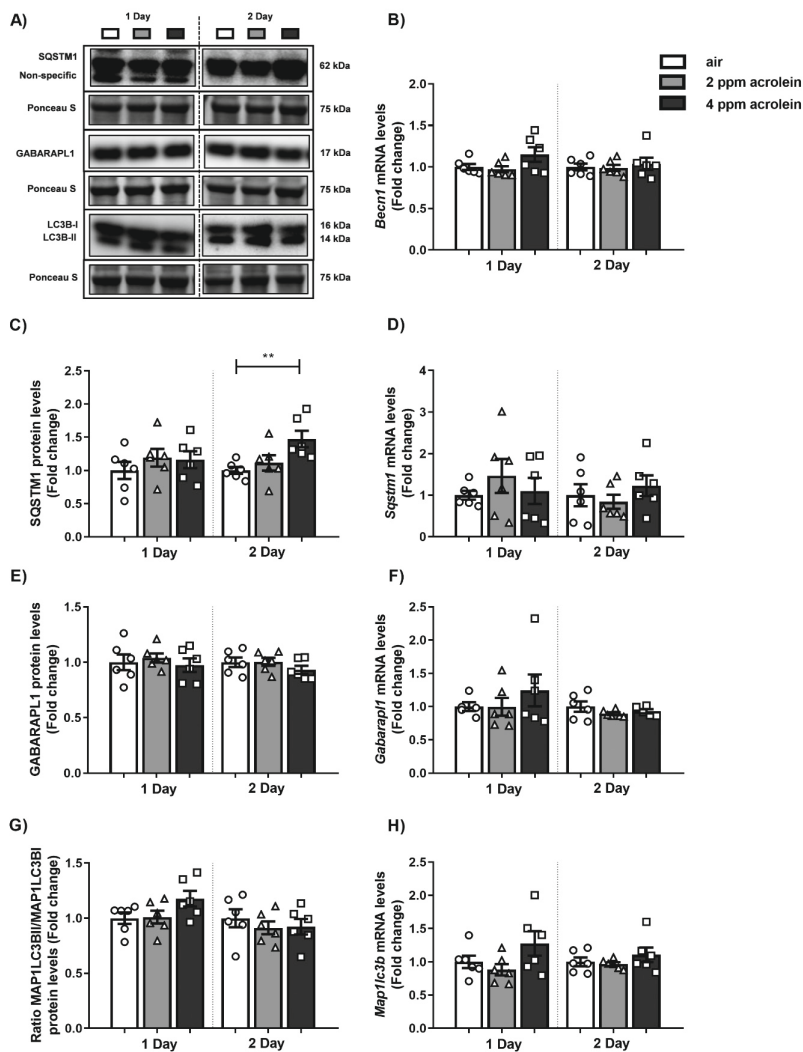


Figure S6. Abundance of autophagy-associated constituents is not affected by acrolein inhalation in rats. Wistar rats were exposed by nose-only inhalation to air (control) or acrolein (2 or 4 ppm) for 4 h/day for 1 or 2 days ($n = 5-6/\text{group}$). General autophagy-associated (A) protein abundance of (C) SQSTM1, (E) GABARAPL1, and (G) ratio MAP1LC3BII/MAP1LC3BI, as well as transcript abundance of (B) *Becn1*, (D) *Sqstm1*, (F) *Gabarapl1*, and (H) *Map1lc3b* in rat lung. Western blot analysis revealed two distinct bands corresponding with expected molecular weights for MAP1LC3B protein, entitled MAP1LC3BI (16 kDa) and MAP1LC3BII (14 kDa). Representative western blot images are shown of one animal/group reflective of the changes in the whole group as quantified in the corresponding graph. The dashed line indicates that the samples of day 1 and day 2 were loaded on (and selected from) different blots. Data are presented as mean fold change compared to air-exposed rats \pm SEM. Individual animals are represented by open circle (air), triangle (2 ppm acrolein) or square (4 ppm acrolein). Statistical differences between 2 or 4 ppm acrolein versus air were tested using an one-way ANOVA followed by a Dunnett's post-hoc test for multiple comparisons or in case of non-normal distribution a Kruskal-Wallis test followed by a Dunn's multiple comparisons test. Statistical significance is indicated as $^{\#}p < 0.1$, $*p < 0.05$ and $**p < 0.01$ compared to air (control).

Table S1. Primers sequences used for real-time quantitative PCR analysis. All primers were designed for rat, except for primers indicated with an asterisks (*) which were initially designed for mice.

Gene	NCBI Reference Sequence	Sense primer (5'-3')	Antisense primer (3'-5')
Reference genes			
<i>B2m</i>	NM_012512.2	TCGCTCGGTGACCGTGATCT	TCCGGTGGATGGCGAGAGTA
<i>Hprt1</i>	NM_012583.2	TGACCAAGTCAACGGGGGACA	GGGGCTGTACTGCTTGACCA
<i>Ppia</i>	NM_017101.1	TCCATGGCAAATGCTGGACCAA	CCTGGACCCAAAACGCTCCA
<i>Rpl13a</i>	NM_173340.2	GCGGATGAACACCAACCCGT	CAGCCTGGCCTCTTTTGGTCT
<i>Tuba1a</i>	NM_022298.1	AGCGCAGCATCCAGTTTGT	CTGTGGTGTGCTCAGCATAGA
Target genes			
<i>Acadl</i>	NM_012819.2	CGGCACAAAAGAACAGATCG	CTCCCAGACCTTTTGGCATT
<i>Aldh2</i>	NM_032416.2	AACGTGGTGGTGATGAAAGT	GTGACCAACCTCAGTGGAAC
<i>Bax</i>	NM_017059.2	CGGCGAATTGGAGATGAACTGG	CTAGCAAAGTAGAAGAGGGCAACC
<i>Bcl2</i>	NM_016993.2	TGTGGATGACTGACTACCTGAACC	CAGCCAGGAGAAAATCAAACAGAGG
<i>Becn1</i>	NM_053739.2; NM_001034117.1	GGTAGCTTTTCTGGACTGTGTGCAGCAG	GTCTTCAATCTTGCCCTTCTCCACGTCC
<i>Bnip3</i>	NM_053420.3	CAGAGCGGCGAGGAGAACCTGCAG	GCTGCTCCCATTCCCATTGCTGAAG
<i>Bnip3l</i>	NM_080888.2	AGGCTAACCTGCAGCACAGT	CACTGCCGATGAAACTGCTA
<i>Ccl2</i>	NM_031530.1	GCCTGTTGTTACACAGTTGCT	AGTTCTCCAGCCGACTCATT
<i>Cox4i1</i>	NM_017202.1	CTGAAGGAGAAGGAGAAGG	CAGTGAAGCCGATGAAGA
<i>Cs</i>	NM_130755.1	GATTGTGCCCAATGTCCTCT	TTCATCTCCGTCATGCCATA
<i>Cxcl1</i>	NM_030845.2	CCCCCATGGTTCAGAAGATTG	TTGTCAGAAGCCAGCGTTCAC
<i>Cyc1</i>	NM_001277194.1	ATGTTGCCACCTTCCTTCGCT	AGGACTGACCATTATGCCGC
<i>Dnm1l</i>	NM_053655.3	TGGAGATGGTGGTCAGGAAC	TTTCGTGCAACTGGAAGTGG
<i>Esrra</i>	NM_001008511.2	TGTGGCCTCTGGCTACCACT	CTTGCTCTCCGCTTGGTGA
<i>Fis1*</i>	NM_001105919.1	GGGCAACTACCGGCTCAAG	GCCATGCCTACCAGTCCATC
<i>Fundc1</i>	NM_001025027.1	TTCCGGACCTATGGTAGAAAAA	CCAACCTTCTGGAATAAAAATCC
<i>Gabaraapl</i>	NM_001044294.1	CAAATGAAGAGCGTCTCCCCGTTG	CAAAGTCCAGAACCTGATGCCGACA
<i>Gabpa</i>	NM_001108841.1	ATGGGGACAACGTAAAAACAAGCCT	AGTTCGCTGCACTGTATCCAA
<i>Hadha</i>	NM_130826.2	GGTGTCCCTGAAGTGTGCT	TCTGTCTGCACGAATGTTCC
<i>Hk2</i>	NM_012735.2	TGATCGCCTGCTTATTCACGG	AACCGCCTAGAAATCTCCAGA
<i>Ldha</i>	NM_017025.2	GCACTAAGCGGTCCCAAAAG	ACAGCACCAACCCCAACAAC
<i>Map1lc3b</i>	NM_022867.2	ACCCTCCCTGCATGCAGCTGTCC	ACCAGGGACATGACGAGTACACAACC
<i>Mfn1*</i>	NM_138976.1	GCTGGCTGTCTTGTGCATGT	TCCAGCTCTGTGGTGACATCTG
<i>Mfn2</i>	NM_130894.4	TTGACTCCAGCCATGTCCAT	GGTGACGATGGAGTTGCATC
<i>Mt-Co2*</i>	MN964117.1	CCATCCCAGGCCGACTAA	ATTTTCAGAGCATTGGCCATAGAA
<i>Ndufb3</i>	NM_001106912.1	GAAGAAGCTTGCTGCACGAGG	ACGCAGCAAACCCCCATTTG
<i>Nfkbia</i>	NM_001105720.2	CCGAGAGTGAGGATGAGGAG	ACAAGTCCACGTTCTTTTGG
<i>Nrf1</i>	NM_001100708.1	GGCGGGGACAGATAGTCCT	CGTCACGGCTTTGCTGATGG
<i>Opa1</i>	NM_133585.3	CAGCTGGCAGAAGATCTCAAG	CATGAGCAGGATTTTGACACC

Table S1. Primers sequences used for real-time quantitative PCR analysis. All primers were designed for rat, except for primers indicated with an asterisks (*) which were initially designed for mice. (continued)

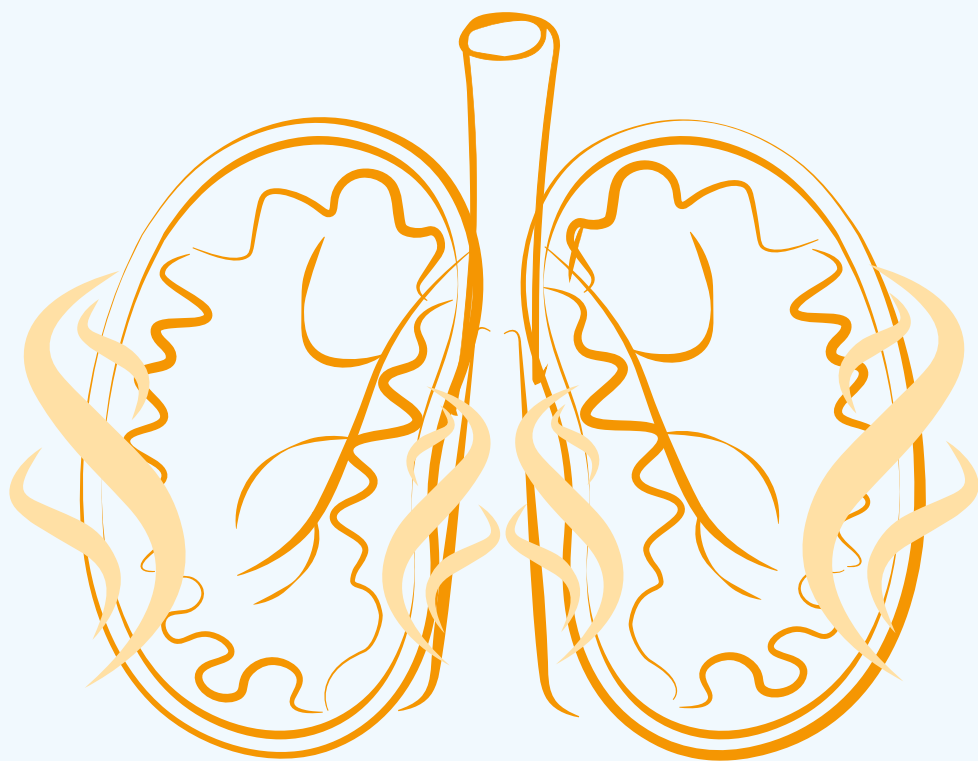
Gene	NCBI Reference Sequence	Sense primer (5'-3')	Antisense primer (3'-5')
<i>Pdk4</i>	NM_053551.2	GCATTTCTACTCGGATGCTCATG	CCAATGTGGCTTGGGTTTCC
<i>Pink1</i>	NM_001106694.1	CCAAACACCTTGGCCTTCTA	CTTAAGATGGCTTCGCTGGA
<i>Pkm</i>	NM_053297.2	GACATTGACTCCGCACCCA	AATTCAGCCGAGCCACATTC
<i>Ppara</i>	NM_013196.2	ACTATGGAGTCCACGCATGTGA	TGTGCTACGCCAGCTTAGC
<i>Ppard</i>	NM_013141.2	ACAGATGAGGACAAACCCACGG	ATGACTGACCCCCACTTGCC
<i>Ppargc1a</i>	NM_031347.1	GGGACATGTGCAGCCAAGACT	GATCTGGGCAAAGAGGCTGGT
<i>Ppargc1b</i>	NM_176075.3	ACTATGATCCCACGTCTGAAGAGTC	CCTTGTCTGAGGTATTGAGGTATTC
<i>Pprc1</i>	NM_001106363.1	TAGACCGGTTACACGCCCA	TCAGGGTTCCTCTTGGGCA
<i>Prkn</i>	NM_020093.1	ACCCACCTACCACAGCTTTT	CAAGGTGAGGGTTGCTTGTC
<i>Sdhb</i>	NM_001100539.1	GAACGGAGACAAAGTACCTGGGG	GATGTTGTGGCAGCGGTAGA
<i>Slc2a1</i>	NM_138827.2	CTTTGTGTCTGCCGTGCTTA	CACATACATGGGCACAAAGC
<i>Slc2a4</i>	NM_012751.1	GGAAGGAAAAGGGCTATGCTG	TGAGGAACCGTCCGAGAATGA
<i>Sod1</i>	NM_017050.1	CGAGCATGGGTTCATGTC	CTGGACCGCATGTTTCTTAG
<i>Sod2</i>	NM_017051.2	ATTAACGCGCAGATCATGCA	CCTCGGTGACGTTTCAATTGT
<i>Sqstm1</i>	NM_175843.5; NM_001393885.1	CTAGGCATCGAGGTTGACATT	CTTGCTGAGTACCACCTTATC
<i>Tfam</i>	NM_031326.2	AATTGCAGCCATGTGGAGGGAG	GCCGGGCTTCCTTCTCTAAGC

Abbreviations: *B2m*: beta-2 microglobulin, *Hprt1*: Hypoxanthine Phosphoribosyltransferase 1, *Ppia*: peptidylprolyl isomerase A, *Rpl13a*: Ribosomal Protein L13A, *Tuba1a*: tubulin, alpha 1A, *Acadl*: acyl-CoA dehydrogenase, long chain, *Aldh2*: aldehyde dehydrogenase 2 family member, *Bax*: BCL2 associated X, apoptosis regulator, *Bcl2*: Bcl2, apoptosis regulator, *Becn1*: Beclin 1, transcript variant 1/2, *Snip3*: BCL2 interacting protein 3, *Snip3l*: BCL2 interacting protein 3-like, *Ccl2*: C-C motif chemokine ligand 2, *Cox4i1*: cytochrome c oxidase subunit 4i1, *Cs*: citrate synthase, *Cxcl1*: C-X-C motif chemokine ligand 1, *Cyc1*: cytochrome c-1, *Dnm1l*: dynamin 1-like, *Esrra*: estrogen related receptor, alpha, *Fis1*: fission, mitochondrial 1, *Fundc1*: FUN14 domain containing 1, *Gabara1l*: GABA type A receptor associated protein like 1, *Gabpa*: GA binding protein transcription factor subunit alpha, *Hadha*: hydroxyacyl-CoA dehydrogenase trifunctional multienzyme complex subunit alpha, *Hk2*: hexokinase 2, *Ldha*: lactate dehydrogenase A, *Map1lc3b*: microtubule-associated protein 1 light chain 3 beta, *Mfn1*: mitofusin 1, *Mfn2*: mitofusin 2, *Mt-Co2*: mitochondrially encoded cytochrome c oxidase II, *Ndufb3*: NADH:ubiquinone oxidoreductase subunit B3, *Nfkb1a*: NFkB inhibitor alpha, *Nrf1*: nuclear respiratory factor 1, *Opal*: OPA1, mitochondrial dynamin like GTPase, *Pdk4*: pyruvate dehydrogenase kinase 4, *Pink1*: Phosphatase and tensin homolog (PTEN) Induced Kinase 1, *Pkm*: pyruvate kinase M1/2, *Ppara*: peroxisome proliferator activated receptor alpha, *Ppard*: Peroxisome proliferator activated receptor delta, *Ppargc1a*: PPARG coactivator 1 alpha, *Ppargc1b*: PPARG coactivator 1 beta, *Pprc1*: PPARG related coactivator 1, *Prkn*: parkin RBR E3 ubiquitin protein ligase, *Sdhb*: succinate dehydrogenase complex iron sulfur subunit B, *Slc2a1*: solute carrier family 2 member 1, *Slc2a4*: solute carrier family 2 member 4, *Sod1*: superoxide dismutase 1, *Sod2*: superoxide dismutase 2, *Sqstm1*: sequestosome 1, transcript variant 1/4, *Tfam*: transcription factor A, mitochondrial

Table S2. Antibodies used for western blotting.

Target	RRID	Company	Product number	Dilution
Primary antibodies				
BNIP3	AB_2259284	Cell Signaling Technology	Cat# 3769S	1:1000
BNIP3L	AB_2688036	Cell Signaling Technology	Cat# 12396	1:1000
CASP3	AB_2341188	Cell Signaling Technology	Cat# 9661	1:1000
ESRRA	AB_1523580	Abcam	Cat# ab76228	1:1000
FUNDC1	AB_10609242	Santa Cruz Biotechnology	Cat# sc-133597	1:500
GABARAPL1	AB_2294415	Proteintech Group	Cat# 11010-1-AP	1:1000
HK2	AB_2232946	Cell Signaling Technology	Cat# 2867	1:1000
MAP1LC3B	AB_915950	Cell Signaling Technology	Cat# 2775	1:1000
NRF1	AB_2154534	Abcam	Cat# ab55744	1:1000
OXPHOS	AB_2629281	MitoScience LLC	Cat# MS604	1:1000
PINK1	AB_10127658	Novus Biologicals	Cat# BC100-494	1:2000
PPARGC1A	AB_10697773	Millipore	Cat# 516557	1:1000
PRKN	AB_2159920	Cell Signaling Technology	Cat# 4211	1:1000
SQSTM1	AB_10624872	Cell Signaling Technology	Cat# 5114	1:1000
TFAM	AB_10682431	Millipore	Cat# DR1071	1:1000
TOMM20	AB_2716623	Abcam	Cat# Ab186734	1:1000
Secondary antibodies				
Goat Anti-Mouse IgG Antibody	AB_2827937	Vector Laboratories	Cat#BA-9200	1:10000
Goat Anti-Rabbit IgG Antibody	AB_2313606	Vector Laboratories	Cat#BA-1000	1:10000
Goat Anti-Rabbit IgG Antibody	AB_2099233	Cell Signaling Technology	Cat#7074S	1:10000

Abbreviations: BNIP3: BCL2 Interacting Protein 3, BNIP3L: BCL2 Interacting Protein 3-Like, CASP3: Caspase 3, ESRRA: Estrogen Related Receptor, Alpha, FUNDC1: FUN14 Domain Containing 1, GABARAPL1: GABA Type A Receptor Associated Protein Like 1, HK2: Hexokinase 2, MAP1LC3B: Microtubule-Associated Protein 1 Light Chain 3 Beta, NRF1: Nuclear Respiratory Factor 1, OXPHOS: oxidative phosphorylation antibody cocktail (containing NDUFB8: NADH:Ubiquinone Oxidoreductase Subunit B8, SDHB: Succinate Dehydrogenase Complex Iron Sulfur Subunit B, UQCRC2: Ubiquinol-Cytochrome C Reductase Core Protein 2, MT-COI: Mitochondrially Encoded Cytochrome C Oxidase I, ATP5F1A: ATP Synthase F1 Subunit Alpha), PINK1: Phosphatase and tensin homolog (PTEN) Induced Kinase 1, PPARGC1A: PPARG Coactivator 1 Alpha, PRKN: Parkin RBR E3 Ubiquitin Protein Ligase, SQSTM1: Sequestosome 1, TFAM: Transcription factor A, Mitochondrial, TOMM20: Translocase Of Outer Mitochondrial Membrane 20



Chapter 5

Impact of sub-acute acrolein inhalation on the molecular regulation of mitochondrial metabolism in rat lung

Christy B.M. Tulen, Pieter A. Leermakers, Sarah E. Schrieder,
Frederik-Jan van Schooten, Antoon Opperhuizen, Alexander H.V. Remels

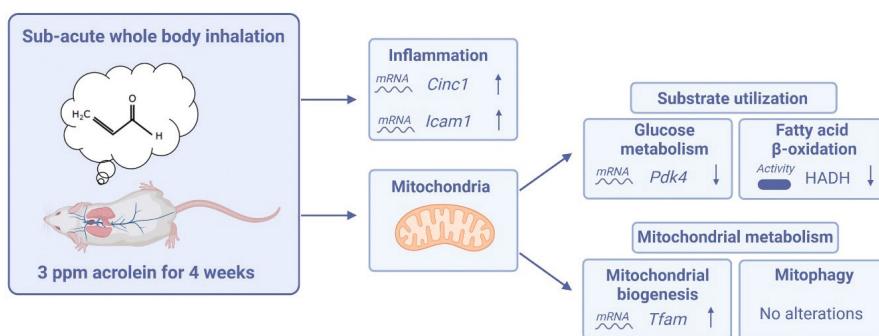
Submitted

Abstract

Nowadays, mitochondria are recognized as key players in the pathogenesis of a variety of smoking-associated lung diseases. Acrolein, a component of cigarette smoke, is a known driver of biological mechanisms underlying smoking-induced respiratory toxicity. The impact of sub-acute acrolein inhalation *in vivo* on key processes controlling mitochondrial homeostasis in cells of the airways however is unknown. In this study, we investigated the activity/abundance of a myriad of molecules critically involved in mitochondrial metabolic pathways and mitochondrial quality control processes (mitochondrial biogenesis and mitophagy) in the lungs of Sprague-Dawley rats that were sub-acutely exposed to filtered air or 3 ppm acrolein by whole-body inhalation (5 h/day, 5 days/week for 4 weeks). Acrolein exposure induced a general inflammatory response in the lung as gene expression analysis revealed an increased expression of *Icam1* and *Cinc1* ($p < 0.1$; $p < 0.05$). Acrolein significantly decreased enzyme activity of hydroxy-acyl-Coenzyme A dehydrogenase ($p < 0.01$), and decreased *Pdk4* transcript levels ($p < 0.05$), suggestive of acrolein-induced changes in metabolic processes. Investigation of constituents of the mitochondrial biogenesis pathways and mitophagy machinery revealed no pronounced alterations. In conclusion, sub-acute inhalation of acrolein did not affect the regulation of mitochondrial metabolism and quality control, which is in contrast to more profound changes after acute exposure in other studies.

Keywords: acrolein, chronic obstructive pulmonary disease, inflammation, mitochondrial metabolism, respiratory toxicity

Graphical abstract



Designed with Biorender.com

Introduction

The volatile carbonyl acrolein is one of the most reactive aldehydes generated during the pyrolysis and combustion of tobacco (1). Exposure to acrolein by tobacco smoking equals or exceeds the total human exposure to this reactive aldehyde from all other sources in the environment such as combustion of animal fats, forest fires, fossil fuels, and plastics (2).

Smoking-associated acrolein emissions are known to irritate the respiratory tract and are responsible for ~88.5% of the known non-cancer respiratory hazard (3, 4). Acrolein-induced cellular toxicity is manifested, amongst others, as oxidative stress, formation of adducts in DNA and proteins, and activation of inflammatory pathways (5). Acrolein is shortlisted for regulation in cigarette smoke (CS) by the World Health Organization Study Group on Tobacco Product Regulation (6, 7), which is based on the relatively high abundance of acrolein in CS, the reactivity of acrolein due to its α,β -unsaturated structure and also the fact that acrolein is one of the representative aldehydes present in CS (1, 8-10). A recent mode-of-action analysis of Yeager *et al.* identified critical cellular processes associated with acrolein-induced respiratory toxicity, respectively inflammation and necrosis in the middle and lower regions of the respiratory tract, as important contributors to chronic obstructive pulmonary disease (COPD) pathogenesis (11). Interestingly, inactivating mutations in aldehyde dehydrogenase 2, an enzyme that detoxifies aldehydes, have been associated with an increased risk of smoking-related chronic airway obstruction in human studies (12). Moreover, activation of aldehyde dehydrogenase activity has been linked to protection against CS-induced cytotoxicity and cell damage in epithelial cells of the airways *in vitro* (13), and to protection from acute acrolein-induced lung damage *in vivo* in mice (14). While it has been suggested that similar biological processes play a role in acrolein-induced toxicity and in the development of COPD, the molecular mechanistic link between smoking-associated acrolein exposure and COPD pathogenesis is incompletely understood.

In recent years, evidence indicates aberrant mitochondrial morphology and a causal role for mitochondrial dysfunction in the pathogenesis of smoking-associated lung diseases, such as COPD (15-17). Interestingly, besides energy production, mitochondria play a prominent role in the regulation of inflammation, oxidative stress and cell death, which are all observed in COPD pathogenesis (15, 16).

As mitochondrial homeostasis is critical for proper cellular function, several processes, such as selective breakdown of mitochondria by mitophagy, mitochondrial biogenesis, and mitochondrial dynamics, play a key role in adaptation of cells of the airways to stress for example in response to inhalation of toxicants (15). In case of damaged or defective mitochondria, degradation will be regulated by two specific mitophagy pathways. One known mitophagy pathway is initiated by mitochondrial receptors

like BCL2/Adenovirus E1B 19 kDa protein-interacting protein 3 (BNIP3), BNIP3-Like (BNIP3L), and FUN14 domain containing 1 (FUNDCl), while the other mitophagy pathway is initiated by a loss of mitochondrial membrane potential, accumulation of phosphatase and tensin homolog (PTEN) induced kinase 1 (PINK1) and recruitment of parkin RBR E3 ubiquitin protein ligase (PRKN) in the outer mitochondrial membrane. These two mitophagy pathways are respectively called receptor- and ubiquitin-mediated mitophagy. Both pathways require recruitment of autophagy proteins to subsequently eliminate proteins by the autophagic-lysosomal pathways (18, 19). On the other hand, mitochondrial biogenesis is involved in the generation of new organelles and is regulated by the peroxisome proliferator-activated receptor (PPAR) gamma (PPARG), coactivator 1 (PPARGC1) signaling pathway (20-22). The continuous fission and fusion of mitochondria is important to control mitochondrial morphology, and facilitates inter-mitochondrial content exchange, monitors mitochondrial distribution, and mediates the release of intermembrane space proteins during apoptosis (23).

Although previous studies convincingly demonstrated disturbances in mitochondrial function and the abovementioned molecular pathways controlling mitochondrial homeostasis in response to repeated inhalation of CS in experimental animals (17, 24-29) as well as in patients with lung disease (24-26, 30-33), it is unclear whether these changes are directly mediated by inhalation of acrolein. Only a few *in vitro* studies have reported impaired mitochondrial morphology and mitochondrial dysfunction in cells of the airways that were acutely or sub-acutely exposed to acrolein *in vitro* (34-36). Interestingly, a previous *in vitro* study suggested that acrolein exposure induces cellular and mitochondrial reactive oxygen species production and leads to oxidative stress in the mitochondrial compartment which was associated with a reduction in mitochondrial function/respiration in human lung epithelial cells and fibroblasts. Moreover, they have demonstrated that acrolein exposure resulted in increased DNA damages in the mitochondrial compartment (34). These findings make it highly likely that acrolein induces oxidative stress in the mitochondrial compartment in cells of the lung. Although, *in vivo* evidence supporting this is largely lacking, we recently reported that acute inhalation of acrolein in rats disrupted the molecular regulation of mitochondrial metabolism in the lung (37). However, sub-acute or chronic exposure studies would be more relevant for assessing the impact of acrolein inhalation on mitochondrial homeostasis in the lungs and airways, as these studies reflect a more realistic smoking-associated acrolein exposure regime. Although one study reported that sub-chronic inhalation of acrolein resulted in structural lung damage and impaired lung function (38), the impact of prolonged inhalation of acrolein on the molecular mechanisms involved in the regulation of mitochondrial metabolism, mitochondrial content and homeostasis (mitochondrial breakdown, mitochondrial biogenesis, and fission/fusion) is currently unknown.

Therefore, in this study, we aimed to investigate the activity and/or abundance of key constituents involved in mitochondrial metabolic pathways and mitochondrial quality control processes in lungs of Sprague Dawley rats after sub-acute whole-body inhalation to filtered air or 3 ppm acrolein (5 h/day, 5 days/week for 4 weeks). We hypothesized that acrolein inhalation would lead to changes in the molecular pathways controlling mitophagy and mitochondrial biogenesis.

Materials and methods

Acrolein administration and exposure of animals

The acrolein administration and exposure of rats were conducted at Purdue University, West-Lafayette, Indiana, United States of America (USA) and previously described by Liu *et al.* (39). The animal study was approved by the Institutional Animal Care and Use Committee at Purdue University.

In short, male Sprague-Dawley rats, (4-months old) were purchased from Envigo RMS, Inc., (Indianapolis, Indiana, USA). All rats were housed in a humidity and temperature controlled room on a 12 h light/12 h dark cycle in the animal facility at Purdue University. *Ad libitum* filtered water and standard rat chow food were provided during the study. After acclimation for 6 days in the animal facility, the acrolein exposures started using a whole-body 50 L exposure chamber (EZ-179, World Precision Instruments, Sarasota, Florida, USA). The final desired concentration of 3 ppm acrolein (CAS No. 107-02-8) was achieved by mixing 350 ppm acrolein in nitrogen (Praxair gas cylinder, Danbury, Connecticut, USA) with filtered air in a 'T' tube with a final total flow of 8 L/min. Monitoring and controlling of the flow rates was conducted by two mass flow meters & controllers (41695K, 41945K, McMaster-Carr, Chicago, Illinois, USA). This acrolein or filtered air flow entered the chamber on one side. A calibrated Volatile Organic Compounds detector (Mocon Baseline, Colorado, USA) monitored the actual concentration of acrolein in the chamber. Before the start of the experiment, a stable acrolein concentration was monitored in the whole exposure chamber for 5 h. 1 h post-start of the exposure the average acrolein concentration was 3.1 ± 0.9 ppm (39). Rats were exposed to 3 ppm acrolein or filtered air (control) for 5 h every day, 5 days per week for 4 weeks. In total, 12 animals were exposed to acrolein and 12 animals to filtered air (control).

Following 4 h after the last dose of exposure (acrolein or filtered air), the rats were euthanized by I.V. administration of an overdose of sodium pentobarbital ((Beuthanasia®; Intervet Inc., Merck, Madison, New Jersey, USA) at 100 mg/kg body weight. Exsanguination was administrated after cessation of heartbeat. Next, the right cranial lung lobe and left caudal lung lobe (\pm trachea) were dissected, snap-frozen in

liquid nitrogen and stored at -80°C until further processing. Frozen lung tissue was crushed using a mortar and powdered lung tissue was stored at -80°C until use.

RNA isolation, synthesis of cDNA and real-time quantitative PCR analysis

Powdered lung tissue (~50-100 mg) was homogenized in 1 mL TRIzol Reagent™ (Invitrogen™, the Netherlands) using a handheld PRO Scientific Bio-Gen PRO2000 homogenizer for two times 10 s at maximum speed. Processing of the homogenates was conducted following the manufacturer's protocol with catalog numbers 15,596,026 and 15,596,018 (Invitrogen™). Purity and quantity of the RNA samples were determined by using the NanoDrop ND 1000 UV-vis spectrophotometer (Isogen Life Sciences, the Netherlands). Before downstream processing, the integrity of total RNA samples was assessed by agarose gel analysis. Approximately 475-2850 ng RNA of each sample dissolved 1:10 in Loading Dye (Invitrogen™) was loaded in a 2% (w/v) agarose gel in 0.5x Tris-borate EDTA stained with Sybr Safe DNA gel Stain (Invitrogen™) and ran for approximately 60 min at 100 Volt. Degraded RNA samples identified by a lower molecular weight smear were excluded for further analysis. Subsequently, cDNA synthesis was conducted using the iScript™ cDNA synthesis kit (Bio-Rad, the Netherlands). In accordance with the manufacturer's protocol 400 ng of total RNA was reverse transcribed including a no reverse transcription control and a no template control. cDNA was diluted 1:50 in Milli-Q and stored in -20°C until further analysis.

Genes of interest were analyzed using real-time quantitative PCR amplification. Firstly, 4.4 µL of 1:50 diluted cDNA, 5 µL 2xSensiMix™ SYBR® & Fluorescein Kit (Bioline, the Netherlands) and 0.6 µL target and species-specific primers were mixed in white LightCycler480 384-multiwell plates (Roche, Switzerland). This was followed by running the plate in the Roche LightCycler480 machine (Roche) using the thermal cycling protocol as suggested by the manufacturer: 10 min at 95°C, 55 cycles of: 10 s at 95°C, 20 s at 60°C. A list of target and species-specific primer sequences analyzed is presented in Table S1. Analysis of melt curves/peaks was conducted using LightCycler480 Software (Roche) and relative gene expression quantification was performed by LinRegPCR software 2014.x (the Netherlands). In order to normalize the expression of mRNA transcripts of interest, the geometric mean was calculated based on the transcript expression of a combination of five reference genes (*B2m*, *Hprt1*, *Ppia*, *Rpl13A*, *Tuba1a*) using GeNorm software 3.4 (Primerdesign, Southampton, USA).

DNA isolation and analysis of mitochondrial DNA copy number

Powdered lung tissue (~10-30 mg) was dissolved in 250 µL lysis buffer (0.1 M Tris/HCl pH 8.5, 0.005 M EDTA pH 8.0, 0.2% (w/v) sodium dodecyl sulphate, 0.2 M NaCl) and 5 µL Proteinase K (Qiagen, USA) (>600 mAU/mL) (1:50) at room temperature and thereafter incubated overnight at 55°C. The next day, again 250 µL lysis buffer was added to the homogenates followed by centrifugation at full speed 25,000 x g for 15 min. Processing of the homogenates was continued by addition of 500 µL isopropanol to the supernatant

and shaking vigorously in order to precipitate the DNA. After washing the DNA pellet twice using 70% ethanol and subsequently evaporation of the ethanol, the DNA pellets were dissolved in 125 μ L TE buffer (10 mM Tris/HCl pH 8.0, 1 mM EDTA pH 8.0). Next, the DNA pellets were incubated at 55°C for 2 h followed by incubation overnight at 4°C. The DNA samples were stored at -20°C until further analysis.

Before downstream processing, purity and quantity of the DNA samples were evaluated by using the NanoDrop ND 1000 UV-vis spectrophotometer (Isogen Life Sciences) followed by dilution of the DNA samples (1:50) in TE buffer. mtDNA copy numbers were assessed by the ratio of the abundance of mtDNA, *mitochondrially encoded cytochrome c oxidase II* (*Mt-co2*), and genomic DNA, *peptidylprolyl isomerase A* (*Ppia*), (Table S1) using real-time quantitative PCR (see paragraph 'RNA isolation, synthesis of cDNA and real-time quantitative PCR analysis').

Western blotting

Powdered lung tissue (~50 mg) was homogenized in 600 μ L Immunoprecipitation lysis buffer (50 mM Tris pH 7.4, 150 mM NaCl, 10% (v/v) glycerol, 0.5% Nonidet P40, 1 mM EDTA) including PhosSTOP Phosphatase and cOmplete, Mini, EDTA-free Protease Inhibitor cocktail tablets (Roche) using a handheld PRO Scientific Bio-Gen PRO2000 homogenizer for 5 s at medium speed. After homogenizing and 15 min of incubation on ice, the whole tissue lysates were rotated for 30 min in the cold room. Next, the samples were centrifuged at 20,000 \times g for 30 min at 4°C. Total protein content was assessed in an aliquot of the supernatant of the whole tissue lysates using Pierce™ BCA Protein Assay Kit according to the manufacturer's protocol (Catalog number 23225 and 23227, Thermo Fischer Scientific, USA, range 20-2000 μ g/mL). Next, the supernatant fraction was diluted in a final concentration of 1 μ g/ μ L in 1 \times Laemmli buffer (0.25 M Tris pH 6.8, 8% (w/v) sodium dodecyl sulphate, 40% (v/v) glycerol, 0.4 M Dithiothreitol, 0.02% (w/v) Bromophenol Blue) and boiled for 5 min at 100°C. The samples were stored at -80°C until running on gel.

The samples (10 μ g of protein per lane) and two or more Precision Plus Protein™ All Blue Standards (#161-0373, Bio-Rad) were loaded and run on a 26-well Criterion XT Precast 4-12% or 12% Bis-Tris gel (Bio-Rad) in 1 \times MES running buffer (Bio-Rad). Next, electrophoresis (100-130 V) for 1 h resulted into separation of the proteins, whereafter electroblotting (Bio-Rad Criterion Blotter) (100 V) for 1 h achieved transfer of the proteins from the gel to a 0.45 μ M Nitrocellulose Transfer membrane (Bio-Rad). Subsequently, total protein quantification was evaluated by staining of the Nitrocellulose membranes with 0.2% Ponceau S in 1% acetic acid (Sigma-Aldrich, the Netherlands) for 5 min, followed by a Milli-Q wash and imaging using the Amersham™ Imager 600 (GE Healthcare, the Netherlands). After washing away the Ponceau S staining, incubation in 3% (w/v) non-fat dry milk (Campina, the Netherlands) in Tween20 Tris-buffered saline (TBST; 20 mM Tris, 137 mM NaCl, 0.1% (v/v) Tween20, pH 7.6) for 1 h at room temperature

resulted in blocking of the membranes. After a wash with TBST, the membranes were cut and incubated with a target-specific primary antibody diluted 1:500-1:2,000 in TBST with 3% (w/v) Bovine Serum Albumin or non-fat dry milk at 4°C overnight (Table S2). The day after, a membrane wash with TBST was followed by incubation with a horseradish peroxidase-conjugated secondary antibody (Table S2) diluted 1:10,000 in 3% (w/v) non-fat dry milk in TBST at room temperature for 1 h. After a wash with TBST, a 3 min incubation of the membranes with either 0.25-1 x Supersignal West FEMTO or 0.5 x Supersignal West PICO Chemiluminescent Substrate (Thermo Fischer Scientific) was followed by visualization of the target proteins using the Amersham™ Imager 600 (GE Healthcare). Original images, if required, have been adjusted for brightness and contrast equally throughout the picture, and were quantified using Image Quant software (GE Healthcare). Ponceau S staining and quantification was used as normalization factor for semi-quantitative western blot analysis, respectively assessed by correction for total protein loading content via quantification over the entire size range of proteins (250 kDa - 10 kDa), with the exception of quantification of a smaller range in case of technical errors (e.g., air bubbles). Because some target-proteins were analyzed on a similar gel/membrane, which is possible due to a different molecular mass, quantification of these proteins was based on normalization on the same Ponceau S staining, respectively Gel I: HK2, DNMT1L, OXPHOS, TOMM20, SQSTM1; Gel II: PRKN, BNIP3L, BNIP3, FUNDC1, PINK1, MAP1LC3B; Gel III: PPARGC1A, NRF1, TFAM, GABARAPL1, ESRRA; Gel IV: AMPK α , CASP3; Gel V: phospho-AMPK α . The presented Ponceau S band (~75 kDa) in the figures is representative for the whole Ponceau S staining, as well as the selected band of the target protein and corresponding Ponceau S band of one animal is reflecting the changes observed in the whole group.

Metabolic enzyme activity assay

Powdered lung tissue (~10-30 mg) was homogenized using a handheld PRO Scientific Bio-Gen PRO2000 homogenizer in 350 μ L SET buffer (pH 7.4: 250 mM sucrose, 2 mM EDTA, 10 mM Tris) for 5 s at medium speed. Following incubation of the homogenates at ice for 15 min, the homogenates were centrifuged at 20,000 x g for 10 min at 4°C. The supernatants were aliquoted for determination of total protein concentration using the Pierce™ BCA Protein Assay Kit according to the manufacturer's protocol (Catalog number 23,225 and 23227, Thermo Fischer Scientific, range 20-2000 μ g/mL) or diluted in 5% Bovine Serum Albumin in Milli-Q (1:4) for further metabolic enzyme activity analysis. All supernatants were stored at -80°C until use.

Hydroxyacyl-Coenzyme A dehydrogenase (HADH). As previously described (EC 1.1.1.35) (40), undiluted samples (in 5% Bovine Serum Albumin) were mixed with reagent (0.22 mM NADH, 100 mM tetrapotassium pyrophosphate pH 7.3) in a 96-well plate (Costar) and thereafter the reaction was initiated by addition of 2.3 mM acetoacetyl-CoA.

Phosphofructokinase 1 (PFK 1). As previously described, (EC 2.7.1.11) (41), undiluted samples (in 5% Bovine Serum Albumin) were mixed with reagent (48.8 mM Tris, 7.4 mM $\text{MgCl}_2 \cdot 6\text{H}_2\text{O}$, 74 mM KCl, 384 μM KCN, 2.8 mM ATP, 1.5 mM DTT, 0.3 mM NADH, 0.375 U/mL aldolase, 0.5625 U/mL glycerol-3-phosphate dehydrogenase and 7.425 U/mL triose phosphate isomerase, pH 8.0) in a 96-well plate (Costar), and subsequently the reaction was initiated by addition of fructose-6-phosphate (30.6 mM) in Tris buffer (49.5 mM, pH 8.0).

In both assays, spectrophotometric analysis of duplicate undiluted samples was conducted at 340 nM at 37°C, 60 readings, interval of 19 s HADH or 30 s PFK 1 using the Multiskan Spectrum plate reader (Thermo Labsystems, the Netherlands). Final metabolic enzyme activity was assessed by slope determination and correction for total protein concentration per sample.

Statistical data analysis

All data are presented as mean fold change compared to air control \pm standard error of the mean (SEM). Statistical analyses as well as graph of the data were performed in Graphpad Prism 8.0 Software (La Jolla, California, USA). Quality evaluation of the data and corresponding exclusion of extreme outliers was conducted by evaluation of *i*. RNA integrity using denaturing agarose gel analysis; *ii*. gene expression melt curve/peak analysis using LightCycler480 Software (Roche); and *iii*. protein degradation by Western blot analysis. Comparison of acrolein *versus* air (control) group was conducted by testing normal distribution of the data with the Shapiro-Wilk test, followed by a two-tailed unpaired parametric t-test or in case of non-normal distribution an unpaired nonparametric Mann-Whitney test. Statistical significant differences were considered when p-values were below 0.05 (* $p < 0.05$) or 0.01 (** $p < 0.01$) and a trend was indicated if p-values were below 0.1 (# $p < 0.1$).

Results

Elevated transcript abundance of key regulators involved in inflammation following sub-acute acrolein exposure

Repeated inhalation of the toxicant acrolein is known to induce inflammation in cells of the airways (42-46). As previously reported in the animals used in this study, an inflammatory response in the vocal fold was observed upon sub-acute acrolein exposure (39). We now investigated the impact of acrolein inhalation on lower regions of the respiratory tract, i.e. peripheral lung tissue, in these animals. In line with previously described acrolein-induced inflammation (39), we observed increased transcript abundance of pro-inflammatory genes *Intracellular adhesion molecule-1* (*Icam1*) ($p<0.1$) and *cytokine-induced neutrophil chemoattractant-1* (*Cinc1*) ($p<0.05$) in lung tissue homogenates of these animals (Fig. 1A). No significant alterations were observed in transcript levels of other analyzed inflammatory genes (Fig. 1A).

Because acrolein is also known to induce oxidative stress resulting in lung damage and epithelial cell apoptosis (5, 11), we next assessed the impact of acrolein inhalation on the abundance of anti-oxidant and apoptosis markers. Remarkably, mRNA levels of anti-oxidant molecules *superoxide dismutase 1* and *2* (*Sod1* and *Sod2*; $p=0.10$, $p=0.24$) and *catalase* (*Cat*) were not different between groups (Fig. 1B and C). In contrast to previous histopathological observations of acrolein-induced epithelial cell death and sloughing in vocal folds (39), significantly lower mRNA levels of the ratio of *BCL2 associated X*, *apoptosis regulator* and *Bcl2*, *apoptosis regulator* (*Bax/Bcl2*) ($p<0.01$) were detected in lung homogenates of these acrolein-exposed animals, while protein levels of cleaved caspase-3, as an indicator for apoptosis, was unaltered (Fig. S1).

In summary, these findings suggest an inflammatory response in rat lung following sub-acute acrolein exposure by whole-body inhalation, while no consistent effects on apoptosis or anti-oxidant defense systems were observed.

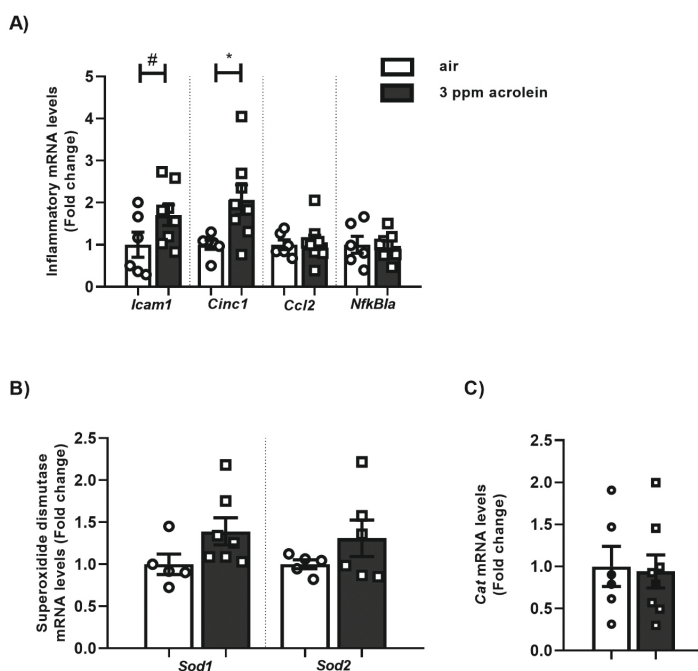


Figure 1. Acrolein-induced increased expression of inflammatory genes in rat lung. Sprague-Dawley rats were sub-acute exposed by whole-body inhalation to air or 3 ppm acrolein (5 h/day, 5 days/week for 4 weeks) (n=6-8/group). Transcript levels of inflammatory markers *Icam1*, *Cinc1*, *Ccl2*, *NfkB1a* (A) as well as mRNA levels of anti-oxidant markers *Sod1* and *Sod2* (B), and *Cat* (C) in rat lung homogenates. Data are presented as mean fold change compared to air-exposed rats \pm SEM. Individual animals are represented by open circles (control) or squares (3 ppm acrolein). Statistical differences between acrolein *versus* air groups were tested using a two-tailed unpaired parametric t-test. Statistical significance is indicated as #p<0.1 and *p<0.05 compared to air-exposed rats.

The regulation of constituents involved in mitochondrial metabolism in response to sub-acute acrolein exposure

Next, we investigated whether or not sub-acute acrolein exposure affected the abundance and activity of molecules involved in key metabolic processes.

First, we assessed expression of *pyruvate dehydrogenase kinase 4 (Pdk4)*, a key metabolic regulatory molecule that is transcriptionally-regulated and is well-known for its control over whether pyruvate (derived from glycolytic processing of glucose) is directed into the tricarboxylic acid cycle in the mitochondria or whether it is converted to lactate (47). We observed that acrolein inhalation resulted in significantly decreased transcript levels of *Pdk4* ($p < 0.05$) (Fig. 2A), which is suggestive of enhanced conversion of pyruvate to acetyl-CoA as fuel for the tricarboxylic acid cycle and further oxidative processing into the mitochondria. Further investigation of expression and activity levels of critical constituents of glycolysis and the tricarboxylic acid cycle (i.e., hexokinase 2 (HK2) and enzyme activity of PFK 1), revealed no significant alterations in response to sub-acute acrolein inhalation compared to air control (Fig. 2B-D). However, upon investigation of constituents of the fatty acid beta-oxidation pathway, we observed that exposure to acrolein resulted in significantly decreased enzyme activity of HADH ($p < 0.01$) (Fig. 3A). This was not observed at the transcript level nor did we observe significant changes in mRNA expression levels of another enzyme of the fatty acid β -oxidation pathway *acyl-CoA dehydrogenase, long chain (Acadl)* (Fig. 3B). Exposure to acrolein also did not affect transcript or protein levels of nuclear- and mitochondrial-encoded sub-units of the electron transport chain complexes or abundance of another mitochondrial protein that we investigated (translocase of outer mitochondrial membrane 20; TOMM20) (Fig. 3C-F).

Subsequently, we investigated the ratio of phosphorylated 5'adenosine monophosphate-activated protein kinase α (phospho-AMPK α)/AMPK α as a marker of energy status, and found a trend to an increased ratio in acrolein-exposed animals relative to air control ($p = 0.08$) (Fig. 3G-H). In addition, quantification of mtDNA copy number revealed no significant changes (Fig. 3I).

In conclusion, these data indicate no pronounced changes in the activity and abundance of constituents of key metabolic processes upon acrolein inhalation for 4 weeks, except decreased *Pdk4* mRNA levels and HADH enzyme activity.

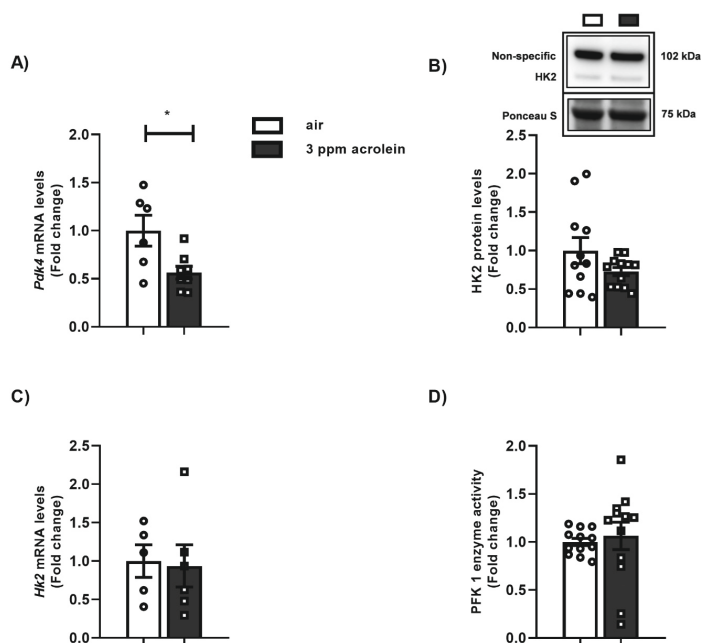


Figure 2. Abundance and activity of glycolysis-associated markers were not different in acrolein- and air-exposed rats. Sprague-Dawley rats were sub-acute exposed by whole-body inhalation to air or 3 ppm acrolein (5 h/day, 5 days/week for 4 weeks) (n=5-12/group). Transcript levels of *Pdk4* (A) were assessed. Moreover, protein abundance of HK2 (B) and transcript levels of *Hk2* (C) and PFK 1 enzyme activity (D) were presented. Representative western blot images, respectively bands of the target-proteins and corresponding normalization bands of the Ponceau S staining, are shown of one animal/group reflective of the changes in the group as quantified in the graph. Data are presented as mean fold change compared to air-exposed rats \pm SEM. Individual animals are represented by open circles (control) or squares (3 ppm acrolein). Statistical differences between acrolein versus air groups were tested using a two-tailed unpaired parametric t-test. Statistical significance is indicated as * p <0.05 compared to air-exposed rats.

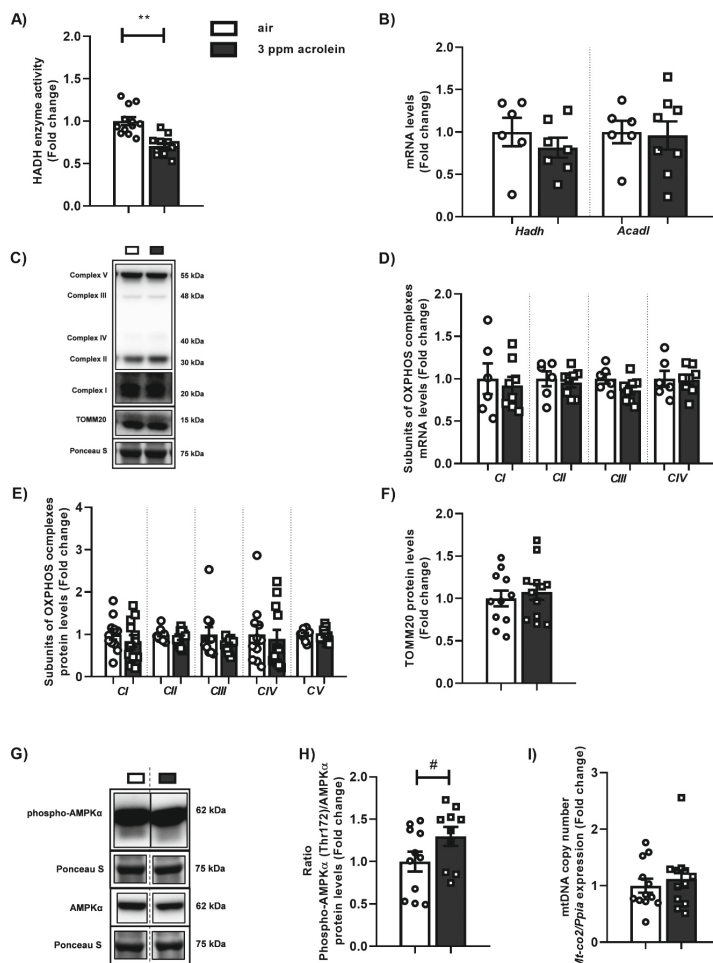


Figure 3. Sub-acute acrolein exposure did not affect the regulation mitochondrial content in rat lung.

Sprague-Dawley rats were sub-acutely exposed by whole-body inhalation to air or 3 ppm acrolein (5 h/day, 5 days/week for 4 weeks) (n=6-12/group). HADH enzyme activity (A) and transcript expression of *Hadh* and *Acadl* (B). Moreover, protein (C-D) and mRNA (E) levels of nuclear- and mitochondrial-encoded constituents of the electron transport chain (i.e. subunits of oxidative phosphorylation complexes I-V) as well as TOMM20 protein levels (C,F) were analyzed in rat lung homogenates. In addition, protein levels of the ratio phospho-AMPKα/AMPKα were shown (G, H). Western blot analysis revealed two distinct bands on two different blots corresponding with expected molecular weights for phospho-AMPKα (Thr172) protein (62 kDa) and AMPKα (62 kDa). Lastly, mitochondrial DNA (mtDNA) copy number (I) was quantified. Representative western blot images, respectively bands of the target-proteins and corresponding normalization bands of the Ponceau S staining, are shown of one animal/group reflective of the changes in the group as quantified in the graph. Data are presented as mean fold change compared to air-exposed rats ± SEM. Individual animals are represented by open circles (control) or squares (3 ppm acrolein). Statistical differences between acrolein versus air groups were tested using a two-tailed unpaired parametric t-test, or in case of non-normal distribution an unpaired nonparametric Mann-Whitney test. Statistical significance is indicated as #p<0.1 and **p<0.01 compared to air-exposed rats.

The molecular regulation of the mitophagy machinery upon sub-acute acrolein exposure

As mitochondrial metabolism and content are regulated by the interplay between mitophagy and mitochondrial biogenesis, and it is possible that these processes balance each other out, we decided to probe these processes as well in the current study.

First, we evaluated the protein and transcript abundance of constituents involved in the two mitophagy pathways, i.e., receptor- and ubiquitin-mediated mitophagy. Evaluation of the abundance of key regulators involved in the mitophagy machinery revealed no significant differences in protein and transcript levels of investigated constituents associated with both mitophagy pathways: receptor- (Fig. 4) and ubiquitin-mediated mitophagy (Fig. S2). Inhalation of acrolein also revealed no changes in protein and mRNA levels of autophagy-associated proteins, which are required to facilitate protein degradation by the autophagic-lysosomal pathway, as shown in Fig. S3. The only exception being protein levels of GABA type A receptor associated protein like 1 (GABARAPL1) which were elevated ($p < 0.1$) compared to air-exposed rats (Fig. S3B).

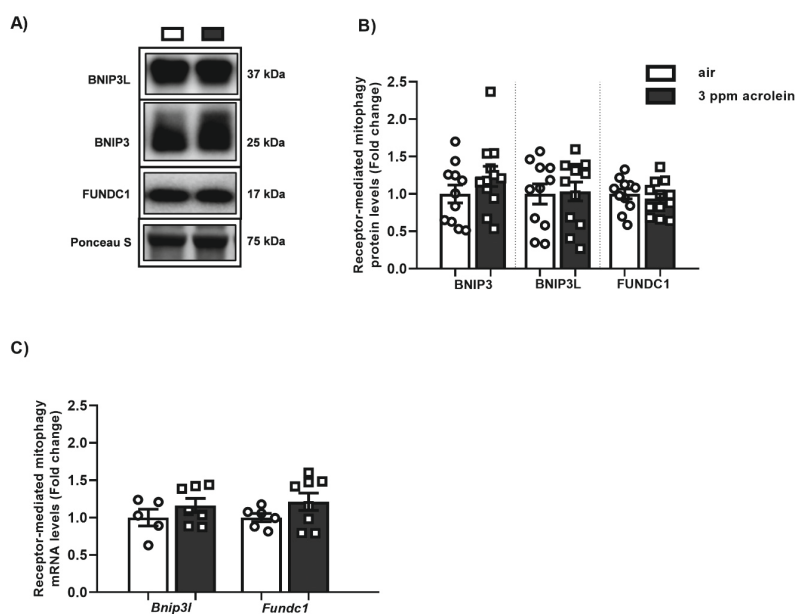


Figure 4. No changes in the abundance of constituents involved in receptor-mediated mitophagy in acrolein-exposed rat lung. Sprague-Dawley rats were sub-acutely exposed by whole-body inhalation to air or 3 ppm acrolein (5 h/day, 5 days/week for 4 weeks) ($n=5-12$ /group). Protein levels of BNIP3, BNIP3L, FUNDC1 (A,B) as well as gene expression of *Bnip3l* and *Fundc1* (C) in rat lung homogenates. Representative western blot images, respectively bands of the target-proteins and corresponding normalization bands of the Ponceau S staining, are shown of one animal/group reflective of the changes in the group as quantified in the graph. Data are presented as mean fold change compared to air-exposed rats \pm SEM. Individual animals are represented by open circles (control) or squares (3 ppm acrolein). Statistical differences between acrolein *versus* air groups were tested using a two-tailed unpaired parametric t-test.

Sub-acute acrolein exposure has minor effects on the abundance of regulatory molecules controlling mitochondrial biogenesis

We next explored whether or not acrolein inhalation has an impact on the protein and transcript abundance of key constituents of the PPARGC1 signaling network, which is the master pathway controlling mitochondrial biogenesis in eukaryotic cells (20-22).

As depicted in Fig. 5F, mRNA levels of *transcription factor a, mitochondrial (Tfam)*, which is a main transcription factor controlling transcription of the mitochondrial genome, was significantly increased ($p < 0.05$) in rat lung following whole-body acrolein inhalation for 4 weeks. Protein and transcript levels of all other analyzed constituents involved in the PPARGC1 signaling network were largely unaltered (Fig. 5).

Mitochondrial dynamics play an essential role in maintaining mitochondrial homeostasis. Despite the largely unaltered abundance of regulators associated with mitophagy and mitochondrial biogenesis in response to acrolein, we did investigate the abundance of markers involved in mitochondrial fission and fusion after sub-acute exposure to acrolein for 4 weeks as previous studies indicated altered mitochondrial morphology in response to *in vitro* acrolein (34) or *in vivo* chronic CS exposure (17, 24). We observed no significant changes in the abundance of analyzed fission- or fusion-associated proteins in the different groups (Fig. S4).

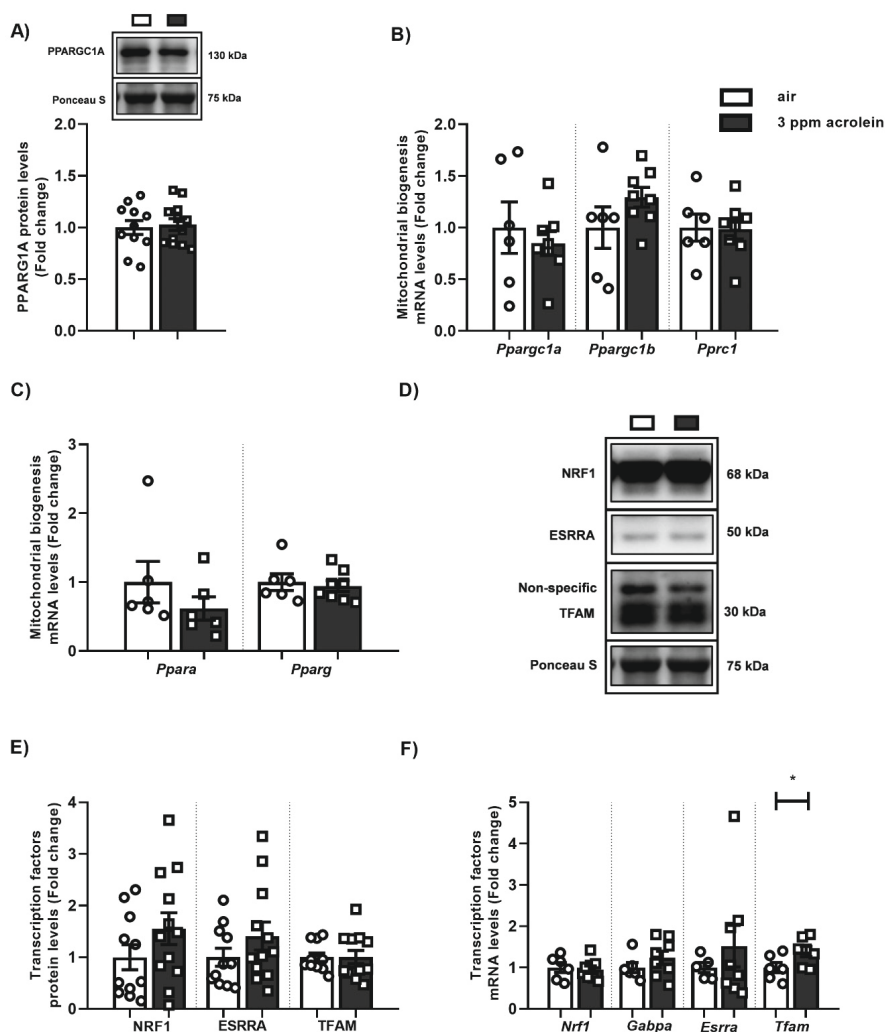


Figure 5. Unaltered abundance of molecules involved in the PPARGC1 network following sub-acute acrolein exposure in rat. Sprague-Dawley rats were sub-acutely exposed by whole-body inhalation to air or 3 ppm acrolein (5 h/day, 5 days/week for 4 weeks) (n=5-12/group). Protein levels of PPARGC1A (A) and mRNA expression of *Ppargc1a*, *Ppargc1b*, *Pprc1* (B) and *Ppara*, *Pparg* (C) as well as protein abundance of co-activated transcription factors NRF1, ESRRRA, TFAM (D, E) and transcript levels of *Nrf1*, *Gabpa*, *Esrra* and *Tfam* (F) in rat lung homogenates. Representative western blot images, respectively bands of the target-proteins and corresponding normalization bands of the Ponceau S staining, are shown of one animal/group reflective of the changes in the group as quantified in the graph. Data are presented as mean fold change compared to air-exposed rats \pm SEM. Individual animals are represented by open circles (control) or squares (3 ppm acrolein). Statistical differences between acrolein versus air groups were tested using a two-tailed unpaired parametric t-test, or in case of non-normal distribution an unpaired nonparametric Mann-Whitney test.

Discussion

In this study, we assessed the impact of a 4-week whole-body acrolein inhalation regime on key regulatory molecules involved in the molecular control of mitochondrial content and homeostasis (mitophagy *versus* mitochondrial biogenesis) in rat lung. Successful acrolein exposure in these exact same animals was supported by significant different body weight changes in acrolein- *versus* air-exposed animals (48), and by our observation of increased inflammatory gene expression which is in line with previous findings reported in the vocal fold of these animals (39). However, we failed to observe significant changes in the expression of anti-oxidant genes and markers for apoptosis. Moreover, while previous literature has convincingly demonstrated changes in the regulation of mitochondrial biogenesis and mitophagy *in vitro* and *in vivo* in response to acute acrolein exposure (34, 37) or *in vivo* (sub-) chronic CS exposure (17, 24-29), we did not observe pronounced changes in the abundance of key constituents involved in these processes in response to acrolein in our study.

The dosage of 3 ppm (6.98 mg/m³) used in this study situates itself in the lower range of the amount of acrolein present in one cigarette (range of 1.3-121.7 µg/cigarette i.e., 2.1-110.4 ppm; varying drastically due to different brands, tobacco and smoking regimes/topography) (8). Environmental presence of acrolein sits in a much lower range (3.6-10.7 ppb) (49). Although exposures to dosages up to 10 ppm acrolein (6-12 h) have been reported in acute *in vivo* inhalation studies (50-52), it was shown that laboratory animals were severely affected by sub-acute exposure to these high doses of acrolein (i.e., 3.7-4.9 ppm acrolein; 6-8 h/day, 5 days/week/6-13 weeks; mortality rate > 50% (38, 42, 53)). Therefore, we opted for a dose of 3 ppm acrolein as being representative for smoking-associated exposure and lung damage, and being shown to be non-lethal and well-tolerated up to a duration of 4 weeks (43, 46, 54).

It has been described in literature that the inflammatory and cell death response following acrolein exposure may depend on the dose and model used (5, 11). In line with the increased immune responses shown in previous sub-acute acrolein-inhalation animal studies (ranging up to 4.9 ppm acrolein-exposure for 6 h/day, 5-7 days/week for a maximum of 13 weeks) (42-46), as well as increased inflammatory gene expression and NF-κB activation reported in the vocal fold in the animals of this study (39), we observed increased inflammatory transcript levels in lung homogenates of acrolein-exposed rats. These findings are in accordance with the previously reported induction of COX-2 by NF-κB activation in rat lung epithelial cells upon acrolein exposure, although we failed to detect measurable expression of COX-2 in our samples (data not shown) (55). Interestingly, a critical role for aldehydes, as component of CS, in the induction of airway inflammation and cytokine production is also shown by van der Toorn *et al.* in mice whole-body exposed for 5 days to water-filtered CS (i.e., low in aldehydes) *versus* CS (56). Our findings on inflammatory gene expression in the lower airways/lungs of

the acrolein-exposed rats supports that acrolein reached the cells of the lower airways or at least elicited an inflammatory response that reached this compartment.

Acrolein is known to lead to oxidative damage in the respiratory tract and to induce activity of anti-oxidant enzymes (11, 51, 57, 58). More specifically, increased intracellular and mitochondrial reactive oxygen species production has been shown in alveolar cell models in response to acute acrolein exposure (34), as well as in acrolein-exposed rats (intra-nasal installation for 5 days/week; 4 weeks) (59), which was suggested to be a critical mechanism underlying acrolein-induced lung inflammation and damage. Remarkably, in our study, mRNA levels of anti-oxidant markers were unchanged in response to acrolein. As only anti-oxidant gene expression has been analysed in this study, no conclusions can be drawn about (anti-) oxidant status and system directly. While there are indications for a role of acrolein in oxidation of DNA, RNA, protein and lipids in cells of the lungs (60, 61), knowledge is lacking about the role of, specifically, *in vivo* sub-acute/chronic acrolein exposure in oxidation of DNA, RNA, protein and lipid as most available studies focuses on *in vitro* as well as acute exposures (57, 58, 62-64). Moreover, it is well-described that acrolein interacts with in particular the sulfhydryl group of cysteine, has a role in depletion of GSH and results in DNA damage or oxidation (11), but the specific role of acrolein in these processes in mitochondria has to be elucidated in particular in the *in vivo* setting. In addition, in contrast to previous histopathological observations of acrolein-induced epithelial cell death (39) as well as previous evidence reporting cell death and apoptosis *in vivo* (51, 59) and *in vitro* (34, 57, 65, 66) upon acrolein exposure, we did not observe an indication for apoptosis in our study. Variability in dose (low or high), exposure duration (acute, sub-acute or chronic), chosen endpoints (activity, protein or gene expression) and model of exposure can explain the differential responses in our model compared to literature and should be taken into account in future studies.

Previous *in vitro* studies have shown that acute acrolein exposure can result in mitochondrial dysfunction, inhibition of mitochondrial enzyme activity, and mtDNA damage in alveolar cell models and in rat liver mitochondria (34, 35, 67). In addition, we recently showed that acute *in vivo* acrolein exposure of rats resulted in significantly decreased protein and transcript abundance of subunits of the electron transport chain (37). Furthermore, aberrant mitochondrial function was observed upon *in vivo* chronic CS exposure (whole-body) (17). We failed to observe changes indicative of alterations in mitochondrial content and energy metabolism in response to acrolein in our study. Although we previously observed a shift to glycolysis in response to acute acrolein inhalation *in vivo* (37), we did not observe pronounced changes in activity and abundance in most of the analyzed constituents associated with glycolysis, tricarboxylic acid cycle and the fatty acid beta-oxidation. However, we did observe lower mRNA expression of *Pdk4*, indicative of decreased inhibition of pyruvate dehydrogenase, resulting in increased conversion of pyruvate to acetyl-coA thereby suggestive of a

reduced conversion of pyruvate to lactate through anaerobic glycolysis. Interestingly, a previous *in vivo* study has shown that *Pdk4* remained partially downregulated after 9 months of CS exposure followed by 3 months of recovery in mice (68) as well as bioinformatics analysis showed downregulated expression of *Pdk4* in COPD patients (69). In addition, we found decreased HADH enzyme activity levels suggestive of a disrupted fatty acid beta-oxidation pathway upon repeated inhalation of acrolein. These acrolein-induced alterations in the abundance and activity of key regulators involved in glycolysis and fatty acid beta-oxidation may suggest a disrupted mitochondria metabolism, however further functional analysis is required.

Mitochondrial function and homeostasis in cells of the airways is maintained by a delicate interplay between mitochondrial biogenesis and mitophagy (15), which is suggested to be disturbed in response to inhaled toxicants, such as acrolein (37), CS (17, 24-29) as well as in COPD patients (24-26, 30-33). More specifically, previous studies detected decreased abundance of constituents associated with mitochondrial biogenesis in acute acrolein exposed rat lung (37), upregulated mitophagy in mice lung after CS-exposure for up to 6 months (24), and increased autophagy in 12-weeks CS-exposed mice (27). We did not observe these type of changes in our study, the explanation for which can be multifactorial as discussed below.

Firstly, the difference between acute changes and potential adaptation in response to prolonged exposure may explain the apparent discrepancies in the abundance of key regulators involved in mitochondrial quality control processes (mitochondrial biogenesis and mitophagy). This potential adaptive impact has been described in a study of Struve *et al.* in which pre-exposure to acrolein vapor (0.6 or 1.8 ppm) for 6 h/day, 5 days/week for 14 days resulted in increased nasal acrolein uptake of inhaled acrolein (1.8 or 3.6 ppm), while an adaptive response in GSH-metabolism was observed in the respiratory nasal regions (54). A differential impact of nose-only acrolein inhalation on the regulation of mitochondrial metabolism was also found in rat lung in response to a different dose (2 *versus* 4 ppm) and time (1-day *versus* 2-day) of exposure (37). These time-dependent adaptive responses can be explained by the immediate cellular effects mediated by a stress response and cellular metabolic and immune alterations acutely initiated after exposure (in the abovementioned study, at day 1 (37)), based on previous ozone and acrolein exposure studies (70-73). Subsequently, the actual extravasation of neutrophils in the lung takes several h and generally peaks on next day (in case of the abovementioned study, at day 2, a combination of this inflammatory peak response and a new immediate exposure response was investigated) (37, 73). This adaptive effect has also been observed in human COPD patients showing a contrasting pattern in expression levels of regulatory molecules controlling mitochondrial biogenesis, respectively increased PPARGC1A abundance has been observed in mild or ex-smoking COPD patients *versus* decreased abundance in moderate and severe COPD lung tissue

(31, 32). Thus, it is important to take this potential adaptive effect into account in studies evaluating repeated toxicant inhalation.

Secondly, it is difficult to compare the impact of the individual aldehyde acrolein, as a component of CS, on the regulation of mitochondrial metabolism with whole CS exposures because of the potential synergistic toxicity of the complex combination of aldehydes (74-76) or other chemicals present in CS. To obtain insight in the impact of the interaction of the various components in CS, for example co-exposure of aldehydes should be studied.

Thirdly, the route and mode of toxicant exposure used in *in vivo* studies vary and can lead to different results. Interestingly, a recent study compared CS whole-body inhalation (as a similar inhalation modality as used in our study) with nose-only inhalation for 4 h/day for 9 weeks. They observed in both systems similar changes in lung inflammation/function and lung proteome, as well as alterations in nasal epithelia (transcriptome). Nevertheless, more severe structural and molecular changes in the upper respiratory tract (i.e., nose), lung inflammation and disruption of the molecular regulation in the respiratory system have been reported in nose-only *versus* whole-body exposed mice, while comparable/similar yields of acrolein relative to the nominal concentration were found in the breathing zones of the exposure chambers (77). This difference could be assigned to local toxicity in case of nose-only inhalation. Other explanations could be less stress or the decreased inhaled dose in the whole-body inhalation exposure system because of deposition losses, such as larger contact surfaces, deposition on the fur, filtering the aerosol through the fur or animals huddle together covering their nose with fur (77-81). However, the optimal translational model for the human situation can still be discussed as the airway anatomy, way of breathing (oral *versus* nasal) (82), and the smoke-topography of humans *versus* the continuous exposure of laboratory rodents is totally different (10, 83). Moreover, it is known that in reflex to inhalation of toxicants, such as acrolein inhalation, breathing parameters are altered in rodents, suggested to serve as a protecting mechanism to reduce deposition in lower airways and alveoli (73, 83-86). Nevertheless, also intra-tracheal instillation of acrolein has been reported in (sub-) acute acrolein exposure studies in mice (14, 59), which is suggested to be even less translational to the human situation of smoking-associated acrolein exposure due to the factors described above such as smoking topography (no inhalation), dosimetry, and local toxicity.

Fourthly, while we did not observe pronounced alterations in markers of mitochondrial metabolism at enzyme activity-, protein- or transcript level, this does not imply that mitochondrial function *per se* is unaltered. As mitochondrial homeostasis and the accompanied interplay between mitochondrial biogenesis, mitophagy and dynamics are fluxes, the measured abundance of key regulators involved in these processes are a snapshot not reflecting actual changes in mitochondrial function or content. However,

as respiration measurements require freshly isolated tissue/cells, and we did not isolate fresh material from our study, we were unable to perform such functional analysis in this study. Nevertheless, previous studies have shown already that acute acrolein exposure induced decreased respiration capacity in cells of the lungs (34, 35) as well as in rat lung microvascular endothelial cells (14). In addition, it is well described that CS(E) exposure resulted in declined mitochondrial respiration in cells of the airways both *in vitro* and *in vivo* (17, 24, 28, 87, 88). Interestingly, a relation between expression levels of markers involved in mitochondrial biogenesis and mitochondrial respiration can be suggested based on various studies. For example, it has been shown that hypoxia triggered elevated protein and mRNA abundance of PPARGC1A in cultured cardiac myocytes, as well as an increased basal oxygen consumption rate (89) implying that a similar tendency in expression and respiration data could be expected. This hypothesis is also supported by studying overexpression of PPARGC1A in primary cultures of rabbit renal proximal tubular cells which induced basal and uncoupled respiration and elevated ATP levels in response to oxidant injury (90), as well as by studying knock-out of PPARGC1A which revealed impaired mitochondrial respiration capacity in mice muscle (91). Although these studies imply a relation between expression levels of markers involved in mitochondrial biogenesis and mitochondrial respiration, we did not observe pronounced changes in the abundance of constituents controlling mitochondrial biogenesis and mitophagy following sub-acute acrolein exposure. Therefore, it seems to be unlikely that respiration is altered if the regulation of underlying pathways (mitochondrial biogenesis and mitophagy) are unchanged. We should however be careful in assuming this relation and drawing this conclusion, as the dynamic nature of processes involved in mitochondrial homeostasis should be taken into account.

Lastly, lung tissue homogenates include various cell types, which could be differently impacted by acrolein compensating each other. However, this seems unlikely as dysregulated mitochondrial function and quality control (i.e., mitochondrial biogenesis and mitophagy) has been previously observed in various cell types (*in vitro*) in response to acute acrolein exposure, e.g., lung fibroblasts, alveolar or bronchial epithelial cells, suggesting that these cell types likely are similar affected by acrolein (34-36, 57, 74, 92, 93).

These multiple considerations as indicated above, respectively duration of exposure and potential adaptation, individual *versus* mixture effect of aldehydes, route and models of toxicant exposure, (functional) read-out parameters and interaction of various cell types in the lung, should be taken into account in designing future studies focusing on elucidating the mechanistic and causal impact of acrolein on mitochondrial dysfunction in the lung.

In conclusion, protein and mRNA levels of key constituents involved in mitochondrial metabolism and quality control were largely unaltered in response to sub-acute acrolein inhalation for 4 weeks in rat lung homogenates, which is in contrast with more pronounced changes in the abundance of these molecules in response to acute inhalation of acrolein *in vivo* as observed in other studies.

Acknowledgements

We would like to thank Prof. Dr. M.P. Sivasankar and Dr. X. Liu of the Department of Speech, Language, and Hearing Sciences, Purdue University, West Lafayette, IN, USA for conducting the acrolein exposure studies and sharing the rat lung for analysis.

Conflicts of Interest

The authors have declared no conflict of interest.

Funding

This research is supported by the Netherlands Food and Consumer Product Safety Authority (NVWA).

Authors' contribution

Conceptualization: Christy B.M. Tulen, Frederik-Jan van Schooten, Antoon Opperhuizen, Alexander H.V. Remels

Investigation: Christy B.M. Tulen, Pieter A. Leermakers, Sarah E. Schrieder

Formal analysis: Christy B.M. Tulen, Pieter A. Leermakers, Sarah E. Schrieder

Writing – original draft: Christy B.M. Tulen

Writing – review and editing: Pieter A. Leermakers, Sarah E. Schrieder, Frederik-Jan van Schooten, Antoon Opperhuizen, Alexander H.V. Remels

References

1. Stevens JF, Maier CS. Acrolein: sources, metabolism, and biomolecular interactions relevant to human health and disease. *Mol Nutr Food Res*. 2008;52(1):7-25.
2. Faroon O, Roney N, Taylor J, Ashizawa A, Lumpkin MH, Plewak DJ. Acrolein environmental levels and potential for human exposure. *Toxicol Ind Health*. 2008;24(8):543-64.
3. Haussmann H-J. Use of hazard indices for a theoretical evaluation of cigarette smoke composition. *Chem Res Toxicol*. 2012;25(4):794-810.
4. Fowles J, Dybing E. Application of toxicological risk assessment principles to the chemical constituents of cigarette smoke. *Tob Control*. 2003;12(4):424-30.
5. Moghe A, Ghare S, Lamoreau B, Mohammad M, Barve S, McClain C, et al. Molecular mechanisms of acrolein toxicity: relevance to human disease. *Toxicol Sci*. 2015;143(2):242-55.
6. World Health Organization & World Health Organization Tobacco Free Initiative. The scientific basis of tobacco product regulation: second report of a WHO study group. World Health Organization; 2008.
7. World Health Organization Framework Convention on Tobacco Control. Partial guidelines for implementation of articles 9 and 10—regulation of the contents of tobacco products and regulation of tobacco product disclosures. 2012.
8. Pauwels C, Klerx WNM, Pennings JLA, Boots AW, van Schooten FJ, Opperhuizen A, et al. Cigarette Filter Ventilation and Smoking Protocol Influence Aldehyde Smoke Yields. *Chem Res Toxicol*. 2018;31(6):462-71.
9. Burns DM, Dybing E, Gray N, Hecht S, Anderson C, Sanner T, et al. Mandated lowering of toxicants in cigarette smoke: a description of the World Health Organization TobReg proposal. *Tob Control*. 2008;17(2):132-41.
10. Cheah NP. Volatile aldehydes in tobacco smoke: source fate and risk. [Ph.D. Dissertation Thesis]. Maastricht, The Netherlands: Maastricht University; 2016.
11. Yeager RP, Kushman M, Chemerynski S, Weil R, Fu X, White M, et al. Proposed Mode of Action for Acrolein Respiratory Toxicity Associated with Inhaled Tobacco Smoke. *Toxicol Sci*. 2016;151(2):347-64.
12. Morita K, Masuda N, Oniki K, Saruwatari J, Kajiwarra A, Otake K, et al. Association between the aldehyde dehydrogenase 2*2 allele and smoking-related chronic airway obstruction in a Japanese general population: a pilot study. *Toxicol Lett*. 2015;236(2):117-22.
13. Jang JH, Bruse S, Liu Y, Duffy V, Zhang C, Oyamada N, et al. Aldehyde dehydrogenase 3A1 protects airway epithelial cells from cigarette smoke-induced DNA damage and cytotoxicity. *Free Radic Biol Med*. 2014;68:80-6.
14. Lu Q, Mundy M, Chambers E, Lange T, Newton J, Borgas D, et al. Alda-1 Protects Against Acrolein-Induced Acute Lung Injury and Endothelial Barrier Dysfunction. *Am J Respir Cell Mol Biol*. 2017;57(6):662-73.
15. Cloonan SM, Choi AM. Mitochondria in lung disease. *J Clin Invest*. 2016;126(3):809-20.
16. Aghapour M, Remels AHV, Pouwels SD, Bruder D, Hiemstra PS, Cloonan SM, et al. Mitochondria: at the crossroads of regulating lung epithelial cell function in chronic obstructive pulmonary disease. *Am J Physiol Lung Cell Mol Physiol*. 2020;318(1):L149-l64.
17. Cloonan SM, Glass K, Laucho-Contreras ME, Bhashyam AR, Cervo M, Pabon MA, et al. Mitochondrial iron chelation ameliorates cigarette smoke-induced bronchitis and emphysema in mice. *Nat Med*. 2016;22(2):163-74.

18. Gomes LC, Scorrano L. Mitochondrial morphology in mitophagy and macroautophagy. *Biochim Biophys Acta*. 2013;1833(1):205-12.
19. Fritsch LE, Moore ME, Sarraf SA, Pickrell AM. Ubiquitin and Receptor-Dependent Mitophagy Pathways and Their Implication in Neurodegeneration. *J Mol Biol*. 2020;432(8):2510-24.
20. Jornayvaz FR, Shulman GI. Regulation of mitochondrial biogenesis. *Essays Biochem*. 2010;47:69-84.
21. Lin J, Handschin C, Spiegelman BM. Metabolic control through the PGC-1 family of transcription coactivators. *Cell Metab*. 2005;1(6):361-70.
22. Scarpulla RC. Metabolic control of mitochondrial biogenesis through the PGC-1 family regulatory network. *Biochim Biophys Acta*. 2011;1813(7):1269-78.
23. Detmer SA, Chan DC. Functions and dysfunctions of mitochondrial dynamics. *Nature Reviews Molecular Cell Biology*. 2007;8(11):870-9.
24. Mizumura K, Cloonan SM, Nakahira K, Bhashyam AR, Cervo M, Kitada T, et al. Mitophagy-dependent necroptosis contributes to the pathogenesis of COPD. *J Clin Invest*. 2014;124(9):3987-4003.
25. Ahmad T, Sundar IK, Lerner CA, Gerloff J, Tormos AM, Yao H, et al. Impaired mitophagy leads to cigarette smoke stress-induced cellular senescence: implications for chronic obstructive pulmonary disease. *Faseb j*. 2015;29(7):2912-29.
26. Chen ZH, Kim HP, Sciurba FC, Lee SJ, Feghali-Bostwick C, Stolz DB, et al. Egr-1 regulates autophagy in cigarette smoke-induced chronic obstructive pulmonary disease. *PLoS One*. 2008;3(10):e3316.
27. Chen ZH, Lam HC, Jin Y, Kim HP, Cao J, Lee SJ, et al. Autophagy protein microtubule-associated protein 1 light chain-3B (LC3B) activates extrinsic apoptosis during cigarette smoke-induced emphysema. *Proc Natl Acad Sci U S A*. 2010;107(44):18880-5.
28. Agarwal AR, Yin F, Cadenas E. Short-term cigarette smoke exposure leads to metabolic alterations in lung alveolar cells. *Am J Respir Cell Mol Biol*. 2014;51(2):284-93.
29. Agarwal AR, Zhao L, Sancheti H, Sundar IK, Rahman I, Cadenas E. Short-term cigarette smoke exposure induces reversible changes in energy metabolism and cellular redox status independent of inflammatory responses in mouse lungs. *Am J Physiol Lung Cell Mol Physiol*. 2012;303(10):L889-98.
30. Hara H, Araya J, Ito S, Kobayashi K, Takasaka N, Yoshii Y, et al. Mitochondrial fragmentation in cigarette smoke-induced bronchial epithelial cell senescence. *Am J Physiol Lung Cell Mol Physiol*. 2013;305(10):L737-46.
31. Hoffmann RF, Zarrintan S, Brandenburg SM, Kol A, de Bruin HG, Jafari S, et al. Prolonged cigarette smoke exposure alters mitochondrial structure and function in airway epithelial cells. *Respir Res*. 2013;14:97.
32. Li J, Dai A, Hu R, Zhu L, Tan S. Positive correlation between PPARGgamma/PGC-1alpha and gamma-GCS in lungs of rats and patients with chronic obstructive pulmonary disease. *Acta Biochim Biophys Sin*. 2010;42(9):603-14.
33. Ito S, Araya J, Kurita Y, Kobayashi K, Takasaka N, Yoshida M, et al. PARK2-mediated mitophagy is involved in regulation of HBEC senescence in COPD pathogenesis. *Autophagy*. 2015;11(3):547-59.
34. Wang HT, Lin JH, Yang CH, Haung CH, Weng CW, Maan-Yuh Lin A, et al. Acrolein induces mtDNA damages, mitochondrial fission and mitophagy in human lung cells. *Oncotarget*. 2017;8(41):70406-21.

35. Agarwal AR, Yin F, Cadenas E. Metabolic shift in lung alveolar cell mitochondria following acrolein exposure. *Am J Physiol Lung Cell Mol Physiol*. 2013;305(10):L764-73.
36. Luo C, Li Y, Yang L, Feng Z, Li Y, Long J, et al. A cigarette component acrolein induces accelerated senescence in human diploid fibroblast IMR-90 cells. *Biogerontology*. 2013;14(5):503-11.
37. Tulen CBM, Snow SJ, Leermakers PA, Kodavanti UP, van Schooten FJ, Opperhuizen A, et al. Acrolein inhalation acutely affects the regulation of mitochondrial metabolism in rat lung. *Toxicology*. 2022;153129.
38. Costa DL, Kutzman RS, Lehmann JR, Drew RT. Altered lung function and structure in the rat after subchronic exposure to acrolein. *Am Rev Respir Dis*. 1986;133(2):286-91.
39. Liu X, Durkes AC, Schrock W, Zheng W, Sivasankar MP. Subacute acrolein exposure to rat larynx in vivo. *Laryngoscope*. 2019;129(9):E313-E7.
40. Bergmeyer H, Gawehn K, Grassl M. 3-Hydroxyacyl-CoA dehydrogenase. *Methods of enzymatic analysis*. 1974;1:474.
41. Ling K, Paetkau V, Marcus F, Lardy HA. [77a] Phosphofructokinase: I. Skeletal Muscle. *Methods in enzymology*. 9: Elsevier; 1966. p. 425-9.
42. Feron VJ, Kruysse A, Til HP, Immel HR. Repeated exposure to acrolein vapour: subacute studies in hamsters, rats and rabbits. *Toxicology*. 1978;9(1-2):47-57.
43. Borchers MT, Wesselkamper S, Wert SE, Shapiro SD, Leikauf GD. Monocyte inflammation augments acrolein-induced Muc5ac expression in mouse lung. *Am J Physiol*. 1999;277(3):L489-97.
44. Borchers MT, Wesselkamper SC, Deshmukh H, Beckman E, Medvedovic M, Sartor M, et al. The role of T cells in the regulation of acrolein-induced pulmonary inflammation and epithelial-cell pathology. *Res Rep Health Eff Inst*. 2009(146):5-29.
45. Dorman DC, Struve MF, Wong BA, Marshall MW, Gross EA, Willson GA. Respiratory tract responses in male rats following subchronic acrolein inhalation. *Inhal Toxicol*. 2008;20(3):205-16.
46. Wang T, Liu Y, Chen L, Wang X, Hu XR, Feng YL, et al. Effect of sildenafil on acrolein-induced airway inflammation and mucus production in rats. *Eur Respir J*. 2009;33(5):1122-32.
47. Zhang S, Hulver MW, McMillan RP, Cline MA, Gilbert ER. The pivotal role of pyruvate dehydrogenase kinases in metabolic flexibility. *Nutr Metab (Lond)*. 2014;11(1):10.
48. Liu X. Airborne challenges to vocal folds: studies on barrier function and inflammation: Purdue University, West Lafayette, Indiana, USA; 2018.
49. De Woskin R, Greenberg M, Pepelko W, Strickland J. Toxicological review of acrolein; in support of summary information on the integrated risk information system (Iris). Washington, DC: US Environmental Protection Agency; 2003. Contract No.: EPA/635/R-03/003.
50. Fabisiak JP, Medvedovic M, Alexander DC, McDunn JE, Concel VJ, Bein K, et al. Integrative metabolome and transcriptome profiling reveals discordant energetic stress between mouse strains with differential sensitivity to acrolein-induced acute lung injury. *Mol Nutr Food Res*. 2011;55(9):1423-34.
51. Park JH, Ku HJ, Lee JH, Park JW. Idh2 Deficiency Exacerbates Acrolein-Induced Lung Injury through Mitochondrial Redox Environment Deterioration. *Oxid Med Cell Longev*. 2017;2017:1595103.

52. Kim JK, Park JH, Ku HJ, Kim SH, Lim YJ, Park JW, et al. Naringin protects acrolein-induced pulmonary injuries through modulating apoptotic signaling and inflammation signaling pathways in mice. *J Nutr Biochem*. 2018;59:10-6.
53. Lyon JP, Jenkins LJ, Jr., Jones RA, Coon RA, Siegel J. Repeated and continuous exposure of laboratory animals to acrolein. *Toxicol Appl Pharmacol*. 1970;17(3):726-32.
54. Struve MF, Wong VA, Marshall MW, Kimbell JS, Schroeter JD, Dorman DC. Nasal uptake of inhaled acrolein in rats. *Inhal Toxicol*. 2008;20(3):217-25.
55. Sarkar P, Hayes BE. Induction of COX-2 by acrolein in rat lung epithelial cells. *Mol Cell Biochem*. 2007;301(1-2):191-9.
56. van der Toorn M, Slebos DJ, de Bruin HG, Gras R, Rezayat D, Jorge L, et al. Critical role of aldehydes in cigarette smoke-induced acute airway inflammation. *Respir Res*. 2013;14(1):45.
57. Roy J, Pallepati P, Bettaieb A, Tanel A, Averill-Bates DA. Acrolein induces a cellular stress response and triggers mitochondrial apoptosis in A549 cells. *Chem Biol Interact*. 2009;181(2):154-67.
58. Arumugam N, Sivakumar V, Thanislass J, Pillai KS, Devaraj SN, Devaraj H. Acute pulmonary toxicity of acrolein in rats--underlying mechanism. *Toxicol Lett*. 1999;104(3):189-94.
59. Sun Y, Ito S, Nishio N, Tanaka Y, Chen N, Isobe K. Acrolein induced both pulmonary inflammation and the death of lung epithelial cells. *Toxicol Lett*. 2014;229(2):384-92.
60. Pizzimenti S, Ciamporcerio E, Daga M, Pettazzoni P, Arcaro A, Cetrangolo G, et al. Interaction of aldehydes derived from lipid peroxidation and membrane proteins. *Front Physiol*. 2013;4:242.
61. Zarkovic N, Cipak A, Jaganjac M, Borovic S, Zarkovic K. Pathophysiological relevance of aldehydic protein modifications. *J Proteomics*. 2013;92:239-47.
62. Li L, Jiang L, Geng C, Cao J, Zhong L. The role of oxidative stress in acrolein-induced DNA damage in HepG2 cells. *Free Radic Res*. 2008;42(4):354-61.
63. Sarkar P. Response of DNA damage genes in acrolein-treated lung adenocarcinoma cells. *Molecular and Cellular Biochemistry*. 2019;450(1):187-98.
64. Baldrige KC, Zavala J, Surratt J, Sexton KG, Contreras LM. Cellular RNA is chemically modified by exposure to air pollution mixtures. *Inhal Toxicol*. 2015;27(1):74-82.
65. Yadav UCS, Ramana KV, Srivastava SK. Aldose reductase regulates acrolein-induced cytotoxicity in human small airway epithelial cells. *Free radical biology & medicine*. 2013;65:15-25.
66. Xiong R, Wu Q, Muskhelishvili L, Davis K, Shemansky JM, Bryant M, et al. Evaluating Mode of Action of Acrolein Toxicity in an In Vitro Human Airway Tissue Model. *Toxicol Sci*. 2018;166(2):451-64.
67. Sun L, Luo C, Long J, Wei D, Liu J. Acrolein is a mitochondrial toxin: effects on respiratory function and enzyme activities in isolated rat liver mitochondria. *Mitochondrion*. 2006;6(3):136-42.
68. Miller MA, Danhorn T, Cruickshank-Quinn CI, Leach SM, Jacobson S, Strand MJ, et al. Gene and metabolite time-course response to cigarette smoking in mouse lung and plasma. *PLoS One*. 2017;12(6):e0178281.
69. Huang X, Li Y, Guo X, Zhu Z, Kong X, Yu F, et al. Identification of differentially expressed genes and signaling pathways in chronic obstructive pulmonary disease via bioinformatic analysis. *FEBS Open Bio*. 2019;9(11):1880-99.

70. Henriquez AR, Snow SJ, Schladweiler MC, Miller CN, Dye JA, Ledbetter AD, et al. Beta-2 Adrenergic and Glucocorticoid Receptor Agonists Modulate Ozone-Induced Pulmonary Protein Leakage and Inflammation in Healthy and Adrenalectomized Rats. *Toxicol Sci.* 2018;166(2):288-305.
71. Henriquez AR, Williams W, Snow SJ, Schladweiler MC, Fisher C, Hargrove MM, et al. The dynamicity of acute ozone-induced systemic leukocyte trafficking and adrenal-derived stress hormones. *Toxicology.* 2021;458:152823.
72. Miller DB, Snow SJ, Schladweiler MC, Richards JE, Ghio AJ, Ledbetter AD, et al. Acute Ozone-Induced Pulmonary and Systemic Metabolic Effects Are Diminished in Adrenalectomized Rats. *Toxicol Sci.* 2016;150(2):312-22.
73. Snow SJ, McGee MA, Henriquez A, Richards JE, Schladweiler MC, Ledbetter AD, et al. Respiratory Effects and Systemic Stress Response Following Acute Acrolein Inhalation in Rats. *Toxicol Sci.* 2017;158(2):454-64.
74. Zhang S, Zhang J, Chen H, Wang A, Liu Y, Hou H, et al. Combined cytotoxicity of co-exposure to aldehyde mixtures on human bronchial epithelial BEAS-2B cells. *Environ Pollut.* 2019;250:650-61.
75. Zhang S, Chen H, Wang A, Liu Y, Hou H, Hu Q. Combined effects of co-exposure to formaldehyde and acrolein mixtures on cytotoxicity and genotoxicity in vitro. *Environ Sci Pollut Res Int.* 2018;25(25):25306-14.
76. LoPachin RM, Gavin T. Molecular mechanisms of aldehyde toxicity: a chemical perspective. *Chem Res Toxicol.* 2014;27(7):1081-91.
77. Kogel U, Wong ET, Szostak J, Tan WT, Lucci F, Leroy P, et al. Impact of whole-body versus nose-only inhalation exposure systems on systemic, respiratory, and cardiovascular endpoints in a 2-month cigarette smoke exposure study in the ApoE(-/-) mouse model. *J Appl Toxicol.* 2021;41(10):1598-619.
78. Wong BA. Inhalation exposure systems: design, methods and operation. *Toxicol Pathol.* 2007;35(1):3-14.
79. Phalen RF, Mannix RC, Drew RT. Inhalation exposure methodology. *Environ Health Perspect.* 1984;56:23-34.
80. Pauluhn J, Mohr U. Inhalation studies in laboratory animals--current concepts and alternatives. *Toxicol Pathol.* 2000;28(5):734-53.
81. Phelps DW, Veal JT, Buschbom RL, Filipy RE, Wehner AP. Tobacco smoke inhalation studies: a dosimetric comparison of different cigarette types. *Arch Environ Health.* 1984;39(5):359-63.
82. Phalen RF, Oldham MJ, Wolff RK. The relevance of animal models for aerosol studies. *Journal of aerosol medicine and pulmonary drug delivery.* 2008;21(1):113-24.
83. Corley RA, Kabilan S, Kuprat AP, Carson JP, Jacob RE, Minard KR, et al. Comparative Risks of Aldehyde Constituents in Cigarette Smoke Using Transient Computational Fluid Dynamics/ Physiologically Based Pharmacokinetic Models of the Rat and Human Respiratory Tracts. *Toxicol Sci.* 2015;146(1):65-88.
84. Lee BP, Morton RF, Lee LY. Acute effects of acrolein on breathing: role of vagal bronchopulmonary afferents. *J Appl Physiol.* 1992;72(3):1050-6.
85. Perez CM, Hazari MS, Ledbetter AD, Haykal-Coates N, Carll AP, Cascio WE, et al. Acrolein inhalation alters arterial blood gases and triggers carotid body-mediated cardiovascular responses in hypertensive rats. *Inhal Toxicol.* 2015;27(1):54-63.

86. Corley RA, Kabilan S, Kuprat AP, Carson JP, Minard KR, Jacob RE, et al. Comparative computational modeling of airflows and vapor dosimetry in the respiratory tracts of rat, monkey, and human. *Toxicol Sci.* 2012;128(2):500-16.
87. Sundar IK, Maremanda KP, Rahman I. Mitochondrial dysfunction is associated with Miro1 reduction in lung epithelial cells by cigarette smoke. *Toxicol Lett.* 2019;317:92-101.
88. Malinska D, Szymanski J, Patalas-Krawczyk P, Michalska B, Wojtala A, Prill M, et al. Assessment of mitochondrial function following short- and long-term exposure of human bronchial epithelial cells to total particulate matter from a candidate modified-risk tobacco product and reference cigarettes. *Food Chem Toxicol.* 2018;115:1-12.
89. Zhu L, Wang Q, Zhang L, Fang Z, Zhao F, Lv Z, et al. Hypoxia induces PGC-1 α expression and mitochondrial biogenesis in the myocardium of TOF patients. *Cell Research.* 2010;20(6):676-87.
90. Rasbach KA, Schnellmann RG. PGC-1 α over-expression promotes recovery from mitochondrial dysfunction and cell injury. *Biochem Biophys Res Commun.* 2007;355(3):734-9.
91. Adhihetty PJ, Uguccioni G, Leick L, Hidalgo J, Pilegaard H, Hood DA. The role of PGC-1 α on mitochondrial function and apoptotic susceptibility in muscle. *Am J Physiol Cell Physiol.* 2009;297(1):C217-25.
92. Moretto N, Facchinetti F, Southworth T, Civelli M, Singh D, Patacchini R. α , β -Unsaturated aldehydes contained in cigarette smoke elicit IL-8 release in pulmonary cells through mitogen-activated protein kinases. *Am J Physiol Lung Cell Mol Physiol.* 2009;296(5):L839-48.
93. Zhang S, Zhang J, Cheng W, Chen H, Wang A, Liu Y, et al. Combined cell death of co-exposure to aldehyde mixtures on human bronchial epithelial BEAS-2B cells: Molecular insights into the joint action. *Chemosphere.* 2020;244:125482.

Supplementary information

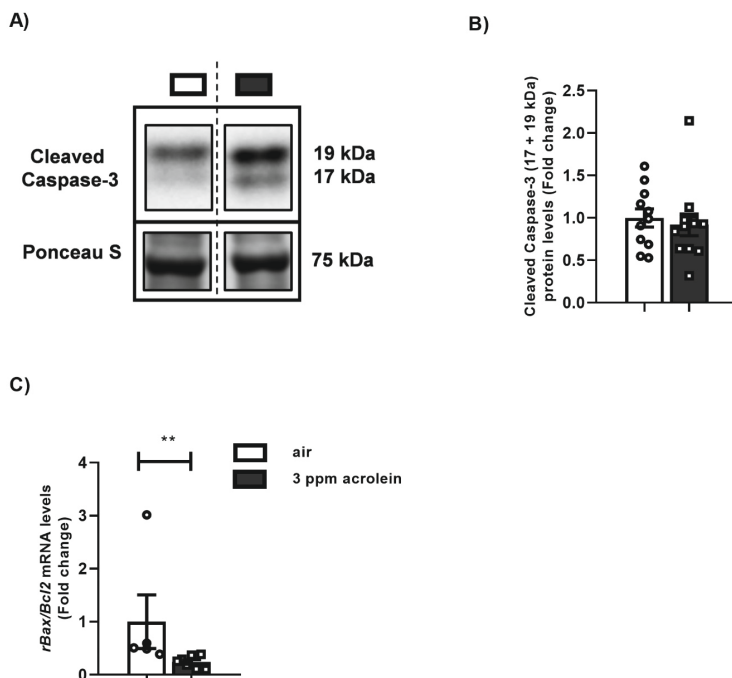


Figure S1. Abundance of apoptosis-associated constituents in sub-acute acrolein exposed rats.

Sprague-Dawley rats were sub-acute exposed by whole-body inhalation to air or 3 ppm acrolein (5 h/day, 5 days/week for 4 weeks) (n=5-12/group). Protein levels of cleaved caspase-3 (**A,B**) and mRNA levels of ratio *Bax/Bcl2* (**C**) were analyzed. Western blot analysis revealed two distinct bands corresponding with expected molecular weights for cleaved caspase-3 protein, (17 + 19 kDa). Representative western blot images, respectively bands of the target-proteins and corresponding normalization bands of the Ponceau S staining, are shown of one animal/group reflective of the changes in the group as quantified in the graph. Data are presented as mean fold change compared to air-exposed rats \pm SEM. Individual animals are represented by open circles (control) or squares (3 ppm acrolein). Statistical differences between acrolein *versus* air groups were tested using an unpaired nonparametric Mann-Whitney test (non-normal distribution). Statistical significance is indicated as **p<0.01 compared to air-exposed rats.

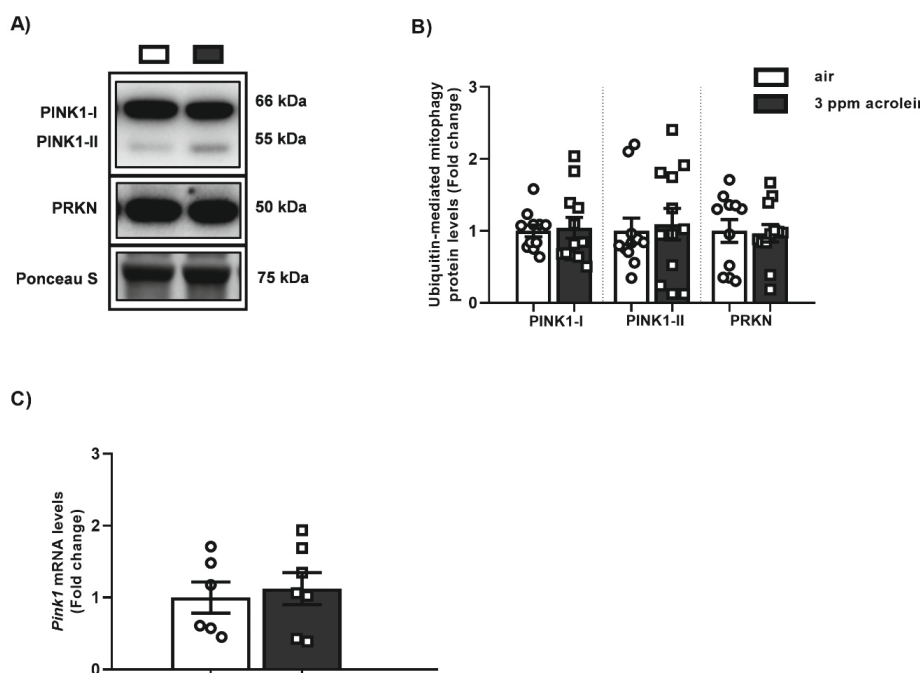


Figure S2. No alterations in the abundance of key indices controlling ubiquitin-mediated mitophagy upon sub-acute acrolein exposure in rats. Sprague-Dawley rats were sub-acutely exposed by whole-body inhalation to air or 3 ppm acrolein (5 h/day, 5 days/week for 4 weeks) (n=6-12/group). Protein abundance of PINK1-I, PINK1-II, PRKN (**A, B**) as well as mRNA levels of *Pink1* (**C**) were analyzed. Western blot analysis revealed two distinct bands corresponding with expected molecular weights for PINK protein, entitled PINK1-I (66 kDa) and PINK1-II (55 kDa). Representative western blot images, respectively bands of the target-proteins and corresponding normalization bands of the Ponceau S staining, are shown of one animal/group reflective of the changes in the group as quantified in the graph. Data are presented as mean fold change compared to air-exposed rats \pm SEM. Individual animals are represented by open circles (control) or squares (3 ppm acrolein). Statistical differences between acrolein *versus* air groups were tested using a two-tailed unpaired parametric t-test, or in case of non-normal distribution an unpaired nonparametric Mann-Whitney test.

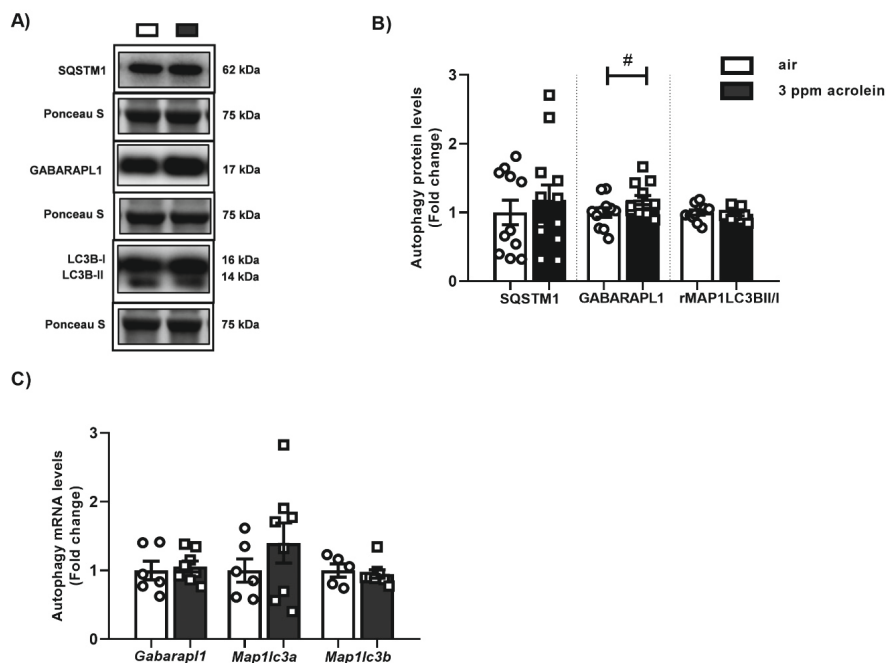


Figure S3. Acrolein exposure did not alter the abundance of molecules associated with autophagy.

Sprague-Dawley rats were sub-acutely exposed by whole-body inhalation to air or 3 ppm acrolein (5 h/day, 5 days/week for 4 weeks) (n=5-12/group). Protein levels of SQSTM1, GABARAPL1, ratio MAP1LC3BII/I (**A,B**) as well as transcript abundance of *Gabarapl1*, *Map1lc3a* and *Map1lc3b* (**C**) in rat lung homogenates. Western blot analysis revealed two distinct bands corresponding with expected molecular weights for MAP1LC3B protein, entitled LC3B-I (16 kDa) and LC3B-II (14 kDa). Representative western blot images, respectively bands of the target-proteins and corresponding normalization bands of the Ponceau S staining, are shown of one animal/group reflective of the changes in the group as quantified in the graph. Data are presented as mean fold change compared to air-exposed rats \pm SEM. Individual animals are represented by open circles (control) or squares (3 ppm acrolein). Statistical differences between acrolein *versus* air groups were tested using a two-tailed unpaired parametric t-test, or in case of non-normal distribution an unpaired nonparametric Mann-Whitney test. Statistical significance is indicated as # $p < 0.1$ compared to air-exposed rats.

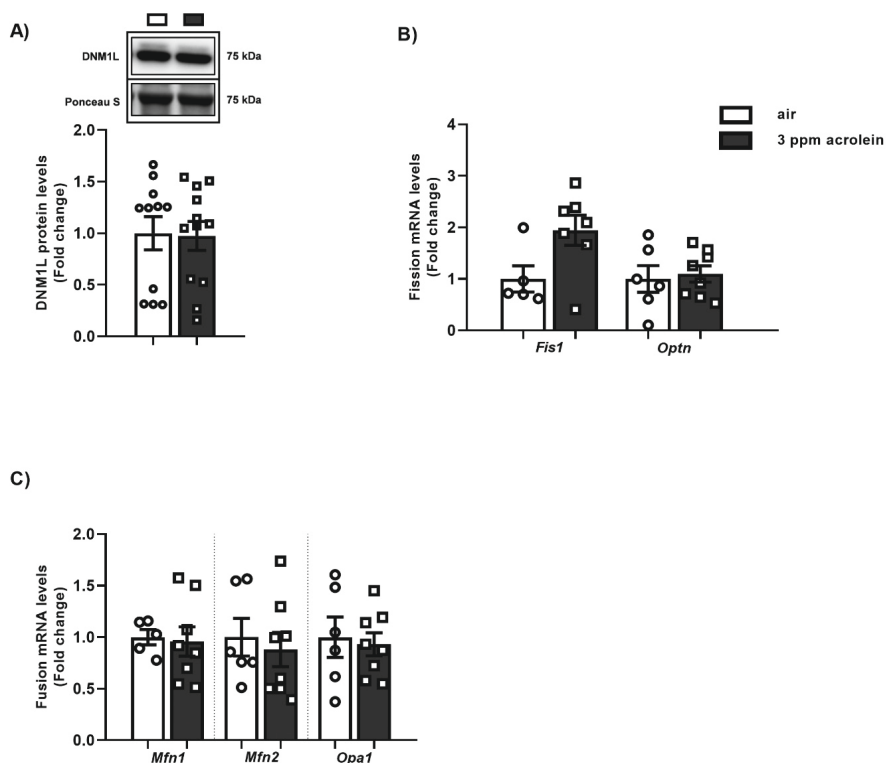


Figure S4. No pronounced impact of sub-acute acrolein exposure on the abundance of fission- and fusion-associated indices in rat lung homogenates. Sprague-Dawley rats were sub-acutely exposed by whole-body inhalation to air or 3 ppm acrolein (5 h/day, 5 days/week for 4 weeks) (n=5-12/group). Abundance of fission-associated indices: DNM1L (**A**), *Fis1* and *Optn* (**B**) as well as of fusion-associated indices *Mfn1*, *Mfn2* and *Opa1* (**C**) were analyzed in rat lung. Representative western blot images, respectively bands of the target-proteins and corresponding normalization bands of the Ponceau S staining, are shown of one animal/group reflective of the changes in the group as quantified in the graph. Data are presented as mean fold change compared to air-exposed rats \pm SEM. Individual animals are represented by open circles (control) or squares (3 ppm acrolein). Statistical differences between acrolein *versus* air groups were tested using a two-tailed unpaired parametric t-test, or in case of non-normal distribution an unpaired nonparametric Mann-Whitney test.

Table S1. Primer sequences of reference and target genes used for real-time quantitative PCR analysis. All primers were designed for rat, except for primers indicated with an asterisks (*) which were initially designed for mice.

Gene	NCBI Reference Sequence	Sense primer (5'-3')	Antisense primer (3'-5')
Reference genes			
<i>B2m</i>	NM_012512.2	TCGCTCGGTGACCGTGATCT	TCCGGTGGATGGCGAGAGTA
<i>Hprt1</i>	NM_012583.2	TGACCAGTCAACGGGGGACA	GGGGCTGTACTGCTTGACCA
<i>Ppia</i>	NM_017101.1	TCCATGGCAAATGCTGGACCAA	CCTGGACCCAAAACGCTCCA
<i>Rpl13a</i>	NM_173340.2	GCGGATGAACACCAACCCGT	CAGCCTGGCCTCTTTTGGTCT
<i>Tuba1a</i>	NM_022298.1	AGCGCAGCATCCAGTTTGT	CTGTGGTGTGCTCAGCATAGA
Target genes			
<i>Acadl</i>	NM_012819.2	CGGCACAAAAGAACAGATCG	CTCCCAGACCTTTTGGCATT
<i>Bax</i>	NM_017059.2	CGGCGAATTGGAGATGAACTGG	CTAGCAAAGTAGAAGAGGGCAACC
<i>Bcl2</i>	NM_016993.2	TGTGGATGACTGACTACCTGAACC	CAGCCAGGAGAAATCAAACAGAGG
<i>Bnip3l</i>	NM_080888.2	AGGCTAACCTGCAGCACAGT	CACTGCCGATGAAACTGCTA
<i>Cat</i>	NM_012520.2	GAATGGCTATGGCTCACACA	CAAGTTTTTGATGCCCTGGT
<i>Ccl2</i>	NM_031530.1	GCCTGTTGTTTCAGATTGCT	AGTTCTCCAGCCGACTCATT
<i>Cox4i1</i> (CIV)	NM_017202.1	CTGAAGGAGAAGGAGAAGG	CAGTGAAGCCGATGAAGA
<i>Cinc1</i>	NM_030845.2	AACCGAAGTCATAGCCACAC	CGCCATCGGTGCAATCTATC
<i>Cycl (CIII)</i>	NM_001277194.1	ATGTTGCCACCTTCCTTCGCT	AGGACTGACCACTTATGCCGC
<i>Esrra</i>	NM_001008511.2	TGTGGCCTCTGGCTACCACT	CTTGCCTCTCCGCTTGGTGA
<i>Fis1</i>	NM_001105919.2	ATGGATGCCAGAGATGAAG	ACGATGCCTCTACGGATGTC
<i>Fundc1</i>	NM_001025027.1	TTCCGGACCTATGTTAGAAAAA	CCAACCTTCTGGAATAAAAAATCC
<i>Gabarapl1</i>	NM_001044294.1	CAAAATGAAGAGCGTCTCCCCGTG	CAAAAGTTCCAGAACCTGATGCCGACA
<i>Gabpa</i>	NM_001108841.1	ATGGGGACAACGTAAAAACAAGCCT	AGTTCCGCTGCACTGTATCCAA
<i>Hadha</i>	NM_130826.2	GGTGTCCCTGAAGTGTGCT	TCTGTCTGCACGAATGTTCC
<i>Hk2</i>	NM_012735.2	TGATCGCCTGCTTATTCACGG	AACCGCCTAGAAATCTCCAGA
<i>Icam1</i>	NM_012967.1	CACCTGACAGTGCTGTACCA	CGGGGCTTGTACCTTGAGTT
<i>Map1lc3a</i>	NM_199500.2	TGTTAGGCTTGCTCTTTTGG	GCAGAGGAAATGACCACAGAT
<i>Map1lc3b</i>	NM_022867.2	ACCCTCCCTGCATGCAGCTGTCC	ACCAGGGACATGACGACGTACACAACC
<i>Mfn1</i>	NM_138976.1	CGGAGGCATATGAAAGTGGC	CCATCAGTTCCTCCCACT
<i>Mfn2</i>	NM_130894.4	TTGACTCCAGCCATGTCCAT	GGTGACGATGGAGTTGCATC
<i>Mt-Co2*</i>	MN964117.1	CCATCCCAGGCCGACTAA	ATTTCCAGAGCATTGGCCATAGAA
<i>Ndufb3 (CI)</i>	NM_001106912.1	GAAGAAGCTTGCTGCACGAGG	ACGCAGCAAACCCCATTTG
<i>Nfkbia</i>	NM_001105720.2	CCGAGAGTGAGGATGAGGAG	ACAAGTCCACGTTTCCTTTGG
<i>Nrf1</i>	NM_001100708.1	GGCGGGGGACAGATAGTCCT	CGTCACGGCTTTGCTGATGG
<i>Opa1</i>	NM_133585.3	CAGCTGGCAGAAGATCTCAAG	CATGAGCAGGATTTTGACACC
<i>Optn</i>	NM_145081.4	AGAAGGAAGAACGCCAGTTG	AAACCCGCATCTACCTGTGA
<i>Pdk4</i>	NM_053551.2	GCATTTCTACTCGGATGCTCATG	CCAATGTGGCTTGGGTTTCC

Table S1. Primer sequences of reference and target genes used for real-time quantitative PCR analysis. All primers were designed for rat, except for primers indicated with an asterisks (*) which were initially designed for mice. (continued)

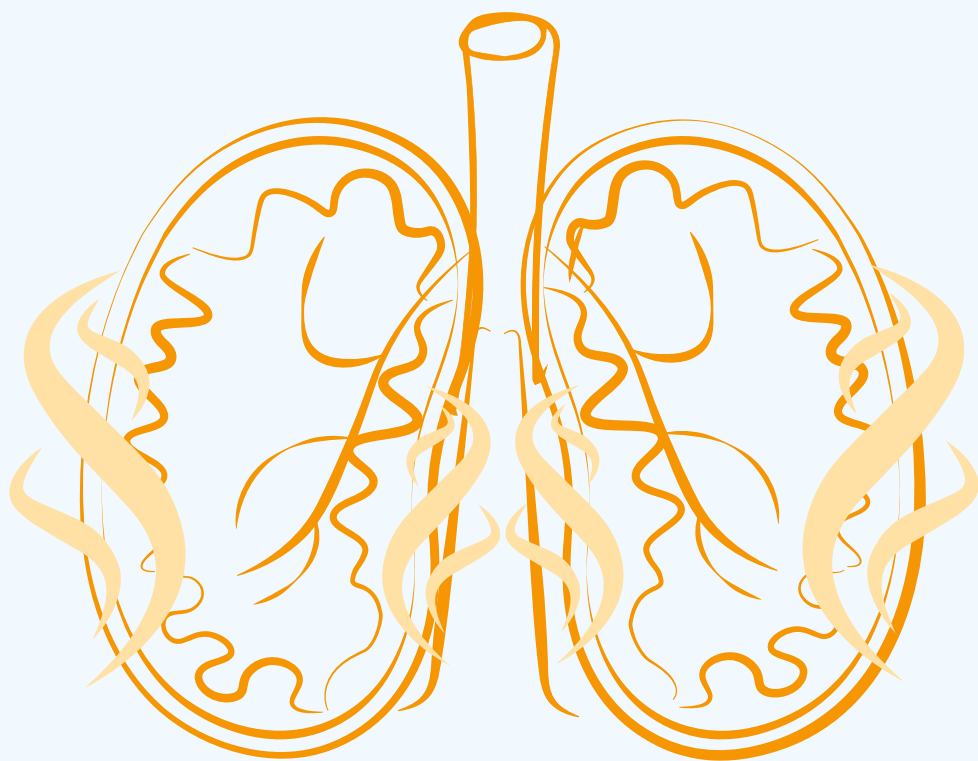
Gene	NCBI Reference Sequence	Sense primer (5'-3')	Antisense primer (3'-5')
<i>Pink1</i>	NM_001106694.1	CCAAACACCTTGGCCTTCTA	CTTAAGATGGCTTCGCTGGA
<i>Ppara</i>	NM_013196.2	ACTATGGAGTCCACGCATGTGA	TTGTCGTACGCCAGCTTTAGC
<i>Pparg</i>	NM_013124.3; NM_001145366.1; NM_001145367.1	AGGACATCCAAGACAACCTG	CTCTGTGACAATCTGCCTGA
<i>Ppargc1a</i>	NM_031347.1	GGGACATGTGCAGCCAAGACT	GATCTGGGCAAAGAGGCTGGT
<i>Ppargc1b</i>	NM_176075.3	ACTATGATCCCACGTCTGAAGAGTC	CCTTGTCTGAGGTATTGAGGTATTC
<i>Pprc1</i>	NM_001106363.1	GATCTTGACTCCAATCGGGA	AGGTTCTTCTGGGCCTGTTT
<i>Sdhb (CII)</i>	NM_001100539.1	GAACGGAGACAAGTACCTGGGG	GATGGTGTGGCAGCGGTAGA
<i>Sod1</i>	NM_017050.1	CGAGCATGGGTTCCATGTC	CTGGACCGCCATGTTTCTTAG
<i>Sod2</i>	NM_017051.2	ATTAACGCGCAGATCATGCA	CCTCGGTGACGTCAGATTGT
<i>Tfam</i>	NM_031326.2	AATTGCAGCCATGTGGAGGGAG	GCCGGGCTTCCTTCTCTAAGC

Abbreviations: *B2m*: beta-2 microglobulin, *Hprt1*: hypoxanthine phosphoribosyltransferase 1, *Ppia*: peptidylprolyl isomerase A, *Rpl13a*: ribosomal protein L13A, *Tuba1a*: tubulin, alpha 1A, *Acadl*: acyl-CoA dehydrogenase, long chain, *Bax*: BCL2 associated X, apoptosis regulator, *Bcl2*: Bcl2, apoptosis regulator, *Bnip3l*: BCL2 interacting protein 3-like, *Cat*: catalase, *Ccl2*: C-C motif chemokine ligand 2, *Cox4i1*: cytochrome c oxidase subunit 4i1, *Cinc1*: cytokine-induced neutrophil chemoattractant-1, *Cyc1*: cytochrome c-1, *Esrra*: estrogen related receptor, alpha, *Fis1*: fission, mitochondrial 1, *Fundc1*: FUN14 domain containing 1, *Gabara1l*: GABA type A receptor associated protein like 1, *Gabpa*: GA binding protein transcription factor subunit alpha, *Hadha*: hydroxyacyl-CoA dehydrogenase trifunctional multienzyme complex subunit alpha, *Hk2*: hexokinase 2, *Icam*: intracellular adhesion molecule 1, *Map1lc3a*: microtubule-associated protein 1 light chain 3 alpha, *Map1lc3b*: microtubule-associated protein 1 light chain 3 beta, *Mfn1*: mitofusin 1, *Mfn2*: mitofusin 2, *Mt-Co2*: mitochondrially encoded cytochrome c oxidase II, *Ndufb3*: NADH:ubiquinone oxidoreductase subunit B3, *Nfkb1a*: NFkB inhibitor alpha, *Nrf1*: nuclear respiratory factor 1, *Opa1*: OPA1, mitochondrial dynamin like GTPase, *Optn*: optineurin, *Pdk4*: pyruvate dehydrogenase kinase 4, *Pink1*: PTEN induced kinase 1, *Ppara*: peroxisome proliferator activated receptor alpha, *Pparg*: peroxisome proliferator activated receptor gamma, *Ppargc1a*: peroxisome proliferator activated receptor gamma, coactivator 1 alpha, *Ppargc1b*: peroxisome proliferator activated receptor gamma, coactivator 1 beta, *Pprc1*: peroxisome proliferator activated receptor gamma, coactivator-related 1, *Sdhb*: succinate dehydrogenase complex iron sulfur subunit B, *Sod1*: superoxide dismutase 1, *Sod2*: superoxide dismutase 2, *Tfam*: transcription factor A, mitochondrial

Table S2. Primary and secondary antibodies used for western blotting.

Target	RRID	Company	Product number	Dilution
Primary antibodies				
AMPK α	AB_10624867	Cell Signaling Technology	Cat#5832	1:1000
Phospho-AMPK α	AB_331250	Cell Signaling Technology	Cat#2535	1:1000
BNIP3	AB_2259284	Cell Signaling Technology	Cat# 3769S	1:1000
BNIP3L	AB_2688036	Cell Signaling Technology	Cat# 12396	1:1000
CASP3	AB_2341188	Cell Signaling Technology	Cat# 9661	1:1000
DNM1L	AB_10950498	Cell Signaling Technology	Cat# 8570	1:1000
ESRRA	AB_1523580	Abcam	Cat# ab76228	1:1000
FUNDC1	AB_10609242	Santa Cruz Biotechnology	Cat# sc-133597	1:500
GABARAPL1	AB_2294415	Proteintech Group	Cat# 11010-1-AP	1:1000
HK2	AB_2232946	Cell Signaling Technology	Cat# 2867	1:1000
MAP1LC3B	AB_915950	Cell Signaling Technology	Cat# 2775	1:1000
NRF1	AB_2154534	Abcam	Cat# ab55744	1:1000
OXPPOS	AB_2629281	MitoScience LLC	Cat# MS604	1:1000
PINK1	AB_10127658	Novus Biologicals	Cat# BC100-494	1:2000
PPARGC1A	AB_10697773	Millipore	Cat# 516557	1:1000
PRKN	AB_2159920	Cell Signaling Technology	Cat# 4211	1:1000
SQSTM1	AB_10624872	Cell Signaling Technology	Cat# 5114	1:1000
TFAM	AB_10682431	Millipore	Cat# DR1071	1:1000
TOMM20	AB_2716623	Abcam	Cat# Ab186734	1:1000
Secondary antibodies				
Goat Anti-Mouse IgG Antibody	AB_2827937	Vector Laboratories	Cat#BA-9200	1:10000
Goat Anti-Rabbit IgG Antibody	AB_2313606	Vector Laboratories	Cat#BA-1000	1:10000
Goat Anti-Rabbit IgG Antibody	AB_2099233	Cell Signaling Technology	Cat#7074S	1:10000

Abbreviations: AMPK α : 5'adenosine monophosphate-activated protein kinase α , phospho-AMPK α : phosphorylated 5'adenosine monophosphate-activated protein kinase α , BNIP3: BCL2 interacting protein 3, BNIP3L: BCL2 interacting protein 3-like, CASP3: caspase-3, ESRRA: estrogen related receptor, α , DNML1: dynamin-1-like, FUNDC1: FUN14 domain containing 1, GABARAPL1: GABA type a receptor associated protein like 1, HK2: hexokinase 2, NRF1: nuclear respiratory factor 1, MAP1LC3B (or LC3B): microtubule-associated protein 1 light chain 3 beta, OXPPOS: oxidative phosphorylation antibody cocktail (containing NDUFB8: NADH:Ubiquinone oxidoreductase subunit B8 (CI), SDHB: succinate dehydrogenase complex iron sulfur subunit B (CII), UQCRC2: ubiquinol-cytochrome C reductase core protein 2 (CIII), MT-COI: mitochondrially encoded cytochrome C oxidase I (CIV), ATP5F1A: ATP synthase F1 subunit α (CV)), PINK1: PTEN induced kinase 1, PPARGC1A: peroxisome proliferator activated receptor gamma, coactivator 1 α , PRKN: parkin RBR E3 ubiquitin protein ligase, SQSTM1: sequestosome 1, TFAM: transcription factor A, mitochondrial, TOMM20: translocase of outer mitochondrial membrane 20



Chapter 6

Smoking-associated exposure of human primary bronchial epithelial cells to aldehydes: Impact on molecular mechanisms controlling mitochondrial content and function

Christy B.M. Tulen, Evert Duistermaat, Johannes W.J.M. Cremers, Walther N.M. Klerx, Paul H.B. Fokkens, Naömi Weibolt, Nico Kloosterboer, Mieke A. Dentener, Eric R. Gremmer, Phyllis J.J. Jessen, Evi J.C. Koene, Lou Maas, Antoon Opperhuizen, Frederik-Jan van Schooten, Yvonne C.M. Staal, Alexander H.V. Remels

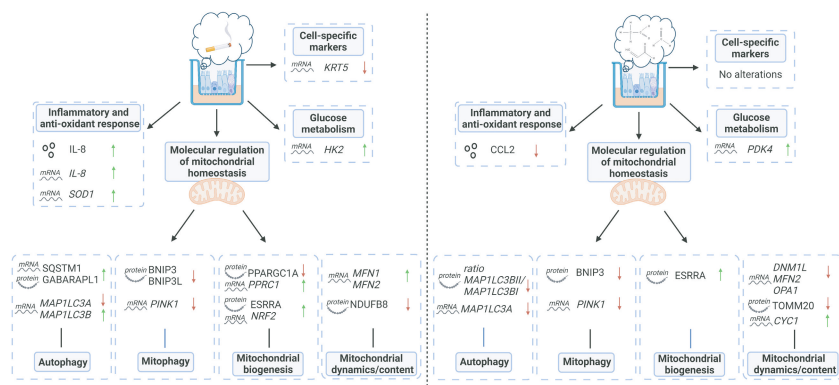
Submitted

Abstract

Chronic obstructive pulmonary disease (COPD) is a devastating lung disease primarily caused by exposure to cigarette smoke (CS). During the pyrolysis and combustion of tobacco, reactive aldehydes such as acetaldehyde, acrolein and formaldehyde are formed, which are known to be involved in respiratory toxicity. Although CS-induced mitochondrial dysfunction has been implicated in the pathophysiology of COPD, the role of aldehydes herein is incompletely understood. To investigate this, we used a physiologically-relevant *in vitro* exposure model of differentiated human primary bronchial epithelial cells (PBEC) exposed to CS (1 cigarette) or a mixture of acetaldehyde, acrolein, and formaldehyde (at relevant concentrations of 1 cigarette) or air in a continuous flow system using a puff-like exposure protocol. Exposure of PBEC to CS resulted in elevated IL-8 cytokine and mRNA levels, increased abundance of constituents associated with autophagy, decreased protein levels of molecules associated with the mitophagy machinery and alterations in the abundance of regulators of mitochondrial biogenesis. Also, decreased transcript levels of basal epithelial cell marker *KRT5* were reported after CS exposure. Only part of these changes were recapitulated in PBEC upon exposure to a combination of acetaldehyde, acrolein and formaldehyde. More specifically, aldehydes decreased *MAP1LC3A* mRNA (autophagy) and BNIP3 protein (mitophagy) and increased ESRR protein (mitochondrial biogenesis). This data suggests that other compounds than aldehydes in CS contribute to CS-induced dysregulation of constituents controlling mitochondrial content and function in airway epithelial cells.

Keywords: acetaldehyde, acrolein, formaldehyde, cigarette smoke, primary bronchial epithelial cells, mitochondria, inhalation toxicology

Graphical abstract



Introduction

Yearly, inhalation of cigarette smoke (CS) is responsible for 6.5 million death as a result of tobacco-related diseases including chronic obstructive pulmonary disease (COPD) (1, 2). CS contains over 6000 chemicals (3). One class of chemicals well known to be generated during the pyrolysis and combustion of tobacco are aldehydes. These include the short-chain aldehydes: acetaldehyde, acrolein and formaldehyde which have similar mechanisms of formation, molecular structures, and chemical properties (4-6). The airways of smokers are exposed to these aldehydes in peak concentrations (7). Smoking-associated exposure to these aldehydes are thought to induce cellular mechanisms underlying respiratory toxicity, in particular studied in response to acrolein (8-10). Taken into consideration the chemical characteristics and detrimental impact on health, these three short-chain aldehydes are considered representative for the chemical class of aldehydes present in CS of all brands and human smoking regimes (4-6, 11) and are shortlisted for regulation in CS by the World Health Organization Study Group on Tobacco Product Regulation (12, 13).

Inhaled toxicants, such as compounds that are abundantly present in CS, are primarily reaching the epithelial cells of the respiratory tract (14), which include a variety of cell types such as ciliated-, club- and goblet cells (15, 16). The mitochondria present in these distinct cell types differ in number and intracellular organization and are essential for proper function of these cell types (e.g., ciliary function and mucus production) (17, 18). Moreover, mitochondria play a key role in the regulation of inflammation, oxidative stress and cell death (17), all of which are processes known to be involved in the pathogenesis of COPD (19). As a relevant example, mitochondrial dysfunction induces production of pro-inflammatory cytokines in alveolar epithelial cells (20). Moreover, based on recent evidence a (mechanistic) link has been suggested between mitochondrial-derived reactive oxygen species mediating mitochondrial dysfunction-induced inflammatory processes which can contribute to the pathogenesis of inflammatory-related diseases, such as COPD (21).

Mitochondrial homeostasis is regulated by several key processes which together coordinate adequate quality control of mitochondria. These processes include mitophagy, mitochondrial biogenesis, mitochondrial fission and fusion (17). Mitophagy is responsible for the breakdown of damaged or defective mitochondria via autophagy. The degradation of mitochondria is triggered by activation of mitochondrial receptors (i.e., receptor-mediated mitophagy) or a loss of membrane potential resulting in accumulation or activation of specific proteins (i.e., ubiquitin-mediated mitophagy) (22). To replenish damaged/removed mitochondria, the generation of new mitochondria (i.e., mitochondrial biogenesis) is facilitated via the Peroxisome Proliferator-Activated Receptor Gamma, Coactivator 1 (PPARGC1) signaling network accompanied by

PPARGC1 alpha co-activators (23, 24). The dynamic processes of fission and fusion are essential in facilitating these mitochondrial quality control processes (25).

Emerging evidence suggests a role for CS-induced mitochondrial dysfunction in the airway pathogenesis of COPD (18, 26, 27). Indeed, abnormal mitochondrial morphology has been observed in airway epithelial cells from COPD patients and in several *in vivo* and *in vitro* smoke exposure experimental models (28-37). Moreover, literature showed an upregulation of key regulators controlling the mitophagy machinery and constituents associated with autophagy in various smoke-exposure *in vitro* models of human bronchial epithelial cells (31, 33, 37-47). Importantly, Cloonan *et al.* also demonstrated that blocking of CS-induced mitochondrial dysfunction prevented the development of COPD-like features such as bronchitis and emphysema in mice (29).

The exact chemical constituents of CS responsible for these mitochondrial abnormalities are unknown. Interestingly, Morita *et al.* previously showed an association between the presence of an inactive allele of aldehyde dehydrogenase (an enzyme that detoxifies aldehydes) and increased incidence of smoking-related chronic airway obstruction in a Japanese population (48). Moreover, it has been shown that *in vivo* acrolein exposure resulted in impaired lung function and structure (49).

Studies assessing the impact of aldehydes on mitochondrial function in cells of the airways are scarce. If available, aldehyde studies primarily focus on the impact of individual aldehydes, in particular the most reactive aldehyde acrolein on mitochondrial metabolism. As CS consists of a complex combination of aldehydes, varying in concentration due to tobacco brand and smoking regime (11), these abovementioned individual aldehydes exposure studies are not representative for the exposure of airways of smokers to aldehydes. Moreover, airborne exposure methods (as we deployed) are not commonly used in both aldehydes and CS studies due to the complexity of these models.

Therefore, the aim of this study was to investigate the impact of a mixture of three aldehydes (representative for CS) on a comprehensive panel of constituents involved in molecular mechanisms controlling mitochondrial content and mitochondrial quality control (mitochondrial biogenesis *versus* mitophagy) by using a physiologically-relevant *in vitro* model of the bronchial epithelium. To this end, fully differentiated human primary bronchial epithelial cells (PBEC) from non-COPD subjects (n=4) were exposed in a continuous flow system using a puff-like exposure protocol to CS (1 cigarette) or a mixture of acetaldehyde, acrolein, and formaldehyde (at relevant concentrations of 1 cigarette) or air (control). After recovery for 6 h or 24 h, we assessed cytotoxicity, inflammatory protein secretion, ciliary beating as well as protein and transcript abundance of key constituents involved in mitochondrial metabolic pathways and quality control. We hypothesized that acute exposure to a mixture of aldehydes, representative for CS, disrupts the molecular regulation of mitochondrial content and mitochondrial function.

Materials and methods

PBEC isolation

Lung tissue used for the isolation of PBEC was obtained from the Maastricht Pathology Tissue Collection (MPTC). The scientific board of the MPTC (MPTC 2010-019) and the local Medical Ethic Committee (METC 2017-0087; date: 10/19/2017) provided approval of use of lung tissue for research purposes. In line with the 'Human Tissue and Medical Research: Code of conduct for responsible use' (2011) (www.federa.org), the available lung tissue within the framework of patient care at Maastricht University Medical Center+ (MUMC+) was handled anonymously coded with respect to patient data, tissue collection, storage and further use. Isolation, culture and characterization of cells was performed by the Primary Lung Culture (PLUC) facility at the MUMC+ as previously described (50, 51). PBEC were isolated from resected lung tissue of 4 patients without known history of chronic lung diseases who underwent surgery for solitary pulmonary nodules. In Table 1, characteristics of the subjects are described.

Table 1. Characteristics of primary human bronchial epithelial cell donors.

Experiment	Primary bronchial epithelial cell donors
N	4
Male/female	3/1
Age (years)	69.75±2.02
Body mass index	28.00±4.38
Pack-years (years)	35.00±15.00 ^s
FEV ₁ absolute (L)	2.73±0.19
Tiffeneau Index	76.06±2.06

Subject characteristics of human primary bronchial epithelial cell donors. Data are presented as mean ± s.e.m.. ^sMissing value for two donors. FEV₁: forced expiratory volume in first second.

PBEC proliferation and differentiation

PBEC of four donors without known history of COPD (5×10^5 cells, passage 1) were thawed, seeded and expanded in T75-flasks (passage 2; Corning Costar, USA) on pre-coated growth areas (coating: bovine serum albumin, human fibronectin, PureCol Type I Collagen Solution) in Pneumacult™-Ex medium including Pneumacult™-Ex Basal medium, Pneumacult™-Ex 50x supplement, hydrocortisone stock solution (96 µg/mL) (all STEMCELL Technologies, GmbH) and 1% penicillin/streptomycin (10.000 U/mL/10.000 µg/mL) (Gibco, USA) following the manufacturer's protocol of Pneumacult™-Ex medium (#5008; STEMCELL Technologies). Every other day, PBEC were washed with Hank's balanced salt solution (HBSS; no calcium, no magnesium, no Phenol Red) (Gibco) followed by refreshment of the Pneumacult™-Ex medium. Upon

reaching 80-90% confluency (approximately 5-7 days of proliferation), PBEC were seeded in a density of 40,000 cells (passage 3) per pre-coated 1.12 cm² polycarbonate insert polycarbonate membrane cell culture inserts (Corning) using the Pneumacult™-Ex medium. Upon reaching 90% confluency (approximately 5-7 days of proliferation) on inserts, PBEC were airlifted by removing apical medium. Differentiation at air-liquid interface (ALI) was maintained for 28-32 days by replacing basolateral medium with Pneumacult™-ALI maintenance medium containing Pneumacult™-ALI Basal medium, Pneumacult™-ALI 10x supplement, Pneumacult™-ALI maintenance 100x supplement, heparin solution (0.2%), hydrocortisone stock solution (96 µg/mL) (all STEMCELL Technologies) and 1% penicillin/streptomycin (10,000 U/mL/10,000 µg/mL) (Gibco) following the manufacturer's protocol of Pneumacult™-ALI maintenance medium (#5001; STEMCELL Technologies). Every other day, PBEC were washed with HBSS both apical and basolateral and subsequently basolateral Pneumacult™-ALI maintenance medium was changed. PBEC were differentiated up to 28-32 days until exposure in an incubator at 37°C and 5% CO₂ in humidified air.

Validation and characterization of differentiation of PBEC at ALI

To validate and characterize our model of differentiation of PBEC using above mentioned culturing protocol at ALI, both mRNA expression and immunohistochemistry staining of cell type-specific markers associated with basal and luminal cells of two representative donors were analysed. Respectively, undifferentiated PBEC (day 0; moment of airlift) and PBEC during differentiation (days 14, 21, and 28 post-airlift) were harvested in TRIzol™ Reagent (Invitrogen™, USA) or fixed in 4% paraformaldehyde in phosphate buffered saline (Thermo Fisher Scientific, USA) to evaluate the abundance of basal and luminal characterization markers reflecting differentiation status by gene expression analysis (see '*RNA isolation and real-time quantitative PCR*' section) and immunohistochemistry (see '*Fixation for paraffin-embedded section and immunohistochemistry staining*' section).

Monitoring PBEC differentiation and monolayer integrity

Several measurements were conducted during the differentiation of the PBEC to validate the development of a basal monolayer into a pseudostratified epithelium of all four donors. Firstly, monolayer integrity was monitored during differentiation of all PBEC cultures of all donors before exposure to CS and aldehydes. The trans-epithelial electrical resistance (TEER) was analysed at day 0 (day of airlift) in apical and basolateral Pneumacult™-Ex medium and post-airlift at day 7, 14, 21, 28 as well as at 24 h before exposure (this timepoint can also be similar to day 28 post-airlift) in apical HBSS or Pneumacult™-ALI maintenance medium and basolateral Pneumacult™-ALI maintenance medium. The Epithelial Volt/Ohm meter (World Precision Instruments, USA) was used to analyse TEER of the PBEC cultures as indication of an intact monolayer of the pseudostratified epithelium. TEER ($\Omega \cdot \text{cm}^2$) was corrected for surface of the 12-wells inserts and background measurements of medium used. Secondly, cell layer permeability was analysed using Fluorescein Isothiocyanate-Dextran (FITC-Dextran)

immediately after analysis of the bead motion in a flow induced by ciliary beating. FITC-dextran solution (Sigma-Aldrich, USA; 1 mg/mL) was prepared in Pneumacult™-ALI maintenance medium. Subsequently 0.5 mL FITC-dextran was added to the apical side of the inserts. After incubation for 2 h in dark in the incubator at 37°C and 5% CO₂ in humidified air, the inserts were transported to a new 12-well plate to prevent spill-over and to guarantee similar incubation times among the inserts. Technical triplicates of 100 µL of the basolateral medium per insert were analysed by fluorescence measurements (Molecular Devices, Spectramax M2) (485/535 nm; intensity 7000) in a 96-well plate (black; Corning Costar). Fluorescence was corrected for background of Pneumacult™-ALI maintenance medium and expressed relative to 2% Triton-X-100 (i.e., cell lysis resulting in complete permeability of the membrane).

Dosimetry and exposure regime

As shown in Fig. S1, an experimental exposure system was designed to directly expose differentiated PBEC cultures in a puff-like manner to CS or a mixture of aldehydes (at relevant concentrations of 1 cigarette) via the air using two Vitrocell® 12/3 CF stainless steel modules for 12-well sized inserts (Vitrocell, Germany). Exposure to CS or aldehydes was conducted by the Health Canada Intense (HCI) exposure regime. To specify, 8 puffs were taken from 1 cigarette (Marlboro Red; taped) or the gaseous mixture of aldehydes in the buffer tank by the smoking machine (VC1, Vitrocell, Germany) following the HCI Bell regime (2 puffs/min, 55 ml puff volume, 2 s puff duration, 4 s puff exhaust time; taped). The generated streams of CS or aldehydes were distributed (and diluted) to the exposure manifold by a mass flow controlled stream of 500 mL/min compressed dry air. Subsequently, streams of 5 mL/min per insert were extracted from the exposure manifold. These streams were individually humidified by passing them through Nafion humidifiers kept in a water bath at 33.8 °C. After humidification the streams were delivered to the cells. As control, the PBEC cultures were exposed to clean compressed air with a similar flow-rate and humidification in the control module.

To match the target concentration of aldehydes present in the mixture to the concentration present in CS of one Marlboro Red cigarette, we analysed the total concentrations of these three aldehydes: acetaldehyde, acrolein and formaldehyde present in a Marlboro Red cigarette. Marlboro Red cigarettes were taped following the World Health Organization SOP1: standard operating procedure for intense smoking of cigarettes (52) and subsequently 'smoked' following the above described HCI regime. Directly prior to the measurement of aldehydes in the CS, the exposure system was primed by smoking 3 cigarettes. After priming, three single cigarettes in a row were smoked to analyse the aldehydes present in the smoke. The mainstream smoke from one cigarette was trapped using a Cambridge filter and Carboxen adsorbent cartridge (extern filter) placed after the smoking machine. Besides the primary trapping cartridge, an additional cartridge was included to measure possible flow through. The circumstances present were: 1 L/min continuous sample flow, exhaust

flow smoking machine complemented with clean compressed air. Extraction and analysis of these trapped aldehydes was followed by the World Health Organization TobLabNet SOP8 for determination of aldehydes in mainstream CS under International Standardization Organization (ISO) and Intense smoking conditions (exception of 1 min extraction instead of 30 min) (53). While flow through was measured for acetaldehyde and formaldehyde in CS (~10-15%), the mean concentrations of all three aldehydes including flow through (mg/m^3) measured in the CS of 1 Marlboro Red cigarette were as expected compared to literature (Table S1) (11). Based on these concentrations, the target concentrations of the mixture of aldehydes was set.

The mixture of 3 aldehydes was generated by evaporating syringe pump controlled flows of the aldehydes in streams of mass flow controlled compressed dry air using two Dimroth evaporators (one for formaldehyde, the other one for acrolein and acetaldehyde). After evaporation, the generated formaldehyde and acrolein/acetaldehyde streams were mixed in a buffer chamber. The target settings of the syringe pumps to reach the target concentration of each aldehyde was calculated using the density and purity of each aldehyde, and the total flow of test atmosphere. For formaldehyde, a flow of $2.55 \mu\text{L}/\text{min}$ 37 wt% formaldehyde solution (Sigma Aldrich) with a density of $1.09 \text{ mg}/\mu\text{L}$ was evaporated in a stream of $5 \text{ L}/\text{min}$ of compressed dry air leading to a calculated concentration of $102.8 \text{ mg}/\text{m}^3$ (83 ppm). A flow of $1.64 \mu\text{L}/\text{min}$ of pure acrolein (Sigma Aldrich) with a density of $0.839 \text{ mg}/\mu\text{L}$ was evaporated in a stream of $5 \text{ L}/\text{min}$ compressed air, together with $27.99 \mu\text{L}/\text{min}$ of pure acetaldehyde (Sigma Aldrich) with a density of $0.76 \text{ mg}/\mu\text{L}$. The calculated concentrations of acrolein and acetaldehyde were $137.5 \text{ mg}/\text{m}^3$ (59 ppm) and $2126 \text{ mg}/\text{m}^3$ (1162 ppm) respectively.

A Total Carbon Analyzer (TCA, Ratfisch, Germany) was used to monitor the concentrations of aldehydes during every exposure. The response of the TCA was used as an indicator of the presence of each of the aldehydes in the gaseous mixture (located before the smoking machine), see an example of the TCA measurement during exposure in Fig. S2. Together with the nominal concentrations (calculated concentrations) this confirmed the exposure of the cells to each of the aldehydes.

PBEC exposure to CS or mixture of aldehydes

PBEC of four donors without known history of COPD were differentiated up to 29-32 days until exposure. 24 h prior to treatment, fully differentiated PBEC were apically and basolaterally washed with HBSS, followed by basolateral replacement of the Pneumacult™-ALI maintenance medium. PBEC were transported in a portable incubator at 37°C to the laboratory for exposure.

After priming the system, as explained above, the PBEC were placed into the Vitrocell® 12/3 CF stainless steel modules (exposure or control module) which were preheated to 37°C and filled with fresh Pneumacult™-ALI maintenance medium. PBEC were exposed

to 8 puffs of CS, aldehydes mixture or compressed dry air following the HCI smoking regime as described in paragraph '*Dosimetry and exposure regime*'. Immediately after exposure to CS or mixture of aldehydes, PBEC were transported to a new 12-well plate in fresh Pneumacult™-ALI maintenance medium. Thereafter, the exposed PBEC were transported in a portable incubator at 37°C for analysis of bead motion induced by ciliary beating or placed in the incubator at 37°C and 5% CO₂ in humidified air for recovery for 6 h or 24 h until harvesting. To control for a possible impact of transport of the PBEC to another lab, exposure in a non-sterile environment, and air-flow in the exposure system, we also included incubator control PBEC cultures in our experiment. The experiments were conducted in triplicates per donor per exposure or control condition.

RNA isolation and real-time quantitative PCR

Following recovery for 6 h or 24 h, total RNA was extracted from the PBEC by lysis in TRIzol™ Reagent (Invitrogen™). The lysates were processed following the manufacturer's instructions (Catalog number 15596026 and 15596018, Invitrogen™) using glycogen blue co-precipitant (Thermo Fisher Scientific). To verify the quantity and quality of the total RNA, the RNA was analysed using the NanoDrop ND 1000 UV-visible spectrophotometer (Isogen Life Sciences, the Netherlands). Next, total RNA (100 or 400 ng) was reverse transcribed into cDNA using iScript™ cDNA synthesis kit (Bio-Rad, the Netherlands) including a no reverse transcription control and a no template control. cDNA was diluted in Milli-Q (1:50) and stored at -20°C until use. Real-time quantitative PCR amplification was performed by mixing 4.4 µL of 1:50 diluted cDNA, 5 µL 2xSensiMix™ SYBR® & Fluorescein Kit (Bioline, the Netherlands) and 0.6 µL primers specific for genes of interest in white LightCycler480 384-multiwell plates (Roche, Switzerland) and subsequently running the thermal cycling protocol: 10 min at 95°C, 55 cycles of 10 s at 95°C, 20 s at 60°C on the LightCycler480 machine (Roche). Table S2 shows the list of target-specific primers used for qPCR analysis.

Qualitative analysis of the melt curves was conducted using LightCycler480 software (Roche) and quantitative gene expression analysis was performed in LinRegPCR software 2014.x (the Netherlands). The geometric mean of a combination of at least two and up to four reference genes (*ACTB*, *B2M*, *PPIA*, *RPL13A*) was calculated in GeNorm software 3.4 (Primerdesign, USA). This geometric mean was used for normalization of the gene expression levels of interest. Samples with no amplification, no plateau phase, too low Cq value or outside 5% of group mean were automatically excluded by LinRegPCR analysis. In addition, qualitative analysis of melt curves and peaks in LightCycler480 software resulted in exclusion of outliers.

DNA isolation and analysis of mitochondrial DNA (mtDNA) copy number

After 24 h of recovery, PBEC were lysed in TRIzol™ Reagent (Invitrogen™) as indicated in the previous paragraph. Isolation of DNA was conducted following the manufacturer's

instructions (MAN0016385; Catalog number 15596026 and 15596018, Invitrogen™). The DNA pellet was dissolved in 50 µL TE buffer (10 mM Tris HCl pH 8.0, 1 mM EDTA pH 8.0). To increase solubility the samples were heated by 55°C for 1 h and stored at 4°C overnight. The next day samples were centrifuged to remove insoluble materials, and supernatants were stored at -20°C until use. The quantity and quality of the DNA was verified by using the NanoDrop ND 1000 UV-visible spectrophotometer (Isogen Life Sciences). 200 ng of DNA (diluted in TE buffer) was analysed by real-time quantitative PCR amplification (see paragraph '*RNA isolation and real-time quantitative PCR*'). Assessment of mtDNA copy numbers was performed by analysing the ratio of mtDNA, mitochondrial encoded *MT-CO2* versus genomic DNA, *ACTB* (Table S2).

Fixation for paraffin-embedded section and immunohistochemistry staining

PBEC inserts were harvested for immunohistochemistry staining at day 0 (undifferentiated; at moment of airlift) and day 28 (differentiated) in order to assess differentiation status. At the day of harvest, the inserts with PBEC were gently washed with ice-cold HBSS (apical and basolateral). Next, 4% paraformaldehyde in phosphate buffered saline was added to the basolateral (1 mL) and apical (0.5 mL) side of the insert. After at least 1.5 h of incubation at room temperature, the paraformaldehyde was replaced by 70% ethanol. Fixed inserts were embedded in paraffin, cut and stained with hematoxyline-eosine (H&E), Periodic acid-Schiff (PAS; polysaccharides and mucosubstances) (Periodic acid solution 0.5% (Sigma 1004821000) and Schiff Reagent (Sigma Aldrich, 3952016-500ML)) or target-specific antibodies as listed in Table S3. The target-specific antibodies were used to verify the differentiation status of the PBEC donors, basal cell and differentiation markers were stained using the antibodies P63 (nuclei), Clara cell secretory protein-16 (CC16; clara cell protein 16), and Acetylated Tubulin (AcTub; present in cilia).

Cytotoxicity assay

Following 6 h or 24 h of recovery after exposure, we collected the apical wash (HBSS) and basolateral medium (Pneumacult™-ALI maintenance medium) in order to measure the lactate dehydrogenase (LDH) activity using a cytotoxicity detection kit (LDH Ref.11644793001; Roche, USA). The cytotoxicity was analysed within 7 days after harvesting according to the manufacturer's protocol including a minor adaptation of dilution of the reagents 1:1 in HBSS. The positive control reflecting maximum cytotoxicity, also called LDHmaximum (LDHmax), was determined by optimal lysis of an incubator-control insert of fully differentiated PBEC at harvesting time-point of 24 h via shaking for 10 min in 2% Triton-X-100. A technical triplo of 1/10 diluted LDHmax in Pneumacult™-ALI maintenance medium was analysed for each experiment to determine the relative LDH response. Colorimetric spectrophotometry (Molecular Devices, Spectramax M2) was used to detect cytotoxicity, where after correction for the background of the medium (apical: HBSS; basolateral: Pneumacult™-ALI maintenance medium) was conducted to calculate cytotoxicity relative to the LDHmax (%).

Inflammatory protein secretion

Following the manufacturer's protocol, including minor modifications, the LEGENDplex™ Human Essential Immune Response Panel (13-plex) (BioLegend, USA) has been used to analyse the level of 13 inflammatory proteins involved in the immune response, respectively Interleukin (IL) 4, IL-2, C-X-C motif Chemokine Ligand (CXCL) 10 (IP-10), IL-1 β , Tumor Necrosis Factor-Alpha (TNF- α), C-C Motif Chemokine Ligand (CCL2; MCP-1), IL-17A, IL-6, IL-10, Interferon Gamma (IFN- γ), IL-12p70, CXCL8 (IL-8), and Free Active Transforming Growth Factor Beta 1 (TGF- β 1). By using FACS (BD FACSCanto II), these interleukins, cytokines and chemokines were measured in the undiluted apical and basolateral supernatant of the PBEC exposed to CS or mixture of aldehydes (6 h or 24 h post-exposure). Thereafter, levels of cytokines and chemokines were calculated based on the standard curve (0.169-10.000 pg/mL).

Protein isolation and western blotting

Following recovery for 6 h or 24 h, total protein of PBEC was isolated in 200 μ L of whole-cell lysis buffer (20 mM Tris pH 7.4, 150 mM NaCl, 1% Nonidet P40 in Milli-Q) or Pierce RIPA buffer (Thermo Fisher Scientific) including PhosSTOP Phosphatase and cComplete, Mini, EDTA-free Protease Inhibitor cocktail tablets (both Roche). Next, whole-cell lysates were mixed by rotation for 30 min at 4°C and centrifuged at 20,000 x g for 30 min at 4°C. Based on the determination of total protein content using the Pierce™ BCA Protein Assay Kit (Catalog number 23225 and 23227, Thermo Fisher Scientific), whole-cell lysates were diluted (1 μ g/ μ L) in a final concentration of 1 x Laemmli buffer (0.25 M Tris pH 6.8, 8% (w/v) sodium dodecyl sulphate, 40% (v/v) glycerol, 0.4 M dithiothreitol, 0.02 % (w/v) Bromophenol Blue). Thereafter, lysates were boiled for 5 min at 100°C and stored at -80°C until analysis. The samples (10 μ g of protein per lane) and corresponding protein ladders (Precision Plus Protein™ All Blue Standards #161-0373, Bio-Rad) were separated on a Criterion XT Precast 4-12 % or 12% Bis-Tris gel (Bio-Rad) in 1 x MES running buffer (Bio-Rad) by electrophoresis (100-130 V for 1 h). Next, transfer of the proteins from the gel to a 0.45 μ M nitrocellulose transfer membrane (Bio-Rad) was conducted by electroblotting (Bio-Rad Criterion Blotter) (100 V for 1 h). Staining of total protein content on the blotted membrane was performed by incubation of 0.2% Ponceau S in 1% acetic acid (Sigma-Aldrich) of the nitrocellulose membranes followed by visualization using the Amersham™ Imager 600 (GE Healthcare, the Netherlands). Staining for the target-specific proteins started with washing off the Ponceau S staining and blocking the membranes for 1 h in 5% (w/v) non-fat dry milk (Campina, the Netherlands) dissolved in Tween20 Tris-buffered saline (TBST; 20 mM Tris, 137 mM NaCl, 0.1% (v/v) Tween20, pH 7.6). After washing with TBST, the membranes were incubated with a target-specific primary antibody diluted in 3% (w/v) bovine serum albumin (Table S4) at 4°C overnight. Next, a TBST wash of the membranes was followed by incubation with a horseradish peroxidase-conjugated secondary antibody (Table S3) diluted in 5% (w/v) non-fat dry milk in TBST for 1 h at room temperature. The membranes were subsequently washed, stained with

either 1 x Supersignal West FEMTO or 0.5 x Supersignal West PICO Chemiluminescent Substrate (Thermo Fisher Scientific), and imaged using the Amersham™ Imager 600. Quantification of the total protein content and target-specific proteins was performed on original unaltered images using Image Quant software (GE Healthcare). Total protein content was quantified using the Ponceau S stained images, if possible, over the entire size range of proteins (250 kDa - 10 kDa). For analysis of target-specific proteins, correction for total protein loading was conducted. As some proteins were analysed on the same gel (different molecular mass), quantification of these proteins was based on normalization on the same Ponceau S staining, respectively *Gel I*: Hexokinase 2 (HK2), Dynamin 1-like (DNM1L), OXPHOS complexes: NADH:Ubiquinone Oxidoreductase Subunit B8 (NDUFB8; CI), Succinate Dehydrogenase Complex Iron Sulfur Subunit B (SDHB; CII), Ubiquinol-Cytochrome C Reductase Core Protein 2 (UQCRC2; CIII), ATP Synthase F1 Subunit Alpha (ATP5F1A; CV), Sequestosome 1 (SQSTM1), Translocase Of Outer Mitochondrial Membrane 20 (TOMM20); *Gel II*: Parkin RBR E3 Ubiquitin Protein Ligase (PRKN), BCL2 Interacting Protein 3-Like (BNIP3L), BCL2 Interacting Protein 3 (BNIP3), FUN14 Domain Containing 1 (FUNDCl), PTEN Induced Kinase 1 (PINK1), Microtubule-Associated Protein 1 Light Chain 3 Beta (MAP1LC3B); *Gel III*: Peroxisome Proliferator-Activated Receptor Gamma, Coactivator 1 Alpha (PPARGC1A), Nuclear Respiratory Factor 1 (NRF1), GABA Type A Receptor Associated Protein Like 1 (GABARAPL1), Estrogen Related Receptor, Alpha (ESRRA).

Representative western blot images in the figures of this manuscript have been adjusted for brightness and contrast equally throughout the picture. Moreover, the included 85 kDa Ponceau S band in the figures is representative for the whole Ponceau S staining and the selected target-specific band shown of one replicate of one donor/experiment is reflective of the mean changes in all donors as quantified in the corresponding graph.

Analysis of bead motion induced by ciliary beating

Immediately after exposure, PBEC were transported in a portable incubator at 37°C for analysis of bead motion induced by ciliary beating. The exposed PBEC were placed on the microscope (Leica Dmi8), and maintained at 37°C and 5% CO₂ in humidified air. Directly before recording videos, 10 µL of 2.1 µM beads (RED PSRF 2.1 µM 2.5% PSFR3961A-1219; Magsphere) diluted 1:50.000 in Pneumacult™-ALI maintenance medium were added to the apical side of the exposed PBEC in the middle of the transwell. Recording of the bead motion started circa 5-10 min after addition of the beads to facilitate spreading of the beads over the well and moving around in a flow induced by ciliary beating. Videos were acquired 30 min until 2.5 h post-exposure using the 4x objective and LEICA DFC7000 GT camera along with the LAS X 3.4.2 software. Videos were recorded in a frame interval of 0.33 s for 20-60 s.

Automatic tracking of the beads was conducted in ImageJ version 1.53 (54) using the MTrackJ plugin for motion tracking and analysis (55). First, we selected videos

recording the motion of the beads at the edge of the well, to have a consistent position within the well because flow speed varies with the position in the well. Moreover, beads were followed outside the mucus because flow speed differs within and outside the mucus. Per exposure condition (CS, mixture of aldehydes or air), if available, 1 to 3 videos per transwell per donor were selected. Videos were loaded into ImageJ and scale was adapted to 0.2065 pixels/ μM . Beads which were located as close as possible to the edge of the transwell and following a smooth path were selected for tracking (Fig. S9A). Within one video (i.e., one transwell), 5-6 beads were tracked for 2.97-5.00 s (i.e., 9-16 time frames) (please see an example in Fig. S9B). Subsequently, mean distance per s was calculated per exposure condition per donor including tracked beads in 1-3 videos, respectively resulting in 5-12 tracked beads per donor exposed to air or CS and 6-23 tracked beads per donor exposed to air or aldehydes. In summary, this results in a total number of tracked beads across all donors of air: 29 *versus* CS: 24 and air: 18 *versus* aldehydes: 41.

Statistical analysis

Statistical analysis and graphing the data was conducted using the GraphPad Prism 8.0 software (USA). The experiments were conducted in biological triplicates per independent donor per condition. The mean of the biological triplicates per donor are represented in the bar charts by open circles (donor 1), triangles (donor 2), squares (donor 3) or diamonds (donor 4). The data are presented as mean fold change (FC) compared to air control \pm standard error of the mean (s.e.m.). Statistical differences between air *versus* CS or air *versus* a mixture of aldehydes were tested using a two-tailed paired parametric t-test. Statistical significance was indicated as p-values are below 0.05 (* $p < 0.05$) or below 0.01 (** $p < 0.01$).

Results

Validation and characterization of differentiation of PBEC at ALI

To validate and characterize our model of differentiation of PBEC at ALI, we analysed mRNA expression of markers associated with basal and luminal cells during differentiation of two donors. Basal epithelial cells are identified by markers: *KRT5*, *KRT14* and the nuclear *TP63*. Moreover, club cells were identified by *SCGB1A1*, ciliated cells with *FOXJ1* and goblet cells with *MUC5AC*.

As depicted in Fig. S3A and B, mRNA levels of basal epithelial cell markers were decreased, whereas increased transcript abundance of markers associated with cilia-, club- and goblet cells were observed in fully differentiated cultures (day 28) compared to non-differentiated cultures (day 0 at moment of air-lift). To further verify differentiation status of the PBEC donors during differentiation (14, 21, 28 days post-airlift), we conducted a H&E staining as well as immunohistochemistry staining of

nuclei, clara cell protein 16, polysaccharides and mucosubstances, and cilia. The presence of a pseudostratified epithelium as well as identification of markers associated with specific cell types of one representative donor are visualized and confirmed at 28 days post-airlift in Fig. S3C and D. Based on these findings, PBEC cultures differentiated for at least 28 days at ALI included several cell types representing the pseudostratified epithelium.

In addition, to monitor monolayer integrity during differentiation, TEER was measured in all PBEC cultures of all donors at different time-points. As depicted in Fig. S4, TEER ($\Omega\cdot\text{cm}^2$) of all PBEC donors increased over time and stabilized at 28 days post-airlift, indicating a confluent intact monolayer before starting the exposures to CS and aldehydes.

No impact of CS or aldehydes exposure on cell viability and monolayer integrity

After validation and characterization of differentiation of PBEC at ALI, we assessed the effects of a single exposure to CS or aldehydes on cell viability and monolayer integrity. Exposure to CS or aldehydes did not impact cell viability 6 h or 24 h post-exposure (Fig. S5A and S5B). Moreover, immediately (± 3 h) after the exposure, permeability of PBEC cultures, as assessed by the FITC-dextran assay, was negligible indicating integrity of the monolayer (Fig. S5C). In addition, we took into account the potential (stressful) impact of the exposure system (e.g., transport, air-flow) by including incubator controls in our study. In general no pronounced impact of the dynamic exposure via air was observed for all analysed markers (incubator *versus* air control), except for a small but significant increase in secretion levels of IL-8, IL-6 and CCL-2 in apical supernatants of PBEC after 6 h of exposure (data not shown). Moreover, small decreases in transcript levels of genes encoding for *IL-8*, autophagy and fission/fusion were observed in response to air-flow (data not shown). These findings support a negligible impact of air-flow *per se* on our cultures.

CS exposure affects inflammatory protein production and anti-oxidant gene expression

Next, we investigated the production of several inflammatory proteins (interleukins, cytokines, chemokines) as well as mRNA expression of inflammatory genes and anti-oxidant enzymes in response to CS or aldehydes. Although IL-8, IL-6 and CCL2 were detectable in both apical and basolateral medium at baseline, only IL-8 levels were found to be significantly increased in the basolateral medium of CS-exposed PBEC (Fig. 1A-1F). Moreover, we observed elevated gene expression of IL-8 in response to CS exposure (Fig. 1G). In general, no profound changes in these inflammatory proteins or inflammatory gene expression were observed in response to aldehydes, except for decreased CCL2 levels in apical medium (Fig. 1C). The secretion of IL-4, IL-2, CXCL10, IL-1 β , TNF- α , IL-17A, IL-10, IFN- γ , IL-12p7 and Free Active TGF- β 1 was in general non detectable (data not shown).

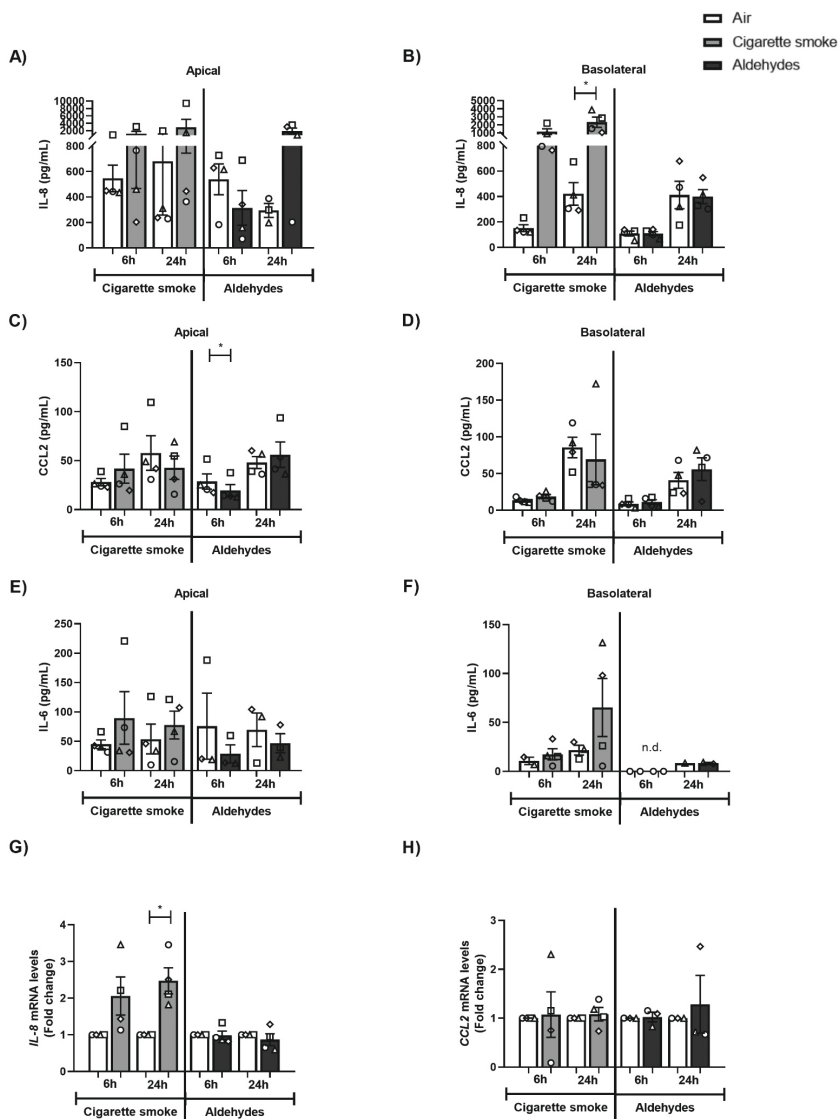


Figure 1. Impact of CS exposure on inflammatory proteins and inflammatory gene expression. Differentiated human primary bronchial epithelial cells (PBEC) from non-COPD subjects were exposed in a continuous flow system using a puff-like exposure protocol to smoke of one Marlboro Red cigarette (CS) or a mixture of aldehydes: acetaldehyde, acrolein, and formaldehyde (at relevant concentrations of 1 cigarette) or air (control) (n=2-4 donors). Following recovery for 6 h or 24 h, supernatants and whole-cell lysates were harvested. Inflammatory protein levels: (A,B) IL-8, (C,D) CCL-2, and (E,F) IL-6 were analysed in apical and basolateral supernatants. Transcript levels of inflammatory markers (G) IL-8 and (H) CCL-2 were analysed in whole-cell lysates. Data are presented as mean fold change compared to air control \pm s.e.m. The mean of biological triplicates per independent donor are represented by open circles, triangles, squares or diamonds. Statistical differences between CS versus air or a mixture of aldehydes versus air were tested using a two-tailed paired parametric t-test. Statistical significance is indicated as * $p < 0.05$ versus air (control).

With respect to the expression of anti-oxidant genes, the transcript levels of *SOD1* were significantly elevated 24 h post-CS exposure, while the expression of *SOD2* was unaltered. Exposure to the aldehydes mixture did not alter anti-oxidant gene expression (Fig. 2A and B).

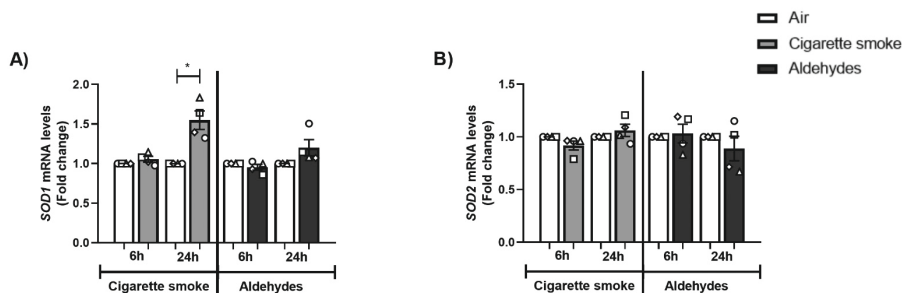


Figure 2. CS exposure affects expression of anti-oxidant genes. Differentiated human primary bronchial epithelial cells (PBEC) from non-COPD subjects were exposed in a continuous flow system using a puff-like exposure protocol to smoke of one Marlboro Red cigarette (CS) or a mixture of aldehydes: acetaldehyde, acrolein, and formaldehyde (at relevant concentrations of 1 cigarette) or air (control) (n=4 donors). Following recovery for 6 h or 24 h, whole-cell lysates were harvested for transcript analysis of oxidative stress markers (**A**) *SOD1* and (**B**) *SOD2*. Data are presented as mean fold change compared to air control \pm s.e.m. The mean of biological triplicates per independent donor are represented by open circles, triangles, squares or diamonds. Statistical differences between CS versus air or a mixture of aldehydes versus air were tested using a two-tailed paired parametric t-test. Statistical significance is indicated as * $p < 0.05$ versus air (control).

In conclusion, although CS exposure affected the secretion levels of IL-8 as well as the transcript abundance of inflammatory and anti-oxidant genes, aldehydes had a minor impact.

Altered abundance of molecules associated with autophagy following CS or aldehydes exposure

Since the autophagosomal pathway has an important role clearing (sub)cellular damage and previous *in vitro* studies suggested that acute exposure of PBEC to CS resulted in increased abundance of components of autophagy (47), we assessed the expression of specific autophagy proteins in response to CS or aldehydes. After 6 h or 24 h of recovery following exposure to CS, protein and transcript levels of SQSTM1 and GABARAPL1 were significantly increased (Fig. 3A-E). These results were not recapitulated in response to exposure aldehydes. The protein ratio of MAP1LC3BII/MAP1LC3BI was not changed post-exposure to CS, while this protein ratio was decreased in PBEC exposed to aldehydes (Fig. 3A and F). Both CS as well as aldehydes exposure resulted in decreased *MAP1LC3A* and/or increased *MAP1LC3B* mRNA abundance (Fig. 3G and H).

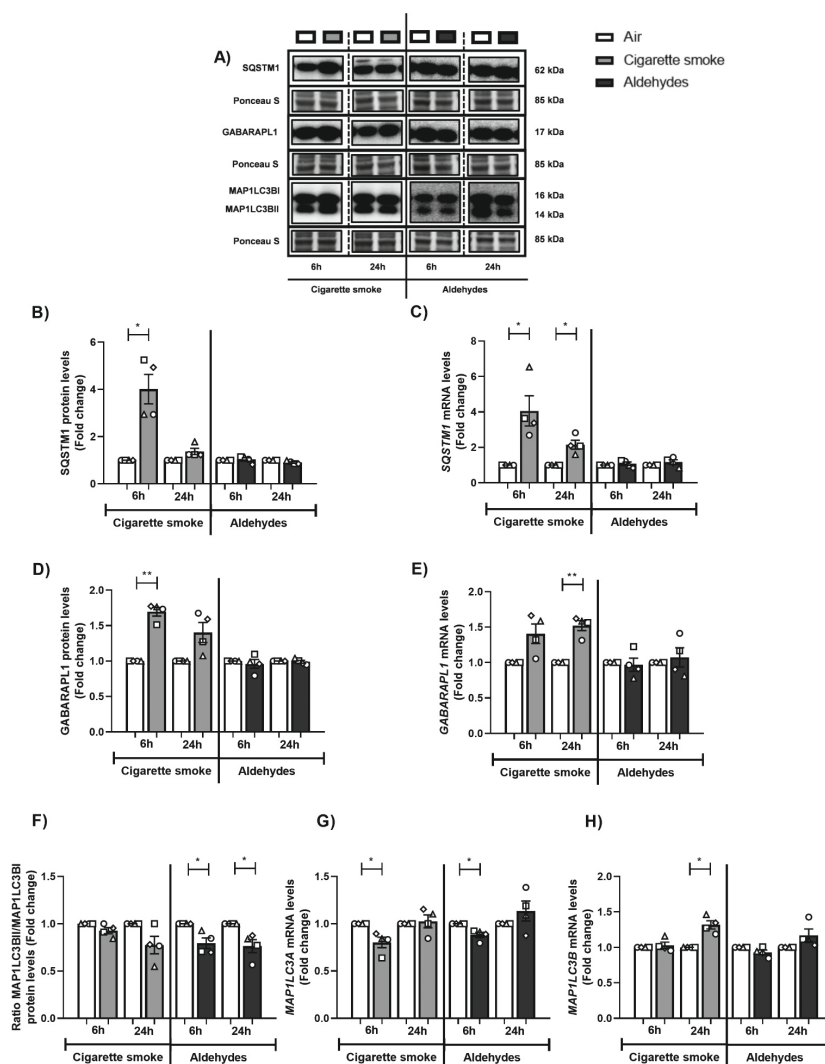


Figure 3. Altered abundance of components of autophagy in response to CS or aldehydes exposure.

Differentiated human primary bronchial epithelial cells (PBEC) from non-COPD subjects were exposed in a continuous flow system using a puff-like exposure protocol to smoke of one Marlboro Red cigarette (CS) or a mixture of aldehydes: acetaldehyde, acrolein, and formaldehyde (at relevant concentrations of 1 cigarette) or air (control) (n=4 donors). Following recovery for 6 h or 24 h, whole-cell lysates were harvested for analysis of the (A, B, D, F) protein and (C, E, G, H) transcript abundance of constituents associated with autophagy, respectively SQSTM1, GABARAPL1, ratio MAP1LC3BII/I, and MAP1LC3A and MAP1LC3B. Representative western blot images are shown of one replicate of one donor/experiment reflective of the changes in all donors as quantified in the corresponding graph. Data are presented as mean fold change compared to air control \pm s.e.m. The mean of biological triplicates per independent donor are represented by open circles, triangles, squares or diamonds. Statistical differences between CS versus air or a mixture of aldehydes versus air were tested using a two-tailed paired parametric t-test. Statistical significance is indicated as * $p < 0.05$ and ** $p < 0.01$ versus air (control).

Exposure to CS decreases expression of components of the mitophagy machinery

Because CS and aldehydes exposure are associated with alterations in the abundance of specific-autophagy proteins and these proteins are critical for facilitating the degradation of damaged or dysfunctional mitochondria (i.e., mitophagy), we further assessed the effect of smoking-associated aldehydes exposure on the abundance of constituents of the mitophagy machinery.

Firstly, we investigated the impact of CS or mixture of aldehydes on the abundance of proteins involved in receptor-mediated mitophagy. As shown in Fig. 4, significantly decreased protein levels of BNIP3L and BNIP3 were observed following CS exposure, while the impact of aldehydes was less pronounced. Moreover, protein levels of FUNDC1 as well as mRNA levels of markers of receptor-mitophagy did not significantly change following CS or aldehydes exposure.

Secondly, the abundance of key regulators involved in ubiquitin-mediated mitophagy was examined. As depicted in Fig. S6, exposure to CS or aldehydes resulted in decreased transcript levels of *PINK1* after 6 h of recovery, while other markers related to ubiquitin-mediated mitophagy were unaltered both at protein and mRNA level.

In summary, although CS had a significant impact on the abundance of key regulators involved in autophagy and mitophagy, the effect of aldehydes on constituents associated with these processes was less pronounced.

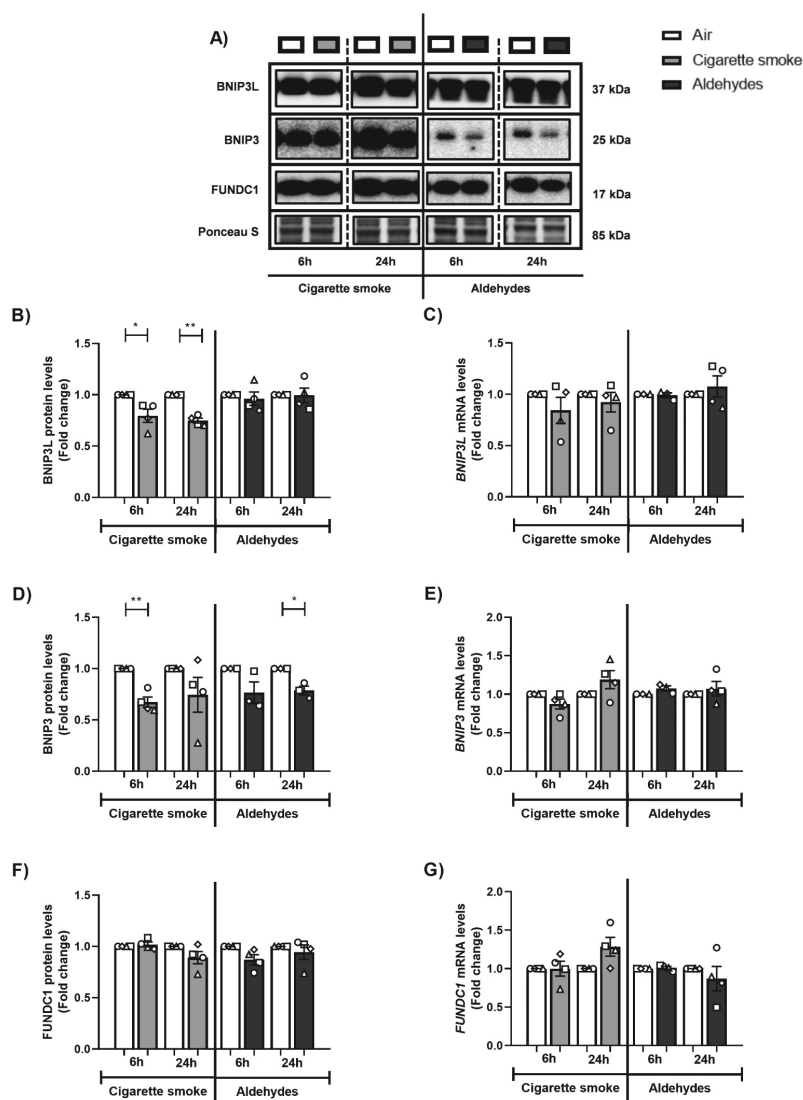


Figure 4. Decreased protein levels of markers associated with receptor-mediated mitophagy upon CS exposure. Differentiated human primary bronchial epithelial cells (PBEC) from non-COPD subjects were exposed in a continuous flow system using a puff-like exposure protocol to smoke of one Marlboro Red cigarette (CS) or a mixture of aldehydes: acetaldehyde, acrolein, and formaldehyde (at relevant concentrations of 1 cigarette) or air (control) (n=3-4 donors). After recovery for 6 h or 24 h, whole-cell lysates were harvested for analysis of (A, B, D, F) protein and (C, E, G) transcript abundance of key regulators involved in receptor-mediated mitophagy: BNIP3L, BNIP3, and FUNDC1. Representative western blot images are shown of one replicate of one donor/experiment reflective of the changes in all donors as quantified in the corresponding graph. Data are presented as mean fold change compared to air control \pm s.e.m. The mean of biological triplicates per independent donor are represented by open circles, triangles, squares or diamonds. Statistical differences between CS *versus* air or a mixture of aldehydes *versus* air were tested using a two-tailed paired parametric t-test. Statistical significance is indicated as * $p<0.05$ and ** $p<0.01$ *versus* air (control).

Alterations in the expression of proteins and genes involved in mitochondrial biogenesis in response to CS

Next, we investigated the abundance of key transcription factors involved in mitochondrial biogenesis, specifically molecules co-activated by PPARGC1. Although we observed decreased protein abundance of PPARGC1A, protein levels of ESRRA and mRNA expression of other co-activators in this pathway (*PPRC1*, *NRF2*) were upregulated in response to CS (Fig. 5 and 6). The abundance of PPARGC1 transcription factors was in general unchanged upon aldehydes exposure, with the exception of significantly elevated ESRRA protein levels 24 h post-exposure to aldehydes.

This data indicates that especially CS exposure resulted in altered expression of constituents controlling mitochondrial biogenesis pathways in PBEC, while the aldehydes present in CS had a minimal impact on the abundance of mitochondrial biogenesis transcription factors.

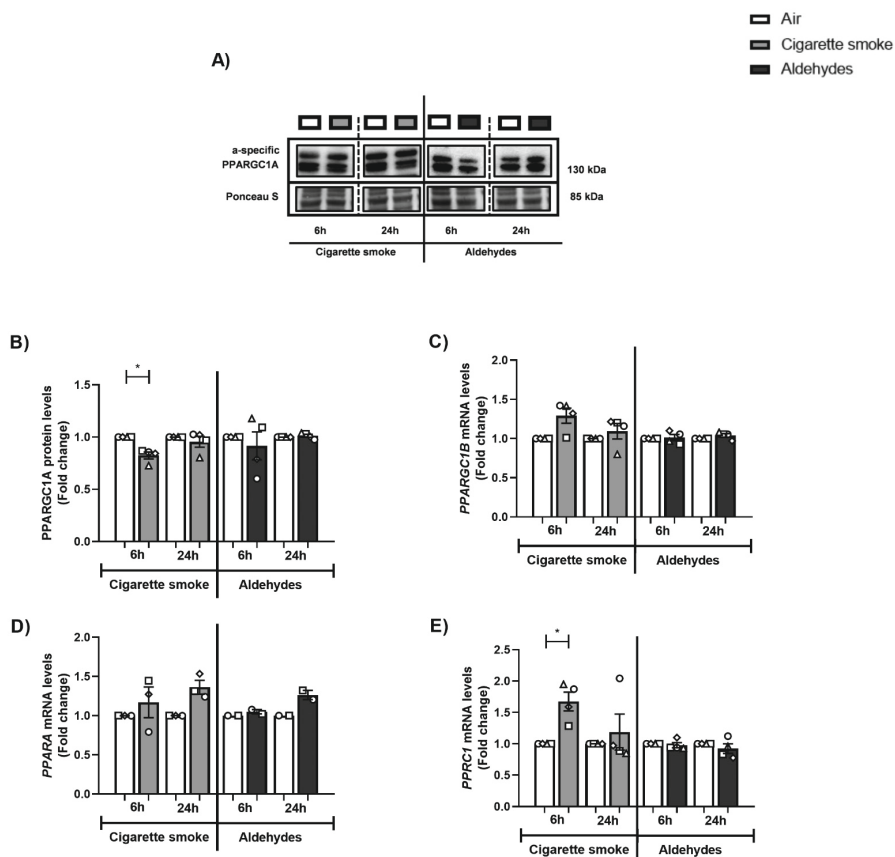


Figure 5. Altered abundance of constituents controlling mitochondrial biogenesis following CS exposure. Differentiated human primary bronchial epithelial cells (PBEC) from non-COPD subjects were exposed in a continuous flow system using a puff-like exposure protocol to smoke of one Marlboro Red cigarette (CS) or a mixture of aldehydes: acetaldehyde, acrolein, and formaldehyde (at relevant concentrations of 1 cigarette) or air (control) (n=3-4 donors). Following recovery for 6 h or 24 h, whole-cell lysates were harvested and **(A, B)** protein levels of PPARGC1A, as well as **(C-E)** transcript levels of PPARGC1 molecules: *PPARGC1B*, *PPARGC1C*, *PPARGC1D* were analysed. Representative western blot images are shown of one replicate of one donor/experiment reflective of the changes in all donors as quantified in the corresponding graph. Data are presented as mean fold change compared to air control \pm s.e.m. The mean of biological triplicates per independent donor are represented by open circles, triangles, squares or diamonds. Statistical differences between CS *versus* air or a mixture of aldehydes *versus* air were tested using a two-tailed paired parametric t-test. Statistical significance is indicated as * $p < 0.05$ *versus* air (control).

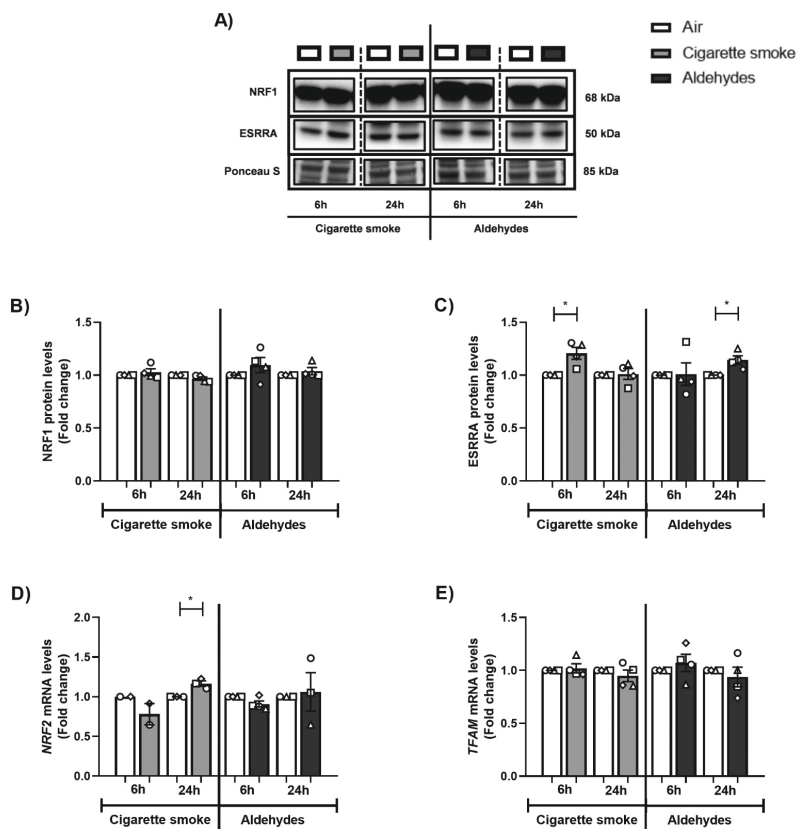


Figure 6. CS exposure results in changes in the abundance of PPARGC1-coactivated transcription factors. Differentiated human primary bronchial epithelial cells (PBEC) from non-COPD subjects were exposed in a continuous flow system using a puff-like exposure protocol to smoke of one Marlboro Red cigarette (CS) or a mixture of aldehydes: acetaldehyde, acrolein, and formaldehyde (at relevant concentrations of 1 cigarette) or air (control) ($n=2-4$ donors). After recovery for 6 h or 24 h, whole-cell lysates were harvested to analyse **(A)** protein levels of **(B)** NRF1 and **(C)** ESSRA. Representative western blot images are shown of one replicate of one donor/experiment reflective of the changes in all donors as quantified in the corresponding graph. Moreover, transcript levels of **(D)** NRF2 and **(E)** TFAM were analysed. Data are presented as mean fold change compared to air control \pm s.e.m. The mean of biological triplicates per independent donor are represented by open circles, triangles, squares or diamonds. Statistical differences between CS *versus* air or a mixture of aldehydes *versus* air were tested using a two-tailed paired parametric t-test. Statistical significance is indicated as * $p<0.05$ *versus* air (control).

CS and aldehydes affect the abundance of mitochondrial fission and fusion regulators

Besides mitophagy and mitochondrial biogenesis, mitochondrial fission and fusion are essential processes in mitochondrial quality control and homeostasis. To study if the CS- and/or aldehydes-induced alterations in the abundance of regulators involved in mitophagy and mitochondrial biogenesis were accompanied by disruption of mitochondrial dynamics, we examined the abundance of fission- and fusion-associated proteins and genes following CS and aldehydes exposure.

Regarding the response of fission-associated markers, we observed minimal decreases in DNM1L protein levels following aldehyde exposure (6 h) (Fig. 7A and B). Transcript level analysis of the fission genes *DNM1L* and *FIS1* showed no differences following exposure to CS or aldehydes compared to air control (Fig. 7C and D). A similar pattern was observed when investigating the expression of fusion-associated genes. mRNA levels of *MFN1* and *MFN2* were increased 24 h post-CS exposure, while *MFN2* and *OPA1* mRNA levels were significantly decreased in response to aldehydes (6 h) (Fig. 7E-G).

Summarized, we observed that exposure to CS resulted in increased transcript abundance of fusion-associated markers 24 h post-stimulation, while aldehyde exposure resulted in a transient decrease in expression of these mitochondrial dynamic fission- and fusion markers.

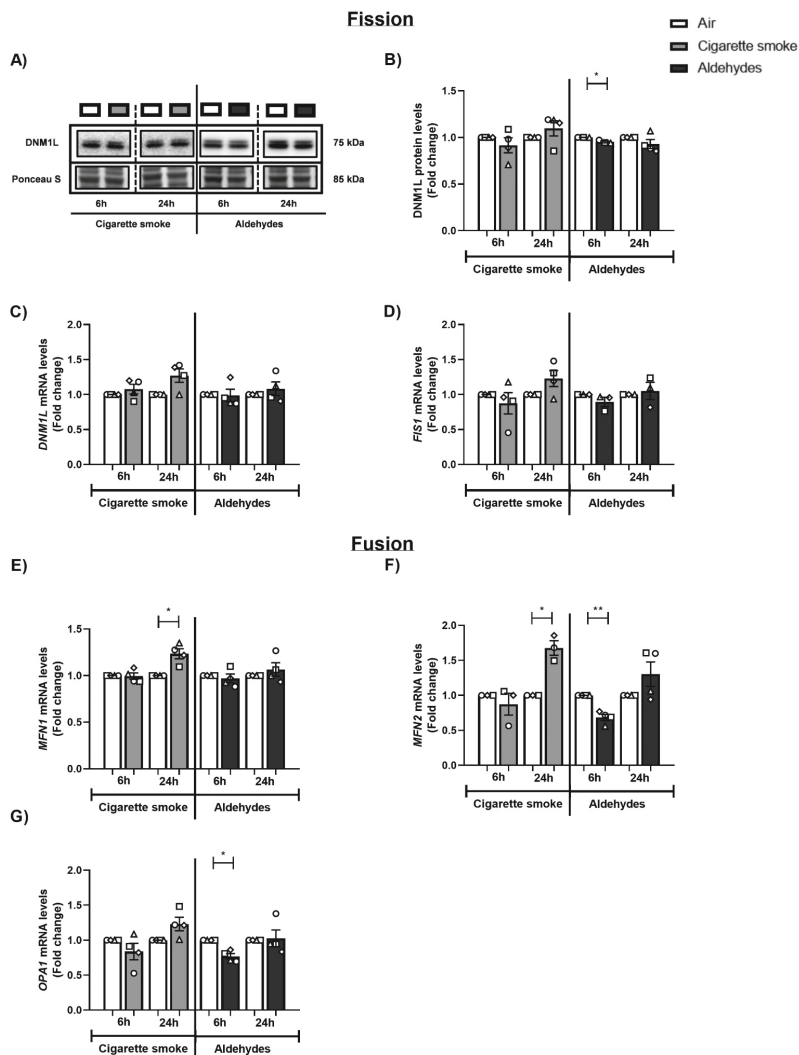


Figure 7. Abundance of mitochondrial fission- and fusion-associated markers is altered upon CS or aldehydes. Differentiated human primary bronchial epithelial cells (PBEC) from non-COPD subjects were exposed in a continuous flow system using a puff-like exposure protocol to smoke of one Marlboro Red cigarette (CS) or a mixture of aldehydes: acetaldehyde, acrolein, and formaldehyde (at relevant concentrations of 1 cigarette) or air (control) (n=3-4 donors). After recovery for 6 h or 24 h, whole-cell lysates were harvested for analysis of fission-associated markers, respectively, (A,B) DNM1L protein as well as (C) *DNM1L* and (D) *FIS1* transcript levels. Representative western blot images are shown of one replicate of one donor/experiment reflective of the changes in all donors as quantified in the corresponding graph. In addition, the expression of fusion-associated genes: (E) *MFN1*, (F) *MFN2* and (G) *OPA1* was analysed. Data are presented as mean fold change compared to air control \pm s.e.m. The mean of biological triplicates per independent donor are represented by open circles, triangles, squares or diamonds. Statistical differences between CS versus air or a mixture of aldehydes versus air were tested using a two-tailed paired parametric t-test. Statistical significance is indicated as *p<0.05 and **p<0.01 versus air (control).

Minor changes in the abundance of subunits of oxidative phosphorylation complexes in response to smoking-associated aldehydes exposure

Next, we assessed whether CS or aldehydes exposure affected the abundance of constituents of the electron transport chain. Protein levels of a subunit of complex I were decreased following exposure to CS (24 h), which was not recapitulated upon aldehyde exposure (Fig. S7A-B). Additionally, protein abundance of investigated subunits of complexes II, III and V were unaltered after exposure (Fig. S7A, C-E). Interestingly, transcript abundance of a subunit of complex I (*NDUFB3*) was not changed, while mRNA levels of complex III (*CYC1*) were elevated after aldehyde exposure (Fig. S8). In addition, exposure to a mixture of aldehydes resulted in a slight decrease in protein abundance of the outer mitochondrial membrane receptor TOMM20 (Fig. S7A and F). Lastly, assessment of mtDNA copy number did not show differences between CS or aldehyde exposure *versus* air control (Fig. S7G).

CS or aldehydes exposure induced expression of genes involved in glucose metabolism

Considering the observed impact on the molecular mechanisms controlling mitochondrial function, we also assessed the abundance of key molecules involved in other metabolic processes (i.e., glycolysis). CS exposure increased transcript abundance of the glycolytic enzyme HK2 (6 h), while protein abundance was unaltered (Fig. 8A-C). This effect was absent in response to aldehydes. Moreover, *PDK4* expression, which regulates the influx of pyruvate into the mitochondria, increased after aldehyde exposure (6 h)(Fig. 8D).

The expression of basal epithelial cell marker KRT5 is decreased after CS exposure

As depicted in Fig. 9A-C, CS exposure resulted in decreased expression of *KRT5*, while other basal epithelial cell markers (*KRT14* and *TP63*) did not change in response to CS. These alterations in the expression of basal cell-specific markers were not recapitulated in response to the mixture of aldehydes. No pronounced impact of CS or aldehydes were detected on club cell marker *SCGB1A1*, ciliogenesis marker *FOXJ1*, and goblet cell differentiation marker *MUC5AC* (Fig. 9D-F).

Impact of CS or aldehydes exposure on cilia bead flow

Because mitochondria are essential for proper function of epithelial cells of the airways (e.g., ciliary function and mucus production), we next investigated the impact of CS-associated aldehydes exposure on the motion of bead in a flow induced by cilia beating. As shown in Fig. S9, no differences were observed in the distance of beads travelled per s in CS or aldehydes-exposed cells compared to air.

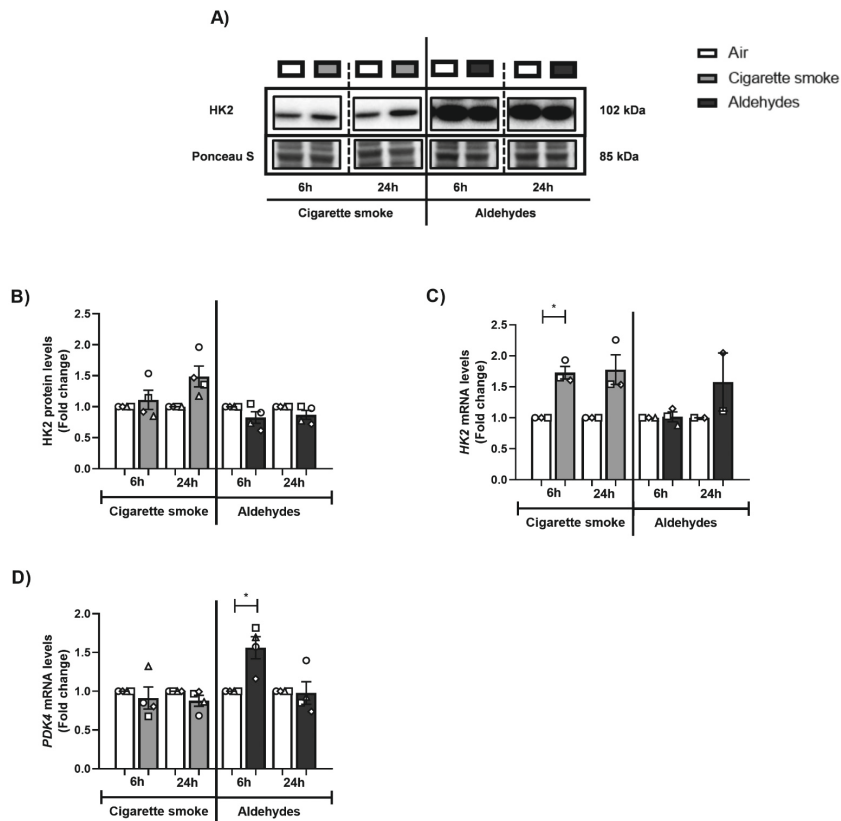


Figure 8. Increased abundance of genes associated with glucose metabolism upon CS or aldehyde exposure. Differentiated human primary bronchial epithelial cells (PBEC) from non-COPD subjects were exposed in a continuous flow system using a puff-like exposure protocol to smoke of one Marlboro Red cigarette (CS) or a mixture of aldehydes: acetaldehyde, acrolein, and formaldehyde (at relevant concentrations of 1 cigarette) or air (control) (n=2-4 donors). After recovery for 6 h or 24 h, whole-cell lysates were harvested to analyse **(A, B)** protein levels of HK2. Representative western blot images are shown of one replicate of one donor/experiment reflective of the changes in all donors as quantified in the corresponding graph. Moreover, transcript levels of **(C) HK2** and **(D) PDK4** were analysed. Data are presented as mean fold change compared to air control \pm s.e.m. The mean of biological triplicates per independent donor are represented by open circles, triangles, squares or diamonds. Statistical differences between CS *versus* air or a mixture of aldehydes *versus* air were tested using a two-tailed paired parametric t-test. Statistical significance is indicated as * $p < 0.05$ *versus* air (control).

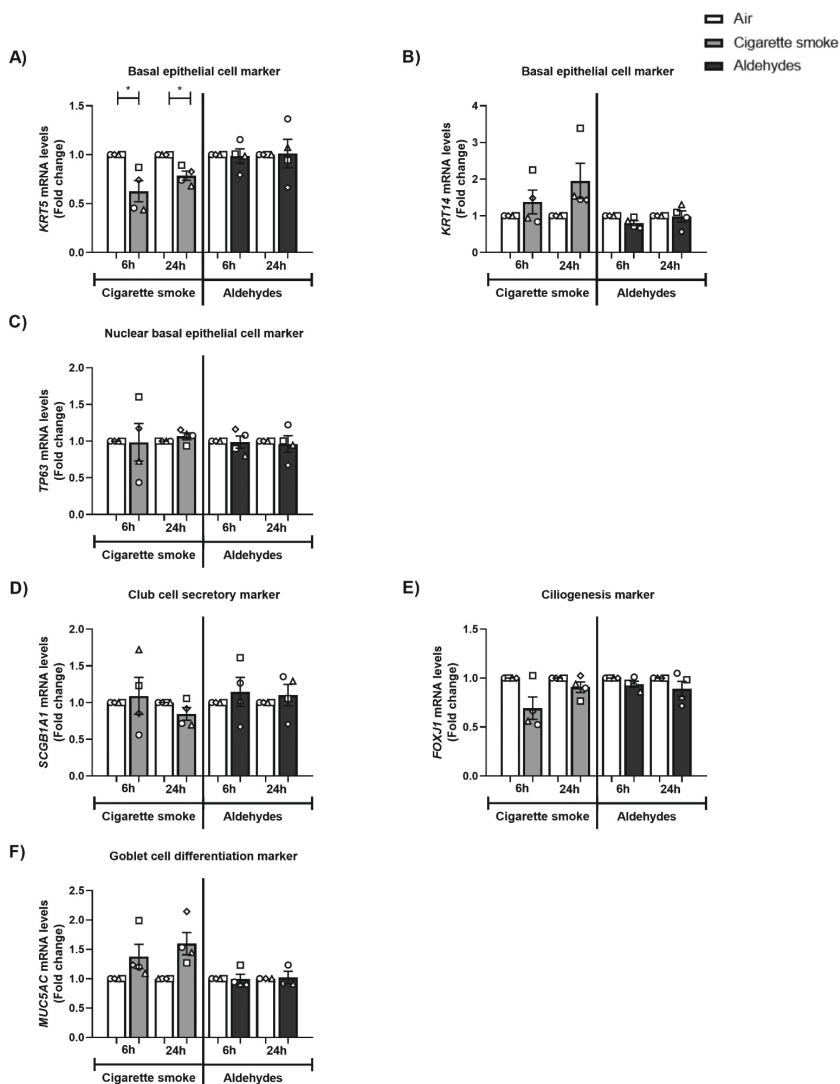


Figure 9. Transcript levels of basal epithelial cell marker *KRT5* are decreased in response to CS exposure. Differentiated human primary bronchial epithelial cells (PBEC) from non-COPD subjects were exposed in a continuous flow system using a puff-like exposure protocol to smoke of one Marlboro Red cigarette (CS) or a mixture of aldehydes: acetaldehyde, acrolein, and formaldehyde (at relevant concentrations of 1 cigarette) or air (control) (n=4 donors). After recovery for 6 h or 24 h, whole-cell lysates were harvested to analyse transcript levels of basal epithelial cell markers (A) *KRT5*, (B) *KRT14* and (C) nuclear basal epithelial cell marker *TP63*. Moreover, the expression of (D) club cell secretory marker *SCGB1A1*, (E) ciliogenesis marker *FOXJ1* and (F) goblet cell differentiation marker *MUC5AC* was analysed. Data are presented as mean fold change compared to air control \pm s.e.m. The mean of biological triplicates per independent donor are represented by open circles, triangles, squares or diamonds. Statistical differences between CS *versus* air or a mixture of aldehydes *versus* air were tested using a two-tailed paired parametric t-test. Statistical significance is indicated as * $p < 0.05$ *versus* air (control).

Discussion

In this study, CS exposure resulted in increased IL-8 secretion as well as elevated transcript levels of anti-oxidant and inflammatory genes. Moreover, the molecular regulation of mitochondrial quality control processes was disrupted in response to CS-exposure, mainly at the level of autophagy and mitophagy. Also, transcript levels of basal epithelial cell marker *KRT5* were declined in response to CS. CS-mediated responses were minimally recapitulated in PBEC cultures exposed to a mixture of aldehydes.

Literature describing inflammation and oxidative stress in response to both CS or aldehydes (acetaldehyde, acrolein and formaldehyde) in *in vivo* and *in vitro* airway models is abundant (8, 9, 56-59). We observed that only CS exposure induced an inflammatory response and anti-oxidant gene expression, whereas the response to aldehydes was less pronounced. It could be suggested that the single exposure to aldehydes (high peak concentrations) that we used may be insufficient to induce an inflammatory response or significantly alter cellular (anti-) oxidant status. In this context, it is important to note that we only measured anti-oxidant gene expression and did not assess (anti-) oxidant status directly.

Studies investigating the impact of CS exposure on the regulation of mitochondrial quality control, content and metabolism in differentiated PBEC models using a continuous flow system combined with a puff-like exposure regime, as the one we deployed, are non-existent in literature. Several studies, however, using CS exposure of cell lines or undifferentiated human primary airway epithelial cells showed that CS or CS extract (CSE) induced autophagy and mitophagy (31, 33, 37-41, 43-46). This is also in line with our previous findings in whole CS-exposed differentiated PBEC (47). Collectively, the CS-mediated autophagy/mitophagy response that we (and others) observed can be interpreted as a cellular response in an effort to clear up CS-induced damage to specific proteins, organelles or other macromolecules. Indeed, it has been previously shown that CS causes damage to mitochondria manifested as aberrant mitochondrial morphology observed in *in vivo* and *in vitro* smoke exposure experimental models (28-37) and mitochondrial dysfunction (i.e., impaired respiration) (34).

An interesting observation in our study was that the abundance of autophagy proteins drastically increased, whereas mitophagy proteins were moderately decreased upon CS exposure. In the case of autophagy, this can be explained in several ways. One possibility would be a blocked autophagy flux (i.e., autophagosome and associated proteins fail to be degraded and thus accumulate). However, we also observed increased autophagy mRNA levels suggestive of another possible explanation, namely an activation of autophagy in response to damage. These two theories have been described

previously as well as conflicting experimental data has been reported regarding the contribution of increased or blocked autophagy to being injurious or protective for the airways and corresponding disease development) (60-64). Future research is necessary to assess the contribution of (blocked) autophagy in response to CS exposure in airway epithelial cells.

In contrast to CS, we observed that aldehydes minimally affect the abundance of autophagy or mitophagy constituents. Previous studies, although limited and in non-primary human lung cells, demonstrated that aldehydes (such as acrolein but also formaldehyde) can stimulate autophagy to a comparable extent as smoke (65-67). Nevertheless, abovementioned findings are difficult to compare with our results, due to variation in dose (25 μ M up to 10 ppm), exposure regimes (gaseous inhalation *versus* exposure in solutions) and cell types analysed (rat lung homogenates *versus* human airway cell lines) in these studies.

With regard to mitochondrial biogenesis, we observed decreased protein levels of PPARGC1A and increased transcript levels of multiple molecules involved in mitochondrial biogenesis in response to CS. These findings suggest a compensatory cellular response to counteract the initiated breakdown of mitochondria. Previous *in vitro* PBEC studies reported a contrary impact of CS exposure on transcript levels of some regulators of the PPARGC1 network (47, 68). Discrepant findings may well be explained by differences in time, dosage and mode-of-exposure. Again, in contrast to CS, aldehydes had no profound impact on mitochondrial biogenesis-associated molecules that we investigated in our study. Previous research however reported decreased expression of constituents of the mitochondrial biogenesis machinery in response to acrolein *in vitro* in cells of the lung and *in vivo* in lung tissue (66, 69). The fact that we did not observe these responses to aldehydes in our model may suggest that this response is limited to certain cell types in the airways, which do not include cells from the bronchial epithelial layer. To our knowledge, the impact of CS-associated acetaldehyde and formaldehyde on the regulation of mitochondrial biogenesis has never been studied in cells of the airways before.

With regard to mitochondrial dynamics, we observed that exposure to CS resulted in increased transcript abundance of fusion-associated markers 24 h post-stimulation, while a transient decrease in expression of both fission- and fusion-markers was observed in response to aldehydes. This is partly in line with our previously published data in differentiated PBEC cultured at ALI and exposed to whole CS (47). Moreover, other *in vivo* and *in vitro* studies have shown that acrolein exposure resulted in increased (transcriptional regulation of) mitochondrial fission (65, 66) and smoke exposure resulted in mitochondrial fragmentation (increased fission) and decreased fusion (30, 33, 34, 41, 44, 45, 70) in cells of the airways. Also discrepancies have been reported in literature after smoke exposure in lung cells (31, 38, 43, 71). These conflicting findings

can be explained by the various exposure models used as well as the dynamic character of the fission and fusion flux. Interestingly, the observation of increased abundance of fusion proteins upon CS-exposure is compatible with alterations in the abundance of regulatory molecules controlling mitochondrial biogenesis and the indications for increased autophagy, which altogether may be interpreted as a stimulated mitochondrial turnover (i.e., increased degradation of mitochondria and increased generation of new mitochondria) after CS exposure.

Although CS-induced mitochondrial dysfunction has been described in airway epithelial cells *in vivo* (29) and *in vitro* (34), we observed no marked changes in the abundance of subunits of oxidative phosphorylation complexes following CS exposure. These findings are in line with our previous study investigating the impact of smoke exposure in various PBEC models (47). Furthermore, the exposure to aldehydes only had a minimal impact on the expression of (subunits of) oxidative phosphorylation complexes. In literature however, aldehyde-induced disruption of mitochondrial function has been shown. Specifically, in response to acetaldehyde in hepatocytes (72), to acrolein in cells of the airways, rat liver mitochondria or rat lung (65, 66, 69, 73, 74) as well as to formaldehyde and acetaldehyde in rat liver mitochondria (75) or formaldehyde in neuroblastoma cells (76). Studying the role of a mixture of aldehydes in differentiated human PBEC *versus* individual aldehydes in non-primary human lung cells may clarify these contrasting results of our study *versus* previous studies.

Several *in vitro* studies, using primary airway epithelial cells or cell lines, showed that CS(E) impacts epithelial barrier integrity, induces cilia toxicity, increases mucus production and changes the presence of cell types in the airway epithelium (77-83), which is in line with pathological alterations observed in COPD patients (84-87). The absence of changes in mRNA expression of cell-type specific markers in our study may be explained by our acute exposure protocol or by the fact that we used fully differentiated cultures, as studies reporting changes are often exposing cells during differentiation and/or using a repeated or chronic exposure protocol of CS(E) or acrolein (77-79, 83, 88).

Although some individual findings that we describe have already been reported in previous studies using other (cell line) models of CS or acrolein exposure, the novelty of our approach and findings is multifaced. These strengths and novelties are outlined in this paragraph and in Fig. 10. Firstly, some strengths can be found in the model. Indeed, the combination of fully differentiated human PBEC with an ALI exposure system can be considered a strength. This model mimics the human situation properly in contrast to studies using submerged cultures of undifferentiated PBEC or immortalized cell lines. Secondly, as previous *in vitro* studies of submerged cultures are using liquid-based exposure modalities (CSE or aldehydes as liquid formulation), our airborne and dynamic exposure method is more reflective for the *in vivo* situation due to the representative

chemical characteristics (gaseous and particulate components). Thirdly, we carefully considered the smoking regime and aimed to mimic the puff-topography (i.e., toxic peak concentrations of aldehydes) of smokers in our *in vitro* model to study the impact of the gaseous and particulate mainstream components of CS or mixture of aldehydes on airway epithelial cells. Previous *in vitro* and *in vivo* studies mainly used continuous whole CS or even liquid-based exposures. The fourth novelty is that we studied for the first time, the impact of simultaneous exposure of three short-chain aldehydes in this experimental set-up. The scarce studies available primarily focus on the impact of individual aldehydes, in particular acrolein (65). Studying this combination of three aldehydes is important due to indications (based on their common mechanisms and previous co-exposure studies) of an additive or synergistic toxicity (89-92). With regard to the data that we obtained, the main novelty is that we investigated a comprehensive panel of essential constituents involved in several molecular mechanisms associated with mitochondrial content and function (mitophagy, mitochondrial dynamics and mitochondrial biogenesis) and compared changes in response to CS and aldehydes, which has never been described before.

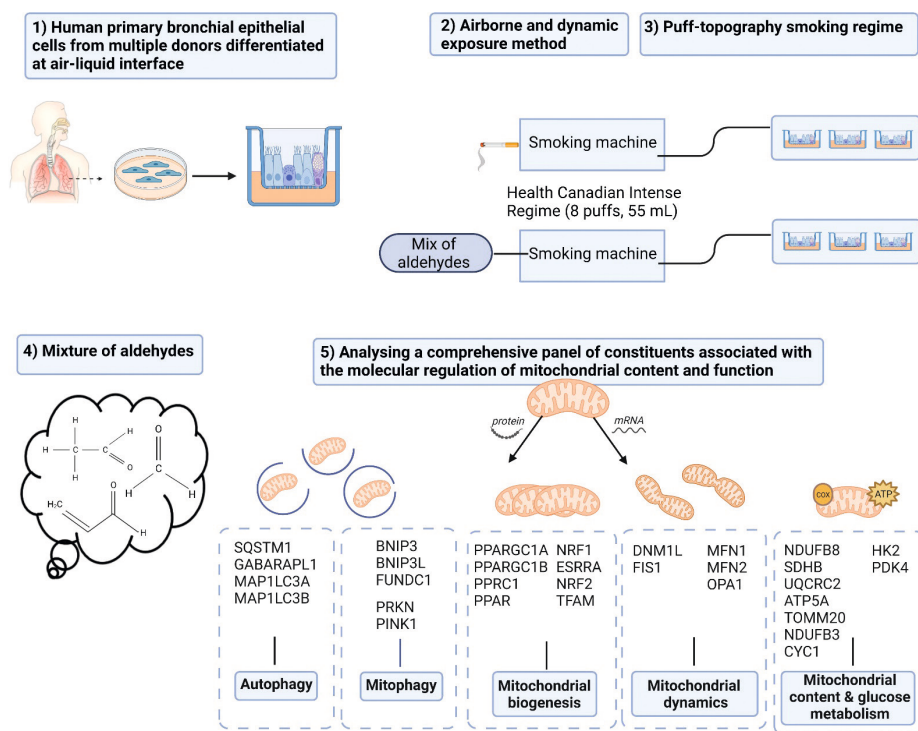


Figure 10. Schematic representation of the strengths and novelties of the study. 1) Use of human primary bronchial epithelial cells from multiple donors which are differentiated at air-liquid interface. 2) The airborne and dynamic exposure method and 3) the smoking regime which mimics the puff-topography are both more reflective for the *in vivo* smoking situation due to the representative chemical characteristics (gaseous and particulate components) of the exposure. 4) Studying the impact of simultaneous exposure of three short-chain aldehydes. 5) Assessment of a comprehensive panel of constituents involved in molecular mechanisms associated with mitochondrial content and function in our sophisticated *in vitro* exposure model. *Designed with Biorender.com*

Obviously, a limitation of our study is that realistic *in vitro* lung models should also include other cell types than epithelial cells e.g., macrophages or fibroblasts. Previous studies showed the potential of such complex co-culture models (93, 94). In addition, with respect to the dosimetry, we were able to reliably assess the levels of the three aldehydes in the mainstream smoke of one cigarette using a standard operating procedure (53), which concentrations were in line with previously reported levels (11). Unfortunately, we were unable to measure levels of these aldehydes in the aldehydes mixture that we generated at the site of the cells. We have however confidence that we generated an aldehydes mixture that is comparable to the concentrations of acetaldehyde, acrolein and formaldehyde present in the mainstream smoke of one Marlboro Red cigarette. This confidence was based on our calculations using the density and purity of each aldehyde in combination with the total flow of test atmosphere as

well as the TCA analyses of the mixture of aldehydes to check whether each compound was present in the generation of the test atmosphere. However, it should be noted as a limitation of our experimental set-up that a mixture of pure aldehydes as used in our study will behave differently from the same quantity of aldehydes present in a mixture with other chemicals, such as in CS. For example, condensation of aldehydes on aerosol particles is more likely in CS. Moreover, as we are interested in the chronic exposure of smoking-associated aldehydes (suggested to be related to COPD pathogenesis), an obvious limitation of our study is the single exposure regime. Nevertheless, acute exposure seems to be partly reflective for changes after chronic exposure as supported by previous evidence. To shortly illustrate this, effects of short-term CS exposure in our study, especially the observed autophagy induction, are in line with observations in lung tissue or PBEC from COPD patients with a long history of smoking (31, 33, 38, 40). This indicates that our short-term CS exposure model reflects, at least in part, changes in airway epithelial cells from chronic smokers. In addition, in line with our findings, airway epithelial cells from mice exposed to CS for a longer period of time also showed elevated autophagy markers (95) and upregulated mitophagy (33). Also, CS-exposure for 6 months disrupted mitochondrial metabolism in BEAS-2B cells (31). Interestingly, Malinska *et al.* compared a short- and long-term CS exposure period (1-week *versus* 12-week CS exposure) in BEAS-2B cells, and they found most changes in mitochondrial function were similar in these two periods, although indications of adaptation were reported after long-term exposure (32).

These limitations could be taken into account in future research to investigate the proposed knowledge gaps. Additional scientific research into the mechanistic and causal involvement of smoking-associated aldehydes in mitochondrial (dys)function in cells of the airways could be of value for supporting regulation of aldehydes in cigarettes. Moreover, further research is required to provide more insight into the potential link between aldehydes, mitochondrial dysfunction and COPD pathogenesis in order to shed light on the potential therapeutical applications targeting aldehydes and/or mitochondria.

Overall, in contrast to our hypothesis, we found no profound impact of aldehydes on molecular mechanisms controlling mitochondrial content and function (compared to CS). This is in contrast to *in vitro* studies which showed that acrolein or co-exposure to acrolein and formaldehyde disrupt processes involved in the regulation of mitochondrial homeostasis in lung cells (65, 73, 89, 92, 96), and conflicting to an *in vivo* study which observed that proper function of aldehyde dehydrogenase protected against the development of CS-induced airway disease (48). Probably, the choice for our sophisticated and novel cell and exposure model, including above-mentioned corresponding limitations e.g., dosimetry, could clarify the limited impact of aldehydes on the molecular regulation of pathways involved in mitochondrial content and function in our study. Besides these study-specific limitations, several

other explanations for the absence of a response to aldehydes could be conceived. Theoretically, the combination of the three aldehydes of interest together with any of the other 6000 chemicals, including other aldehydes, present in CS could introduce an additive or synergistic toxicity which we did not address in our study. For example, a recent study reported enhanced lung carcinogenicity by co-exposure to tobacco compound Nitrosamine 4-Methylnitrosamino-1-(3-pyridyl)-1-butanone combined with acetaldehyde, formaldehyde or carbon dioxide in mice (97). Moreover, potentially, compounds other than these three aldehydes may contribute to mito-toxicity of CS (e.g., carbon monoxide, nicotine, polycyclic aromatic hydrocarbons).

In conclusion, this study shows that *in vitro* exposure of differentiated PBEC to CS disrupts the molecular regulation of mitochondrial content and mitochondrial quality control, while only part of these changes were recapitulated in response to exposure to a representative combination of aldehydes. These findings suggest that other compounds than aldehydes in CS contribute to CS-induced disruption of the regulation of mitochondrial content and function in airway epithelial cells. Although there is an indication that aldehydes have an impact on molecular mechanisms controlling mitochondrial content and function, additional research should be conducted to scientifically support the regulation of aldehydes (or other chemicals) in CS.

Acknowledgements

The authors would like to thank Dr. Niki L. Reynaert of the Primary Lung Culture Facility (PLUC; Maastricht University Medical Center+, the Netherlands) for providing advice. Furthermore, we would like to thank Dr. Gerco den Hartog (RIVM, the Netherlands) for the assistance with making the videos of the bead motion induced by ciliary beating.

Competing interests

The authors have declared no conflict of interest.

Funding

This research is supported by the Netherlands Food and Consumer Product Safety Authority (NVWA).

Data availability

N/A

Authors' contribution

Conceptualization: Christy. B.M. Tulen, Antoon Opperhuizen, Frederik-Jan van Schooten, Yvonne C.M. Staal, Alexander H.V. Remels

Formal analysis: Christy B.M. Tulen, Evert Duistermaat, Johannes W.J.M. Cremers, Walther N.M. Klerx, Paul. H.B. Fokkens, Naömi Weibolt, Eric R. Gremmer, Phyllis J.J. Jessen, Evi J.C. Koene, Lou Maas

Investigation: Christy B.M. Tulen, Evert Duistermaat, Johannes W.J.M. Cremers, Walther N.M. Klerx, Paul. H.B. Fokkens, Naömi Weibolt, Nico Kloosterboer, Mieke A. Dentener, Eric R. Gremmer, Phyllis J.J. Jessen, Evi J.C. Koene, Lou Maas

Methodology: Nico Kloosterboer, Mieke A. Dentener

Writing – Drafting: Christy. B.M. Tulen

Writing – Revising: Evert Duistermaat, Johannes W.J.M. Cremers, Walther N.M. Klerx, Paul. H.B. Fokkens, Naömi Weibolt, Nico Kloosterboer, Mieke A. Dentener, Eric R. Gremmer, Phyllis J.J. Jessen, Evi J.C. Koene, Lou Maas, Antoon Opperhuizen, Frederik-Jan van Schooten, Yvonne C.M. Staal, Alexander H.V. Remels

References

1. GBD 2015 Tobacco Collaborators. Smoking prevalence and attributable disease burden in 195 countries and territories, 1990-2015: a systematic analysis from the Global Burden of Disease Study 2015. *Lancet*. 2017;389(10082):1885-906.
2. Celli BR, Wedzicha JA. Update on Clinical Aspects of Chronic Obstructive Pulmonary Disease. *N Engl J Med*. 2019;381(13):1257-66.
3. Rodgman A, Perfetti TA. The chemical components of tobacco and tobacco smoke: CRC press; 2013.
4. Burns DM, Dybing E, Gray N, Hecht S, Anderson C, Sanner T, et al. Mandated lowering of toxicants in cigarette smoke: a description of the World Health Organization TobReg proposal. *Tob Control*. 2008;17(2):132-41.
5. Cheah NP. Volatile aldehydes in tobacco smoke: source fate and risk. [Ph.D. Dissertation Thesis]. Maastricht, The Netherlands: Maastricht University; 2016.
6. Corley RA, Kabilan S, Kuprat AP, Carson JP, Jacob RE, Minard KR, et al. Comparative Risks of Aldehyde Constituents in Cigarette Smoke Using Transient Computational Fluid Dynamics/ Physiologically Based Pharmacokinetic Models of the Rat and Human Respiratory Tracts. *Toxicol Sci*. 2015;146(1):65-88.
7. Bos PMJ, Soeteman-Hernández LG, Talhout R. Risk assessment of components in tobacco smoke and e-cigarette aerosols: a pragmatic choice of dose metrics. *Inhal Toxicol*. 2021;33(3):81-95.
8. Yeager RP, Kushman M, Chemerynski S, Weil R, Fu X, White M, et al. Proposed Mode of Action for Acrolein Respiratory Toxicity Associated with Inhaled Tobacco Smoke. *Toxicol Sci*. 2016;151(2):347-64.
9. Bernardini L, Barbosa E, Charão MF, Brucker N. Formaldehyde toxicity reports from in vitro and in vivo studies: a review and updated data. *Drug Chem Toxicol*. 2020:1-13.
10. National Research Council (US) Committee. Emergency and Continuous Exposure Guidance Levels for Selected Submarine Contaminants. Washington (DC): National Academies Press (US); 2009.
11. Pauwels C, Klerx WNM, Pennings JLA, Boots AW, van Schooten FJ, Opperhuizen A, et al. Cigarette Filter Ventilation and Smoking Protocol Influence Aldehyde Smoke Yields. *Chem Res Toxicol*. 2018;31(6):462-71.
12. World Health Organization Framework Convention on Tobacco Control. Partial guidelines for implementation of articles 9 and 10—regulation of the contents of tobacco products and regulation of tobacco product disclosures. 2012.
13. World Health Organization & World Health Organization Tobacco Free Initiative. The scientific basis of tobacco product regulation: second report of a WHO study group. World Health Organization; 2008.
14. Hiemstra PS, Grootaers G, van der Does AM, Krul CAM, Kooter IM. Human lung epithelial cell cultures for analysis of inhaled toxicants: Lessons learned and future directions. *Toxicol In Vitro*. 2018;47:137-46.
15. Crapo JD, Barry BE, Gehr P, Bachofen M, Weibel ER. Cell number and cell characteristics of the normal human lung. *American Review of Respiratory Disease*. 1982;126(2):332-7.
16. Hiemstra PS, McCray PB, Bals R. The innate immune function of airway epithelial cells in inflammatory lung disease. *European respiratory journal*. 2015;45(4):1150-62.

17. Cloonan SM, Choi AM. Mitochondria in lung disease. *J Clin Invest.* 2016;126(3):809-20.
18. Aghapour M, Remels AHV, Pouwels SD, Bruder D, Hiemstra PS, Cloonan SM, et al. Mitochondria: at the crossroads of regulating lung epithelial cell function in chronic obstructive pulmonary disease. *Am J Physiol Lung Cell Mol Physiol.* 2020;318(1):L149-L64.
19. MacNee W. Pathogenesis of Chronic Obstructive Pulmonary Disease. *Clinics in Chest Medicine.* 2007;28(3):479-513.
20. Hoffmann RF, Jonker MR, Brandenburg SM, de Bruin HG, Ten Hacken NHT, van Oosterhout AJM, et al. Mitochondrial dysfunction increases pro-inflammatory cytokine production and impairs repair and corticosteroid responsiveness in lung epithelium. *Sci Rep.* 2019;9(1):15047.
21. Patergnani S, Bouhamida E, Leo S, Pinton P, Rimessi A. Mitochondrial Oxidative Stress and "Mito-Inflammation": Actors in the Diseases. *Biomedicines.* 2021;9(2).
22. Fritsch LE, Moore ME, Sarraf SA, Pickrell AM. Ubiquitin and Receptor-Dependent Mitophagy Pathways and Their Implication in Neurodegeneration. *J Mol Biol.* 2020;432(8):2510-24.
23. Lin J, Handschin C, Spiegelman BM. Metabolic control through the PGC-1 family of transcription coactivators. *Cell Metab.* 2005;1(6):361-70.
24. Scarpulla RC. Metabolic control of mitochondrial biogenesis through the PGC-1 family regulatory network. *Biochim Biophys Acta.* 2011;1813(7):1269-78.
25. Mishra P, Chan DC. Mitochondrial dynamics and inheritance during cell division, development and disease. *Nat Rev Mol Cell Biol.* 2014;15(10):634-46.
26. Hara H, Kuwano K, Araya J. Mitochondrial Quality Control in COPD and IPF. *Cells.* 2018;7(8).
27. Ryter SW, Rosas IO, Owen CA, Martinez FJ, Choi ME, Lee CG, et al. Mitochondrial Dysfunction as a Pathogenic Mediator of Chronic Obstructive Pulmonary Disease and Idiopathic Pulmonary Fibrosis. *Ann Am Thorac Soc.* 2018;15(Suppl 4):S266-s72.
28. Agarwal AR, Yin F, Cadenas E. Short-term cigarette smoke exposure leads to metabolic alterations in lung alveolar cells. *Am J Respir Cell Mol Biol.* 2014;51(2):284-93.
29. Cloonan SM, Glass K, Laucho-Contreras ME, Bhashyam AR, Cervo M, Pabon MA, et al. Mitochondrial iron chelation ameliorates cigarette smoke-induced bronchitis and emphysema in mice. *Nat Med.* 2016;22(2):163-74.
30. Hara H, Araya J, Ito S, Kobayashi K, Takasaka N, Yoshii Y, et al. Mitochondrial fragmentation in cigarette smoke-induced bronchial epithelial cell senescence. *Am J Physiol Lung Cell Mol Physiol.* 2013;305(10):L737-46.
31. Hoffmann RF, Zarrintan S, Brandenburg SM, Kol A, de Bruin HG, Jafari S, et al. Prolonged cigarette smoke exposure alters mitochondrial structure and function in airway epithelial cells. *Respir Res.* 2013;14:97.
32. Malinska D, Szymanski J, Patalas-Krawczyk P, Michalska B, Wojtala A, Prill M, et al. Assessment of mitochondrial function following short- and long-term exposure of human bronchial epithelial cells to total particulate matter from a candidate modified-risk tobacco product and reference cigarettes. *Food Chem Toxicol.* 2018;115:1-12.
33. Mizumura K, Cloonan SM, Nakahira K, Bhashyam AR, Cervo M, Kitada T, et al. Mitophagy-dependent necroptosis contributes to the pathogenesis of COPD. *J Clin Invest.* 2014;124(9):3987-4003.
34. Sundar IK, Maremanda KP, Rahman I. Mitochondrial dysfunction is associated with Miro1 reduction in lung epithelial cells by cigarette smoke. *Toxicol Lett.* 2019;317:92-101.

35. Valdivieso Á G, Dugour AV, Sotomayor V, Clauzure M, Figueroa JM, Santa-Coloma TA. N-acetyl cysteine reverts the proinflammatory state induced by cigarette smoke extract in lung Calu-3 cells. *Redox Biol.* 2018;16:294-302.
36. van der Toorn M, Rezayat D, Kauffman HF, Bakker SJ, Gans RO, Koëter GH, et al. Lipid-soluble components in cigarette smoke induce mitochondrial production of reactive oxygen species in lung epithelial cells. *Am J Physiol Lung Cell Mol Physiol.* 2009;297(1):L109-14.
37. Wu K, Luan G, Xu Y, Shen S, Qian S, Zhu Z, et al. Cigarette smoke extract increases mitochondrial membrane permeability through activation of adenine nucleotide translocator (ANT) in lung epithelial cells. *Biochem Biophys Res Commun.* 2020;525(3):733-9.
38. Ahmad T, Sundar IK, Lerner CA, Gerloff J, Tormos AM, Yao H, et al. Impaired mitophagy leads to cigarette smoke stress-induced cellular senescence: implications for chronic obstructive pulmonary disease. *Faseb j.* 2015;29(7):2912-29.
39. Chen ZH, Kim HP, Sciurba FC, Lee SJ, Feghali-Bostwick C, Stolz DB, et al. Egr-1 regulates autophagy in cigarette smoke-induced chronic obstructive pulmonary disease. *PLoS One.* 2008;3(10):e3316.
40. Ito S, Araya J, Kurita Y, Kobayashi K, Takasaka N, Yoshida M, et al. PARK2-mediated mitophagy is involved in regulation of HBEC senescence in COPD pathogenesis. *Autophagy.* 2015;11(3):547-59.
41. Kyung SY, Kim YJ, Son ES, Jeong SH, Park JW. The Phosphodiesterase 4 Inhibitor Roflumilast Protects against Cigarette Smoke Extract-Induced Mitophagy-Dependent Cell Death in Epithelial Cells. *Tuberc Respir Dis.* 2018;81(2):138-47.
42. Mizumura K, Justice MJ, Schweitzer KS, Krishnan S, Bronova I, Berdyshev EV, et al. Sphingolipid regulation of lung epithelial cell mitophagy and necroptosis during cigarette smoke exposure. *Faseb j.* 2018;32(4):1880-90.
43. Park EJ, Park YJ, Lee SJ, Lee K, Yoon C. Whole cigarette smoke condensates induce ferroptosis in human bronchial epithelial cells. *Toxicol Lett.* 2019;303:55-66.
44. Son ES, Kim SH, Ryter SW, Yeo EJ, Kyung SY, Kim YJ, et al. Quercetogetin protects against cigarette smoke extract-induced apoptosis in epithelial cells by inhibiting mitophagy. *Toxicol In Vitro.* 2018;48:170-8.
45. Song C, Luo B, Gong L. Resveratrol reduces the apoptosis induced by cigarette smoke extract by upregulating MFN2. *PLoS One.* 2017;12(4):e0175009.
46. Zhang M, Shi R, Zhang Y, Shan H, Zhang Q, Yang X, et al. Nix/BNIP3L-dependent mitophagy accounts for airway epithelial cell injury induced by cigarette smoke. *J Cell Physiol.* 2019;234(8):14210-20.
47. Tulen CBM, Wang Y, Beentjes D, Jessen PJJ, Ninaber DK, Reynaert NL, et al. Dysregulated mitochondrial metabolism upon cigarette smoke exposure in various human bronchial epithelial cell models. *Dis Model Mech.* 2022;15(3).
48. Morita K, Masuda N, Oniki K, Saruwatari J, Kajiwar A, Otake K, et al. Association between the aldehyde dehydrogenase 2*2 allele and smoking-related chronic airway obstruction in a Japanese general population: a pilot study. *Toxicol Lett.* 2015;236(2):117-22.
49. Costa DL, Kutzman RS, Lehmann JR, Drew RT. Altered lung function and structure in the rat after subchronic exposure to acrolein. *Am Rev Respir Dis.* 1986;133(2):286-91.
50. van Wetering S, van der Linden AC, van Sterkenburg MA, de Boer WI, Kuijpers AL, Schalkwijk J, et al. Regulation of SLPI and elafin release from bronchial epithelial cells by neutrophil defensins. *Am J Physiol Lung Cell Mol Physiol.* 2000;278(1):L51-8.

51. van Wetering S, Zuyderduyn S, Ninaber DK, van Sterkenburg MAJA, Rabe KF, Hiemstra PS. Epithelial differentiation is a determinant in the production of eotaxin-2 and -3 by bronchial epithelial cells in response to IL-4 and IL-13. *Mol Immunol*. 2007;44(5):803-11.
52. World Health Organization T. SOP 1 - Standard operating procedure for intense smoking of cigarettes. WHO; 2012.
53. World Health Organization TobLabNet. SOP 8 - Standard operating procedure for determination of aldehydes in mainstream cigarette smoke under ISO and intense smoking conditions. 2018.
54. Rasband WS. ImageJ. In: U. S. National Institutes of Health B, Maryland, USA, editor. 1997-2018.
55. Meijering E, Dzyubachyk O, Smal I. Methods for cell and particle tracking. *Methods Enzymol*. 2012;504:183-200.
56. Mio T, Romberger DJ, Thompson AB, Robbins RA, Heires A, Rennard SI. Cigarette smoke induces interleukin-8 release from human bronchial epithelial cells. *Am J Respir Crit Care Med*. 1997;155(5):1770-6.
57. Moretto N, Facchinetti F, Southworth T, Civelli M, Singh D, Patacchini R. alpha,beta-Unsaturated aldehydes contained in cigarette smoke elicit IL-8 release in pulmonary cells through mitogen-activated protein kinases. *Am J Physiol Lung Cell Mol Physiol*. 2009;296(5):L839-48.
58. Dwivedi AM, Upadhyay S, Johanson G, Ernstgard L, Palmberg L. Inflammatory effects of acrolein, crotonaldehyde and hexanal vapors on human primary bronchial epithelial cells cultured at air-liquid interface. *Toxicol In Vitro*. 2018;46:219-28.
59. Nyunoya T, Mebratu Y, Contreras A, Delgado M, Chand HS, Tesfaigzi Y. Molecular processes that drive cigarette smoke-induced epithelial cell fate of the lung. *Am J Respir Cell Mol Biol*. 2014;50(3):471-82.
60. Mizumura K, Cloonan S, Choi ME, Hashimoto S, Nakahira K, Ryter SW, et al. Autophagy: Friend or Foe in Lung Disease? *Ann Am Thorac Soc*. 2016;13 Suppl 1(Suppl 1):S40-7.
61. Jiang S, Sun J, Mohammadtursun N, Hu Z, Li Q, Zhao Z, et al. Dual role of autophagy/mitophagy in chronic obstructive pulmonary disease. *Pulmonary Pharmacology & Therapeutics*. 2019;56:116-25.
62. Monick MM, Powers LS, Walters K, Lohan N, Zhang M, Gerke A, et al. Identification of an autophagy defect in smokers' alveolar macrophages. *J Immunol*. 2010;185(9):5425-35.
63. Fujii S, Hara H, Araya J, Takasaka N, Kojima J, Ito S, et al. Insufficient autophagy promotes bronchial epithelial cell senescence in chronic obstructive pulmonary disease. *Oncoimmunology*. 2012;1(5):630-41.
64. Barnes PJ, Baker J, Donnelly LE. Autophagy in asthma and chronic obstructive pulmonary disease. *Clin Sci (Lond)*. 2022;136(10):733-46.
65. Wang HT, Lin JH, Yang CH, Haung CH, Weng CW, Maan-Yuh Lin A, et al. Acrolein induces mtDNA damages, mitochondrial fission and mitophagy in human lung cells. *Oncotarget*. 2017;8(41):70406-21.
66. Tulen CBM, Snow SJ, Leermakers PA, Kodavanti UP, van Schooten FJ, Opperhuizen A, et al. Acrolein inhalation acutely affects the regulation of mitochondrial metabolism in rat lung. *Toxicology*. 2022:153129.
67. Liu QP, Zhou DX, Lv MQ, Ge P, Li YX, Wang SJ. Formaldehyde inhalation triggers autophagy in rat lung tissues. *Toxicol Ind Health*. 2018;748233718796347.

68. Vanella L, Li Volti G, Distefano A, Raffaele M, Zingales V, Avola R, et al. A new antioxidant formulation reduces the apoptotic and damaging effect of cigarette smoke extract on human bronchial epithelial cells. *Eur Rev Med Pharmacol Sci*. 2017;21(23):5478-84.
69. Luo C, Li Y, Yang L, Feng Z, Li Y, Long J, et al. A cigarette component acrolein induces accelerated senescence in human diploid fibroblast IMR-90 cells. *Biogerontology*. 2013;14(5):503-11.
70. Aravamudan B, Kiel A, Freeman M, Delmotte P, Thompson M, Vassallo R, et al. Cigarette smoke-induced mitochondrial fragmentation and dysfunction in human airway smooth muscle. *Am J Physiol Lung Cell Mol Physiol*. 2014;306(9):L840-54.
71. Ballweg K, Mutze K, Königshoff M, Eickelberg O, Meiners S. Cigarette smoke extract affects mitochondrial function in alveolar epithelial cells. *Am J Physiol Lung Cell Mol Physiol*. 2014;307(11):L895-907.
72. Farfán Labonne BE, Gutiérrez M, Gómez-Quiroz LE, Königsberg Fainstein M, Bucio L, Souza V, et al. Acetaldehyde-induced mitochondrial dysfunction sensitizes hepatocytes to oxidative damage. *Cell Biol Toxicol*. 2009;25(6):599-609.
73. Agarwal AR, Yin F, Cadenas E. Metabolic shift in lung alveolar cell mitochondria following acrolein exposure. *Am J Physiol Lung Cell Mol Physiol*. 2013;305(10):L764-73.
74. Sun L, Luo C, Long J, Wei D, Liu J. Acrolein is a mitochondrial toxin: effects on respiratory function and enzyme activities in isolated rat liver mitochondria. *Mitochondrion*. 2006;6(3):136-42.
75. Van Buskirk JJ, Frisell WR. Inhibition by formaldehyde of energy transfer and related processes in rat liver mitochondria. II. Effects on energy-linked reactions in intact mitochondria and phosphorylating particles. *Arch Biochem Biophys*. 1969;132(1):130-8.
76. Zerín T, Kim JS, Gil HW, Song HY, Hong SY. Effects of formaldehyde on mitochondrial dysfunction and apoptosis in SK-N-SH neuroblastoma cells. *Cell Biol Toxicol*. 2015;31(6):261-72.
77. Schamberger AC, Staab-Weijnitz CA, Mise-Racek N, Eickelberg O. Cigarette smoke alters primary human bronchial epithelial cell differentiation at the air-liquid interface. *Sci Rep*. 2015;5:8163.
78. Kuehn D, Majeed S, Guedj E, Dulize R, Baumer K, Iskandar A, et al. Impact assessment of repeated exposure of organotypic 3D bronchial and nasal tissue culture models to whole cigarette smoke. *J Vis Exp*. 2015(96).
79. Aufderheide M, Scheffler S, Ito S, Ishikawa S, Emura M. Ciliotoxicity in human primary bronchiolar epithelial cells after repeated exposure at the air-liquid interface with native mainstream smoke of K3R4F cigarettes with and without charcoal filter. *Experimental and Toxicologic Pathology*. 2015;67(7-8):407-11.
80. Tatsuta M, Kan-o K, Ishii Y, Yamamoto N, Ogawa T, Fukuyama S, et al. Effects of cigarette smoke on barrier function and tight junction proteins in the bronchial epithelium: protective role of cathelicidin LL-37. *Respir Res*. 2019;20(1):251.
81. Yu Q, Chen X, Fang X, Chen Q, Hu C. Caveolin-1 aggravates cigarette smoke extract-induced MUC5AC secretion in human airway epithelial cells. *Int J Mol Med*. 2015;35(5):1435-42.
82. Brekman A, Walters MS, Tilley AE, Crystal RG. FOXJ1 prevents cilia growth inhibition by cigarette smoke in human airway epithelium in vitro. *Am J Respir Cell Mol Biol*. 2014;51(5):688-700.
83. Gindele JA, Kiechle T, Benediktus K, Birk G, Brendel M, Heinemann F, et al. Intermittent exposure to whole cigarette smoke alters the differentiation of primary small airway epithelial cells in the air-liquid interface culture. *Scientific Reports*. 2020;10(1):6257.

84. Rigden HM, Alias A, Havelock T, O'Donnell R, Djukanovic R, Davies DE, et al. Squamous Metaplasia Is Increased in the Bronchial Epithelium of Smokers with Chronic Obstructive Pulmonary Disease. *PLoS one*. 2016;11(5):e0156009-e.
85. Crystal RG. Airway basal cells. The “smoking gun” of chronic obstructive pulmonary disease. *American journal of respiratory and critical care medicine*. 2014;190(12):1355-62.
86. Jeffery PK. Comparison of the structural and inflammatory features of COPD and asthma Giles F. Filley Lecture. *Chest*. 2000;117(5):251S-60S.
87. Saetta MT, G.; Baraldo, S.; Zanin, A.; Braccioni, F.; Mapp, C. E.; Maestrelli, P.; Cavallero, G.; Papi, A.; Fabbri, L. M. Goblet cell hyperplasia and epithelial inflammation in peripheral airways of smokers with both symptoms of chronic bronchitis and chronic airflow limitation. *American journal of respiratory and critical care medicine*. 2000;161(3):1016-21.
88. Xiong R, Wu Q, Muskhelishvili L, Davis K, Shemansky JM, Bryant M, et al. Evaluating Mode of Action of Acrolein Toxicity in an In Vitro Human Airway Tissue Model. *Toxicol Sci*. 2018;166(2):451-64.
89. Zhang S, Zhang J, Chen H, Wang A, Liu Y, Hou H, et al. Combined cytotoxicity of co-exposure to aldehyde mixtures on human bronchial epithelial BEAS-2B cells. *Environ Pollut*. 2019;250:650-61.
90. LoPachin RM, Gavin T. Molecular mechanisms of aldehyde toxicity: a chemical perspective. *Chem Res Toxicol*. 2014;27(7):1081-91.
91. Zhang S, Chen H, Wang A, Liu Y, Hou H, Hu Q. Combined effects of co-exposure to formaldehyde and acrolein mixtures on cytotoxicity and genotoxicity in vitro. *Environ Sci Pollut Res Int*. 2018;25(25):25306-14.
92. Zhang S, Zhang J, Cheng W, Chen H, Wang A, Liu Y, et al. Combined cell death of co-exposure to aldehyde mixtures on human bronchial epithelial BEAS-2B cells: Molecular insights into the joint action. *Chemosphere*. 2020;244:125482.
93. Iskandar AR, Xiang Y, Frentzel S, Talikka M, Leroy P, Kuehn D, et al. Impact Assessment of Cigarette Smoke Exposure on Organotypic Bronchial Epithelial Tissue Cultures: A Comparison of Mono-Culture and Coculture Model Containing Fibroblasts. *Toxicol Sci*. 2015;147(1):207-21.
94. van Riet S, van Schadewijk A, de Vos S, Vandeghinste N, Rottier RJ, Stolk J, et al. Modulation of Airway Epithelial Innate Immunity and Wound Repair by M(GM-CSF) and M(M-CSF) Macrophages. *J Innate Immun*. 2020;12(5):410-21.
95. Chen ZH, Lam HC, Jin Y, Kim HP, Cao J, Lee SJ, et al. Autophagy protein microtubule-associated protein 1 light chain-3B (LC3B) activates extrinsic apoptosis during cigarette smoke-induced emphysema. *Proc Natl Acad Sci U S A*. 2010;107(44):18880-5.
96. Liu D, Cheng Y, Tang Z, Mei X, Cao X, Liu J. Toxicity mechanism of acrolein on DNA damage and apoptosis in BEAS-2B cells: Insights from cell biology and molecular docking analyses. *Toxicology*. 2022;466:153083.
97. Peterson LA, Oram MK, Flavin M, Seabloom D, Smith WE, O'Sullivan MG, et al. Coexposure to Inhaled Aldehydes or Carbon Dioxide Enhances the Carcinogenic Properties of the Tobacco-Specific Nitrosamine 4-Methylnitrosamino-1-(3-pyridyl)-1-butanone in the A/J Mouse Lung. *Chem Res Toxicol*. 2021;34(3):723-32.

Supplementary information

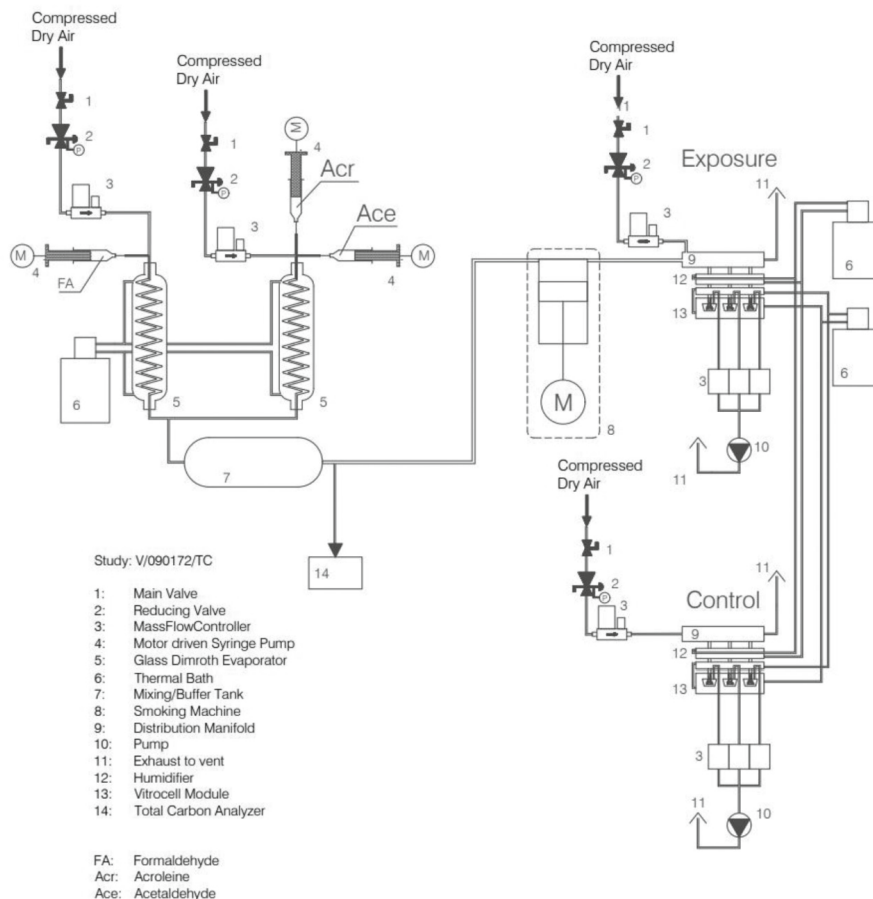


Figure S1. Schematic representation of CS and aldehydes exposure system. Schematic representation of the designed exposure system used to direct expose differentiated PBEC cultures to cigarette smoke (CS) or a comparable dose mixture of aldehydes via the air using two Vitrocell® 12/3 CF stainless steel modules for 12-well sized inserts (Vitrocell, Germany). The mixture of 3 aldehydes was generated by evaporating syringe pump controlled flows of the aldehydes in streams of mass flow controlled compressed dry air using two Dimroth evaporators (one for formaldehyde, the other one for acrolein and acetaldehyde). After evaporation, the generated formaldehyde and acrolein/acetaldehyde streams were mixed in a buffer chamber. A Total Carbon Analyzer (TCA, Rattisch, Germany) was used to monitor the concentrations of aldehydes during every exposure. PBEC were exposed to 8 puffs of CS, gaseous mixture of aldehydes or compressed dry air following the Health Canada Intense smoking regime. The generated streams of CS or aldehydes were distributed (and diluted) to the exposure manifold by a mass flow controlled stream of 500 mL/min compressed dry air. Subsequently, streams of 5 mL/min per insert were extracted from the exposure manifold. These streams were individually humidified by passing them through Nafion humidifiers kept in a water bath at 33.8 °C. After humidification the streams were delivered to the cells. As control, the PBEC cultures were exposed to clean compressed air with a similar flow-rate and humidification in the control module.

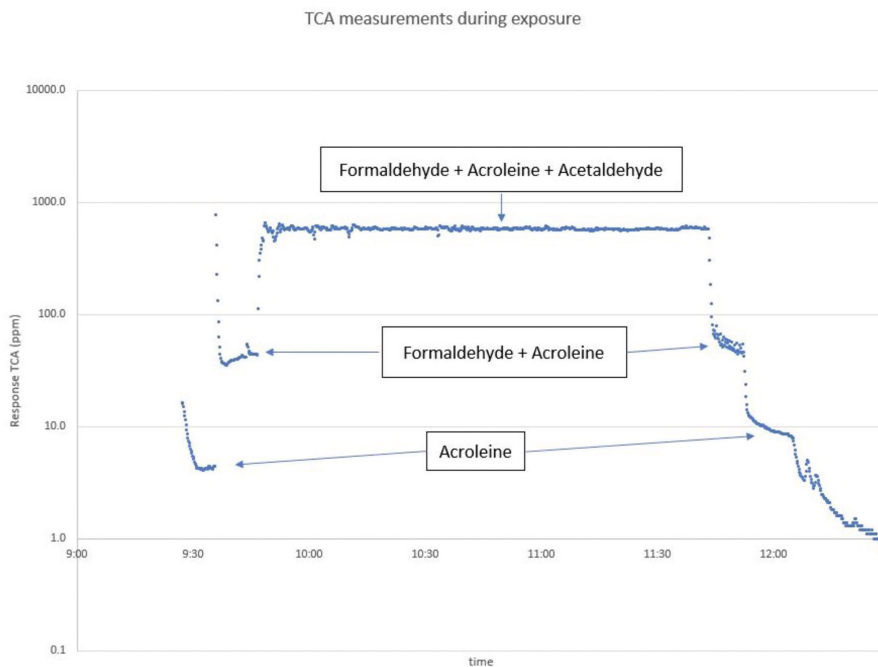


Figure S2. Monitoring of the aldehydes present in the mixture using a total carbon analyzer. A Total Carbon Analyzer (TCA, Ratfisch, Germany) was used to monitor the concentrations of aldehydes during every exposure. The response of the TCA was used as an indicator of the presence of each of the aldehydes in the gaseous mixture (located before the smoking machine). Generation started with formaldehyde (with a slight overshoot in the beginning). After stabilization, the generation of acrolein was started (also with a slight overshoot in the beginning) before initiating the acetaldehyde generation. After the last exposure the generation of acetaldehyde was stopped first, followed by acrolein and, after stabilization, also the generation of formaldehyde was terminated. This example of a sequence of one exposure experiment is showing the attribution of each individual aldehyde to the measured total concentration.

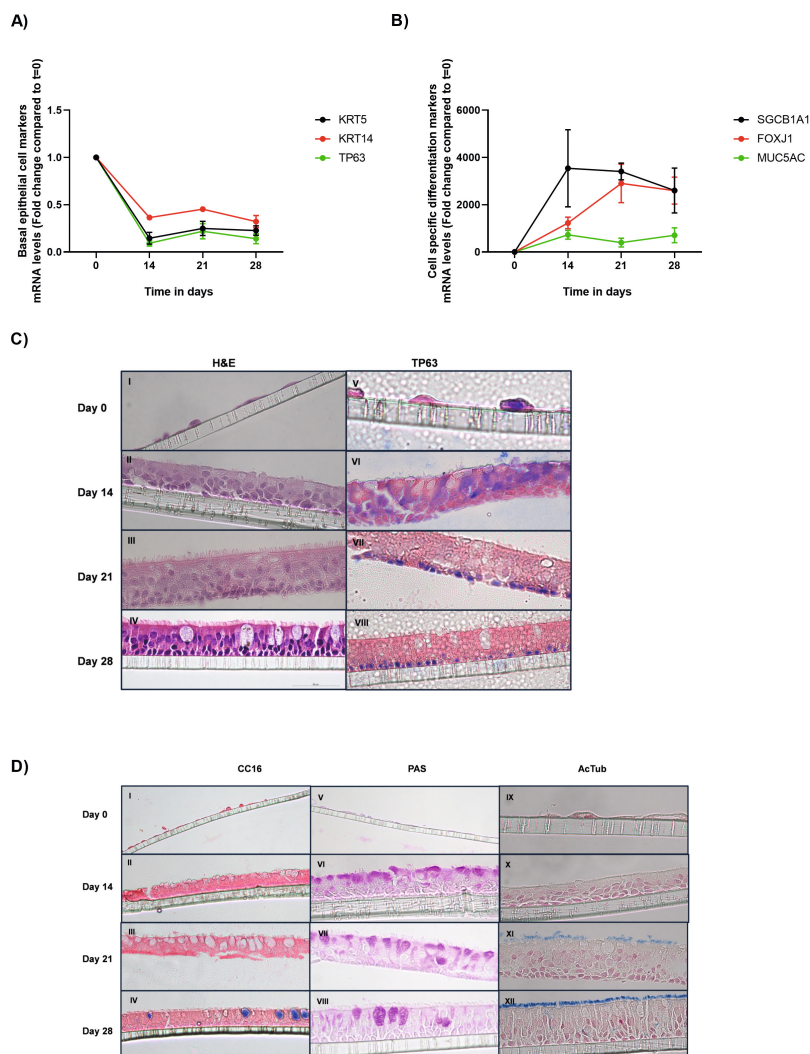


Figure S3. Validation and characterization of differentiation of PBEC. Validation and characterization of differentiation of human primary bronchial epithelial cells (PBEC) monitored at several time-points: day 0 (moment of air-lift) and days 14, 21 and 28 post-airlift. **(A)** mRNA expression of markers associated with basal epithelial cells: Keratin 5 (*KRT5*; black), Keratin 14 (*KRT14*; red), and nuclear Tumor protein 63 (*TP63*; green) are presented. **(B)** Expression of genes representing specific cell types: club cells (*Secretoglobulin Family 1A Member 1*; *SCGB1A1*) (black), ciliated cells (*Forkhead Box J1*; *FOXJ1*) (red) and goblet cells (*Mucin 5AC*, *Oligomeric Mucus/Gel-Forming*; *MUC5AC*) (green) are presented. Data are presented as the mean fold change of the two donors (i.e., the mean of biological triplicates per donor were averaged) per time-point compared to day 0 (moment of air-lift) \pm s.e.m. Further verification of the differentiation status of PBEC at different time points is conducted by **(C)** a hematoxyline-eosine (H&E) staining (I-IV) and TP63 (nuclei) (V-VIII) as well as by **(D)** immunohistochemistry stainings with target-specific antibodies: CC16 (clara cell protein 16) (I-IV), Periodic acid-Schiff (PAS; polysaccharides and mucosubstances) (V-VIII), and Acetylated Tubulin (cilia) (IX-XII). Microscopy images (magnification 200X or 400X) of one representative donor were shown.

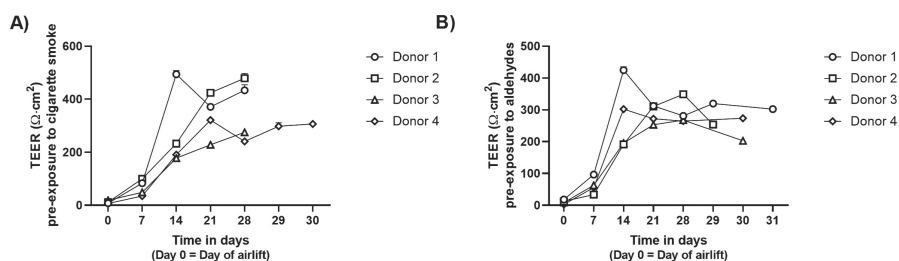


Figure S4. Monolayer integrity of PBEC during differentiation. The monolayer integrity, trans-epithelial electrical resistance (TEER; $\Omega \cdot \text{cm}^2$) was monitored during differentiation of the PBEC of all donors (n=4) in all inserts before exposure to (A) CS and (B) aldehydes. Data are presented as mean TEER per donor \pm s.e.m. The mean of replicates per independent donor (experiment) (n=9-90) are represented by open circles, triangles, squares or diamonds.

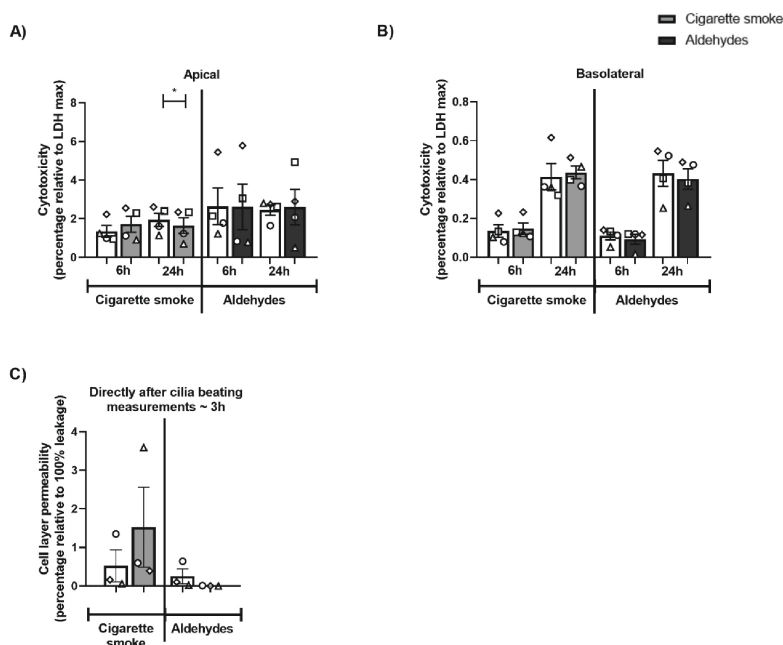


Figure S5. No impact of CS or aldehydes exposure on cytotoxicity and monolayer integrity. Differentiated human primary bronchial epithelial cells (PBEC) from non-COPD subjects were exposed in a continuous flow system using a puff-like exposure protocol to smoke of one Marlboro Red cigarette (CS) or a mixture of aldehydes: acetaldehyde, acrolein, and formaldehyde (at relevant concentrations of 1 cigarette) or air (control) (n=3-4 donors). (A) After recovery for 6 h or 24 h, cytotoxicity was analysed by the LDH assay (percentage relative to LDH max). (B) Moreover, following exposure and cilia beating analysis (± 3 h of recovery), cell layer permeability was analysed (percentage relative to 100% leakage control). Data are presented as mean fold change compared to relative positive control \pm s.e.m. The mean of biological triplicates per independent donor are represented by open circles, triangles, squares or diamonds. Statistical differences between CS *versus* air or a mixture of aldehydes *versus* air were tested using a two-tailed paired parametric t-test. Statistical significance is indicated as *p<0.05 *versus* air (control).

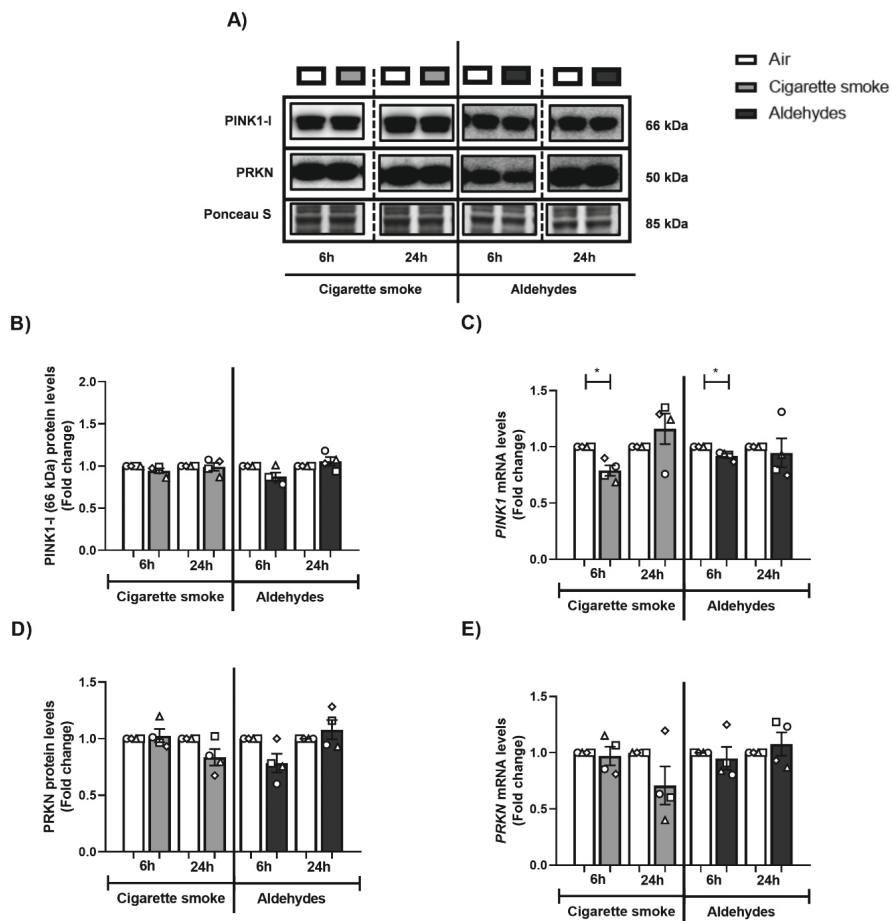


Figure S6. Exposure to CS or aldehydes resulted in decreased gene expression of *PINK1*. Differentiated human primary bronchial epithelial cells (PBEC) from non-COPD subjects were exposed in a continuous flow system using a puff-like exposure protocol to smoke of one Marlboro Red cigarette (CS) or a mixture of aldehydes: acetaldehyde, acrolein, and formaldehyde (at relevant concentrations of 1 cigarette) or air (control) (n=4 donors). Following recovery for 6 h or 24 h, whole cell lysates were harvested for analysis of the abundance of key regulators involved in ubiquitin-mediated mitophagy, respectively protein (**A, B, D**) *PINK1-I* (66 kDa) and *PRKN* as well as transcript (**C, E**) *PINK1* and *PRKN*. Representative western blot images are shown of one replicate of one donor/experiment reflective of the changes in all donors as quantified in the corresponding graph. Data are presented as mean fold change compared to air control \pm s.e.m. The mean of biological triplicates per independent donor are represented by open circles, triangles, squares or diamonds. Statistical differences between CS *versus* air or a mixture of aldehydes *versus* air were tested using a two-tailed paired parametric t-test. Statistical significance is indicated as * $p < 0.05$ *versus* air (control).

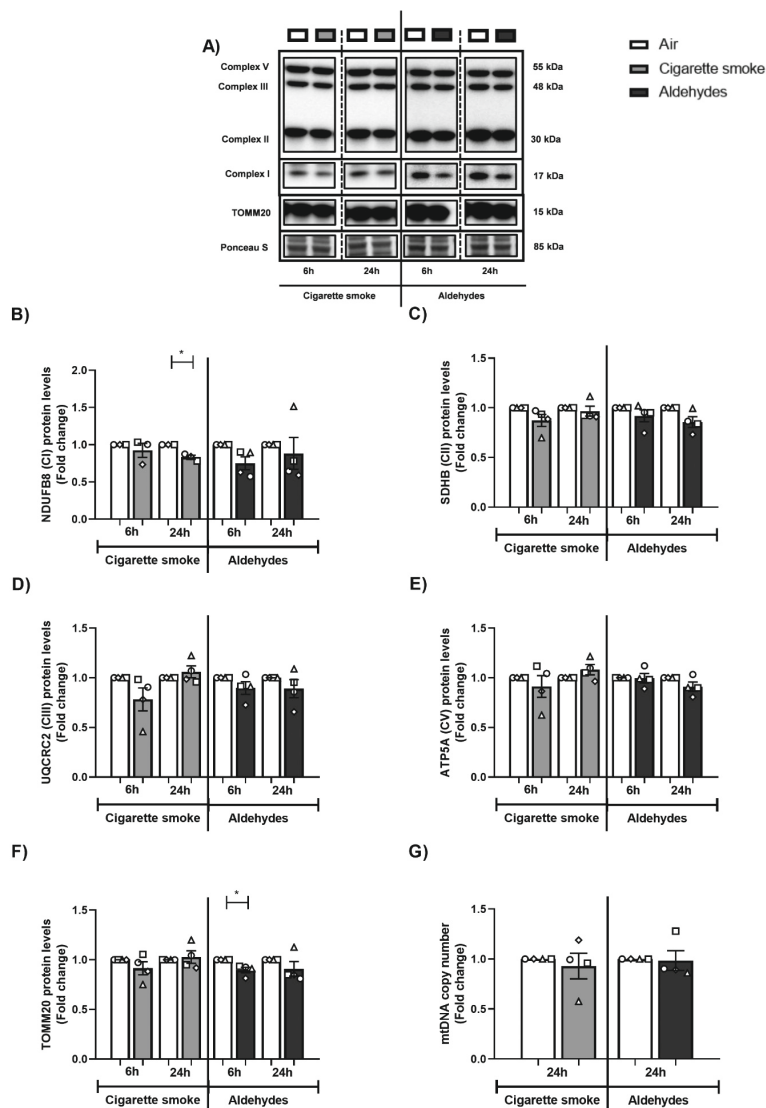


Figure S7. Minor alterations in protein levels of subunits of oxidative phosphorylation complexes following CS or aldehyde exposure. Differentiated human primary bronchial epithelial cells (PBEC) from non-COPD subjects were exposed in a continuous flow system using a puff-like exposure protocol to smoke of one Marlboro Red cigarette (CS) or a mixture of aldehydes: acetaldehyde, acrolein, and formaldehyde (at relevant concentrations of 1 cigarette) or air (control) (n=3-4 donors). After recovery for 6 h or 24 h, whole cell lysates were harvested to analyze (A) protein levels of subunits of (B) NDUFB8 (complex I), (C) SDHB (complex II), (D) UQCRC2 (complex III), (E) ATP5A (complex V), (F) TOMM20 and (G) mtDNA copy number (*MT-CO2/ACTB*). Representative blot images are shown of one replicate of one donor/experiment reflective of the changes in all donors as quantified in the corresponding graph. Data are presented as mean fold change compared to air control \pm s.e.m. The mean of biological triplicates per independent donor are represented by open circles, triangles, squares or diamonds. Statistical differences between CS versus air or a mixture of aldehydes versus air were tested using a two-tailed paired parametric t-test. Statistical significance is indicated as *p<0.05 versus air (control).

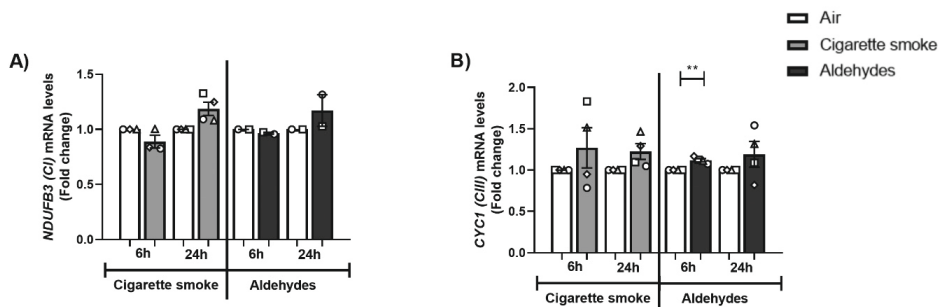


Figure S8. Minimal changes in mRNA expression of subunits of oxidative phosphorylation complexes upon smoking-associated aldehydes exposure. Differentiated human primary bronchial epithelial cells (PBE) from non-COPD subjects were exposed in a continuous flow system using a puff-like exposure protocol to smoke of one Marlboro Red cigarette (CS) or a mixture of aldehydes: acetaldehyde, acrolein, and formaldehyde (at relevant concentrations of 1 cigarette) or air (control) (n=2-4 donors). After recovery for 6 h or 24 h, whole cell lysates were harvested to analyze transcript levels of (A) *NDUFB3 (CI)*, and (B) *CYC1 (CIII)*. Data are presented as mean fold change compared to air control \pm s.e.m. The mean of biological triplicates per independent donor are represented by open circles, triangles, squares or diamonds. Statistical differences between CS versus air or a mixture of aldehydes versus air were tested using a two-tailed paired parametric t-test. Statistical significance is indicated as **p<0.01 versus air (control).

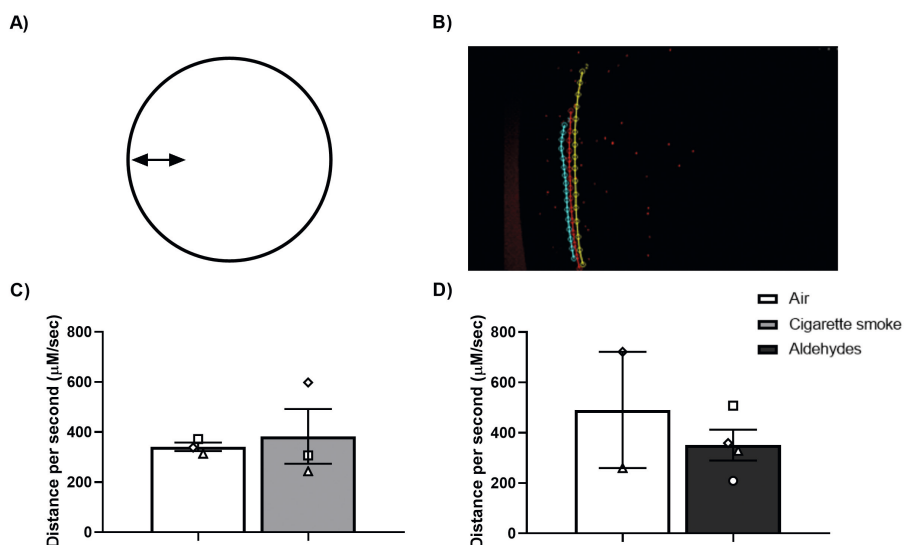


Figure S9. Bead motion induced by ciliary beating in response to CS or aldehydes exposure. Differentiated human primary bronchial epithelial cells (PBEC) from non-COPD subjects were exposed in a continuous flow system using a puff-like exposure protocol to smoke of one Marlboro Red cigarette (CS) or a mixture of aldehydes: acetaldehyde, acrolein, and formaldehyde (at relevant concentrations of 1 cigarette) or air (control) ($n=2-4$ donors). Immediately after exposure, $2.1 \mu\text{M}$ beads were added to the apical side of the exposed PBEC in the middle of the transwell. The exposed PBEC were placed on the microscope (Leica Dmi8), and maintained at 37°C and 5% CO_2 in humidified air. Videos of the bead motion were acquired 30 min until 2.5 h post-exposure using the $4\times$ objective and LEICA DFC7000 GT camera along with the LAS X 3.4.2 software, respectively in a frame interval of 0.33 s for 20-60 s. **(A)** Beads which were located as close as possible to the edge of the transwell, outside the mucus droplet and following a smooth path were selected for tracking. Automatic tracking of the beads was conducted in ImageJ using the MTrackJ plugin (scale: $0.2065 \text{ pixels}/\mu\text{M}$), **(B)** see an example of tracking of 3 beads of donor 3: CS exposure. Per exposure condition (CS, aldehydes, air), if available, 1 to 3 videos per transwell per donor were selected. Within one video (i.e., one transwell), 5-6 beads were tracked for 2.97-5.00 s (i.e., 9-16 time frames). Mean distance per s was calculated per exposure condition per donor \pm s.e.m., respectively including tracked beads in 1-3 videos resulting in **(C)** 5-12 automatic tracked beads per donor exposed to air or CS or **(D)** 6-23 tracked beads per donor exposed to air or aldehydes. In summary, this results in a total number of tracked beads across all donors of air: 29 versus CS: 24 and air: 18 versus aldehydes: 41. Means per independent donor are represented by open circles, triangles, squares or diamonds. Statistical differences between CS *versus* air or a mixture of aldehydes *versus* air were tested using a two-tailed paired parametric t-test.

Table S1. Dosimetry. Concentration analysis of acetaldehyde, acrolein and formaldehyde in the mainstream smoke of one Marlboro Red cigarette (CS) to match the target concentration of the aldehydes present in the gaseous mixture. Marlboro Red cigarettes (taped) were smoked for 8 puffs following the Health Canada Intense Bell regime (2 puffs/min, 55 ml puff volume, 2 s puff duration, 4 s puff exhaust time) using a smoking machine (VC1, Vitrocell, Germany). After priming the system by smoking 3 cigarettes in a row, the mainstream smoke from one cigarette was trapped using a Cambridge filter and Carboxen adsorbent cartridge (extern filter) directly after the smoking machine. Besides the primary trapping cartridge, an additional cartridge was included to measure possible flow through. Measurements were conducted under the following circumstances: 500 mL/min dilution flow; 1 L/min sample flow – continuous, exhaust flow smoking machine complemented with clean compressed air. Data are presented as mean concentration of individual aldehyde (mg/m³) as measured in the trapped mainstream smoke of 3 individual cigarettes including flow through \pm s.d.

Source	Exposure component	Acetaldehyde (mg/m ³)	Acrolein (mg/m ³)	Formaldehyde (mg/m ³)
Literature (1)	Marlboro Red cigarette	2121.4	227.5	105.2
Study	Marlboro Red cigarette	2127.1 \pm 264.5	137.7 \pm 38.3	103.4 \pm 15.3

Table S2. Human primers sequences used for real-time quantitative PCR analysis.

Gene	Sense primer (5'-3')	Antisense primer (3'-5')
Reference genes		
<i>ACTB</i>	AAGCCACCCCACTTCTCTCTAA	AATGCTATCACCTCCCCTGTGT
<i>B2M</i>	CTGTGCTCGCGTACTCTCTCTT	TGAGTAAACCTGAATCTTTGGAGTACGC
<i>PPIA</i>	CATCTGCACTGCCAAGACTGA	TTCATGCCTTCTTTCACCTTTGC
<i>RPL13A</i>	CCTGGAGGAGAAGAGGAAAGAGA	TTGAGGACCTCTGTGTATTTGTCAA
Target genes		
<i>BNIP3</i>	AGCGCCCGGATGCA	CCCGTTCCCATTATTGCTGAA
<i>BNIP3L</i>	CTGCGAGGAAAATGAGCAGTCTCT	GCCCCCAATTTTCCCATTG
<i>CCL2</i>	AGCAGCAAGTGTCCCAAAGAAGCT	CCTTGGCCACAATGGTCTTGAA
<i>MT-CO2</i>	ACCTGCGACTCCTTGACGTT	GGGGGCTTCAATCGGGAGTA
<i>CYC1 (CIII)</i>	GAGCACGACCATCGAAAACG	CGATATGCCAGCTTCCGACT
<i>DNM1L</i>	CGACTCATTAAATCATATTTTCTCATTGTCAG	TGCATTACTGCCTTTGGCACACT
<i>FIS1</i>	CCTGGTGCAGGAGCAAGTACAA	TCCTTGCTCCCTTTGGGCAG
<i>FOXJ1</i>	TCGTATGCCACGCTCATCTG	CTTGTAGATGGCCGACAGGG
<i>FUNDC1</i>	GAAACGAGCGAACAAGAGCAG	GCAAAAAGCCTCCCACAAAT
<i>GABARAPL1</i>	ATCGGAAAAAGGAAGGAGAAAAAGATC	CAGGCACCTGGCTTTTGG
<i>HK2</i>	GTAAATACAGTGGATCTCAATCTTCGGG	CAAGGATTTGAGATGATTTCGTATTCA
<i>IL-8</i>	TTAGAACTATTAAACAGCCAAAACCTCCACA	CAAGTTTCAACCAGCAAGAAATTACTAATATTG
<i>KRT5</i>	GGAGTTGGACCAGTCAACATC	TGGAGTAGTAGCTTCCACTGC
<i>KRT14</i>	TGGATCGCAGTCATCCAGAG	ATCGTGACATCCATGACCT
<i>MAP1LC3A</i>	CCTGGACAAGACCAAGTTTGTG	GTCTTTCTCTGCTCGTAGATG
<i>MAP1LC3B</i>	ACCATGCCGTCGGAGAAGAC	TCTCGAATAAGTCGGACATCTTCTACTCT
<i>MFN1</i>	CTGAGGATGATTGTTAGCTCCACG	CAGGCGAGCAAAAGTGGTAGC
<i>MFN2</i>	TGGACCACCAAGGCCAAGGA	TCTCGCTGGCATGCTCCAC
<i>MUC5AC</i>	AGCAGGGTCCTCATGAAGGTGGAT	AATGAGGACCCAGACTGGCTGAA
<i>NDUFB3 (CI)</i>	TCAGATTGCTGTCTCAGACATGG	TGGTGTCCTTCTATCTTCCA
<i>NRF2</i>	CTCACCTGGGAACAGAACAGGAA	ACCCAAGAAATGCAGTCTCGAGC
<i>OPA1</i>	TACCAAAGGCATTTTGTAGATTCTGAGTT	GCATGCGCTGTATACGCCAA
<i>PDK4</i>	CCTGTGAGACTCGCCAACA	TCCACCAAATCCATCAGGCTC
<i>PINK1</i>	GAAAGCCGAGCTACCAAGA	AGCACATTTGCGGCTACTCG
<i>PPARA</i>	CAGAACAAGGAGGCGGAGGTC	AGGTCCAAGTTTGCGAAGC
<i>PPARGC1B</i>	GGCGCTTTGAAGTGTTTGGTGA	TGATGAAGCCGTACTTCTCGCCT
<i>PPRC1</i>	GCCTTTTGATCTCTGCTTTGGG	AAGTCTTCCCGGTTGGAGTCAAG
<i>PRKN</i>	GGTTTGCTTCTGCGGGAATG	CTTTCATCGACTCTGTAGGCCTG
<i>SCGB1A1</i>	TTCAGCGTGTATCGAAACCC	ACAGTGAGCTTTGGGCTATTTTT
<i>SOD1</i>	GGTCCTCACTTAAATCCTCTAT	CATCTTTGTGTCAGCAGTCACATT
<i>SOD2</i>	TGACAAAACCTCAGCCCTAACG	TGATGGCTTCCAGCAACTCCC
<i>SQSTM1</i>	GGTGCACCCCAATGTGATCT	CGCAGACGTACACAAGTCG
<i>TFAM</i>	GAAAGATTCCAAGAAGCTAAGGGTGATT	TCCAGTTTTCTTTACAGCTTTCAGCTTTT
<i>TP63</i>	CCCGTTTCGTGAGAACACAC	CATAAGTCTCACGGCCCTC

Abbreviations: *ACTB*: Actin B, *B2M*: Beta-2 Microglobulin, *PPIA*: Peptidylprolyl Isomerase A, *RPL13A*: Ribosomal Protein L13A, *BNIP3*: BCL2 Interacting Protein 3, *BNIP3L*: BCL2 Interacting Protein 3-Like, *CCL2*: C-C Motif Chemokine Ligand 2, *MT-CO2*: Mitochondrially Encoded Cytochrome C Oxidase II, *CYC1*: Cytochrome C1, *DNM1L*: Dynamin 1-Like, *FIS1*: Fission, Mitochondrial 1, *FOXJ1*: Forkhead Box J1, *FUNDC1*: FUN14 Domain Containing 1, *GABARAPL1*: GABA Type A Receptor Associated Protein Like 1, *HK2*: Hexokinase 2, *IL-8*: Interleukin 8, *KRT5*: Keratin 5, *KRT14*: Keratin 14, *MAP1LC3A*: Microtubule-Associated Protein 1 Light Chain 3 Alpha, *MAP1LC3B*: Microtubule-Associated Protein 1 Light Chain 3 Beta, *MFN1*: Mitofusin 1, *MFN2*: Mitofusin 2, *MUC5AC*: Mucin 5AC, Oligomeric Mucus/Gel-Forming, *NDUFB3*: NADH:Ubiquinone Oxidoreductase Subunit B3, *NRF2*: Nuclear Respiratory Factor 2, *OPA1*: OPA1, Mitochondrial Dynamin Like GTPase, *PK4*: Pyruvate Dehydrogenase Kinase 4, *PINK1*: PTEN Induced Kinase 1, *PPARA*: Peroxisome Proliferator Activated Receptor Alpha, *PPARGC1B*: Peroxisome Proliferator-Activated Receptor Gamma, Coactivator 1 Beta, *PPRC1*: Peroxisome Proliferator-Activated Receptor Gamma, Coactivator-Related 1, *PRKN*: Parkin RBR E3 Ubiquitin Protein Ligase, *SOD1*: Superoxide Dismutase 1, *SOD2*: Superoxide Dismutase 2, *SCGB1A1*: Secretoglobulin Family 1A Member 1, *SQSTM1*: Sequestosome 1, (transcript variant 1/4), *TFAM*: Transcription Factor A, Mitochondrial, *TP63*: Tumor Protein P63

Table S3. Target-specific antibodies used for immunohistochemistry staining.

Target	Antibody	Company	Product number	Dilution factor
Acetylated Tubulin	Mouse anti-human Acetylated a tubulin	Sigma	Cat# T7451	1:20.000
Clara cell secretory protein-16	Mouse anti-human CC16, clone AY1E6kn	Sanbio	Cat# HM2178	1:200
P63	Rabbit monoclonal P63	Abcam	Cat# ab124762	1:200

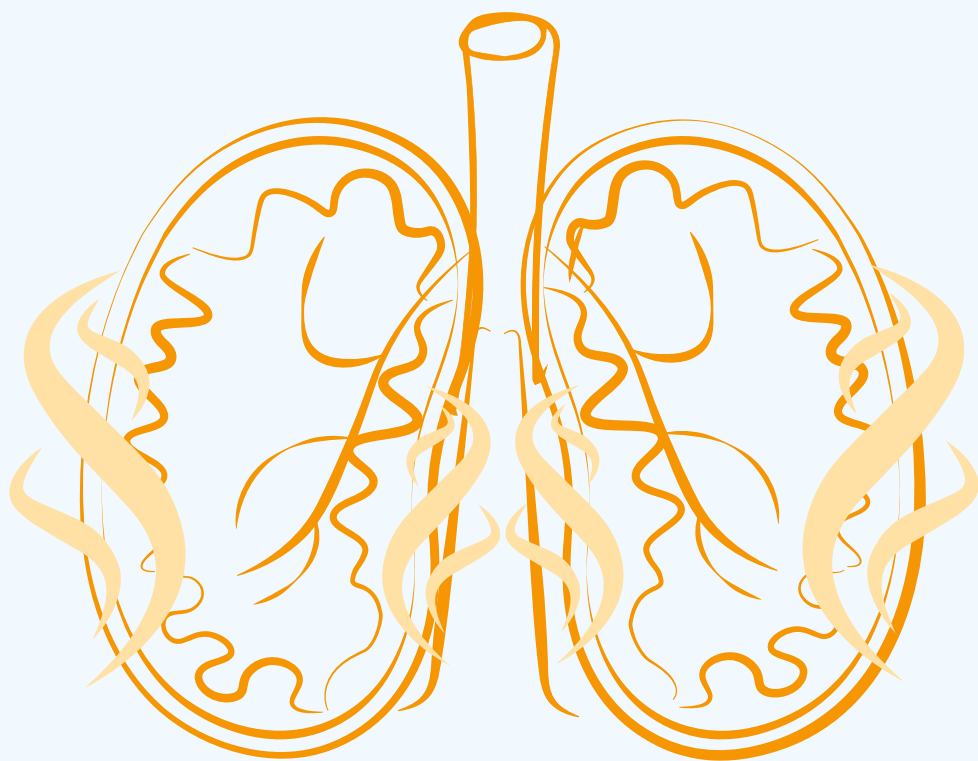
Table S4. Antibodies used for western blotting.

Target	RRID	Company	Product number	Dilution factor
Primary antibodies				
BNIP3	AB_2259284	Cell Signaling Technology	Cat# 3769S	1:1000
BNIP3L	AB_2688036	Cell Signaling Technology	Cat# 12396	1:1000
DNM1L	AB_10950498	Cell Signaling Technology	Cat# 8570	1:1000
ESRRA	AB_1523580	Abcam	Cat# ab76228	1:1000
FUNDC1	AB_10609242	Santa Cruz Biotechnology	Cat# sc-133597	1:500
GABARAPL1	AB_2294415	Proteintech Group	Cat# 11010-1-AP	1:1000
HK2	AB_2232946	Cell Signaling Technology	Cat# 2867	1:1000
MAP1LC3B	AB_915950	Cell Signaling Technology	Cat# 2775	1:1000
NRF1	AB_2154534	Abcam	Cat# ab55744	1:1000
OXPHOS	AB_2629281	MitoScience LLC	Cat# MS604	1:1000
PINK1	AB_10127658	Novus Biologicals	Cat# BC100-494	1:2000
PPARGC1A	AB_10697773	Millipore	Cat# 516557	1:1000
PRKN	AB_2159920	Cell Signaling Technology	Cat# 4211	1:1000
SQSTM1	AB_10624872	Cell Signaling Technology	Cat# 5114	1:1000
TOMM20	AB_2716623	Abcam	Cat# Ab186734	1:1000
Secondary antibodies				
Goat Anti-Mouse IgG Antibody	AB_2827937	Vector Laboratories	Cat#BA-9200	1:10000
Goat Anti-Rabbit IgG Antibody	AB_2313606	Vector Laboratories	Cat#BA-1000	1:10000

Abbreviations: BNIP3: BCL2 Interacting Protein 3, BNIP3L: BCL2 Interacting Protein 3-Like, DNML: Dynamin 1-Like, ESRRA: Estrogen Related Receptor, Alpha, FUNDC1: FUN14 Domain Containing 1, GABARAPL1: GABA Type A Receptor Associated Protein Like 1, HK2: Hexokinase 2, MAP1LC3B: Microtubule-Associated Protein 1 Light Chain 3 Beta, NRF1: Nuclear Respiratory Factor 1, OXPHOS: oxidative phosphorylation antibody cocktail (containing NDUF8: NADH:Ubiquinone Oxidoreductase Subunit B8 (CI), SDHB: Succinate Dehydrogenase Complex Iron Sulfur Subunit B (CII), UQCRC2: Ubiquinol-Cytochrome C Reductase Core Protein 2 (CIII), ATP5F1A: ATP Synthase F1 Subunit Alpha (CV)), PINK1: PTEN Induced Kinase 1, PPARGC1A: Peroxisome Proliferator-Activated Receptor Gamma, Coactivator 1 Alpha, PRKN: Parkin RBR E3 Ubiquitin Protein Ligase, SQSTM1: Sequestosome 1, TOMM20: Translocase Of Outer Mitochondrial Membrane 20

References

1. Pauwels C, Klerx WNM, Pennings JLA, Boots AW, van Schooten FJ, Opperhuizen A, et al. Cigarette Filter Ventilation and Smoking Protocol Influence Aldehyde Smoke Yields. *Chem Res Toxicol*. 2018;31(6):462-71.



Chapter 7

Summary and general discussion

Summary and discussion of the main findings

The overall aim of this thesis was to elucidate the mechanistic involvement of smoking-associated aldehydes on the molecular regulation of mitochondrial function in epithelial cells of the airways and lungs, in the context of chronic obstructive pulmonary disease (COPD) pathogenesis. We hypothesized that exposure to aldehydes impairs the molecular pathways regulating mitochondrial content, mitochondrial function and metabolism in epithelial cells of the lungs and airways. A variety of experimental *in vivo* and *in vitro* airway models were used to investigate the research question. These included peripheral lung tissue and primary bronchial epithelial cells (PBEC) from COPD patients at different stages of the disease (**Chapter 2**), PBEC from non-COPD patients exposed to several types/regimes of cigarette smoke (CS) (**Chapter 3**) or a mixture of aldehydes (**Chapter 6**), and two *in vivo* rat models of (inhalatory) acrolein exposure (**Chapters 4 and 5**).

Chapter 2 provided new insights in the regulation of molecular mechanisms controlling mitochondrial turnover in COPD patients. Transcriptional expression of molecules controlling mitochondrial biogenesis was downregulated, whereas *TFAM* (mitochondrial biogenesis) and *BNIP3L* (mitophagy) were upregulated in peripheral lung tissue from very severe COPD patients. These alterations were, in general, not recapitulated in PBEC. The analysis of a comprehensive panel of molecules involved in the molecular regulation of mitochondrial content and function using precious and rare lung tissue as well as PBEC from COPD patients is new in the field and therefore provided valuable and novel data regarding the disrupted transcriptional regulation of constituents controlling mitochondrial biogenesis and mitophagy in COPD. Nevertheless, our research did not investigate if the observed changes were caused by the disease itself (e.g., inflammation and oxidative stress) or are due to exposure to CS. However, we could speculate that inflammation can induce mitochondrial dysfunction as indicated in literature and the other way around that mitochondrial dysfunction can trigger inflammation thereby predisposing to COPD (1-4). Moreover, previous studies have shown that exposure to CS or CS extract resulted in dysregulated mitochondrial morphology and function in various experimental airway models *in vitro* (5-22) and *in vivo* (9, 14, 18, 23-27) as well as aberrant mitochondrial morphology and function has been observed in COPD patients (5, 6, 9, 14, 16, 28, 29), suggesting that the long smoking history of these patients may play an essential role in the observed changes.

Also, discrepancies observed in the findings in peripheral lung tissue *versus* PBEC in **Chapter 2** may suggest a role for interactions between different cell types comprising the heterogeneous microenvironment *in vivo*. Whereas peripheral lung tissue is reflective of this heterogeneous microenvironment consisting of various cell populations (30, 31), the undifferentiated PBEC are representative of a basal cell layer and differentiated PBEC of a pseudostratified epithelium outside the normal cellular microenvironment.

Therefore, these PBEC models are limited to specific cell types, while the involvement of other distinct cell types in the lung may elicit different responses and/or interactions. For example, the interplay of epithelial cells with immune cells might be involved in the (interaction) response observed in peripheral lung tissue. Nevertheless, it was previously reported that air-liquid interface cultures of PBEC from COPD patients displayed a deformed epithelium similar to the lungs of these patients (e.g., reduced antibacterial activity or limited regeneration capacity) (32, 33), suggesting that (epigenetic) alterations of epithelial cells as a result of the lung microenvironment in these patients are (at least partially) displayed in the culture phenotype (34). In line with this theory, we observed changes in transcript levels of genes indicative of impaired ciliogenesis and increased goblet cell formation in differentiated PBEC from COPD patients, which was confirmed in airway epithelium of COPD patients (smokers) and *in vitro* small airway epithelial cells exposed to whole CS in literature (35-39). However, these (epigenetic) changes in epithelial cell populations seems not responsible for the regulation of mitochondrial metabolism and turnover processes.

Although, in **Chapter 2**, we only observed pronounced differences in the regulation of mitochondrial quality control processes in peripheral lung tissue, not in PBEC, from COPD patients, we continued with the PBEC model in **Chapters 3 and 6**. This model was chosen as differentiated PBEC cultures are representative for the human bronchial epithelium and relevant for the purpose of inhalation toxicology exposure studies.

CS exposure is a major risk factor for the development of COPD (40), and it has been demonstrated that exposure to CS or CS extract resulted in dysregulated mitochondrial function in various *in vitro* (5-22) and *in vivo* (9, 14, 18, 23-27) airway models as indicated above. However, the impact of smoke inhalation on the molecular regulation of mitochondrial metabolism, content and quality control is incompletely understood. Therefore, we focused on the assessment of a comprehensive panel of key regulatory molecules involved in mitochondrial metabolism in several *in vitro* models in **Chapter 3**.

As nowadays a lot of attention is being paid to the development of advanced *in vitro* models to support the transition from *in vivo* to *in vitro* (also for the purpose of studies in the field of inhalation toxicology), we investigated the applicability and relevance of various primary cell *in vitro* models in the context of our research question in **Chapter 3**. In general, three types of *in vitro* models can be identified: cell cultures (cell lines or primary culture, 2D *versus* 3D cultures), lung-on-a-chip- models and, *ex vivo* human precision cut lung slices. As discussed by Hiemstra *et al.*, it is challenging to develop a cell culture *in vitro* model for inhalation toxicology testing mimicking the human situation, as this means that appropriate models should display mucociliary differentiation, barrier formation and metabolic activity (34). Although immortalized or tumour cell lines are widely used in CS research due to their extended life-span and easy-to-handle and inexpensive nature, they are mostly not capable to show the

three characteristics which are essential for an appropriate cellular model as explained above. Therefore, we used PBEC in our studies, which are capable to display these features as well as donor-specific characteristics. Drawbacks of this PBEC model are the limited access to PBEC as it requires patient material, inter-donor variability which can be a pro for generalization but also a con for reproducibility purposes, short lifespan, and labour-intensive and costly culturing procedure (34). Besides the culture system, also the exposure system is of importance in the development of an appropriate *in vitro* method to study the inhalation toxicity of chemicals. The widely recognized method of adding liquid chemicals to the culture medium of 2D cultures or at the apical or basolateral side of 3D air-liquid interface cultures is not representative for the gaseous/aerosol exposure of chemicals in the human situation. Therefore, lately, more sophisticated systems have been developed in-house or are commercially available to expose 3D air-liquid interface PBEC cultures to particles, aerosols or gaseous mixtures via a cloud or air-distribution system (34). These exposure models more realistic and more accurately reflect the exposure to airborne compounds.

Thus, in **Chapter 3**, we compared different PBEC models and types/regimes of CS exposure. The four *in vitro* culture models that we used included human PBEC from non-COPD donors. These different cultures were reflecting various cell types of the bronchiolar epithelium, respectively cell models representing 1) an intact pseudostratified epithelium (differentiated PBEC), 2) damaged/open epithelial cell layer (undifferentiated PBEC), and 3) repair of the epithelial layer (exposure followed by cessation of a differentiating PBEC culture). Moreover, these models were exposed to different CS exposure types and regimes (whole CS/CS extract, acute/repeated). We observed elevated expression of molecules controlling autophagy and mitophagy in response to CS independently of the model used. The impact of smoke exposure on the regulation of mitochondrial metabolic processes and biogenesis was different in the various models. These changes were partially sustained in the model of chronic exposure during differentiation and subsequent cessation. These findings highlighted the importance of tailoring the experimental model to the research question in the context of inhalation (toxicology) studies by taking into account both the cellular model and exposure type/regime. Interestingly, a recent study by Mastalerz *et al.* also validated various *in vitro* PBEC models, comparing differentiation status (undifferentiated/differentiated) and dose, route (apical/basolateral), type of exposure (CS extract/whole CS), and time (acute/chronic) of exposure. They identified effective exposure of PBEC as expression of 10 smoke exposure-regulated genes instead of commonly used indices, such as cell viability. Although their totally different nature, three models seemed to be as effective in upregulation of 6-7 of these genes. Differentiated PBEC cultures were observed to be most susceptible to whole CS exposure, while CS extract exposure of undifferentiated PBEC was reflective for investigating bronchial epithelial injury. Chronic exposure of PBEC to CS extract was relevant in case of chronic exposure assessment (41). Based on our findings and literature, we can conclude that

the most suitable, susceptible and representative model for the human situation are differentiated PBEC cultured at air-liquid interface exposed via air which should be used for future research into the toxicological impact of whole CS (including the volatile compounds such as aldehydes).

Whereas **Chapter 3** revealed insights into the impact of CS on the molecular regulation of mitochondria using advanced *in vitro* models, these cellular models used still have their limitations. For example, these cellular exposure *in vitro* models are not reflective of the systemic interaction in the human body for which more advanced models should be considered, e.g., organ-on-a-chip, microfluidics, organoids, induced pluripotent stems cells (34) and co-culture models consisting of diverse cell types including for example epithelial cells and macrophages or fibroblasts (42, 43). Moreover, single-cell sequencing could identify cell-population-specific mechanisms and interaction in the context of COPD, as recently shown (44). These promising methods might be even more suitable to evaluate cell-specific mechanisms associated with the regulation of mitochondrial turnover and metabolism in response to smoke implicated in COPD pathogenesis in the future.

Although we found similarities between CS-induced dysregulation of mitochondrial turnover processes in PBEC and observations in peripheral lung tissue homogenates from very severe COPD patients (**Chapter 2 and 3**), we did not investigate the causality between CS-induced mitochondrial dysfunction and COPD development. Nevertheless, a causal link has previously been proved by Cloonan *et al.* showing that prevention of CS-induced mitochondrial dysfunction in a mouse model of COPD significantly ameliorated CS-induced development of emphysema and bronchitis (23). Based on these findings, it might be of value to investigate the impact of smoke exposure in PBEC from COPD and non-COPD patients. This is important, as in the current studies we have only investigated the molecular regulation of components controlling mitochondrial metabolism and content in unexposed PBEC from non-COPD *versus* COPD patients (**Chapter 2**), as well as in CS-exposed PBEC from non-COPD patients (**Chapter 3**).

In conclusion, whether or not the observed transcript and/or protein changes in **Chapters 2 and 3** significantly contribute to the development of COPD, are responsible for alterations in mitochondrial function or may represent compensatory mechanisms has to be assessed in future research. This knowledge could contribute to the development of novel and innovative mitochondrial-targeted therapies in the context of COPD. Emerging evidence already describes the potential of mitochondrial-targeted therapy aimed at improving mitochondrial function or rescue/reverse mitochondrial dysfunction to protect against the development of (CS-induced) COPD and/or optimizing lung function. As summarized in previous reviews, these therapeutical applications are targeting mitochondrial transfer (stem cells), inhibition of mitophagy (Quercetogetin), mitochondrial dynamics (Drp1 inhibitors: Mdivi-1, P110), mitochondrial reactive

oxygen species scavengers/antioxidants (e.g., MitoTEMPO, MitoQ, Tiron, SS-31, N-acetylcysteine), iron chelators (Deferiprone), stimulation of mitochondrial biogenesis (AMPK activators, SIRT1 overexpression/activation) and mitochondrial therapy (mitochondrial transplantation/mitoception) (45-47). Other mitochondrial-targeted therapies are focusing on ameliorating mitochondrial respiration by targeting reprogramming of mitochondria influenced by lifestyle, modification of let-7/lin28axis, and miRNAs: hypoxamirs or mitomirs. Moreover, a new direction in this field focuses on the crosstalk between microbes and mitochondria, e.g., microbial metabolites which are sources for mitochondrial oxidation, altered fatty acids affecting mitochondrial function and stimulators of mitochondrial biogenesis, for example pyrroloquinonline quinone (48).

Besides *in vitro* models, we also deployed *in vivo* models to investigate our research question. The use of animals in inhalation toxicology should be carefully considered. Animal research is still essential for investigation of causes, diagnoses and treatment of diseases and could contribute to unravel our research question. However, it is widely recognized that animals are not small humans and therefore it might be hard to translate findings from animal studies to the human situation. The study of Morissette *et al.* reported differences and similarities in the gene expression in lung of human and mice in response to CS exposure suggesting to study pathways instead of single genes (49). The challenges and pro's/con's of using animal models in case of inhalation toxicology studies are also discussed in paragraph 'Dosimetry' of the discussion. In the context of the focus of this thesis, it has already been shown that CS-exposure of rodents results in aberrant mitochondrial morphology and function (9, 14, 18, 23-27). However, the impact of smoking-associated aldehydes on processes involved in mitochondrial health remains to be elucidated. Only limited *in vitro* and *in vivo* studies have shown indications of an impact of acrolein on the dysregulation of mitochondrial function and energy metabolism in airway models (50-54), while it is unknown if acrolein can disrupt regulation of underlying processes. In this context, we analyzed the effect of exposure to acrolein (known to be the most reactive aldehyde abundantly present in CS) in lung tissue from rats. These studies were already performed by collaborators, preventing the need to conduct similar experiments and thereby unnecessary use of animals (reduce; **Chapters 4 and 5**).

In **Chapter 4**, acute nose-only exposure of acrolein in rats revealed a dose- and time-dependent impact on the molecular regulation of mitochondrial metabolism, respectively decreased protein and transcript levels of molecules controlling mitochondrial biogenesis and subunits of the electron transport chain. Interestingly, we observed differential effects upon exposure to acrolein for 1 or 2 days, which could be suggestive of a compensatory/repair response to mitochondrial damage elicited by acute acrolein exposure. Moreover, this difference could be explained by analysis of immediate cellular effects (stress/metabolic/immune) at day 1 (55-58) *versus* analysis

of a combination of the peak inflammatory response (originating from the exposure on day 1) and an immediate cellular effect derived from the second exposure at day 2.

Our findings in **Chapter 4** are mostly in line with prior evidence that demonstrated a detrimental impact of CS exposure on the regulation of mitochondrial morphology and homeostasis in cells of the lungs and airways *in vitro* (5-22) and *in vivo* (9, 14, 18, 23-27). Therefore, it might be suggested that acrolein could be one of the chemicals responsible for these alterations. However, as not acute but chronic smoke inhalation is one of the major risk factors for the development of COPD, we subsequently investigated also the impact of a longer exposure of the lungs and airways of rats to acrolein (sub-acute; 4 weeks).

In contrast to the profound changes observed after acute acrolein exposure in rat lung, no pronounced alterations were observed upon subacute acrolein exposure by whole-body inhalation in **Chapter 5**.

Whereas dosages used were in a similar range and both studies used a continuous exposure regime (**Chapters 4 and 5**), the factors duration of exposure (days *versus* weeks), or route of exposure (nose-only *versus* whole-body inhalation) seems to be critical in determining the impact of acrolein on mito-toxicity. This will be discussed in more detail in paragraph 'Dosimetry' of this discussion. Also, it has to be noted that we did not assess mitochondrial function directly (only the molecular mechanisms known to regulate this) or characteristics of COPD (e.g., emphysema/bronchitis) in **Chapters 4 and 5**, limiting conclusions regarding any potential impact of acrolein on this.

In conclusion, although associations between acrolein inhalation and disrupted molecular regulation of mitochondrial metabolism were observed upon acute exposure in rat lung (**Chapter 4**), this was not recapitulated after 4 weeks of exposure (**Chapter 5**). Based on our findings, no conclusions can be drawn about the causal link between acrolein, potential mitochondrial dysfunction or even induced alterations in COPD features (e.g., mucus hypersecretion, tissue remodeling: emphysema or airway enlargement). While it has been previously shown that sub-chronic inhalation of acrolein impaired lung structure and function (59), and acrolein has been associated with mucus hypersecretion and emphysema (60), future studies should asses in more detail the effect of prolonged inhalation of aldehydes on the development of COPD. Moreover, also the impact of short- and long-term exposure to other aldehydes, formaldehyde, acetaldehyde and crotonaldehyde, on the regulation of mitochondrial mechanisms involved in mitochondrial homeostasis in cells of the lungs/airways as well as on the development of COPD should be investigated. The possibilities for future research in this context will be described in paragraph 'Future research'.

It should be noted that exact mimicking of human smoking (and subsequently aldehydes exposure) is very challenging in both *in vivo* and *in vitro* models. Whereas, the individual aldehyde acrolein has been primarily studied in literature, as well as in our *in vivo* studies (**Chapters 4 and 5**), these studies are not reflective of the mixture of aldehydes present in CS. It should be considered that it has been previously shown that simultaneous exposure to acrolein and formaldehyde might result in additive or even synergistic toxicity in human/rat nasal, alveolar or bronchiolar epithelial cells (61-64). Also, it has been suggested that aldehydes based on their common molecular mechanism can interact leading to additive/synergistic toxicity (65). Moreover, human smoking occurs in a puff-like manner which is difficult to mimic in conventional CS exposure set-ups. We tried to overcome these challenges through investigating the impact of a mixture of acetaldehyde, acrolein and formaldehyde (in a composition and dose range comparable to CS) on differentiated PBEC *in vitro* using a continuous flow system combined with a puff-like exposure protocol in **Chapter 6**.

Exposure to CS in this model elicited (in general) similar changes as we observed in previous chapters of this thesis, respectively elevated Interleukin 8 cytokine and mRNA levels, increased abundance of constituents associated with autophagy, decreased protein levels of molecules associated with the mitophagy machinery and alterations in the abundance of regulators of mitochondrial biogenesis. The mixture of aldehydes failed to induce these changes (**Chapter 6**).

The observation of a lack of impact of this aldehydes mixture could be due to various reasons. One explanation could be a difference in behaviour of an individual mixture of these three aldehydes (as used in our study) *versus* the aldehydes present in CS together with the other circa 6000 chemicals. Aldehydes present in CS may interact with these other constituents, e.g., condensation of aldehydes on aerosol particles in CS, which potentially result in additive or synergistic toxicity. For example, it has been suggested that a mixture of these aldehydes with particulate matter might have an additive or synergistic effect as illustrated in an *in vivo* mice study upon exposure to acrolein and/or carbonaceous particles analysing antibacterial and antiviral defences in the lung (66). Moreover, another mice study have shown increased (severity of) lung carcinogenicity upon exposure to the tobacco specific compound Nitrosamine 4-Methylnitrosamino-1-(3-pyridyl)-1-butanone (NNK) in combination with exposure to formaldehyde, acetaldehyde or carbon dioxide (67). Additional studies are required to elucidate the underlying molecular mechanisms of the observed mixture interactions. The second explanation could be that mito-toxicity of CS might be induced by compounds other than these three aldehydes of interest, e.g., carbon monoxide, nicotine, nitrosamines, polycyclic aromatic hydrocarbons. For example, benzo(a)pyrene and 2,3,7,8-tetrachlorodibenzodioxin (TCDD) induced mitochondrial respiratory dysfunction in the pancreas of mice (68). Unfortunately, the effects in lung tissue were not investigated in this study. Another example is the role

of nicotine on mitochondrial dysfunction, which has been assessed in various *in vitro* and *in vivo* models. These studies observed alterations in mitochondrial respiration, mitochondrial biogenesis, mitophagy and dynamics as well as oxidative stress and calcium homeostasis in lung and non-lung cells (69). Research into this topic of mitotoxicity induced by CS-constituents, however, is limited. The third possible explanation which might play a role in the limited effects observed could be the challenges faced regarding the dosimetry of aldehydes, as further explained in paragraph 'Dosimetry'. Lastly, as previously discussed, the differentiated PBEC model is not reflective of the heterogeneous microenvironment of the lung, and it should be further investigated if the (interaction between) various cell populations play a role in the effect of aldehydes and mitochondrial dysfunction.

In future *in vitro* studies, as previously discussed, time of exposure should carefully be reconsidered. Ideally, differentiated PBEC are exposed several times a day instead of once to the mix of aldehydes or CS *in vitro*, as well as for a longer time period to mimic more realistic the smoking behaviour of smokers. Chronic exposure models seems to be more reflective for the pathological changes observed in COPD patients in the airway epithelium, as these alterations are demonstrated in general upon repeated/chronic exposure and/or upon exposure during differentiation (39, 70-73). In addition, a recent *in vitro* using PBEC cultured at air-liquid interface showed that single exposure to non-toxic doses of acrolein resulted in inflammation and oxidative stress in differentiated PBEC cultures, while repeated exposure for 10 days to acrolein induced functional and structural changes of the cultures comparable to COPD features (70). Practical challenges such as labour-intensity, costly medium, and sensitivity and survival time of primary cultures should be tackled before chronic exposure cell culture research could be performed in similar scale as cell line research. Nevertheless, acute exposure regimes as used in our *in vitro* studies are relevant. Observations of CS-induced autophagy in **Chapters 3 and 6**, are comparable to the previously reported changes in lung tissue or PBEC from COPD patients (5, 9, 14, 16) and are in line with findings in mice exposed to CS for a longer period of time (26). In addition, in **Chapter 3**, changes in the molecular control of autophagy upon acute smoke exposure were shown to persist, at least in part, upon chronic exposure to whole CS during differentiation and upon subsequent discontinuation of whole CS exposure. Lastly, bronchial epithelial cells exposed 1-week *versus* 12-weeks to CS showed mostly similar changes in mitochondrial function, whereas adaptation might be suggested upon long-term exposure (21).

Based on this thesis, since we only studied the impact of an individual mixture of three aldehydes and acute exposure (**Chapter 6**), we can not draw any conclusion regarding mixture mitotoxicity of aldehydes with other tobacco-compounds or chronic exposure of aldehydes. Future studies should focus on chronic exposure and mixture toxicology of tobacco compounds.

Dosimetry

It is difficult to compare levels of aldehydes associated with CS in smokers to doses and route of exposures used in *in vivo* and *in vitro* studies.

Dose

The amount of aldehydes to which individual smokers are exposed varies highly. This depends on tobacco brand, (added) amount and type of sugars in tobacco, smoking topography (74-82) and obviously the number of cigarettes smoked per day. This has been illustrated in a study by Pauwels *et al.*, who reported a highly variable amount of aldehydes per cigarette due to various tobacco brands and smoking regimes (82). Therefore, it is hard to define a general level of exposure for experimental purposes. *In vitro* studies in general use lower dosages of exposure of CS or related compounds compared to *in vivo* studies (closer to the human peak exposures during smoking) due to factors such as sensitivity of cell cultures. The dosages of acrolein used in our *in vivo* studies (2-4 ppm; **Chapters 4 and 5**) are situated at the (lower) range of levels found in one cigarette (82), but higher than environmental exposure (83). Dose-dependent changes upon acrolein exposure in the modulation of inflammatory responses and cellular processes associated with mitochondrial metabolism has been observed in **Chapter 4** and in a previously published study with exact same animals (56).

With respect to our *in vitro* research, in **Chapter 3**, PBEC were exposed to whole CS (2 mg CS-derived particles) or CS extract, both from one Kentucky 3R4F research cigarette. In case of CS extract used, the dose of exposure (of aldehydes) cannot be defined as we did not characterize our mixture, and levels are difficult to compare with other studies using extract in literature. Moreover, volatile components present in the gaseous/aerosol phase of CS are (in theory) not present in CS extract (liquid), while they are assumed to be present in whole CS (but aldehydes levels unknown/not defined in our study). In **Chapter 6**, PBEC were exposed to 8 puffs of one Marlboro Red cigarette (following Health Canadian Intense regime) or a mixture of acetaldehyde, acrolein and formaldehyde which was theoretically similar in concentration and proportion compared to CS. Specifically, the levels of these three aldehydes present in CS (one cigarette) were assessed by a standard operating procedure (84) and corresponded to previously reported levels (82). Subsequently, the generation of the mixture of aldehydes was matched to CS based on the combination of the calculated amount of aldehydes present in the mixture using the density and purity of each aldehyde and the total flow of the test atmosphere. Moreover, it was also checked whether each aldehyde was present in the generation of the test atmosphere using the Total Carbon Analyzer. However, unfortunately (due to technical difficulties) we were unable to measure exact levels of these aldehydes in the generated mixture of aldehydes (at the site of the cells). For this, a reliable method should be developed. Although, as previously mentioned, dosimetry might play a role in the limited effects observed, we have confidence that the

concentrations of acetaldehyde, acrolein and formaldehyde in the aldehydes mixture, which we generated, is comparable to the levels as present in the mainstream smoke of one Marlboro Red cigarette.

The dose of aldehydes exposure is also influenced by tobacco brand, as indicated before. We carefully considered the choice for used tobacco brand Marlboro Red in **Chapter 6** over 3R4F cigarettes as generally used in literature and in **Chapter 3**. As in **Chapter 6**, we aimed to mimic the human situation as close as possible by using a common tobacco brand and physiologically-relevant exposure regime, we have chosen for the leading commercially-available Marlboro Red cigarettes in combination with the Health Canadian Intense smoking regime. The exposure concentrations of three target aldehydes present in Marlboro Red cigarettes are shown to be in the higher range of 11 analyzed tobacco brands upon Health Canadian Intense machine smoking (82). Although, this tobacco brand is not commonly used in research, comparison of our data with other 3R4F studies is still relevant as the concentrations of aldehydes are comparable for Marlboro Red and 3R4F following Health Canadian Intense regime (82). Other factors, which make it even more difficult to compare our results with other smoke inhalation toxicology studies, are the common use of non-primary cells or continuously smoking profiles which will be discussed in the next paragraphs.

In summary, it is challenging to compare exposure levels in all chapters because of limited characterization of the exact dose, and the influence of type/phase of smoke (whole CS *versus* CS extract) and tobacco brand on the composition and corresponding dose of exposure.

Deposition and uptake

The levels of exposure to acrolein, CS or a mixture of aldehydes does not per definition correlate with the levels of deposition and uptake in the lungs (*in vivo*) or in PBEC (*in vitro*).

With respect to *in vivo* research, there are differences in deposition and uptake between humans and animals depending on various factors, besides obvious ones as concentration of components and rate of airflow. Firstly, the airway anatomy/geometry and airway dimensions (length, diameter, thickness of tissue) in experimental animals, e.g., rats, are totally different compared to humans (85-87). Secondly, species-specific respiratory physiology can play a role by extrapolating animal data to the human situation (mode of breathing and rate of ventilation/filtering) (86). Besides the deposition pattern (influences by origin of breathing), also the clearance of inhaled substances affect the potential toxic effect and is species dependent (86, 88, 89). For example, enzyme-dependent metabolic processes vary in activity in lung of humans *versus* rodents (90). Lastly, in rodents (including rats) reflex reactions may influence the dosimetry and parasympathetic system (56, 91-94). This alteration in breathing

parameters has been also shown in exact similar rats as used in our study in **Chapter 4**, respectively upon acute acrolein (nose-only) exposure and measured immediately post-exposure (56).

Interestingly, Corley *et al.* also highlighted the relevance of taking breathing simulations (oral; as present in the human situation) into account in risk analysis of CS-associated aldehydes such as acrolein, acetaldehyde and formaldehyde (91). Moreover, they predicted that rats have the highest nasal extraction efficiency, followed by monkeys and humans and showed higher uptake of acrolein in the lower tracheobronchial tissue in human compared to rats or monkeys by computational fluid dynamics models (92).

With respect to *in vitro* studies, the dose-uptake is examined to a lesser extent. A recent study by Xiong *et al.* assessed the cellular uptake of acrolein after a 10-min exposure (12.5-100 μM) in relation to key molecular events: protein carbonyls and GSH-ACR adduct formation in two pulmonary cell lines (NHBE *versus* lung cancer). It was shown that NHBE cells are more sensitive to acrolein exposure and it was shown that cell susceptibility to acrolein exposure is closely associated with acrolein uptake and formation of GSH-ACR adducts (95).

Summarized, although deposition and uptake were not analysed in our studies, these factors should be taken into account in future research when considering the effect of exposure to specific (potential lowering of) aldehydes dosages, as present in CS, in the lungs (*in vivo*) or in PBEC (*in vitro*).

Route and regime of exposure

First and foremost, the exposure routes used in our animal studies are all different from the human situation, because rats and humans have a different origin of breathing (85). In case of *in vivo* experiments, several options of commonly-used exposure routes are nose-only (**Chapter 4**), whole-body (**Chapter 5**) or intratracheal instillation. It has been described that nose-only exposure leads to more local toxicity (nose), while whole-body inhalation might result in a lower inhaled dose (deposition losses, such as larger contact surfaces, deposition on or filtering the aerosol through the fur, or nose covered by fur from other animals due to huddling together) (96-100). The influence of the route of exposure on toxicity has been illustrated in a recent study in which mice were exposed to CS via nose-only inhalation *versus* whole-body inhalation. More severe structural and molecular changes in the upper respiratory tract (i.e., nose), lung inflammation and aberrant molecular regulation of the respiratory system were observed following nose-only exposure relative to whole-body inhalation. Nevertheless, comparable changes regarding lung inflammation/function, lung proteome, and nasal epithelia (transcriptome) have been shown in both exposure routes. With respect to aldehyde levels in the breathing zones of these exposure chambers, comparable/similar yields of acrolein relative to the nominal concentration have been detected (98). In line with these

findings, we also observed more pronounced disruptions in the molecular regulation of mitochondrial metabolism in **Chapter 4** (nose-only; acute acrolein exposure) *versus* **Chapter 5** (whole-body; sub-acute acrolein exposure). However, it should be noted that our studies also differ in duration of exposure which could be of influence as previously discussed. Besides the route of exposure, also the exposure regime should be discussed. The continuous exposure of laboratory rodents as used in previous research as well as in our models in **Chapters 4 and 5** does not accurately reflect the puff-topography that human smokers usually display (91, 101). According to our knowledge, puff-regime exposure studies does not exist in animals in the context of CS (or related compounds), which should be taken into account in design of future inhalation toxicology studies.

With respect to *in vitro* models, exposure route can differ due to the generally-used droplet exposure of soluble chemicals in medium in 2D models *versus* the more realistic used airborne exposure systems to mimic inhalation in 3D models. Moreover, the continuous exposure regimes used in most *in vitro* models differ from the multiple high peak intervals of toxicants where smokers are normally exposed to during puff inhalation. In **Chapter 6** we tried to overcome these limitations by using a physiologically relevant model using a puff-like exposure regime via a continuous flow system.

Taken all these dosimetry factors (dose, deposition, uptake, exposure route and regime) into consideration, it is hard to set a 'general' exposure level to aldehydes and method to be used in experimental studies. Also, these factors complicate translation of the results from *in vitro* and *in vivo* to the human situation as airborne exposure systems and smoking topography (puff-like manner exposure) are underrepresented in current literature and should be taken into account in future studies.

Future research

In the paragraphs above, several opportunities and implications for future research have been discussed, in particular related to choice of experimental model, dosimetry, duration of exposure and mixture toxicology. More advanced *in vitro* models mimicking the microenvironment in the lung are required to contribute to the aim to reduce, replace and refine animal experiments into a transition to *in vitro* inhalation toxicology research in the future. Besides these limitations and considerations of the experimental set-ups which should be overcome in future research, studies are necessary to unravel: 1. the role of aldehydes in the development of COPD, 2. the relation between aldehydes exposure and mitochondrial dysfunction in cells of the airways and lungs, and 3. the causal impact of aldehyde-induced mitochondrial dysfunction in the development of COPD.

Role of aldehydes in the development of COPD

While aldehydes are shown to be respiratory toxic (102), whether or not exposure to aldehydes increases the risk for development of COPD has to be investigated. Only old studies in dogs and sheeps indicated a link between acrolein and pulmonary edema, which was to a lesser extent induced after formaldehyde exposure (103, 104). Moreover, a few other studies suggested a link between acrolein (60, 105-107) or formaldehyde (108) exposure to the pathogenesis of (features of) COPD. For example, it has been shown that acrolein could induce mRNA expression of MU5CAC and glycoproteins in rat lung (106, 107) and acrolein has been linked to emphysema by triggering an imbalance in protease-anti-protease (60). In addition, also elevated levels of acrolein have been shown in plasma and lung tissue supernatant from COPD patients (109). Furthermore, a key role for aldehyde dehydrogenase (ALDH) has been suggested in the pathogenesis of COPD. To specify, increased ALDH enzyme expression in bronchoalveolar lavage fluid from COPD patients, as well as the inactive form of ALDH2 has been suggested to be related to impaired lung function, chronic obstruction and pathological toxicity of the airways (110-113).

Less is known about the respiratory toxicity of other short-chain aldehydes of interest in relation to COPD pathogenesis, such as formaldehyde, acetaldehyde, and crotonaldehyde. Additional studies are required to increase knowledge regarding the causal and mechanistic relationship between CS-associated aldehydes and COPD development. This can be achieved by conducting mixture toxicity studies into (chronic) inhalation of several aldehydes *versus* individual aldehydes and the impact on COPD endpoints such as mucus hypersecretion and damaged epithelium. With respect to the investigation of COPD in animal models, it should be recognized that COPD initiated in animals is not representative for COPD in human patients. For example, chronic exposure to CS (6 months) will result in mild emphysema and pulmonary lesions in small rodents, however this not comparable to GOLDIII and GOLDIV status (114-116). Therefore, advanced *in vitro* models including various cell types and chronic exposure regimes are preferred.

Aldehydes and mitochondrial dysfunction in cells of the airways and lungs

As discussed in the introduction of this thesis, it has been shown in several *in vivo* and *in vitro* studies of lung and non-lung tissue/cells that exposure to aldehydes, in particular acrolein, formaldehyde, acetaldehyde and crotonaldehyde, result in abnormal mitochondrial morphology, disrupted mitochondrial bioenergetics, oxidative stress and apoptosis, mtDNA damage and reduced mitochondrial membrane potential and mtDNA copy number (50-54, 117-128). However, literature is scarce and focussed on *in vitro* studies using cell lines in combination with acrolein exposure, whereas the impact of formaldehyde and acetaldehyde has been mainly investigated in non-lung cells. While this thesis tried to contribute to the knowledge about the impact of acrolein (or mixture of aldehydes) on the molecular regulation of mitochondrial

content, function and metabolism, future research should focus also on mitochondrial function *per se* in response to individual aldehydes, mixtures of aldehydes and/or in combination with other CS compounds. Mitochondrial function measurements are challenging in frozen tissue of animal studies or advanced 3D cultures. Recently, some research groups described solutions to analyse respiratory capacity in frozen samples (129), or to conduct oxidative respiration measurements in air-liquid interface cultures, for example development of an in-house method (130) or a more approachable method using Seahorse (131). Additional relevant analyses to investigate the link between aldehydes and mitochondrial dysfunction in cells of the airways and lungs are transmission electron microscopy, histology or functional assays of electron transport chain complexes, enzymes involved in mitochondrial (energy) metabolism or focussing on mitochondrial-regulated physiological processes such as mucus secretion or mucociliary function.

Does aldehyde-induced mitochondrial dysfunction lead to the development of COPD?

Genetic modifications or pharmacological interventions might be used to investigate the (suggested) causal relationship between aldehyde-induced mitochondrial dysfunction in cells of the lung and airways and COPD pathogenesis. This research should focus on preventing, scavenging or rescuing aldehyde-induced damage, mitochondrial (dys) function or COPD development. Examples of these interventions are ALDH (de-)activity (alda-1) or aldehyde scavengers, supplementation with a mitochondrial iron chelator or fed a low-iron diet or deficiency, or defective or stimulated COPD susceptibility genes (e.g., *IRP2*). Using those last interventions, it has been shown by Cloonan *et al.* that prevention of CS-induced mitochondrial dysfunction in a mouse model of COPD significantly ameliorated CS-induced development of emphysema and bronchitis (23). Whether the same holds true for aldehydes remains to be established.

Targeting aldehydes in COPD therapy

Although additional research is required to investigate the exact relation between aldehydes, mitochondrial dysfunction and COPD as discussed in the previous paragraph, it can be suggested that aldehydes are implicated in the pathogenesis of COPD via dysregulated mitochondrial function and therefore neutralizing aldehydes might be a potential approach for COPD therapy. Compared to the studies mentioned previously which focus on targeting mitochondria, less studies are focusing on specifically targeting aldehydes (metabolism). The studies available are, in particular, investigating therapeutic targets in relation to ALDH2 and exposure to acrolein.

Firstly, some studies are targeting ALDH using alda-1, an agonist of mitochondrial ALDH. Alda-1 as therapeutic target was mainly investigated in the context of acute

lung injury. For example, it has been shown that administration of alda-1 protected against acrolein-induced lung injury which was manifested as a reduction in edema and inflammation in mice. Moreover, *in vitro* exposure to alda-1 mitigated the acrolein-induced increase in endothelial monolayer permeability in rat lung microvascular endothelial cells, while inhibition of mitochondrial respiration upon acrolein exposure was not prevented by alda-1 treatment (132). In recent studies, it was demonstrated that alda-1 treatment prior to hypoxia exposure alleviated the mitochondrial dysfunction in lung vascular endothelial cells (133) and continuous delivery of alda-1 attenuated the development of hypoxia-induced lung injury in mice (134). In addition, it has been shown that alda-1 treatment protected against whole-body heating-induced acute lung injury in mice (135) and alda-1 also reduced pyroptosis and ferroptosis, processes involved in sepsis-induced acute lung injury (136). Lastly, alda-1 might suppress lung tumor progression (137) and alda-1 has been shown to trigger the clearance of reactive aldehydes resulting in prevention of pulmonary epithelial barrier dysfunction upon severe hemorrhagic shock (138). Albeit in other cell types than lung cells, a few studies investigated the potential of alda-1 as therapeutic target in non-lung injury related diseases by showing their attenuating impact on hepatic fibrosis, hepatic steatosis, atherosclerosis, heart failure, cardiomyopathy and ischemia-reperfusion in several organs including myocardium, liver, brain, spinal cord, eye, intestine, and kidney (139-144). Summarized, there seems to be therapeutic potential for alda-1 in the context of aldehydes-induced mitochondrial dysfunction, but additional fundamental and clinical research is required to investigate the potential of this agonist.

Secondly, aldehyde scavengers might be an effective therapeutic target of which especially acrolein scavengers have been studied. Nitrogen-containing carbonyl compounds are capable of scavenging aldehydes and are known to counteract acrolein-induced protein carbonylation (60). Examples of these compounds are anti-hypertensive hydralazine (145), methoxyamine (146) and glycooxidation inhibitors, aminoguanidine and carnosine (147). Another compound suggested to have acrolein-scavenging properties is erdosteine (60). This is an antioxidant, respectively a thiol-containing molecule with a sulfhydryl group as active metabolite, and is already used in treatment of COPD as a mucolytic agent (148). Another compound, dimercaprol, has been described as an acrolein scavenger in *in vitro* and animal studies focusing on neural diseases. To be more specific, dimercaprol is reported to be effective in detoxifying acrolein *in vitro* by prevention of acrolein-induced cell death in a dose-dependent manner in PC-12 cells, and *in vivo* reduced acrolein levels were detected in case of spinal cord contusion injury in rat (149). Moreover, dimercaprol provides neuroprotection *in vivo* in a rat model of Parkinson's disease (150). Formaldehyde- or acetaldehyde-scavengers are less well studied, however metformin is suggested to be a potential formaldehyde scavenger in HepG2 cells (151).

In summary, extensive further research is required to investigate 1) the exact role of aldehydes in (deregulation of) mitochondrial metabolism and COPD pathogenesis and 2) the potential application of therapeutic strategies specifically targeting aldehydes in the context of lung disease.

Implications for regulation of aldehydes in CS

By investigating the impact of several aldehydes (relevant for CS-exposure) on the molecular pathways regulating mitochondrial content and function in epithelial cells of the lungs and airways, this thesis aimed to provide scientific evidence to support future regulation of aldehyde content in CS. Reduction of aldehyde content in cigarettes can be achieved by decreasing sugar content, selection of specific tobacco types and design of a cigarette (e.g., cigarette filter ventilation) (74, 82, 152). Although we provided evidence that acute exposure of the lungs and airways to acrolein (and CS) impaired the molecular regulation of mitochondrial content, function and metabolism, unfortunately no conclusive recommendations can be provided regarding future regulation of aldehydes in CS based on our findings. However, our findings combined with previous literature could be taken into account by policy makers in their consideration for the mandated lowering/regulation of aldehydes ((added) sugars) in CS and limit emission of CS-associated aldehydes in tobacco products.

Based on this thesis, knowledge gaps are identified as future research should focus on the elucidation of the (causal) relationship between aldehydes, mitochondrial dysfunction and COPD pathogenesis as described in the paragraph above.

Moreover additional research is required to prove if and to what level a reduction of specific aldehydes per cigarette can have health benefits. Only a few studies investigated the dose-effect of acrolein *in vitro* showing differential cytotoxic impact of high dose of acrolein (cytotoxic) *versus* low dose of acrolein (no cytotoxicity) in human bronchial epithelial cells (153). In the case of acrolein, this dose dependent effect has also been shown with respect to the immunology response, which also depended on the cell type. Acute high doses of acrolein have been shown to result in an inhibition of the innate immune and inflammatory responses resulting in increased susceptibility to infections, and in contrast chronic low doses of acrolein may lead to inflammation, oxidative stress, or a response leading to tissue injury (102, 154). In addition, a dose-dependent impact of acrolein exposure on the regulation of mitochondrial quality control processes and mitochondrial metabolism (e.g., membrane potential, ATP content) has been shown *in vivo* (0-2-4 ppm acrolein for 1 or 2 days) in rat lung (**Chapter 4**) and *in vitro* (0-100 μ M) in cells of the airways (50). These studies did however not take into account physiologically-relevant exposure regimes, as smokers are normally exposed to peak-exposure levels (puff regime), several times (i.e., cigarettes) a day, for several years.

Conclusion

In conclusion, we investigated the hypothesis that exposure to CS or associated-aldehydes impaired the molecular regulation of mitochondrial biogenesis, mitophagy and mitochondrial dynamics in cells of the lungs and airways, in the context of COPD development. In general, we observed changes in the molecular regulation of autophagy/mitophagy and mitochondrial biogenesis both in peripheral lung homogenates from very severe COPD patients, *in vitro* PBEC exposed to CS, and *in vivo* in rat upon acute acrolein exposure. Remarkably, no pronounced impact was observed in PBEC models from COPD patients, in PBEC following exposure to a mixture of aldehydes *in vitro* or after sub-acute acrolein exposure of rats. The heterogeneous results observed in the various studies in this thesis might be explained by the differences in experimental set-up: *in vivo* versus *in vitro*, dosimetry and duration of exposure, disease status, exposure type, but may also arise from limitations of the models used and read-outs that were assessed. Besides these characteristics, it is important to take into account the translational impact of our findings to the human situation in future studies, but also to consider what is the most informative and applicable model matching the research question. Moreover, future research should focus on the role of aldehydes in the development of COPD, the relation between aldehydes exposure and mitochondrial dysfunction in cells of the airways and lungs, and the causal impact of aldehyde-induced mitochondrial dysfunction in the development of COPD.

References

1. Cloonan SM, Choi AMK. Mitochondria: commanders of innate immunity and disease? *Current Opinion in Immunology*. 2012;24(1):32-40.
2. Marchi S, Guilbaud E, Tait SWG, Yamazaki T, Galluzzi L. Mitochondrial control of inflammation. *Nature Reviews Immunology*. 2022.
3. López-Armada MJ, Riveiro-Naveira RR, Vaamonde-García C, Valcárcel-Ares MN. Mitochondrial dysfunction and the inflammatory response. *Mitochondrion*. 2013;13(2):106-18.
4. Cloonan SM, Choi AM. Mitochondria in lung disease. *J Clin Invest*. 2016;126(3):809-20.
5. Hoffmann RF, Zarrintan S, Brandenburg SM, Kol A, de Bruin HG, Jafari S, et al. Prolonged cigarette smoke exposure alters mitochondrial structure and function in airway epithelial cells. *Respir Res*. 2013;14:97.
6. Hara H, Araya J, Ito S, Kobayashi K, Takasaka N, Yoshii Y, et al. Mitochondrial fragmentation in cigarette smoke-induced bronchial epithelial cell senescence. *Am J Physiol Lung Cell Mol Physiol*. 2013;305(10):L737-46.
7. Sundar IK, Maremanda KP, Rahman I. Mitochondrial dysfunction is associated with Miro1 reduction in lung epithelial cells by cigarette smoke. *Toxicol Lett*. 2019;317:92-101.
8. Ballweg K, Mutze K, Königshoff M, Eickelberg O, Meiners S. Cigarette smoke extract affects mitochondrial function in alveolar epithelial cells. *Am J Physiol Lung Cell Mol Physiol*. 2014;307(11):L895-907.
9. Mizumura K, Cloonan SM, Nakahira K, Bhashyam AR, Cervo M, Kitada T, et al. Mitophagy-dependent necroptosis contributes to the pathogenesis of COPD. *J Clin Invest*. 2014;124(9):3987-4003.
10. Park EJ, Park YJ, Lee SJ, Lee K, Yoon C. Whole cigarette smoke condensates induce ferroptosis in human bronchial epithelial cells. *Toxicol Lett*. 2019;303:55-66.
11. Wu K, Luan G, Xu Y, Shen S, Qian S, Zhu Z, et al. Cigarette smoke extract increases mitochondrial membrane permeability through activation of adenine nucleotide translocator (ANT) in lung epithelial cells. *Biochem Biophys Res Commun*. 2020;525(3):733-9.
12. Aravamudan B, Kiel A, Freeman M, Delmotte P, Thompson M, Vassallo R, et al. Cigarette smoke-induced mitochondrial fragmentation and dysfunction in human airway smooth muscle. *Am J Physiol Lung Cell Mol Physiol*. 2014;306(9):L840-54.
13. Aravamudan B, Thompson M, Sieck GC, Vassallo R, Pabelick CM, Prakash YS. Functional Effects of Cigarette Smoke-Induced Changes in Airway Smooth Muscle Mitochondrial Morphology. *J Cell Physiol*. 2017;232(5):1053-68.
14. Ahmad T, Sundar IK, Lerner CA, Gerloff J, Tormos AM, Yao H, et al. Impaired mitophagy leads to cigarette smoke stress-induced cellular senescence: implications for chronic obstructive pulmonary disease. *Faseb j*. 2015;29(7):2912-29.
15. Son ES, Kim SH, Ryter SW, Yeo EJ, Kyung SY, Kim YJ, et al. Quercetin protects against cigarette smoke extract-induced apoptosis in epithelial cells by inhibiting mitophagy. *Toxicol In Vitro*. 2018;48:170-8.
16. Ito S, Araya J, Kurita Y, Kobayashi K, Takasaka N, Yoshida M, et al. PARK2-mediated mitophagy is involved in regulation of HBEC senescence in COPD pathogenesis. *Autophagy*. 2015;11(3):547-59.

17. Kyung SY, Kim YJ, Son ES, Jeong SH, Park JW. The Phosphodiesterase 4 Inhibitor Roflumilast Protects against Cigarette Smoke Extract-Induced Mitophagy-Dependent Cell Death in Epithelial Cells. *Tuberc Respir Dis.* 2018;81(2):138-47.
18. Chen ZH, Kim HP, Sciurba FC, Lee SJ, Feghali-Bostwick C, Stolz DB, et al. Egr-1 regulates autophagy in cigarette smoke-induced chronic obstructive pulmonary disease. *PLoS One.* 2008;3(10):e3316.
19. Song C, Luo B, Gong L. Resveratrol reduces the apoptosis induced by cigarette smoke extract by upregulating MFN2. *PLoS One.* 2017;12(4):e0175009.
20. Valdivieso Á G, Dugour AV, Sotomayor V, Clauzure M, Figueroa JM, Santa-Coloma TA. N-acetyl cysteine reverts the proinflammatory state induced by cigarette smoke extract in lung Calu-3 cells. *Redox Biol.* 2018;16:294-302.
21. Malinska D, Szymanski J, Patalas-Krawczyk P, Michalska B, Wojtala A, Prill M, et al. Assessment of mitochondrial function following short- and long-term exposure of human bronchial epithelial cells to total particulate matter from a candidate modified-risk tobacco product and reference cigarettes. *Food Chem Toxicol.* 2018;115:1-12.
22. Vanella L, Li Volti G, Distefano A, Raffaele M, Zingales V, Avola R, et al. A new antioxidant formulation reduces the apoptotic and damaging effect of cigarette smoke extract on human bronchial epithelial cells. *Eur Rev Med Pharmacol Sci.* 2017;21(23):5478-84.
23. Cloonan SM, Glass K, Laucho-Contreras ME, Bhashyam AR, Cervo M, Pabon MA, et al. Mitochondrial iron chelation ameliorates cigarette smoke-induced bronchitis and emphysema in mice. *Nat Med.* 2016;22(2):163-74.
24. Agarwal AR, Yin F, Cadenas E. Short-term cigarette smoke exposure leads to metabolic alterations in lung alveolar cells. *Am J Respir Cell Mol Biol.* 2014;51(2):284-93.
25. Agarwal AR, Zhao L, Sancheti H, Sundar IK, Rahman I, Cadenas E. Short-term cigarette smoke exposure induces reversible changes in energy metabolism and cellular redox status independent of inflammatory responses in mouse lungs. *Am J Physiol Lung Cell Mol Physiol.* 2012;303(10):L889-98.
26. Chen ZH, Lam HC, Jin Y, Kim HP, Cao J, Lee SJ, et al. Autophagy protein microtubule-associated protein 1 light chain-3B (LC3B) activates extrinsic apoptosis during cigarette smoke-induced emphysema. *Proc Natl Acad Sci U S A.* 2010;107(44):18880-5.
27. Araya J, Tsubouchi K, Sato N, Ito S, Minagawa S, Hara H, et al. PRKN-regulated mitophagy and cellular senescence during COPD pathogenesis. *Autophagy.* 2019;15(3):510-26.
28. Li J, Dai A, Hu R, Zhu L, Tan S. Positive correlation between PPARgamma/PGC-1alpha and gamma-GCS in lungs of rats and patients with chronic obstructive pulmonary disease. *Acta Biochim Biophys Sin.* 2010;42(9):603-14.
29. Peng H, Yang M, Chen ZY, Chen P, Guan CX, Xiang XD, et al. Expression and methylation of mitochondrial transcription factor a in chronic obstructive pulmonary disease patients with lung cancer. *PLoS One.* 2013;8(12):e82739.
30. Khan Y, Lynch D. *Histology, Lung: Treasure Island (FL): StatPearls Publishing; Jan 2022 - Updated 2022 May 8.*
31. Altorki NK, Markowitz GJ, Gao D, Port JL, Saxena A, Stiles B, et al. The lung microenvironment: an important regulator of tumour growth and metastasis. *Nat Rev Cancer.* 2019;19(1):9-31.

32. Amatngalim GD, Schrumpf JA, Henic A, Dronkers E, Verhoosel RM, Ordonez SR, et al. Antibacterial defense of human airway epithelial cells from chronic obstructive pulmonary disease patients induced by acute exposure to nontypeable *Haemophilus influenzae*: modulation by cigarette smoke. *Journal of innate immunity*. 2017;9(4):359-74.
33. Staudt MR, Buro-Auriemma LJ, Walters MS, Salit J, Vincent T, Shaykhiev R, et al. Airway Basal stem/progenitor cells have diminished capacity to regenerate airway epithelium in chronic obstructive pulmonary disease. *American journal of respiratory and critical care medicine*. 2014;190(8):955-8.
34. Hiemstra PS, Grootaers G, van der Does AM, Krul CAM, Kooter IM. Human lung epithelial cell cultures for analysis of inhaled toxicants: Lessons learned and future directions. *Toxicol In Vitro*. 2018;47:137-46.
35. Rigden HM, Alias A, Havelock T, O'Donnell R, Djukanovic R, Davies DE, et al. Squamous Metaplasia Is Increased in the Bronchial Epithelium of Smokers with Chronic Obstructive Pulmonary Disease. *PloS one*. 2016;11(5):e0156009-e.
36. Crystal RG. Airway basal cells. The “smoking gun” of chronic obstructive pulmonary disease. *American journal of respiratory and critical care medicine*. 2014;190(12):1355-62.
37. Saetta MT, G.; Baraldo, S.; Zanin, A.; Braccioni, F.; Mapp, C. E.; Maestrelli, P.; Cavallero, G.; Papi, A.; Fabbri, L. M. Goblet cell hyperplasia and epithelial inflammation in peripheral airways of smokers with both symptoms of chronic bronchitis and chronic airflow limitation. *American journal of respiratory and critical care medicine*. 2000;161(3):1016-21.
38. Jeffery PK. Comparison of the structural and inflammatory features of COPD and asthma. *Giles F. Filley Lecture. Chest*. 2000;117(5):251S-60S.
39. Gindele JA, Kiechle T, Benediktus K, Birk G, Brendel M, Heinemann F, et al. Intermittent exposure to whole cigarette smoke alters the differentiation of primary small airway epithelial cells in the air-liquid interface culture. *Scientific Reports*. 2020;10(1):6257.
40. Global Initiative For Chronic Obstructive Lung Disease. *Global Strategy for Diagnosis, Management, and Prevention of Chronic Obstructive Lung Disease: 2022 Report*. 2022.
41. Mastalerz M, Dick E, Chakraborty A, Hennen E, Schamberger AC, Schröppel A, et al. Validation of in vitro models for smoke exposure of primary human bronchial epithelial cells. *Am J Physiol Lung Cell Mol Physiol*. 2022;322(1):L129-148.
42. Iskandar AR, Xiang Y, Frentzel S, Talikka M, Leroy P, Kuehn D, et al. Impact Assessment of Cigarette Smoke Exposure on Organotypic Bronchial Epithelial Tissue Cultures: A Comparison of Mono-Culture and Coculture Model Containing Fibroblasts. *Toxicol Sci*. 2015;147(1):207-21.
43. van Riet S, van Schadewijk A, de Vos S, Vandeghinste N, Rottier RJ, Stolk J, et al. Modulation of Airway Epithelial Innate Immunity and Wound Repair by M(GM-CSF) and M(M-CSF) Macrophages. *J Innate Immun*. 2020;12(5):410-21.
44. Sauler M, McDonough JE, Adams TS, Kothapalli N, Barnthaler T, Werder RB, et al. Characterization of the COPD alveolar niche using single-cell RNA sequencing. *Nature Communications*. 2022;13(1):494.
45. Aghapour M, Remels AHV, Pouwels SD, Bruder D, Hiemstra PS, Cloonan SM, et al. Mitochondria: at the crossroads of regulating lung epithelial cell function in chronic obstructive pulmonary disease. *Am J Physiol Lung Cell Mol Physiol*. 2020;318(1):L149-164.
46. Caldeira DAF, Weiss DJ, Rocco PRM, Silva PL, Cruz FF. Mitochondria in Focus: From Function to Therapeutic Strategies in Chronic Lung Diseases. *Front Immunol*. 2021;12:782074.

47. Sheu SS, Nauduri D, Anders MW. Targeting antioxidants to mitochondria: a new therapeutic direction. *Biochim Biophys Acta*. 2006;1762(2):256-65.
48. Agrawal A, Mabalirajan U. Rejuvenating cellular respiration for optimizing respiratory function: targeting mitochondria. *Am J Physiol Lung Cell Mol Physiol*. 2016;310(2):L103-13.
49. Morissette MC, Lamontagne M, Bérubé JC, Gaschler G, Williams A, Yauk C, et al. Impact of cigarette smoke on the human and mouse lungs: a gene-expression comparison study. *PLoS One*. 2014;9(3):e92498.
50. Wang HT, Lin JH, Yang CH, Haung CH, Weng CW, Maan-Yuh Lin A, et al. Acrolein induces mtDNA damages, mitochondrial fission and mitophagy in human lung cells. *Oncotarget*. 2017;8(41):70406-21.
51. Fabisiak JP, Medvedovic M, Alexander DC, McDunn JE, Concel VJ, Bein K, et al. Integrative metabolome and transcriptome profiling reveals discordant energetic stress between mouse strains with differential sensitivity to acrolein-induced acute lung injury. *Mol Nutr Food Res*. 2011;55(9):1423-34.
52. Agarwal AR, Yin F, Cadenas E. Metabolic shift in lung alveolar cell mitochondria following acrolein exposure. *Am J Physiol Lung Cell Mol Physiol*. 2013;305(10):L764-73.
53. Roy J, Palapati P, Bettaieb A, Tanel A, Averill-Bates DA. Acrolein induces a cellular stress response and triggers mitochondrial apoptosis in A549 cells. *Chem Biol Interact*. 2009;181(2):154-67.
54. Luo C, Li Y, Yang L, Feng Z, Li Y, Long J, et al. A cigarette component acrolein induces accelerated senescence in human diploid fibroblast IMR-90 cells. *Biogerontology*. 2013;14(5):503-11.
55. Miller DB, Snow SJ, Schladweiler MC, Richards JE, Ghio AJ, Ledbetter AD, et al. Acute Ozone-Induced Pulmonary and Systemic Metabolic Effects Are Diminished in Adrenalectomized Rats. *Toxicol Sci*. 2016;150(2):312-22.
56. Snow SJ, McGee MA, Henriquez A, Richards JE, Schladweiler MC, Ledbetter AD, et al. Respiratory Effects and Systemic Stress Response Following Acute Acrolein Inhalation in Rats. *Toxicol Sci*. 2017;158(2):454-64.
57. Henriquez AR, Snow SJ, Schladweiler MC, Miller CN, Dye JA, Ledbetter AD, et al. Beta-2 Adrenergic and Glucocorticoid Receptor Agonists Modulate Ozone-Induced Pulmonary Protein Leakage and Inflammation in Healthy and Adrenalectomized Rats. *Toxicol Sci*. 2018;166(2):288-305.
58. Henriquez AR, Williams W, Snow SJ, Schladweiler MC, Fisher C, Hargrove MM, et al. The dynamicity of acute ozone-induced systemic leukocyte trafficking and adrenal-derived stress hormones. *Toxicology*. 2021;458:152823.
59. Costa DL, Kutzman RS, Lehmann JR, Drew RT. Altered lung function and structure in the rat after subchronic exposure to acrolein. *Am Rev Respir Dis*. 1986;133(2):286-91.
60. Moretto N, Volpi G, Pastore F, Facchinetti F. Acrolein effects in pulmonary cells: relevance to chronic obstructive pulmonary disease. *Ann N Y Acad Sci*. 2012;1259:39-46.
61. Zhang S, Zhang J, Chen H, Wang A, Liu Y, Hou H, et al. Combined cytotoxicity of co-exposure to aldehyde mixtures on human bronchial epithelial BEAS-2B cells. *Environ Pollut*. 2019;250:650-61.
62. Zhang S, Chen H, Wang A, Liu Y, Hou H, Hu Q. Combined effects of co-exposure to formaldehyde and acrolein mixtures on cytotoxicity and genotoxicity in vitro. *Environ Sci Pollut Res Int*. 2018;25(25):25306-14.

63. Cassee FR, Stenhuis WH, Groten JP, Feron VJ. Toxicity of formaldehyde and acrolein mixtures: in vitro studies using nasal epithelial cells. *Exp Toxicol Pathol*. 1996;48(6):481-3.
64. Zhang S, Zhang J, Cheng W, Chen H, Wang A, Liu Y, et al. Combined cell death of co-exposure to aldehyde mixtures on human bronchial epithelial BEAS-2B cells: Molecular insights into the joint action. *Chemosphere*. 2020;244:125482.
65. LoPachin RM, Gavin T. Molecular mechanisms of aldehyde toxicity: a chemical perspective. *Chem Res Toxicol*. 2014;27(7):1081-91.
66. Jakab GJ. The toxicologic interactions resulting from inhalation of carbon black and acrolein on pulmonary antibacterial and antiviral defenses. *Toxicol Appl Pharmacol*. 1993;121(2):167-75.
67. Peterson LA, Oram MK, Flavin M, Seabloom D, Smith WE, O'Sullivan MG, et al. Coexposure to Inhaled Aldehydes or Carbon Dioxide Enhances the Carcinogenic Properties of the Tobacco-Specific Nitrosamine 4-Methylnitrosamino-1-(3-pyridyl)-1-butanone in the A/J Mouse Lung. *Chem Res Toxicol*. 2021;34(3):723-32.
68. Ghosh J, Chowdhury AR, Srinivasan S, Chattopadhyay M, Bose M, Bhattacharya S, et al. Cigarette Smoke Toxins-Induced Mitochondrial Dysfunction and Pancreatitis Involves Aryl Hydrocarbon Receptor Mediated Cyp1 Gene Expression: Protective Effects of Resveratrol. *Toxicological Sciences*. 2018;166(2):428-40.
69. Malińska D, Więckowski MR, Michalska B, Drabik K, Prill M, Patalas-Krawczyk P, et al. Mitochondria as a possible target for nicotine action. *J Bioenerg Biomembr*. 2019;51(4):259-76.
70. Xiong R, Wu Q, Muskhelishvili L, Davis K, Shemansky JM, Bryant M, et al. Evaluating Mode of Action of Acrolein Toxicity in an In Vitro Human Airway Tissue Model. *Toxicol Sci*. 2018;166(2):451-64.
71. Kuehn D, Majeed S, Guedj E, Dulize R, Baumer K, Iskandar A, et al. Impact assessment of repeated exposure of organotypic 3D bronchial and nasal tissue culture models to whole cigarette smoke. *J Vis Exp*. 2015(96).
72. Schamberger AC, Staab-Weijnitz CA, Mise-Racek N, Eickelberg O. Cigarette smoke alters primary human bronchial epithelial cell differentiation at the air-liquid interface. *Sci Rep*. 2015;5:8163.
73. Aufderheide M, Scheffler S, Ito S, Ishikawa S, Emura M. Ciliotoxicity in human primary bronchiolar epithelial cells after repeated exposure at the air-liquid interface with native mainstream smoke of K3R4F cigarettes with and without charcoal filter. *Experimental and Toxicologic Pathology*. 2015;67(7-8):407-11.
74. Talhout R, Opperhuizen A, van Amsterdam JG. Sugars as tobacco ingredient: Effects on mainstream smoke composition. *Food Chem Toxicol*. 2006;44(11):1789-98.
75. Fagerson IS. Thermal degradation of carbohydrates; a review. *Journal of Agricultural and Food Chemistry*. 1969;17(4):747-50.
76. Mattonai M, Tamburini D, Colombini MP, Ribechini E. Timing in Analytical Pyrolysis: Py(HMDS)-GC/MS of Glucose and Cellulose Using Online Micro Reaction Sampler. *Anal Chem*. 2016;88(18):9318-25.
77. Mattonai M, Ribechini E. A comparison of fast and reactive pyrolysis with insitu derivatisation of fructose, inulin and Jerusalem artichoke (*Helianthus tuberosus*). *Anal Chim Acta*. 2018;1017:66-74.
78. Roemer E, Schorp MK, Piadé JJ, Seeman JI, Leyden DE, Haussmann HJ. Scientific assessment of the use of sugars as cigarette tobacco ingredients: a review of published and other publicly available studies. *Crit Rev Toxicol*. 2012;42(3):244-78.

79. Leffingwell J. BA basic chemical constituents of tobacco leaf and differences among tobacco types. Oxford UK: Blackwell Science; 1999. 265-84 p.
80. Cahours X, Verron T, Purkis S. Effect of sugar content on acetaldehyde yield in cigarette smoke. *Beiträge zur Tabakforschung International/Contributions to Tobacco Research*.25(2):381-95.
81. Seeman JI, Laffoon SW, Kassman AJ. Evaluation of relationships between mainstream smoke acetaldehyde and “tar” and carbon monoxide yields in tobacco smoke and reducing sugars in tobacco blends of U.S. commercial cigarettes. *Inhal Toxicol*. 2003;15(4):373-95.
82. Pauwels C, Klerx WNM, Pennings JLA, Boots AW, van Schooten FJ, Opperhuizen A, et al. Cigarette Filter Ventilation and Smoking Protocol Influence Aldehyde Smoke Yields. *Chem Res Toxicol*. 2018;31(6):462-71.
83. De Woskin R, Greenberg M, Pepelko W, Strickland J. Toxicological review of acrolein; in support of summary information on the integrated risk information system (Iris). Washington, DC: US Environmental Protection Agency; 2003. Contract No.: EPA/635/R-03/003.
84. World Health Organization TobLabNet. SOP 8 - Standard operating procedure for determination of aldehydes in mainstream cigarette smoke under ISO and intense smoking conditions. 2018.
85. Hofmann W, Koblinger L, Martonen TB. Structural differences between human and rat lungs: implications for Monte Carlo modeling of aerosol deposition. *Health Phys*. 1989;57 Suppl 1:41-6; discussion 6-7.
86. Phalen RF, Oldham MJ, Wolff RK. The relevance of animal models for aerosol studies. *Journal of aerosol medicine and pulmonary drug delivery*. 2008;21(1):113-24.
87. Miller FJ, Mercer RR, Crapo JD. Lower Respiratory Tract Structure of Laboratory Animals and Humans: Dosimetry Implications. *Aerosol Science and Technology*. 1993;18(3):257-71.
88. Movia D, Bruni-Favier S, Prina-Mello A. In vitro Alternatives to Acute Inhalation Toxicity Studies in Animal Models-A Perspective. *Front Bioeng Biotechnol*. 2020;8:549.
89. Bogdanffy MS, Keller D. Metabolism of xenobiotics by the respiratory tract. *Toxicology of the Lung*. 1999;3:383-407.
90. Oesch F, Fabian E, Landsiedel R. Xenobiotica-metabolizing enzymes in the lung of experimental animals, man and in human lung models. *Archives of Toxicology*. 2019;93(12):3419-89.
91. Corley RA, Kabilan S, Kuprat AP, Carson JP, Jacob RE, Minard KR, et al. Comparative Risks of Aldehyde Constituents in Cigarette Smoke Using Transient Computational Fluid Dynamics/ Physiologically Based Pharmacokinetic Models of the Rat and Human Respiratory Tracts. *Toxicol Sci*. 2015;146(1):65-88.
92. Corley RA, Kabilan S, Kuprat AP, Carson JP, Minard KR, Jacob RE, et al. Comparative computational modeling of airflows and vapor dosimetry in the respiratory tracts of rat, monkey, and human. *Toxicol Sci*. 2012;128(2):500-16.
93. Lee BP, Morton RF, Lee LY. Acute effects of acrolein on breathing: role of vagal bronchopulmonary afferents. *J Appl Physiol*. 1992;72(3):1050-6.
94. Perez CM, Hazari MS, Ledbetter AD, Haykal-Coates N, Carll AP, Cascio WE, et al. Acrolein inhalation alters arterial blood gases and triggers carotid body-mediated cardiovascular responses in hypertensive rats. *Inhal Toxicol*. 2015;27(1):54-63.

95. Xiong R, Wu Q, Bryant M, Rosenfeldt H, Healy S, Cao X. In vitro dosimetry analyses for acrolein exposure in normal human lung epithelial cells and human lung cancer cells. *Environ Toxicol Pharmacol*. 2021;83:103576.
96. Wong BA. Inhalation exposure systems: design, methods and operation. *Toxicol Pathol*. 2007;35(1):3-14.
97. Phalen RF, Mannix RC, Drew RT. Inhalation exposure methodology. *Environ Health Perspect*. 1984;56:23-34.
98. Kogel U, Wong ET, Szostak J, Tan WT, Lucci F, Leroy P, et al. Impact of whole-body versus nose-only inhalation exposure systems on systemic, respiratory, and cardiovascular endpoints in a 2-month cigarette smoke exposure study in the ApoE(-/-) mouse model. *J Appl Toxicol*. 2021;41(10):1598-619.
99. Pauluhn J, Mohr U. Inhalation studies in laboratory animals--current concepts and alternatives. *Toxicol Pathol*. 2000;28(5):734-53.
100. Phelps DW, Veal JT, Buschbom RL, Filipy RE, Wehner AP. Tobacco smoke inhalation studies: a dosimetric comparison of different cigarette types. *Arch Environ Health*. 1984;39(5):359-63.
101. Cheah NP. Volatile aldehydes in tobacco smoke: source fate and risk. [Ph.D. Dissertation Thesis]. Maastricht, The Netherlands: Maastricht University; 2016.
102. Yeager RP, Kushman M, Chemerynski S, Weil R, Fu X, White M, et al. Proposed Mode of Action for Acrolein Respiratory Toxicity Associated with Inhaled Tobacco Smoke. *Toxicol Sci*. 2016;151(2):347-64.
103. Hales CA, Barkin PW, Jung W, Trautman E, Lamborghini D, Herrig N, et al. Synthetic smoke with acrolein but not HCl produces pulmonary edema. *J Appl Physiol* (1985). 1988;64(3):1121-33.
104. Hales CA, Musto SW, Janssens S, Jung W, Quinn DA, Witten M. Smoke aldehyde component influences pulmonary edema. *J Appl Physiol* (1985). 1992;72(2):555-61.
105. Deshmukh HS, Shaver C, Case LM, Dietsch M, Wesselkamper SC, Hardie WD, et al. Acrolein-activated matrix metalloproteinase 9 contributes to persistent mucin production. *Am J Respir Cell Mol Biol*. 2008;38(4):446-54.
106. Borchers MT, Wert SE, Leikauf GD. Acrolein-induced MUC5ac expression in rat airways. *Am J Physiol*. 1998;274(4):L573-81.
107. Borchers MT, Carty MP, Leikauf GD. Regulation of human airway mucins by acrolein and inflammatory mediators. *Am J Physiol*. 1999;276(4):L549-55.
108. Tian M, Xia P, Yan L, Gou X, Giesy JP, Dai J, et al. Toxicological Mechanism of Individual Susceptibility to Formaldehyde-Induced Respiratory Effects. *Environ Sci Technol*. 2022;56(10):6511-24.
109. Yasuo M, Droma Y, Kitaguchi Y, Ito M, Imamura H, Kawakubo M, et al. The relationship between acrolein and oxidative stress in COPD: in systemic plasma and in local lung tissue. *Int J Chron Obstruct Pulmon Dis*. 2019;14:1527-37.
110. Tu C, Mammen MJ, Li J, Shen X, Jiang X, Hu Q, et al. Large-scale, ion-current-based proteomics investigation of bronchoalveolar lavage fluid in chronic obstructive pulmonary disease patients. *J Proteome Res*. 2014;13(2):627-39.
111. Morita K, Masuda N, Oniki K, Saruwatari J, Kajiwarra A, Otake K, et al. Association between the aldehyde dehydrogenase 2*2 allele and smoking-related chronic airway obstruction in a Japanese general population: a pilot study. *Toxicol Lett*. 2015;236(2):117-22.
112. Kuroda A, Hegab AE, Jingtao G, Yamashita S, Hizawa N, Sakamoto T, et al. Effects of the common polymorphism in the human aldehyde dehydrogenase 2 (ALDH2) gene on the lung. *Respir Res*. 2017;18(1):69.

113. Oyama T, Isse T, Ogawa M, Muto M, Uchiyama I, Kawamoto T. Susceptibility to inhalation toxicity of acetaldehyde in Aldh2 knockout mice. *Frontiers in Bioscience-Landmark*. 2007;12(5):1927-34.
114. Churg A, Cosio M, Wright JL. Mechanisms of cigarette smoke-induced COPD: insights from animal models. *Am J Physiol Lung Cell Mol Physiol*. 2008;294(4):L612-31.
115. Churg A, Sin DD, Wright JL. Everything prevents emphysema: are animal models of cigarette smoke-induced chronic obstructive pulmonary disease any use? *Am J Respir Cell Mol Biol*. 2011;45(6):1111-5.
116. Churg A, Wright JL. Testing drugs in animal models of cigarette smoke-induced chronic obstructive pulmonary disease. *Proc Am Thorac Soc*. 2009;6(6):550-2.
117. Sun L, Luo C, Long J, Wei D, Liu J. Acrolein is a mitochondrial toxin: effects on respiratory function and enzyme activities in isolated rat liver mitochondria. *Mitochondrion*. 2006;6(3):136-42.
118. Sisson JH, Tuma DJ, Rennard SI. Acetaldehyde-mediated cilia dysfunction in bovine bronchial epithelial cells. *Am J Physiol*. 1991;260(2 Pt 1):L29-36.
119. Farfán Labonne BE, Gutiérrez M, Gómez-Quiroz LE, Konigsberg Fainstein M, Bucio L, Souza V, et al. Acetaldehyde-induced mitochondrial dysfunction sensitizes hepatocytes to oxidative damage. *Cell Biol Toxicol*. 2009;25(6):599-609.
120. Van Buskirk JJ, Frisell WR. Inhibition by formaldehyde of energy transfer and related processes in rat liver mitochondria. II. Effects on energy-linked reactions in intact mitochondria and phosphorylating particles. *Arch Biochem Biophys*. 1969;132(1):130-8.
121. Zerin T, Kim JS, Gil HW, Song HY, Hong SY. Effects of formaldehyde on mitochondrial dysfunction and apoptosis in SK-N-SH neuroblastoma cells. *Cell Biol Toxicol*. 2015;31(6):261-72.
122. Ma H, Lin J, Li L, Ding Z, Huang P, Song X, et al. Formaldehyde reinforces pro-inflammatory responses of macrophages through induction of glycolysis. *Chemosphere*. 2021;282:131149.
123. Li S, Wei P, Zhang B, Chen K, Shi G, Zhang Z, et al. Apoptosis of lung cells regulated by mitochondrial signal pathway in crotonaldehyde-induced lung injury. *Environ Toxicol*. 2020;35(11):1260-73.
124. Zhang S, Zhang B, Zhang Q, Zhang Z. Crotonaldehyde exposure induces liver dysfunction and mitochondrial energy metabolism disorder in rats. *Toxicol Mech Methods*. 2021;31(6):425-36.
125. Liu XY, Yang ZH, Pan XJ, Zhu MX, Xie JP. Crotonaldehyde induces oxidative stress and caspase-dependent apoptosis in human bronchial epithelial cells. *Toxicol Lett*. 2010;195(1):90-8.
126. Yang BC, Pan XJ, Yang ZH, Xiao FJ, Liu XY, Zhu MX, et al. Crotonaldehyde induces apoptosis in alveolar macrophages through intracellular calcium, mitochondria and p53 signaling pathways. *J Toxicol Sci*. 2013;38(2):225-35.
127. Pei Z, Zhuang Z, Sang H, Wu Z, Meng R, He EY, et al. α,β -Unsaturated aldehyde crotonaldehyde triggers cardiomyocyte contractile dysfunction: role of TRPV1 and mitochondrial function. *Pharmacol Res*. 2014;82:40-50.
128. Clapp PW, Lavrich KS, van Heusden CA, Lazarowski ER, Carson JL, Jaspers I. Cinnamaldehyde in flavored e-cigarette liquids temporarily suppresses bronchial epithelial cell ciliary motility by dysregulation of mitochondrial function. *Am J Physiol Lung Cell Mol Physiol*. 2019;316(3):L470-l86.
129. Acin-Perez R, Benador IY, Petcherski A, Veliova M, Benavides GA, Lagarrigue S, et al. A novel approach to measure mitochondrial respiration in frozen biological samples. *Embo j*. 2020;39(13):e104073.

130. Xu W, Janocha AJ, Leahy RA, Klatte R, Dudzinski D, Mavrakis LA, et al. A novel method for pulmonary research: assessment of bioenergetic function at the air-liquid interface. *Redox Biol.* 2014;2:513-9.
131. Mavin E, Verdon B, Carrie S, Saint-Criq V, Powell J, Kuttruff CA, et al. Real-time measurement of cellular bioenergetics in fully differentiated human nasal epithelial cells grown at air-liquid-interface. *Am J Physiol Lung Cell Mol Physiol.* 2020;318(6):L1158-l64.
132. Lu Q, Mundy M, Chambers E, Lange T, Newton J, Borgas D, et al. Alda-1 Protects Against Acrolein-Induced Acute Lung Injury and Endothelial Barrier Dysfunction. *Am J Respir Cell Mol Biol.* 2017;57(6):662-73.
133. Patil SS, Hernández-Cuervo H, Fukumoto J, Narala VR, Saji S, Borra M, et al. Alda-1 attenuates hyperoxia-induced mitochondrial dysfunction in lung vascular endothelial cells. *Aging (Albany NY).* 2019;11(12):3909-18.
134. Sidramagowda Patil S, Hernández-Cuervo H, Fukumoto J, Krishnamurthy S, Lin M, Alleyn M, et al. Alda-1 Attenuates Hyperoxia-Induced Acute Lung Injury in Mice. *Front Pharmacol.* 2020;11:597942.
135. Tsai HY, Hsu YJ, Lu CY, Tsai MC, Hung WC, Chen PC, et al. Pharmacological Activation Of Aldehyde Dehydrogenase 2 Protects Against Heatstroke-Induced Acute Lung Injury by Modulating Oxidative Stress and Endothelial Dysfunction. *Front Immunol.* 2021;12:740562.
136. Cao Z, Qin H, Huang Y, Zhao Y, Chen Z, Hu J, et al. Crosstalk of pyroptosis, ferroptosis, and mitochondrial aldehyde dehydrogenase 2-related mechanisms in sepsis-induced lung injury in a mouse model. *Bioengineered.* 2022;13(3):4810-20.
137. Li K, Guo W, Li Z, Wang Y, Sun B, Xu D, et al. ALDH2 Repression Promotes Lung Tumor Progression via Accumulated Acetaldehyde and DNA Damage. *Neoplasia.* 2019;21(6):602-14.
138. Hua T, Yang M, Zhou Y, Chen L, Wu H, Liu R. Alda-1 Prevents Pulmonary Epithelial Barrier Dysfunction following Severe Hemorrhagic Shock through Clearance of Reactive Aldehydes. *Biomed Res Int.* 2019;2019:2476252.
139. Ma X, Luo Q, Zhu H, Liu X, Dong Z, Zhang K, et al. Aldehyde dehydrogenase 2 activation ameliorates CCl(4) -induced chronic liver fibrosis in mice by up-regulating Nrf2/HO-1 antioxidant pathway. *J Cell Mol Med.* 2018;22(8):3965-78.
140. Kornfeld OS, Hwang S, Disatnik MH, Chen CH, Qvit N, Mochly-Rosen D. Mitochondrial reactive oxygen species at the heart of the matter: new therapeutic approaches for cardiovascular diseases. *Circ Res.* 2015;116(11):1783-99.
141. Pan C, Xing JH, Zhang C, Zhang YM, Zhang LT, Wei SJ, et al. Aldehyde dehydrogenase 2 inhibits inflammatory response and regulates atherosclerotic plaque. *Oncotarget.* 2016;7(24):35562-76.
142. Panisello-Roselló A, Lopez A, Folch-Puy E, Carbonell T, Rolo A, Palmeira C, et al. Role of aldehyde dehydrogenase 2 in ischemia reperfusion injury: An update. *World J Gastroenterol.* 2018;24(27):2984-94.
143. Mali VR, Palaniyandi SS. Regulation and therapeutic strategies of 4-hydroxy-2-nonenal metabolism in heart disease. *Free Radic Res.* 2014;48(3):251-63.
144. Ning S, Budas GR, Churchill EN, Chen CH, Knox SJ, Mochly-Rosen D. Mitigation of radiation-induced dermatitis by activation of aldehyde dehydrogenase 2 using topical alda-1 in mice. *Radiat Res.* 2012;178(1):69-74.
145. Burcham PC, Pyke SM. Hydralazine inhibits rapid acrolein-induced protein oligomerization: role of aldehyde scavenging and adduct trapping in cross-link blocking and cytoprotection. *Mol Pharmacol.* 2006;69(3):1056-65.

146. Wondrak GT, Cervantes-Laurean D, Roberts MJ, Qasem JG, Kim M, Jacobson EL, et al. Identification of alpha-dicarbonyl scavengers for cellular protection against carbonyl stress. *Biochem Pharmacol.* 2002;63(3):361-73.
147. Vistoli G, Orioli M, Pedretti A, Regazzoni L, Canevotti R, Negrisoli G, et al. Design, synthesis, and evaluation of carnosine derivatives as selective and efficient sequestering agents of cytotoxic reactive carbonyl species. *ChemMedChem.* 2009;4(6):967-75.
148. Rahman I. Pharmacological antioxidant strategies as therapeutic interventions for COPD. *Biochim Biophys Acta.* 2012;1822(5):714-28.
149. Tian R, Shi R. Dimercaprol is an acrolein scavenger that mitigates acrolein-mediated PC-12 cells toxicity and reduces acrolein in rat following spinal cord injury. *J Neurochem.* 2017;141(5):708-20.
150. Shi L, Lin Y, Jiao Y, Herr SA, Tang J, Rogers E, et al. Acrolein scavenger dimercaprol offers neuroprotection in an animal model of Parkinson's disease: implication of acrolein and TRPA1. *Transl Neurodegener.* 2021;10(1):13.
151. Mai X, Zhou F, Lin P, Lin S, Gao J, Ma Y, et al. Metformin scavenges formaldehyde and attenuates formaldehyde-induced bovine serum albumin crosslinking and cellular DNA damage. *Environ Toxicol.* 2020;35(11):1170-8.
152. Baker RR, da Silva JRP, Smith G. The effect of tobacco ingredients on smoke chemistry. Part I: Flavourings and additives. *Food Chem Toxicol.* 2004;42:3-37.
153. Stijns MMJPE, Randall MJ, Bast A, Haenen GRMM. Adaptation to acrolein through upregulating the protection by glutathione in human bronchial epithelial cells: The materialization of the hormesis concept. *Biochemical and Biophysical Research Communications.* 2014;446(4):1029-34.
154. Moghe A, Ghare S, Lamoreau B, Mohammad M, Barve S, McClain C, et al. Molecular mechanisms of acrolein toxicity: relevance to human disease. *Toxicol Sci.* 2015;143(2):242-55.

Impact paragraph

Worldwide tobacco epidemic – societal impact

Although it is known for years that tobacco smoking is harmful for health and a preventable cause of death, smoking is still a worldwide problem as 22.3% of the global population is using tobacco products. In addition, more than 8 million people die due to tobacco smoking globally each year, including 1.2 million deaths due to second-hand tobacco smoke (1). Also in the Netherlands, 1 out of 5 people is smoking and smoking is an important cause of illness and death as approximately >19.000 smokers die yearly (2, 3). Moreover, tobacco use has substantial societal and economic effects as 9.4% of the burden of disease is due to smoking in the Netherlands (2).

Last decades, several measures are taken by the World Health Organization (WHO) Framework Convention on Tobacco Control (FCTC) and the WHO Study Group on Tobacco Product Regulation (TobReg) to address the worldwide tobacco epidemic. Their focus is to prevent initiation of tobacco use, promote cessation of tobacco use and protect against exposure to second-hand tobacco smoke. Altogether, these measures aim to reduce tobacco-related morbidity and mortality. Moreover, WHO FCTC acknowledges that regulation of contents and composition of emissions of tobacco products (Articles 9 and 10) is required in order to reduce attractiveness, addictiveness as well as toxicity of tobacco products. Although quitting smoking is the preferred option to reduce the detrimental impact of tobacco on human health and the economy, less harmful tobacco products can be beneficial for the smokers' health given the addictiveness of tobacco consumption. Regulation of chemicals present in tobacco products is largely lacking, except for nicotine, carbon monoxide and tar. Moreover, it is not conclusively proven yet that lowering of specific components in tobacco will contribute to a reduced risk of mortality and morbidity of smokers. Based on toxicity data, one of thousands of toxicants suggested to be potential for mandated lowering by the WHO FCTC are the chemical group of aldehydes which, in the context of cigarette smoke (CS), mainly include acetaldehyde, acrolein and formaldehyde. (4, 5)

With regard to the morbidity and mortality numbers described above, it has to be mentioned that tobacco smoking is an important main risk factor for several respiratory diseases including chronic obstructive pulmonary disease (COPD) (6). COPD is a leading cause of death globally (7, 8). Mainly symptomatic treatments are available focusing on ameliorating lung function and reducing exacerbation (risk), however no cure exists for COPD patients (6, 9). COPD is a multifactorial disease in which, besides inflammation and oxidative stress, mitochondrial dysfunction is suggested to play a role (10, 11). Nowadays, mitochondrial dysfunction has been firmly implicated in the pathogenesis of COPD (12, 13), and CS-induced abnormalities in mitochondrial morphology and function have been described in literature (12-16). However, the underlying molecular mechanisms controlling mitochondrial content, metabolism and function (mitochondrial biogenesis, mitophagy, mitochondrial dynamics) in (epithelial)

cells of the lungs and airways are incompletely understood in COPD patients as well as upon exposure to CS and CS-associated aldehydes. Therefore, the aim of this thesis was to investigate the impact of several aldehydes (relevant for CS-exposure) on the molecular pathways regulating mitochondrial function in epithelial cells of the lungs and airways in the context of COPD.

Impact on fundamental and applied science

Our findings in **Chapter 2** provided novel insights in the extent of abnormalities in the molecular regulation (mitochondrial biogenesis *versus* mitophagy) of mitochondrial metabolism in COPD peripheral lung tissue. Directionality of the observed alterations in gene- and protein expression was dependent on disease status, showing more pronounced changes in very severe COPD patients. Moreover, as we observed discrepancies in the findings in different (cellular) compartments of the airways and lungs, this data emphasized the importance of using models reflecting different parts of the airways and lungs. Based on our results, the next step is to investigate if the observed alterations in mitochondrial turnover processes in lung tissue homogenates play a significant role in the pathogenesis of COPD, are responsible for alterations in mitochondrial function or may represent compensatory mechanisms. Our findings accompanied by additional data from future studies would contribute to filling this knowledge gap and discovering potential new therapy targets for COPD.

As in science there is an urgent request for transition from use of *in vivo* to *in vitro* models, we contributed to this aim by analyzing the relevance and applicability of various cellular and smoke exposure *in vitro* models in the context of our research question. The findings in **Chapter 3** highlighted the importance of making a thought-out choice for an *in vitro* exposure model, which is tailored to the specific research question. By comparing more advanced models using differentiated primary bronchial epithelial cell cultures exposed to whole CS to more simple conventional models using submerged primary bronchial epithelial cell cultures and CS extract, we aimed to encourage future inhalation toxicology researchers to carefully consider if and when it is needed to use more complex models over the more simple *in vitro* models. This study hopefully creates more awareness for the pitfall to assume that more complex models are ‘better’, while in particular cases the simple models are sufficient to answer the research question and thereby save time and money.

Taken into account the findings of **Chapters 2 and 3**, our studies support the value of comparison of various experimental models to consider applicability for respiratory (toxicology) studies. In the future, even more complex models mimicking the human lung environment (e.g., co-cultures, organs-on-chip) should be included in this research field.

Furthermore, in this thesis, we studied the regulation of mitochondrial metabolism in response to noxious particles, i.e., CS and aldehydes, in several *in vivo* and *in vitro* models. We observed differences in degree of effect of CS, mix of aldehydes or acrolein exposure *in vivo* or *in vitro*, following an acute or sub-acute exposure regime (**Chapters 4, 5, 6**). Heterogeneity observed in the results of these studies could be explained by the variety in models used (*in vivo* rat (lung) *versus in vitro* human primary bronchial epithelial cells), route (nose-only, whole-body) and duration of exposure (acute *versus* sub-acute), mixture (CS or three aldehydes) *versus* the individual aldehyde acrolein, and dosimetry. These studies elaborate the knowledge about fundamental pathways involved in the regulation of molecules associated with mitochondrial biogenesis, mitophagy and mitochondrial dynamics in response to CS or aldehydes, which is a suggested mechanism to predispose to COPD. Future studies could focus on the (potential additive/synergistic) impact of (other) compounds (individually or in a mixture) emitted by CS on the function of mitochondria to contribute to and/or strengthen the evidence reported in our studies. It is important to take into account the translational impact of our findings to the human situation, but also to consider what is the most informative and applicable model matching the research question. This data again underscores the importance of a considered choice for the use of a specific research model. The innovative model developed in **Chapter 6** contributes to the transition to *in vitro* research (replace). This model (puff-like exposure, differentiated cultures) could be of value for future research in the field of inhalation toxicology of noxious particles and unravelling molecular mechanisms underlying respiratory diseases. Moreover, we also used lung material from animal studies which were designed and conducted by collaborating research groups (reduce; **Chapters 4 and 5**) and we build on their already published findings (17, 18). By reusing these samples from previous executed animal studies, the needless repeating of animal studies and corresponding unnecessary use of animals is prevented. In conclusion, lessons learned from our studies could be used for design of future studies in this research field, taking into account the challenges faced regarding dosimetry (e.g., dose, peak-exposure mimicking puff topography), mixture toxicology, exposure duration and route, and model used.

Lastly, the knowledge from our studies combined with additional insights about the causal and mechanistic impact of several aldehydes (relevant for CS-exposure) on the molecular pathways controlling mitochondrial content, mitochondrial function and metabolism in epithelial cells of the lungs and airways in the context of COPD could contribute to detect, investigate and develop potential therapeutic applications targeting aldehydes-induced mitochondrial dysfunction in COPD therapy in the future.

Impact on regulation

Despite the initiation by the WHO FCTC to approach the tobacco epidemic by aiming to reduce harmful components present in CS, minimal progress has been made last years with respect to regulation of specific chemicals. This research project aimed to provide additional scientific evidence to fill the knowledge gaps regarding the impact of aldehydes emitted by CS on epithelial cells of the airways, in particular related to the molecular regulation of mitochondrial content/function. The evidence described in this thesis aims to provide, together with other (previous) research, a scientific basis to potential regulate aldehydes content/composition of emissions in CS in the future. Nevertheless, as described in **Chapters 4, 5, 6** our findings regarding the impact of a mixture of aldehydes *versus* individual aldehydes were inconclusive making it hard to draw any conclusions and recommendations for future regulation only based on our data. Therefore, policy makers should critically review and take into account all available scientific literature and acknowledge the current knowledge gaps in their consideration for the mandated lowering/regulation of aldehydes ((added) sugars) in CS and limit emission of CS-associated aldehydes in tobacco products. Our research creates more awareness of the need and potential for regulation of the contents and composition of emissions of tobacco products, in particular sugars and additives in tobacco (smoke). Decreasing sugar yield, selection of specific tobacco types and design of a cigarette (e.g., cigarette filter ventilation) are ways to reduce aldehyde content in cigarettes (19-21). In addition, the amount of aldehydes exposure of a smoker depends on smoking behavior/topography (21). In follow-up of our research, additional studies are necessary to prove if a reduction of specific aldehydes in CS is required and to what extent this should be in order to induce a beneficial health effect for smokers in relation to mitochondrial (dys)function and COPD development. In addition, based on our findings, it is interesting for other researchers to investigate the impact of exposure to aldehydes or other CS-components alone or possible (additive/synergistic) interaction with other compounds in the mix of thousands of chemicals present in CS.

Target groups

The findings from this thesis are relevant for several target groups. First and foremost, the research described in this thesis is relevant for other researchers in the field of respiratory diseases and inhalation toxicology. We aimed to contribute to the knowledge about the underlying molecular mechanisms involved in the regulation of mitochondrial content, function and metabolism in (epithelial) cells of the airways and lungs in response to smoking-associated aldehydes exposure in the context of COPD. By investigating this, we hope to extend knowledge in this research field, set a basis for further research and might reveal therapeutic targets for this disease. With respect to inhalation toxicology, we also aimed to provide insight in differences and similarities

between the various *in vitro* models and *in vivo* models, emphasizing the importance of tailoring the model to the research question. In addition, we deployed a sophisticated (puff-like) exposure model for differentiated primary bronchial epithelial cells to a mixture of aldehydes and CS, which could be used in future research in the field of inhalation toxicology but is also applicable to research disciplines outside this area. Secondly, as described in the paragraphs above, our study is relevant for policy makers. Although our findings did not provide conclusive evidence for regulation of aldehydes in CS, it is relevant for policy makers to include our findings in the review of available scientific literature to consider the potential (health) impact of the regulation/lowering of aldehydes ((added) sugars) to the emission of CS-associated aldehydes in tobacco products and acknowledge the current knowledge gaps.

Conclusion

In conclusion, the research described in this thesis provides a comprehensive overview of the impact of CS and aldehydes on the regulation of processes involved in mitochondrial content, function and metabolism in the context of COPD using various *in vitro* and *in vivo* exposure models of the airways and lungs. By comparing various experimental models, our study highlights the importance of making considered choices for experimental model and exposure type/regime tailoring the research question. Moreover, our data contribute to the knowledge about aldehydes-induced mitochondrial toxicity in (epithelial) cells of the lungs and airways. These findings may be of value for both researchers in the field of respiratory diseases and inhalation toxicology. Furthermore, our study provided additional data which could be taken into account by policy makers to consider potential (health) impact by future regulation (lowering) of aldehydes levels in CS. Altogether, this thesis contributes to reducing the detrimental impact of smoking on society, economy and health status, in particular with regard to COPD.

References

1. World Health Organization. Factsheet Tobacco: WHO; 2022 [updated 05/24/2022. Available from: <https://www.who.int/news-room/fact-sheets/detail/tobacco>
2. Rijksinstituut voor Volksgezondheid en Milieu. Volksgezondheid Toekomst Verkenning 2018 - Een gezond vooruitzicht synthese. 2018.
3. Gezondheidsenquête/Leefstijlmonitor. CBS i.s.m. RIVM en Trimbos-Instituut; 2021.
4. Burns DM, Dybing E, Gray N, Hecht S, Anderson C, Sanner T, et al. Mandated lowering of toxicants in cigarette smoke: a description of the World Health Organization TobReg proposal. *Tob Control*. 2008;17(2):132-41.
5. World Health Organization & World Health Organization Tobacco Free Initiative. The scientific basis of tobacco product regulation: second report of a WHO study group. World Health Organization; 2008.
6. Global Initiative For Chronic Obstructive Lung Disease. Global Strategy for Diagnosis, Management, and Prevention of Chronic Obstructive Lung Disease: 2022 Report. 2022.
7. GBD 2015 Mortality and Causes of Death Collaborators. Global, regional, and national life expectancy, all-cause mortality, and cause-specific mortality for 249 causes of death, 1980-2015: a systematic analysis for the Global Burden of Disease Study 2015. *Lancet*. 2016;388(10053):1459-544.
8. GBD 2019 Diseases and Injuries Collaborators. Global burden of 369 diseases and injuries in 204 countries and territories, 1990-2019: a systematic analysis for the Global Burden of Disease Study 2019. *Lancet*. 2020;396(10258):1204-22.
9. Matera MG, Cazzola M, Page C. Prospects for COPD treatment. *Curr Opin Pharmacol*. 2021;56:74-84.
10. MacNee W. Pathogenesis of Chronic Obstructive Pulmonary Disease. *Clinics in Chest Medicine*. 2007;28(3):479-513.
11. Ryter SW, Rosas IO, Owen CA, Martinez FJ, Choi ME, Lee CG, et al. Mitochondrial Dysfunction as a Pathogenic Mediator of Chronic Obstructive Pulmonary Disease and Idiopathic Pulmonary Fibrosis. *Ann Am Thorac Soc*. 2018;15(Suppl 4):S266-s72.
12. Hoffmann RF, Zarrintan S, Brandenburg SM, Kol A, de Bruin HG, Jafari S, et al. Prolonged cigarette smoke exposure alters mitochondrial structure and function in airway epithelial cells. *Respir Res*. 2013;14:97.
13. Hara H, Araya J, Ito S, Kobayashi K, Takasaka N, Yoshii Y, et al. Mitochondrial fragmentation in cigarette smoke-induced bronchial epithelial cell senescence. *Am J Physiol Lung Cell Mol Physiol*. 2013;305(10):L737-46.
14. Sundar IK, Maremanda KP, Rahman I. Mitochondrial dysfunction is associated with Mito1 reduction in lung epithelial cells by cigarette smoke. *Toxicol Lett*. 2019;317:92-101.
15. Ballweg K, Mutze K, Königshoff M, Eickelberg O, Meiners S. Cigarette smoke extract affects mitochondrial function in alveolar epithelial cells. *Am J Physiol Lung Cell Mol Physiol*. 2014;307(11):L895-907.
16. Aghapour M, Remels AHV, Pouwels SD, Bruder D, Hiemstra PS, Cloonan SM, et al. Mitochondria: at the crossroads of regulating lung epithelial cell function in chronic obstructive pulmonary disease. *Am J Physiol Lung Cell Mol Physiol*. 2020;318(1):L149-l64.

17. Snow SJ, McGee MA, Henriquez A, Richards JE, Schladweiler MC, Ledbetter AD, et al. Respiratory Effects and Systemic Stress Response Following Acute Acrolein Inhalation in Rats. *Toxicol Sci.* 2017;158(2):454-64.
18. Liu X, Durkes AC, Schrock W, Zheng W, Sivasankar MP. Subacute acrolein exposure to rat larynx in vivo. *Laryngoscope.* 2019;129(9):E313-E7.
19. Talhout R, Opperhuizen A, van Amsterdam JG. Sugars as tobacco ingredient: Effects on mainstream smoke composition. *Food Chem Toxicol.* 2006;44(11):1789-98.
20. Baker RR, da Silva JRP, Smith G. The effect of tobacco ingredients on smoke chemistry. Part I: Flavourings and additives. *Food Chem Toxicol.* 2004;42:3-37.
21. Pauwels C, Klerx WNM, Pennings JLA, Boots AW, van Schooten FJ, Opperhuizen A, et al. Cigarette Filter Ventilation and Smoking Protocol Influence Aldehyde Smoke Yields. *Chem Res Toxicol.* 2018;31(6):462-71.

Nederlandse samenvatting

Wereldwijde tabak epidemie

Het roken van tabak heeft een desastreuze invloed op de gezondheid en daarmee een significante impact op de maatschappij wereldwijd. Hoewel het al tientallen jaren bekend is dat roken schadelijk is voor de gezondheid en sterfte- en ziektelast als gevolg van sigarettenrook voorkomen zouden kunnen worden, rookt momenteel nog steeds 22.3% van de wereldbevolking.

Roken van sigaretten is de meest voorkomende vorm van tabak consumptie. Gedurende de verbranding van tabak worden meer dan 6000 chemische componenten gevormd, waaronder verschillende reactieve aldehyden. De korte-keten aldehyden: acroleïne, acetaldehyde en formaldehyde behoren tot de meest respiratoir toxische stoffen aanwezig in sigarettenrook.

De afgelopen decennia zijn er verschillende maatregelen geïnitieerd door de Wereldgezondheidsorganisatie (WHO) Framework Convention on Tobacco Control (FCTC) en de WHO Study Group on Tobacco Product Regulation (TobReg) om de tabak epidemie aan te pakken. Naast de focus op preventie van starten met roken, bevordering van stoppen met roken en bescherming tegen blootstelling aan tweedehands tabaksrook, erkennen zij ook de urgentie van de toekomstige regulering van inhoud en samenstelling van tabaksproducten zoals beschreven in de artikelen 9 en 10 van WHO FCTC. Deze artikelen richten zich op het verminderen van de aantrekkelijkheid, mate van verslaving en toxiciteit van tabaksproducten. Momenteel zijn alleen de stoffen nicotine, teer en koolstofmonoxide gereguleerd, en staan onder andere de aldehyden: acroleïne, acetaldehyde, formaldehyde op de lijst voor potentiële regulering in sigarettenrook.

Mitochondriële dysfunctie in epitheelcellen van de longen en luchtwegen

Blootstelling aan sigarettenrook is een van de voornaamste risicofactoren voor het ontwikkelen van chronische obstructieve long ziekte (COPD). COPD is belangrijke doodsoorzaak wereldwijd. Echter, de onderliggende moleculaire mechanismen die ten grondslag liggen aan de pathogenese van de multifactoriële ziekte COPD zijn niet volledig bekend. Naast de belangrijke rol van inflammatie, oxidatieve stress en remodeleren van de luchtwegwand, suggereert recente literatuur betrokkenheid van mitochondriële dysfunctie in de pathogenese van COPD. Adequate functie van mitochondria is essentieel voor het functioneren van de longcellen, aangezien mitochondria zowel noodzakelijk zijn voor de energieproductie alsook betrokken zijn in het controleren van cellulaire processen zoals inflammatie, oxidatieve stress en celdood. Mitochondriële homeostase is hierbij afhankelijk van dynamische processen,

zoals de aanmaak van nieuwe mitochondria (mitochondriële biogenese), de afbraak van beschadigde of dysfunctionele mitochondria (mitofagie) en de flux van fusie of splijting van mitochondria. Enkele studies rapporteren afwijkingen in mitochondriële morfologie en mitochondriële functie in luchtwegcellen of in longweefsel van COPD-patiënten, en daarnaast ook in respons op sigarettenrook in verschillende *in vitro* en *in vivo* modellen. Bovendien is een causaal verband tussen mitochondriële dysfunctie en de ontwikkeling van COPD reeds aangetoond in een muis model. In deze studie toonden de onderzoekers aan dat het voorkomen van dysfunctie van de mitochondriën in een muismodel van rook-geïnduceerd COPD tot gevolg had dat de ernst van emfyseem en bronchitis afnamen. Echter ontbreekt kennis met betrekking tot welke moleculaire mechanismen ten grondslag liggen aan de rook-geïnduceerde mitochondriële dysfunctie (in de longen en luchtwegen van COPD patiënten) en daarnaast is het onbekend welke stoffen in sigarettenrook verantwoordelijk zijn voor de mitochondriële dysfunctie.

Aangezien sigarettenrook bestaat uit een mengsel van duizenden chemische stoffen, is het momenteel onbekend welke exacte componenten de veroorzakers zijn van mitochondriële schade geïnduceerd door sigarettenrook. De aldehyden worden aangewezen als mogelijke kritische stoffen in sigarettenrook. Dit wordt ondersteund door enkele *in vitro* studies waarin longcellen werden blootgesteld aan individuele aldehyden (voornamelijk longepitheel cellijnen blootgesteld aan acroleïne), wat leidde tot verstoring van processen betrokken bij mitochondriële homeostase. Echter, uitgebreid onderzoek naar de impact van aldehyden op de regulatie van de essentiële regulatoren betrokken bij aanmaak en afbraak van mitochondria, fusie en splijting van mitochondriën en mitochondrieel metabolisme in geavanceerde *in vitro* modellen (primaire culturen) en *in vivo* modellen ontbreekt in de huidige literatuur. Bovendien is aanvullend wetenschappelijk bewijs vereist om de wettelijke regulering (verlaging) van de aldehyden acetaldehyde, acroleïne en formaldehyde in sigarettenrook te onderbouwen. Dit proefschrift heeft als doel om hieraan bij te dragen door middel van het ontrafelen van de moleculaire mechanismen die ten grondslag liggen aan mitochondriële dysfunctie in (epitheel) cellen van de longen en luchtwegen in reactie op blootstelling aan aldehyden.

In dit proefschrift werd daarom de volgende hypothese onderzocht: aldehyden aanwezig in sigarettenrook verstoren de moleculaire regulatie van mitochondriële functie in epitheelcellen van de longen en luchtwegen wat bijdraagt aan het risico op COPD. Om deze hypothese te onderzoeken hebben wij verschillende experimentele modellen gebruikt: 1) perifeer longweefsel van COPD patiënten, 2) primaire kweken van humane bronchiale epitheelcellen van COPD patiënten en non-COPD patiënten (*in vitro*) en 3) diermodellen (*in vivo*). Deze modellen verschillen in blootstelling met betrekking tot sigarettenrook en aldehyden (mix van aldehyden of acroleïne), blootstellingsduur (acuut *versus* sub-acuut), type blootstelling (gas of extract, mengsel *versus* individuele chemische stof), blootstellingsroute, en dosimetrie. In deze modellen

werd onder andere de regulatie van mitochondriële biogenese en afbraak (mitofagie) onderzocht door middel van analyse van de expressie van genen en eiwitten die hierbij betrokken zijn en daarnaast ook het aantal kopieën mitochondrieel DNA (i.e., maat voor mitochondriële content) en activiteit van enzymen betrokken in metabole processen.

Verstoringen in de moleculaire regulatie van mitochondriële biogenese en mitofagie in perifeer longweefsel van COPD-patiënten

In aanvulling op de huidige literatuur is onderzoek nodig om te analyseren hoe moleculaire regulatoren van mitochondriële biogenese en mitofagie verstoord zijn in longcellen van COPD patiënten. Bovendien dient te worden onderzocht of de regulatie van deze moleculaire processen verschilt in diverse regio's van de long, bijvoorbeeld in perifeer longweefsel *versus* bronchiale epitheelcellen. Daarom werd in **hoofdstuk 2** gen- en eiwitexpressie onderzocht van moleculen betrokken bij deze processen (o.a. biogenese en afbraak van mitochondriën, fusie en splijting) in perifeer longweefsel van COPD patiënten in verschillende stadia van het ziekteproces en in (on) gedifferentieerde primaire bronchiale epitheelcellen van COPD en non-COPD patiënten. Een verlaagde mRNA expressie van regulatoren betrokken bij mitochondriële biogenese werd aangetoond in perifeer longweefsel van zeer ernstig zieke COPD patiënten, wat positief gecorreleerd bleek met long functie parameters. Daarentegen waren mRNA levels van transcriptie factor *TFAM* (biogenese) en *BNIP3L* (mitofagie) verhoogd in patiënten met zeer ernstige COPD, hetgeen negatief correleerde met longfunctie. Deze veranderingen werden echter niet geobserveerd op eiwit niveau of in primaire bronchiale epitheelcellen.

Toekomstig onderzoek zal moeten uitwijzen of deze veranderingen significant bijdragen aan de pathogenese van COPD, ten grondslag liggen aan veranderingen in mitochondriële functie of eventueel compensatiemechanismen zijn.

Deregulatie van mitochondrieel metabolisme na sigaretten-rook blootstelling in verschillende humane bronchiale epitheelcel modellen

Aangezien het niet volledig duidelijk is hoe sigarettenrook de moleculaire regulatie van mitochondrieel metabolisme en processen die daar bij betrokken zijn beïnvloedt in de bronchiale epitheelcellen van de luchtwegen, hebben wij dit in **hoofdstuk 3** onderzocht.

Vier verschillende experimentele modellen van blootstelling aan sigarettenrook of sigarettenrook extract (beiden gemaakt van Kentucky 3R4F referentie sigaretten)

werden gebruikt. (1) gedifferentieerde primaire bronchiale epitheelcellen gekweekt op air-liquid interface werden acuut blootgesteld aan sigarettenrook, (2) primaire bronchiale epitheelcellen gekweekt op air-liquid interface werden chronisch blootgesteld aan sigarettenrook tijdens differentiatie gevolgd door het stoppen van de blootstelling, (3) ongedifferentieerde primaire bronchiale epitheelcellen submerged gekweekt werden acuut blootgesteld aan sigarettenrook en (4) ongedifferentieerde primaire bronchiale epitheelcellen submerged gekweekt werden blootgesteld aan sigarettenrook extract. Deze modellen reflecteren verschillende typen en/of stadia van schade aan het bronchiaal epithelium, relevant om de respons op blootstelling aan respiratoir toxische stoffen te bestuderen. De gedifferentieerde primaire bronchiale epitheelcel culturen reflecteren een intact pseudo-gestratificeerd epithelium (inclusief basale cellen, secretoire club cellen en trilhaarcellen), terwijl ongedifferentieerde primaire bronchiale epitheelcel culturen bestaan uit basale cel typen wat overeenkomt met een beschadigde, gedeeltelijk 'ontmaskerde/onbeschermde' epitheel laag. Herstel van het bronchiaal epitheel werd onderzocht in het model waarin chronische sigarettenrook blootstelling tijdens differentiatie van de primaire bronchiale epitheelcellen werd gevolgd door stopzetten van de blootstelling. Bovendien werden deze modellen verschillend blootgesteld: sigarettenrook (inclusief componenten aanwezig in de verschillende fases: gas en deeltjes) *versus* waterig sigarettenrook extract (zonder vluchtige componenten).

Eiwit- en transcriptniveaus evenals enzymactiviteit van essentiële moleculen die betrokken zijn bij de regulatie van mitochondriële biogenese, mitofagie, fusie- en splijting van mitochondria en mitochondrieel energiemetabolisme werden in deze modellen bestudeerd. Verhoging van de gen- en eiwitexpressie van moleculen die geassocieerd worden met autofagie en receptor-gemedieerde mitofagie werd waargenomen in de verschillende *in vitro* primaire bronchiale epitheelcel modellen, zowel na acute als ook na chronische blootstelling (hoewel minder uitgesproken). Deze resultaten suggereren een impact van sigarettenrook op de regulatie van processen betrokken bij afbraak van mitochondria in zowel een intact, beschadigd als tijdens herstel van het bronchiaal epithelium. Echter, het aantal kopieën mitochondrieel DNA (i.e. maat voor mitochondriële content) en de gen- en eiwitexpressie van onderdelen van de elektronen transport keten evenals expressie van moleculen betrokken bij fusie/splijting van mitochondria leken grotendeels onveranderd na blootstelling aan sigarettenrook in de modellen. Ten slotte, in de gedifferentieerde primaire bronchiale epitheelcel culturen werden veranderingen in de moleculaire controle van mitochondriële biogenese waargenomen en ook detecteerden wij een verhoogd glycolyse metabolisme in reactie op blootstelling aan sigarettenrook. De beschreven veranderingen bleven gedeeltelijk in stand in het model van chronische blootstelling tijdens differentiatie, en de daaropvolgende stopzetting van blootstelling. De overeenkomsten laten zien dat rook blootstelling een verandering in de regulatie van mitofagie en mitochondriële biogenese induceert in de verschillende modellen, terwijl

de waargenomen verschillen in de regulatie van mitochondriële (metabole) processen in de verschillende modellen het belang benadrukken van het afstemmen van het *in vitro* model op de onderzoeksvraag.

Inhalatie van acroleïne heeft effect op de moleculaire regulatie van mitochondrieel metabolisme en functie in longweefsel van ratten

In welke mate inhalatie van acroleïne (als component van sigarettenrook) invloed heeft op processen die mitochondrieel metabolisme en mitochondriële content/functie reguleren *in vivo* is nauwelijks beschreven in de literatuur.

Daarom hebben wij, in **hoofdstuk 4**, het effect van inhalatie van acroleïne via de neus (0-2-4 ppm; 4 uur/dag voor 1 of 2 dagen) onderzocht op de enzymactiviteit, eiwit- en genexpressie van regulatoren van mitochondrieel metabolisme in de longen van ratten. De impact van acute acroleïne blootstelling op de enzymactiviteit, eiwit- en genexpressie van regulatoren van mitochondriële functie was dosis- en tijdsafhankelijk. Er werd voornamelijk een verlaagde mRNA- en eiwit expressie van regulatoren betrokken bij mitochondriële biogenese en expressie van onderdelen van de elektronentransportketen waargenomen. Moleculen betrokken bij mitofagie bleken onveranderd.

Vervolgens, hebben wij dit, in **hoofdstuk 5**, verder onderzocht door te kijken naar het effect van acroleïne na langdurige blootstelling. Deze langdurige blootstelling is potentieel een meer representatief blootstellingsregime voor de chronische blootstelling van rokers. In deze studie werden ratten blootgesteld aan acroleïne gedurende 4 weken ('whole body'; 0-3 ppm; 5 uur per dag/5 dagen/week). Genexpressie van inflammatoire genen was verhoogd na acroleïne blootstelling. Daarnaast resulteerde acroleïne blootstelling in een verlaagde enzymactiviteit en/of transcriptie niveaus van regulatoren betrokken bij de verbranding van vetzuren en glucose metabolisme, wat mogelijk duidt op veranderingen in metabole processen (substraat gebruik). Expressie van regulatoren betrokken bij biogenese en afbraak van mitochondriën bleken onveranderd.

Het in meer detail begrijpen van het effect van acroleïne (alsook andere aldehyden) op de functie van mitochondriën zal moeten uitwijzen of aldehyden in sigarettenrook bijdragen aan mitochondriële dysfunctie en of dit daarom ook een argument zal zijn voor de regulering van aldehyden in sigarettenrook.

Impact van aldehyden op de moleculaire mechanismen die mitochondriële content en functie reguleren in humane primaire bronchiale epitheelcellen

Zoals eerder aangegeven focust de huidige maar schaarse literatuur in dit veld zich voornamelijk op onderzoek naar blootstelling van longcellijnen aan individuele aldehyden (met name acroleïne). Relevanter echter zijn studies naar de impact van een mengsel van aldehyden in meer geavanceerde *in vitro* modellen van primaire cel culturen waarbij een fysiologisch relevant blootstelling regime (puf-regime) wordt gebruikt. Dit ontbreekt momenteel in de literatuur. Daarom hebben wij in **hoofdstuk 6** een *in vitro* model ontwikkeld om te onderzoeken wat de invloed is van een mengsel van acetaldehyde, acroleïne en formaldehyde op de moleculaire regulatie van mitochondriële content en functie in gedifferentieerde humane primaire bronchiale epitheelcellen. Hiertoe hebben wij primaire bronchiale epitheelcel culturen van 4 non-COPD donoren blootgesteld aan de rook van één sigaret (Marlboro Red) of een vergelijkbaar mengsel van acetaldehyde, acroleïne en formaldehyde of lucht (controle) in een systeem met een continue luchtflow waarbij een puf-regime werd aangehouden (Health Canadian Intense regime, 8 puffen). Blootstelling aan sigarettenrook of een mengsel van aldehyden resulteerde niet in een verhoogde celdood. Na blootstelling aan sigarettenrook werden verhoogde eiwit en mRNA levels van Interleukine-8 waargenomen. Bovendien toonde eiwit- en genexpressie data van de aan sigarettenrook blootgestelde gedifferentieerde primaire bronchiale epitheelcellen een verhoogde expressie van autofagie regulatoren aan, terwijl de eiwitexpressie van regulatoren betrokken in receptor-gemedieerde mitofagie verlaagd was. Veranderingen in de regulatie van mitochondriële biogenese werden ook waargenomen in respons op sigarettenrook. Deze veranderingen in de expressie van regulatoren betrokken bij de regulatie van mitochondriële content/functie (mitofagie/biogenese) werden slechts gedeeltelijk ook waargenomen na blootstelling aan het mengsel van aldehyden. Bovendien had sigarettenrook blootstelling een effect op de genexpressie van marker *KRT5* (basaal celtype) (verlaging), terwijl andere basale en lumbale celtypen aanwezig in het bronchiale epitheel en de trilhaar bewegingen niet beïnvloed leken te worden door blootstelling aan sigarettenrook of een mengsel van aldehyden. Samenvattend suggereren deze bevindingen dat andere componenten dan aldehyden aanwezig in sigarettenrook bijdragen aan de rook-geïnduceerde veranderingen in (de regulatie van) mitochondriële functie in epitheelcellen van de luchtwegen.

Samenvatting, discussie en conclusie

Dit proefschrift had als doel om te onderzoeken wat de impact is van aldehyden (als componenten van sigarettenrook) op de moleculaire regulatie van mitochondriële functie in epitheelcellen van de longen en luchtwegen in de context van COPD.

In aanvulling op de huidige literatuur waarin een (causale) relatie tussen sigarettenrook, mitochondriële dysfunctie en COPD wordt gesuggereerd, hebben wij aangetoond dat de transcriptionele regulatie van mitochondriële biogenese en mitofagie verstoord is in het perifere longweefsel van zeer ernstig zieke COPD patiënten. Dit werd echter niet in dezelfde mate waargenomen in primaire bronchiale epitheelcellen van COPD patiënten (**hoofdstuk 2**). De waargenomen verschillen tussen de verschillende compartimenten van de luchtwegen/longen suggereren een rol voor (interacties tussen) verschillende celtypen die aanwezig zijn in de heterogene micro-omgeving in de long waarvoor het perifere longweefsel representatief is, terwijl primaire bronchiale epitheelcellen slechts een basaal cel type of een intact pseudo-gestratificeerd epithelium reflecteren.

Vervolgens heeft **hoofdstuk 3** meer inzicht gegeven in het effect van verschillende type sigarettenrook blootstelling op de moleculaire regulatie van mitochondrieel metabolisme en processen die daarbij betrokken zijn in verschillende cel modellen welke representatief zijn voor diverse soorten bronchiaal epitheel (schade). De waargenomen overeenkomsten en verschillen in de expressie en enzymactiviteit van componenten betrokken bij mitochondriële metabole processen en aanmaak/afbraak van mitochondria in de verschillende experimentele modellen benadrukken het belang van het afstemmen van het *in vitro* model op de onderzoeksvraag.

Aangezien het onbekend is welke van de duizenden stoffen in sigarettenrook verantwoordelijk zijn voor deze rook-geïnduceerde verstoring van de regulatie van mitochondriële functie en aldehyden worden erkend als één van de schadelijkste componenten, hebben wij de rol van acroleïne hierin onderzocht. Afwijkingen in de moleculaire regulatie van mitochondrieel metabolisme werden waargenomen na acute (1-2 dagen) acroleïne blootstelling van ratten (**hoofdstuk 4**). Dit effect werd echter niet (of in mindere mate) waargenomen na een langere *in vivo* acroleïne blootstelling (4 weken) (**hoofdstuk 5**).

Adaptatie na langdurige blootstelling kan een mogelijke verklaring zijn voor deze verschillende resultaten. Hoewel de gebruikte doseringen en het continue blootstellingsregime in deze studies overeenkwamen, lijken duur van blootstelling (dagen *versus* weken) en blootstellingsroute (neus *versus* whole-body) cruciaal te zijn bij het bepalen van de impact van acroleïne op mito-toxiciteit. Bovendien, zijn mitochondriële functie *per se* of kenmerken van COPD (emfyseem/bronchitis) niet geanalyseerd in deze studies, waardoor er geen conclusies kunnen worden

getrokken over de relatie tussen acroleïne inhalatie en mitochondriële functie en/of de ontwikkeling van COPD. Ten slotte, is alleen acroleïne blootstelling onderzocht waardoor we niets kunnen concluderen over andere aldehyden en/of de mogelijke invloed van andere chemische componenten aanwezig in sigarettenrook (in combinatie met aldehyden) op mito-toxiciteit in cellen van de longen.

Aangezien het relevanter is om, in de context van sigarettenrook, studies uit te voeren waarin geavanceerde *in vitro* modellen van humane primaire cel culturen worden blootgesteld aan een mengsel van aldehyden via een fysiologisch blootstelling regime (puf-regime), hebben wij dit gebruikt voor het onderzoeken van onze hypothese in **hoofdstuk 6**. Hoewel een verstoring in de inflammatoire respons alsook in de regulatie van mitochondriële content/functie (mitofagie/biogenese) werd waargenomen in respons op sigarettenrook, werden deze bevindingen slechts gedeeltelijk bevestigd na blootstelling aan het mengsel van aldehyden. Er zijn verschillende verklaringen voor deze discrepanties. Ten eerste, het mengsel van aldehyden gedraagt zich mogelijk anders dan de aldehyden zoals aanwezig in het complexe mengsel van sigarettenrook. Ten tweede, het kan niet worden uitgesloten dat andere chemische componenten aanwezig in sigarettenrook verantwoordelijk zijn voor de rook-geïnduceerde mito-toxiciteit in cellen van de longen. Ten derde dienen de uitdagingen met betrekking tot de dosimetrie te worden opgelost om direct terug te kunnen meten welke hoeveelheid aldehyden de cellen hebben bereikt om vervolgens meer inzicht te krijgen in effecten van dosimetrie. Ten vierde zou het mogelijk kunnen zijn, zoals eerder gesuggereerd, dat de heterogene micro-omgeving in de long en respectievelijk interactie tussen verschillende cel populaties een rol speelt bij de relatie tussen aldehyden blootstelling, mitochondriële dysfunctie, en COPD ontwikkeling. Vervolgonderzoek met bijvoorbeeld co-culturen kunnen bijdragen om dit effect onderzoeken.

Concluderend vormen de bovenstaande resultaten van de onderzoeken omtrent blootstelling aan aldehyden geen overtuigend bewijs om de regulering (verlaging) van aldehyden in sigarettenrook te ondersteunen. Desalniettemin, draagt ons onderzoek bij aan het beschikbare wetenschappelijke bewijs met betrekking tot de impact van de blootstelling aan aldehyden via sigarettenrook op de moleculaire mechanismen die ten grondslag liggen aan mitochondriële dysfunctie in de (epitheel) cellen van de longen en luchtwegen van rokers. Deze aanvullende wetenschappelijk kennis creëert meer bewustzijn van de potentie en noodzaak van het reguleren van de inhoud en samenstelling van emissies van tabak producten, in het bijzonder suikers en additieven, en dient in overweging te worden genomen door beleidsmakers.

Ten slotte hebben wij op basis van onze bevindingen en de huidige literatuur verschillende 'knowledge gaps' geïdentificeerd. Toekomstig onderzoek zal zich kunnen focussen op:

1. *De rol van aldehyden in de ontwikkeling van COPD*

Suggesties voor onderzoek: langdurige blootstellingen aan individuele aldehyden, mengsels van aldehyden en/of in combinatie met andere chemische stoffen aanwezig in sigarettenrook in in vivo of geavanceerde in vitro modellen (e.g., co-culturen) dienen te worden gecombineerd met eindpunten gerelateerd aan COPD ontwikkeling zoals slijm hypersecretie of beschadigingen aan het epitheel.

2. *De relatie tussen blootstelling aan aldehyden en mitochondriële dysfunctie in cellen van de longen en luchtwegen.*

Suggesties voor onderzoek: het effect van individuele aldehyden, mengsels van aldehyden en/of in combinatie met andere chemische stoffen aanwezig in sigarettenrook op de mitochondriële functie per se in cellen van de luchtwegen en longen kan worden geanalyseerd door middel van geavanceerde respiratie metingen, microscopie, activiteit van enzymen betrokken bij mitochondrieel energie metabolisme of analyse van fysiologische processen waarin mitochondria een grote rol spelen zoals slijm secretie en trilhaar bewegingen.

3. *De causale rol van aldehyde-geïnduceerde mitochondriële dysfunctie in de ontwikkeling van COPD.*

Suggesties voor onderzoek: genetische modificaties of farmacologische interventies welke zich richten op het voorkomen, opruimen of redden van door aldehyde veroorzaakte schade, mitochondriële (dys)functie of COPD ontwikkeling kunnen bijdrage aan het ontrafelen van de relatie tussen aldehyden, mitochondriële dysfunctie en de ontwikkeling van COPD.

Naast bovenstaande punten, moet worden onderzocht of het verlagen van de aldehyde levels (dosis-respons studies) in sigaretten (rook) kan bijdragen aan gezondheidswinst van rokers, specifiek met betrekking tot een gunstig effect op mitochondriële dysfunctie in de context van COPD ontwikkeling.

Deze toekomstige onderzoeken kunnen bijdragen aan het verkennen van de mogelijkheden om COPD therapieën te ontwikkelen die zich richten op mitochondria en/of aldehyden.

Samenvattend, kunnen we concluderen dat, op basis van ons onderzoek, het op dit moment onduidelijk is of aldehyden bijdragen aan het risico op COPD via het induceren van mitochondriële dysfunctie. Aanvullend wetenschappelijk onderzoek zal nodig zijn om het mechanistische en causale effect van aldehyden op de regulatie van mitochondriële processen/functie in de longen en luchtwegen verder te onderzoeken.

Dankwoord

‘What you do in the dark, puts you in the light’

Na ontelbaar veel dagen in de celkweek, talloze qPCR en Western blot analyses in het lab en het (her)schrijven van manuscripten tot in de late avond uren achter mijn laptop, is daar dan nu eindelijk het moment om mijn proefschrift te gaan verdedigen in de ‘spotlights’! Dit betekent dat het einde van mijn PhD traject is aangebroken, een avontuur met pieken en dalen, trots en teleurstelling, zoals die horen bij het doen van onderzoek. Dit proefschrift zou niet tot stand zijn gekomen zonder de inzet en betrokkenheid van velen van jullie die ik hiervoor graag wil bedanken.

Allereerst, gaat mijn dank en waardering uit naar mijn promotieteam. Dank voor de kans die jullie mij hebben geboden om te promoveren en het vertrouwen wat jullie mij hebben gegeven gedurende het project.

Antoon, hartelijk dank voor het vertrouwen en de vrijheid die je mij hebt gegeven om mij te laten starten met dit project en er mijn eigen invulling aan te geven. Dankzij jou, verloren wij niet uit het oog dat het minstens net zo belangrijk is om de vertaalslag te maken van wetenschappelijke inzichten naar maatschappelijke impact en beleid.

Frederik-Jan, dank voor het bieden en faciliteren van een promotie plek op de afdeling Farmacologie en Toxicologie. Ik heb veel geleerd over het doen van wetenschappelijk onderzoek de afgelopen jaren en heb mij bovendien altijd gesteund gevoeld in het uitvoeren van ons onderzoek, of dit nu was in Maastricht of op het RIVM. Daarnaast ben ik dankbaar voor de mogelijkheden om al vroeg in mijn PhD traject de kans te krijgen om af te reizen naar congressen om ons onderzoek te presenteren en een netwerk op te bouwen. De bemoedigende en motiverende woorden tijdens de laatste fase van mijn PhD, hielpen mij om met een positieve blik de eindsprint in te zetten.

Alex, ik wil jou bedanken voor de intensieve en enthousiaste begeleiding tijdens mijn promotietraject. Vanaf dag één stond jouw deur altijd open voor grote en kleine vragen, of dit nu was tijdens de wekelijkse meetings of even tussendoor. Door jouw input en kritische blik, heb ik de afgelopen jaren veel geleerd over het doen van onderzoek, scherper opschrijven van wetenschappelijke manuscripten, presenteren van de hoofdboodschap en ook het geven van onderwijs en begeleiden van studenten. Jouw onuitputtelijke enthousiasme voor wetenschappelijk onderzoek en vele ideeën werkten aanstekelijk, inspireerden, en motiveerden op de momenten dat ik het soms even niet meer zag zitten. Daarnaast heb ik veel gehad aan en geleerd van alle (inter-) nationale samenwerkingen die jij tijdens mijn PhD hebt geïnitieerd. Ten slotte, waren de congressen die wij samen hebben bezocht naast interessante ook leuke uitstapjes. Ik heb onze samenwerking altijd als erg prettig ervaren en ben dankbaar voor het vertrouwen wat jij mij hebt gegeven om mijzelf te ontwikkelen tot onafhankelijk onderzoeker.

Furthermore, I would like to gratefully thank the assessment committee Prof. dr. M.K.C. Hesselink, Prof. dr. D.J. Conklin, Prof. dr. F. Franssen, Prof. dr. H.I. Heijink, and Prof. dr. D.T.H.M. Sijm for their time and effort to evaluate my thesis.

Mijn PhD project was een samenwerking tussen Maastricht Universiteit, de Nederlandse Voedsel en Warenautoriteit (NVWA) en het Rijksinstituut voor Volksgezondheid en Milieu (RIVM). Ik ben dan ook dankbaar voor de kansen die dit heeft geboden. Het was leerzaam om samen te werken met de experts op het RIVM en ook gebruik te maken van de faciliteiten aldaar. Ik wil alle collega's van de tabaksgroep, GZB en in het bijzonder VTS bedanken voor het warme welkom en alle hulp tijdens de periodes dat ik in Bilthoven aan het werk was. In het bijzonder, Reinskje bedankt voor het delen van jouw kennis en inzichten met betrekking tot tabaksonderzoek. Yvonne, bedankt voor het meedenken bij het opzetten van de blootstellingsexperimenten en de input en hulp die jij mij op het RIVM en op afstand hebt geboden. Het was fijn om altijd bij jou terecht te kunnen om te overleggen over alle uitdagingen die op ons pad kwamen. Evert, Hans, Walther, Naomi, en Paul, bedankt voor jullie ondersteuning bij het opzetten van het blootstellingssysteem en uitvoeren van de chemische analyse van de rook/aldehyden-experimenten, ook al hebben wij hiervoor heel wat tegenslagen moeten overwinnen. In het bijzonder, Evert bedankt dat jij altijd klaar stond om met jouw expertise mij te helpen en mij vanaf het begin het vertrouwen gaf dat wij de experimenten links- of rechtsom zouden laten slagen. Gerco, bedankt voor alle hulp bij het in beeld brengen van de trilhaar bewegingen in onze PBEC modellen. Ik heb veel geleerd van jouw microscopie expertise. Eric, ik waardeer het dat je altijd klaar stond om mijn (logistieke) vragen te beantwoorden, mij wegwijs te maken op het lab en de assistentie bij de multiplex cytokines/chemokines analyses. GZB PhDs, bedankt voor de gezellige koffie-, lunch- en markt momenten tijdens mijn tijd in Bilthoven, ondanks dat ik vaak last-minute aan kwam schuiven vanuit de celkweek, kijk ik er met veel plezier op terug.

As I am convinced that working together in sciences will bring projects to the next level, I am thankful for all the inspiring and fruitful national and international collaborations during my PhD. I hope that these collaborations contribute to innovative steps in our field of research.

Pieter Hiemstra, Ying Wang, Daan Beentjes and Dennis Ninaber from Leiden University, thank you for the interesting collaboration which resulted in our manuscript about the differences between various *in vitro* airway models exposed to cigarette smoke. I have learned a lot from working on and writing of our manuscript together. In particular, I would like to gratefully thank Ying for your dedication and hard work to make it possible to publish our paper.

Urmila Kodavanti and Samantha Snow from the United States Environmental Protection Agency, thank you for sharing with us your precious samples of your animal exposure

study. I have enjoyed collaborating with you and would like to thank you for your valuable guidance and input for writing our manuscript. Moreover, thank you for the hospitality during my stay in Durham Urmila, and pleasant drive to the SOT in Baltimore Sam. The lunch and dinner meetings with you and your colleagues of the EPA during the SOTs were inspiring.

Preeti Sivasankar and Xinxin Liu from Purdue University, thank you for conducting the acrolein exposure studies and sharing your rat lung samples for analysis. I really appreciate your support in publishing our article.

Daniel Conklin and Jordan Finch from Louisville University, I would like to thank you for setting up our collaboration with regards to the impact of aldehydes inhalation in mice and the interesting discussions during the SOTs. Hopefully, this collaboration will be continued in the future.

Dunja Bruder and Mahyar Aghapour from Otto-von-Guericke University, thank you for unravelling together the impact of cigarette smoke extract and pneumococci on the molecular regulation of mitochondrial pathways. Our discussions about the data provided me new insights and I enjoyed our efficient way of working. Mahyar, it was fun to join together the ERS lung conference in Estoril, Portugal.

Bernd Schmeck and Birke Benedikter from Universities of Giessen and Marburg Lung Center as well as Cheryl van de Wetering, Caspar Schiffers and Niki Reynaert from the department of Respiratory Medicine, I would like to thank you all for your enthusiasm to work together on our complex manuscript, your willingness to share precious material and your critical input. Your support made it possible to investigate the abundance of molecules controlling mitochondrial turnover in various parts of the lung from COPD patients.

In addition, Birke, I would like to thank you for your curiosity-driven research mentality, which makes it interesting to work together on detecting extracellular vesicles in our aldehydes and cigarette smoke exposure experiments. Although it is still work under construction, I hope our effort will be rewarded in due time.

Special thanks to the PLUC facility coordinators and users, especially to Mieke, Niki, Nico and Lorena, as you were always eager to help, advise and share your knowledge about doing research with PBEC. Your (ad-hoc) guidance and support have helped me a lot during all the challenges faced in setting up our ALI-PBEC exposure model.

Bovendien, wil ik graag iedereen van het pulmonologie lab bedanken dat ik altijd welkom was op jullie lab. In het bijzonder: Marco bedankt voor alle (praktische) hulp, Pieter bedankt voor het delen van al jouw kennis met betrekking tot western

blotting en constructieve feedback bij het schrijven van meerdere manuscripten en Wessel, als mede-AIO van Alex, bedankt voor het altijd bereid zijn om mijn vragen te beantwoorden, te helpen bij het opzetten van experimenten en delen van jouw buffers.

Naast het inhoudelijke onderzoek, heb ik mij ingezet om de jaarvergadering van de Nederlandse Vereniging voor Toxicologie te organiseren samen met andere PhD's en professionals werkzaam bij verschillende universiteiten, bedrijven en kennisinstellingen. Ik wil graag Victoria, Gina, Charlotte en Lennart, evenals Juliëtte, Paul, Peter, Martijn en Suzanne bedanken voor de fijne samenwerking. Het gaf mij positieve energie om samen met jullie een interessant congres programma samen te stellen, ondanks de uitdagingen die kwamen kijken bij de overschakeling naar een hybride platform.

Uiteraard wil ik ook alle collega's bedanken van de vakgroep Farmacologie en Toxicologie voor zowel de inhoudelijke bijdragen, kritische vragen tijdens presentaties en behulpzaamheid in of buiten het lab, als ook voor de gezellige momenten tijdens lab-day-outs en kerstdiners.

Philippe, ik herinner mij nog goed de eerste ontmoeting waarbij jij gelijk aangaf dat als er iets was ik het altijd mocht komen vragen. Dit is na vijf jaar niet veranderd. Jouw deur staat altijd open, of dit nu is voor een wetenschappelijk vraag, sparren over protocollen of experimenten, een ontspannen koffietje of een klaag uurtje. De SOT in 2019 en aansluitende reis naar Washington en New York waren onvergetelijk. Bedankt voor de fijne samenwerking, onze goede gesprekken, en de gezelligheid de afgelopen jaren!

Marie-José en Lou, bedankt voor de prettige samenwerking. Jullie stonden altijd klaar om mij te assisteren in het lab, en ik wil jullie dan ook enorm bedanken voor de vele qPCRs en Western blots die jullie gerund hebben. Bovendien, Ger, bedankt voor de gezellige koffiemomenten en de reis in de States die mij altijd zal bijblijven. Josephina, bedankt voor de secretariële ondersteuning tijdens mijn PhD.

Finally, I would like to thank all the PhDs in the department for their support, helpfulness and fun over the past five years. Thanks for the numerous coffees, lunches, and nice events together such as iceskating, indoor-skiing, after-work drinks, and 'ambtenaren' carnaval, which made my time in Maastricht also enjoyable! George, we were officemates as of day 1 and I would like to thank you for the 1001 coffee walks we made together, sometimes full of laughter and sometimes full of complaints. Efcharistó! Kim, bedankt voor jouw Limburgse gastvrijheid waaronder de gezellige BBQ's in jouw tuin. Shan, thank you for your delicious self-made treats and your kindness to always help me out in the lab. Wenbo, thanks for joining and motivating me until late in the lab, I have enjoyed sharing our travel journeys and planning our next trips. Robert, bedankt

voor de inspirerende en enthousiaste start van de dag met een koffie op kantoor, ik word altijd vrolijk van jouw outfit complimenten. Nicole, ik wil je bedanken voor de gezellige laatste weken samen op kantoor, hopelijk heeft al ons geklets, gezucht en gesteun je niet teveel afgeleid. Irene en Michele, ik vond het leuk en leerzaam om samen als PhDs van Alex te brainstormen en te werken aan onze projecten die veel raakvlakken hadden. Carmen, Charlotte, Ellen, Julen, Kristyna, Laura, Letao, Merel, Ming, Narek, Sara, Stefan, Sven, Thanos, Timme, Victor, Zhengwen THANKS!

Ten slotte, wil ik graag de stagiaires Sarah, Juliana, Phyllis en Evi bedanken die mij hebben geholpen tijdens mijn project. Ik heb met veel plezier met jullie samengewerkt, en jullie hebben ook mij veel geleerd over de begeleiding van studenten gedurende een project.

Will en Alex van de spoelkeuken, dank voor de altijd vrolijke groeten en spoed-autoclaveer klusjes, en Eddy voor het enthousiast opzoeken en afleveren van al mijn pakketjes.

Montse, although you were not directly involved in my PhD project, I would like to thank you for your inspiring enthusiasm which motivated me to choose for a PhD. You guided me along my first steps in the lab during my Master thesis, and gave me the confidence to start my PhD journey. Last years, I often thought about and referred to your relativizing words if experiments failed or something went wrong in the lab: 'Don't worry, that's how the lab works'.

Nienke, onze wegen kruisten elkaar voor het eerst tijdens onze MSc thesis periode in Wageningen waar wij beide onder begeleiding van Montse afstudeerden. Wij sleepten elkaar door vele labuurtjes heen en ook toen al zorgde jij altijd voor de relaxte sfeer. Wat een aangename verrassing was het toen wij opnieuw met elkaar in het lab belandden, dit keer als PhD studenten bij het RIVM in de zomer van 2020. Terwijl velen op vakantie waren en thuiswerken de norm was door COVID-19, motiveerden wij elkaar opnieuw de lange lab dagen in de celkweek door. De ijs-wandelingetjes zorgden ervoor dat wij toch nog wat zonnestralen opvingen. Heel veel succes met het afronden van jouw PhD project. Wie weet kruisen onze carrière paden elkaar opnieuw in de toekomst, dat zou toch leuk zijn.

Dank aan al mijn lieve familie en vrienden, die altijd voor mij klaarstaan en zorgden voor momenten van ontspanning naast mijn PhD project. Dank voor jullie betrokkenheid, interesse en steun!

Natuurlijk wil ik mijn dierbare middelbare-school vriendinnen Anja, Anne, Charlotte, Femke en Josefen bedanken voor al jullie support en betrokkenheid bij mijn project maar bovenal ook voor alles wat niets met mijn PhD te maken had de afgelopen jaren. Terwijl

we op het gymnasium al regelmatig werden aangesproken op ons eindeloze gepraat tijdens de les, zijn we ook nu nog steeds nooit uitgepraat! Hoewel ik als enige richting het zuiden vertrok, betekende uit het oog zeker niet uit het hart. Ik zal beloven dat ik vanaf nu niet meer last-minute zal afhaken bij een weekendje weg of concert omdat ik voor mijn 'cell babies' moet zorgen. Op naar nog vele mooie momenten met elkaar.

Wie had dat gedacht lieve Joëlle, toen wij elkaar ontmoetten in de collegebanken in 2013 tijdens de minor Farmacie in Utrecht en een onvoldoende kregen voor onze essay opdracht, dat we nu 10 jaar verder beide een doctorstitel op zak zouden hebben! Het was heel fijn dat onze PhD projecten zo gelijk op liepen en wij onze struggles en successen konden delen tijdens de verschillende fases van onze projecten. Bedankt voor jouw luisterende oor tijdens onze (telefoon)gesprekken, maar bovendien ook voor de leuke momenten samen waarbij wij herinneringen ophaalden, het nu bespraken of juist vooruit blikten op de toekomst.

Oud-huisgenootjes – Daniela, Ida, Jocelyn, Lianne, Sanne, Dorianne, Bianca, Katja, Lysbet, Roëlle, Sophie – hoewel onze studententijd alweer ver achter ons ligt, voelt het bij jullie nog altijd als thuiskomen, en alsof we gisteren nog met elkaar aan de keukentafel op de Kapelstraat in Wageningen zaten! Dank voor alle gezellige momenten, en de ontspannen weekendjes skiën of surfen. Katja, jij mag jezelf ondertussen al trots doctor noemen, het was extra leuk dat onze wegen elkaar ook kruisten op TOX congressen zoals de NVT en de SOT in San Diego.

Bedankt voor de gezellige borrels en dansjes op festivals Gloriaantjes. Heerlijk om even alle PhD stress te vergeten! Dankjulliewel voor alle gezellige etentjes in Brabant Christianne, Lenna, en Noortje waarbij ik als 'import zuiderling' mocht aansluiten. Altijd lachen én goede gesprekken met jullie onder het genot van een portje Babette, Fijke en Noortje. Ik zal ervoor zorgen dat we onze whatsapp naam weer eer aan doen door ein-de-lijk terug te verhuizen naar de randstad, komen jullie op bezoek? Bedankt voor de spontane koffietjes en drankjes in Utrecht, Annemarie, Jessy & Miriam. Teuni, wat toevallig dat wij beide voor onze PhD in Maastricht belandden. Hoewel aan de andere kant van de campus, bespraken wij het wel en wee van ons PhD leven tijdens onze gezellige lunchbreaks bij UNS30 of UM sports.

Thanks voor de memorabele impulsieve reis door Indonesië Bab! Het was echt de beste afleiding en oplaad vakantie die ik mij maar kon wensen voordat ik aan de aller, allerlaatste loodjes van mijn proefschrift begon. Ik heb genoten van onze zonnige avonturen in Bali en Java, en kijk hier met een glimlach op terug. Terima kasih!

Clubgenootjes van WatDan!? Amber, Jessy, Laura, Mara, Nicolet & Tessa, dank voor de gezelligheid afgelopen jaren, of dit nu was in de vorm van etentjes, feestjes of weekendjes

Maastricht! Hoewel mijn project soms abracadabra uit te leggen was, waardeer ik jullie interesse en ben ik blij dat jullie de 3 keywords hebben onthouden, toch!?

Dankjulliewel, Nienke en Annemiek, voor de waardevolle vriendschap die al heel ver terug gaat. Ondanks dat onze levens soms even een andere weg inslaan, kruisen ze altijd weer waarbij we verder gaan waar we gebleven waren!

Lieve familie Rutgrink en Tulen, bedankt voor jullie onvoorwaardelijke betrokkenheid, interesse, steun, en bovenal gezelligheid tijdens de vele dierbare momenten samen! Ik kijk ernaar uit dat ik straks ook weer kan aanschuiven bij de doordeweekse familie momenten! Peettante Marion en peetoom Wim, dank voor de bijzondere rol die jullie in mijn leven vervullen.

Lieve papa en mama, bedankt voor jullie steun! Ik ben jullie zeer dankbaar voor het vertrouwen dat jullie ons gegeven hebben om je eigen weg in te slaan, jullie aanmoediging om door te zetten en onafhankelijk te kunnen zijn, de behulpzame en soms kritische adviezen, en natuurlijk jullie onvoorwaardelijke zorgzaamheid. De liefdevolle thuisbasis in Noordwijkerhout heeft het mogelijk gemaakt om deze mijlpaal te bereiken!

Lieve zussen, Anne en Renske, onze bijzondere en fantastische reis met z'n drieën naar Fiji en Nieuw-Zeeland direct na het opsturen van mijn proefschrift naar de leescommissie was de ultieme mogelijkheid om af te schakelen en zijn dierbare, mooie herinneringen voor het leven!

Lieve Rens, bedankt voor jouw warmte, vrolijkheid, zorgzaamheid, relativeringsvermogen en kunst om altijd weer een glimlach op mijn gezicht te toveren, dat waardeer ik echt enorm. Ik ben trots op en heb bewondering voor hoe jij in het leven staat!

Lieve An, dank voor alles!! Het opgroeien als tweelingzussen is iets unieks, en betekent in ons geval een 'soulmate' voor het leven. Hoewel wij van jongs af aan al onze eigen levens hebben opgebouwd, staan wij (ook op afstand) samen sterk en hebben we aan één woord of blik genoeg om elkaar te begrijpen. Ik kan jou niet genoeg bedanken voor jouw onvoorwaardelijke steun, eerlijke adviezen, motiverende peptalks, afleiding tijdens onze talloze mooie reizen en de deur die altijd openstaat in Amsterdam. Ik ben trots op en heb bewondering voor jouw positieve mindset en grenzeloze ambitie!

Thank you all for joining and supporting me during this PhD journey!

Bedankt voor jullie bijdragen, op welke manier dan ook!

Christy

About the author

Curriculum vitae



Christy Tulen was born in Leiden, the Netherlands on August 28th 1993. She graduated from the gymnasium at Teylingen College Leeuwenhorst in Noordwijkerhout in 2011. Pursuing her interest in human nutrition and health, she started the Bachelor's program Nutrition and Health at Wageningen University, the Netherlands. During the bachelor's phase of her studies, she completed a minor in Pharmacy at Utrecht University, the Netherlands. In 2014, she continued her

studies being enrolled in the master program Nutrition and Health and specialized in Molecular Nutrition and Toxicology at Wageningen University. She performed her master internship at the department of Nutrition, Metabolomics and Genomics focussing on the characterisation of SLC25A47 in isolated mitochondria of hepatocytes. In 2016, she received her Masters' degree from Wageningen University.

She started as a PhD-student at the department of Pharmacology and Toxicology at Maastricht University, the Netherlands in 2018. Her PhD project was a collaboration between Maastricht University, the National Institute for Public Health and the Environment (RIVM), and the Food and Consumer Product Safety Authority (NVWA). The overall aim of this PhD project was to elucidate the mechanistic involvement of smoking-associated aldehydes on the molecular regulation of mitochondrial function and content in epithelial cells of the airways and lungs, in the context of chronic obstructive pulmonary disease pathogenesis. In this project various types of experimental airway and inhalation models were used in collaboration with (inter-) national research institutes and universities.

Besides research, she was involved in teaching in the bachelor curricula Biomedical Sciences and Medicine at the Faculty of Health, Medicine and Life Sciences at Maastricht University. These teaching activities included supervising of practica, guiding problem-based learning groups and supervising bachelor and master interns. During her PhD, she followed various courses and actively participated in (inter-) national conferences by giving oral- and poster presentations awarded by prizes and supported by several travel grants. She was also a member of the organizing committee of the Dutch Society of Toxicology (NVT) annual meeting 2020/2021.

List of publications

Tulen, C.B.M., van de Wetering, C., Schiffers, C.H.J., Benedikter, B.J., Leermakers, P.A., Boukhaled, J.A., Drittij, M.J., Schmeck, B.T., Reynaert, N.L., Opperhuizen, A., van Schooten, F.J., Remels, A.H.V. Alterations in the transcript abundance of molecules controlling mitochondrial turnover in peripheral lung tissue from chronic obstructive pulmonary disease patients. *Submitted*

Tulen, C.B.M., Leermakers, P.A., Schrieder, S.E., van Schooten, F.J., Opperhuizen, A., Remels, A.H.V. Impact of sub-acute acrolein inhalation on the molecular regulation of mitochondrial metabolism in rat lung. *Submitted*

Tulen, C.B.M., Duistermaat, E., Cremers, J.W.J.M., Klerx, W.N.M., Fokkens, P.H.B., Weibolt, N., Kloosterboer, N., Dentener, M.A., Gremmer, E.R., Jessen, P.J.J., Koene, E.J.C., Maas, L., Opperhuizen, A., van Schooten, F.J., Staal, Y.C.M., Remels, A.H.V. Smoking-associated exposure of human primary bronchial epithelial cells to aldehydes: Impact on molecular mechanisms controlling mitochondrial content and function. *Submitted*

Tulen, C.B.M., Opperhuizen, A., van Schooten, F.J., Remels, A.H.V. (2023). Disruption of the molecular regulation of mitochondrial metabolism in airway and lung epithelial cells by cigarette smoke: are aldehydes the culprit? *Cells*, 12(2), 299. DOI: 10.3390/cells12020299

Tulen, C.B.M.*, Wang, Y.*, Beentjes, D., Jessen, P.J.J., Ninaber, D.K., Reynaert, N.L., van Schooten, F.J., Opperhuizen, A., Hiemstra, P.S., Remels, A.H.V. (2022). Dysregulated mitochondrial metabolism upon cigarette smoke exposure in various human bronchial epithelial cell models. *Dis Model Mech*, 15(3), dmm049247. DOI: 10.1242/dmm.049247

*These authors contributed equally to this work

Tulen, C.B.M., Snow, S.J., Leermakers, P.A., Kodavanti, U.P., van Schooten, F.J., Opperhuizen, A., Remels, A.H.V. (2022). Acrolein inhalation acutely affects the regulation of mitochondrial metabolism in rat lung. *Toxicology*, 469, 153129. DOI: 10.1016/j.tox.2022.153129

Aghapour, M., **Tulen, C.B.M.**, Abdi Sarabi, M., Weinert, S., Müsken, M., Relja, B., van Schooten, F.J., Jeron, A., Braun-Dullaeus, R., Remels, A.H., Bruder, D. (2022). Cigarette smoke extract disturbs mitochondria-regulated airway epithelial cell responses to pneumococci. *Cells*, 11(11), 1771. DOI: 10.3390/cells11111771

Vangrieken, P., Al-Nasiry, S., Bast, A., Leermakers, P.A., **Tulen, C.B.M.**, Schiffers, P.M.H., van Schooten, F.J., Remels, A.H.V. (2021). Placental mitochondrial abnormalities in preeclampsia. *Reprod Sci*, 28(8), 2186–2199. DOI: 10.1007/s43032-021-00464-y

Vangrieken, P., Al-Nasiry, S., Bast, A., Leermakers, P.A., **Tulen, C.B.M.**, Janssen, G.M.J., Kaminski, I., Geomini, I., Lemmens, T., Schiffers, P.M.H., van Schooten, F.J., Remels, A.H.V. (2021). Hypoxia-induced mitochondrial abnormalities in cells of the placenta. *PloS One*, 16(1), e0245155. DOI: 10.1371/journal.pone.0245155

Ogger, P.P., Silva, J.D., Aghapour, M., Mahmutovic Persson, I., **Tulen, C.B.M.**, Jurkowska, R., Ubags, N.D. (2020). Early Career Members at the ERS Lung Science Conference 2020: metabolic alterations in lung ageing and disease. *Breathe* (Sheff), 16(3), 200063. DOI: 10.1183/20734735.0063-2020

van 't Erve, I.* , **Tulen, C.B.M.***, Jansen, J., van Laar, A.D.E., Minnema, R., Schenk, P.R., Wolvers, D., van Rossum, C.T.M., Verhagen, H. (2017). Overview of elements within national food-based dietary guidelines. *Eur. J. Nutr. Food Saf.*, 6(4), 172-227. DOI:10.9734/EJNFS/2016/32645

*These authors contributed equally to this work

